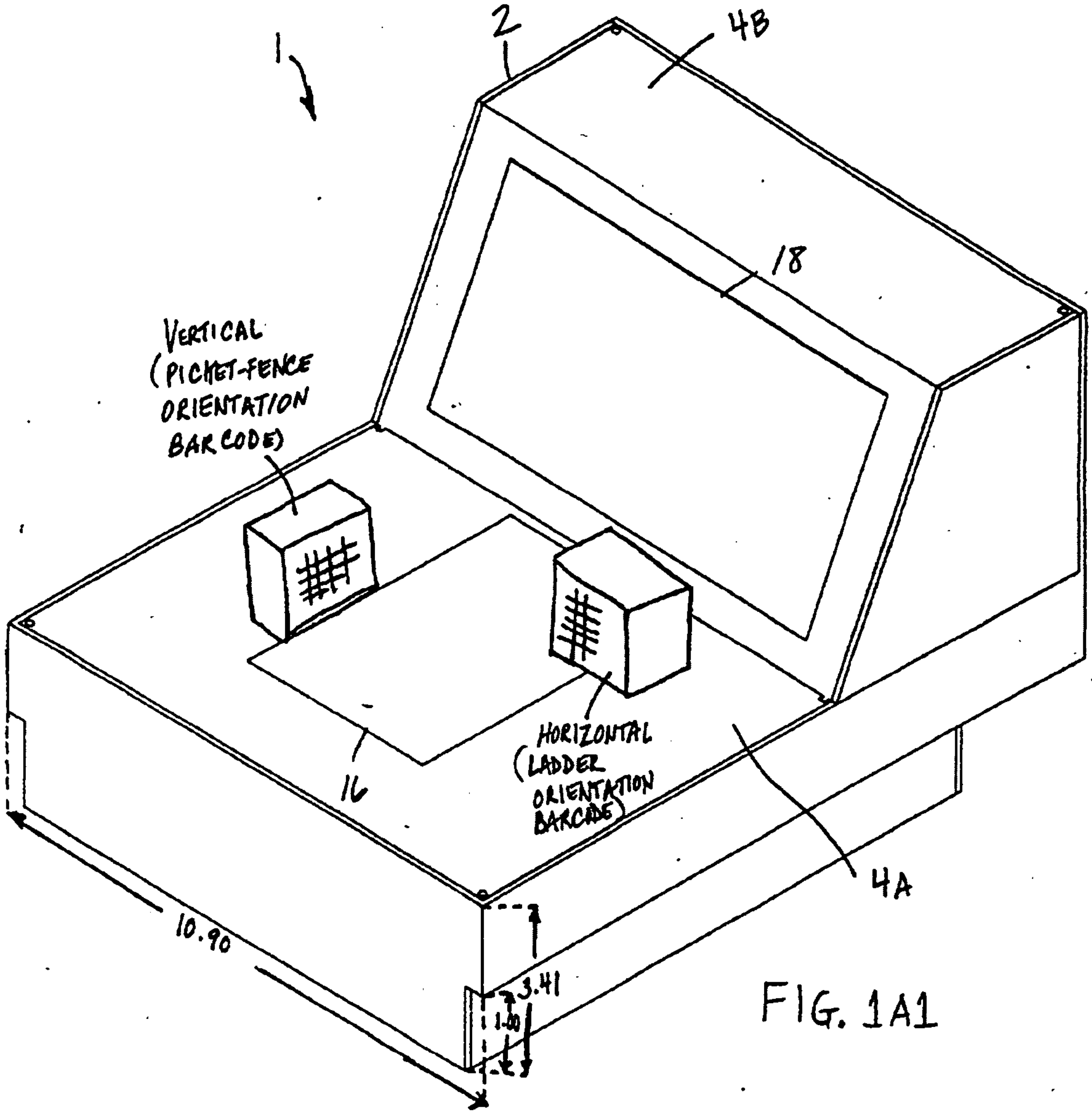
1
2
4B
18
VERTICAL (PICKET-FENCE ORIENTATION BARCODE)
HORIZONTAL (LADDER ORIENTATION BARCODE)
16
4A
10.90
3.41
1.00

FIG. 1A1

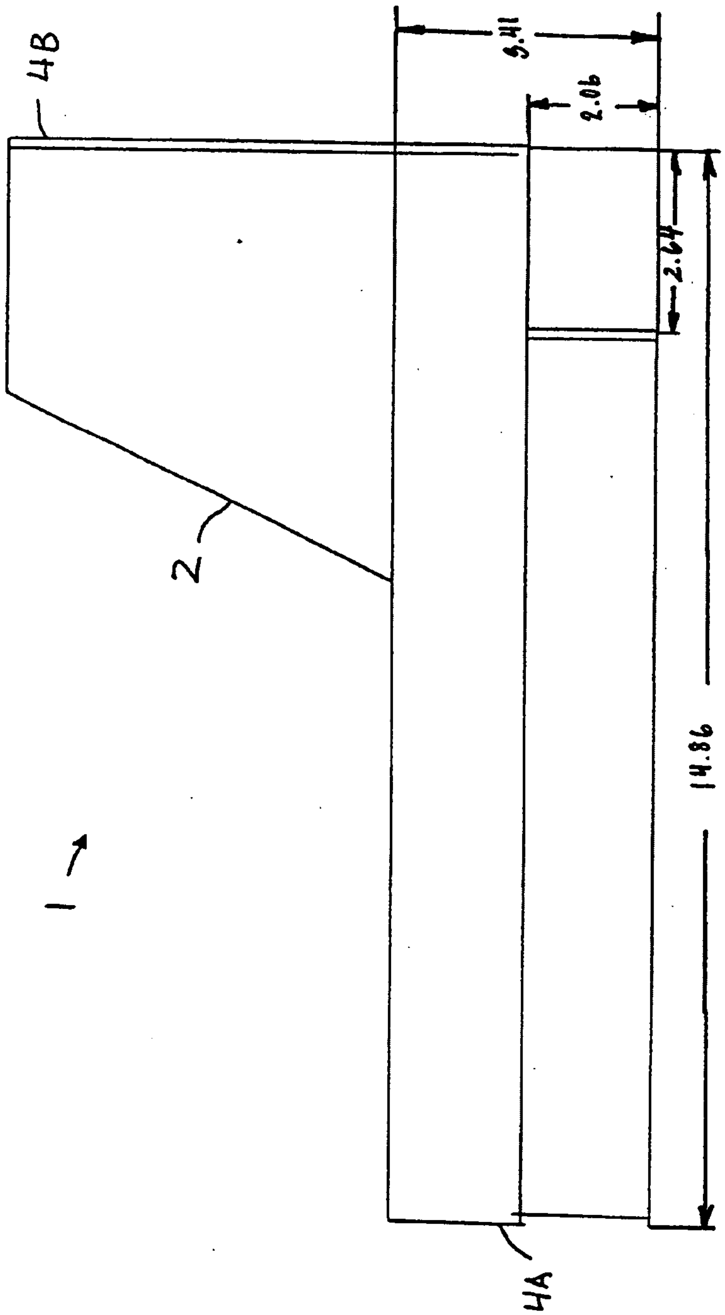

FIG. 1A2

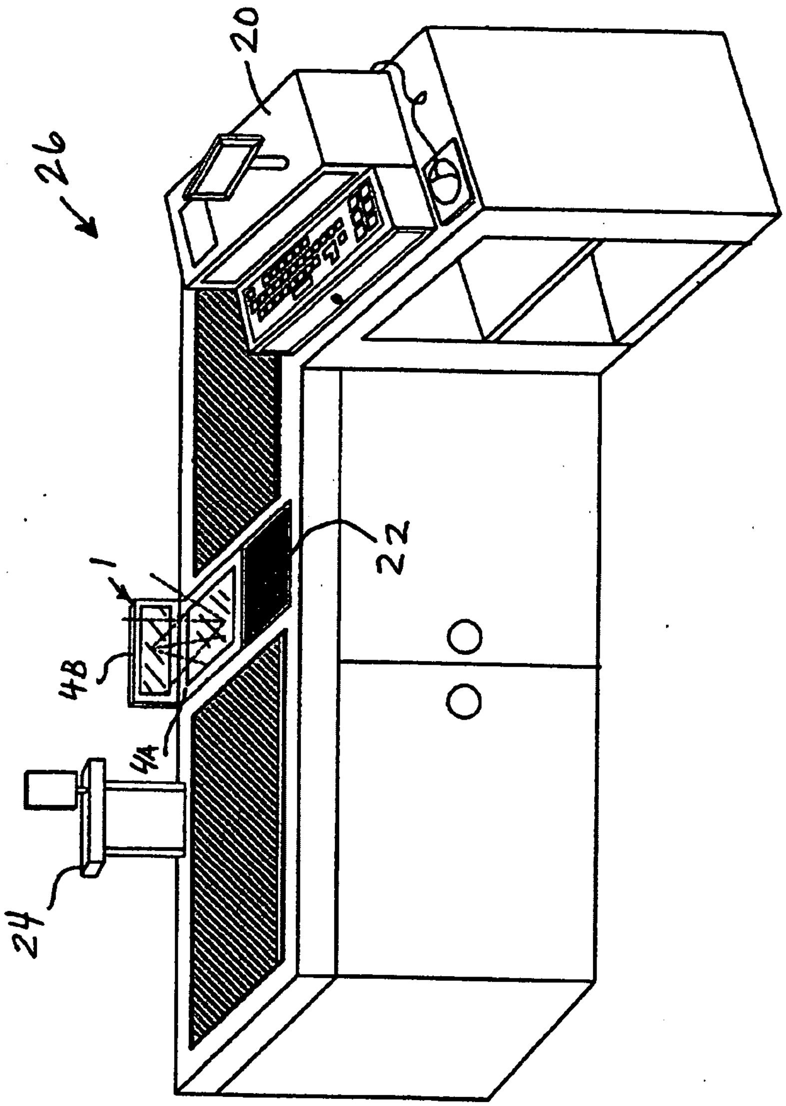

FIG. 1B

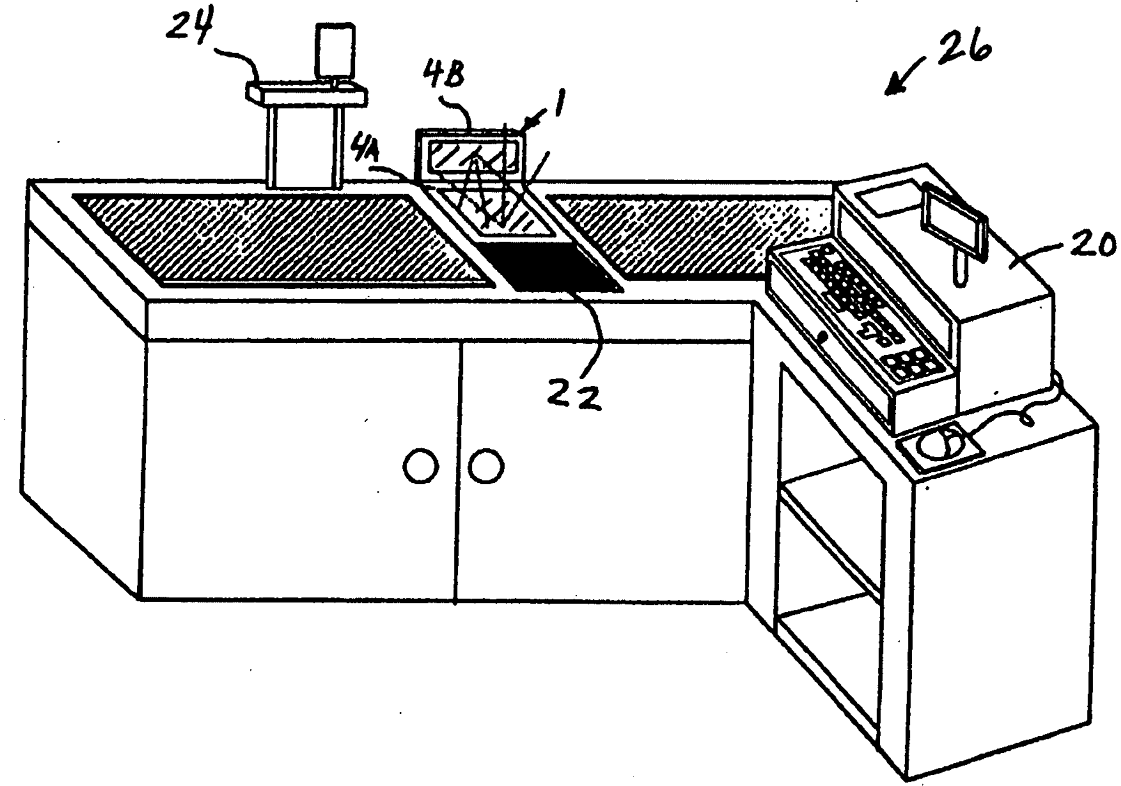

FIG. 1B1

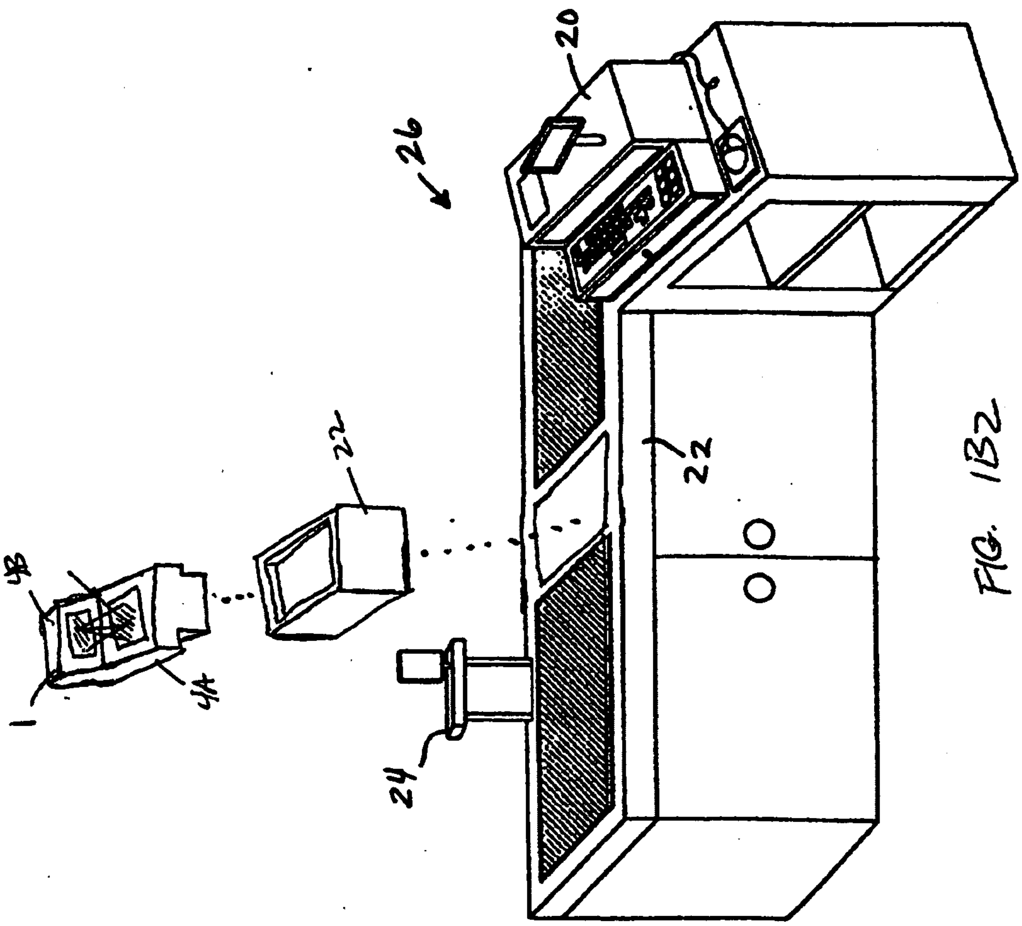

FIG. 1B2

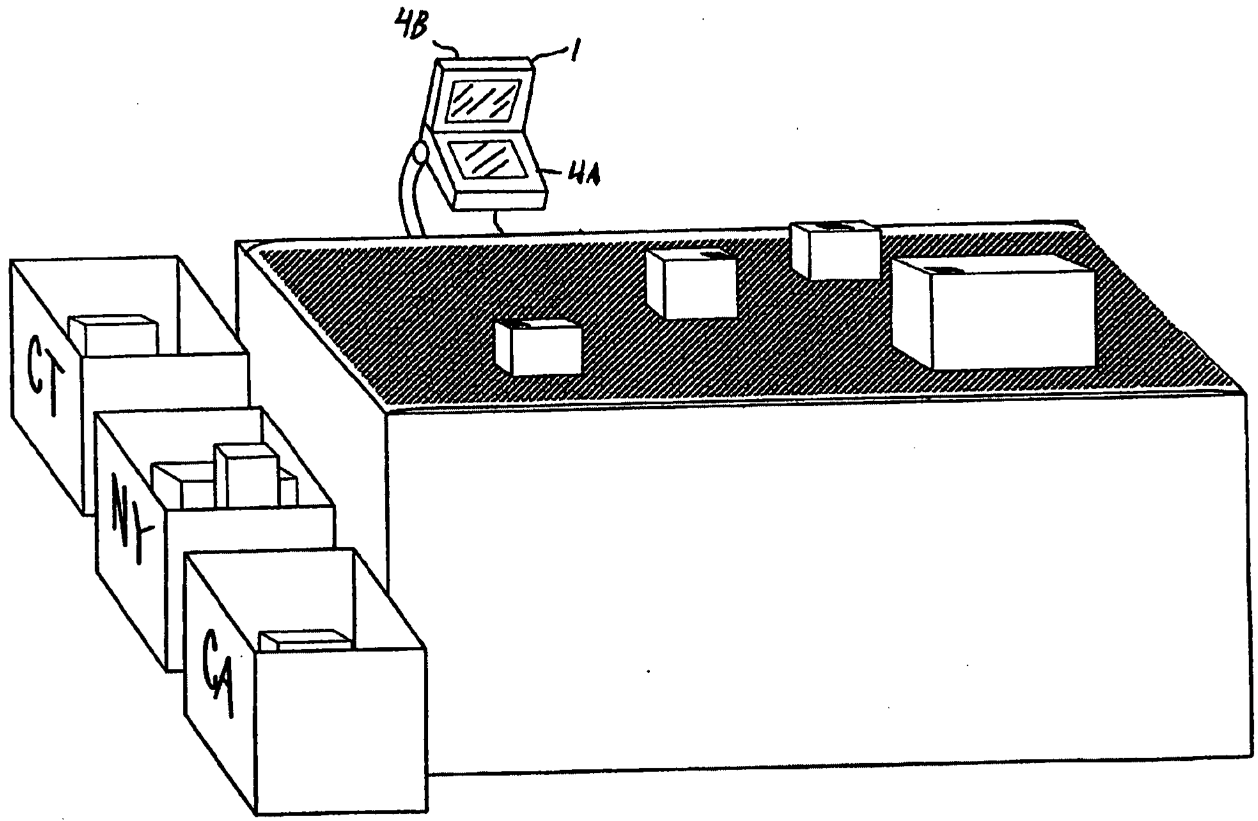

FIG. 1C

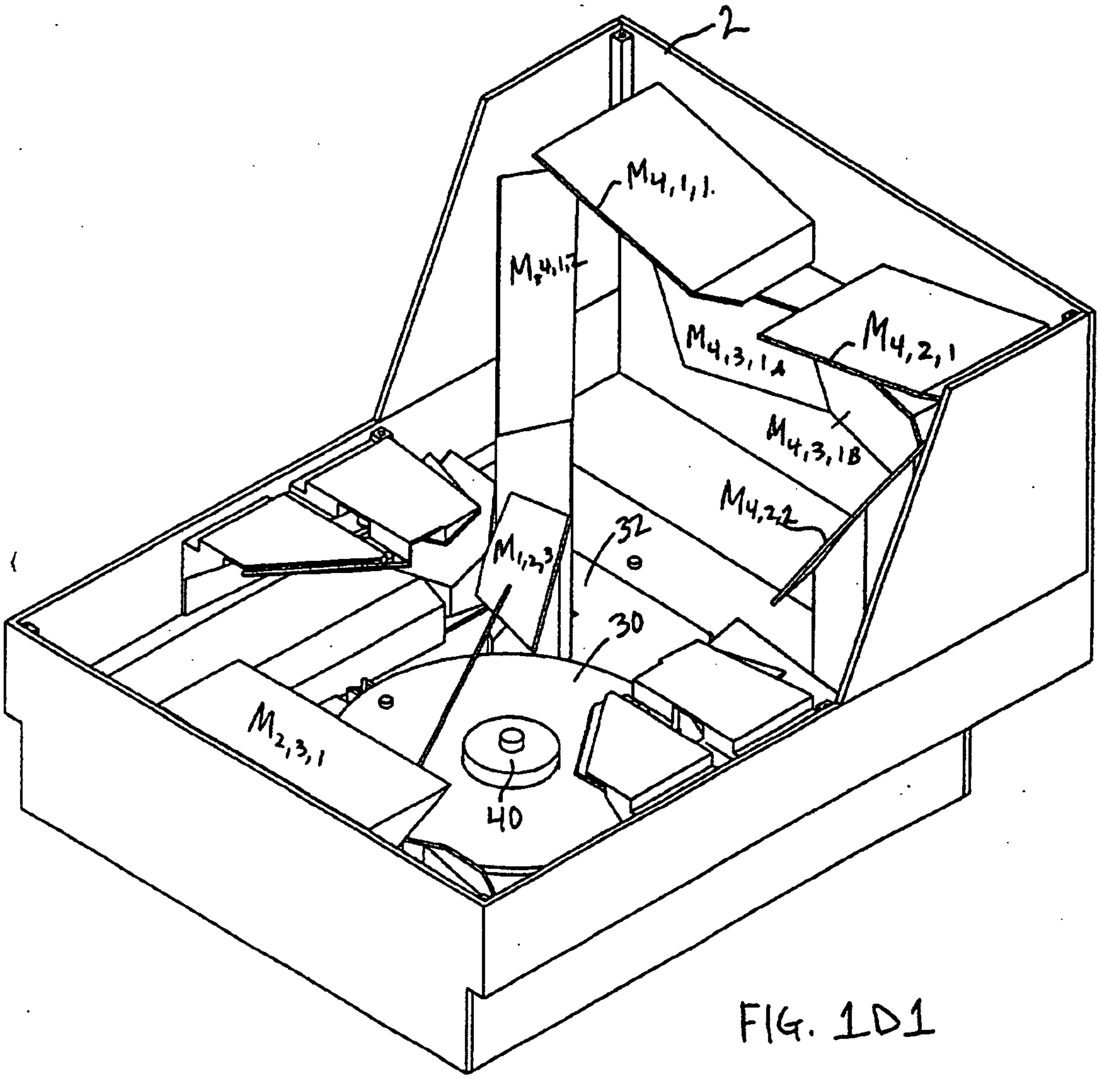

FIG. 1D1

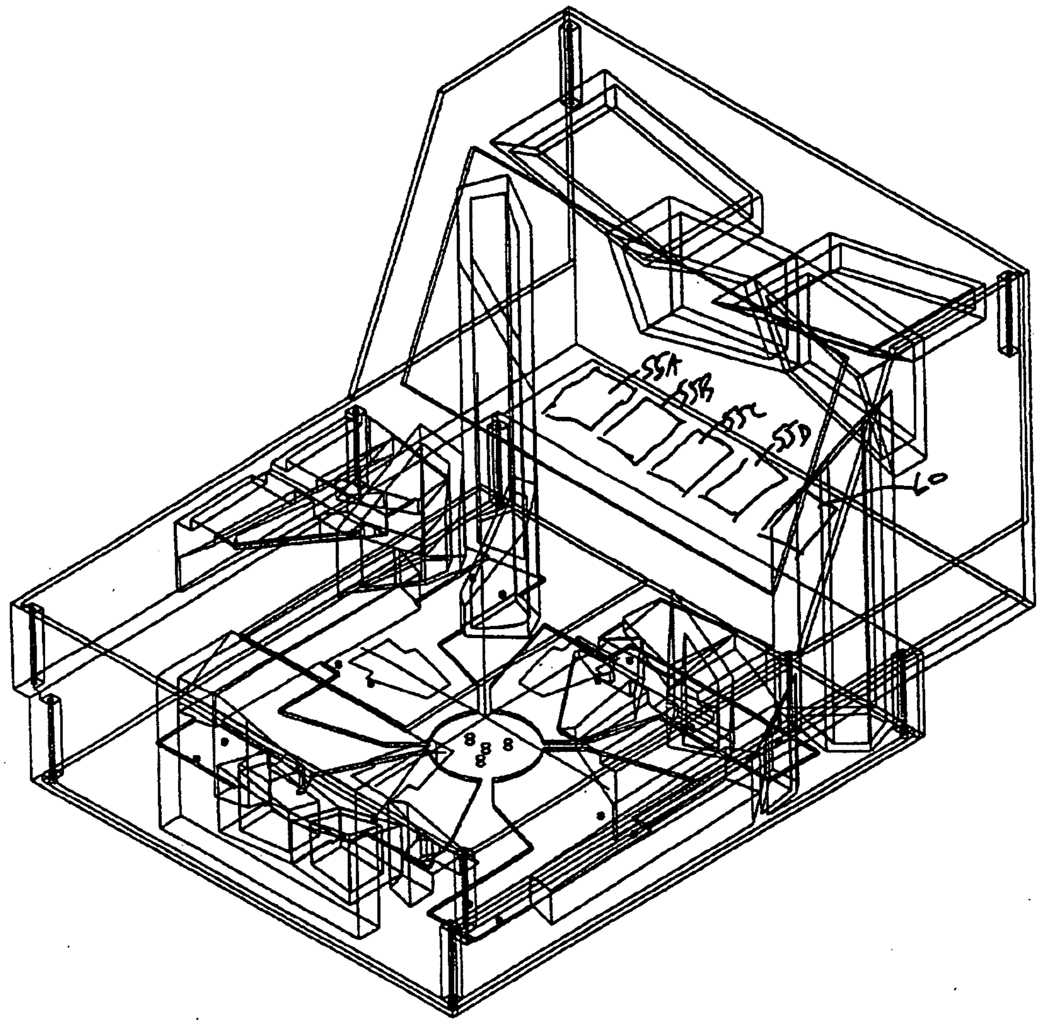

FIG. 1D2

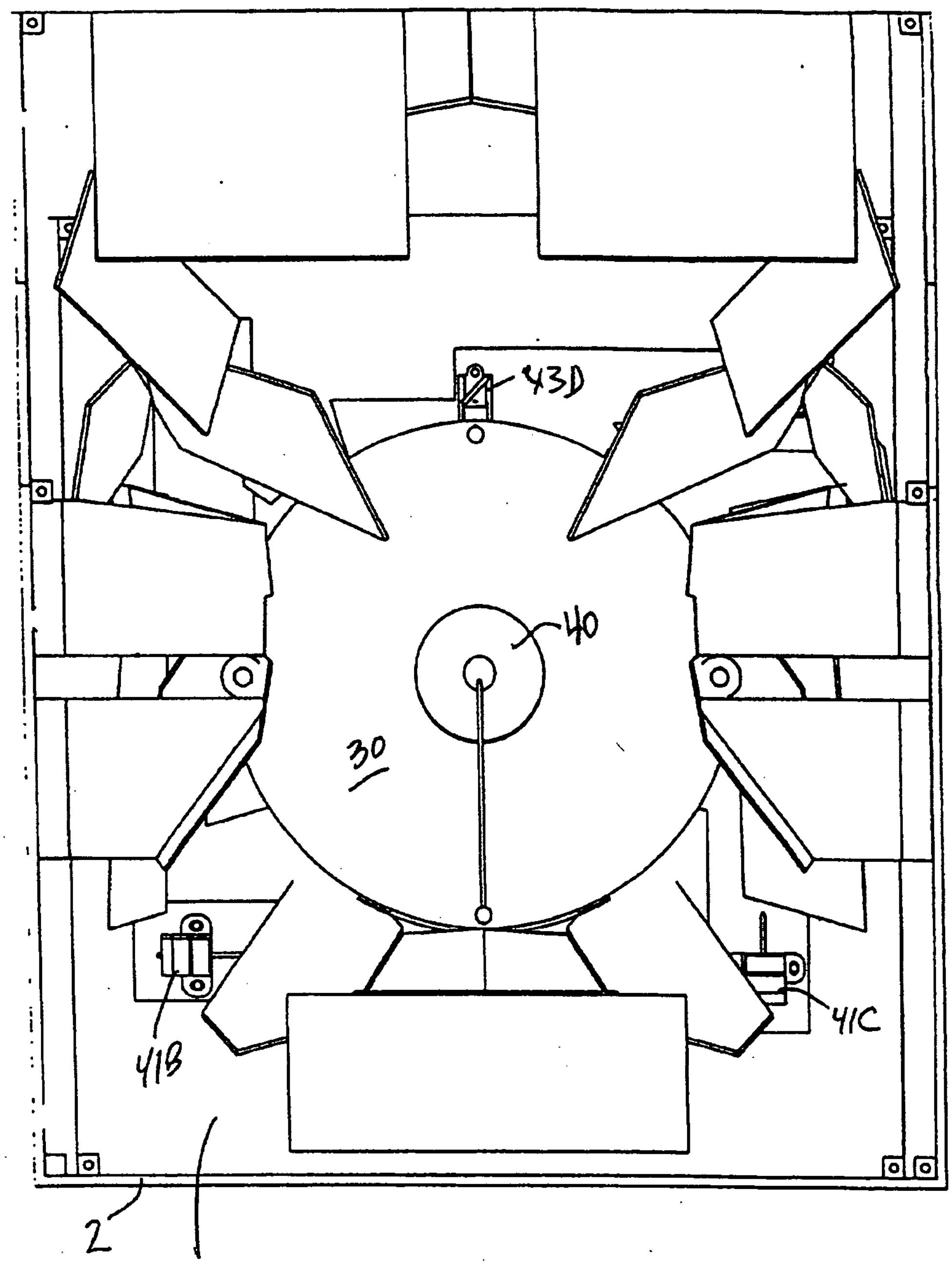

FIG. 1E

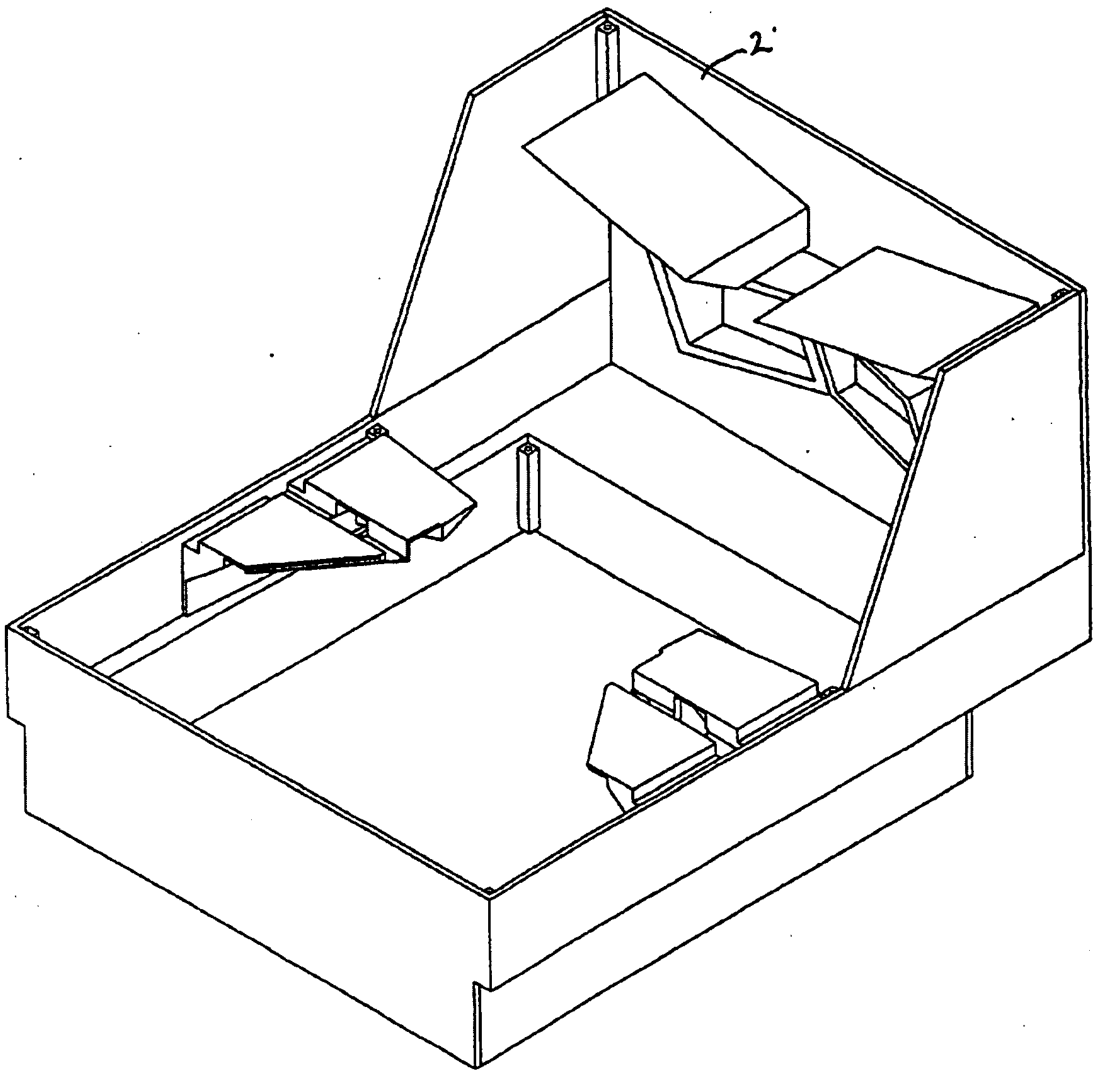

FIG. 1F

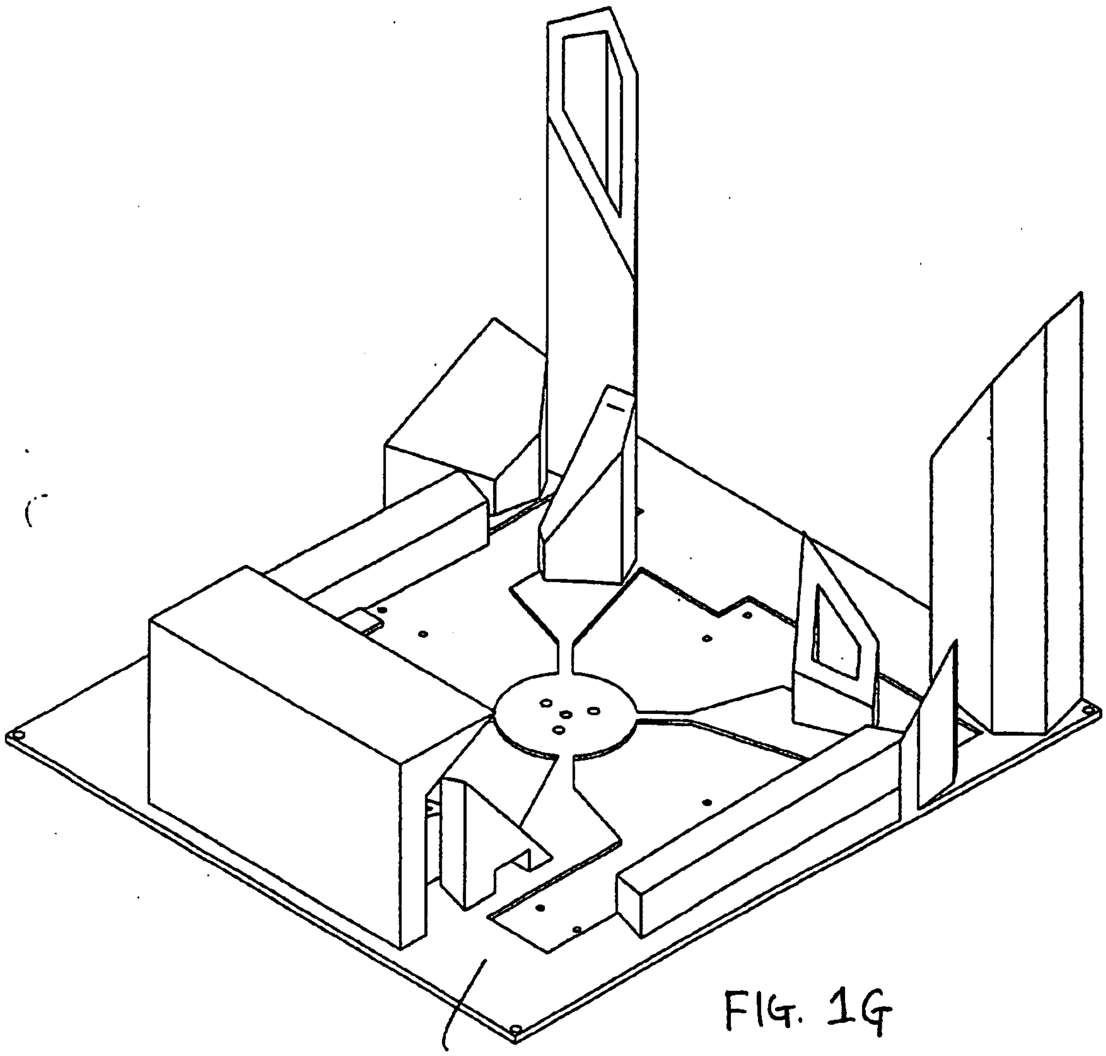

42

FIG. 1G

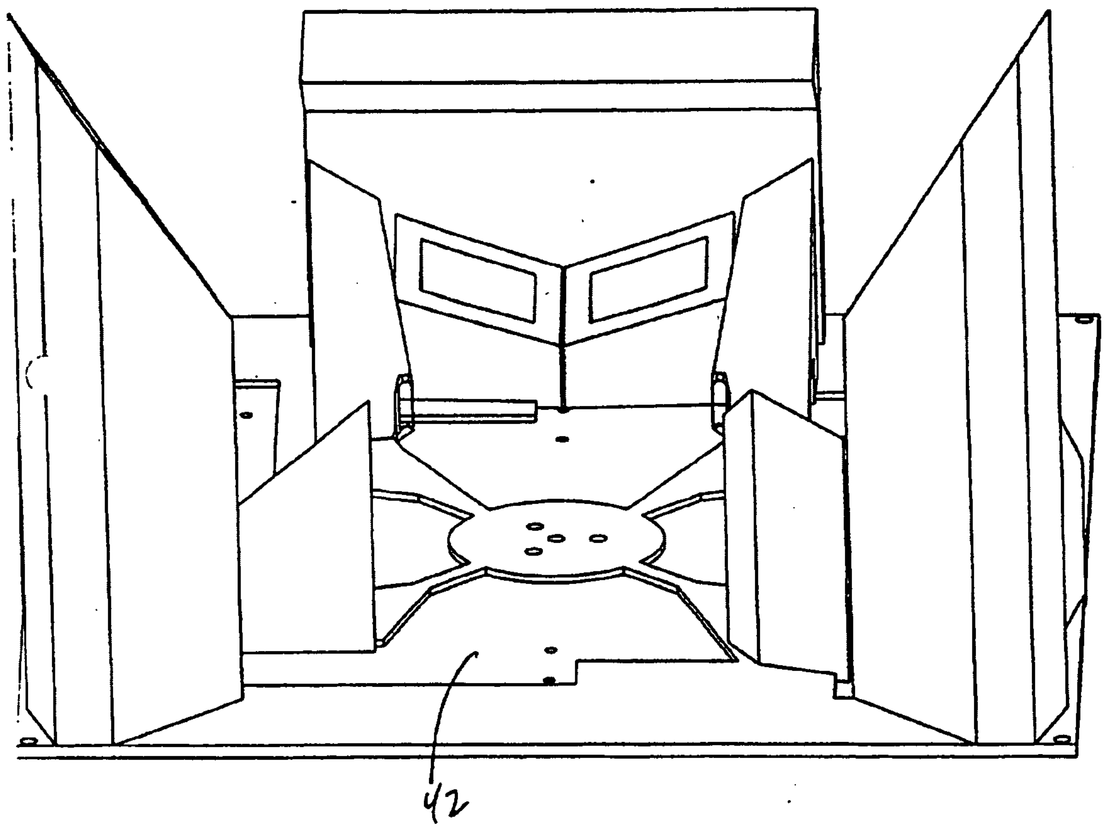

FIG. 1H

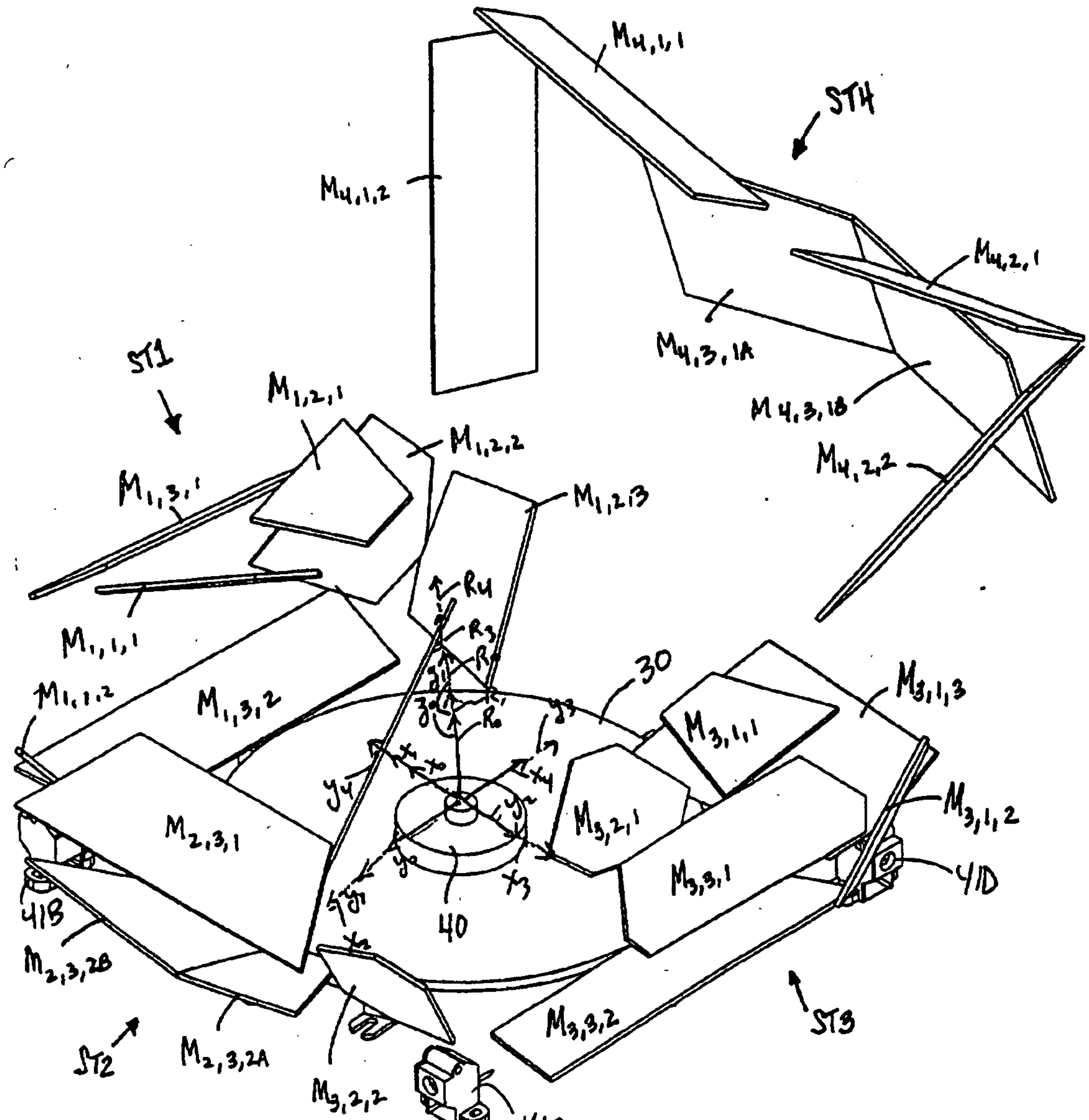

FIG. 2A1

Define: $R_1, R_2, R_3\, R_4, R_0$

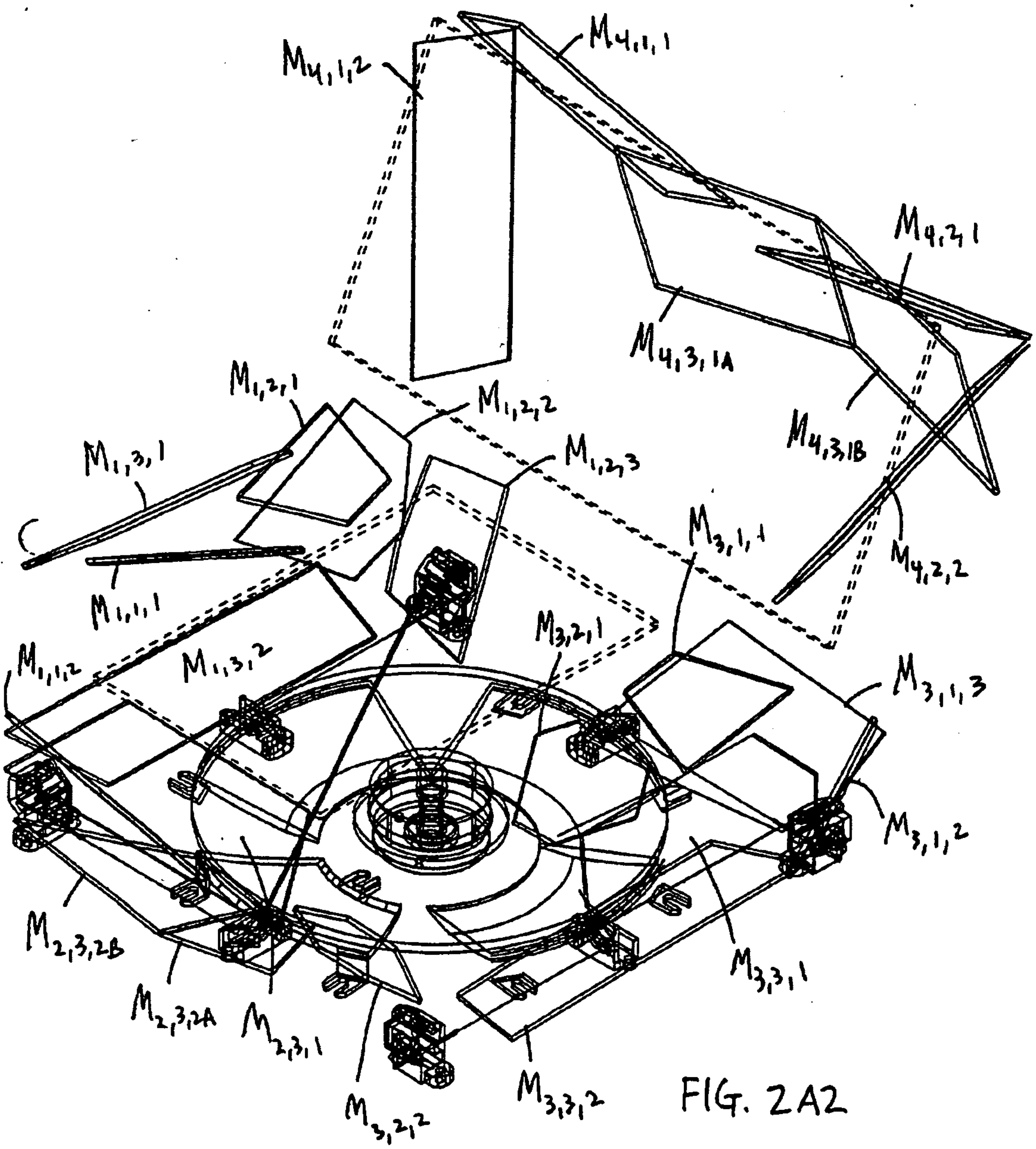
$M_{4,1,2}$
$M_{4,1,1}$
$M_{4,2,1}$
$M_{4,3,1A}$
$M_{4,3,1B}$
$M_{4,2,2}$
$M_{1,2,1}$
$M_{1,2,2}$
$M_{1,3,1}$
$M_{1,2,3}$
$M_{1,1,1}$
$M_{3,1,1}$
$M_{3,2,1}$
$M_{1,1,2}$
$M_{1,3,2}$
$M_{3,1,3}$
$M_{3,1,2}$
$M_{2,3,2B}$
$M_{3,3,1}$
$M_{2,3,2A}$
$M_{2,3,1}$
$M_{3,2,2}$
$M_{3,3,2}$

FIG. 2A2

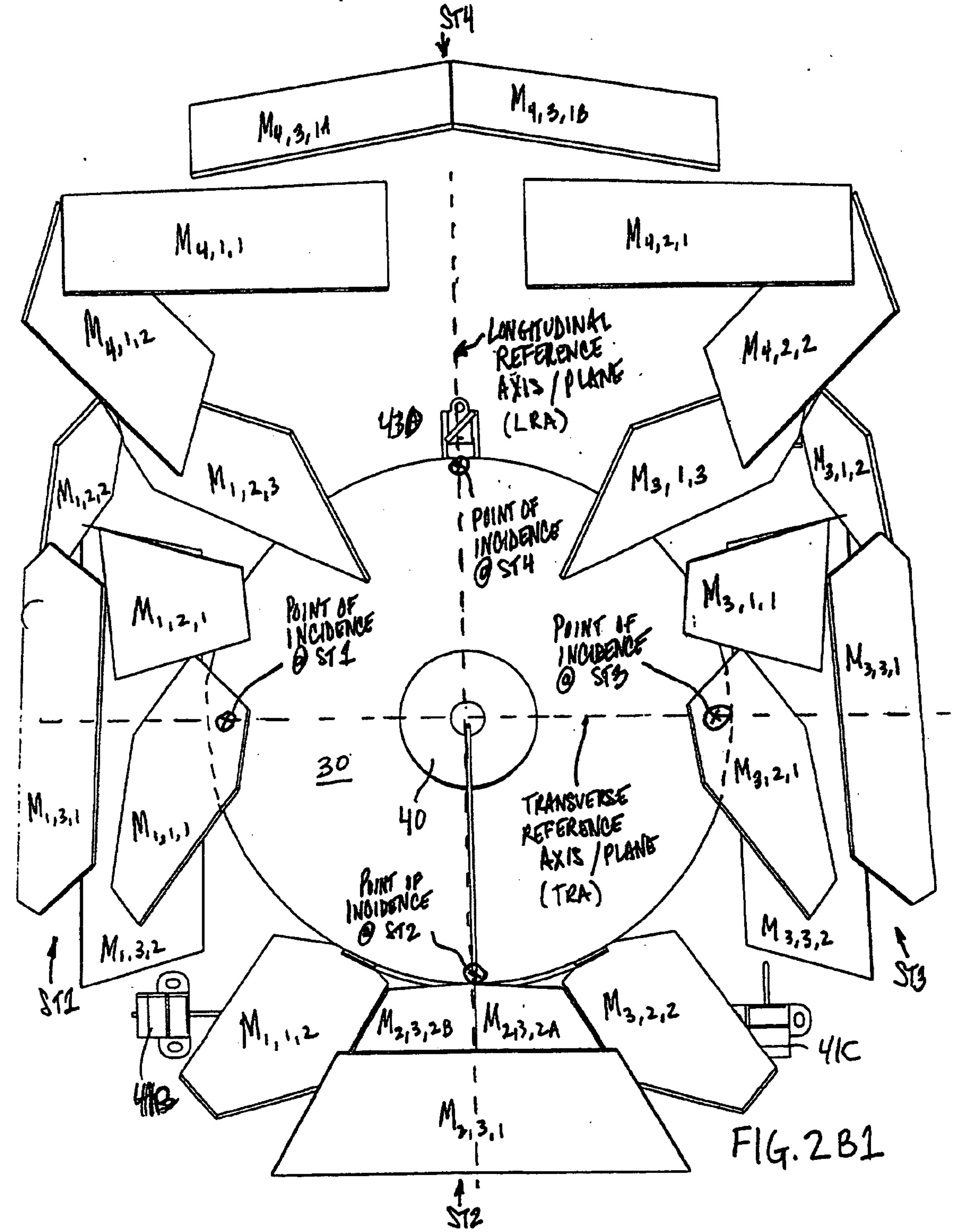
ST4
$M_{4,3,1A}$
$M_{4,3,1B}$
$M_{4,1,1}$
$M_{4,2,1}$
$M_{4,1,2}$
$M_{4,2,2}$
LONGITUDINAL REFERENCE AXIS / PLANE (LRA)
43B
$M_{1,2,2}$
$M_{1,2,3}$
$M_{3,1,3}$
$M_{3,1,2}$
POINT OF INCIDENCE @ ST4
$M_{1,2,1}$
$M_{3,1,1}$
POINT OF INCIDENCE @ ST1
POINT OF INCIDENCE @ ST3
$M_{3,3,1}$
30
40
$M_{3,2,1}$
$M_{1,3,1}$
$M_{1,1,1}$
TRANSVERSE REFERENCE AXIS / PLANE (TRA)
POINT OF INCIDENCE @ ST2
$M_{1,3,2}$
$M_{3,3,2}$
ST1
ST3
$M_{1,1,2}$
$M_{2,3,2B}$
$M_{2,3,2A}$
$M_{3,2,2}$
41C
41B
$M_{2,3,1}$
ST2

FIG. 2B1

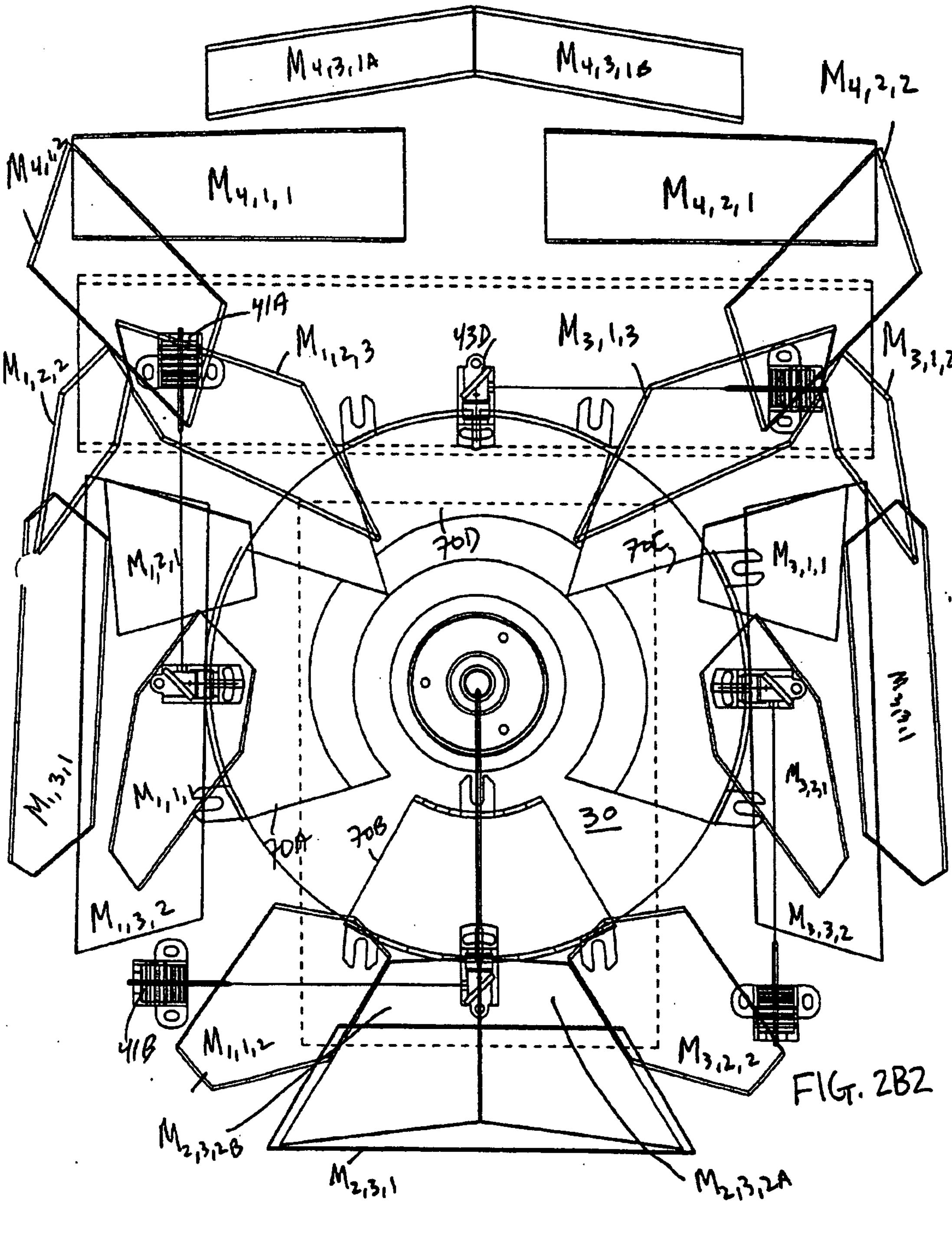

$M_{4,3,1A}$
$M_{4,3,1B}$
$M_{4,2,2}$
$M_{4,1,2}$
$M_{4,1,1}$
$M_{4,2,1}$
41A
$M_{1,2,3}$
43D
$M_{3,1,3}$
$M_{3,1,2}$
$M_{1,2,2}$
70D
70E
$M_{1,2,1}$
$M_{3,1,1}$
$M_{3,3,1}$
$M_{1,3,1}$
$M_{1,1,1}$
$M_{3,2,1}$
70A
70B
30
$M_{1,3,2}$
$M_{3,3,2}$
41B
$M_{1,1,2}$
$M_{3,2,2}$
$M_{2,3,2B}$
$M_{2,3,1}$
$M_{2,3,2A}$

FIG. 2B2

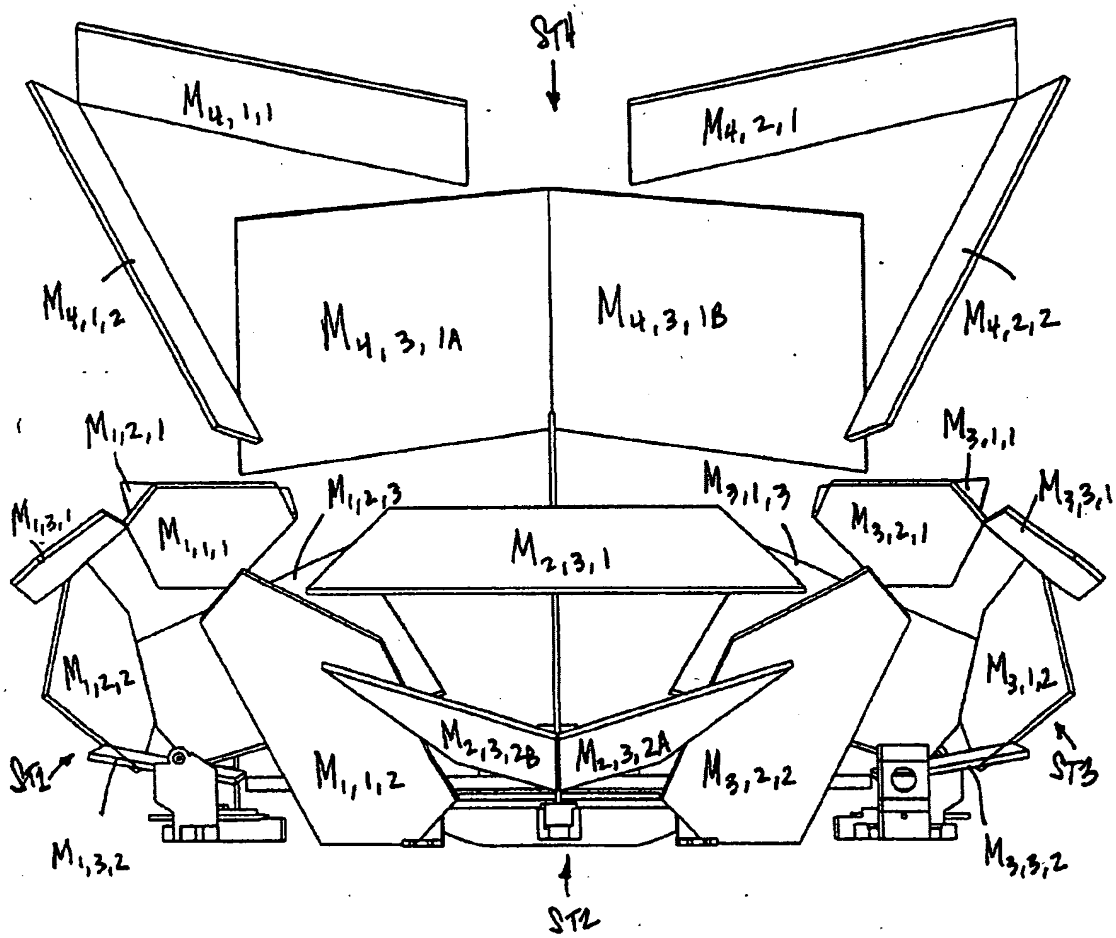
ST4
$M_{4,1,1}$
$M_{4,2,1}$
$M_{4,1,2}$
$M_{4,3,1A}$
$M_{4,3,1B}$
$M_{4,2,2}$
$M_{1,2,1}$
$M_{3,1,1}$
$M_{1,3,1}$
$M_{1,1,1}$
$M_{1,2,3}$
$M_{3,1,3}$
$M_{3,2,1}$
$M_{3,3,1}$
$M_{2,3,1}$
$M_{1,2,2}$
$M_{3,1,2}$
$M_{2,3,2B}$
$M_{2,3,2A}$
ST1
$M_{1,1,2}$
$M_{3,2,2}$
ST3
$M_{1,3,2}$
$M_{3,3,2}$
ST2

FIG. 2C1

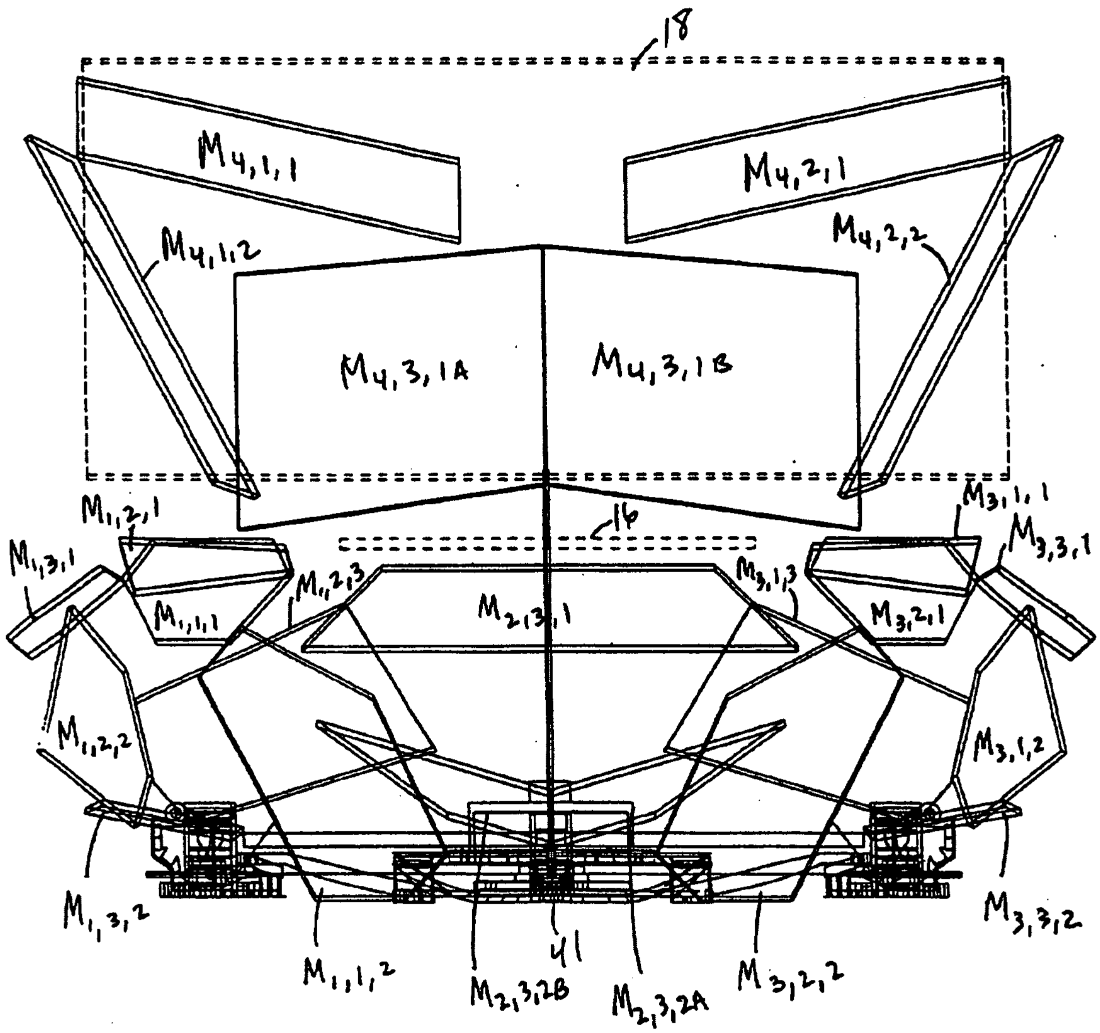
18
M4,1,1
M4,2,1
M4,1,2
M4,2,2
M4,3,1A
M4,3,1B
16
M1,2,1
M1,3,1
M1,1,1
M1,2,3
M2,3,1
M3,1,3
M3,1,1
M3,3,1
M3,2,1
M1,2,2
M3,1,2
M1,3,2
M1,1,2
M2,3,2B
41
M2,3,2A
M3,2,2
M3,3,2

FIG. 2C2

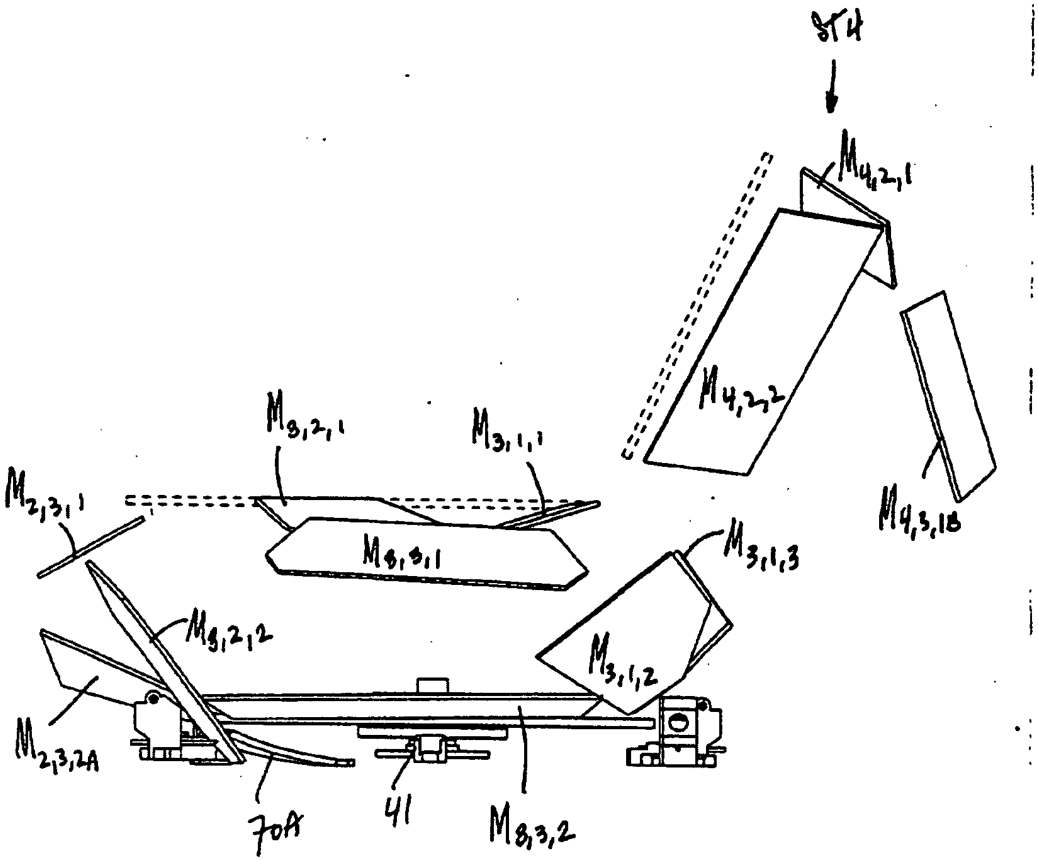
ST4
$M_{4,2,1}$
$M_{4,2,2}$
$M_{4,3,1B}$
$M_{3,2,1}$
$M_{3,1,1}$
$M_{2,3,1}$
$M_{3,3,1}$
$M_{3,1,3}$
$M_{3,2,2}$
$M_{3,1,2}$
$M_{2,3,2A}$
70A
41
$M_{3,3,2}$

FIG. 2D1

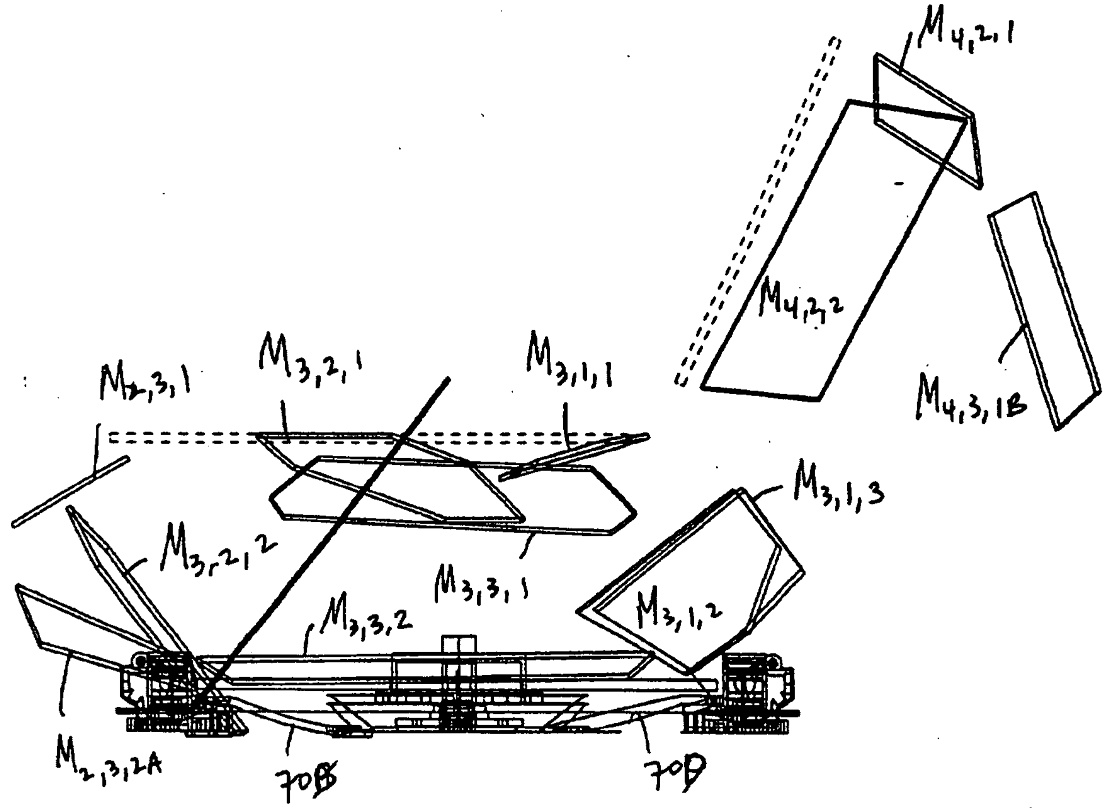
M4,2,1
M4,2,2
M4,3,1B
M2,3,1
M3,2,1
M3,1,1
M3,2,2
M3,3,1
M3,1,3
M3,1,2
M3,3,2
M2,3,2A
70B
70D

FIG. 2D2

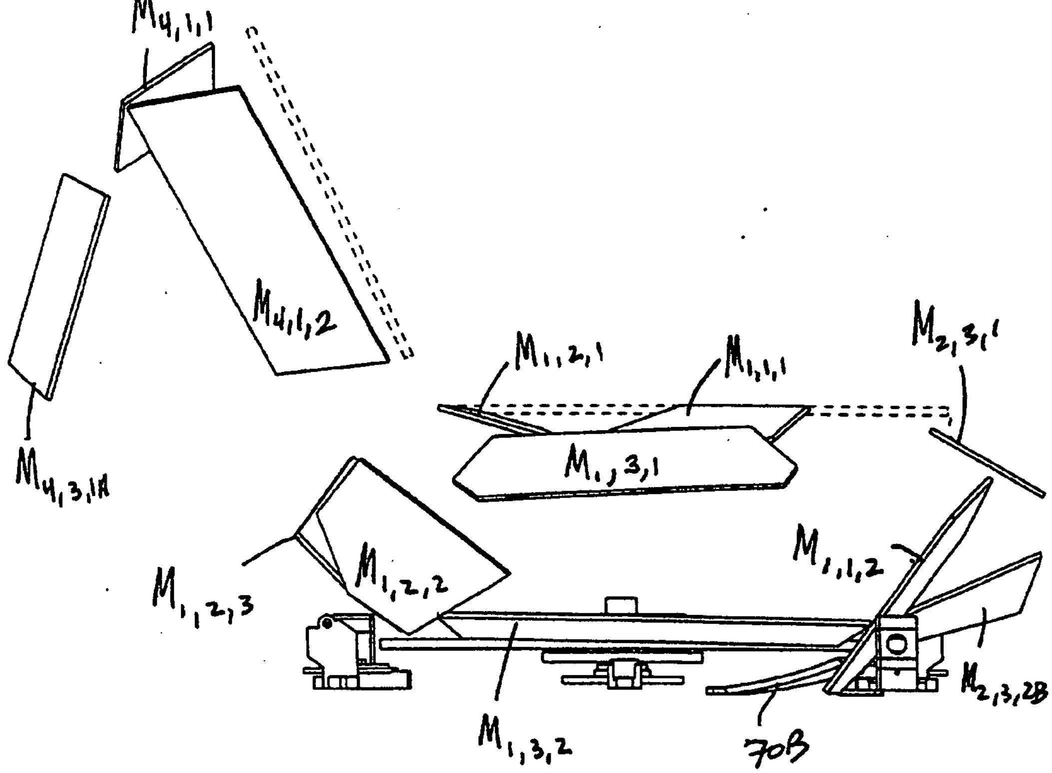
M4,1,1
M4,1,2
M4,3,1A
M1,2,1
M1,1,1
M2,3,1
M1,3,1
M1,2,3
M1,2,2
M1,1,2
M2,3,2B
M1,3,2
70B

FIG. 2E1

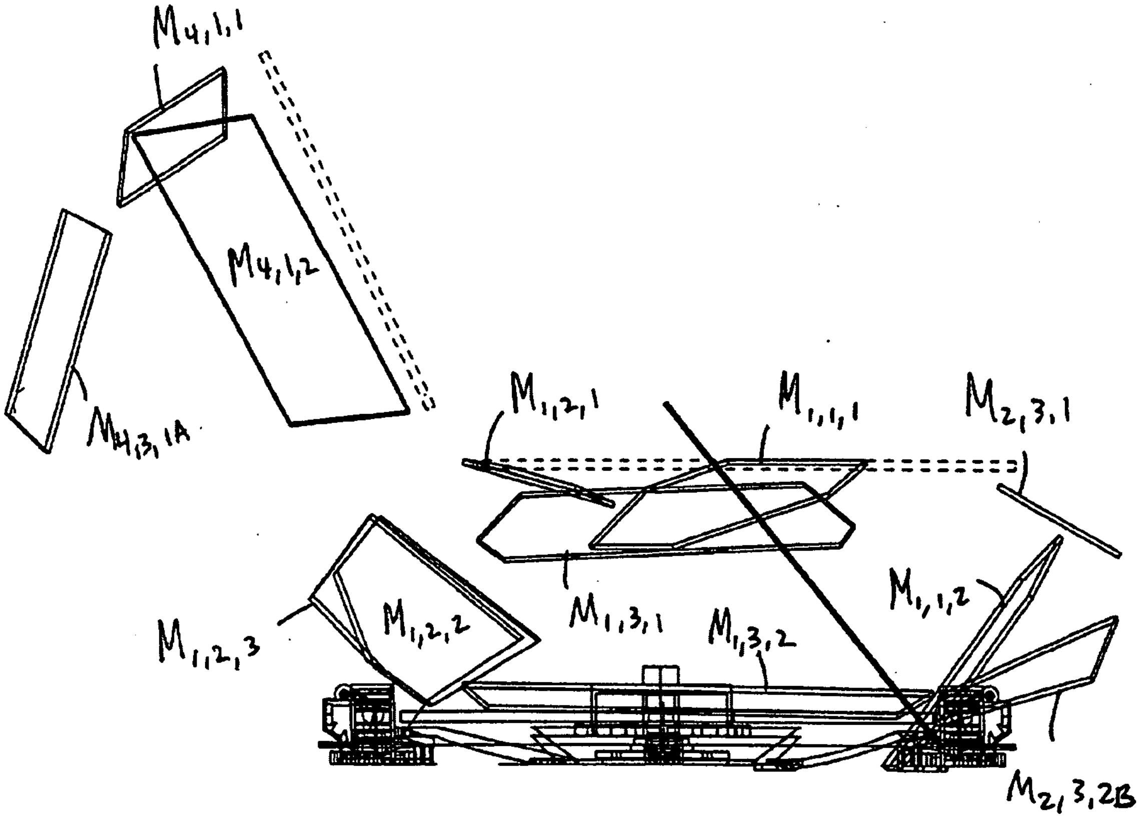
M4,1,1
M4,1,2
M4,3,1A
M1,2,1
M1,1,1
M2,3,1
M1,3,1
M1,1,2
M1,2,3
M1,2,2
M1,3,2
M2,3,2B

FIG. 2E2

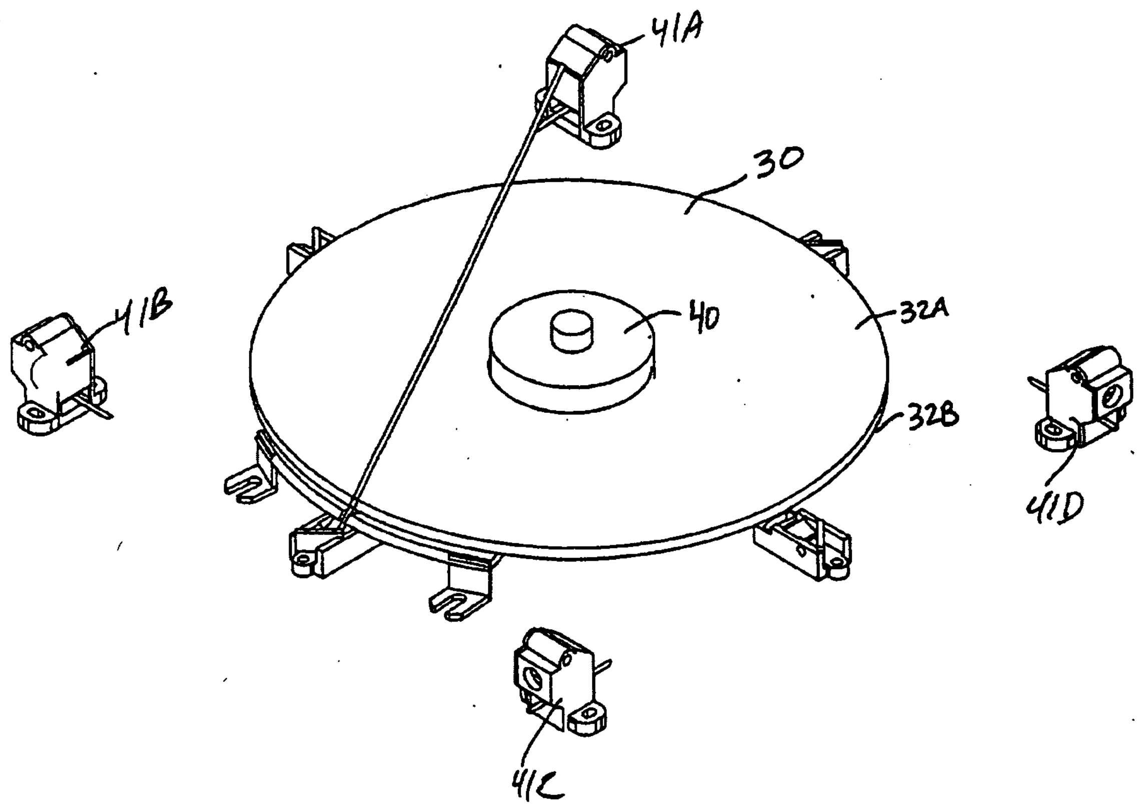

FIG. 2F1

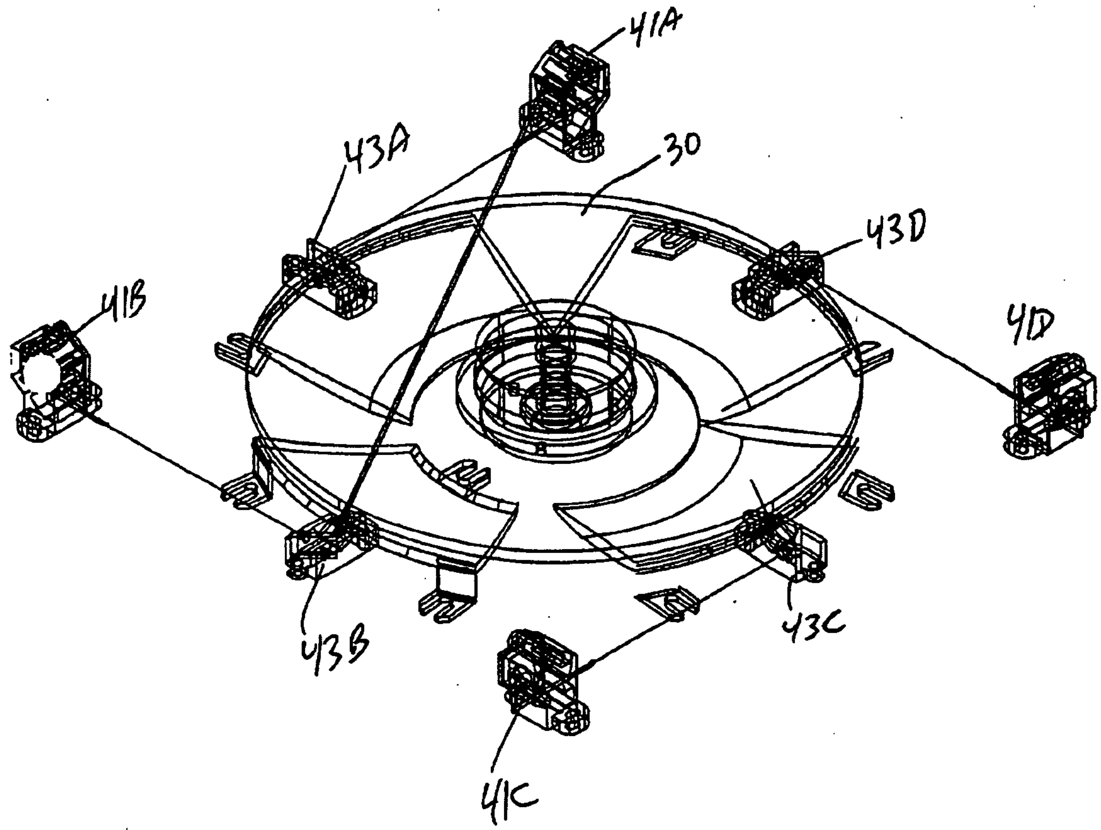

FIG. 2F2

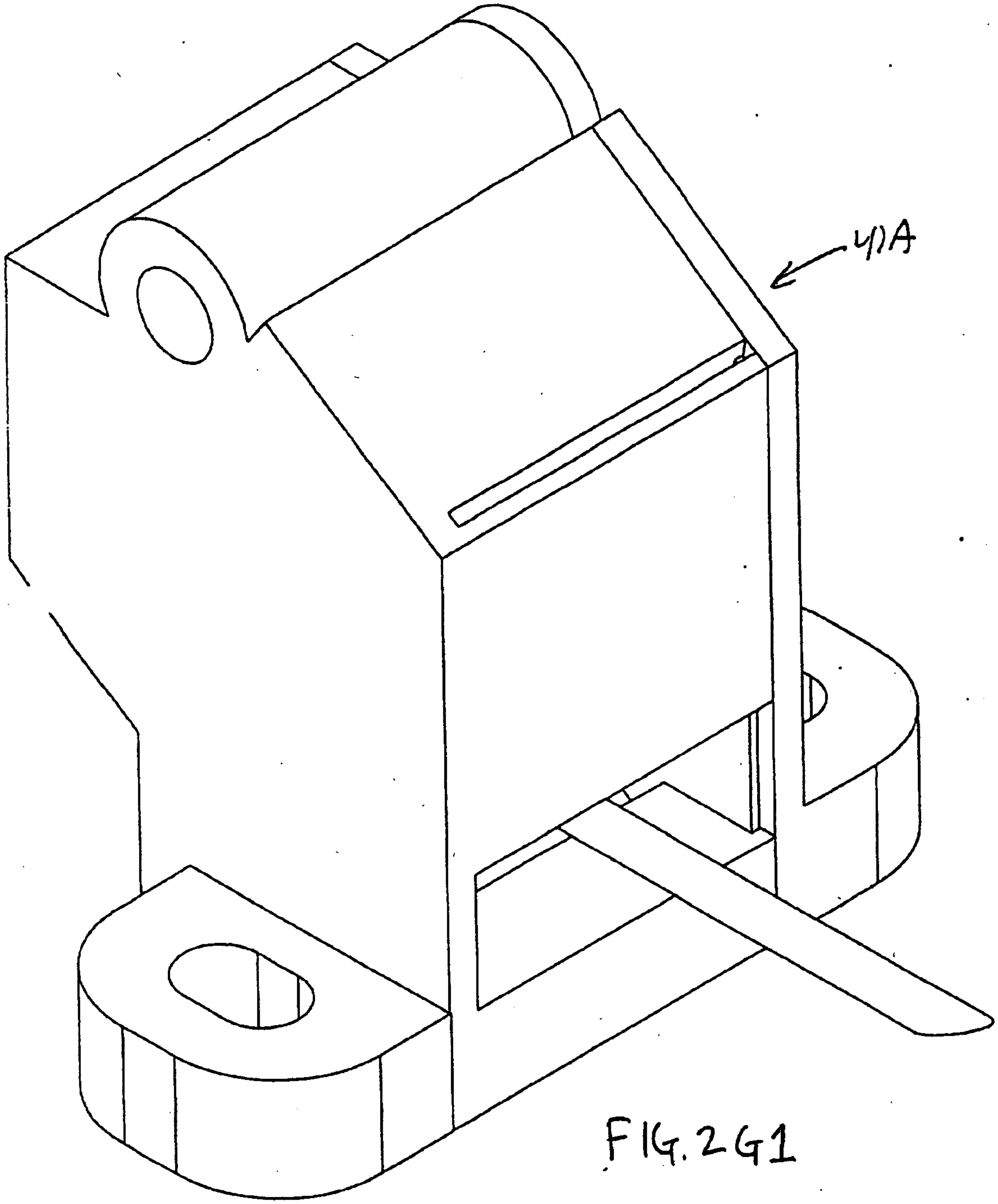

FIG. 2G1

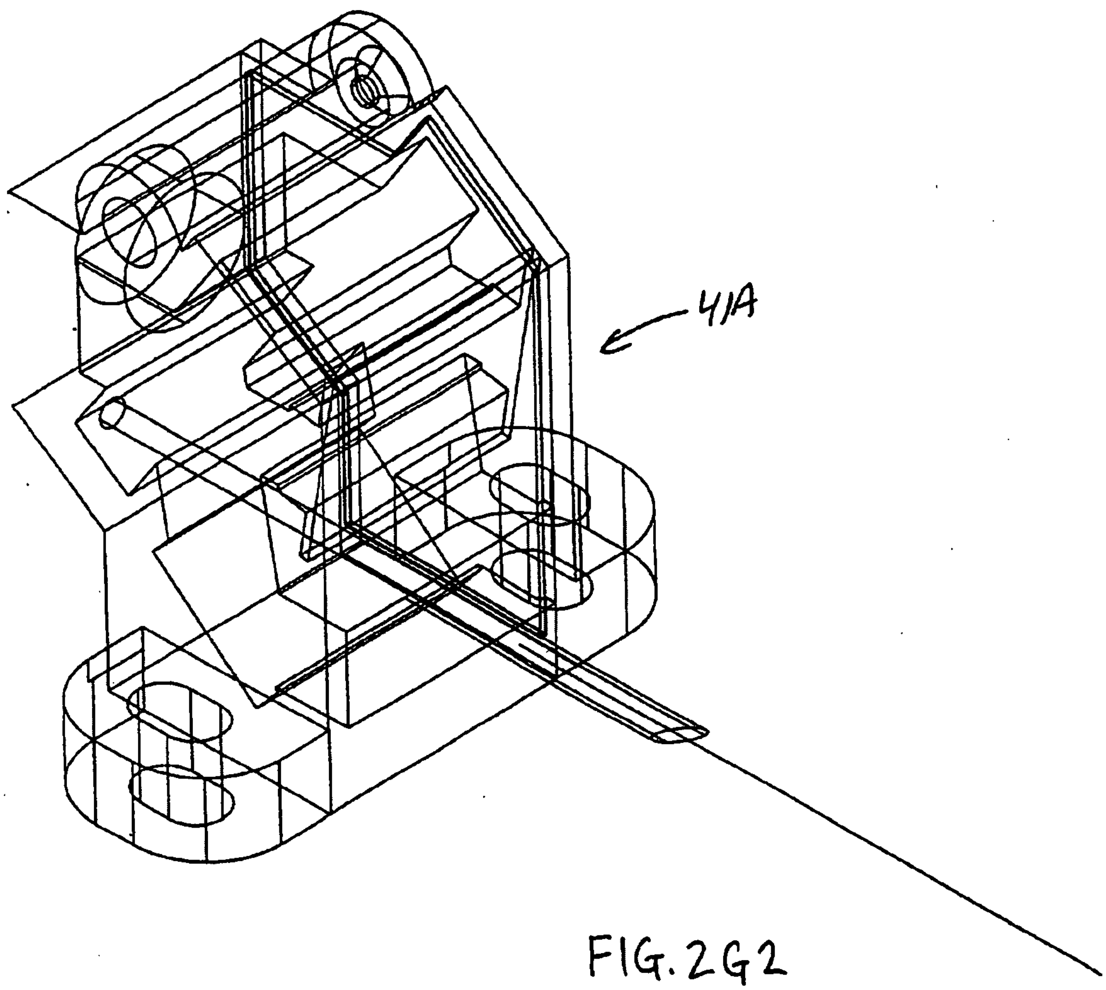

FIG. 2G2

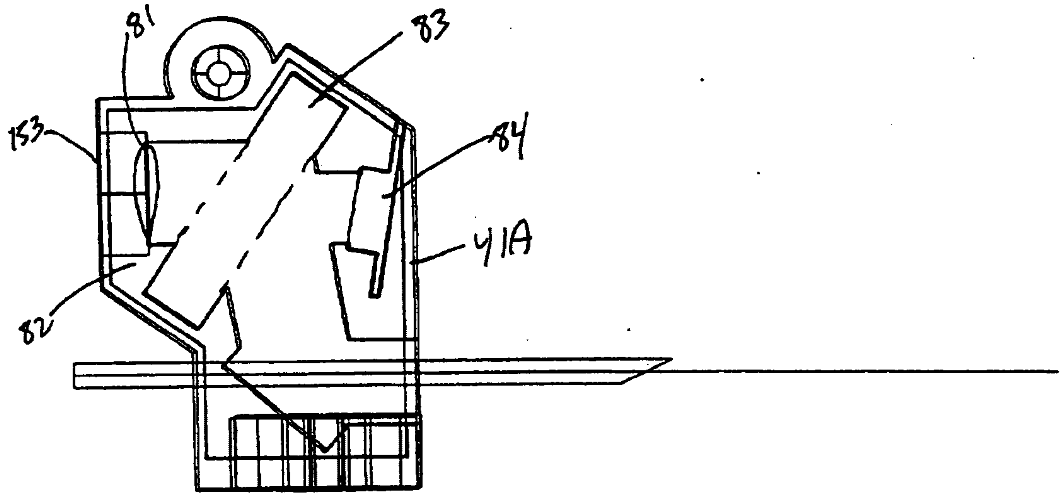

FIG. 2G3

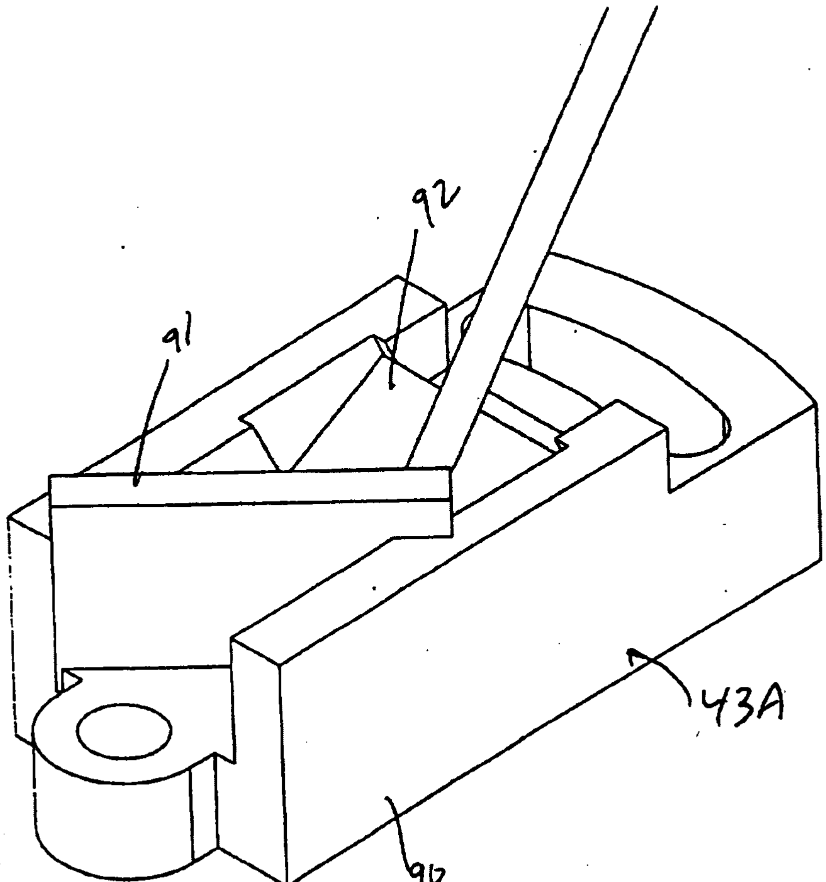

FIG. 2H1

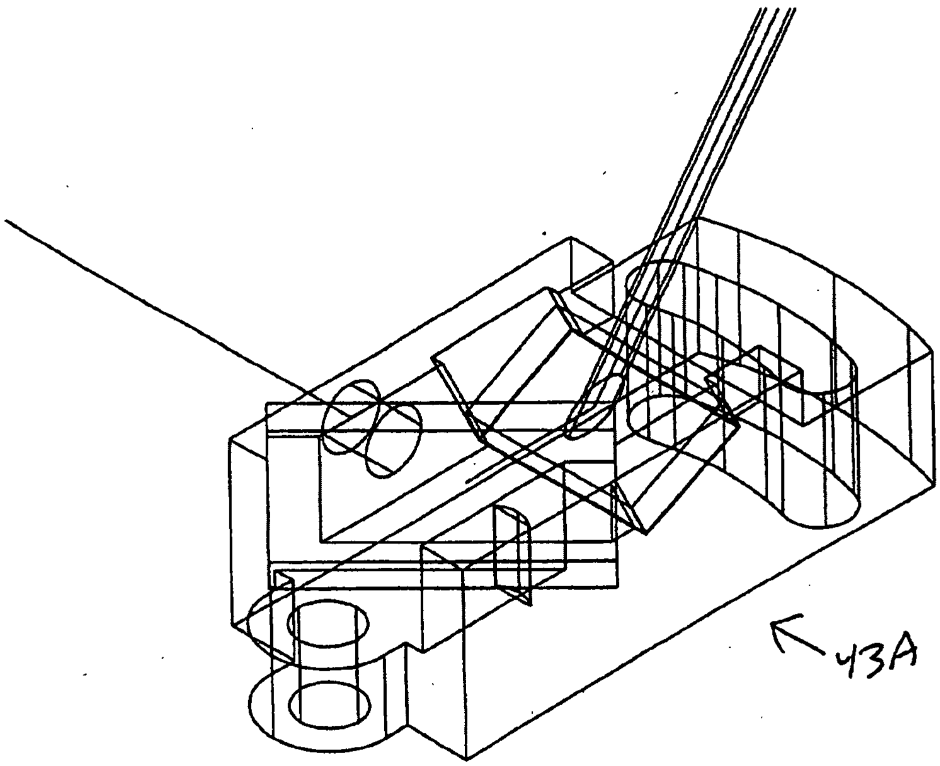

FIG. 2H2

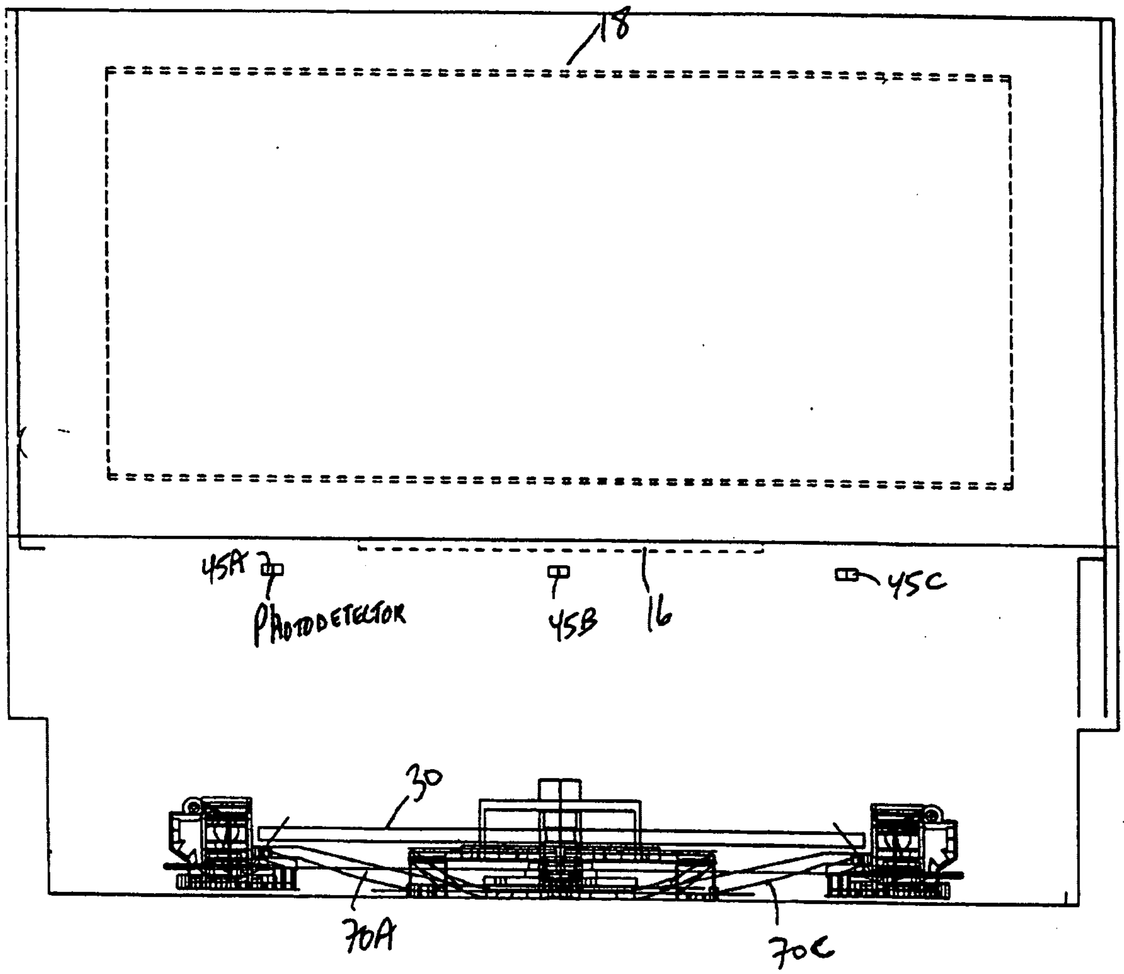

FIG. 2I1

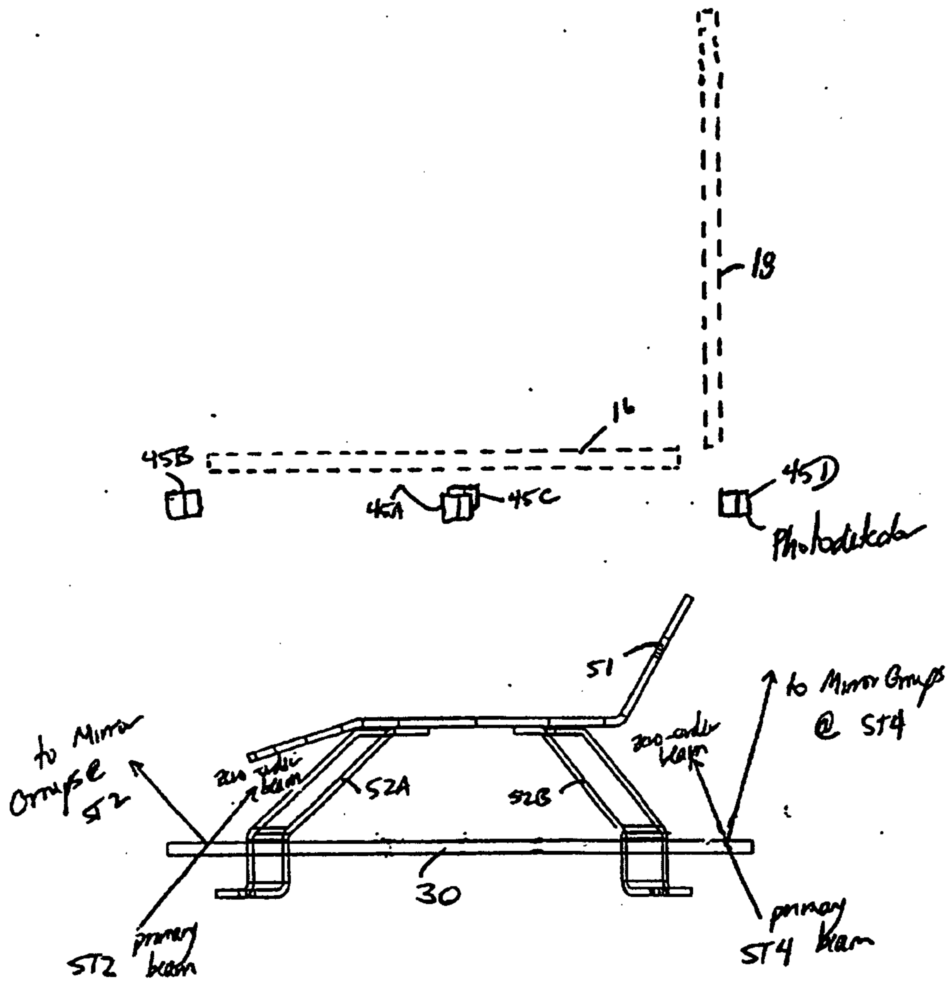
18
16
45B
45A
45C
45D
Photodetector
51
to Mirror Groups @ ST2
zero order beam
52A
52B
zero order beam
to Mirror Groups @ ST4
30
ST2
primary beam
primary beam
ST4

FIG. 2I2

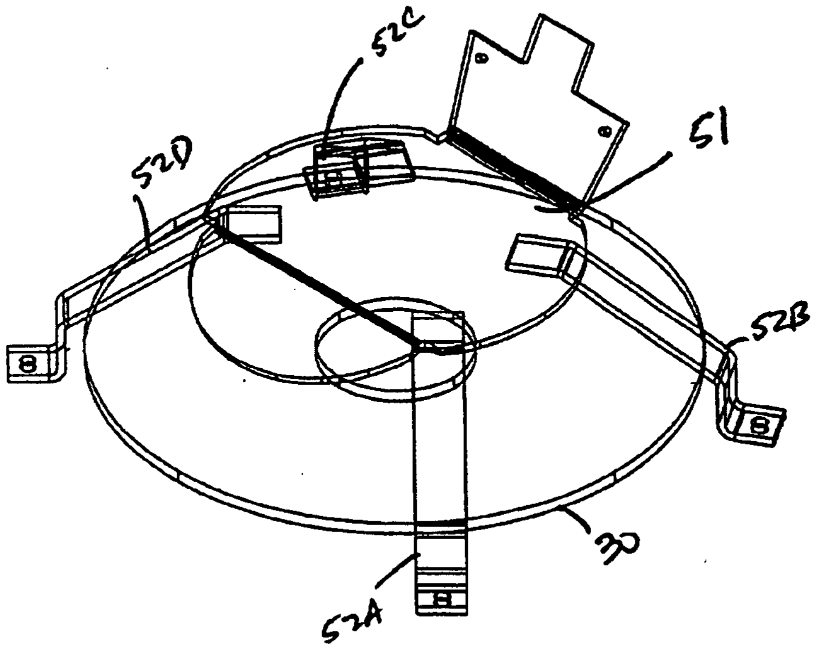

FIG 2I3

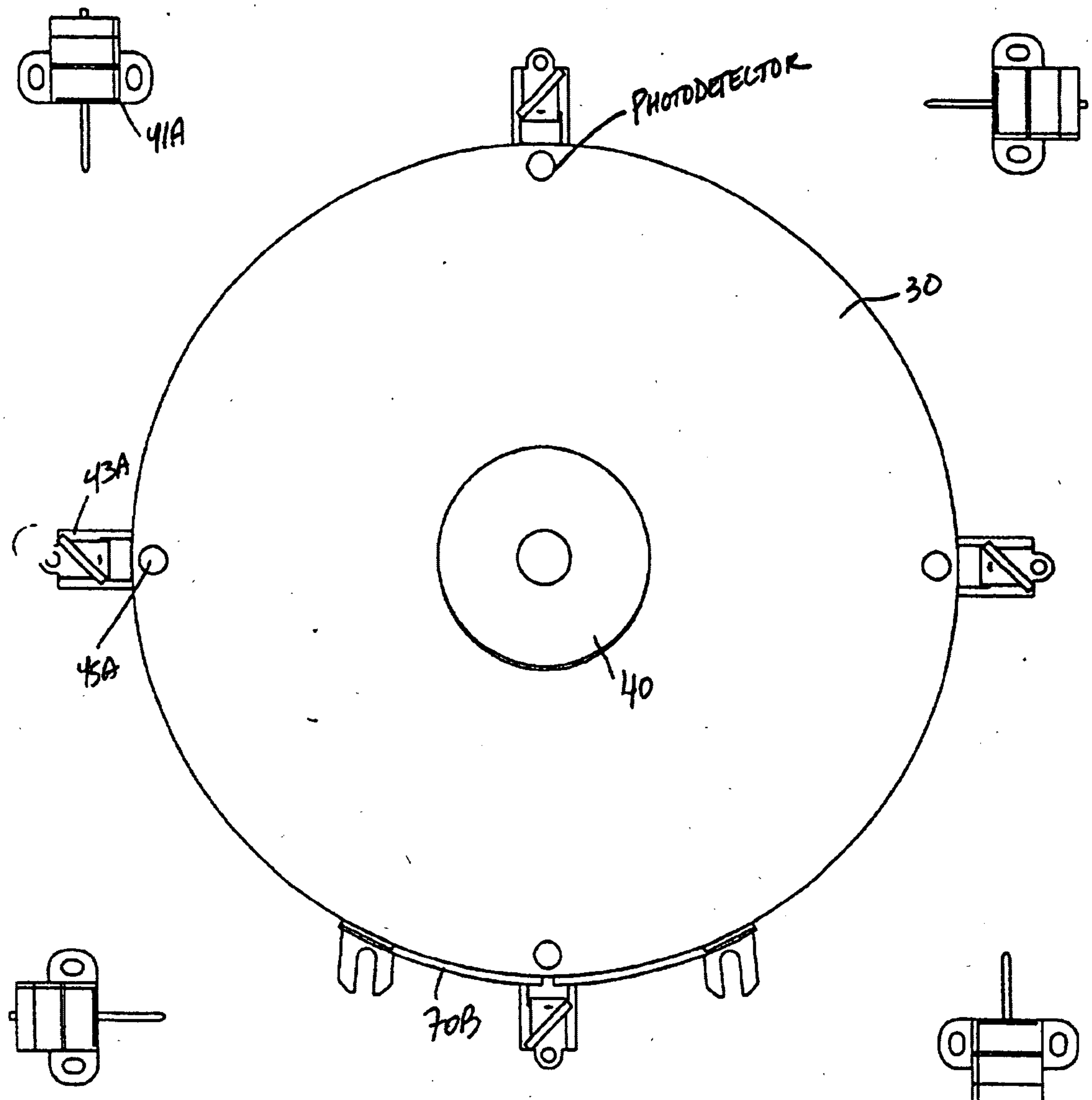

FIG. 2J1

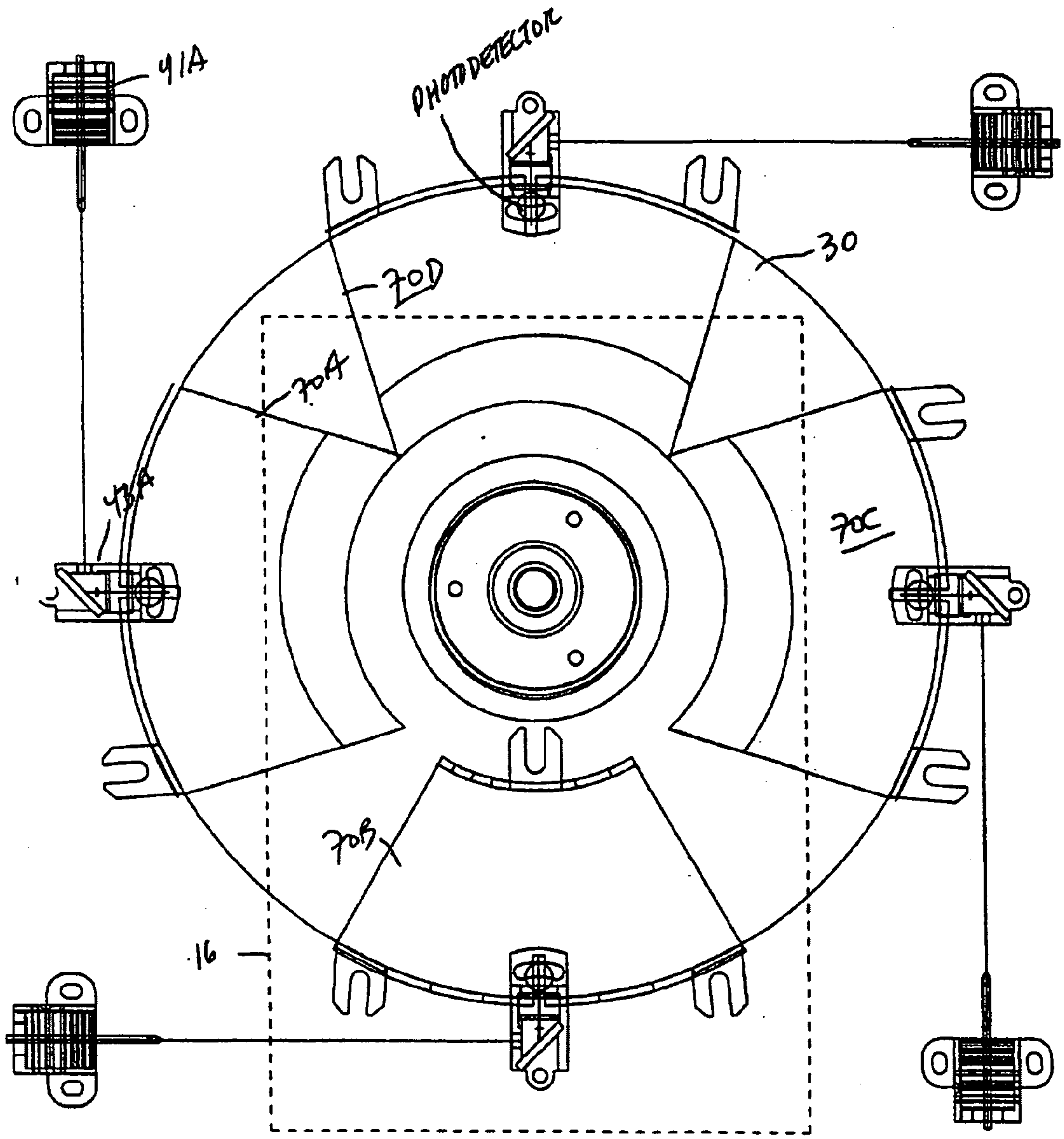

FIG. 2J2

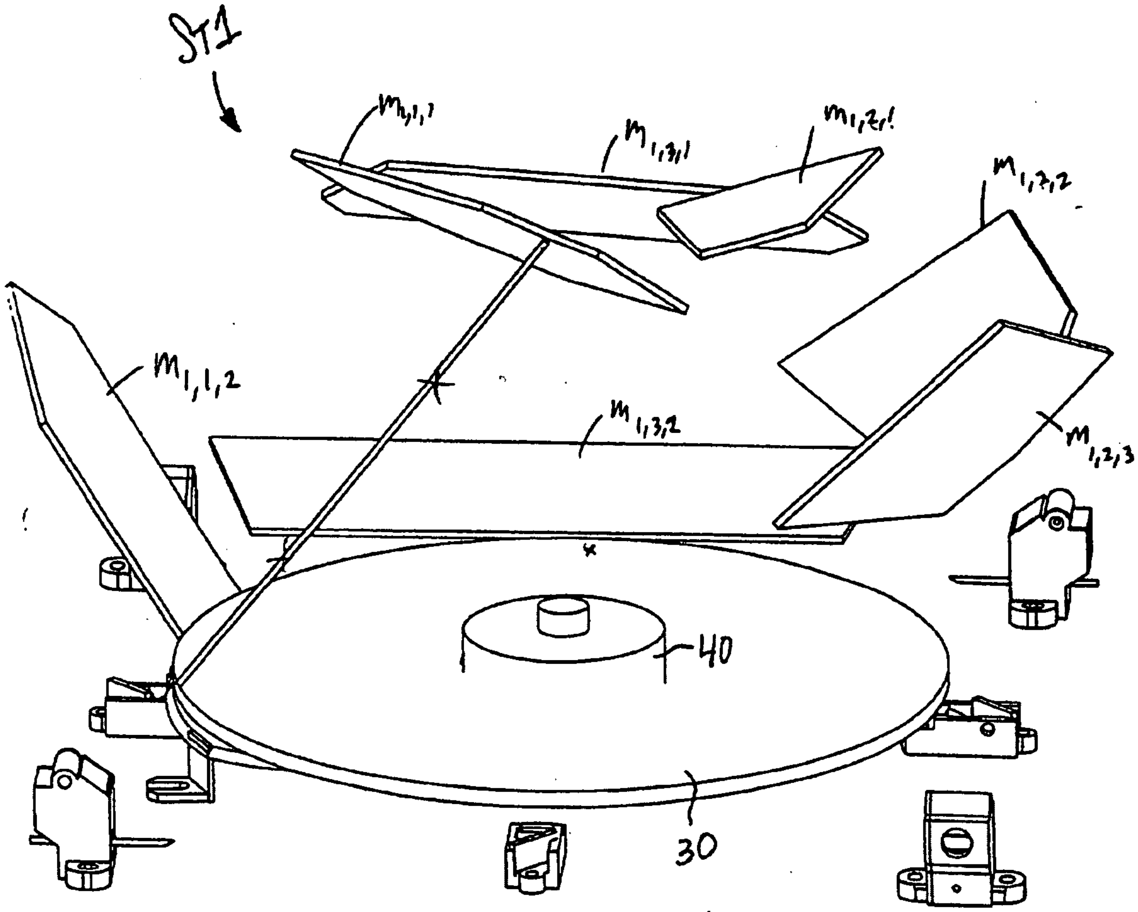

FIG. 2K

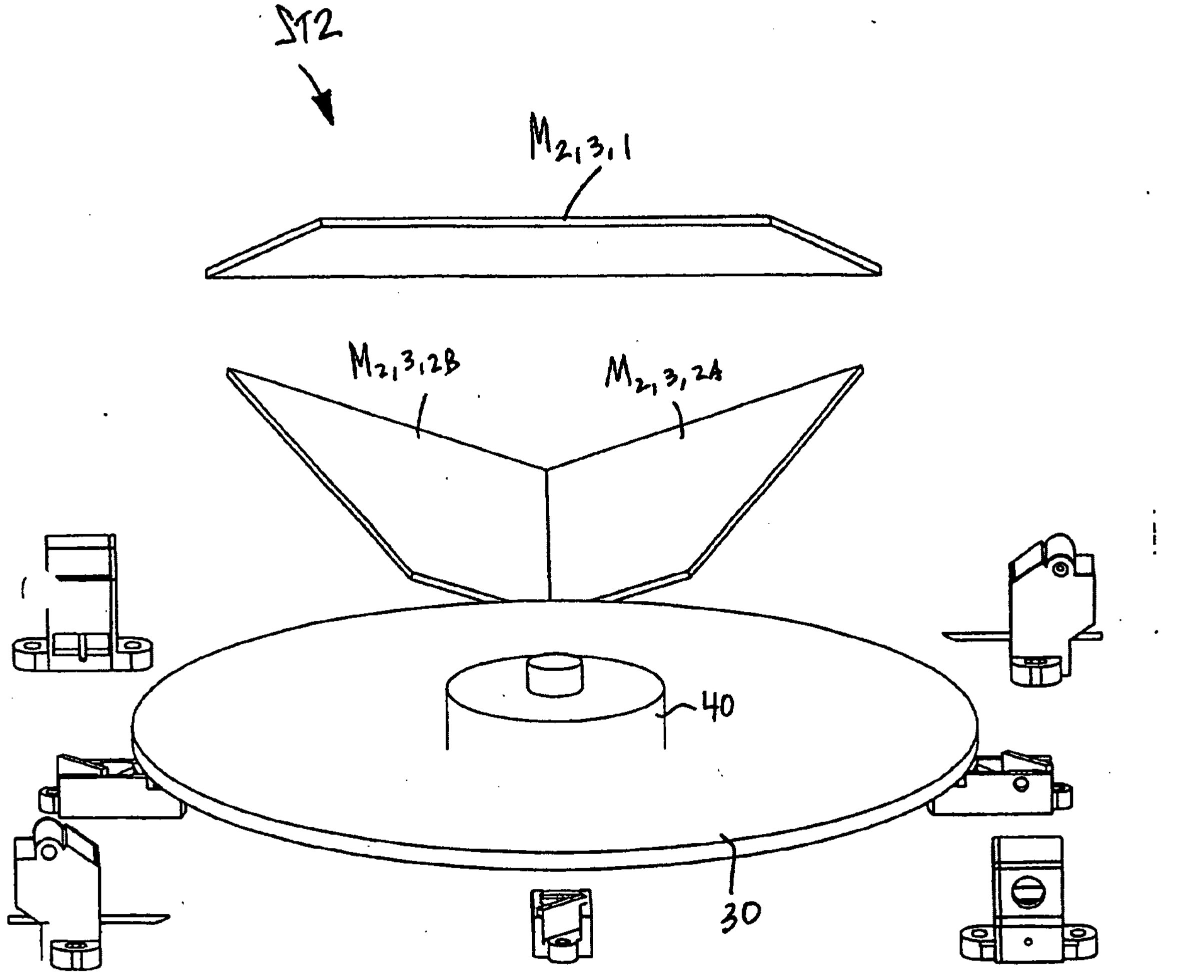

FIG. 2L

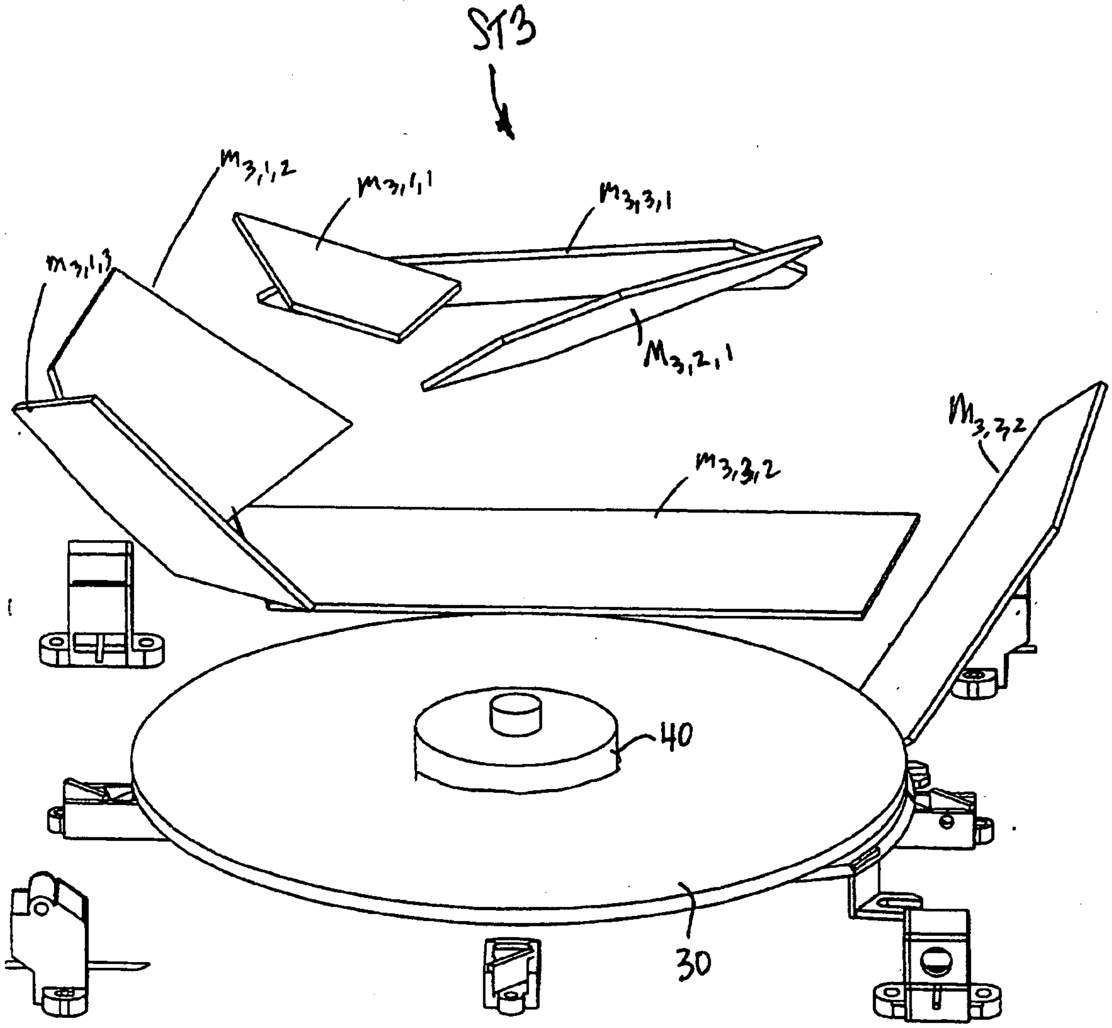

FIG. 2M

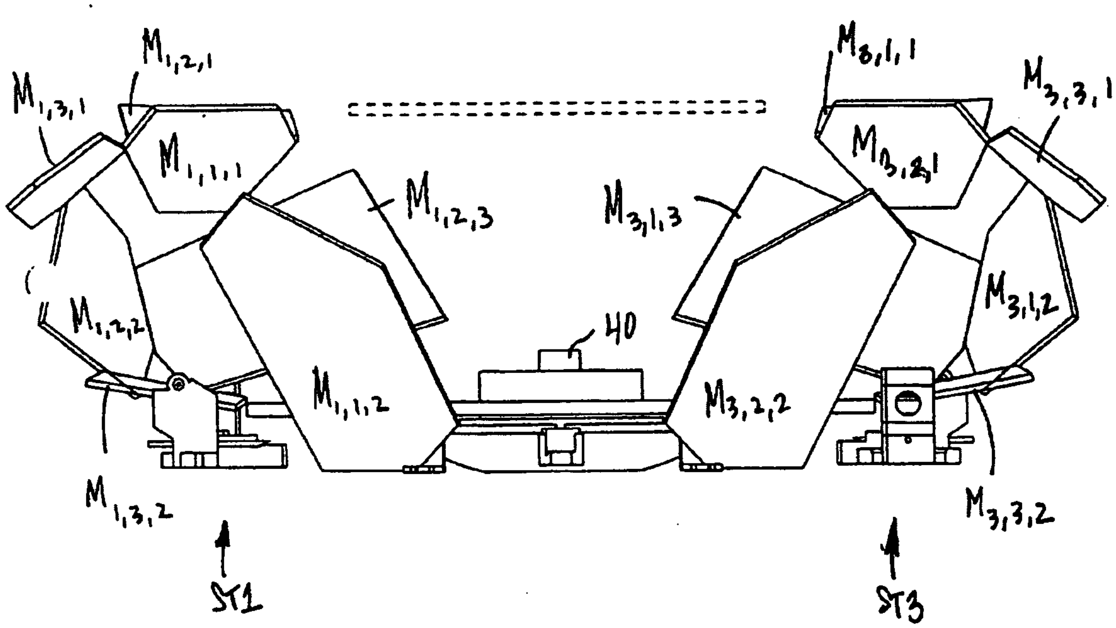

M1,2,1
M1,3,1
M1,1,1
M1,2,3
M1,2,2
M1,1,2
M1,3,2
ST1
40
M3,1,1
M3,3,1
M3,2,1
M3,1,3
M3,1,2
M3,2,2
M3,3,2
ST3

FIG. 2N

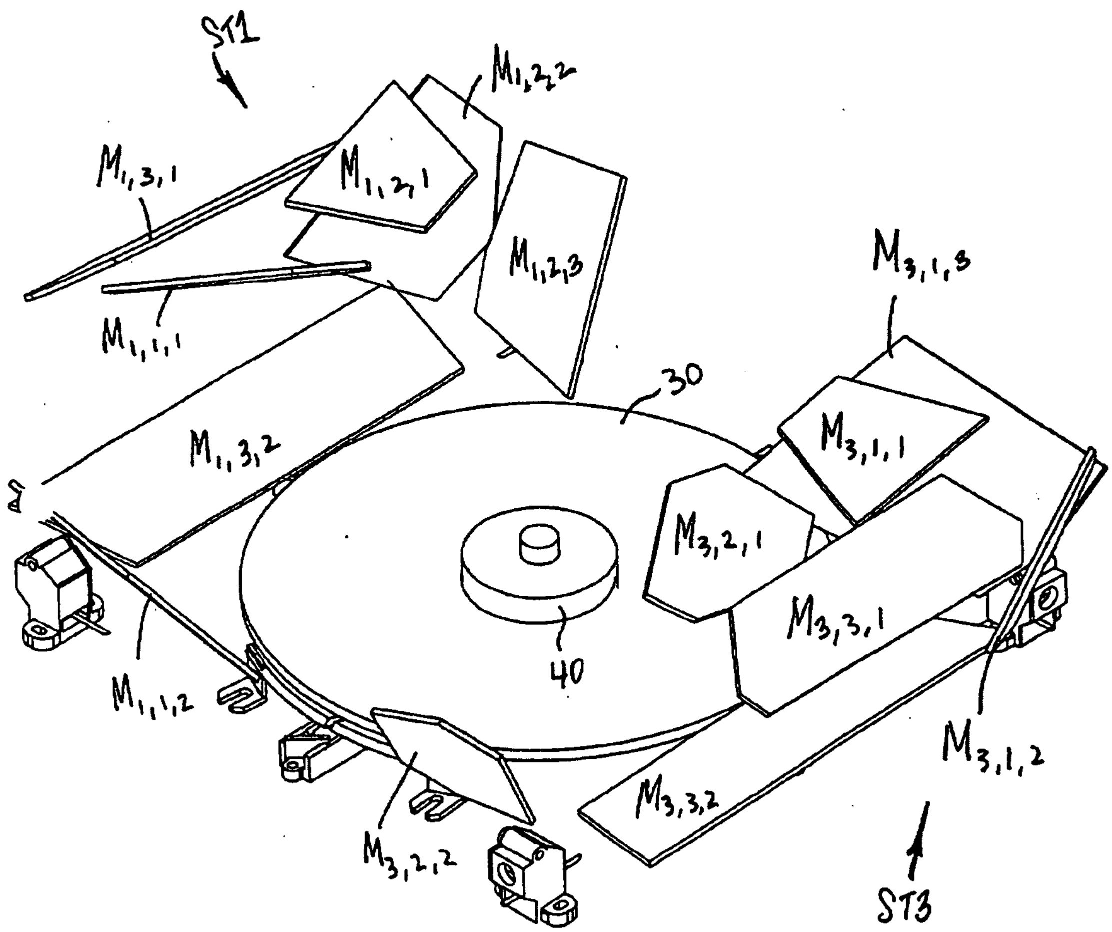
ST1
M1,2,2
M1,3,1
M1,2,1
M1,2,3
M1,1,1
M3,1,3
30
M1,3,2
M3,1,1
M3,2,1
M3,3,1
40
M1,1,2
M3,1,2
M3,3,2
M3,2,2
ST3

FIG. 20

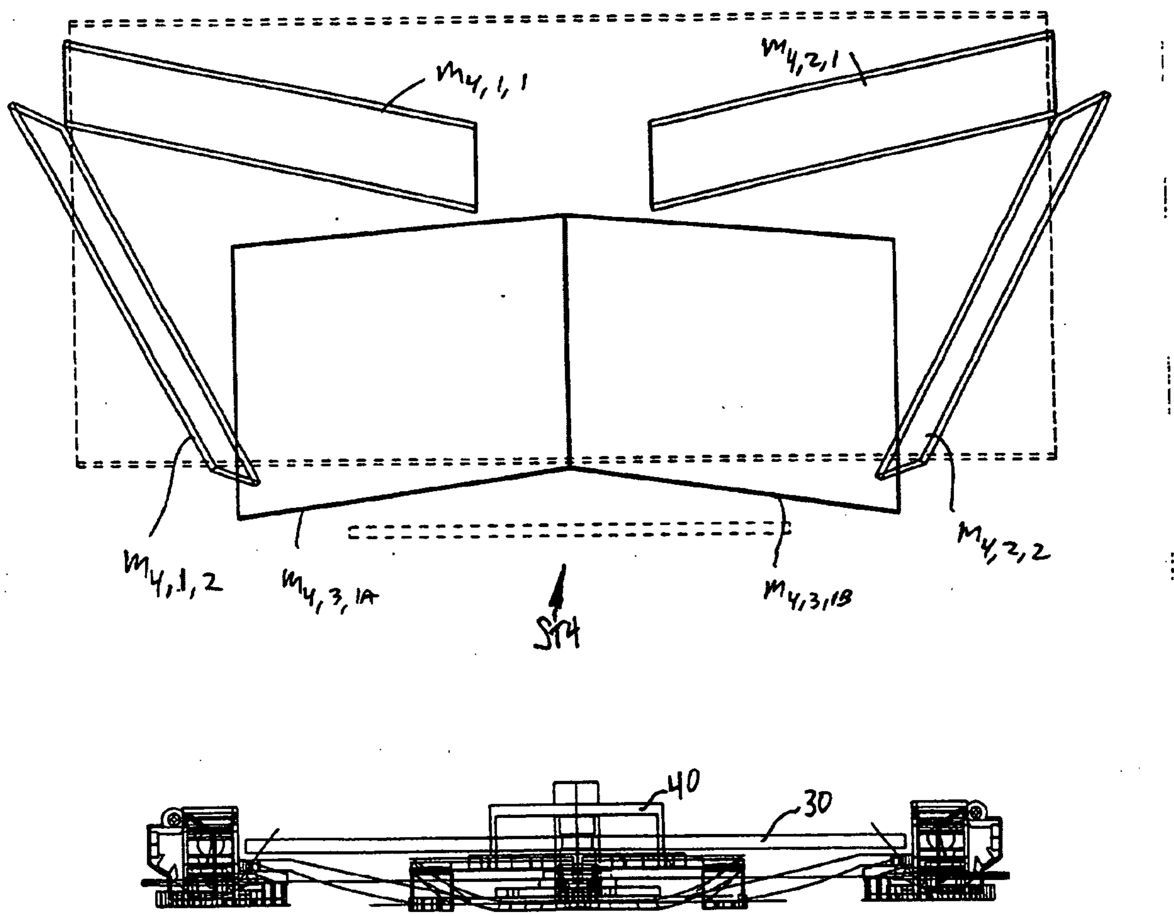

FIG. 2P

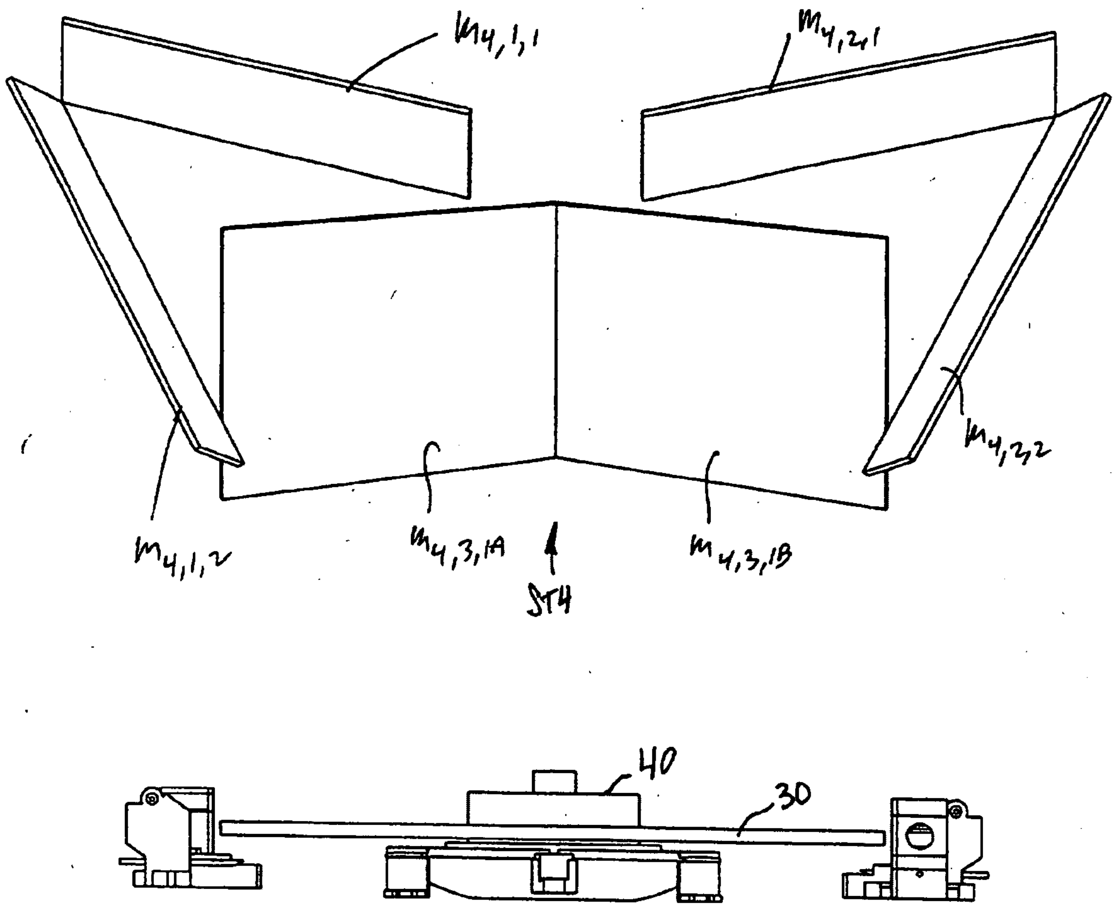

FIG. 2Q

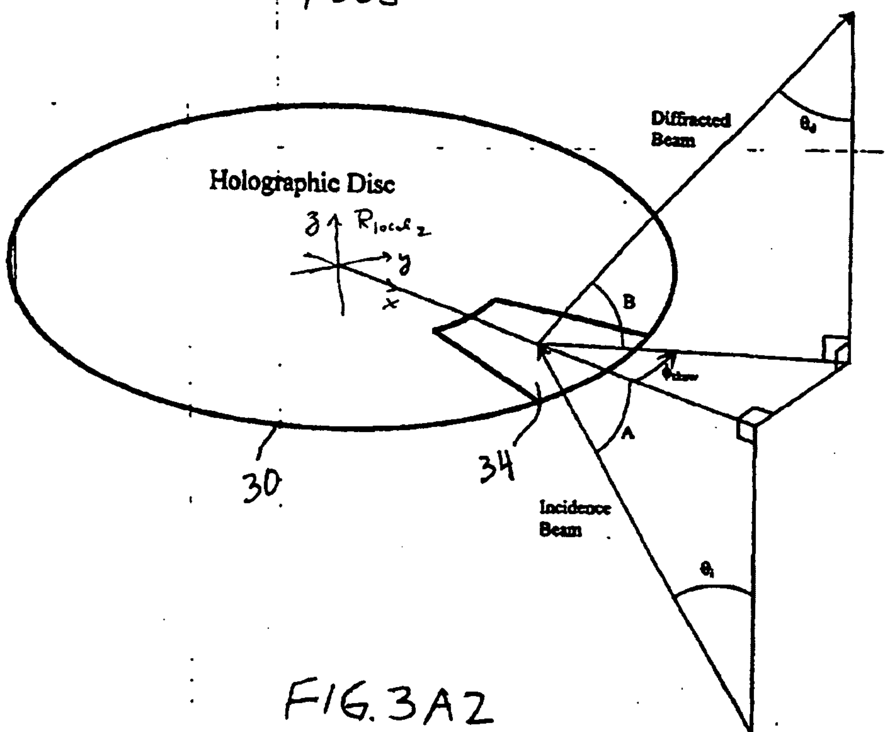

FIG. 3A2

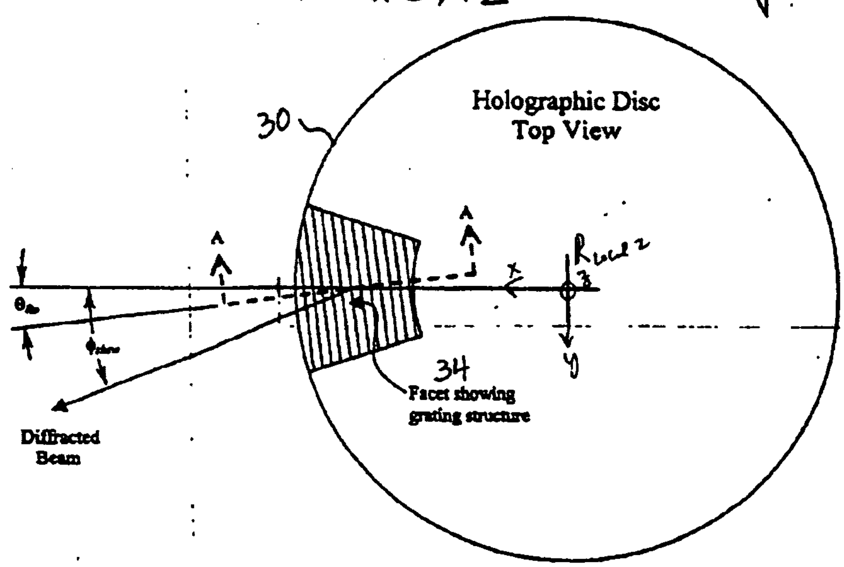

FIG. 3A3

ELEVATION AND SKEW ANGLE CHARACTERISTICS OF FACETS ON HOLOGRAPHIC SCANNING DISK OF THE PRESENT INVENTION

FACET GROUP NO.		FACET NO.
G1	HIGH ELEVATION ANGLE LEFT SKEW ANGLE	7
		9
		11
G2	HIGH ELEVATION ANGLE RIGHT SKEW ANGLE	8
		10
		12
G3	LOW ELEVATION ANGLE NO/ZERO SKEW ANGLE	1
		2
		3
		4
		5
		6

FIG. 3A4

MG2@ST1 MG1@ST1 M$3@ST1

	A	B	C	D	E	F	G	H	I	J	K	L	M	N	O	P
1	**Station 1**	(Local Co-ordinates)				(left)										
2		(right) Negative skew				Positive Skew				No Skew		(zero)				
3	First Mirror	x	y	z		x	y	z		x	y	z				
4		2.55	-1.80	2.70		3.80	2.30	2.77		4.30	1.60	2.52				
5		4.15	-2.27	2.77		4.10	1.88	2.40		4.95	2.15	2.04				
6	$m_{1,2,1}$	3.95	0.23	2.05	$m_{4,1}$	3.80	0.14	1.80	$m_{4,3,1}$	5.20	2.00	1.83				
7		2.42	-0.24	2.25		3.10	-0.80	1.80		5.00	-1.80	1.66				
8		2.55	-1.80	2.70		2.50	-0.16	2.45		4.70	-2.10	1.87				
9						2.65	0.76	2.77		4.10	-1.60	2.40				
10						3.80	2.30	2.77		4.30	1.60	2.52				
11																
12	Second Mirror	x	y	z		x	y	z		x	y	z				
13		4.00	-2.63	0.05		1.70	4.10	1.30		3.10	2.60	-0.03				
14		4.90	-1.40	0.77		3.00	4.45	1.98		4.50	3.00	0.22				
15	$m_{1,2,2}$	4.60	-3.20	2.18	$m_{4,2}$	3.40	3.99	1.50	$m_{1,3,2}$	4.35	-2.30	0.30				
16		3.70	-4.10	1.06		2.30	2.43	-0.63		3.00	-2.00	0.04				
17		4.00	-2.63	0.05		1.40	2.57	-0.63		3.10	2.60	-0.03				
18						1.00	2.99	-0.20								
19						1.70	4.10	1.30								
20																
21	Third Mirror	x	y	z												
22		4.41	-4.10	1.10												
23		1.97	-3.30	2.20												
24	$m_{1,2,3}$	1.12	-1.60	0.80												
25		2.51	-2.00	0.10												
26		3.53	-2.70	0.10												
27		4.41	-4.10	1.10												
28																

FIG. 3B

m63⑨ST2

	A	B	C	D	E	F	G	H	I	J	K	L	M	N	O	P
30																
31	**Station 2**	(Local Co-ordinates)														
32			Negative skew				Positive Skew				No Skew				No Skew	
33	First Mirror	x	y	z		x	y	z		x	y	z				
34										3.75	-1.60	2.51				
35										5.10	-2.40	1.73				
36								m2,3,1		5.10	2.40	1.73				
37										3.75	1.60	2.51				
38										3.75	-1.60	2.51				
39																
40																
41																
42	Second Mirror	x	y	z		x	y	z		x	y	z		x	y	z
43										3.00	0.00	-0.11		3.00	0.00	-0.11
44										4.80	0.00	0.38		4.80	0.00	0.38
45										5.07	-2.26	1.07		5.07	2.26	1.07
46								m3,3,24		5.07	-2.26	1.07		5.07	2.26	1.07
47										3.06	-1.00	0.17		3.06	1.00	0.17
48										3.00	0.00	-0.11		3.00	0.00	-0.11
49																
50										(Split mirror for generating two sets of horizontal lines)						
51																
52																

m2,3,23

FIG. 3C

Mirror Summary

Mirror Shapes

mG2@ST3 mG1@ST3 MG3@ST3

	A	B	C	D	E	F	G	H	I	J	K	L	
54	**Station 3**	(Local Co-ordinates)											
55		(V) Negative skew				(L) Positive Skew					No Skew		
56	First Mirror	x	y	z		x	y	z		x	y	z	
57		3.80	-2.30	2.77		2.55	1.80	2.70		4.30	-1.60	2.52	
58		4.10	-1.88	2.40		4.15	2.27	2.77		4.95	-2.15	2.04	
59		3.80	-0.14	1.80	$m_{3,1,1}$	3.95	-0.23	2.05		5.20	-2.00	1.83	$m_{3,3,1}$
60	$m_{3,2,1}$	3.10	0.80	1.80		2.42	0.24	2.25		5.00	1.80	1.66	
61		2.50	0.16	2.45		2.55	1.80	2.70		4.70	2.10	1.87	
62		2.65	-0.76	2.77						4.10	1.60	2.40	
63		3.80	-2.30	2.77						4.30	-1.60	2.52	
64													
65	Second Mirror	x	y	z		x	y	z		x	y	z	
66		1.70	-4.10	1.30		4.00	2.63	0.05		3.10	-2.60	-0.03	
67		3.00	-4.45	1.98		4.90	1.40	0.77		4.50	-3.00	0.22	$m_{3,3,2}$
68		3.40	-3.99	1.50	$m_{3,1,2}$	4.60	3.20	2.18		4.35	2.30	0.30	
69	$m_{3,2,2}$	2.30	-2.43	-0.63		3.70	4.10	1.06		3.00	2.00	0.04	
70		1.40	-2.57	-0.63		4.00	2.63	0.05		3.10	-2.60	-0.03	
71		1.00	-2.99	-0.20									
72		1.70	-4.10	1.30									
73													
74	Third Mirror	x	y	z		x	y	z					
75						4.41	4.10	1.10					
76						1.97	3.30	2.20					
77						1.12	1.60	0.80					
78					$m_{3,1,3}$	2.51	2.00	0.10					
79						3.53	2.70	0.10					
80						4.41	4.10	1.10					
81													

FIG. 3D

Mirror Summary

Mirror Shapes

47/335

MG2@STY MG1@STY MG3@STY

	A	B	C	D	E	F	G	H	I	J	K	L	M	N	O	P
83	**Station 4**	(Local Co-ordinates)														
84		(R) Negative skew				(L) Positive Skew				No Skew				No Skew		
85	First Mirror	x	y	z		x	y	z		x	y	z		x	y	z
86		4.90	-0.80	6.41		4.90	0.80	6.41		6.70	0.00	5.61		6.70	0.00	5.61
87		6.10	-0.80	5.65	M4,1,1	6.10	0.80	5.65		7.40	0.00	3.32		7.40	0.00	3.32
88	M4,2,1	6.00	-4.50	6.47		6.00	4.50	6.47	M4,3	6.95	-3.00	2.90		6.95	3.00	2.90
89		4.90	-4.50	7.17		4.90	4.50	7.17		6.20	-3.00	5.34		6.20	3.00	5.34
90		4.90	-0.80	6.41		4.90	0.80	6.41		6.70	0.00	5.61		6.70	0.00	5.61
91																
92										(Split mirror for generating two sets of horizontal lines)						
93																
94	Second Mirror	x	y	z		x	y	z		x	y	z				
95		2.85	-3.20	3.37	M4,1,2	2.85	3.20	3.37								
96		4.20	-2.80	3.23		4.20	2.80	3.23								
97	M4,2,2	5.95	-4.50	6.46		5.95	4.50	6.46								
98		4.60	-4.95	6.68		4.60	4.95	6.68								
99		2.85	-3.20	3.37		2.85	3.20	3.37								
100																

M4,3,1B

FIG. 3E

Mirror Summary

Mirror Shapes

*** Table of I	Dependent Parameters for both the Scanner and the Disk ***				DiskStr.	4a			
Box height (inches):			N/A	(See Note 1)	Problem items are				
Box width (inches):			N/A	(See Note 2)	highlighted (red).				
Max angle B (degrees):			62.00	(See Note 3)					
Min angle B (degrees):			38.00	(See Note 3)					
Total facet angular sweep (degrees):			358.14	(See Note 4)					
Min (angle A - angle B) (degrees):			0.00	(See Note 6)					
Max beam speed (inches per second):			13704						
Min beam speed (inches per second):			7156						
Power at data detector (nW):			872						
Signal voltage (volts):			5.47	(See Note 7)					
Signal voltage at max DOF limits (volts):			3.45	(See Note 7)	0.91	Max bandwidth (MHz) for		7.5	mil bars
CDRH:	P-avg. Class 2?	Class 2A?	P-pulse Class 1?						
	YES	YES	YES	(See Note 8)					
IEC:	Single pulse	P-avg. 0.25s	Pulse train correction						
	PASS	PASS	PASS	(See Note 8)					

Note 1: If this entry is highlighted (red) then the value exceeds the specified value for the box height (Cell G21). Go to cells G417 to G456 to identify the problem entries and make the necessary inner radius adjustments in Cells G215 to G254.

Note 2: This entry is not used in the box design, but it gives an indication of the box dimensions that would be established by the width of the tops of the mirrors.

Note 3: Generally, the B angles should range between 40 degrees and 70 degrees. Holograms with smaller or larger angles may be difficult to construct.

Note 4: This entry must be less than, but within a few degrees of, 360 degrees. To satisfy this requirement, it may be necessary to make adjustments to the focal distances and/or the length of the scan lines.

FIG. 3F

Note 6: This value must be greater than 0.5 degrees to avoid feedback into the laser from disk surface reflections. If it is too small, adjustments must be made to the B angles of the problem facets (See Cells X468 to X507).

Note 7: The signal voltage must be greater than some value established by the signal processor requirements. Typically, this value should be greater than 2 volts. If this value is less than 2 volts, either the laser power must be increased or the focal distances must be decreased.

Note 8: All CDRH/IEC entries must be YES or PASS. If not, laser power must be reduced. (Modify laser power in Cell B799.)

d = distance from disk to base of scanner (inches):						0						
Rotational speed of disk (rpm)						5200						
DiskStratos_4.xls						650 nm	358.14					
Facet	Diffraction Focal length (inches)	Geometrical Focal length (inches)	Angle A (degrees)	Angle B (degrees)	Angle of Diffraction (degrees)	Focal plane scan line length (inches)	Scan Angle (degrees)	Scan mult. Factor (m)	Rotation Angle (degrees)	Accounting for dead time for laser beam 1.15 (degrees)	Light Collection Factor	Maximum Collection Area (ignoring notch) (sq. in.)
	Given		Given	Given								
1	12.6	12.73	52	38.00	52.00	9.750	42.61	1.62	26.24	27.39	1.00	2.28
2	11.5	11.68	52	40.00	50.00	9.750	45.95	1.62	28.35	29.50	0.80	1.81
3	12.7	12.94	52	42.00	48.00	9.750	42.00	1.58	26.66	27.81	0.92	2.09
4	11.5	11.68	52	44.00	46.00	9.750	45.95	1.57	29.19	30.34	0.71	1.62
5	12.7	12.94	52	48.00	42.00	9.750	42.00	1.50	27.97	29.12	0.79	1.79
6	12.0	12.21	52	52.00	38.00	9.750	44.22	1.46	30.28	31.43	0.64	1.47
7	14.7	15.08	52	58.00	32.00	9.750	36.69	1.31	27.99	29.14	0.87	1.97
8	14.7	15.08	52	58.00	32.00	9.750	36.69	1.31	27.99	29.14	0.87	1.97
9	13.5	13.80	52	60.00	30.00	9.750	39.71	1.30	30.65	31.80	0.71	1.61
10	13.5	13.80	52	60.00	30.00	9.750	39.71	1.30	30.65	31.80	0.71	1.61
11	14.8	15.19	52	62.00	28.00	9.750	36.46	1.25	29.19	30.34	0.83	1.88
12	14.8	15.19	52	62.00	28.00	9.750	36.46	1.25	29.19	30.34	0.83	1.88

FIG. 3G1

Notch size in mirror

TG (12/21/99)

3.5 mm x 5.1 m (3.5 mm x 6.5 mm at disk)

Design

Collection

NOTE: If any entry in these two columns is less than 0.5 degrees (highlighted in red), the corresponding B angle should be changed. This is accomplished by modifying the "Distance from rotational axis" entry for that line (cells G46 to G85).

	Area (includes notch loss of 0.035 sq. inches)	Beam speed at center of scan line (inches/sec)	Beam speed at max depth of field (inches/sec)	Beam speed at min depth of field (inches/sec)	Beam skew angle (degrees)	Facet count function 1 = facet 0 = no facet	Number of facets 12 / Max freq.	Min Freq.	Bandwidth		Angle A - Angle B (Absolute value) (degrees)
1	2.27	11052	13704	8400	0	1	0.914	0.560	0.354		14.00
2	1.81	10150	12798	7502	0	1	0.853	0.500	0.353		12.00
3	2.08	10895	13468	8321	0	1	0.898	0.555	0.343		10.00
4	1.63	9858	12429	7286	0	1	0.829	0.486	0.343		8.00
5	1.79	10383	12835	7930	0	1	0.856	0.529	0.327		4.00
6	1.47	9544	11929	7158	0	1	0.795	0.477	0.318		0.00
7	1.97	10492	12634	8351	28	1	0.842	0.557	0.286		6.00
8	1.97	10492	12634	8351	-28	1	0.842	0.557	0.286		6.00
9	1.62	9524	11640	7407	28	1	0.776	0.494	0.282		8.00
10	1.62	9524	11640	7407	-28	1	0.776	0.494	0.282		8.00
11	1.88	10068	12106	8027	28	1	0.807	0.535	0.272		10.00
12	1.88	10068	12106	8027	-28	1	0.807	0.535	0.272		10.00

FIG. 3G2

51/335

Avg. LA (in.)	13.83	Average angle B (degrees):	52.00		Average:	1.42						
Avg waist loo	13.34	Maximum angle B (degrees):	62.00	SUMS --->	480.46		344.36	358.14	9.66	21.89	21.89	<---SUMS
Approximate minimum bus width:		N/A	inches							Vmax (in/s):	13704	
(Based on large mirror as limitation)					Total facet angular sweep (degrees):			358.14		Vmin (in/s):	7159	
										Ratio	1.91	

*** Master Hologram Exposure Information ***

DiskStrates_4.xls

650 nm

Gelatin Refractive Indexes		Wavelengths (microns)	
Before processing:	1.53	Scanner:	0.66
After processing:	1.4	Exposure:	0.488

Distance from beam incidence point on disk to 488 nm reference point: 0 inch

Facet	Grating spacing at scan region (microns) Design wavelength = 0.66 microns
1	0.4631
2	0.4794
3	0.4794
4	0.4869
5	0.5089
6	0.5279
7	0.5674
8	0.5674
9	0.5838
10	0.5825
11	0.5980
12	0.5960

Facet	Diffraction angle from annulus (degrees)	Diffraction angle from reference point (degrees)	Exposure angles at reference point at 488 nm: Reference Beam (degrees)	Object Beam (degrees)	alpha-1 (degrees)	beta-1 (degrees)	phi (degrees)	theta-1 (degrees)	L (microns)	theta-2 (degrees)	alpha-2 (degrees)	beta-2 (degrees)
1	52.00	52.80	25.13	38.99	26.00	34.25	85.92	30.17	0.46	20.20	14.12	24.28
2	50.00	50.00	25.48	37.42	26.00	33.17	86.46	29.83	0.47	19.85	15.31	23.60
3	48.00	48.00	25.79	35.82	26.00	32.66	87.01	29.07	0.48	19.50	15.52	22.49
4	46.00	46.00	26.12	34.20	26.00	30.92	87.59	28.58	0.49	19.14	16.72	21.56
5	42.00	42.00	26.81	30.90	26.00	28.53	88.77	27.32	0.51	18.39	17.16	19.61
6	38.00	38.00	27.53	27.83	26.00	26.09	90.00	26.06	0.53	17.59	17.59	17.59
7	32.00	32.00	28.64	22.38	26.00	22.34	91.92	24.17	0.57	16.33	18.86	14.41
8	32.00	32.00	28.64	22.38	26.00	22.34	91.92	24.17	0.57	16.33	18.86	14.41
9	30.00	30.00	29.02	20.64	26.00	20.92	92.58	23.51	0.58	15.90	18.98	13.32
10	30.00	30.00	29.02	20.64	26.00	20.92	92.58	23.51	0.58	15.90	18.98	13.32
11	28.00	28.00	29.40	18.89	26.00	19.59	93.25	22.84	0.60	15.47	18.71	12.22
12	28.00	28.00	29.40	18.89	26.00	19.59	93.25	22.84	0.60	15.47	18.71	12.22

FIG. 3H

DiskStr. •8

*** Modified Exposure Angles to Correct for Post-processing Residual Gelatin Swell ***														
DiskStratos_4.xls						650	nm							
Percent gelatin swell (from measurements) delta-t/t:				20%										
	Exposure angles at 488 nm			Exposure angles to compensate for swell										
	Reference	Object		Reference	Object		gamma(sw)	gamma(0)	A	B	C	Z	alpha-0	beta-0
Facet	Beam	Beam		Beam	Beam									
	(degrees)	(degrees)		(degrees)	(degrees)									
1	25.13	38.99		23.85	40.50		-4.08	-4.90	1.99	0.17	0.69	0.26	15.33	25.12
2	25.45	37.42		24.34	38.70		-3.54	-4.25	1.99	0.15	0.68	0.27	15.62	24.12
3	25.78	35.82		24.83	36.88		-2.99	-3.58	1.99	0.12	0.67	0.27	15.93	23.10
4	26.12	34.20		25.35	35.04		-2.41	-2.90	1.99	0.10	0.65	0.28	16.25	22.04
5	26.81	30.90		26.41	31.31		-1.23	-1.48	2.00	0.05	0.63	0.29	16.90	19.86
6	27.53	27.53		27.53	27.53		0.00	0.00	2.00	0.00	0.60	0.30	17.58	17.58
7	28.64	22.38		29.28	21.77		1.92	2.31	2.00	-0.08	0.56	0.32	18.65	14.03
8	28.64	22.38		29.28	21.77		1.92	2.31	2.00	-0.08	0.56	0.32	18.65	14.03
9	29.02	20.64		29.89	19.83		2.58	3.10	1.99	-0.11	0.55	0.33	19.01	12.81
10	29.02	20.64		29.89	19.83		2.58	3.10	1.99	-0.11	0.55	0.33	19.01	12.81
11	29.40	18.89		30.50	17.89		3.25	3.90	1.99	-0.14	0.53	0.33	19.37	11.58
12	29.40	18.89		30.50	17.89		3.25	3.90	1.99	-0.14	0.53	0.33	19.37	11.58

FIG. 3I

*** Analysis of the Focus Shift and Out-of-locus Spot Size for Converging Reference Beam ***

(Not applicable for Stratos)

Convergence of the reference beam:				-1477	mm			
Focal length of parabolic mirror:				58.62	mm			
Distance from parabolic mirror to detector:				60	mm			
Facet	Design Focal length (mm)	Par. Mirror Eff. width (mm)	Required foc. length (mm)	Object distance (mm)	Image distance (mm)	Image shift (mm)	Spot size at detector (mm)	
								0.88
1	317.50	40	404.42	-14856.75	59.05	-0.95	0.64	Distance (Cell E621) may have to be adjusted
2	292.10	40	364.09	31841.43	58.71	-1.29	0.88	so that the maximum spot size at the detector is
3	322.58	40	412.69	-11828.19	59.11	-0.89	0.60	approximately the same when the 1/2 depth of field value
4	292.10	40	364.09	31841.43	58.71	-1.29	0.88	is negative as it is when the 1/2 depth of field value is positive.
5	322.58	40	412.69	-11828.19	59.11	-0.89	0.60	(The 1/2 depth of field value is located at Cell G19)
6	304.80	40	384.03	-48230.76	58.89	-1.11	0.75	
7	373.38	40	499.67	-4485.04	59.60	-0.40	0.27	
8	373.38	40	499.67	-4485.04	59.60	-0.40	0.27	
9	342.90	40	446.55	-6818.26	59.33	-0.67	0.45	
10	342.90	40	446.55	-6818.26	59.33	-0.67	0.45	
11	375.92	40	504.23	-4375.15	59.62	-0.38	0.25	
12	375.92	40	504.23	-4375.15	59.62	-0.38	0.25	

FIG. 3J

Focal distances and distances to the window for the Stratos scanner
LDD 12/7/99 RPH

Facet	Diffraction Focal length (inches) Given	Distance to horizontal window (inches)	Difference (inches)	Distance to vertical window (inches)	Difference (inches)	Operator side Distance to horizontal window (inches)	Difference (inches)
1	12.5	8.5	4	10.2	2.3	8	4.5
2	11.5	8.8	2.7	10.2	1.3	8.42	3.08
3	12.7	9.2	3.5	10.2	2.5	8.85	3.85
4	11.5	9.5	2	10.2	1.3	9.25	2.25
5	12.7	9.8	2.9	10.2	2.5	9.7	3
6	12	10.2	1.8	10.2	1.8	10.1	1.9
7	14.7	10.6	4.1	14.1	0.6		
8	14.7	9.7	5	14.1	0.6		
9	13.5	11.2	2.3	13.8	-0.3		
10	13.5	9.8	3.7	13.8	-0.3		
11	14.8	11.1	3.7	13.6	1.2		
12	14.8	9.6	5.2	13.6	1.2		

The horizontal window lines from the even numbered vertical facets 8, 10, 12 are near the vertical window.

FIG. 3K

55/335

* CDRH/IEC Calculations to Verify that the Scanner Meets the Laser Class Requirements ***

The number of overlapping lines (N-overlap) must be determined from the scanner data.
A safe assumption for our scanners is to consider that two scan lines are overlapped
ONLY when the difference between their diffraction angles (B) is less than 2 degrees.
All else being equal, the slowest scan lines (largest angle B) will be the worst case scan lines.

N-overlap:	1	
Motor speed (rpm):	5200	
Alpha-min (radians):	0.0015	(from standard)
FWHM P-divergence of laser (deg.):	8	(Linked from Tmc spreadsheet)
FWHM S-divergence of laser (deg.):	30	(Linked from Tmc spreadsheet)
Focal length of collimating lens (mm):	6.1	(Linked from Tmc spreadsheet)
Angle of incidence at MF plate (deg.):	29.23	
Angle of diffraction at MF plate (deg.):	42.12	
X-p (mm):	0.87	
X-s (mm):	3.93	
Average source dimension (mm):	2.40	
Distance to aperture (mm):	200	(actual distance or 200 mm, whichever is greater)
Alpha (radians):	0.012	
C6:	7.996	

Facet	Laser power at window (mW)	tc (200) 7 mm transit time at d = 200 mm (seconds)	ti (actual) 7 mm transit time at actual d (seconds)	P x ti (Joules)		Facet count
1	0.86	3.95856E-05	3.95856E-05	0.0000339		1
2	0.86	3.96549E-05	3.96549E-05	0.0000341		1
3	0.86	4.08001E-05	4.08001E-05	0.0000351		1
4	0.86	4.08315E-05	4.08315E-05	0.0000352		1
5	0.86	4.28115E-05	4.28115E-05	0.0000370		1
6	0.87	4.40086E-05	4.40086E-05	0.0000381		1
7	0.87	4.90358E-05	4.90358E-05	0.0000425		1
8	0.87	4.90358E-05	4.90358E-05	0.0000425		1
9	0.87	4.96126E-05	4.96126E-05	0.0000430		1
10	0.87	4.96126E-05	4.96126E-05	0.0000430		1
11	0.87	5.14525E-05	5.14525E-05	0.0000446		1
12	0.87	5.14525E-05	5.14525E-05	0.0000446		1

FIG. 3L1

Sums:			0.000(DiskStr.	0.0000446 4a	These values are the sums of the worst case (largest) overlap values		
Duty Cycle:	0.004459213						
Paverage is the sum of the overlap Pi x ti products divided by the sum of the ti times times the duty cycle							
Paverage is, therefore, the sum of the overlap Pi x ti products times the rps of the motor.							
CDRH calculations and results							
			Class 1	Class 2?	Class 2A?		
Pavg. (mW):		0.003869		YES	YES		
P (single pulse) (mW): (Maximum allowed)		8.27					
P (single pulse) (Actual)		0.67	YES				
IEC calculations and results							
IEC condition A (Single pulse)					PASS/FAIL		
P (single pulse) (mW): (Maximum allowed)		70.6			PASS		
IEC condition B (average power in a 0.25 second pulse train)							
Pavg. allowed (mW):		7.92			PASS/FAIL		
Pavg. scanner (mW):		0.0039			PASS		
IEC condition C (pulse train correction factor)							
(For this calculation, you need to insert the sum of the pulse times in the overlapping scan lines)							
T-total (seconds): (sum of pulse times in overlap scan lines)		0.000051					
Pmax (mW):		66.1					
Number of pulses in train:		21.67					
Correction factor:		0.4635					
Pmax (PT corrected)(mW):		30.63			PASS/FAIL		
Pw (including overlap)		0.67			PASS		

FIG. 3L2

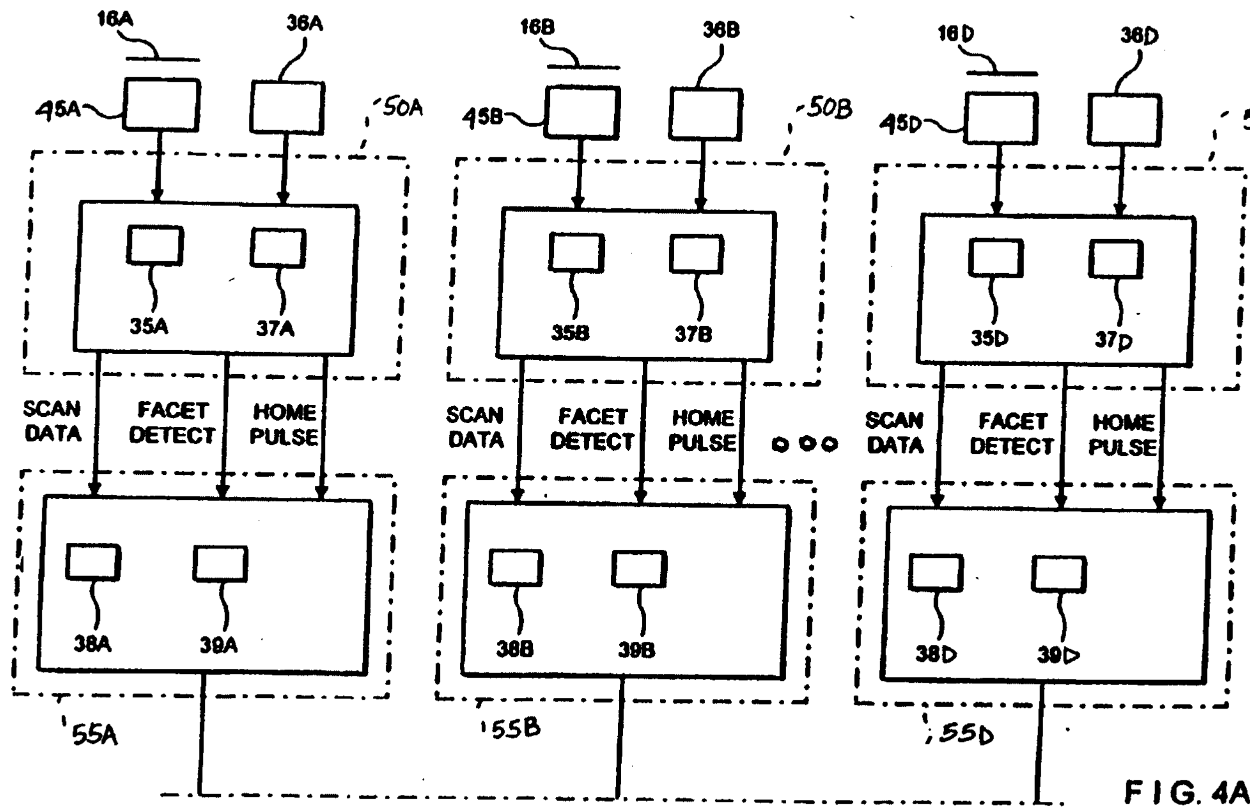
16A
36A
45A
50A
35A
37A
SCAN DATA
FACET DETECT
HOME PULSE
38A
39A
55A
16B
36B
45B
50B
35B
37B
SCAN DATA
FACET DETECT
HOME PULSE
38B
39B
55B
16D
36D
45D
50D
35D
37D
SCAN DATA
FACET DETECT
HOME PULSE
38D
39D
55D

FIG. 4A

58/335

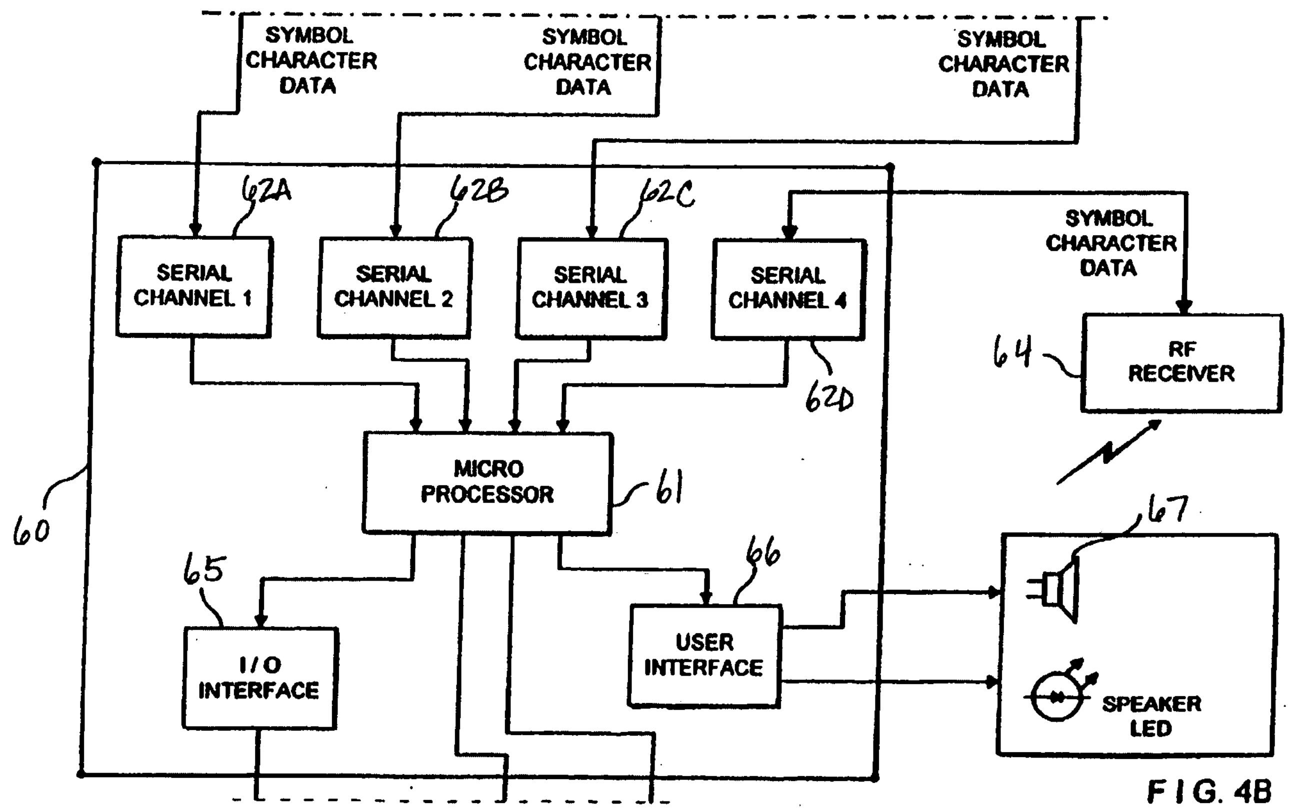
SYMBOL CHARACTER DATA
SYMBOL CHARACTER DATA
SYMBOL CHARACTER DATA
SYMBOL CHARACTER DATA
62A
62B
62C
62D
SERIAL CHANNEL 1
SERIAL CHANNEL 2
SERIAL CHANNEL 3
SERIAL CHANNEL 4
64
RF RECEIVER
60
MICRO PROCESSOR
61
67
65
66
I/O INTERFACE
USER INTERFACE
SPEAKER LED

F I G. 4B

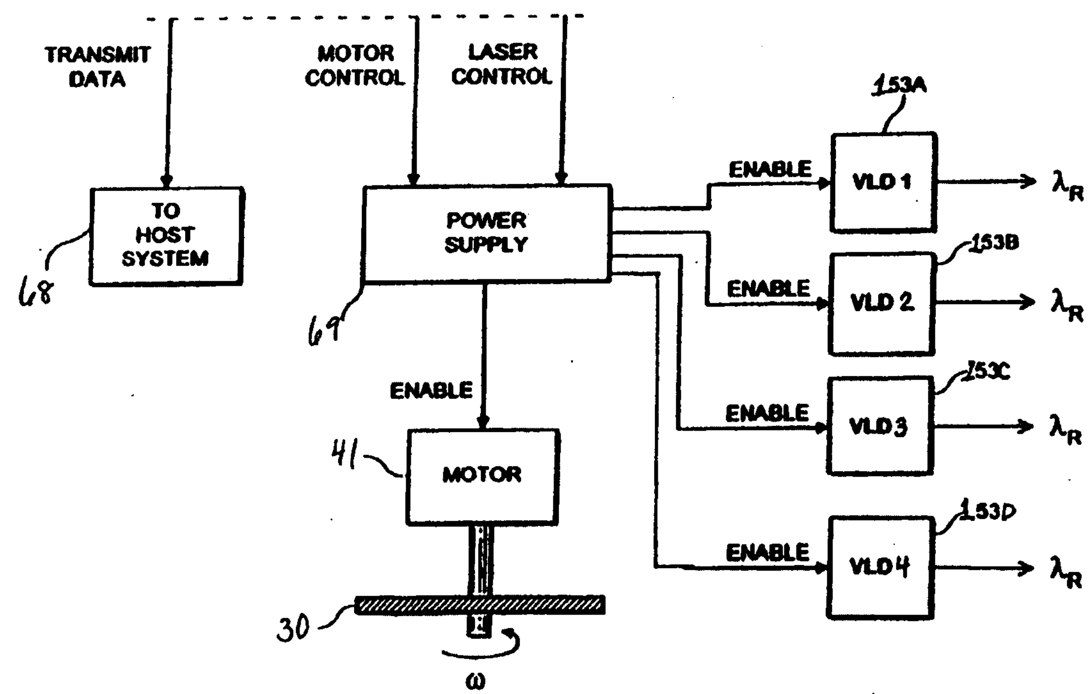
TRANSMIT DATA
MOTOR CONTROL
LASER CONTROL
TO HOST SYSTEM
68
POWER SUPPLY
69
ENABLE
MOTOR
41
30
ω
ENABLE
ENABLE
ENABLE
ENABLE
VLD 1
VLD 2
VLD 3
VLD 4
153A
153B
153C
153D
λ_R
λ_R
λ_R
λ_R

FIG. 4C

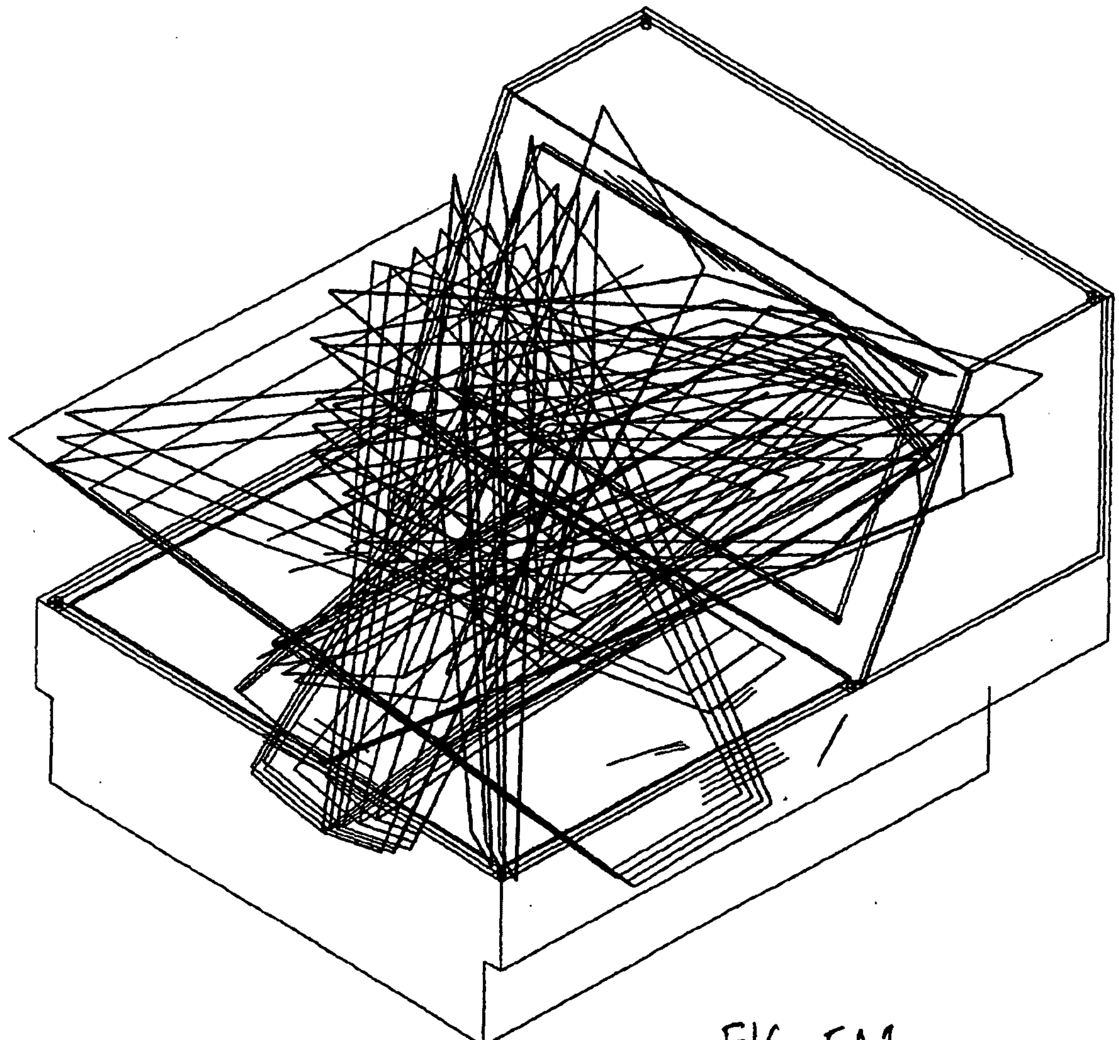

FIG. 5A1

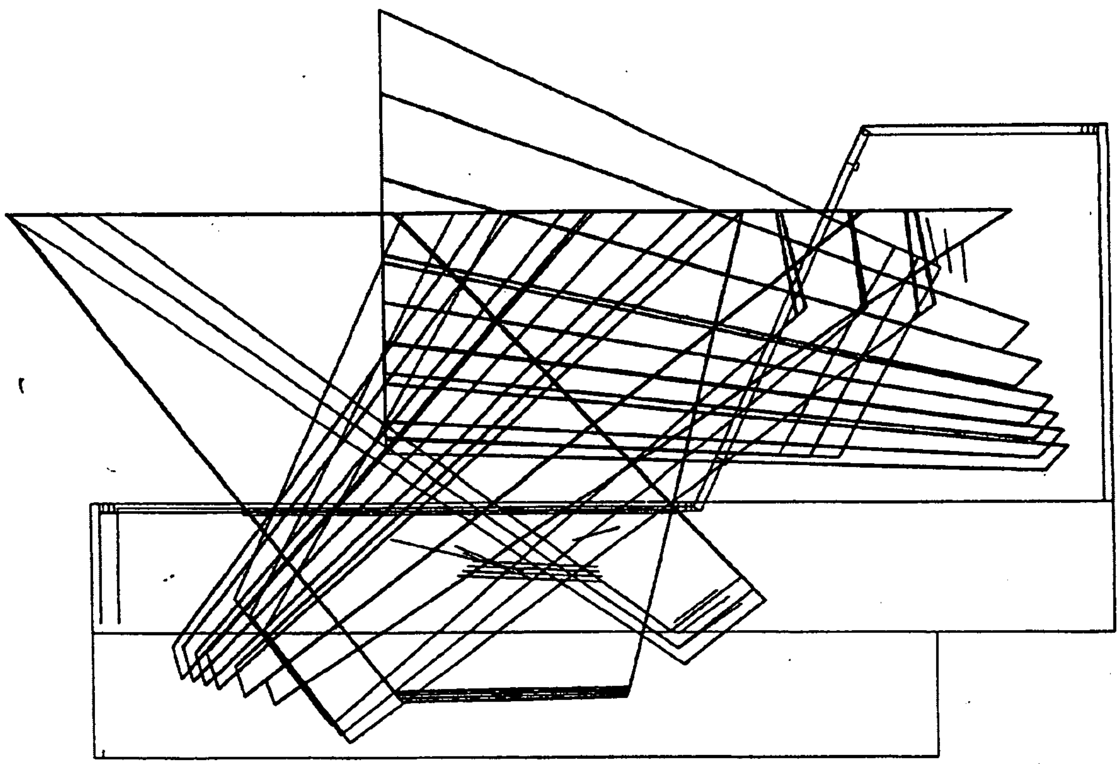

FIG. 5A2

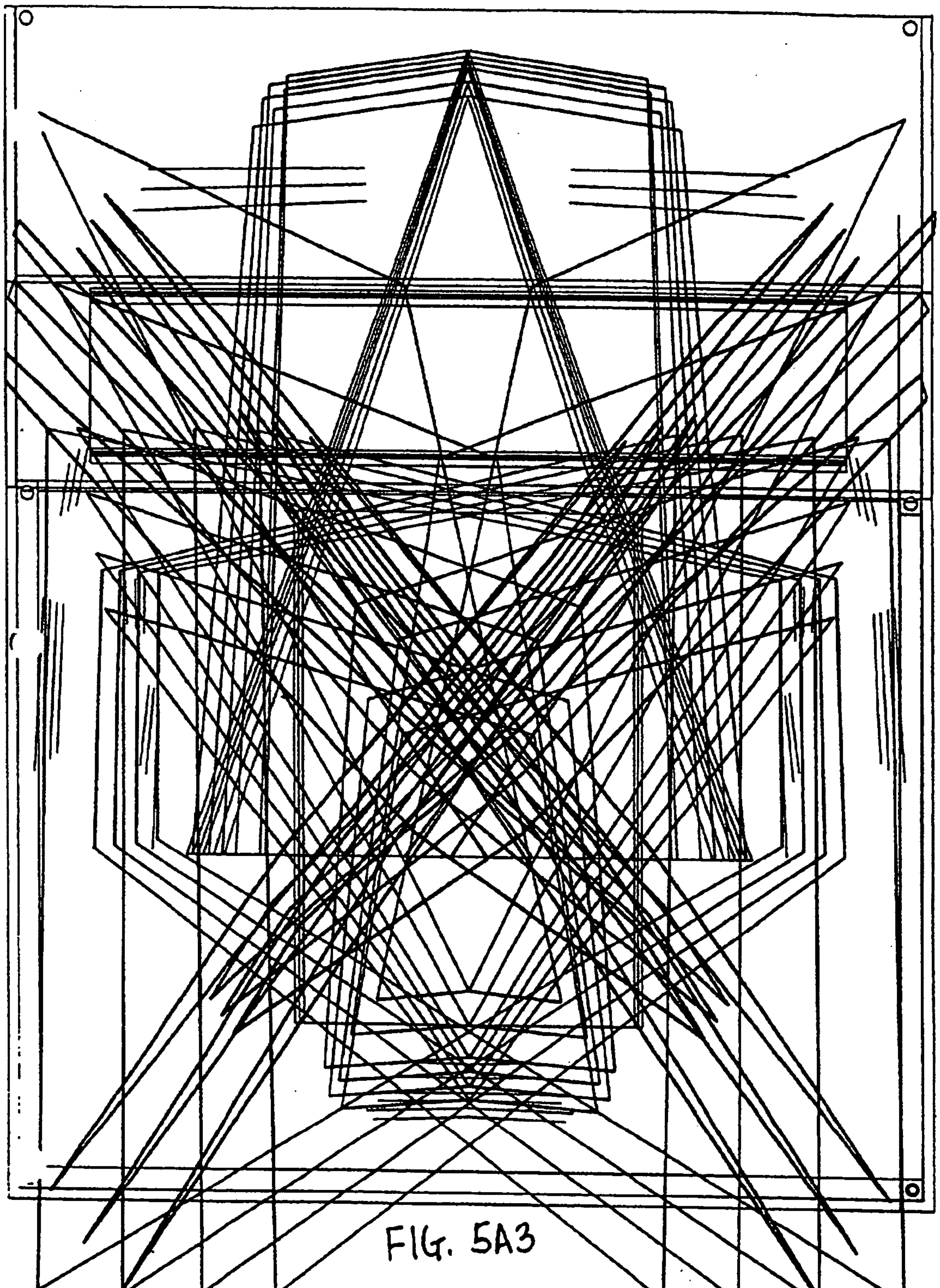

FIG. 5A3

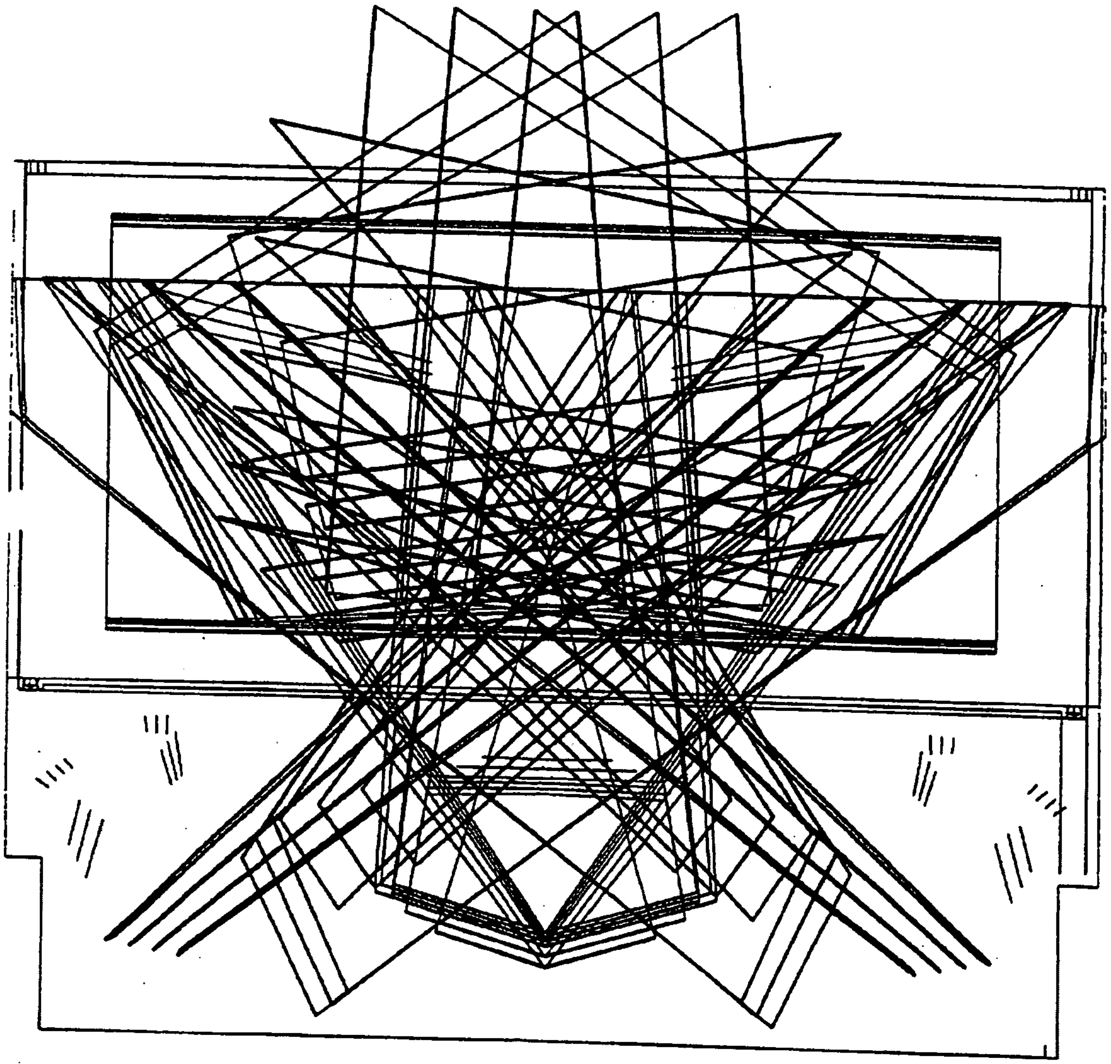

FIG. 5A4

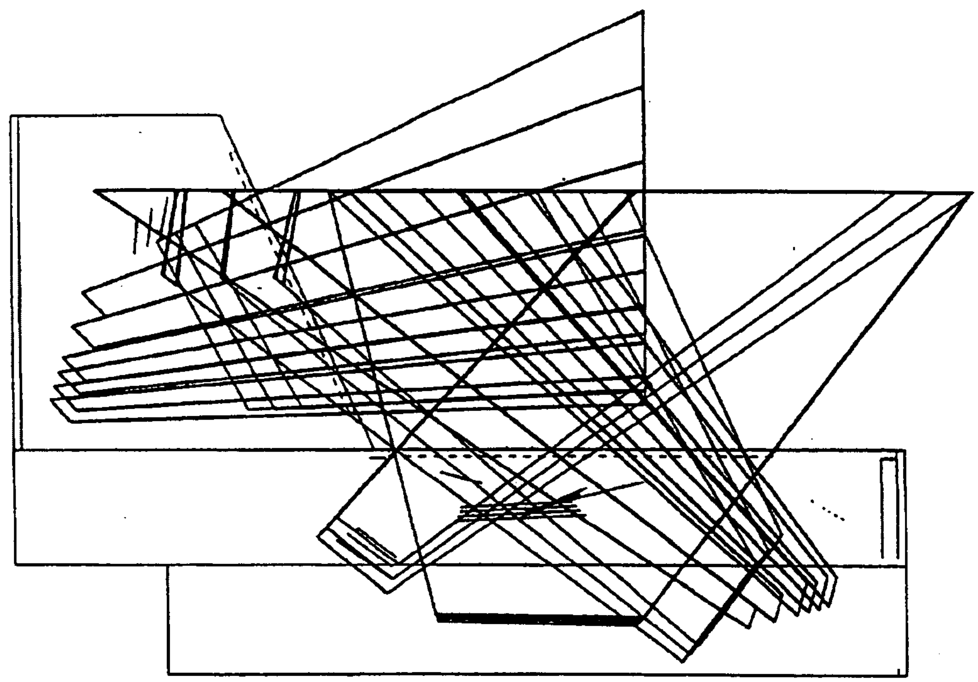

FIG. 5A5

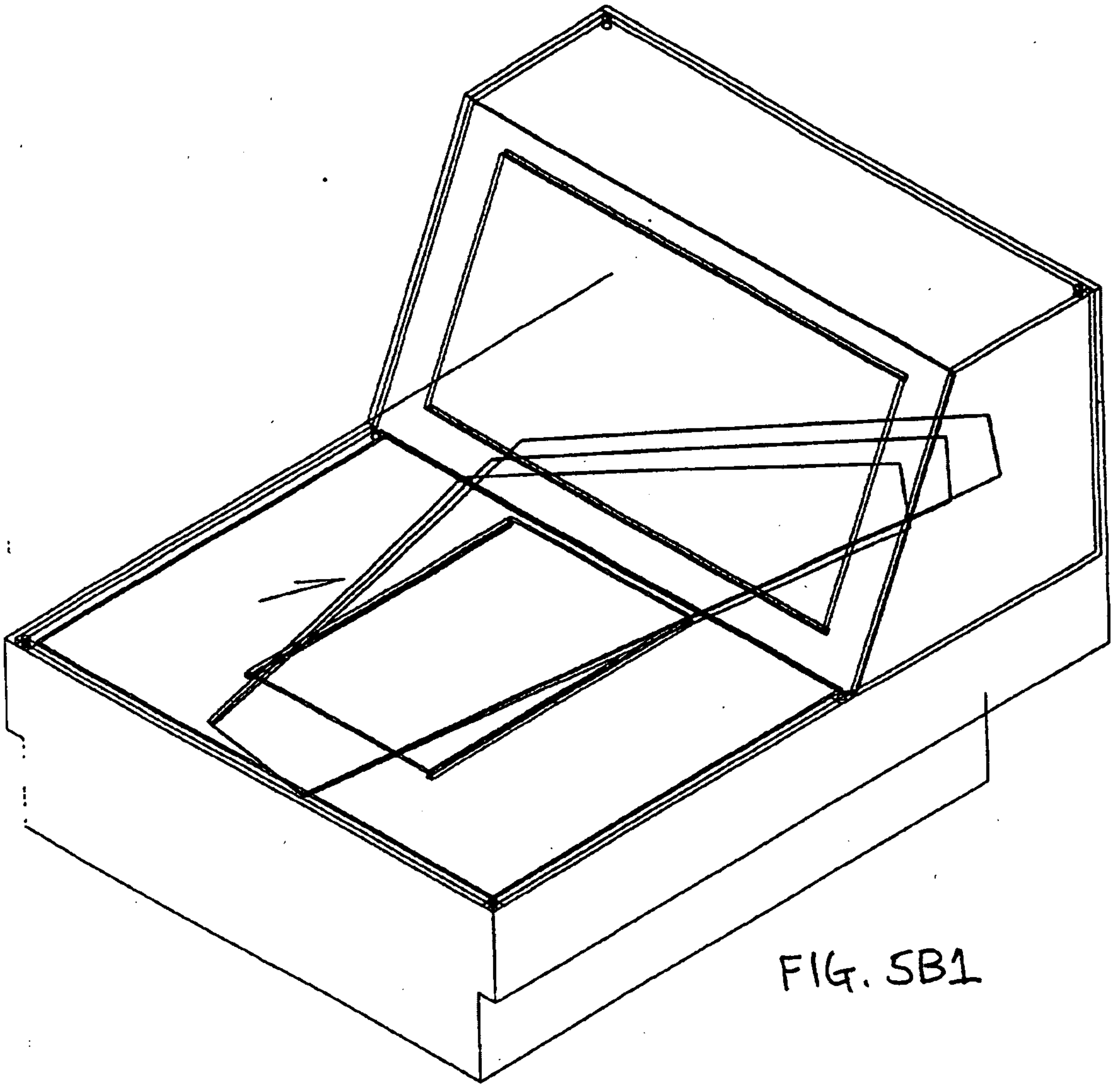

FIG. 5B1

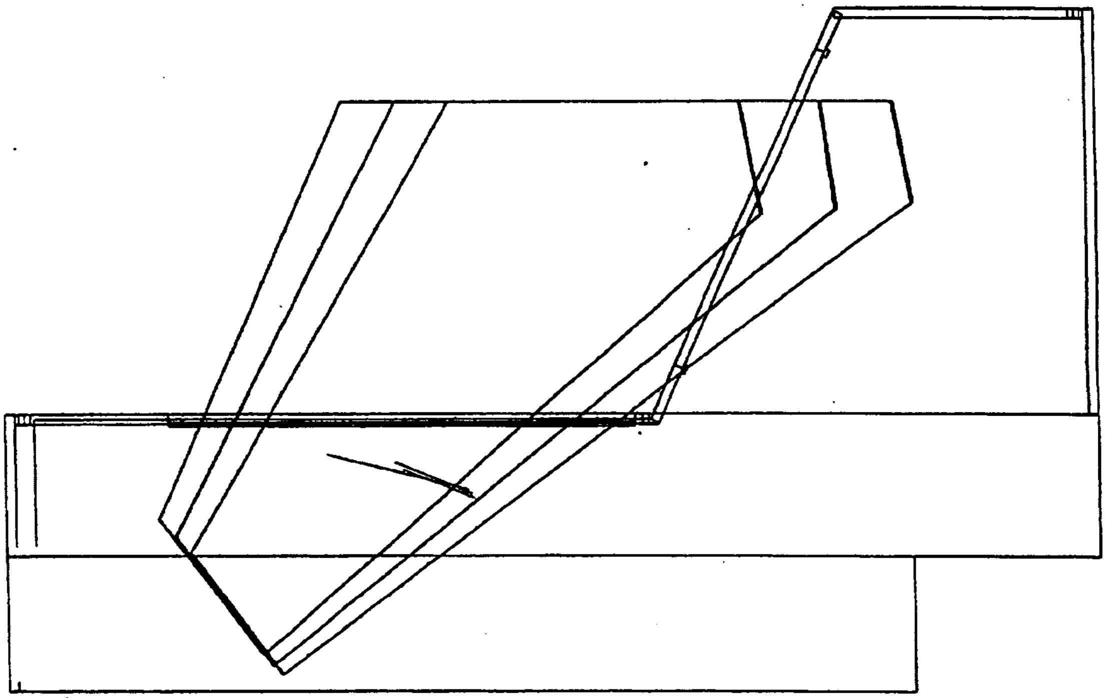

FIG. 5B2

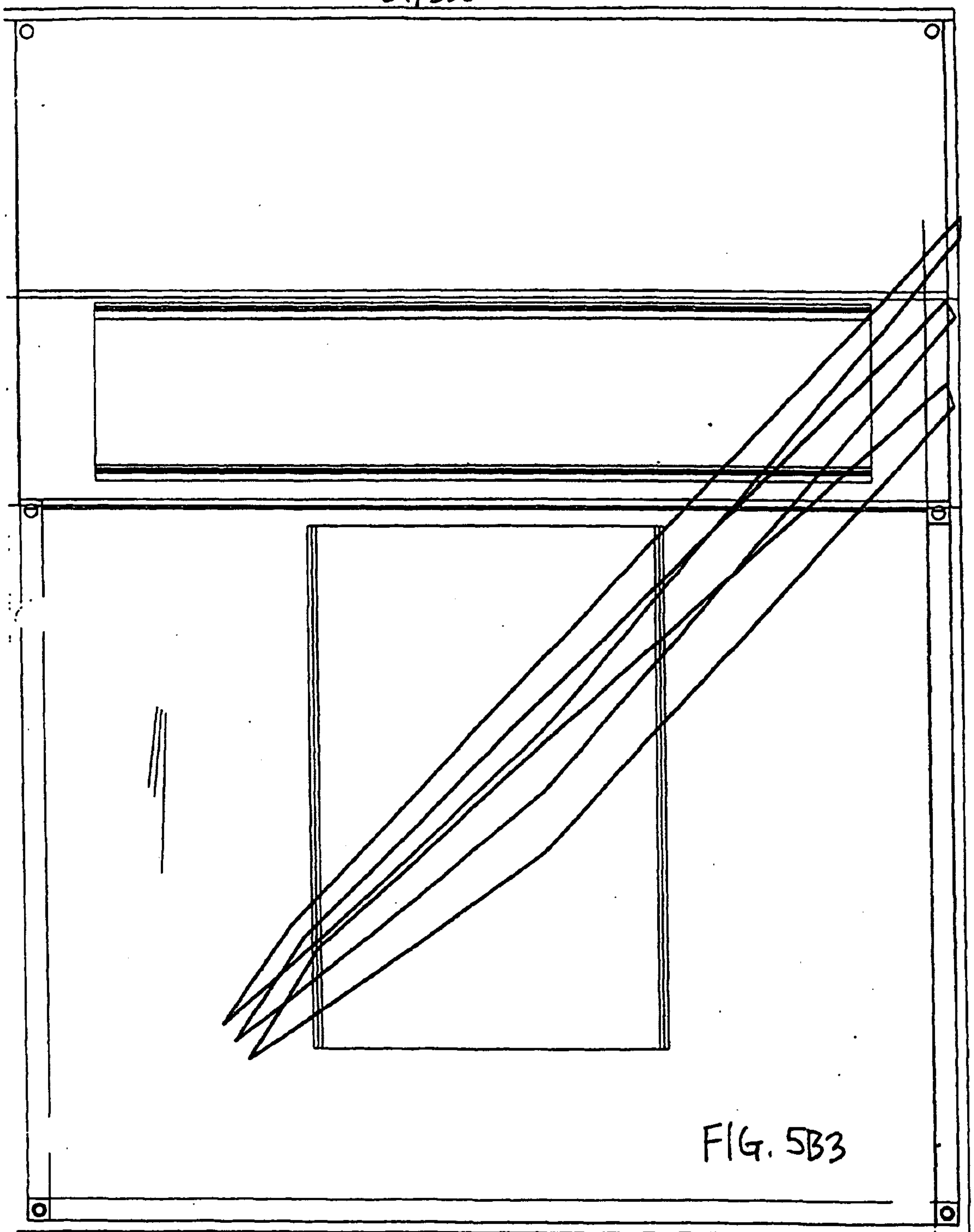

FIG. 5B3

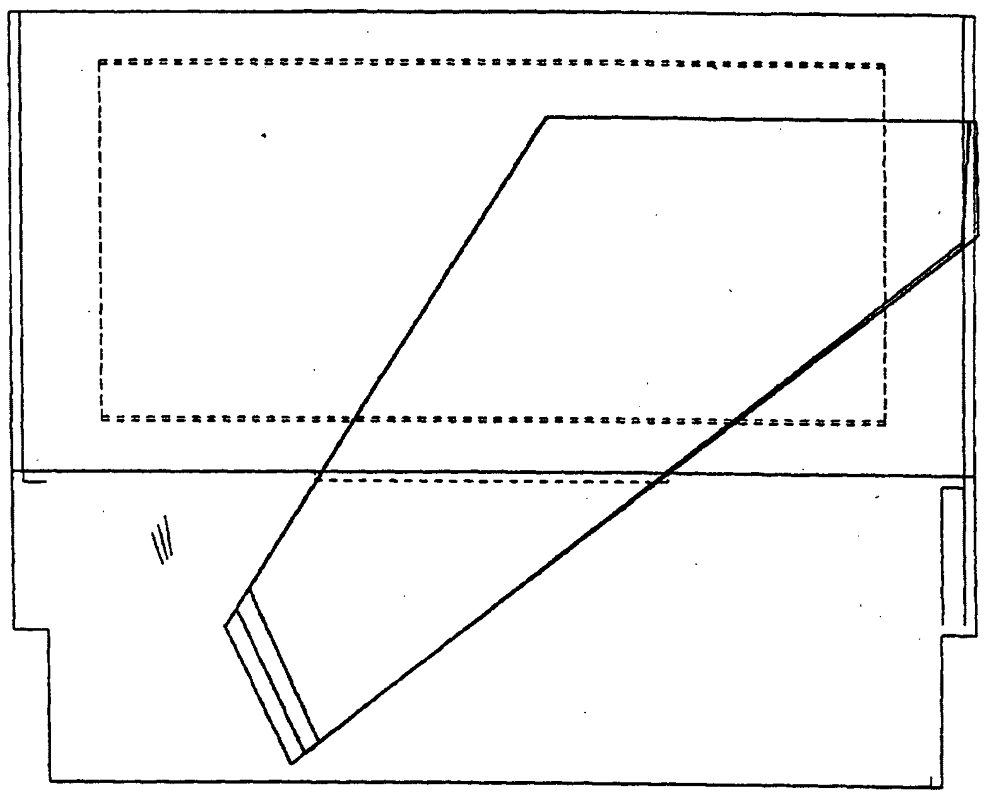

FIG. 5B4

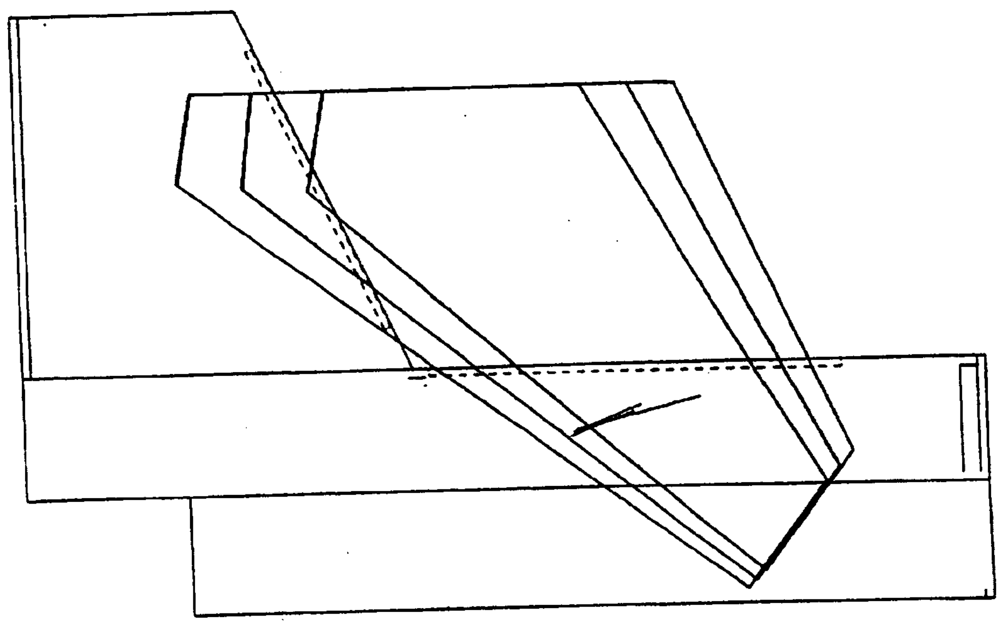

FIG. 5B5

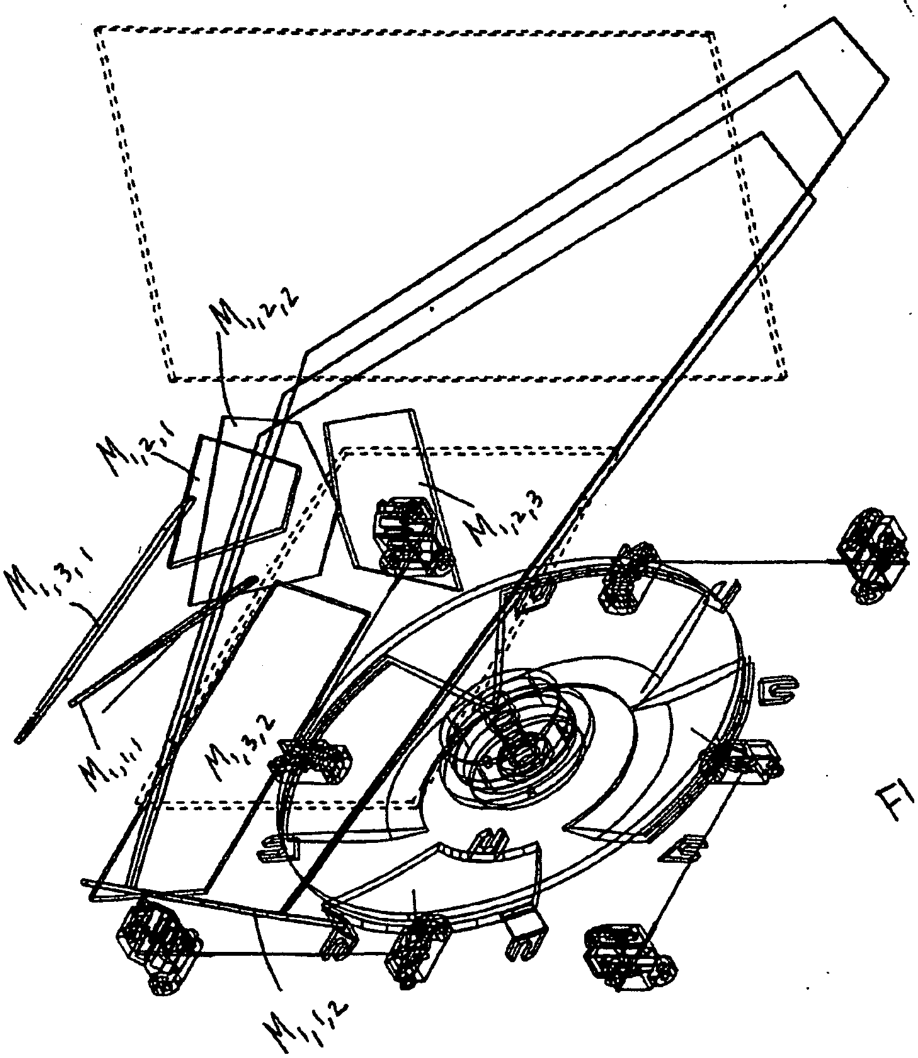

FI

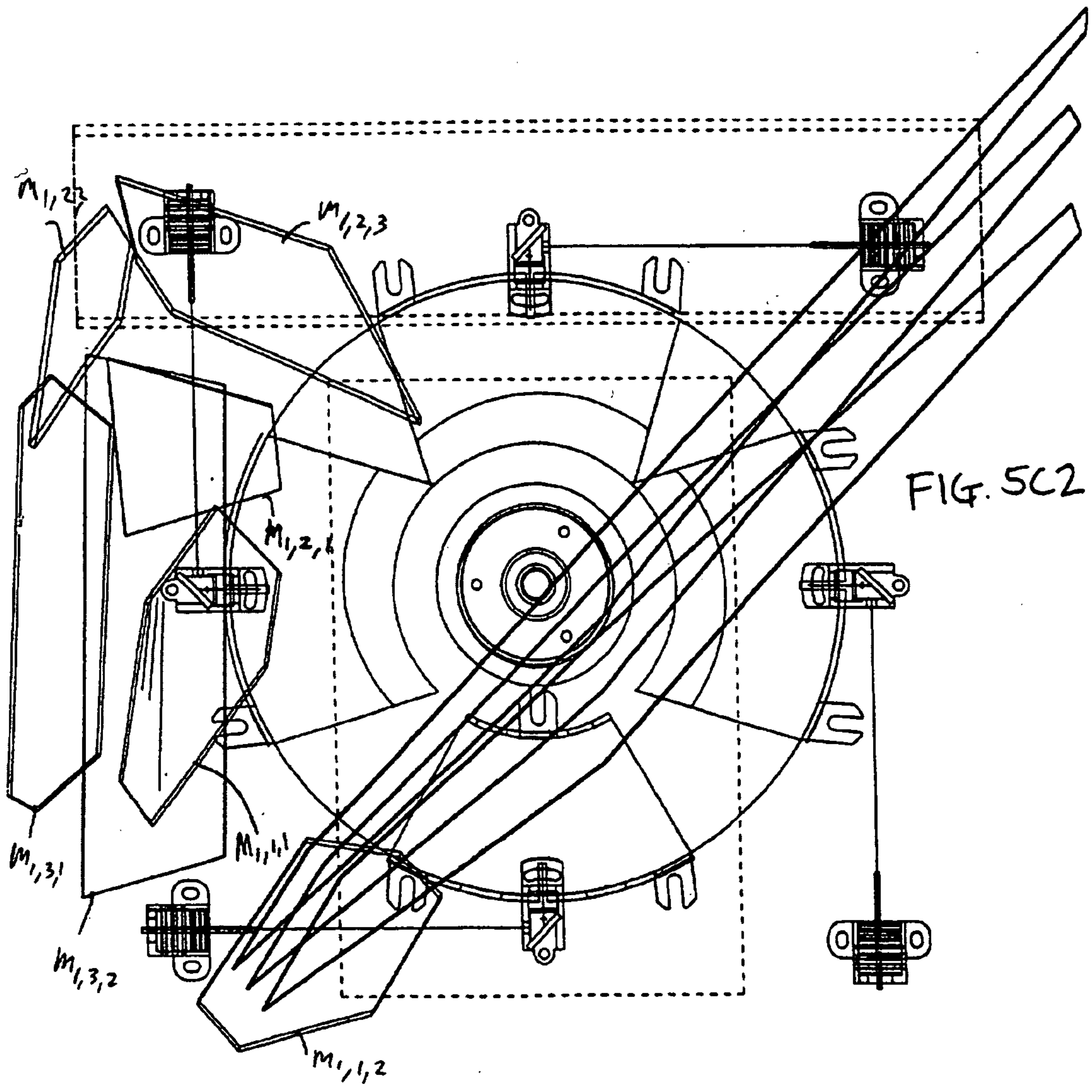

FIG. 5C2

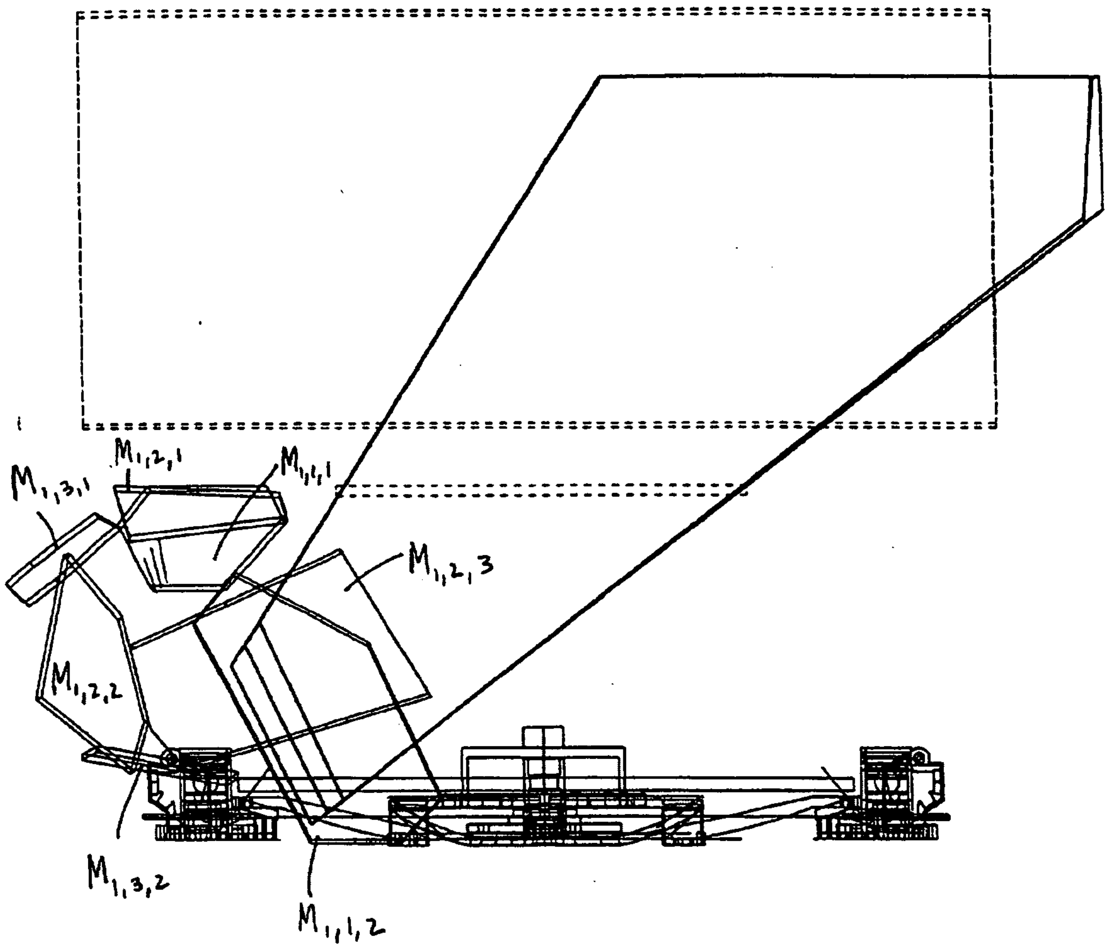

FIG. 5C3

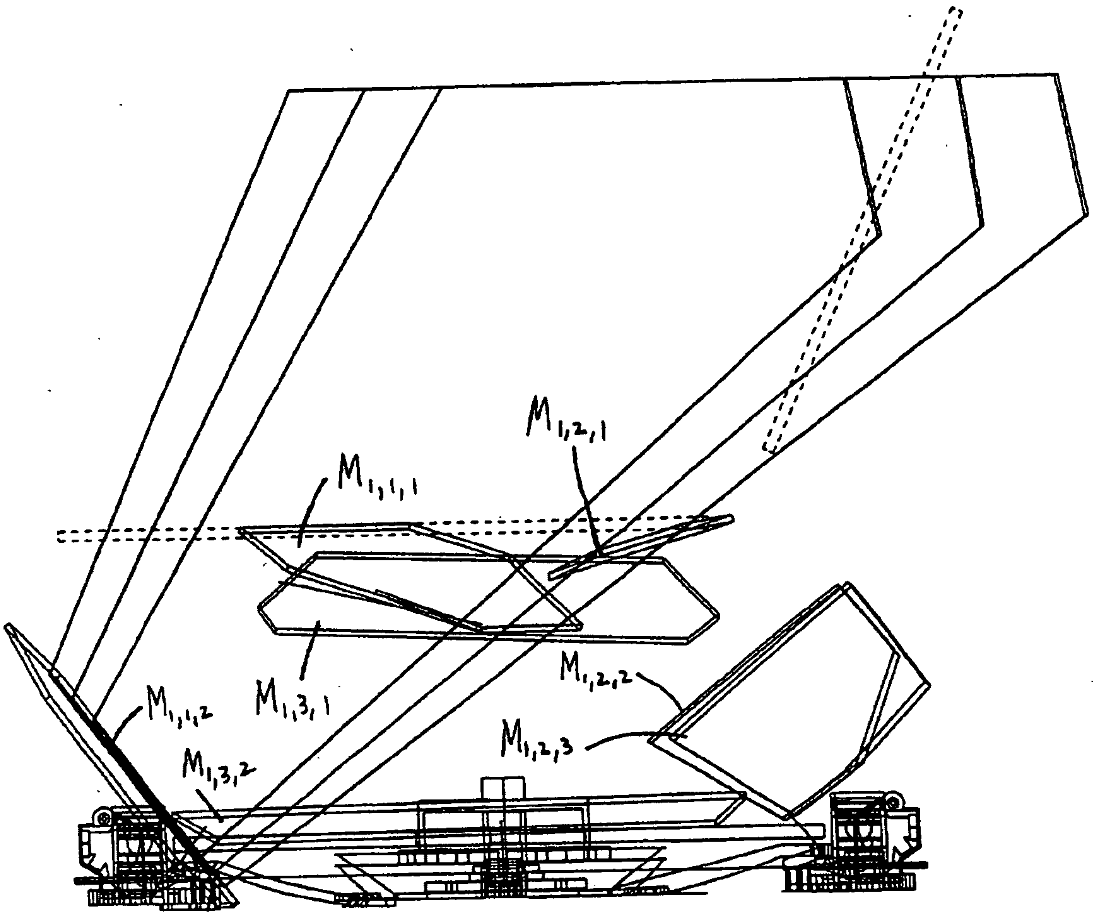

FIG. 5C4

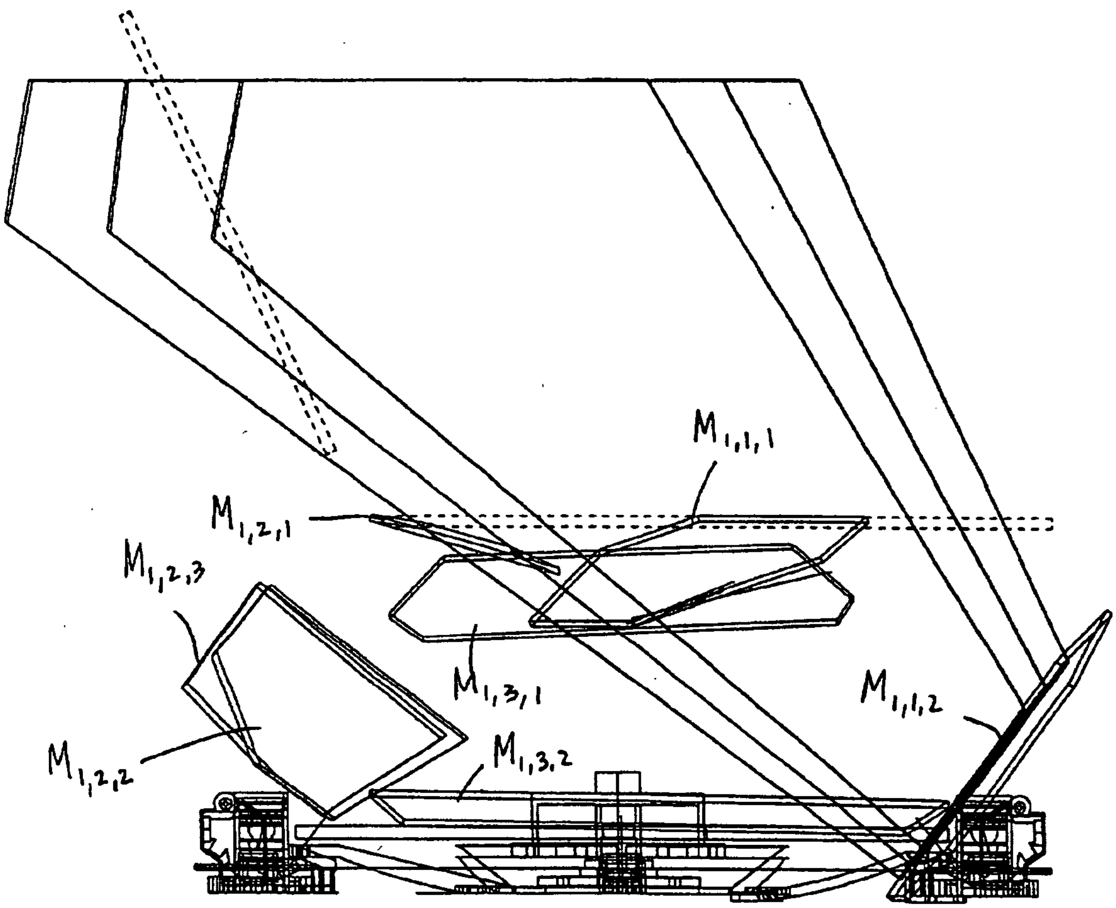

FIG. 5C5

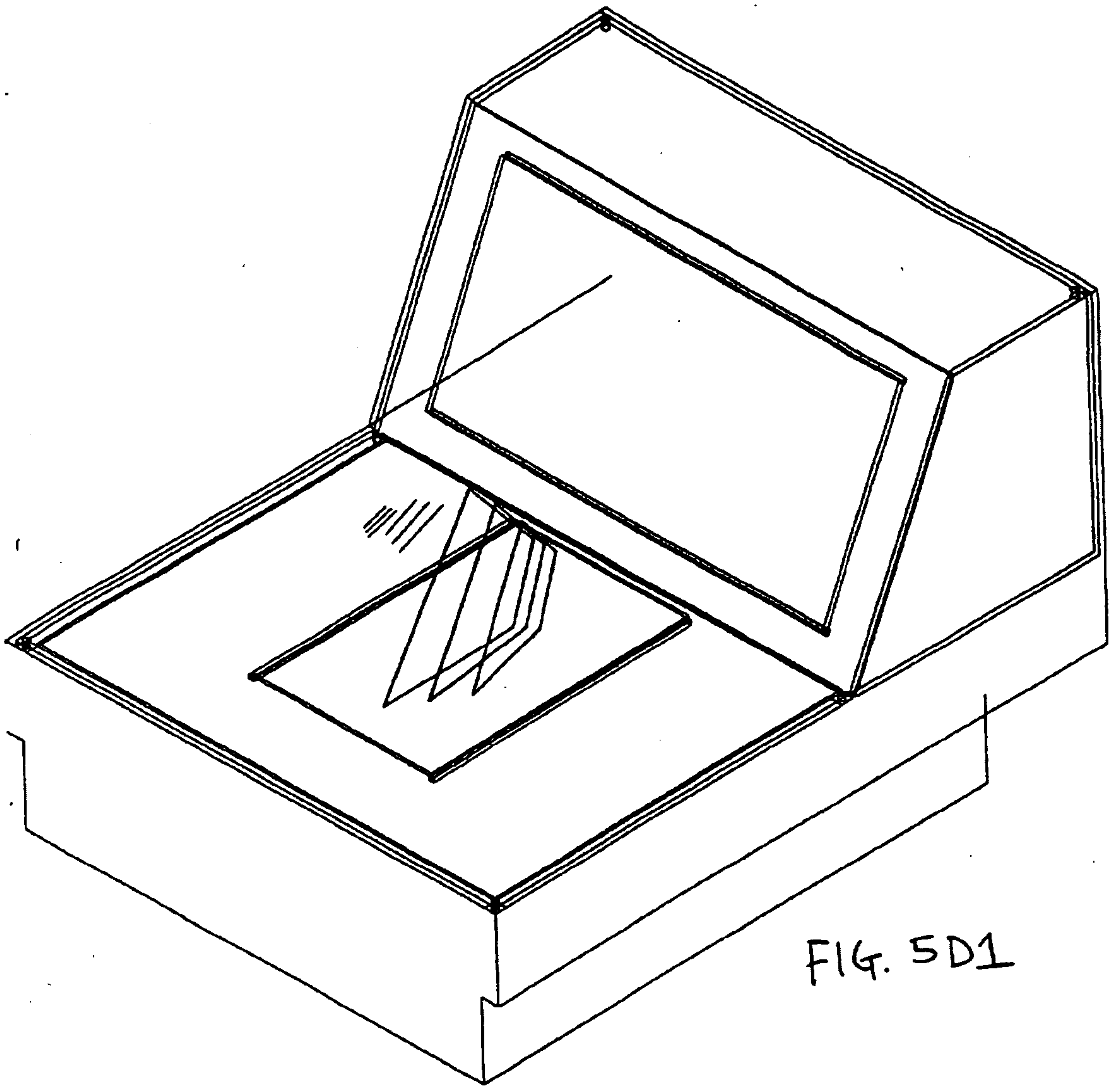

FIG. 5D1

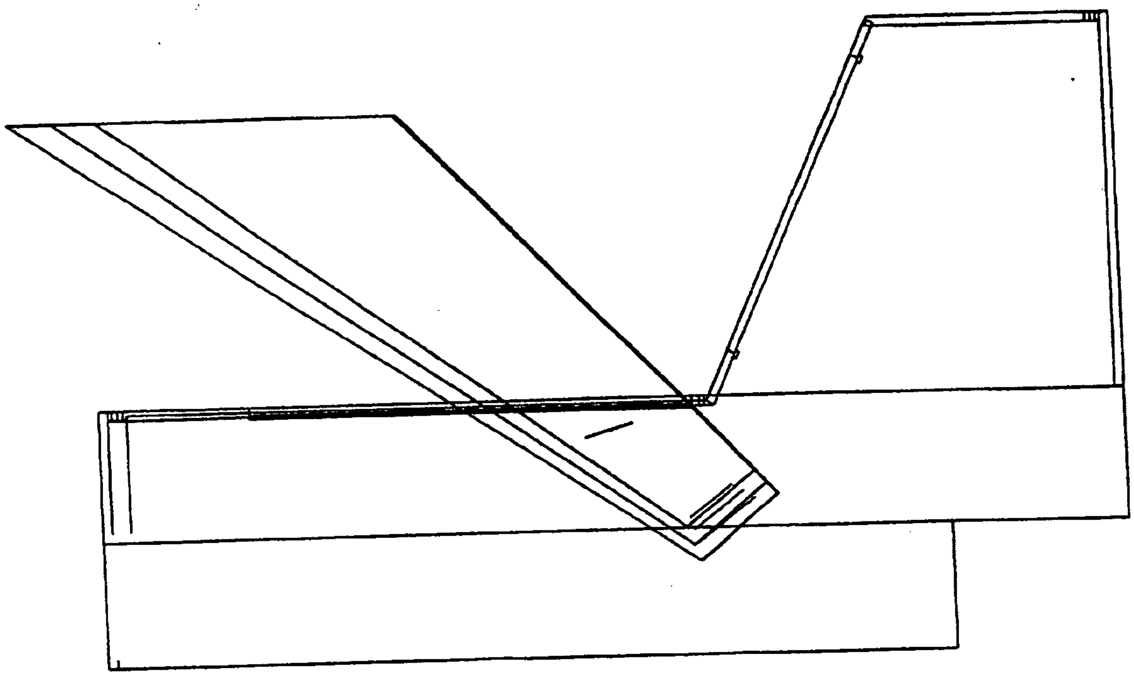

FIG. 5D2

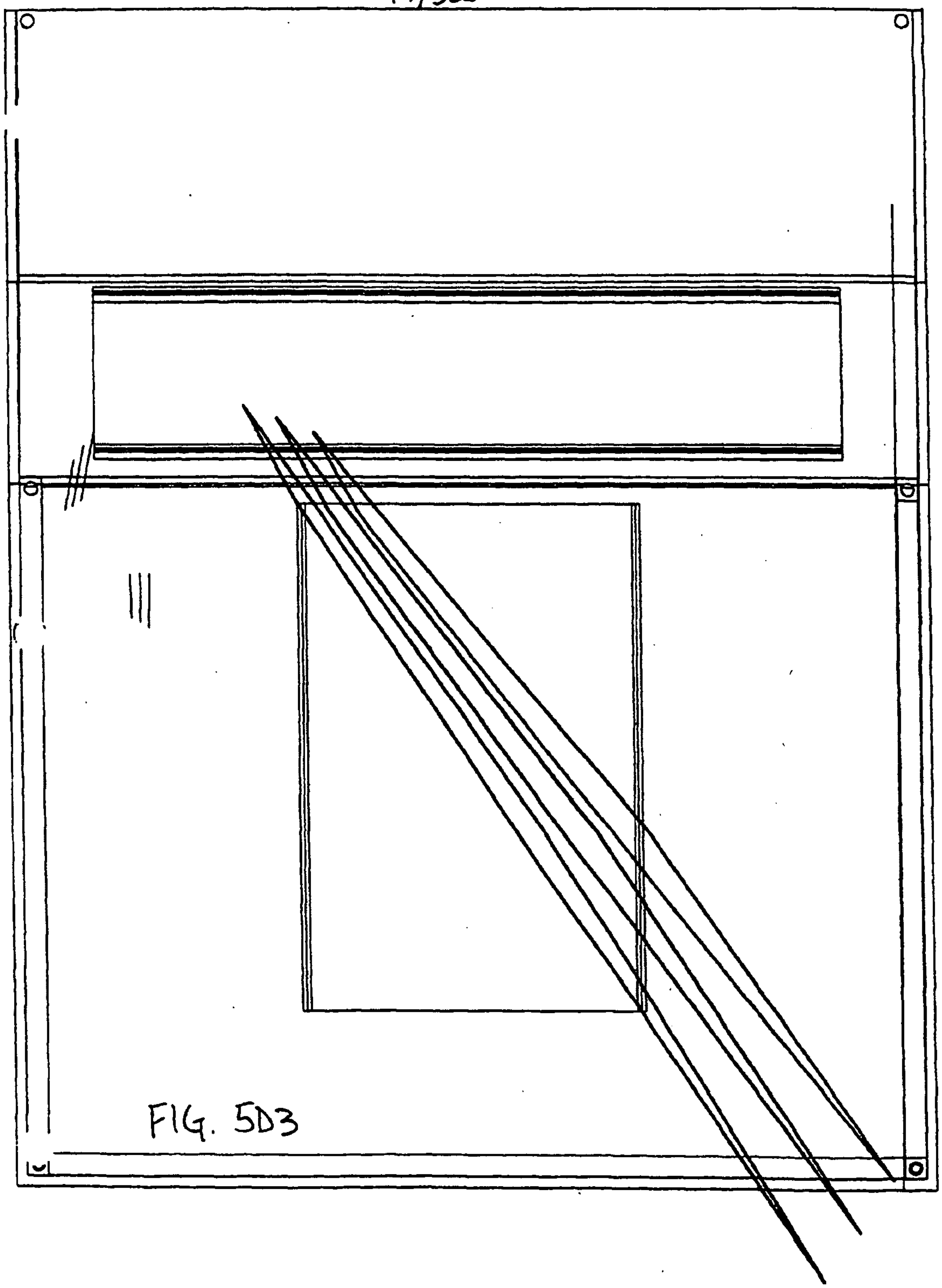

FIG. 5D3

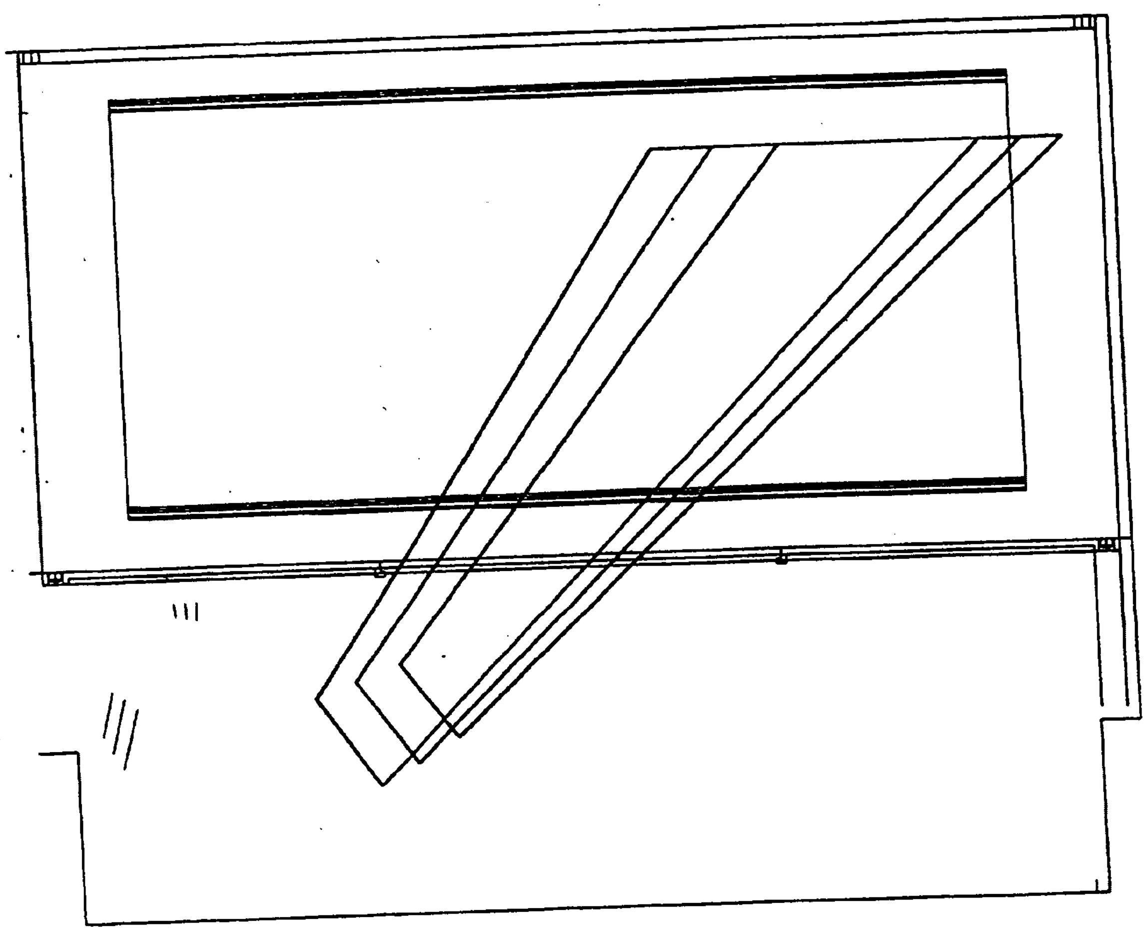

FIG. 5D4

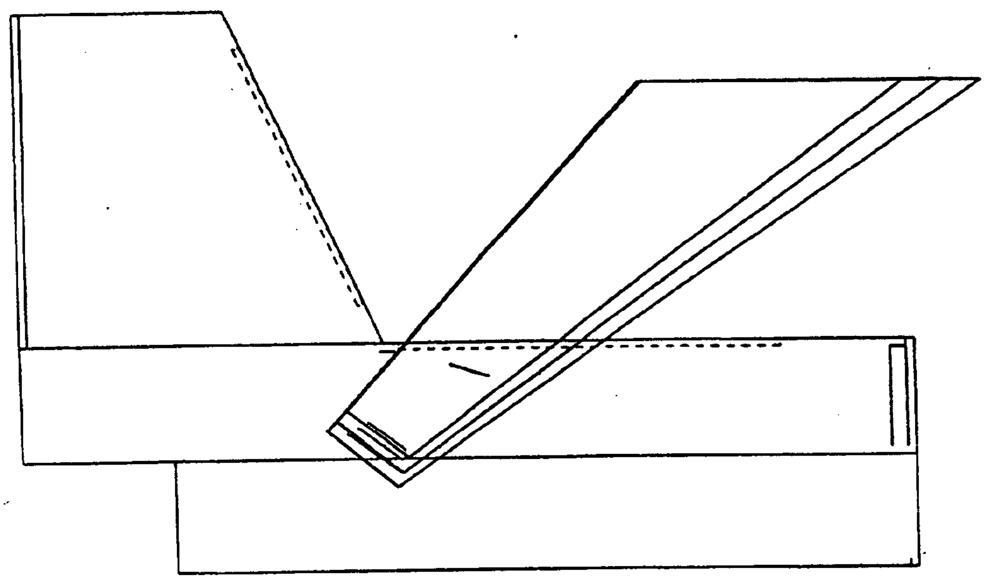

FIG. 5D5

80/335

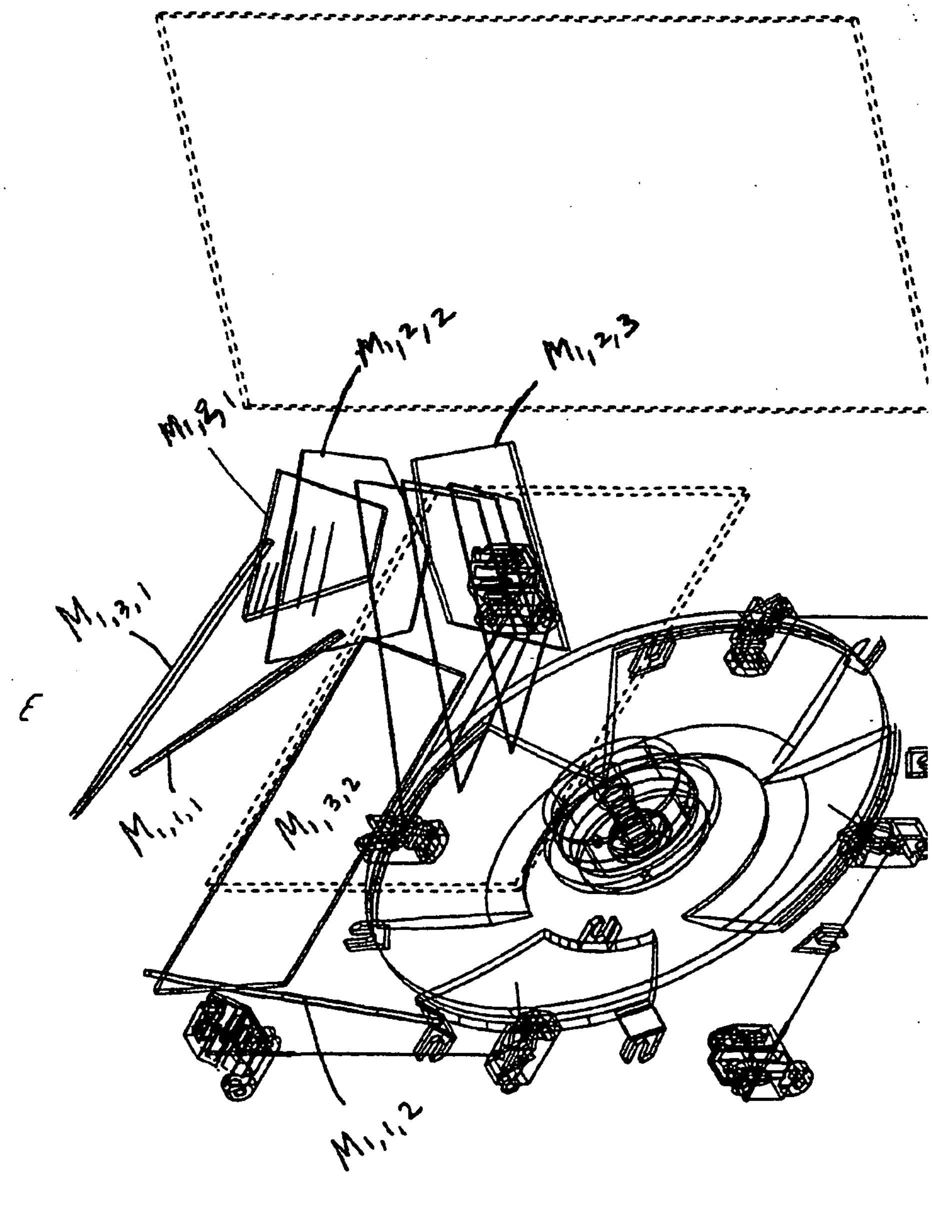

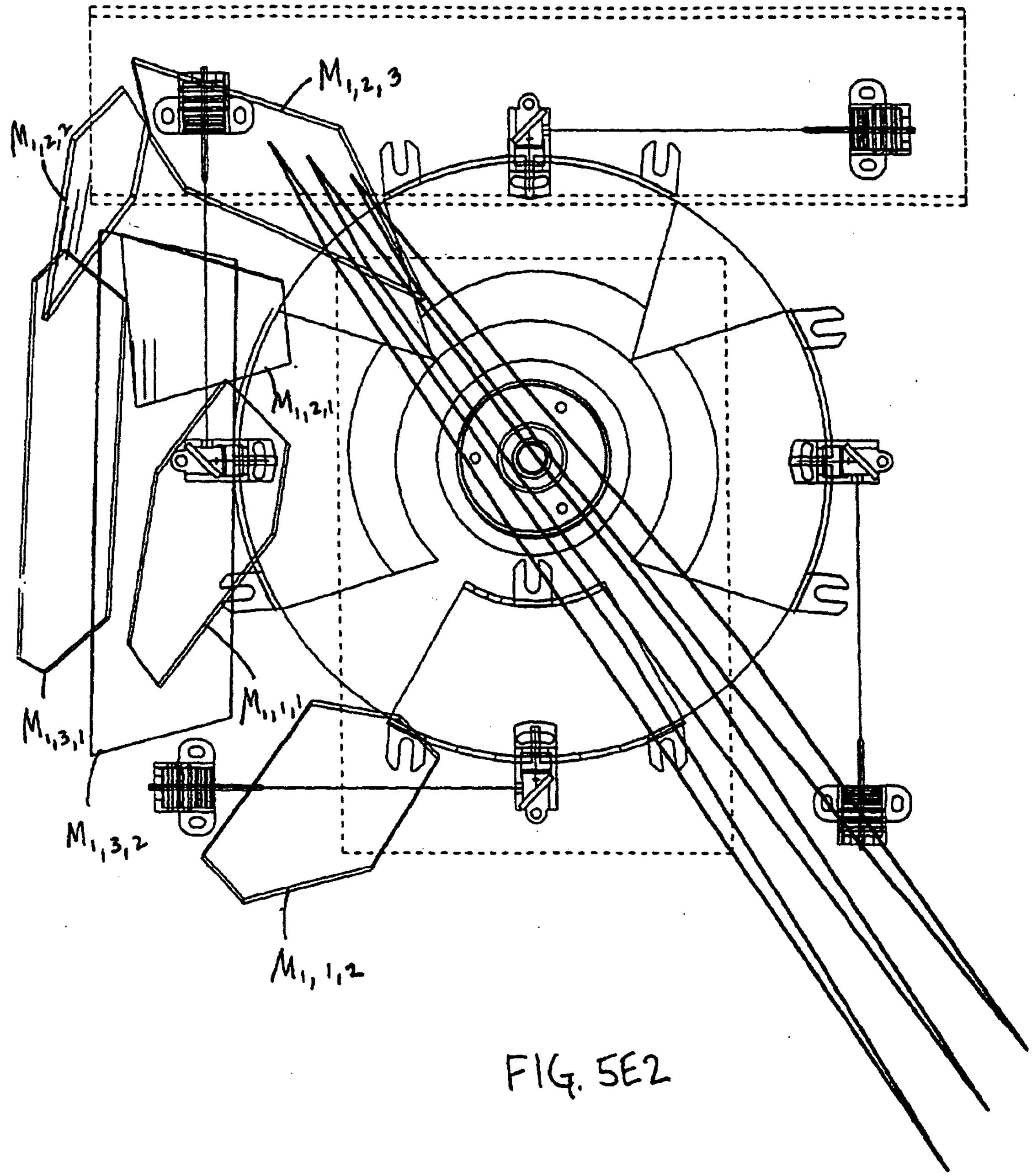

FIG. 5E2

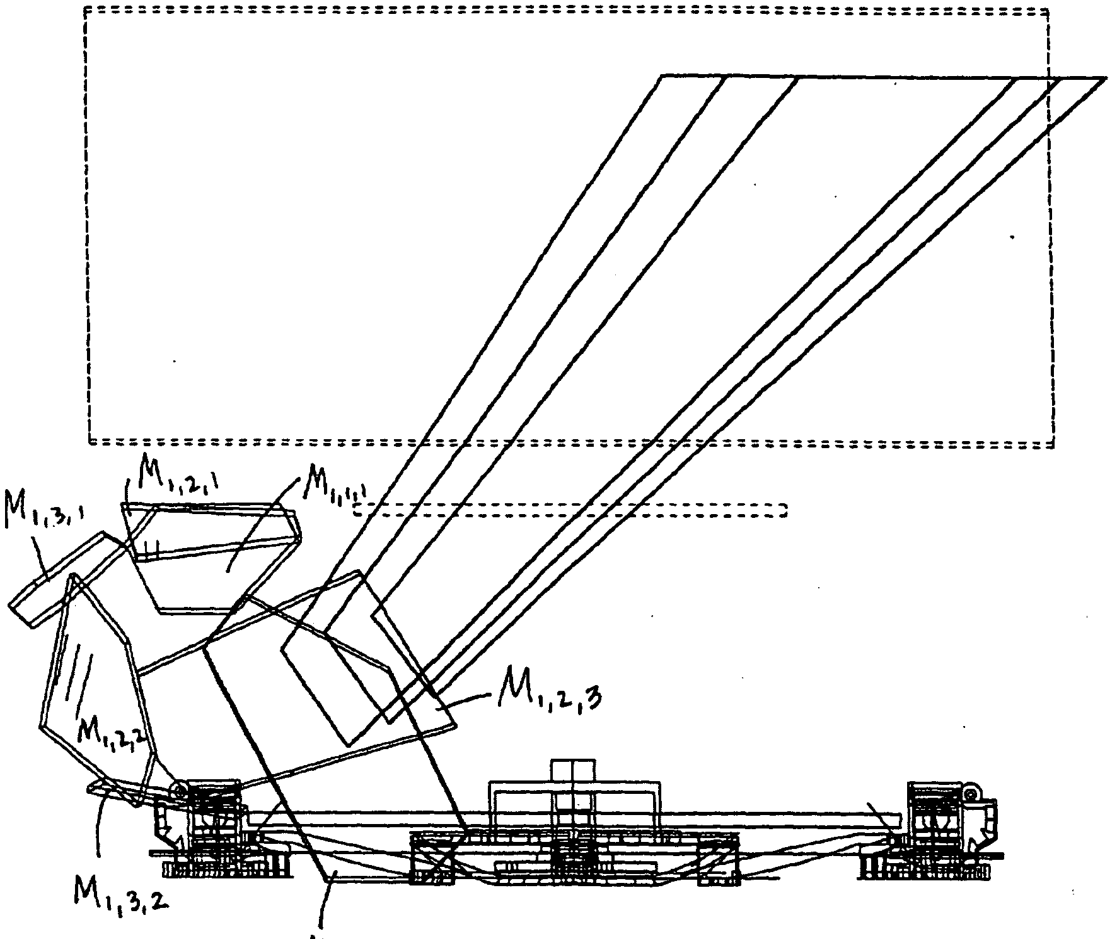

FIG. 5E3

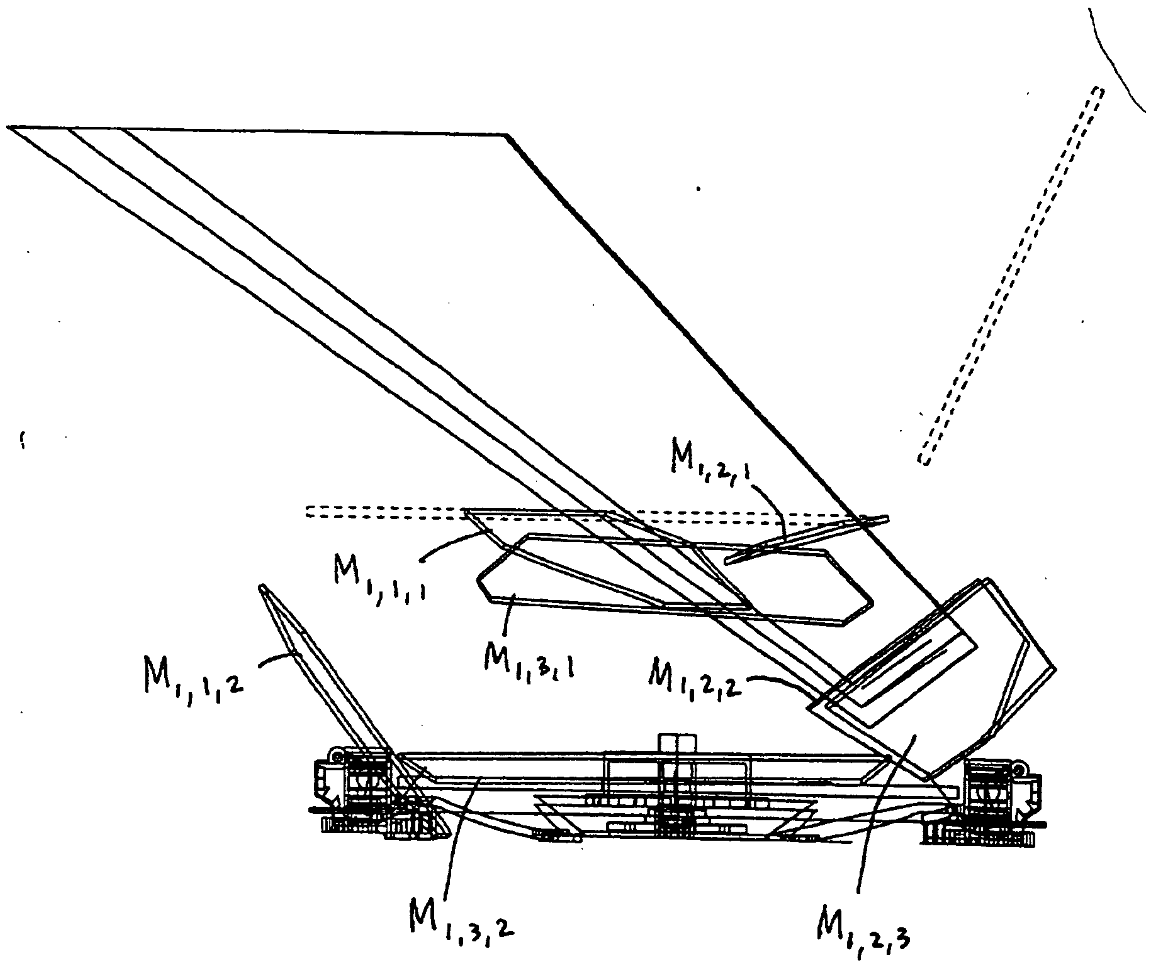

FIG. 5E4

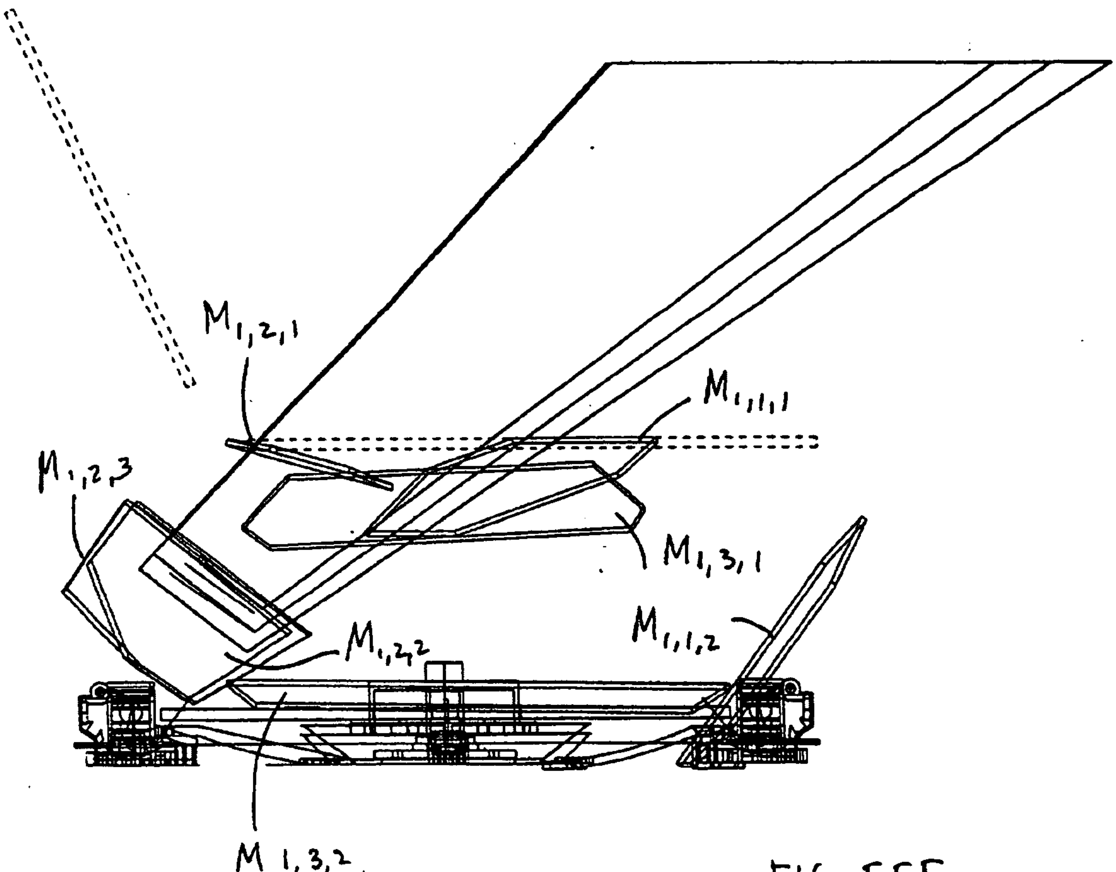

FIG. 5E5

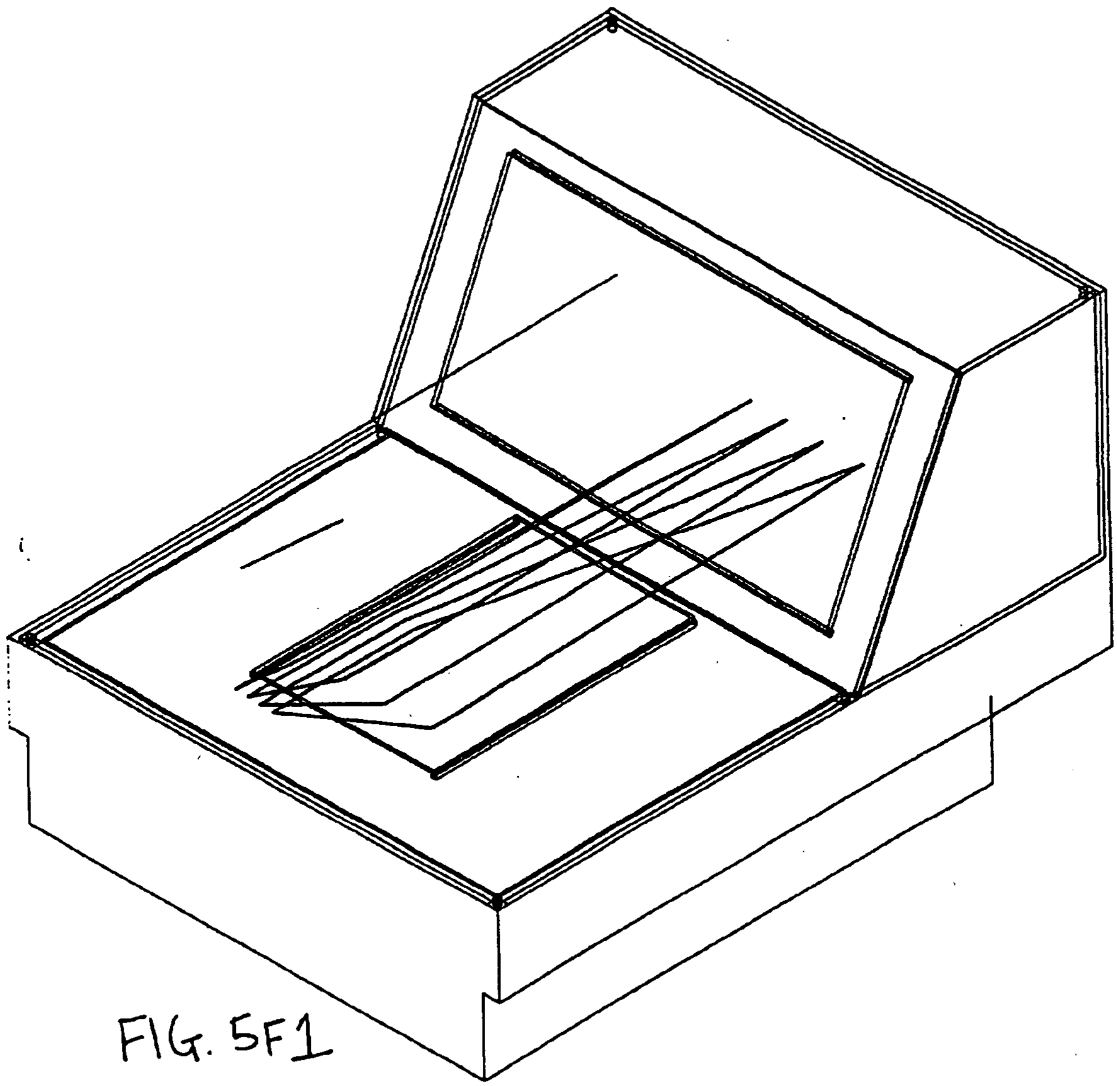

FIG. 5F1

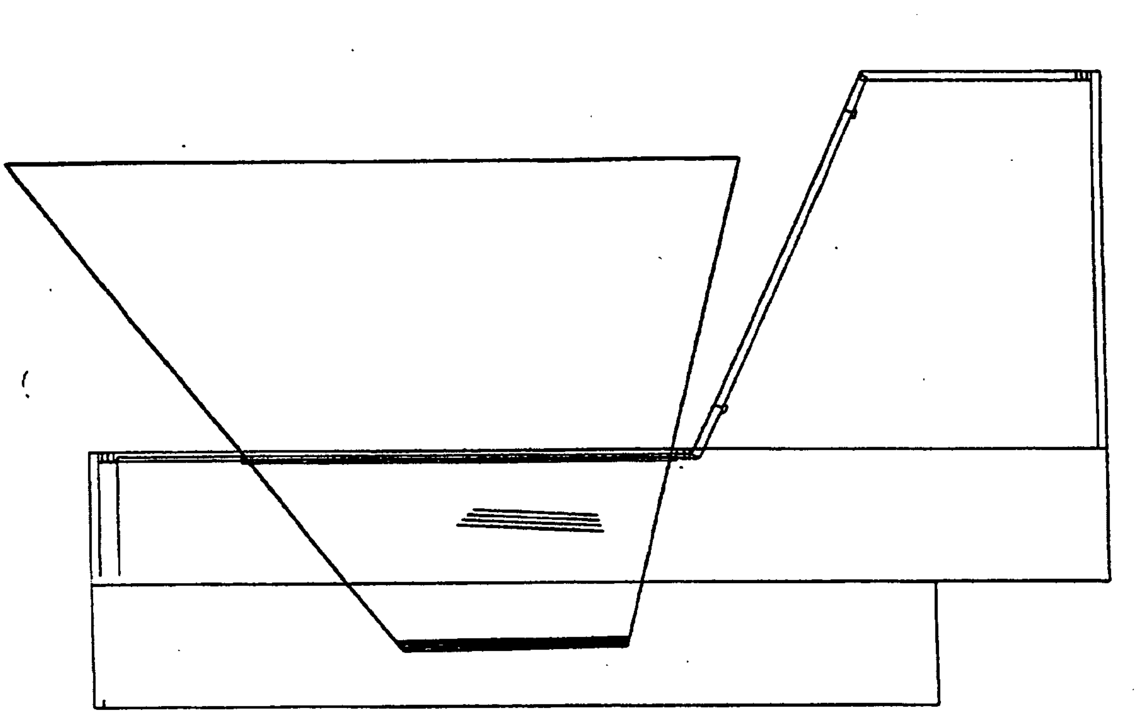

FIG. 5F2

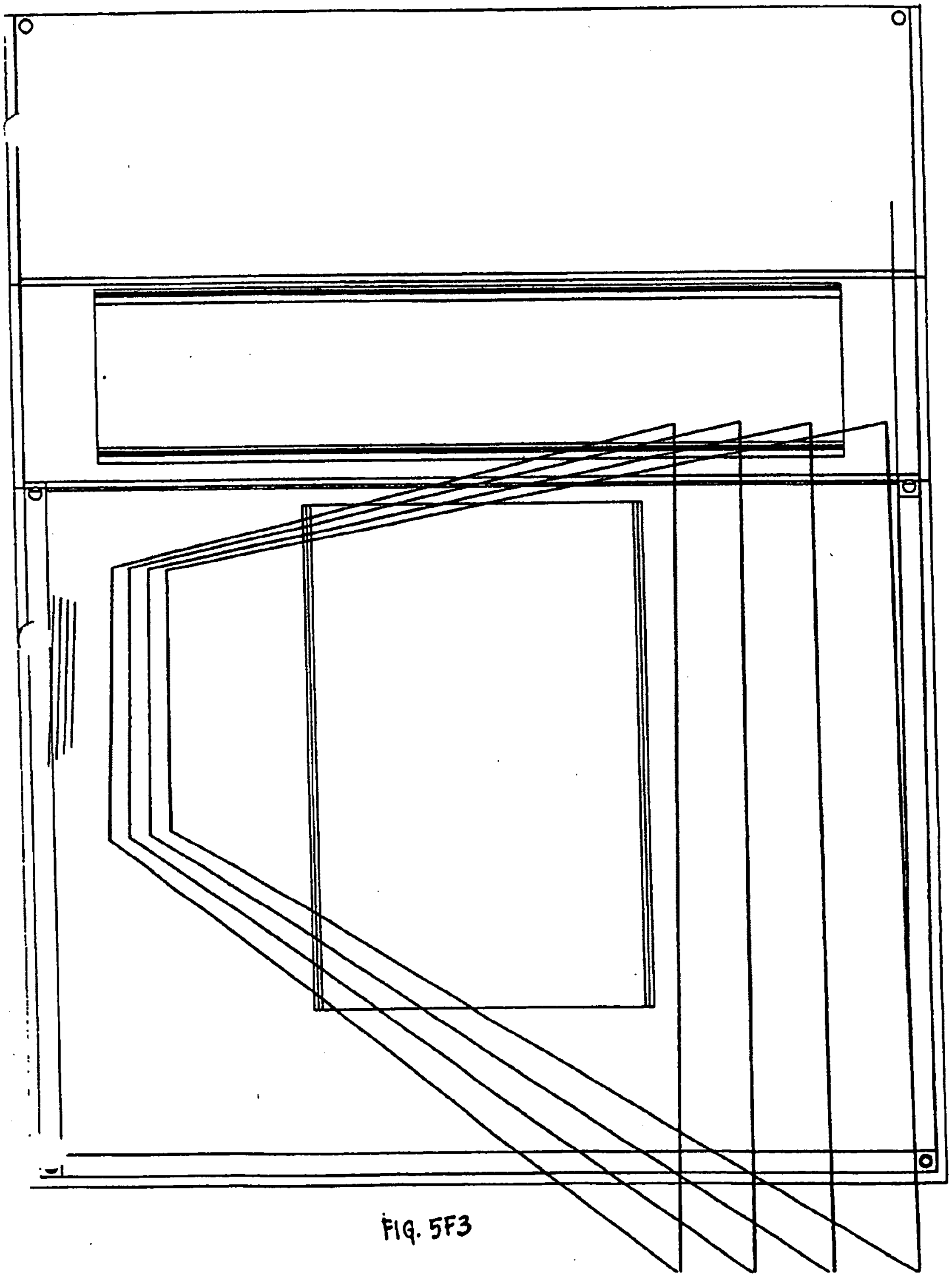

FIG. 5F3

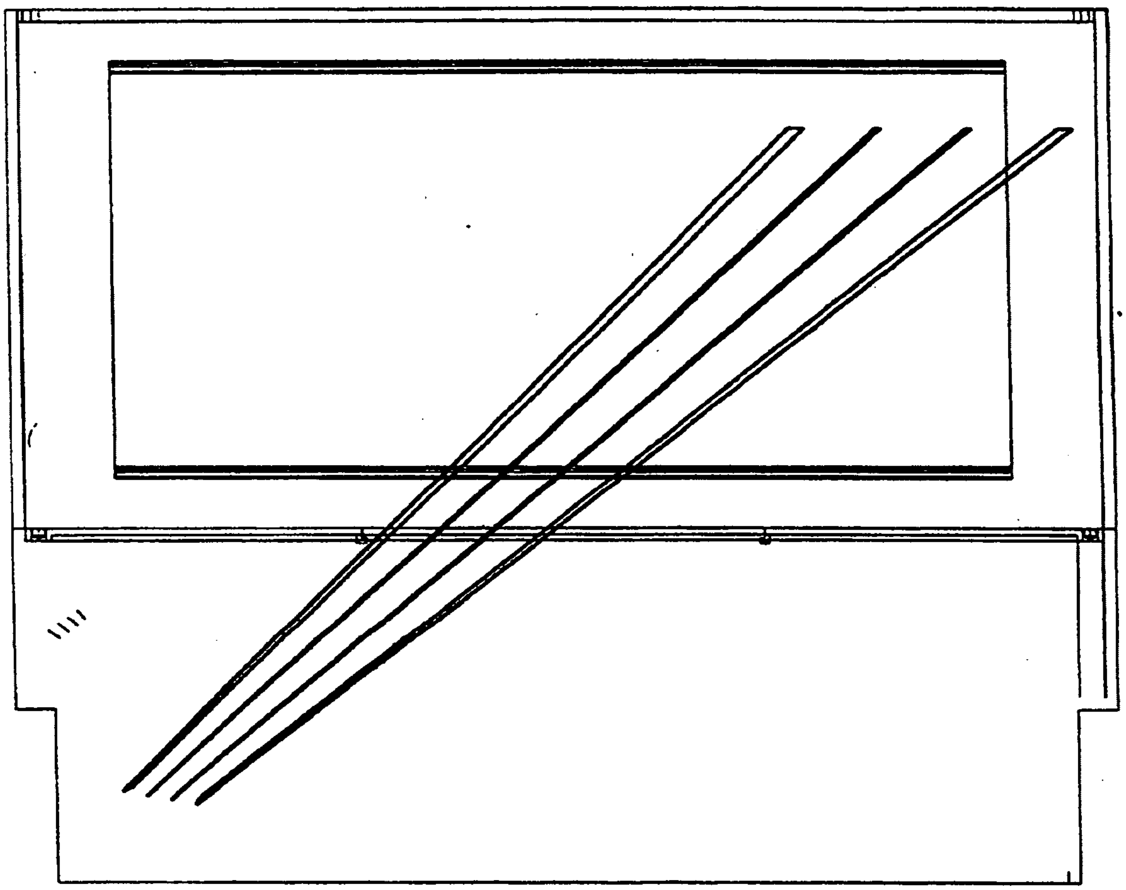

FIG. 5F4

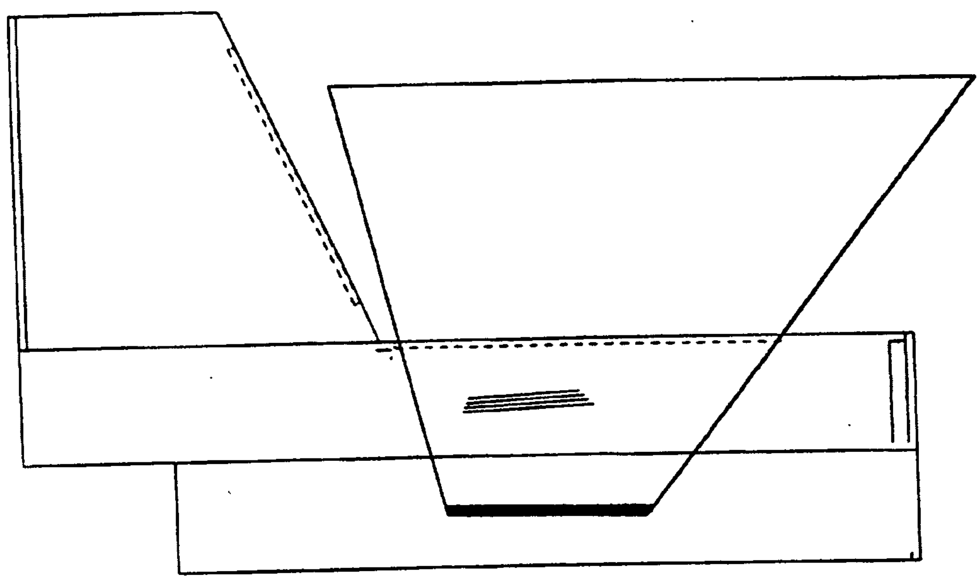

FIG. 5F5

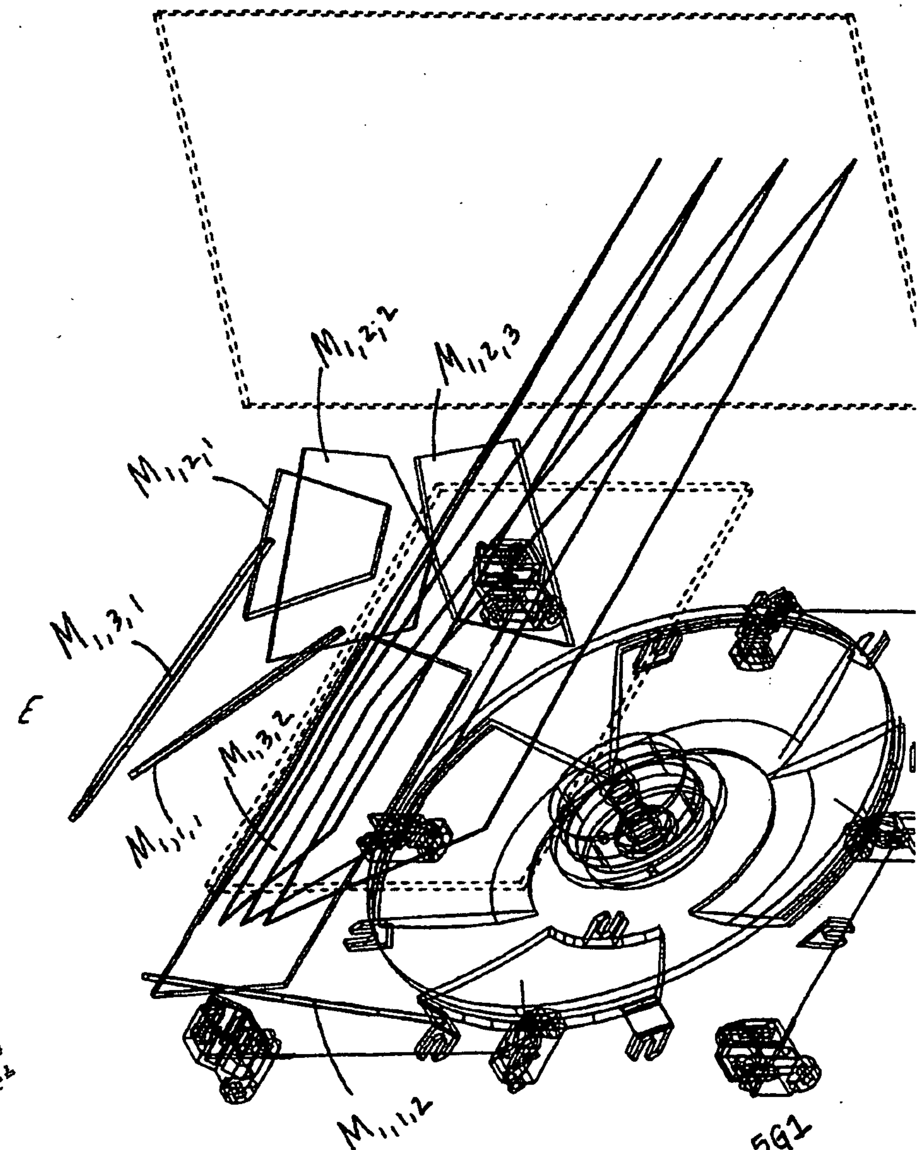

FIG. 5G1

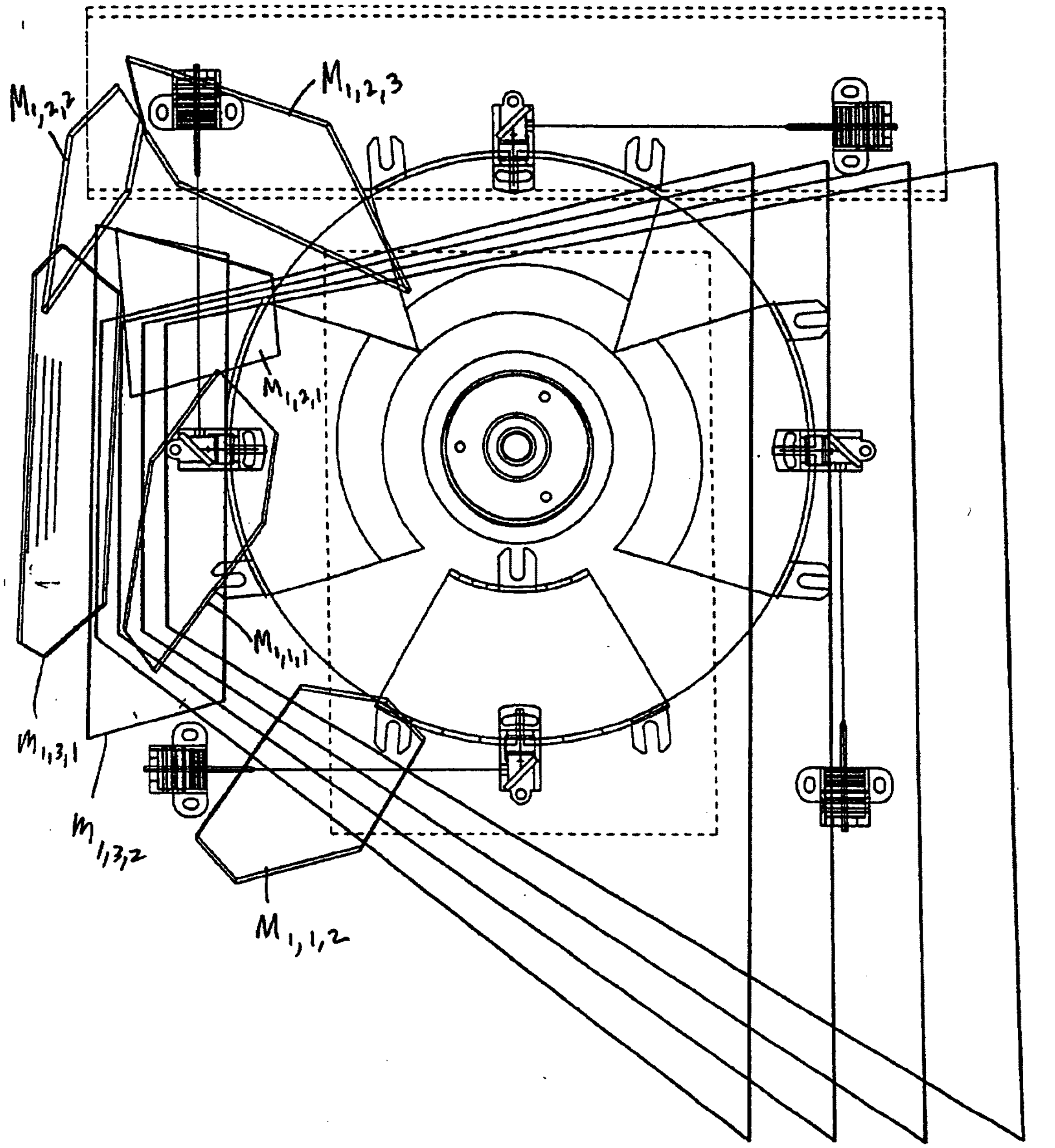

FIG. 5G2

92/335

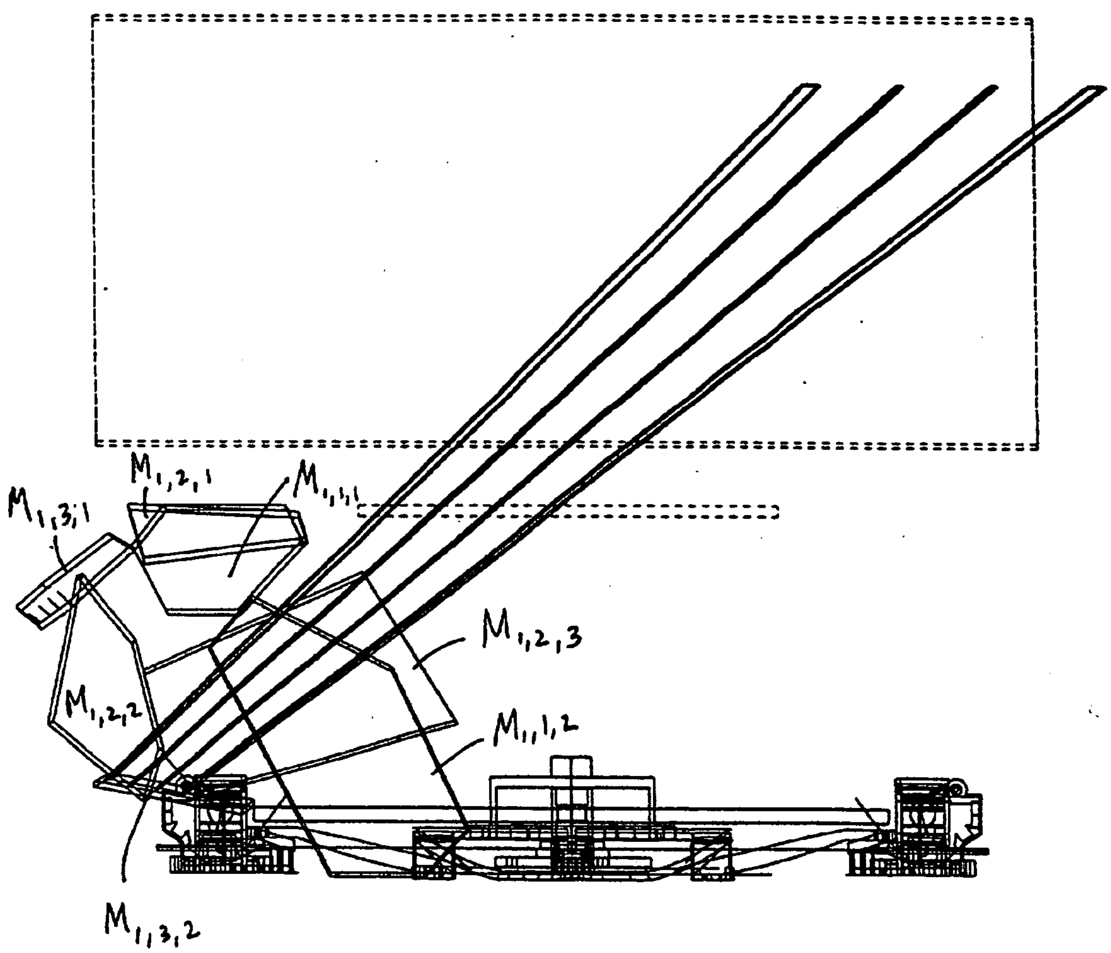

FIG 5G3

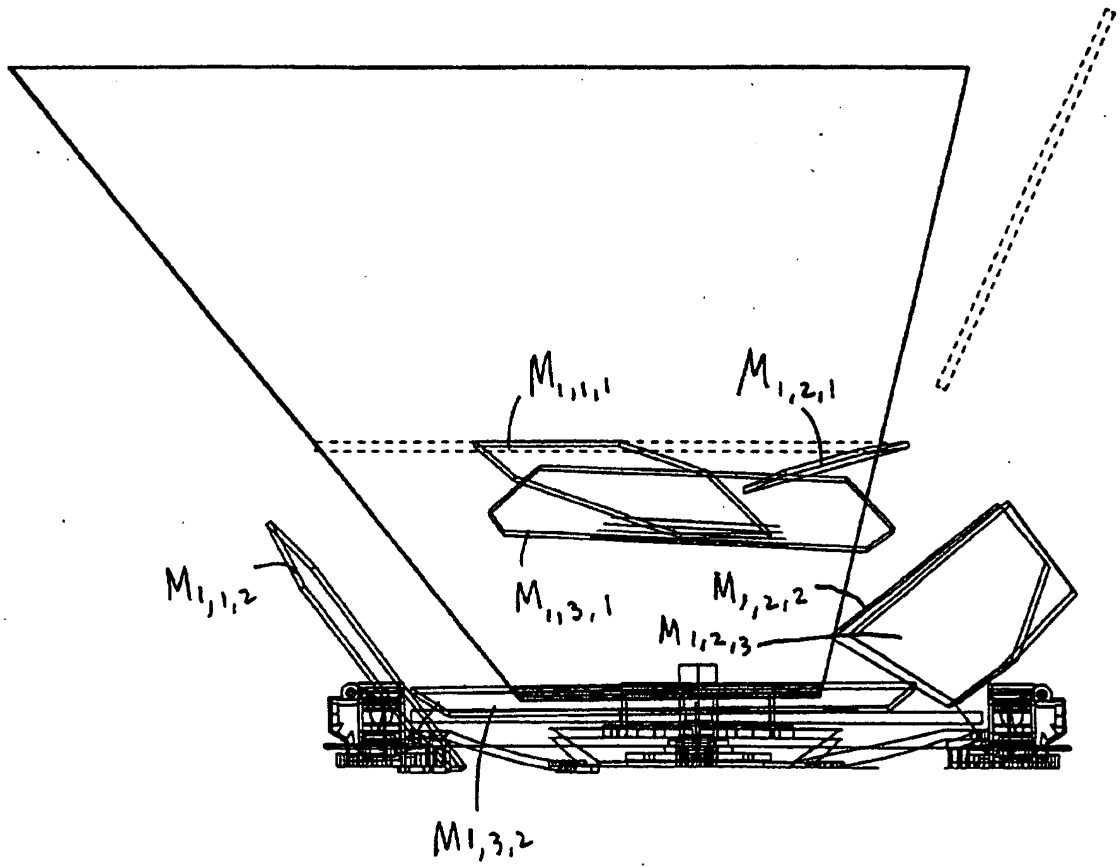

FIG. 5G4

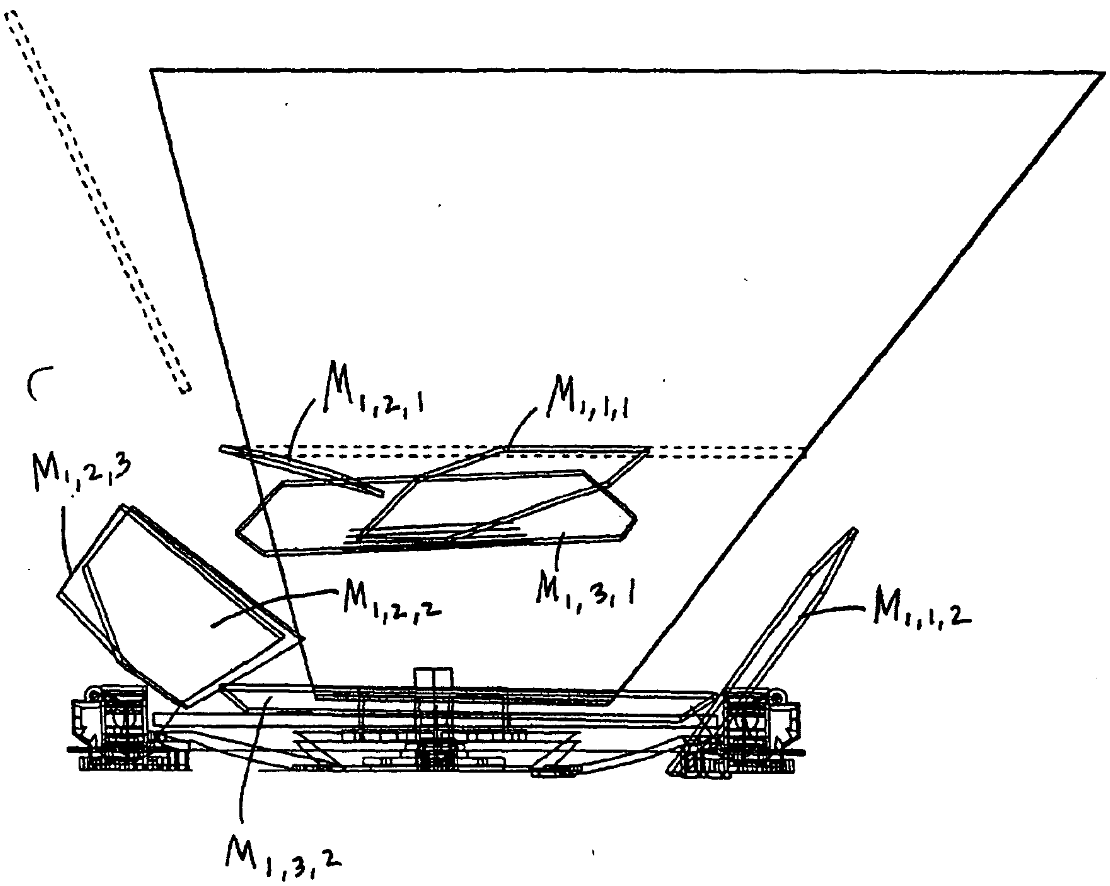

FIG. 5G5

95/335

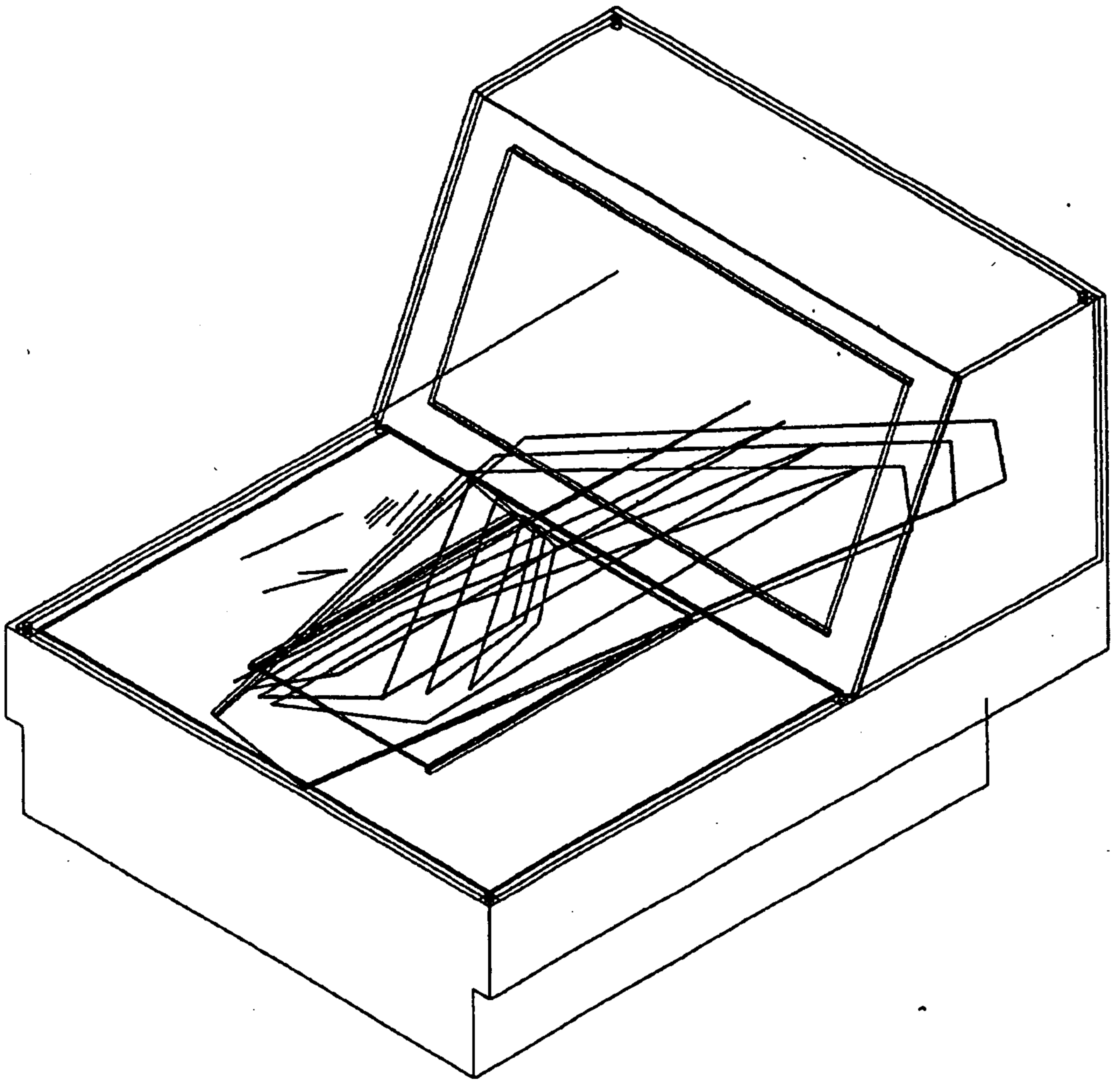

5H1

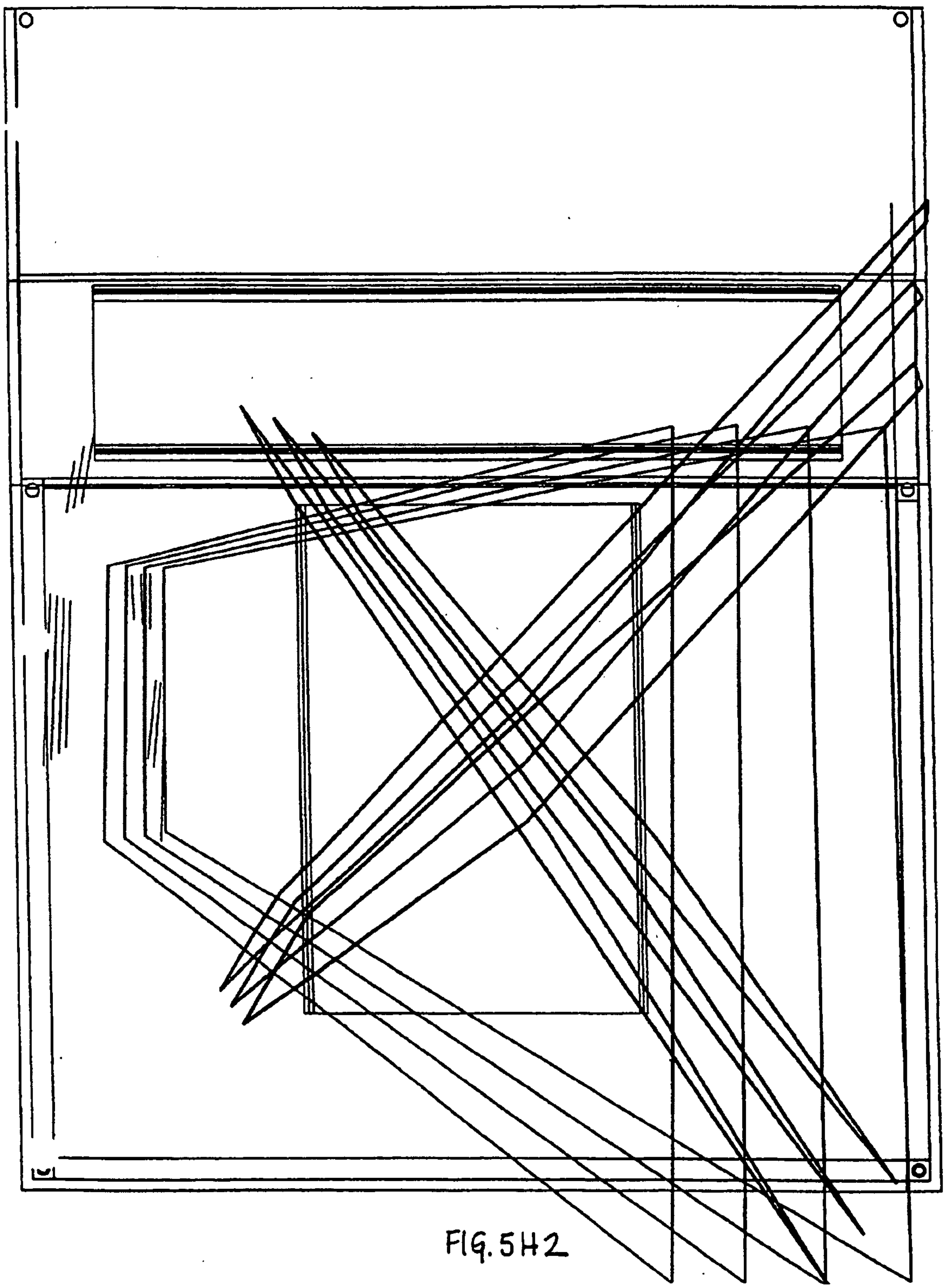

FIG. 5H2

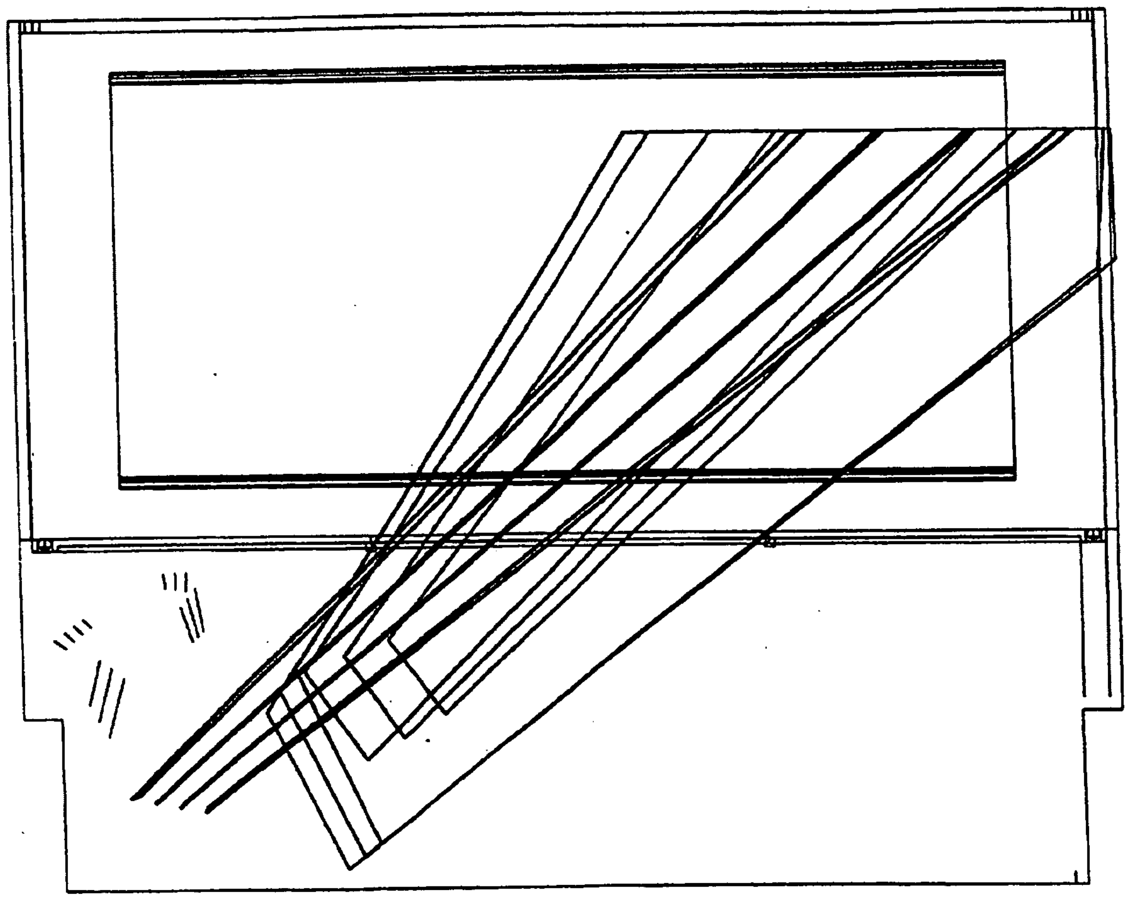

FIG. 5H3

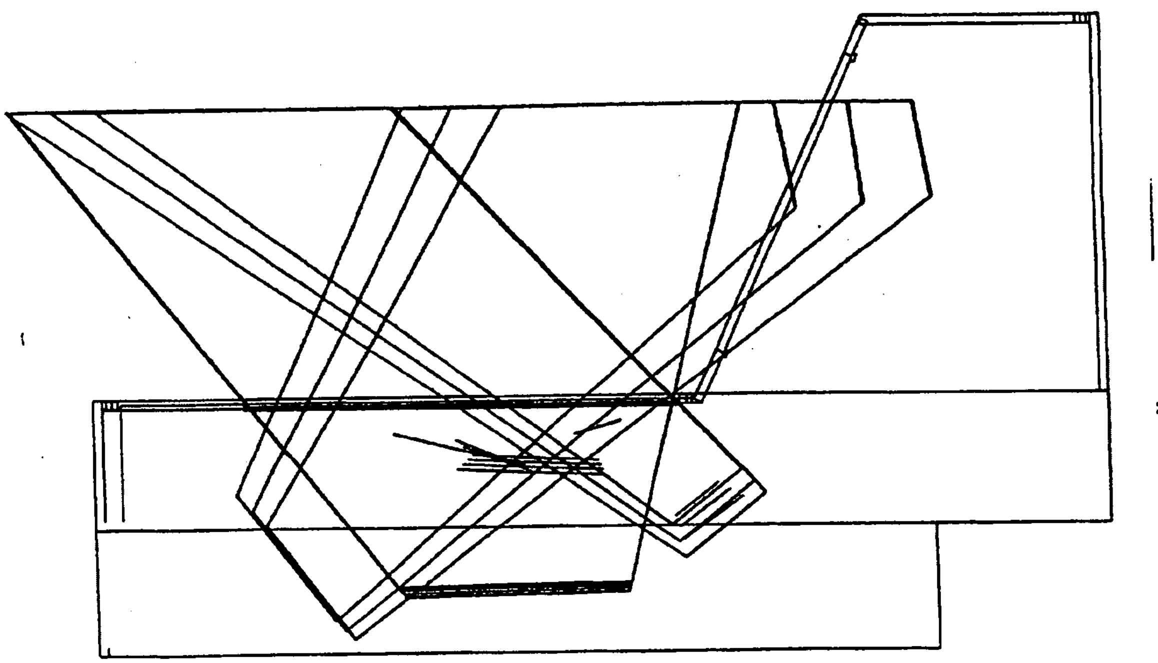

FIG. 5H4

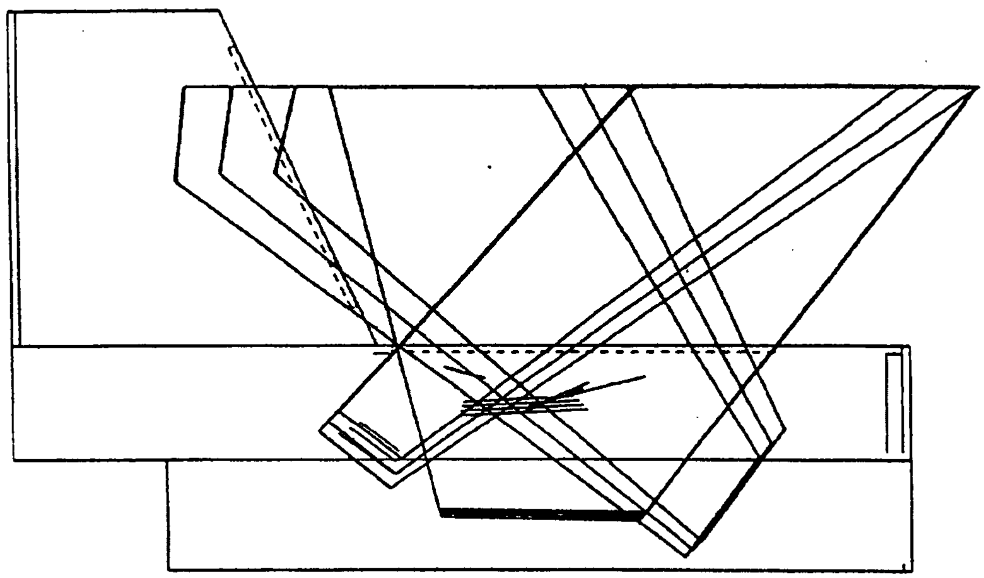

FIG. 5H5

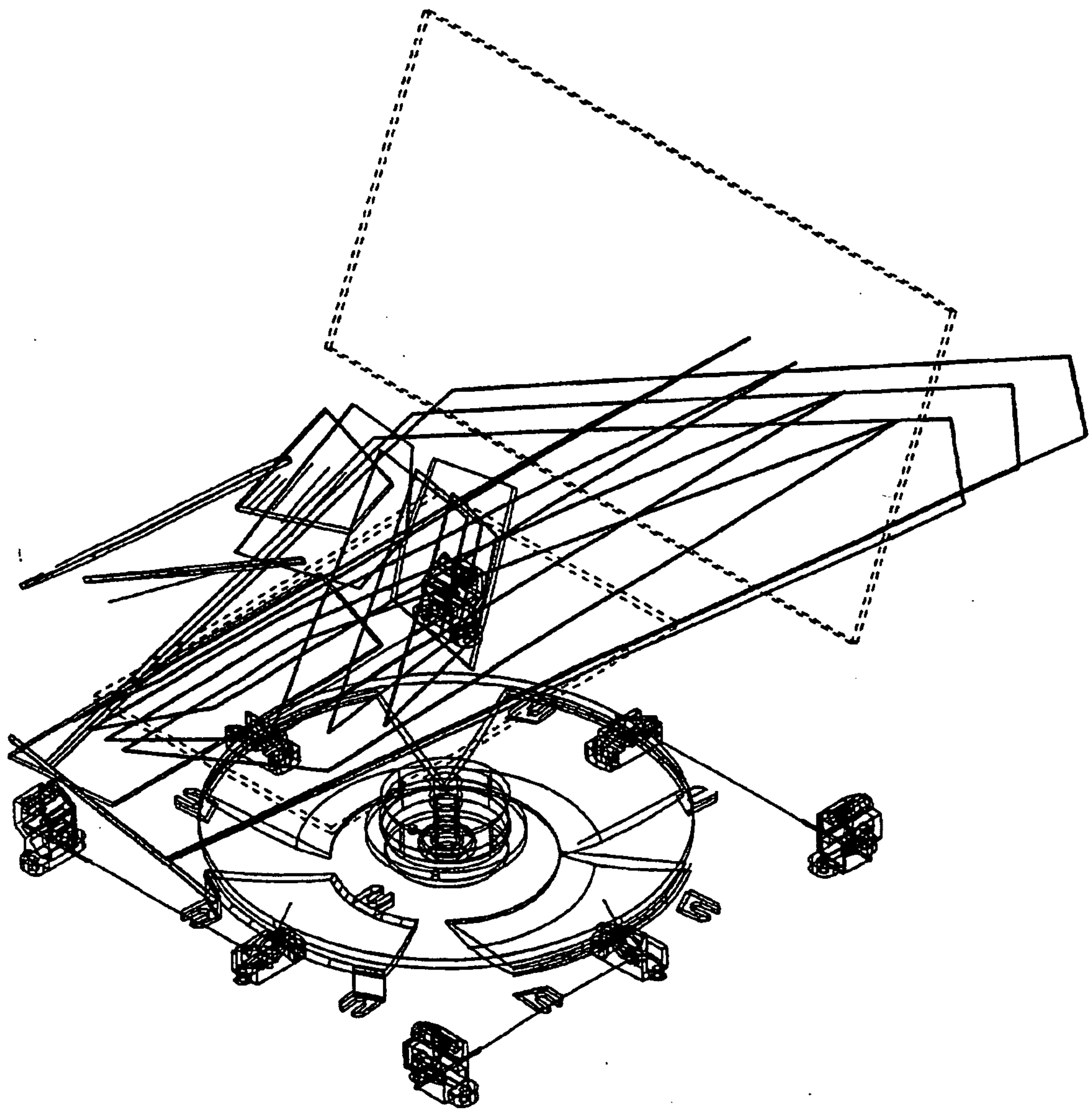

FIG. 5H6

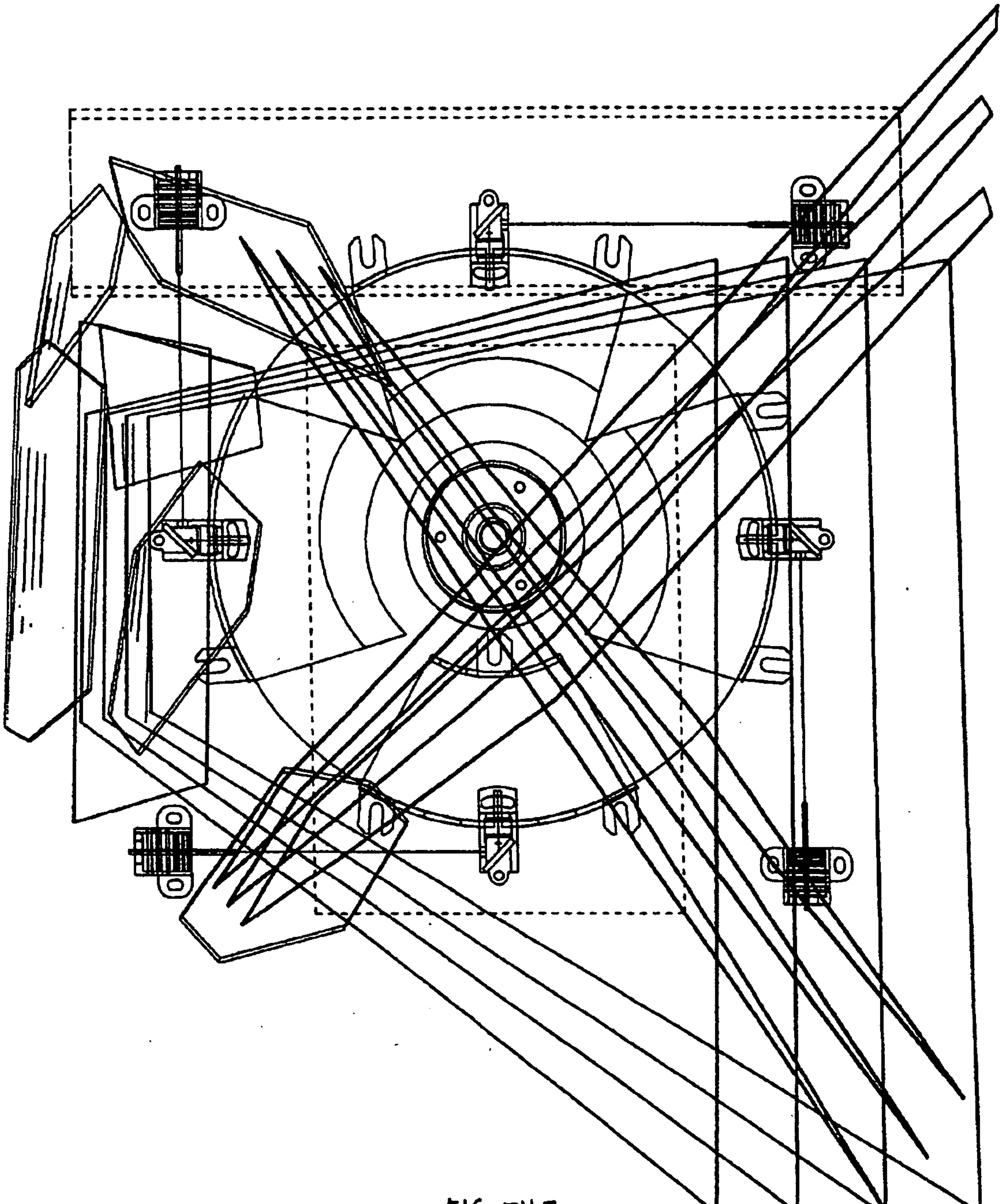

FIG. 5H7

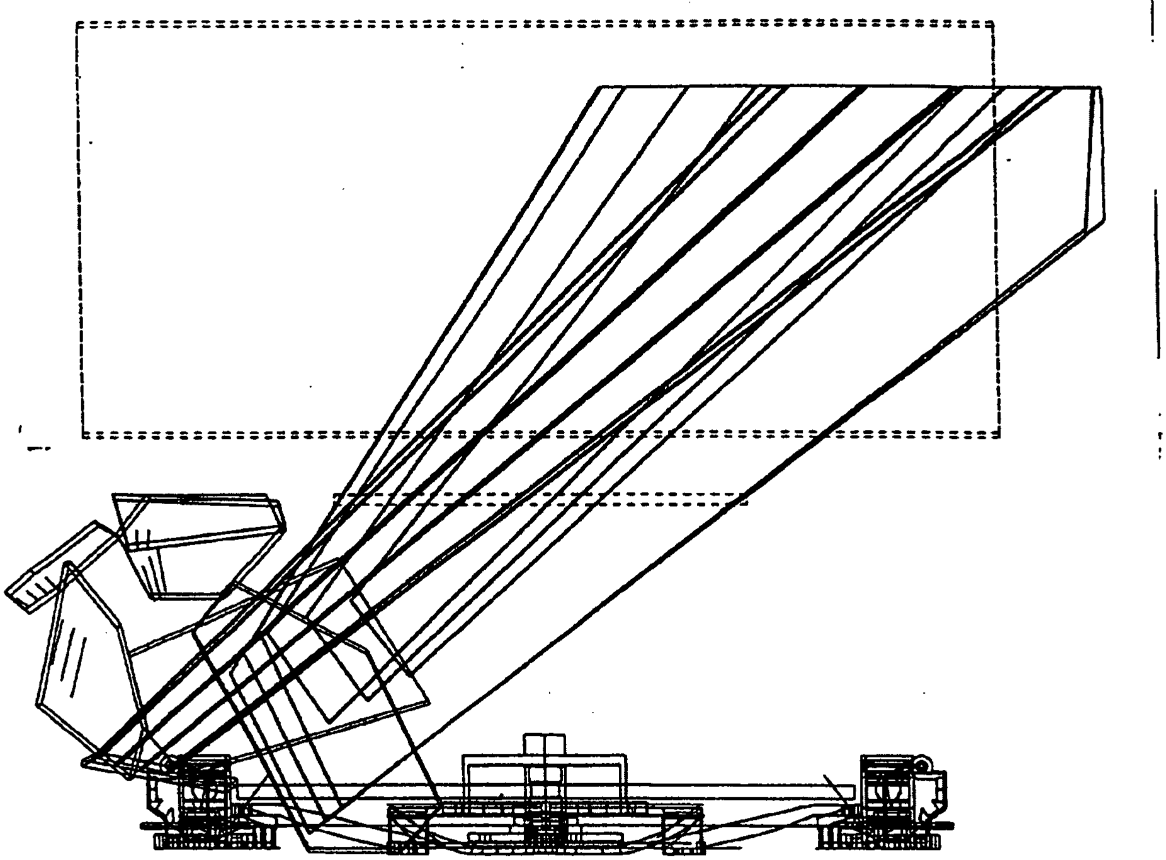

FIG. 5H8

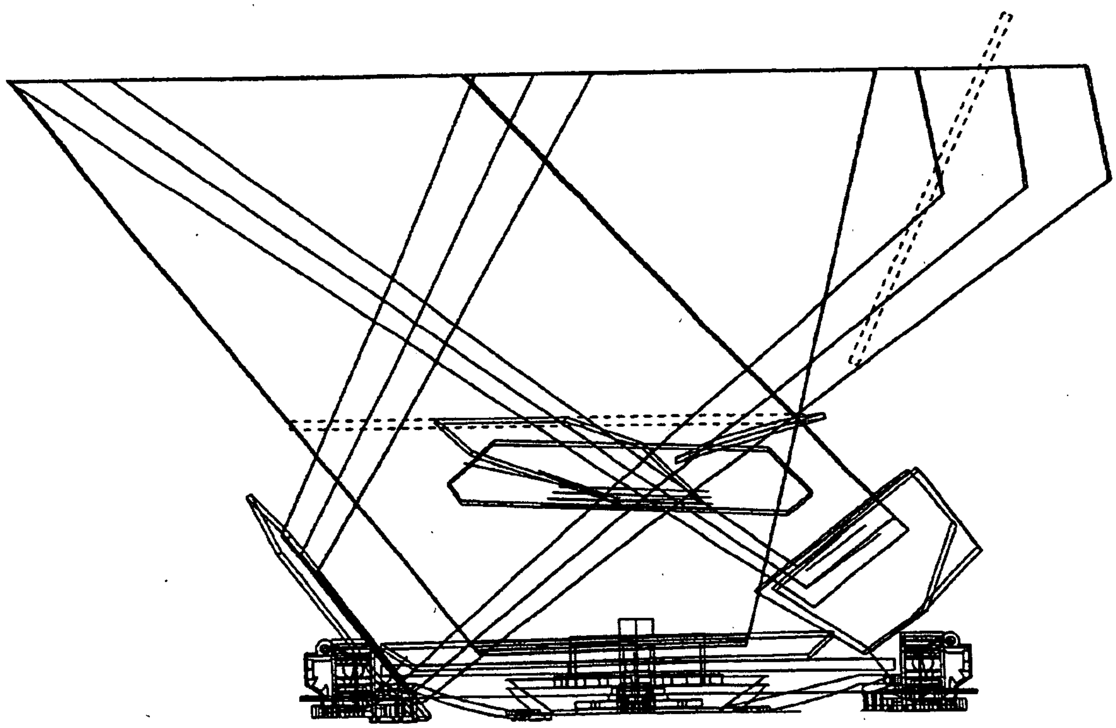

FIG. 5H9

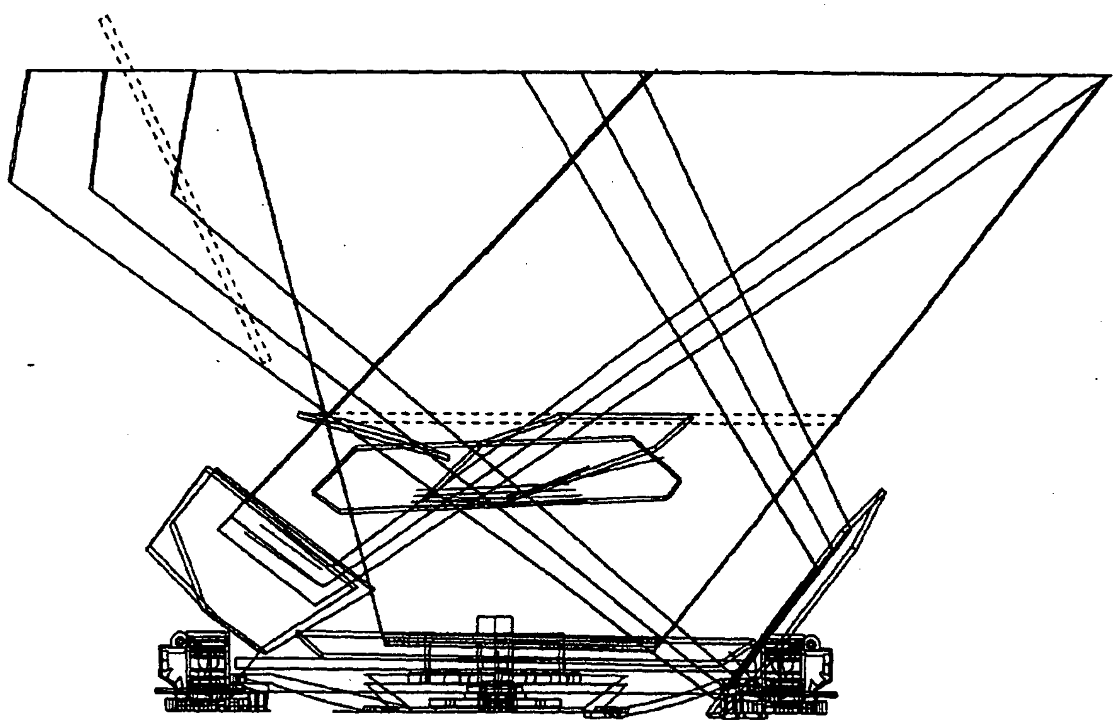

FIG. 5H10

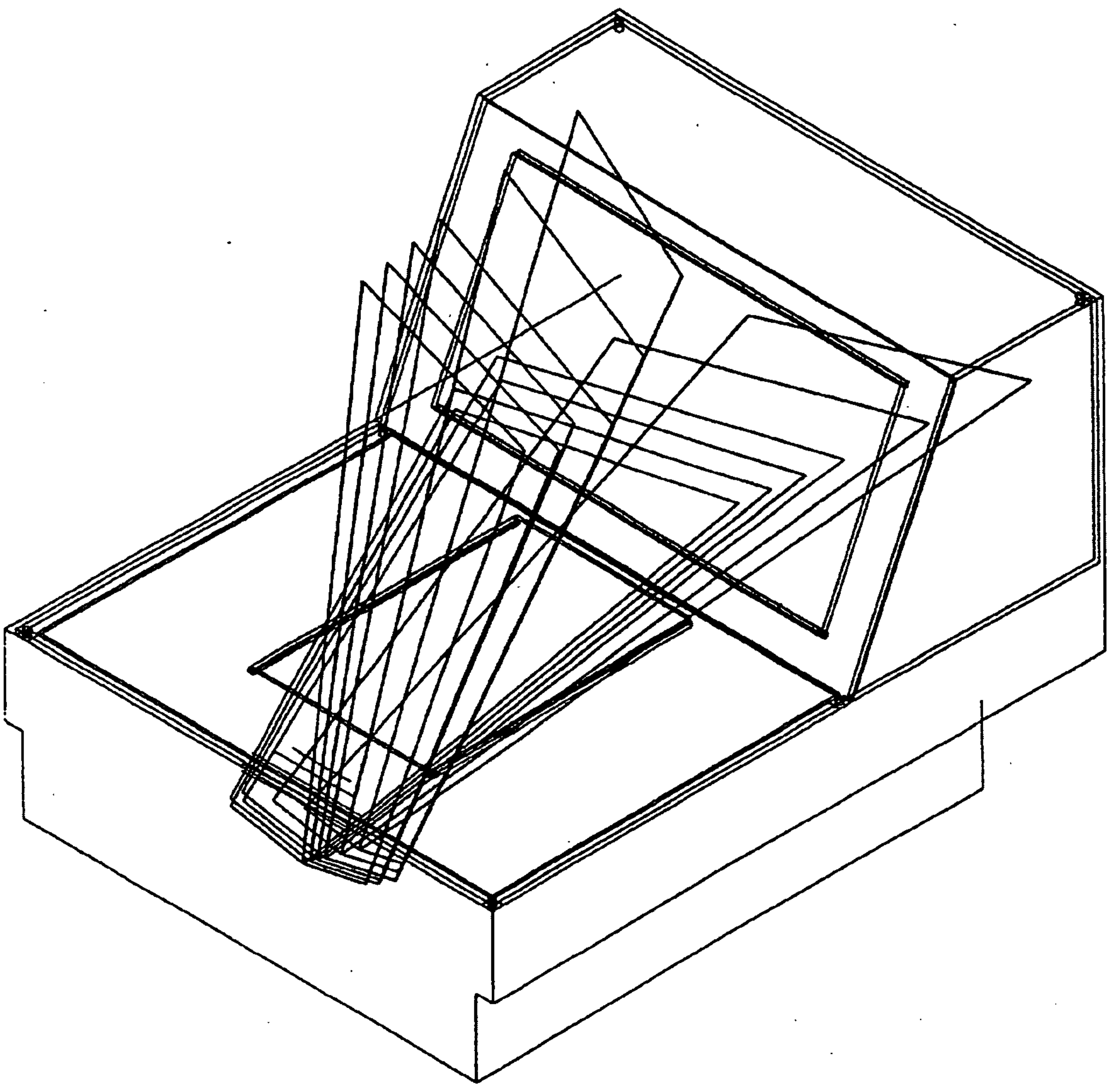

FIG. 5I1

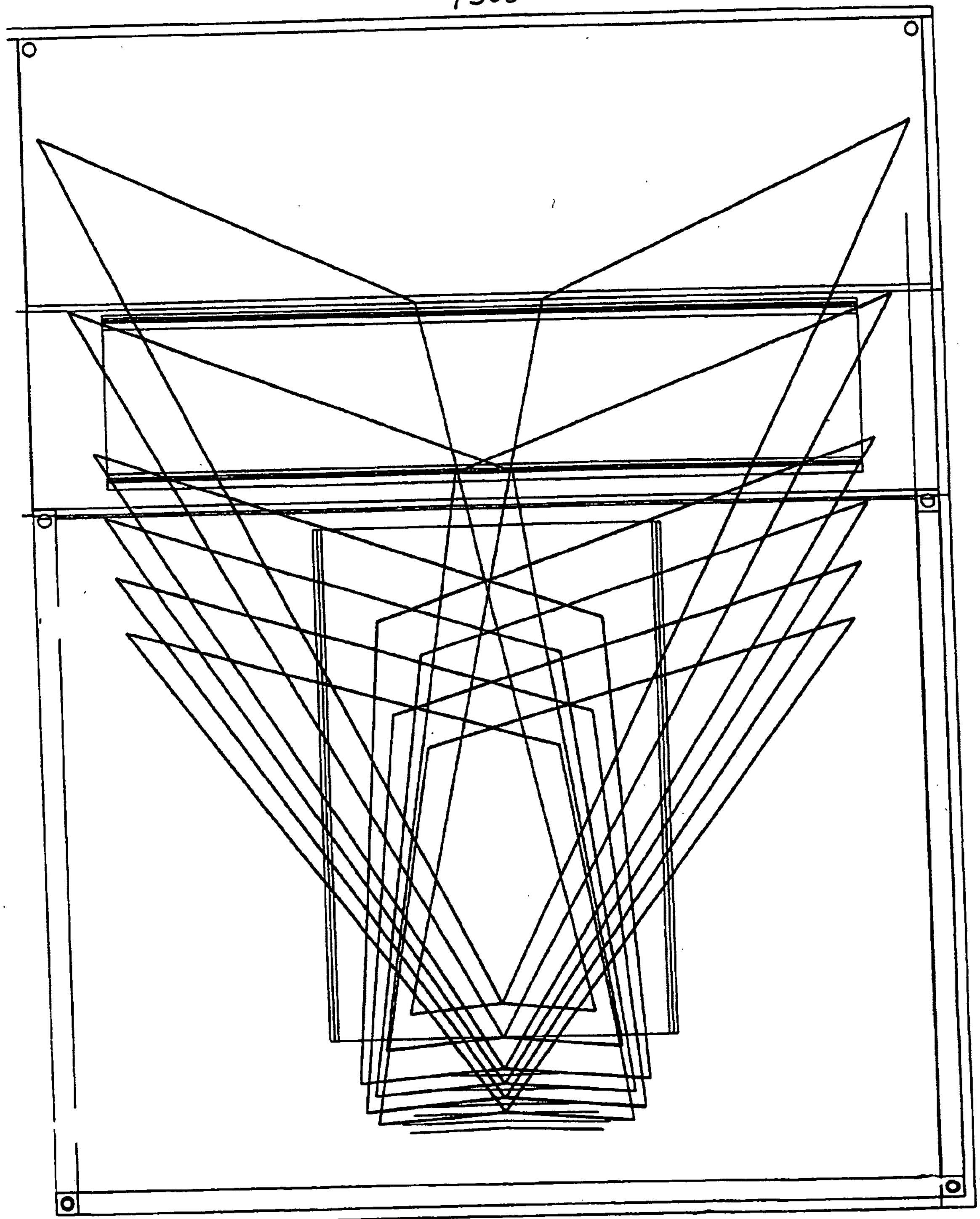

FIG. 512

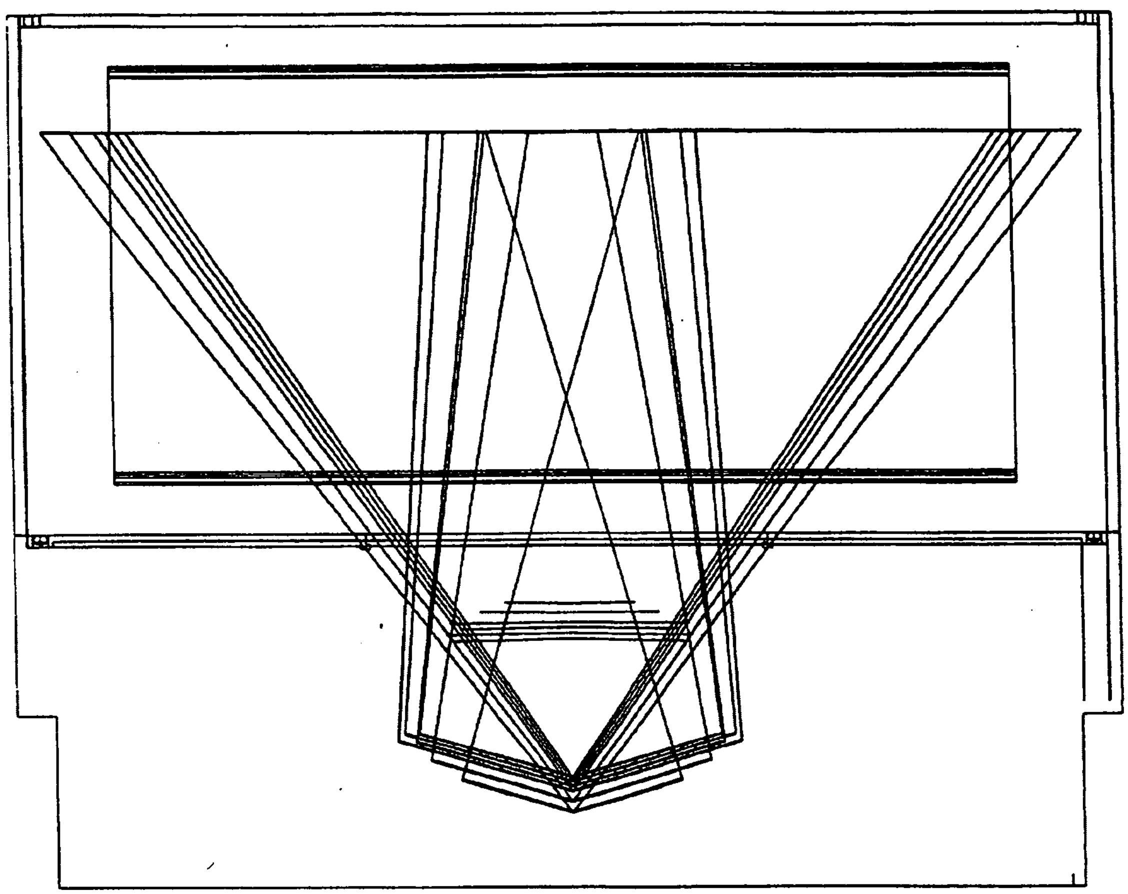

FIG. 5I3

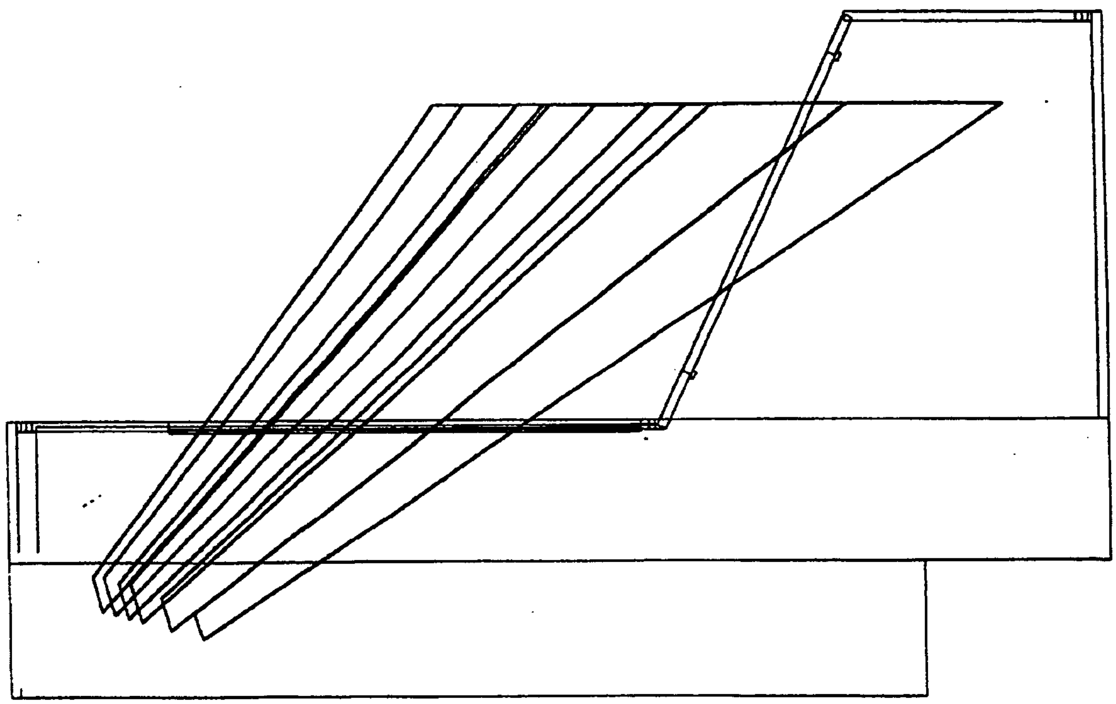

FIG. 5I4

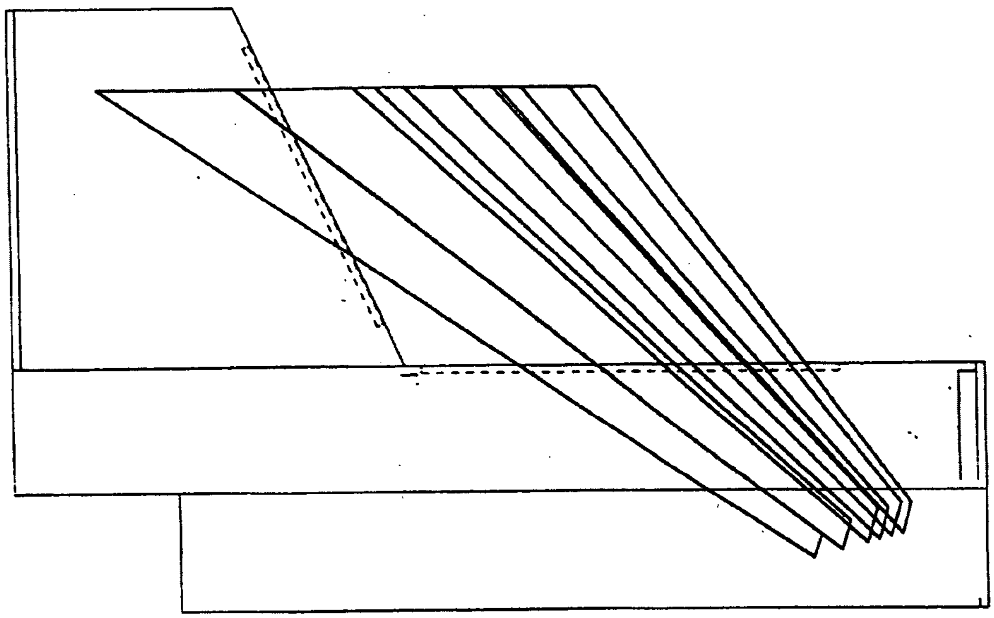

FIG. 5I5

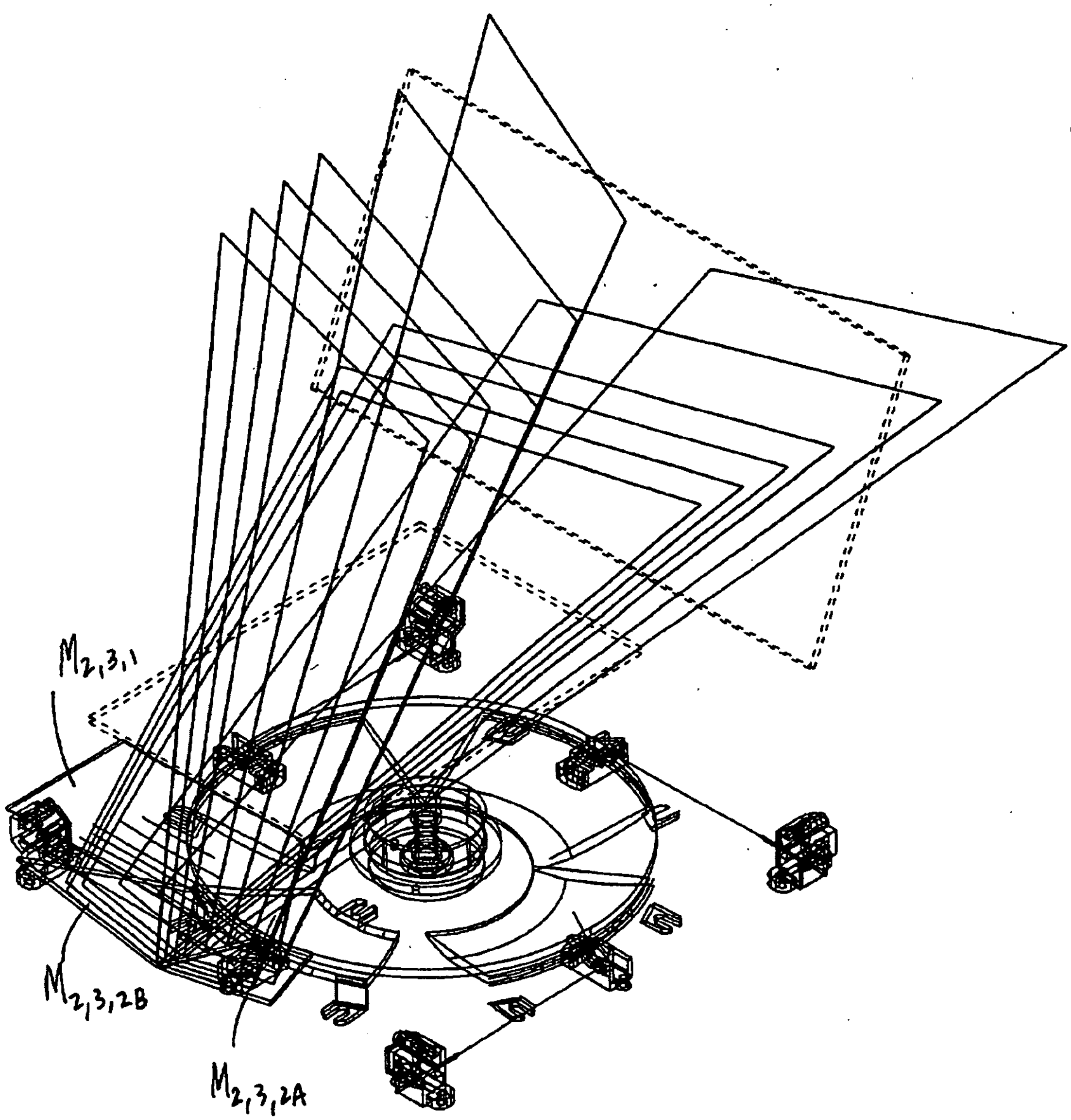

FIG 5J1

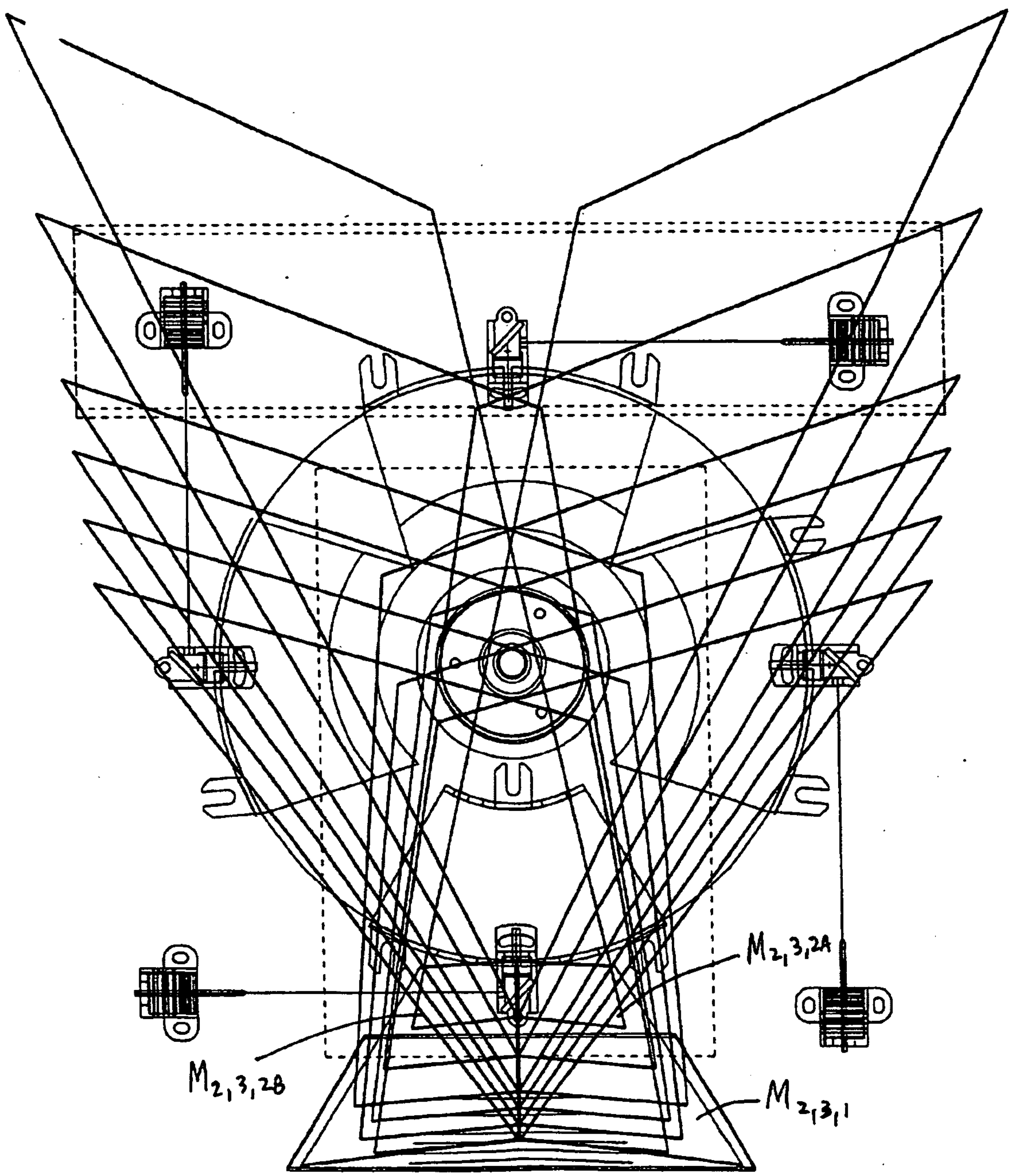

FIG. 5J2

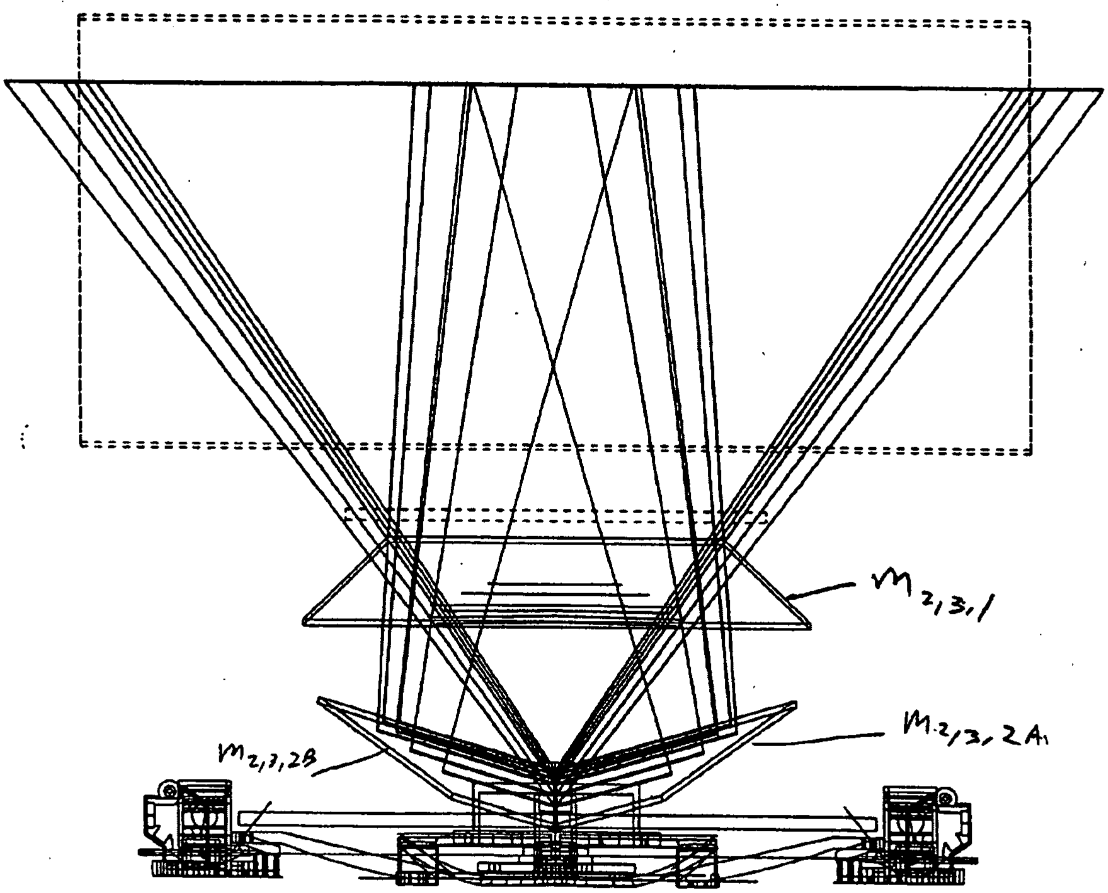

FIG 5J3

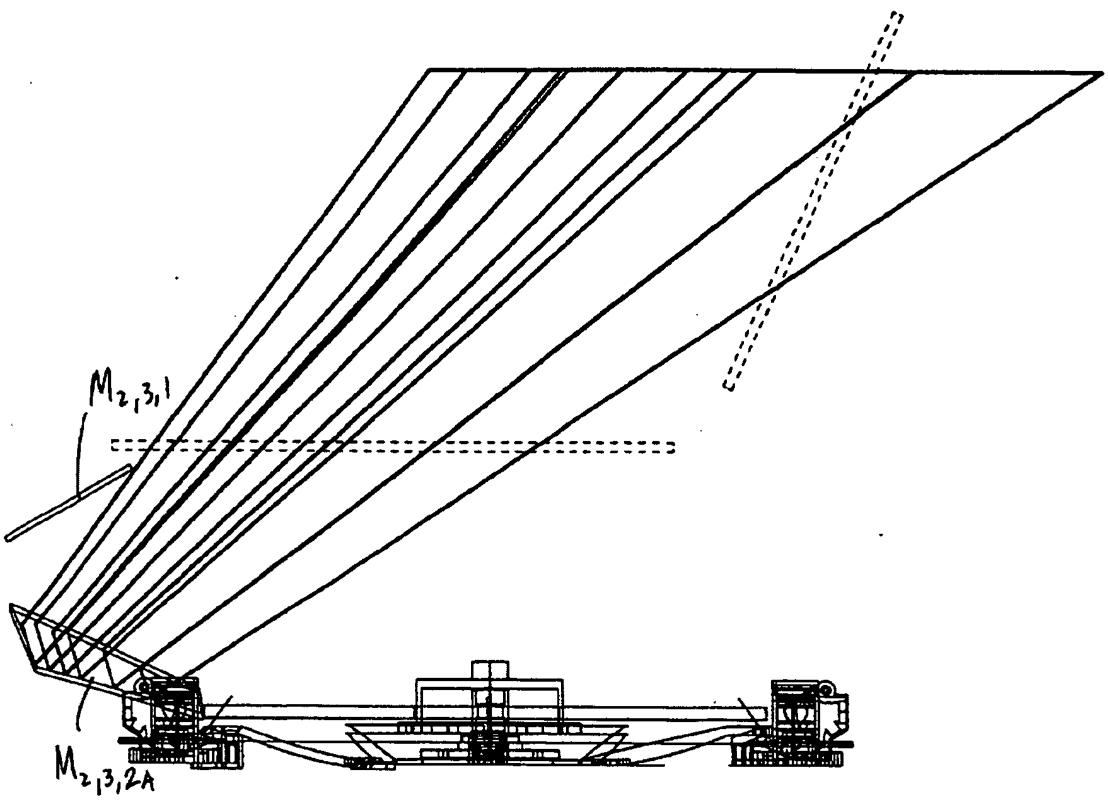

FIG. 5J4

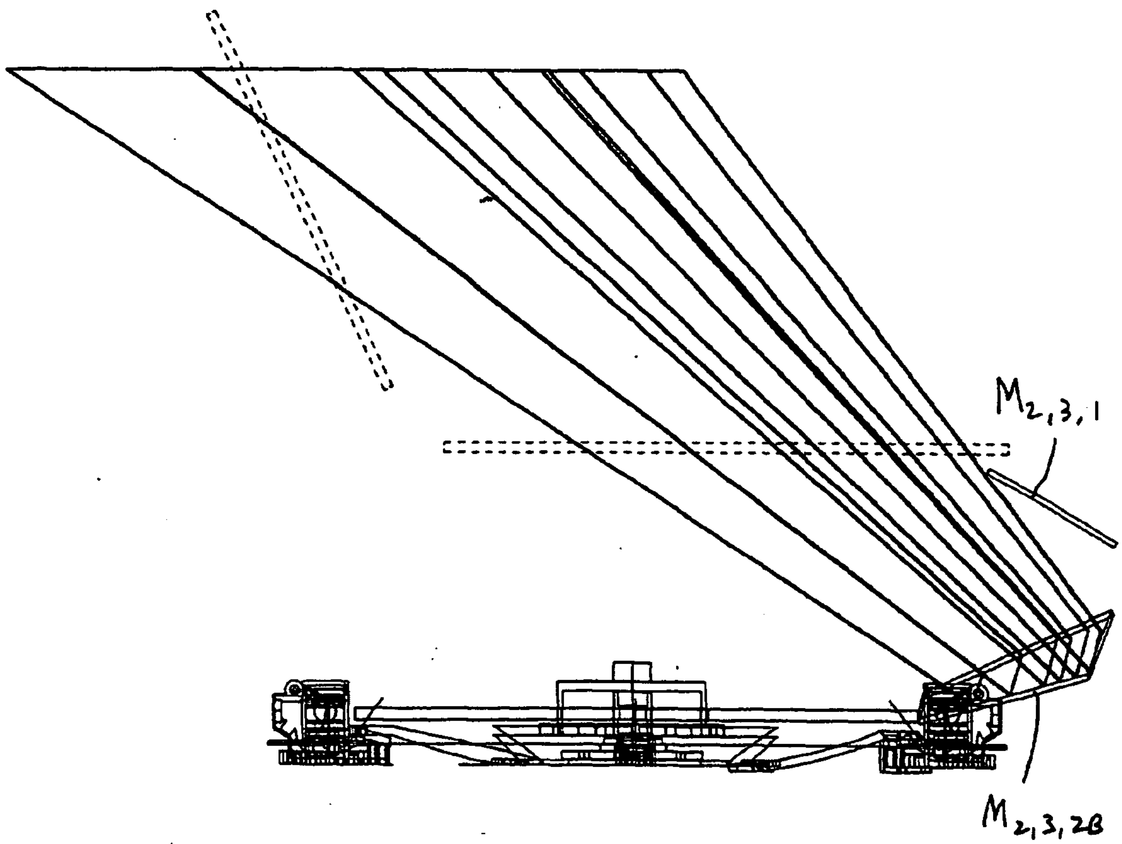

FIG. 5J5

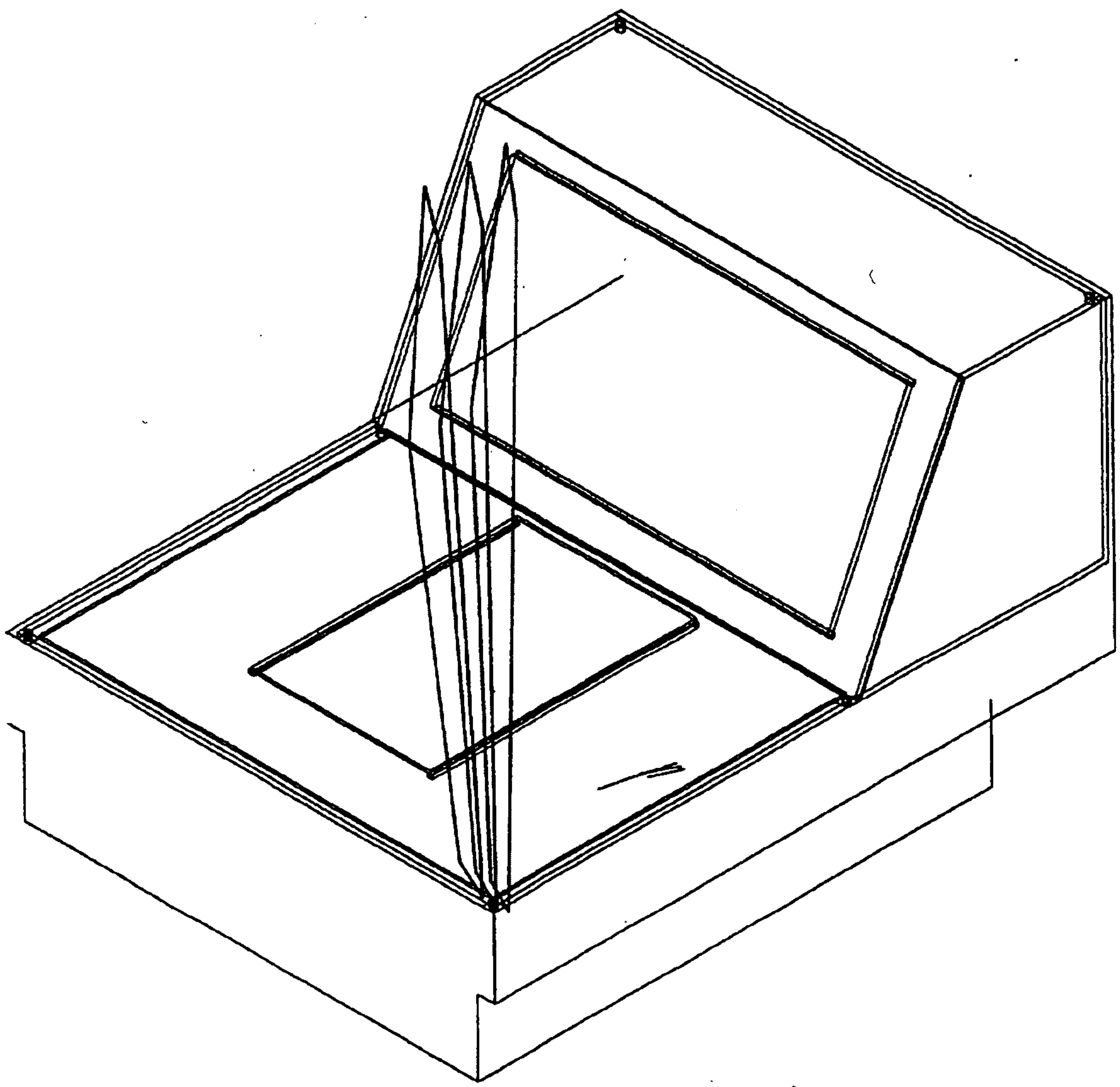

FIG. 5K1

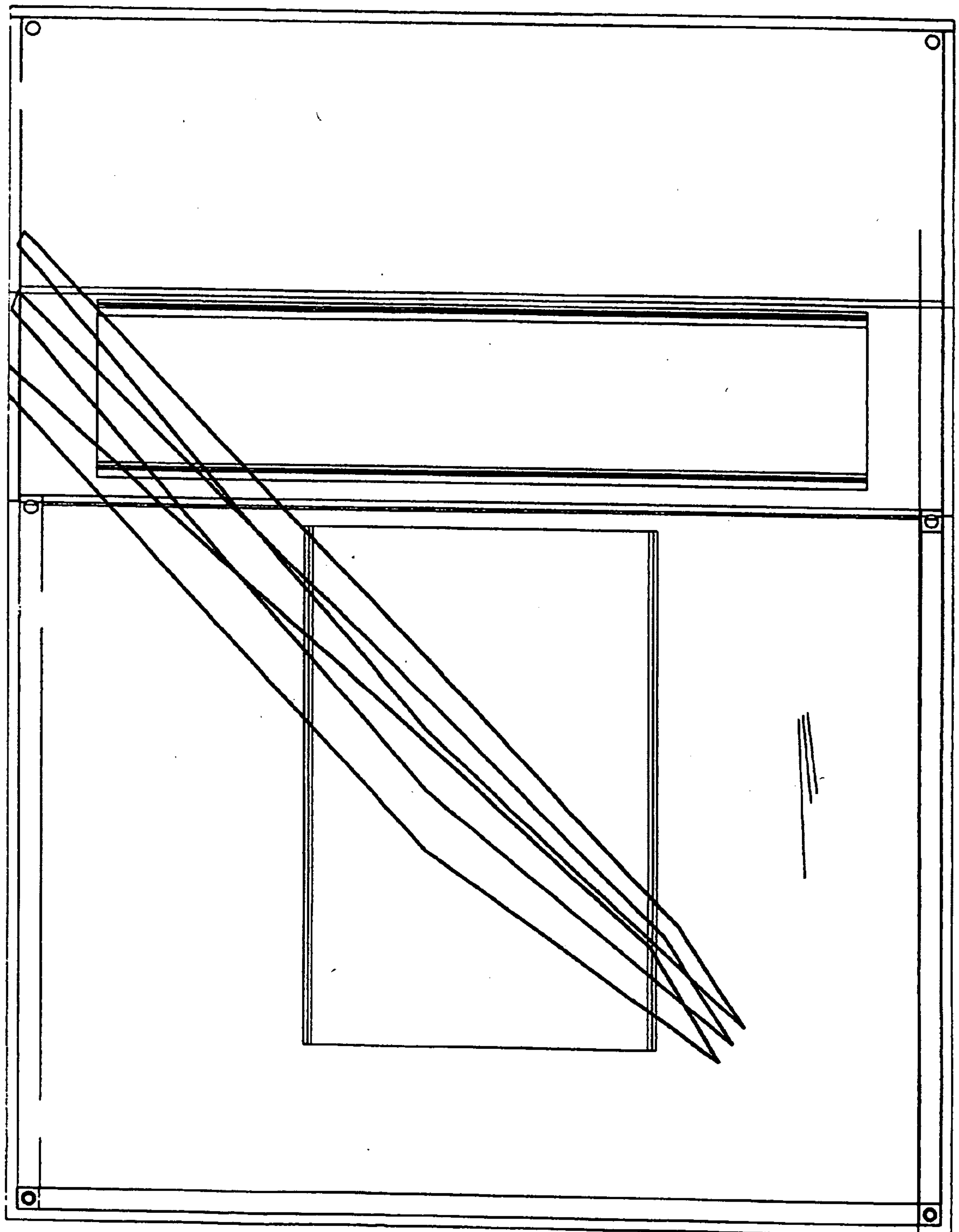

FIG. 5K2

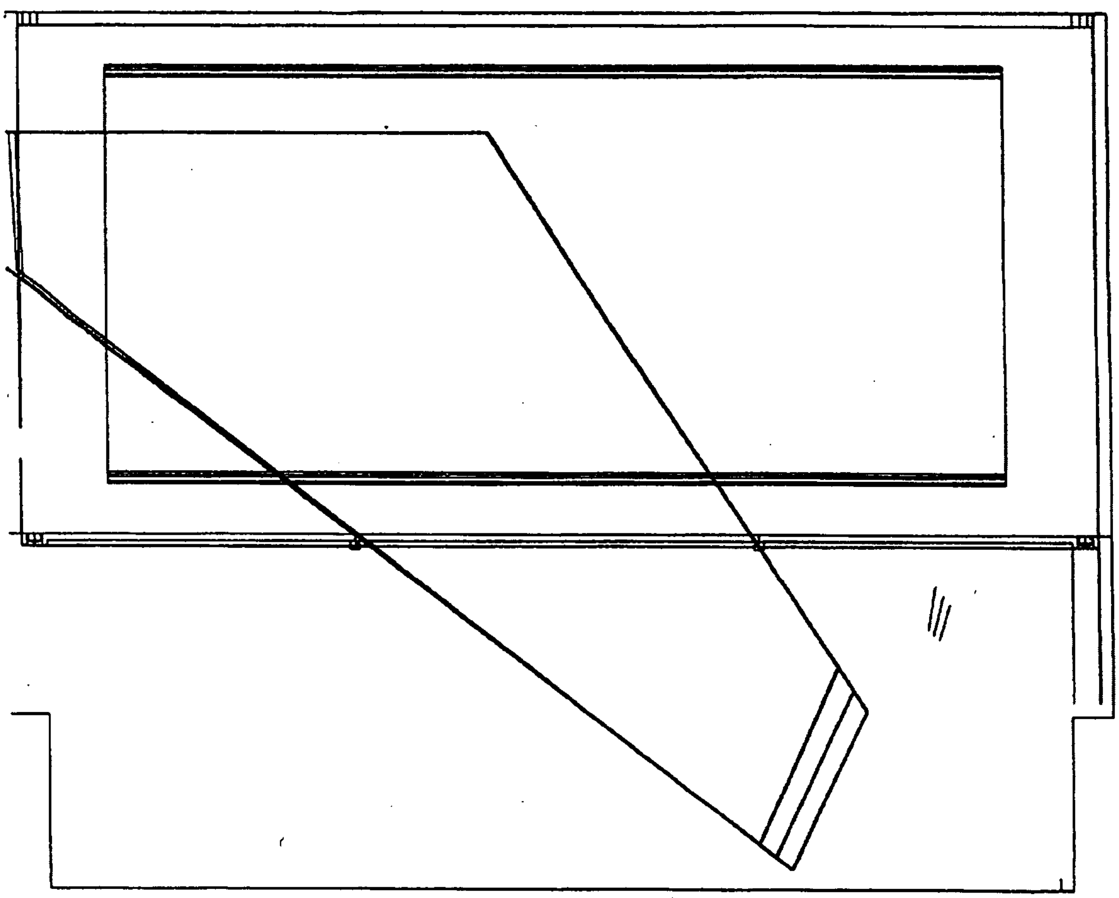

FIG 5K3

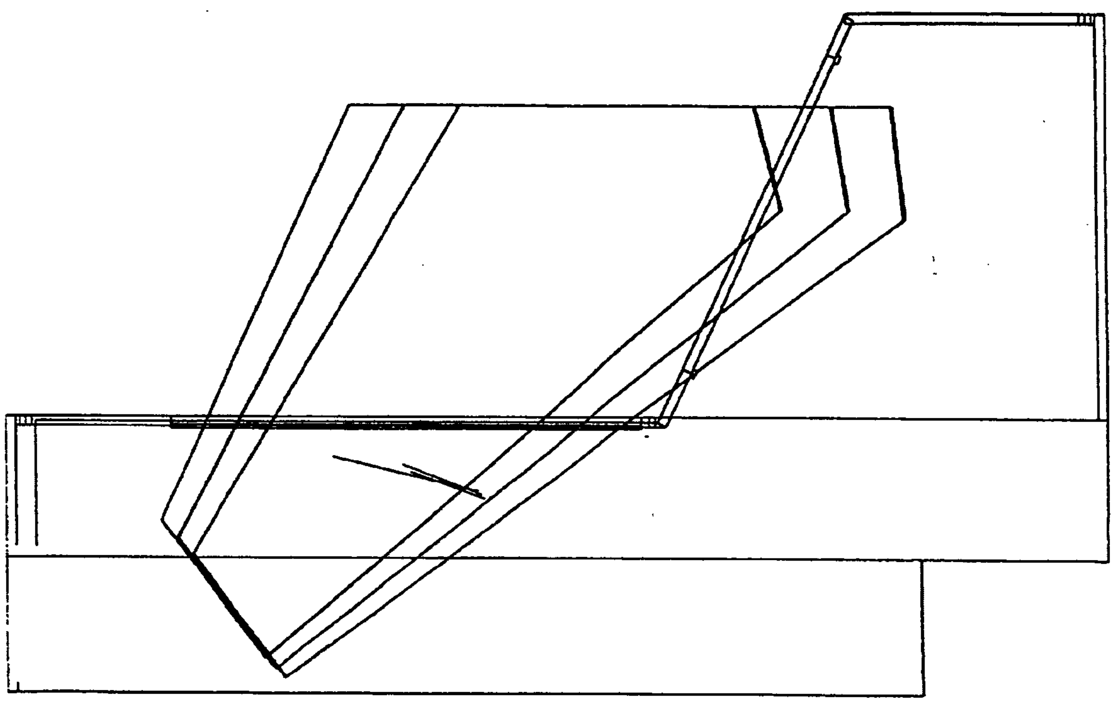

FIG. 5K4

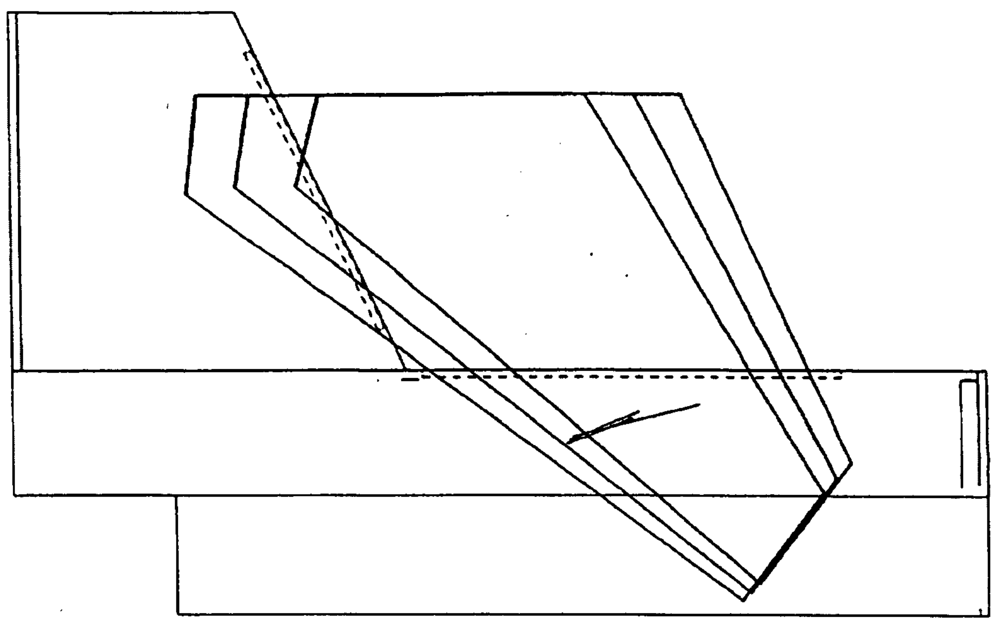

FIG. 5K5

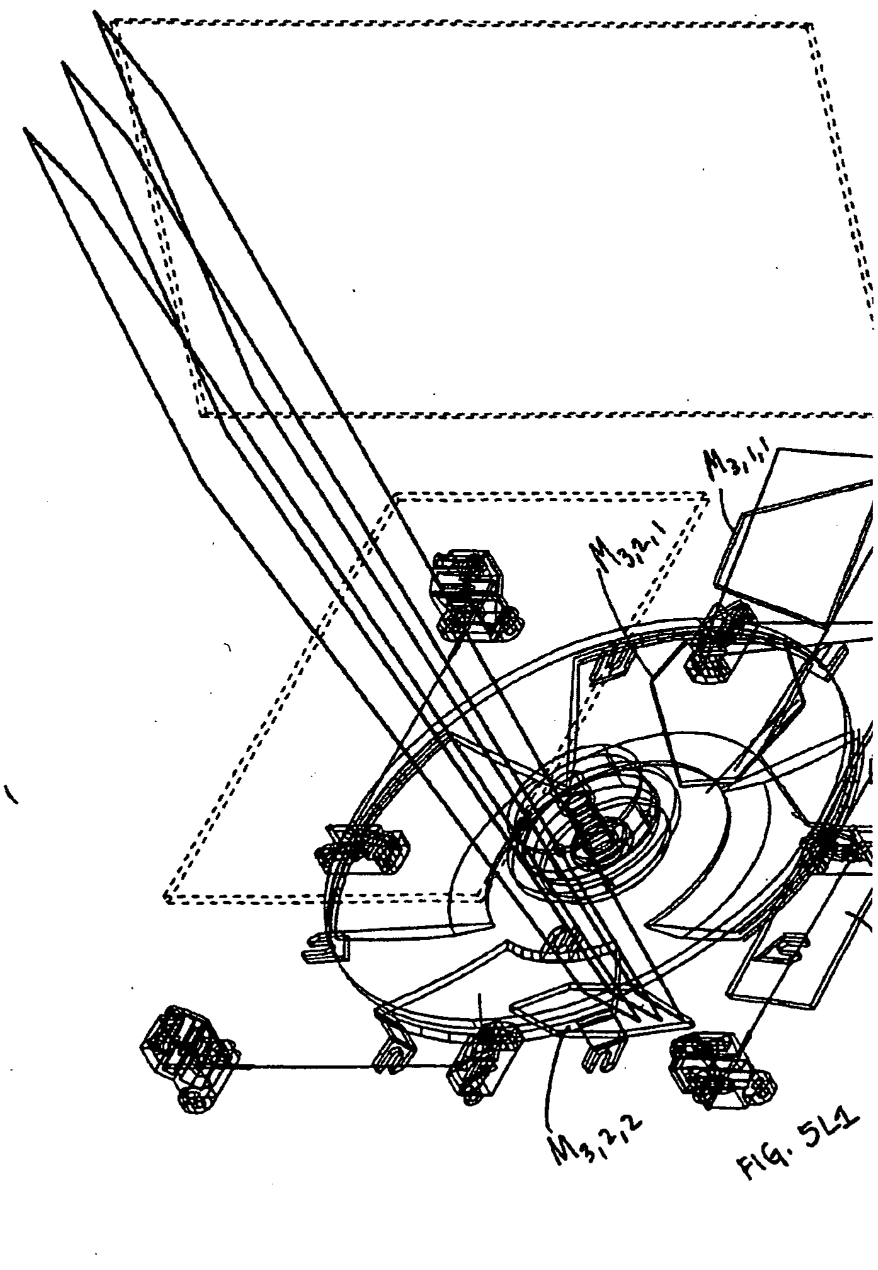

FIG. 5L1

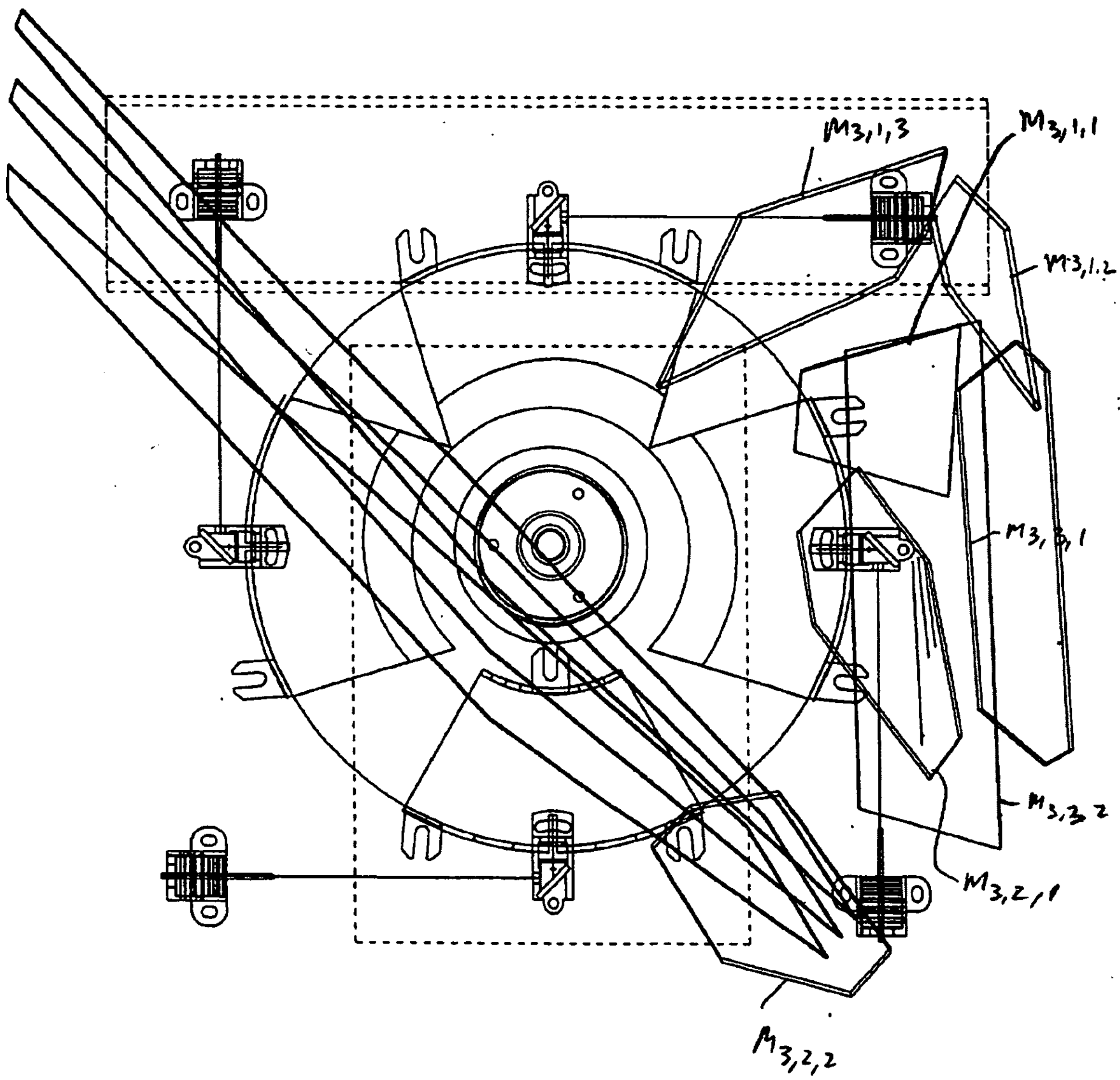

FIG. 5L2

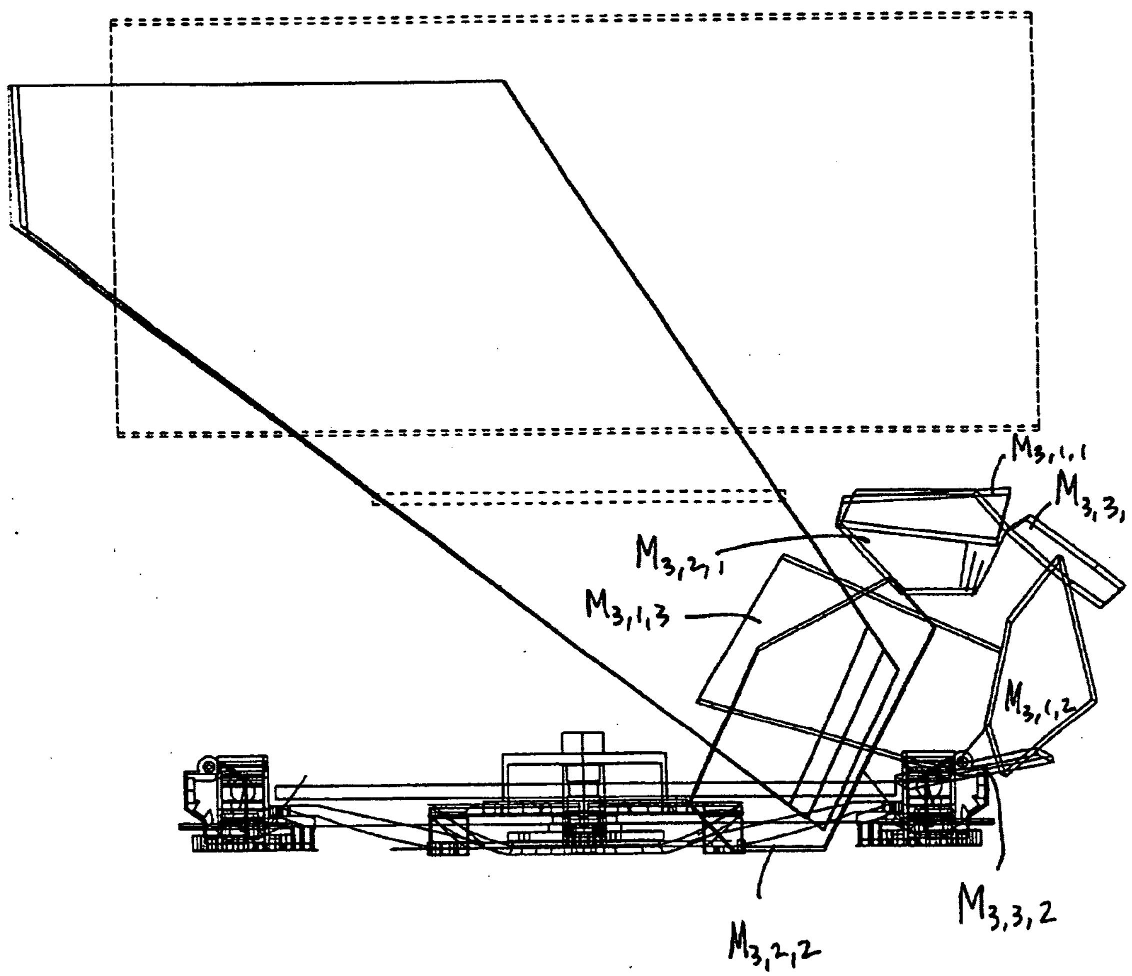

FIG. 5L3

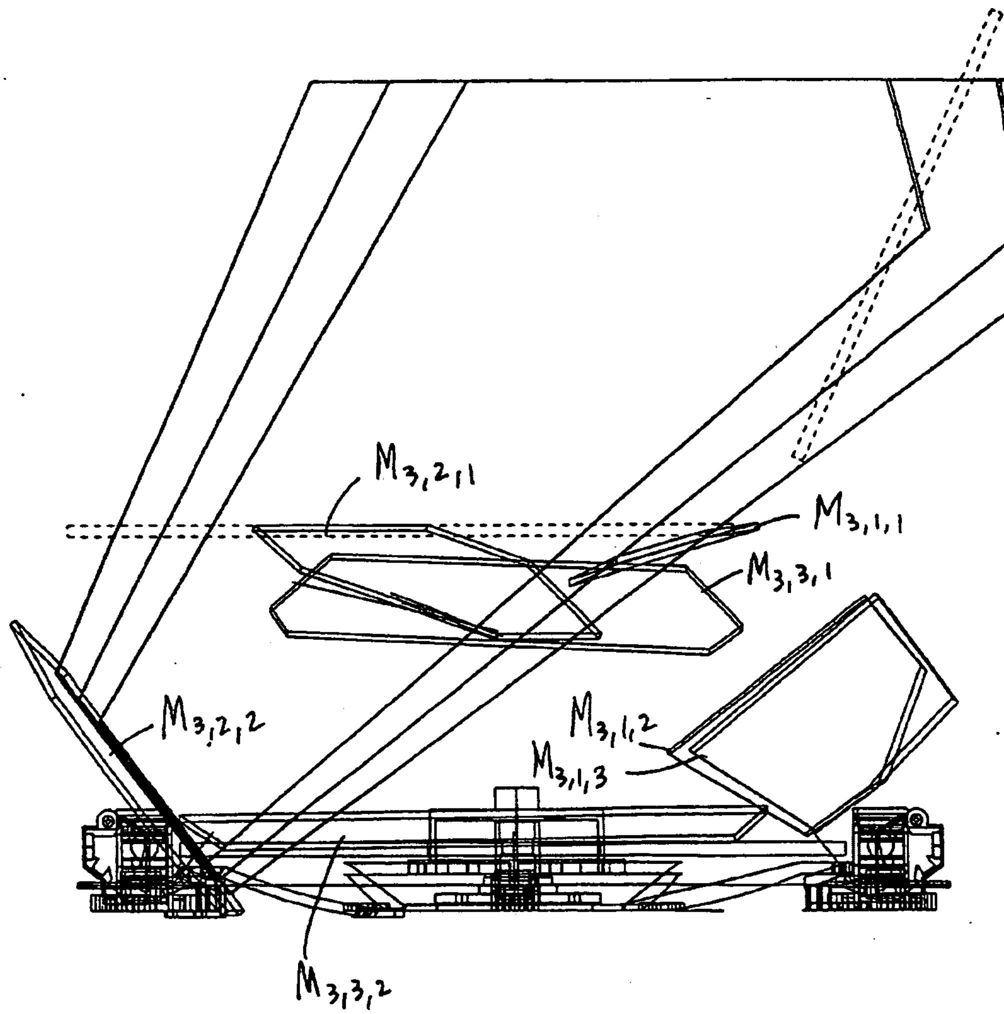

FIG, 5L4

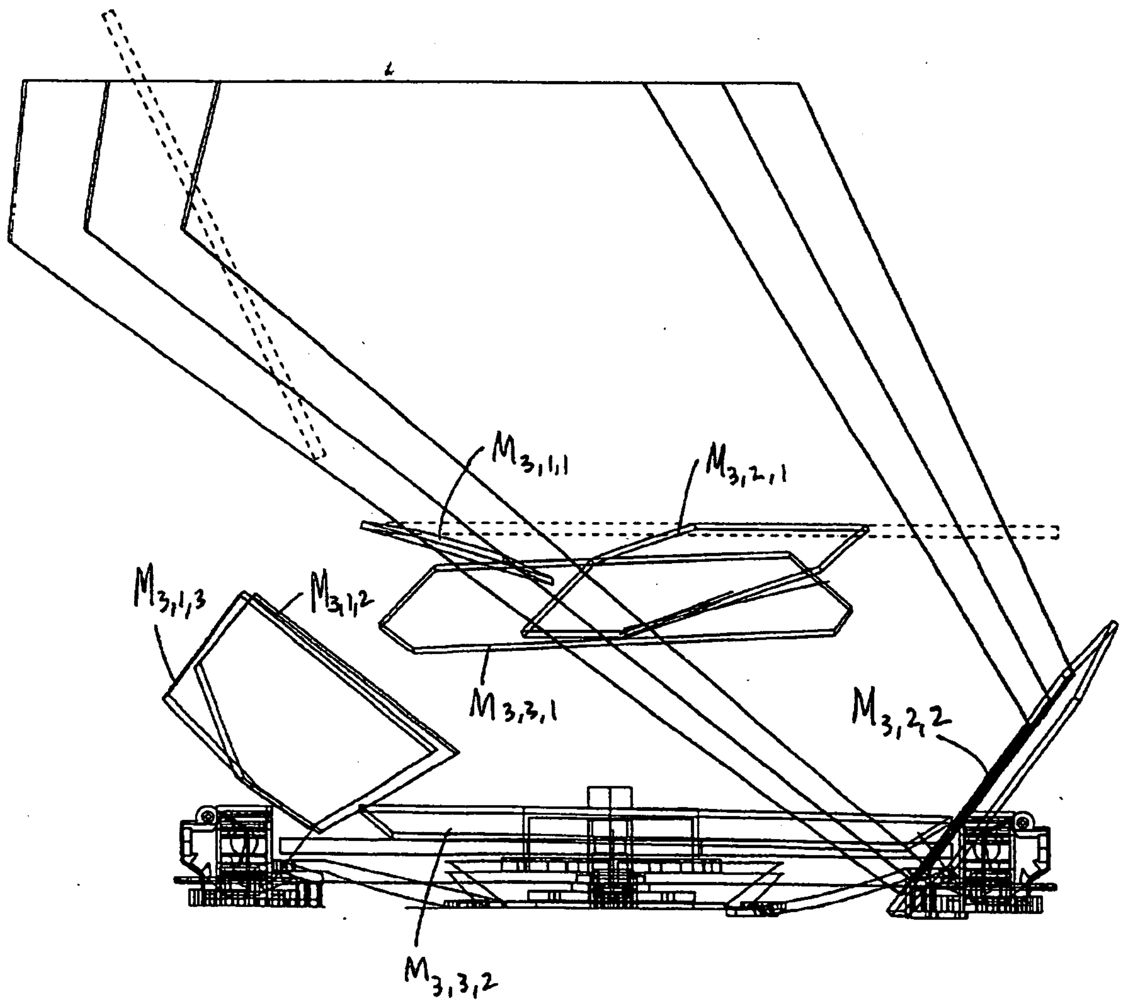

FIG. 5L5

125/335

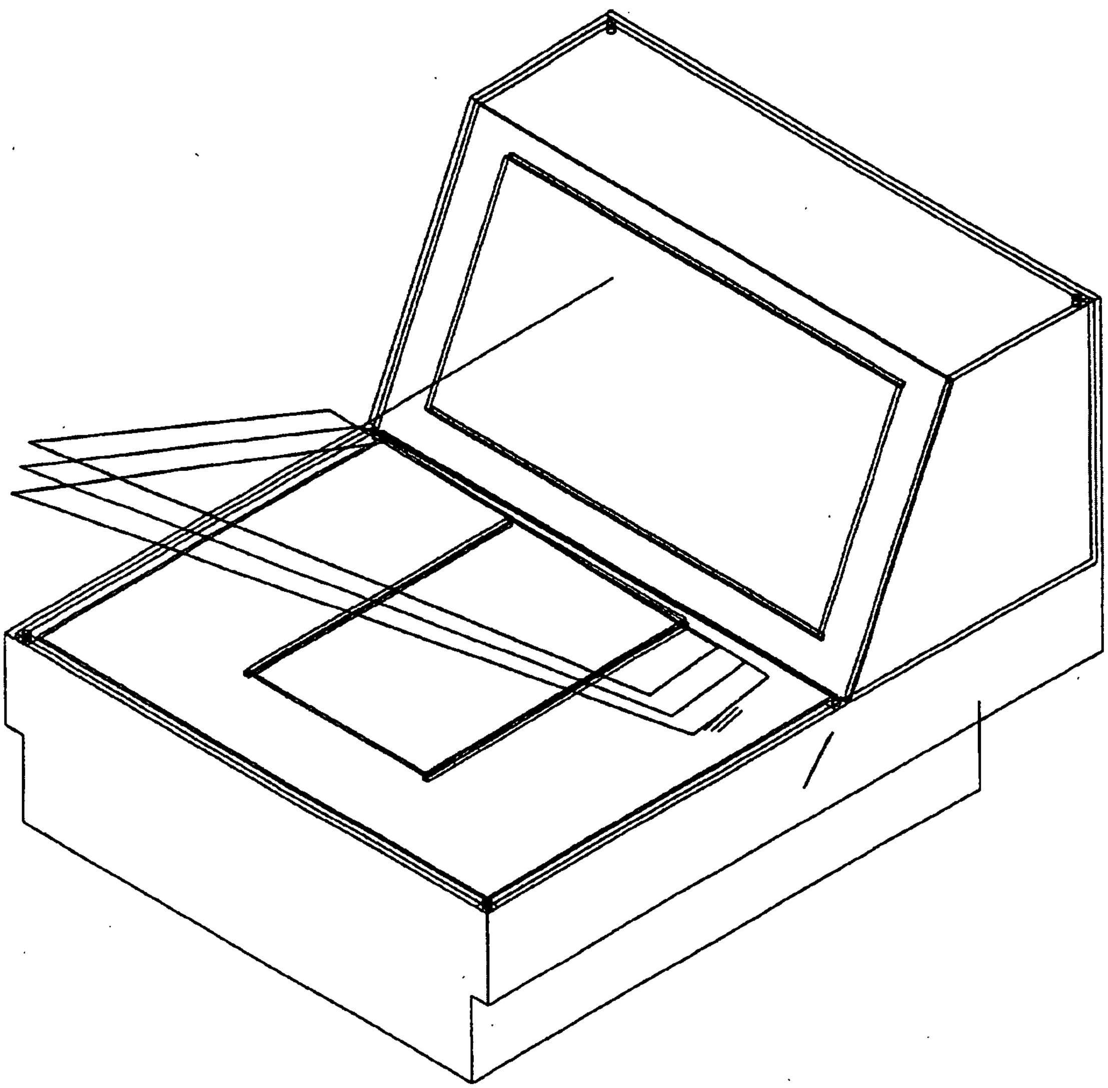

FIG. 5M1

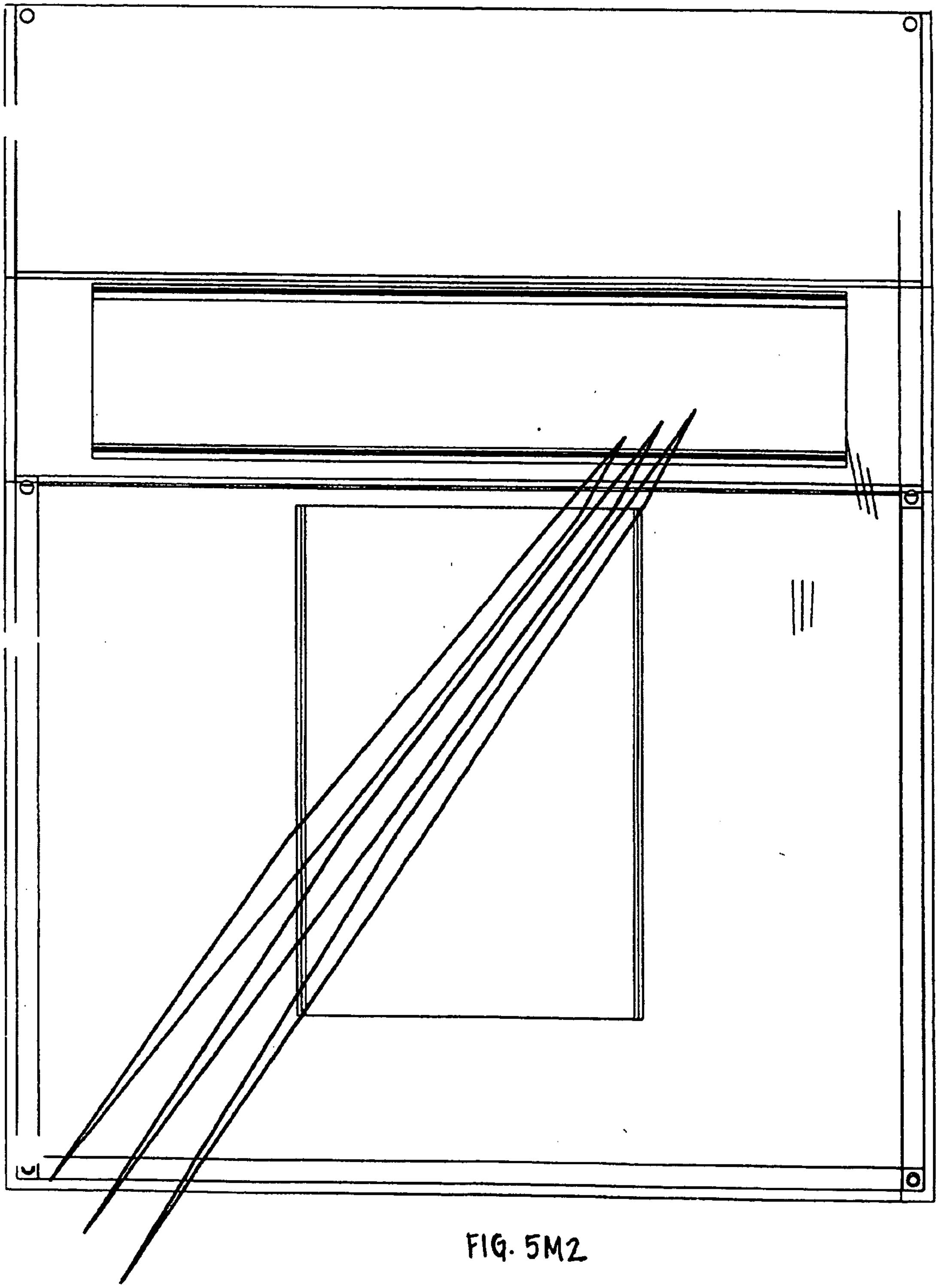

FIG. 5M2

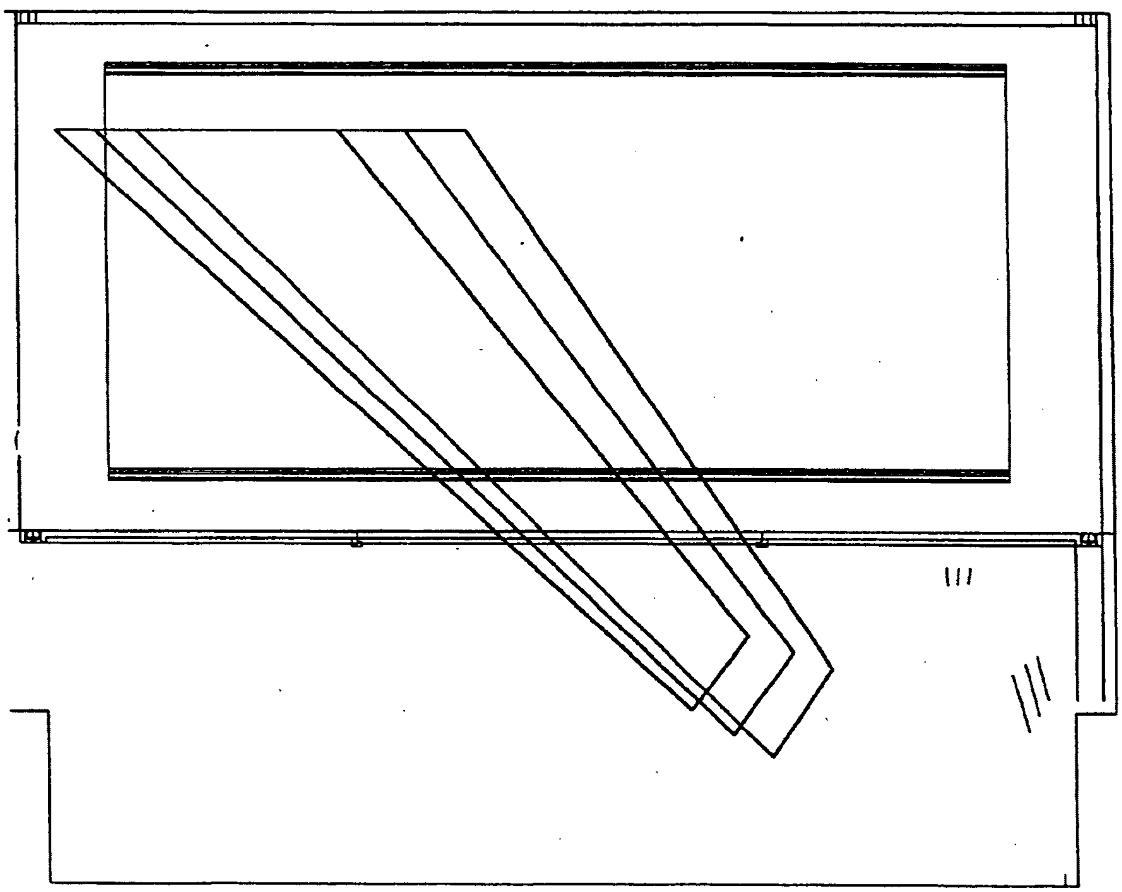

FIG. 5M3

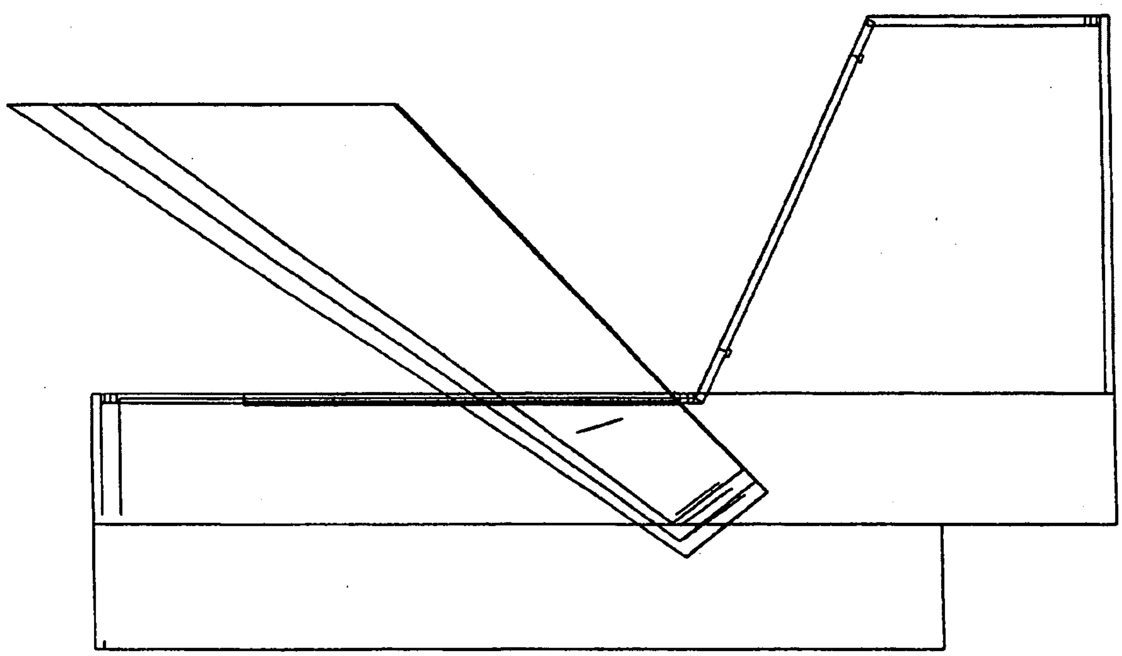

FIG. 5M4

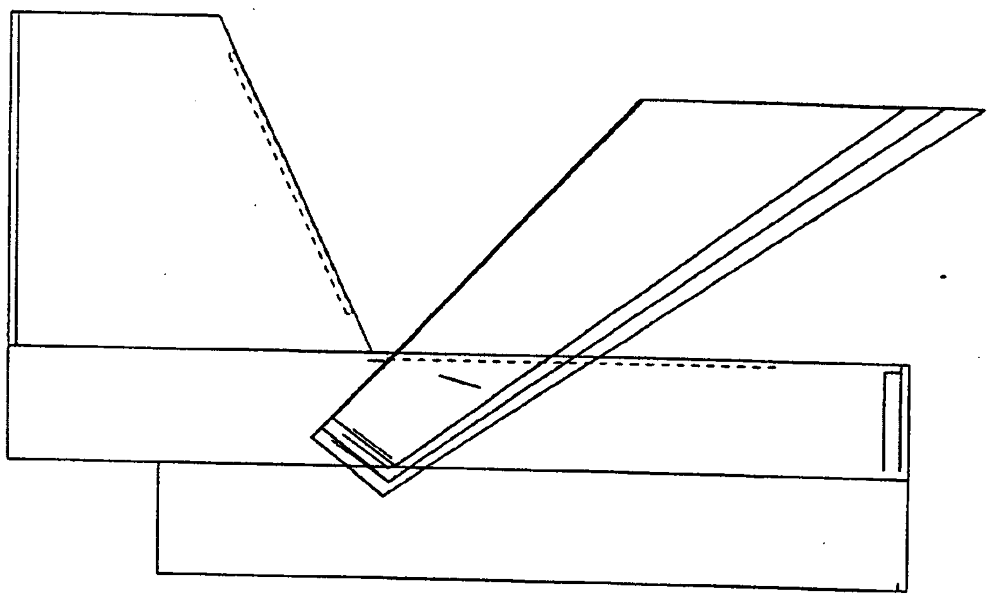

FIG. 5M5

130/335

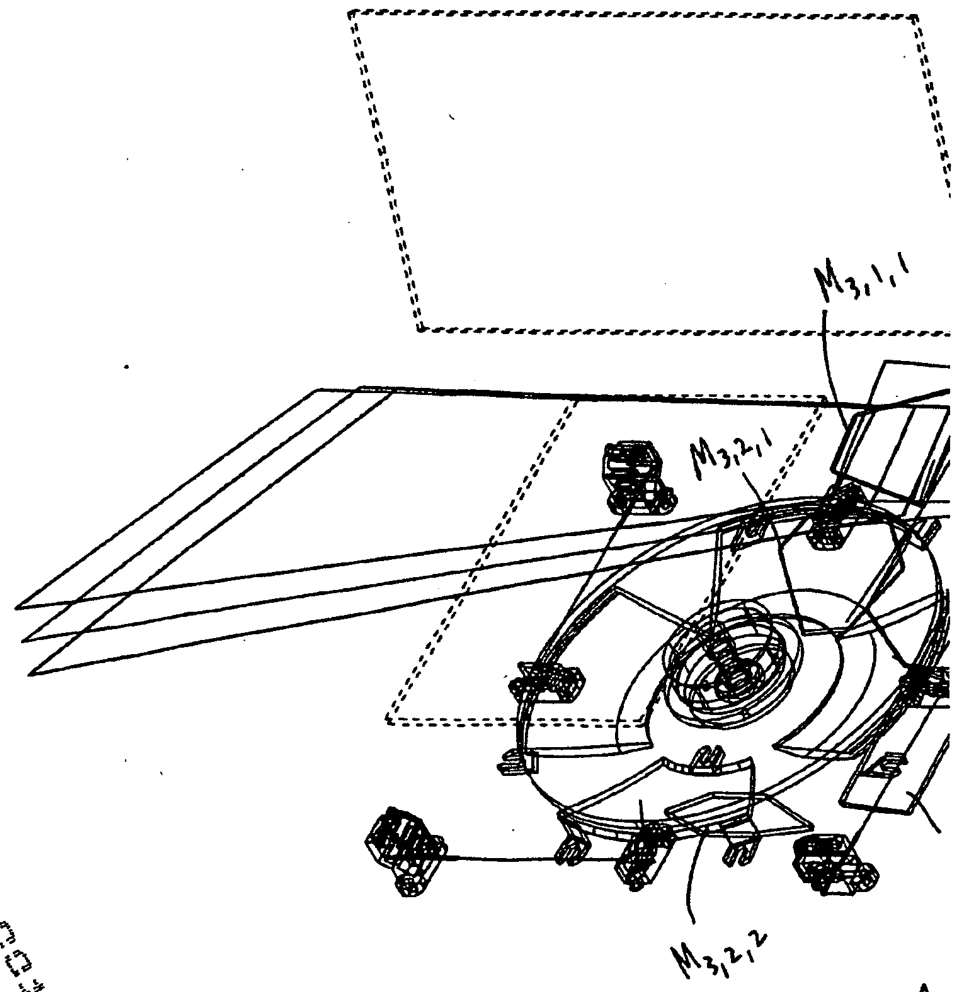

FIG. 5N1

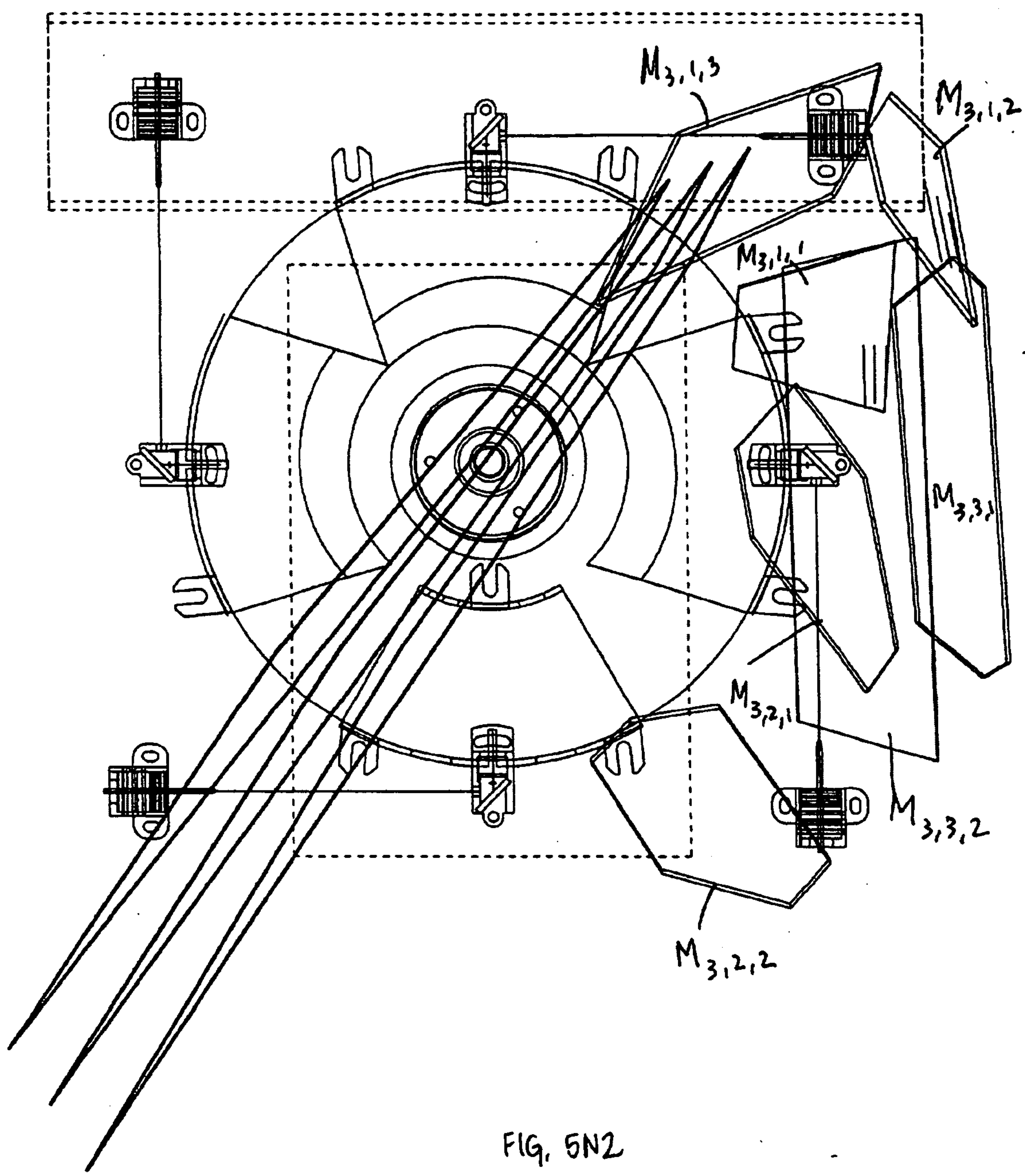

FIG. 5N2

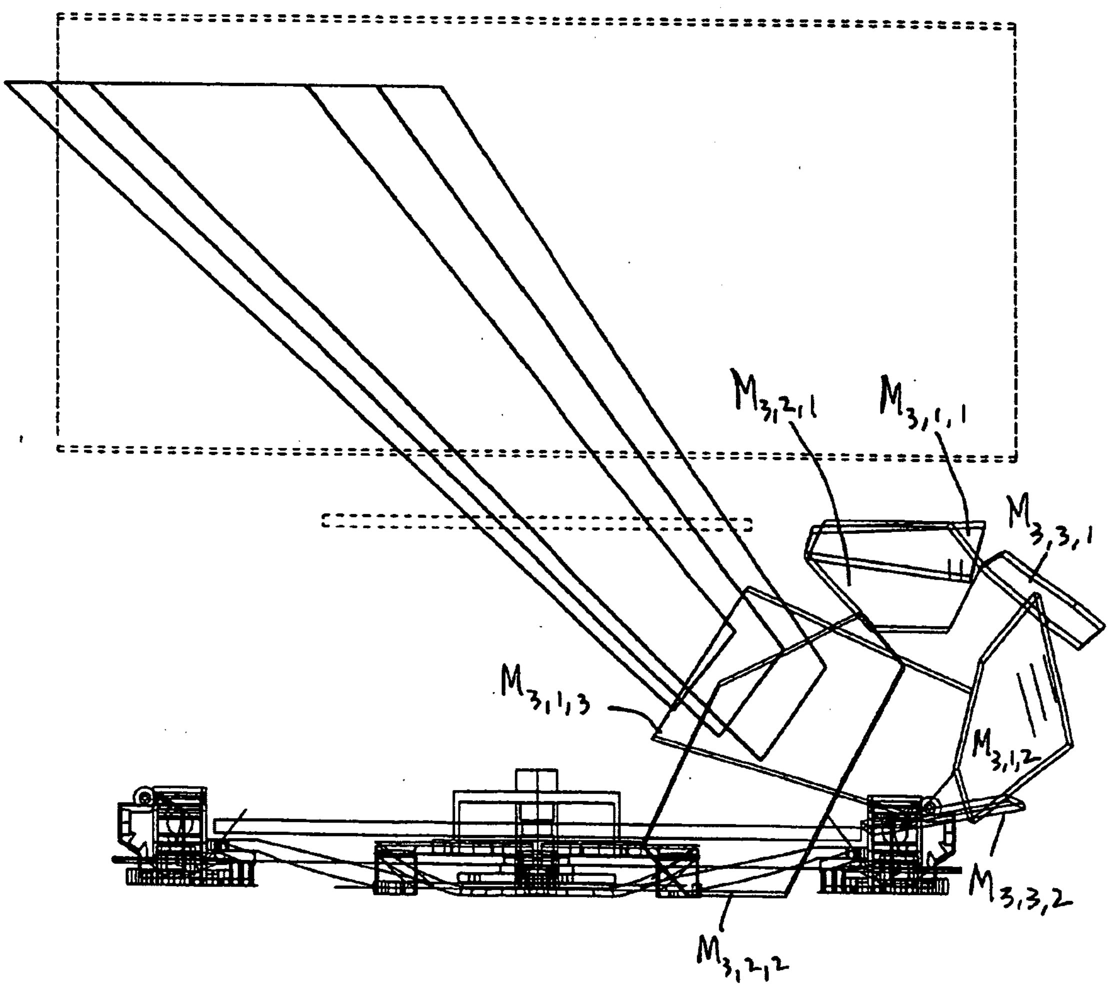

FIG.5N3

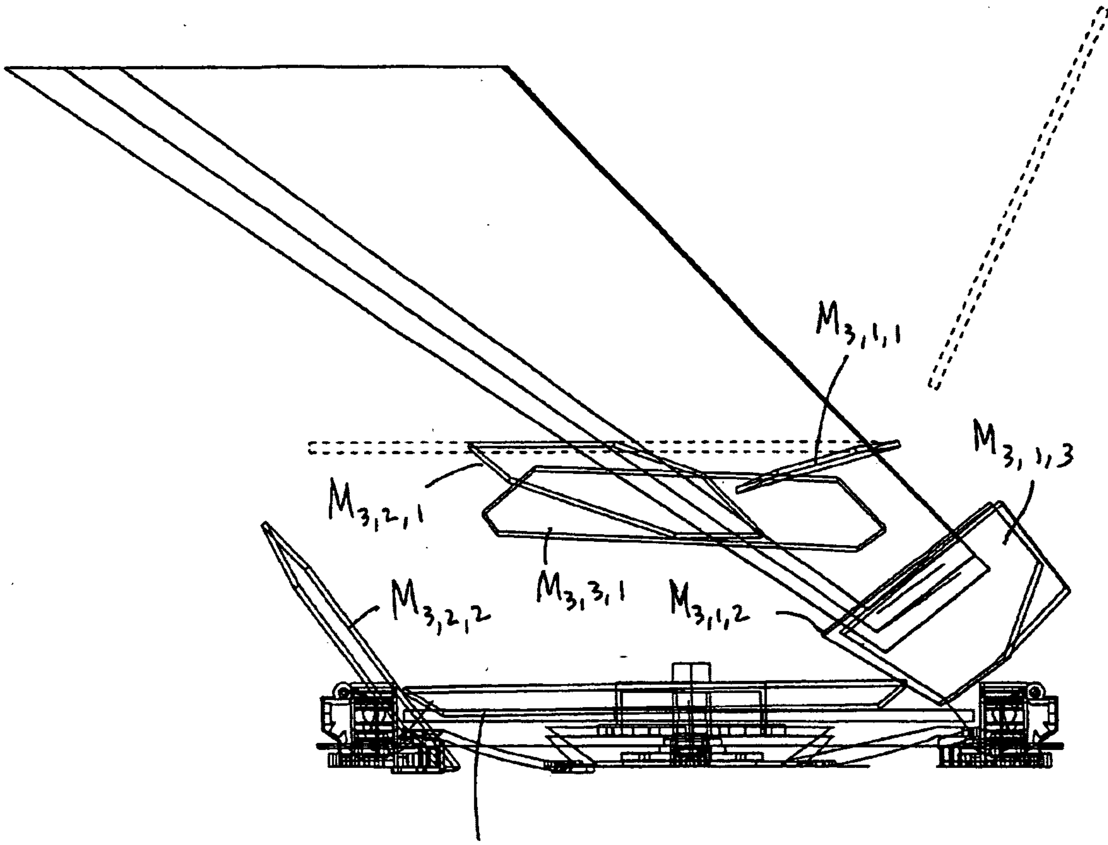

FIG. 5N4

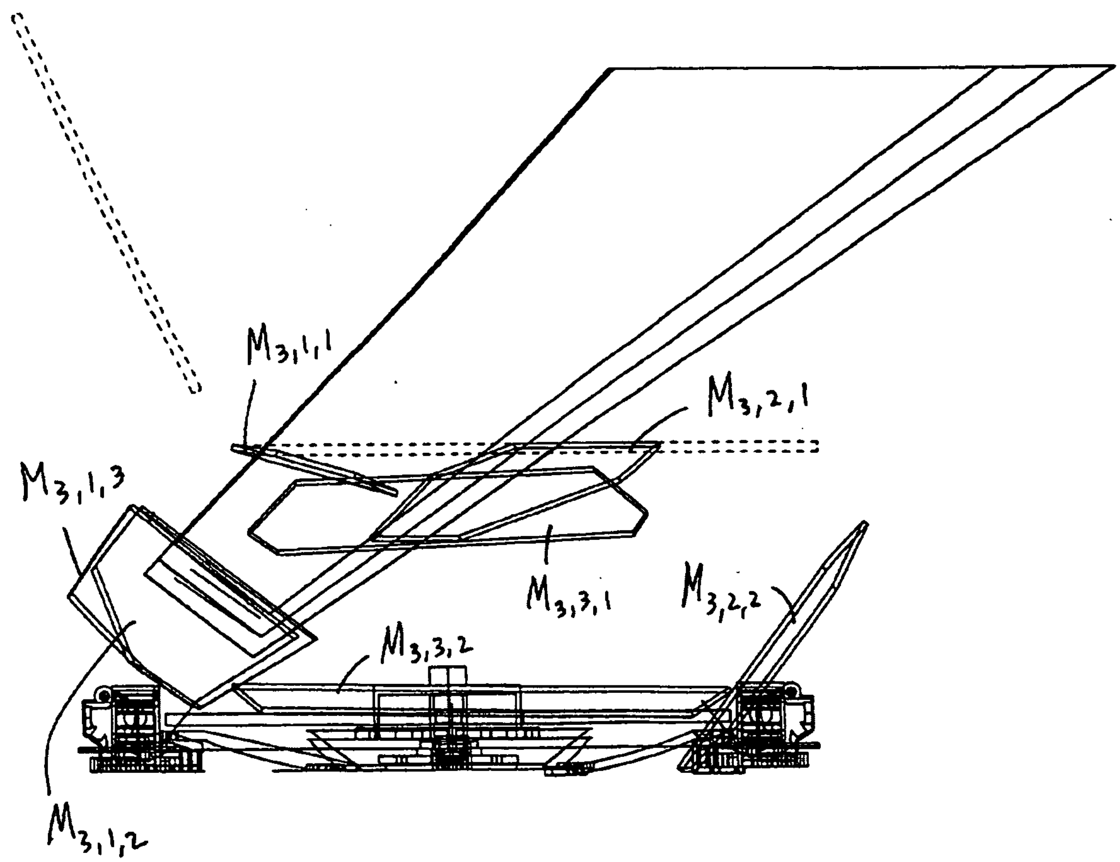

FIG. 5N5

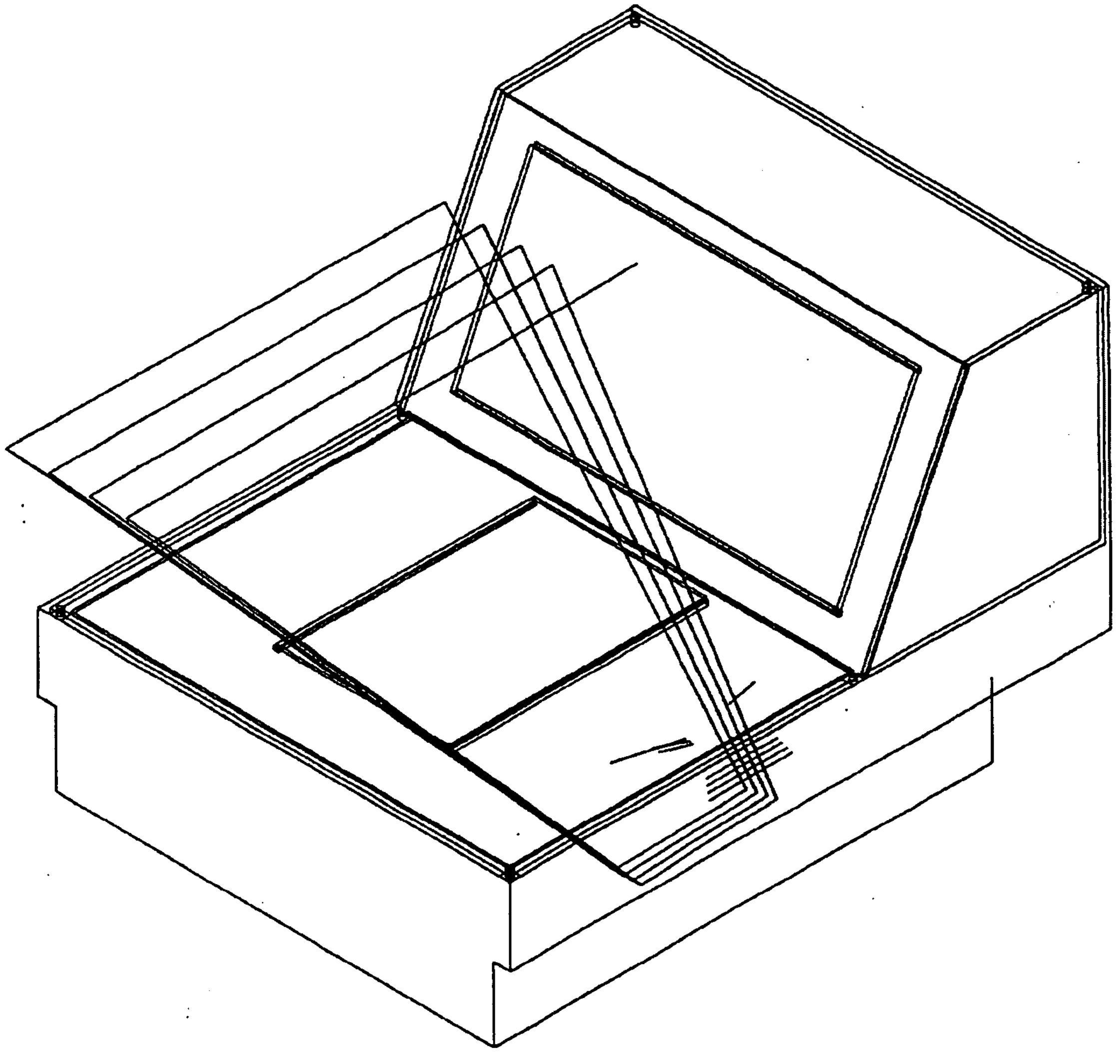

FIG. 501

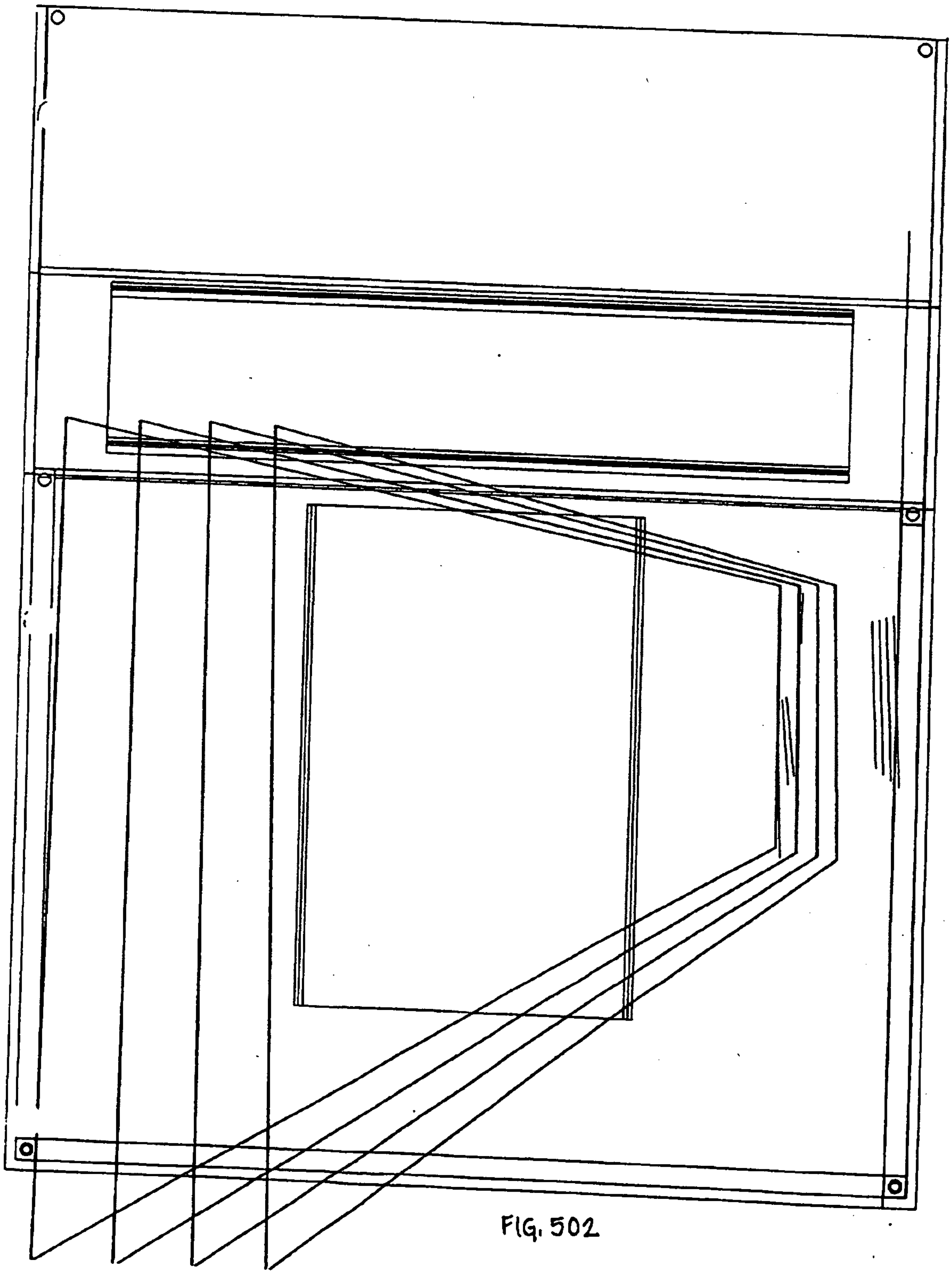

FIG. 502

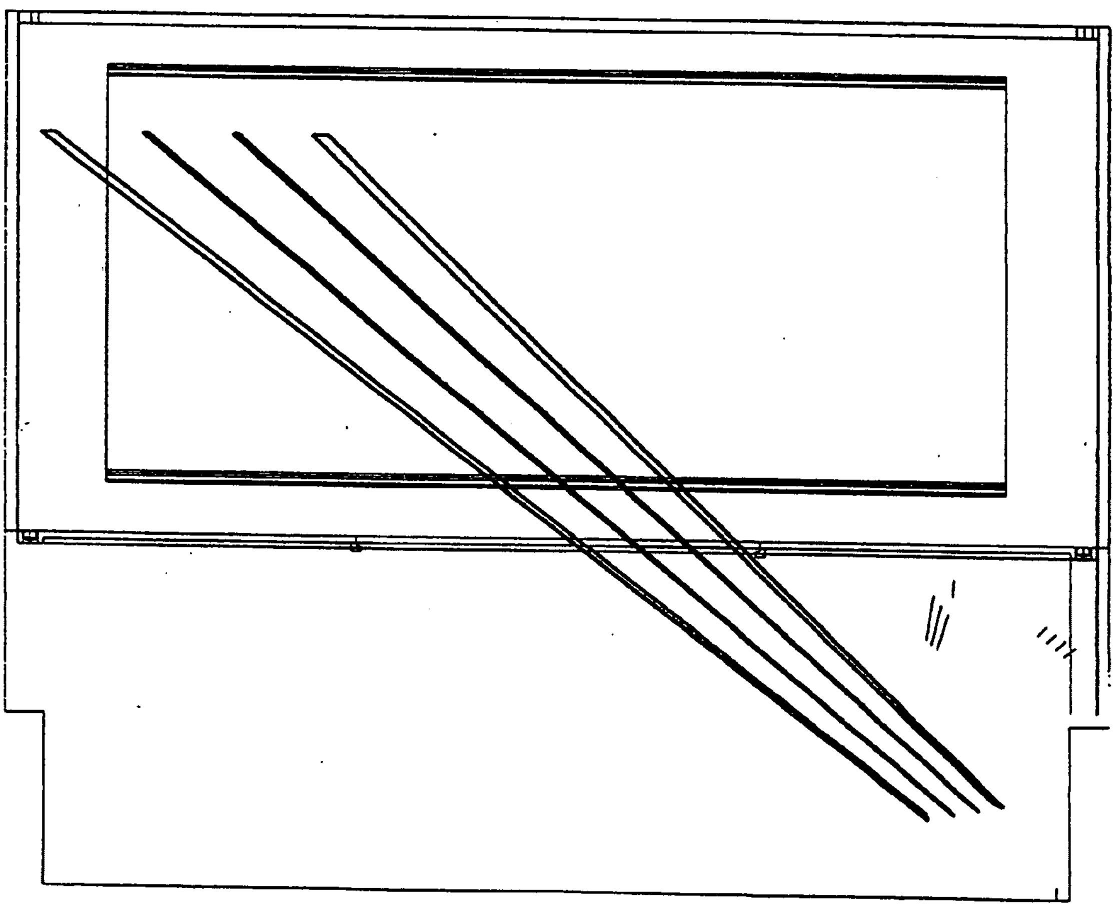

FIG. 503

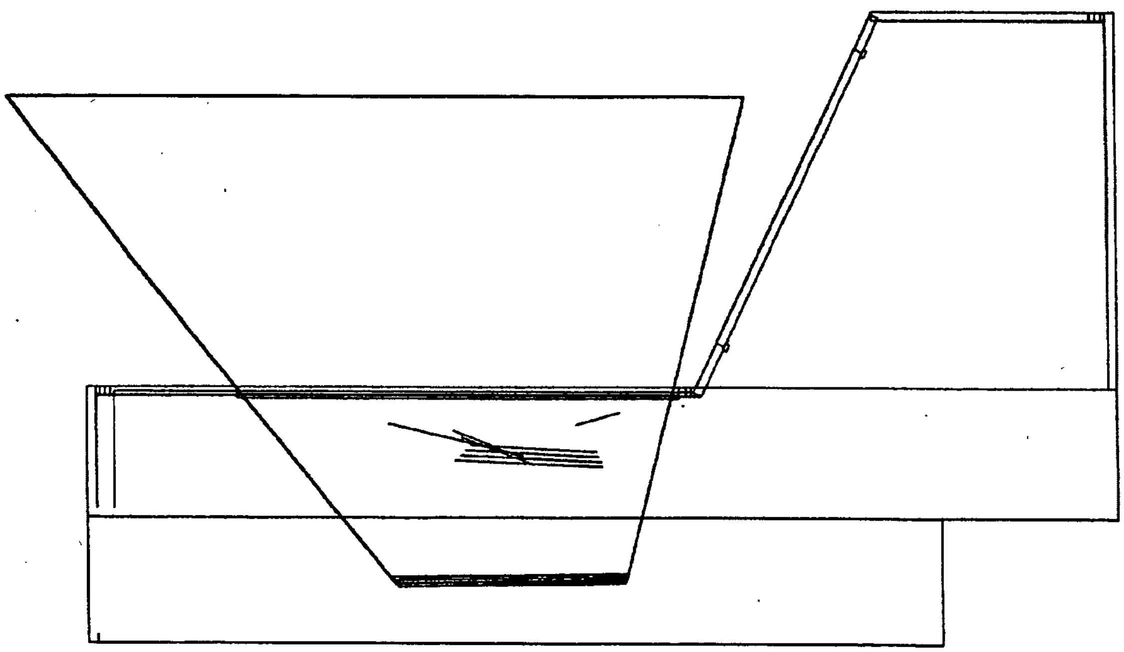

FIG. 504

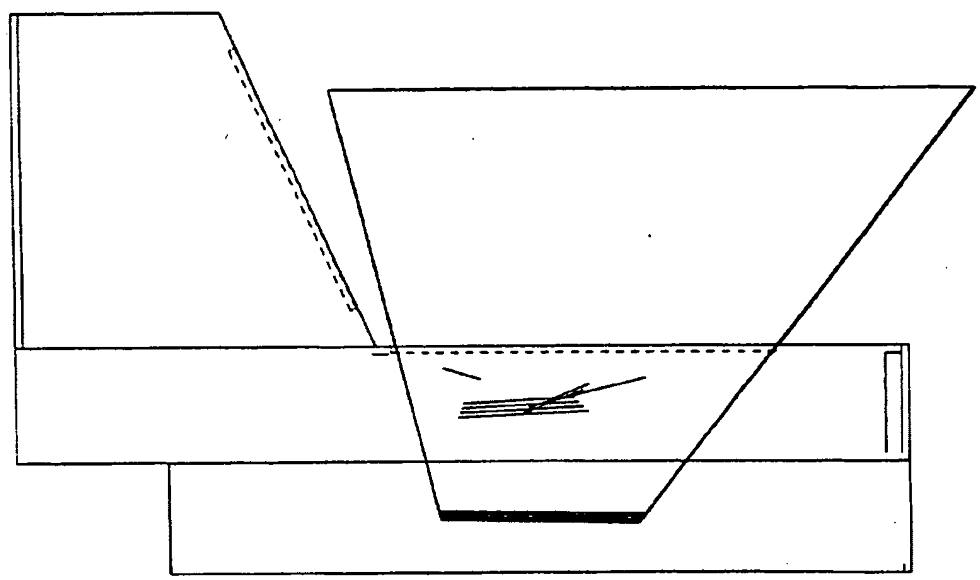

FIG. 505

140/335

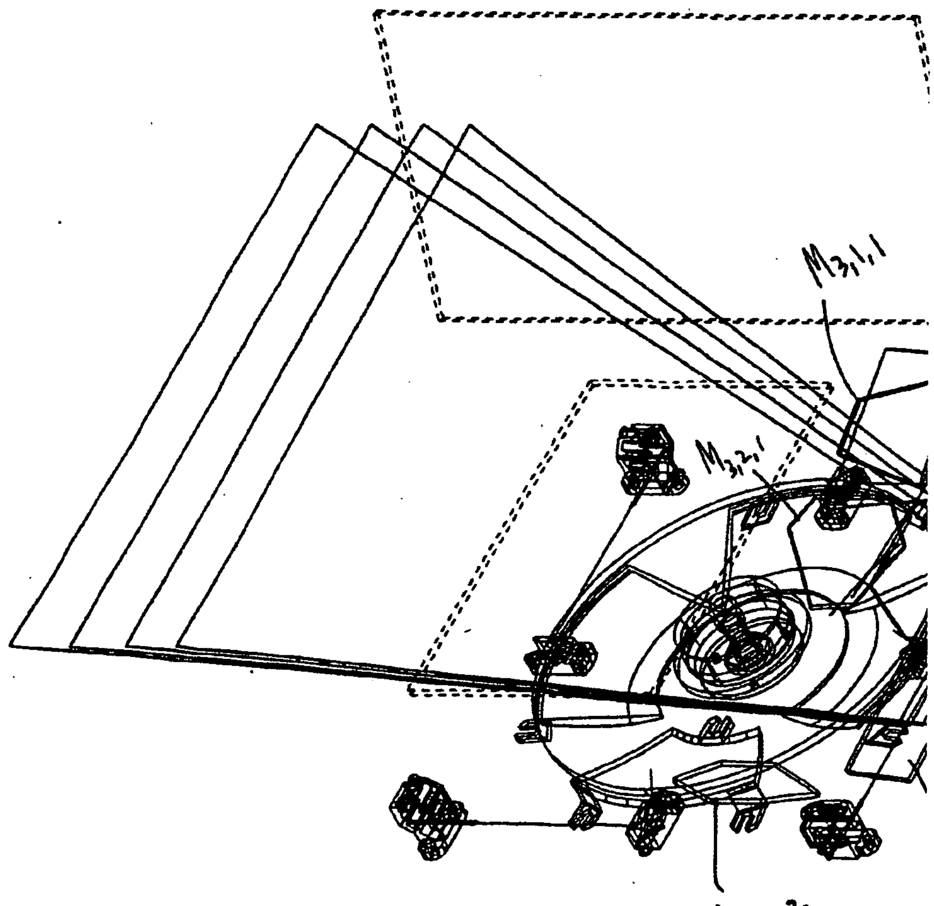

FIG. 5D

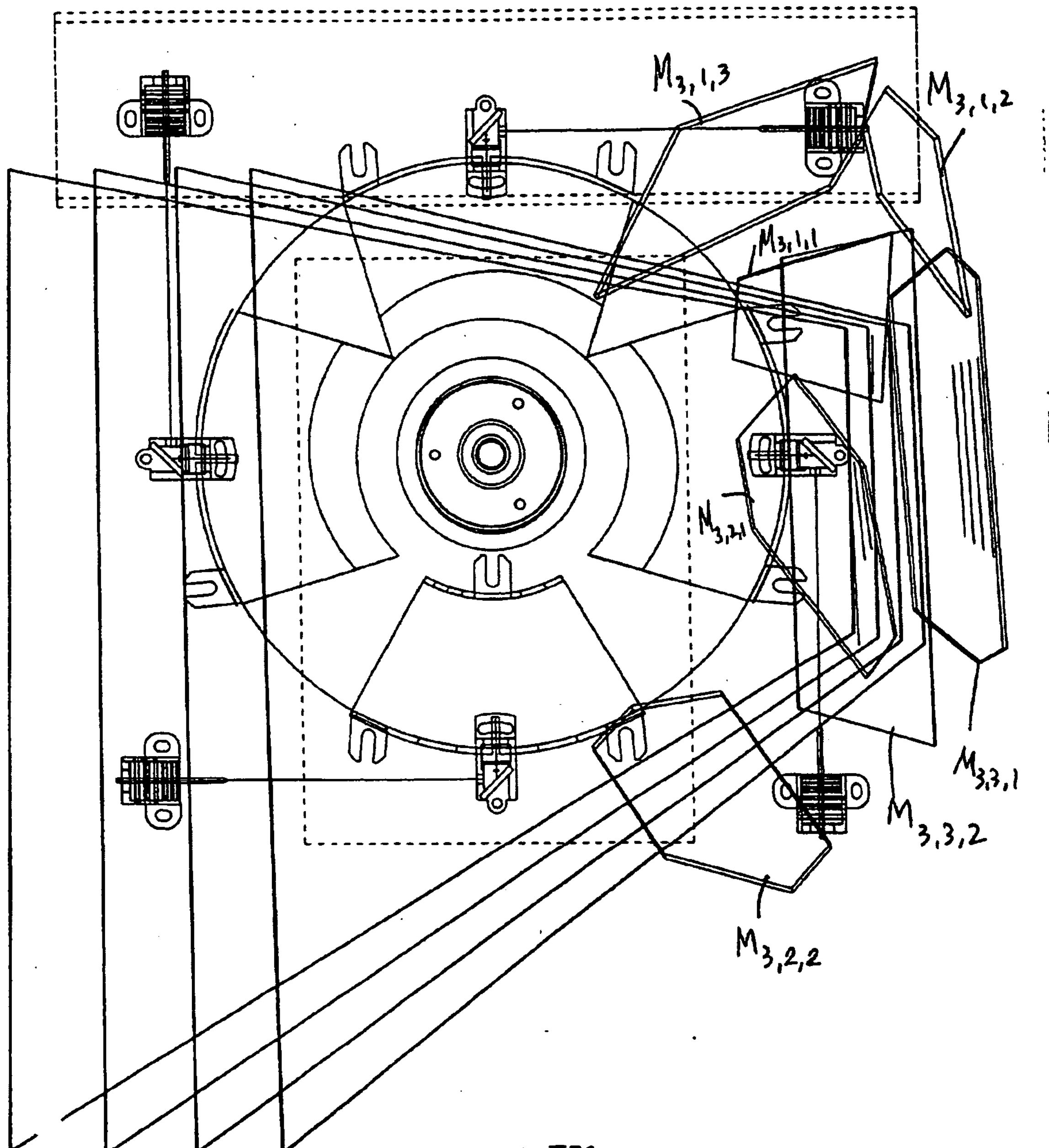

FIG. 5P2

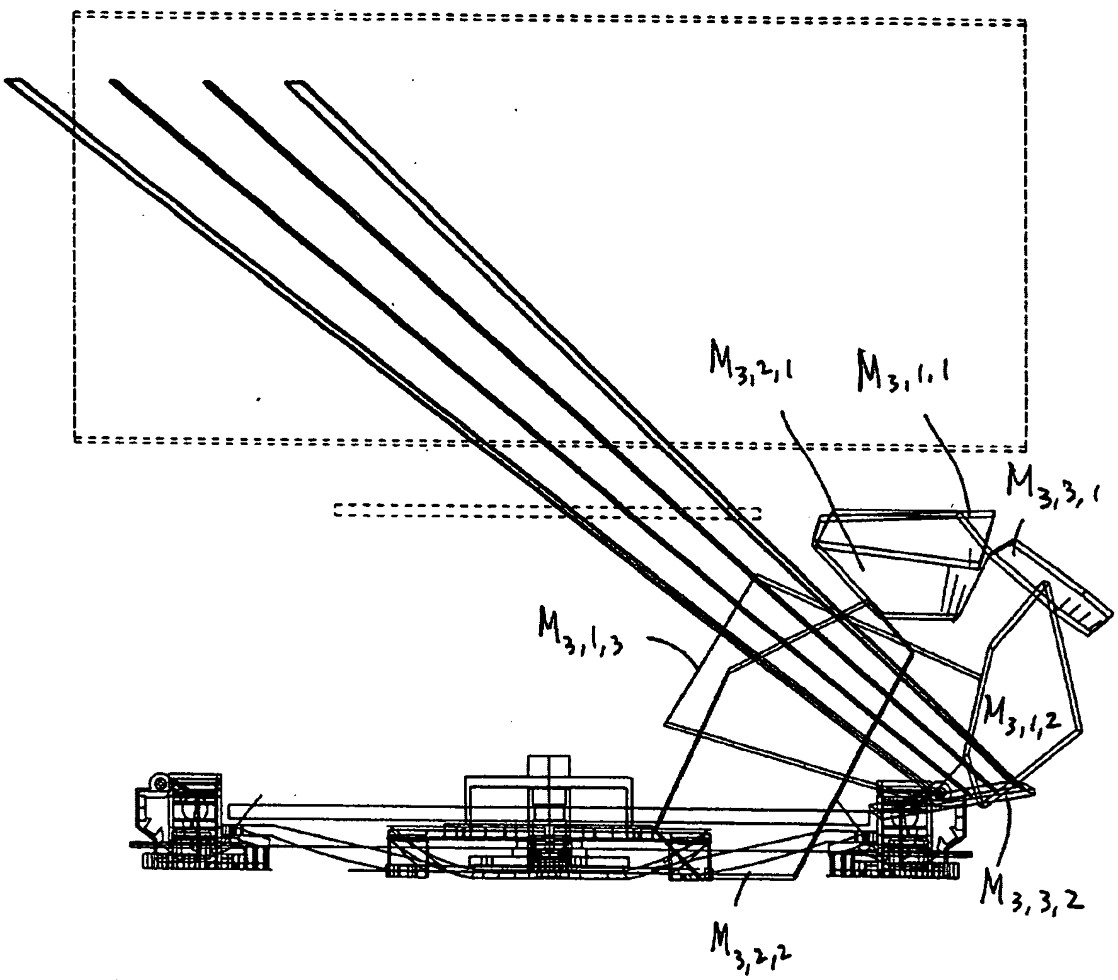

FIG. 5P3

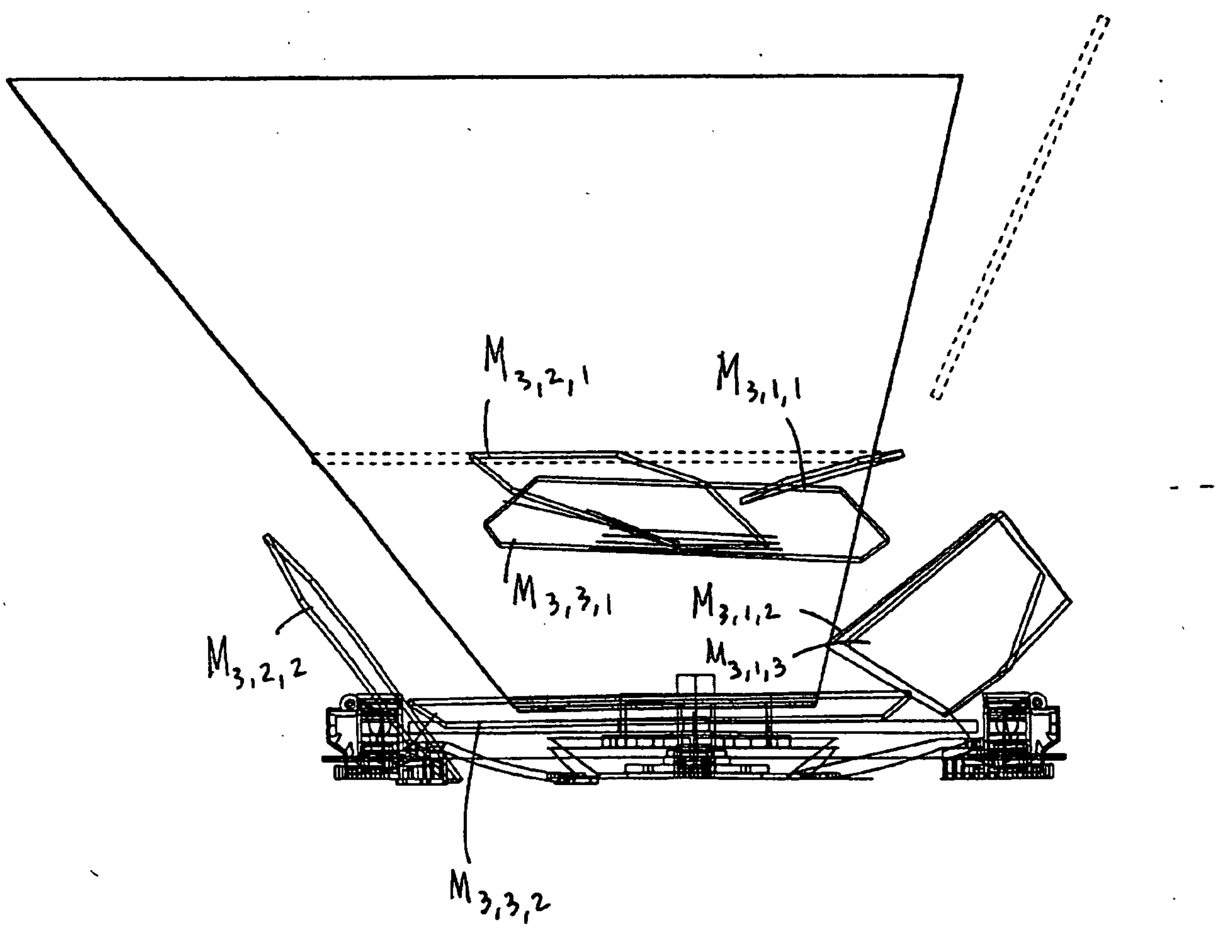

FIG. 5P4

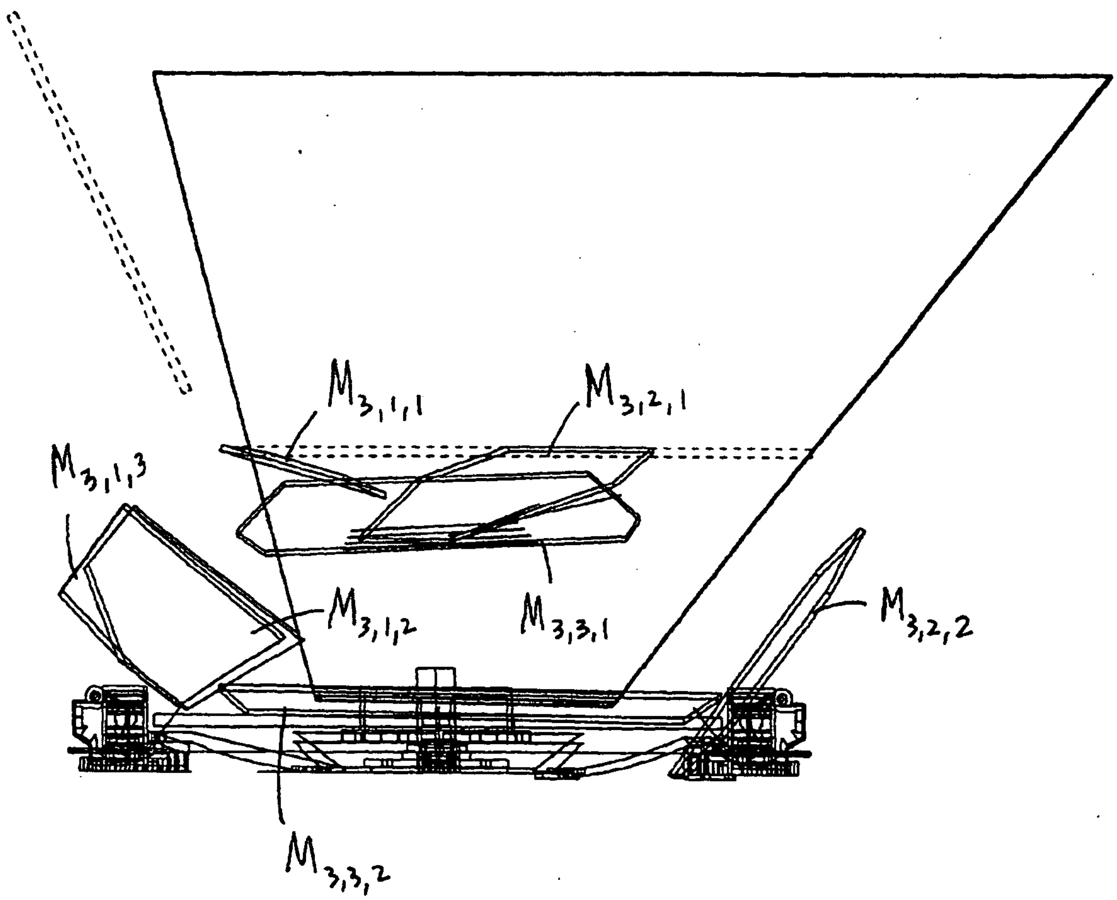

FIG. 5P5

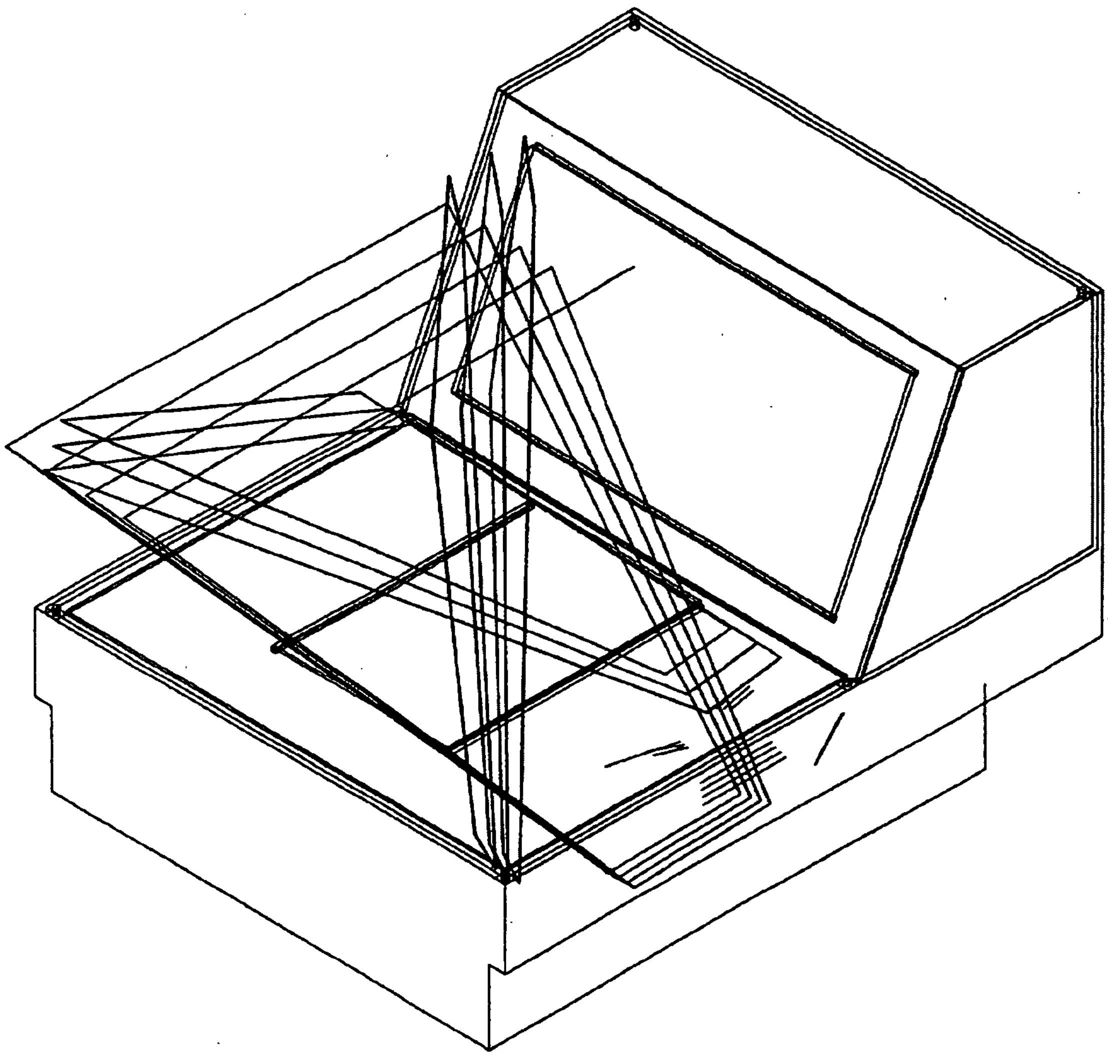

FIG. 5Q1

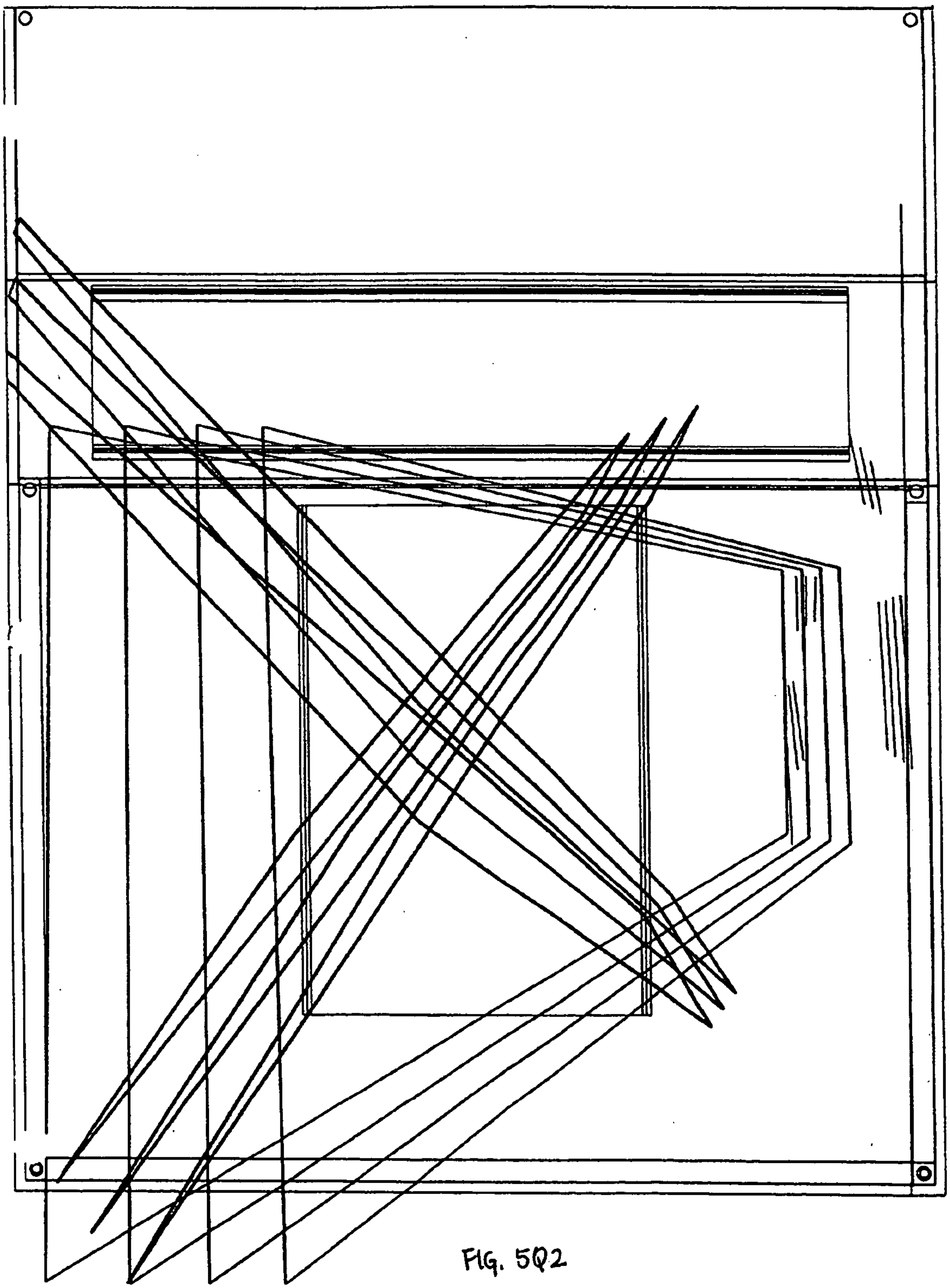

FIG. 5Q2

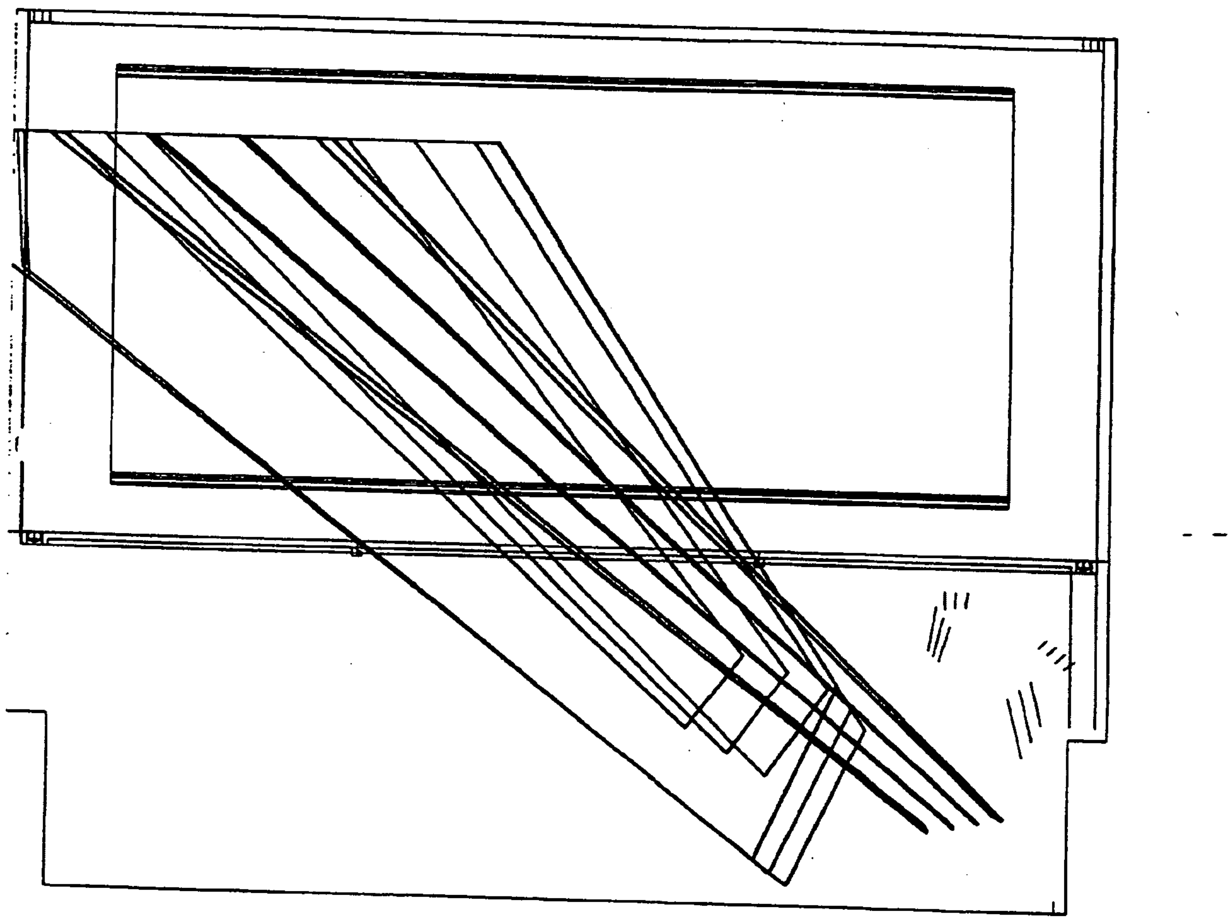

FIG. 5Q3

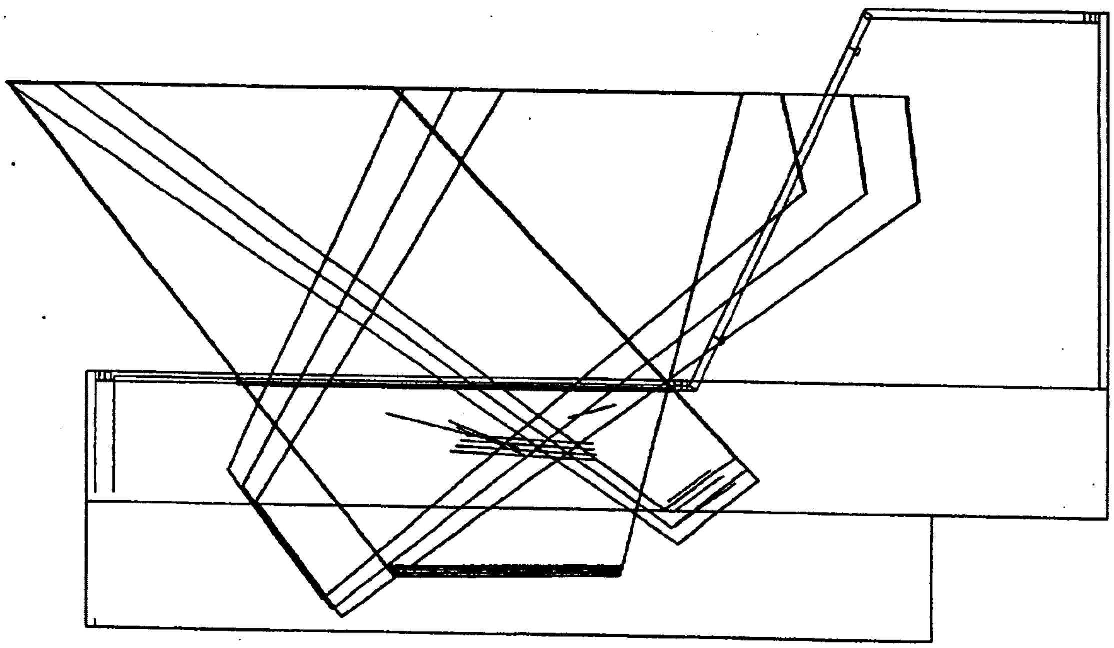

FIG. 5Q4

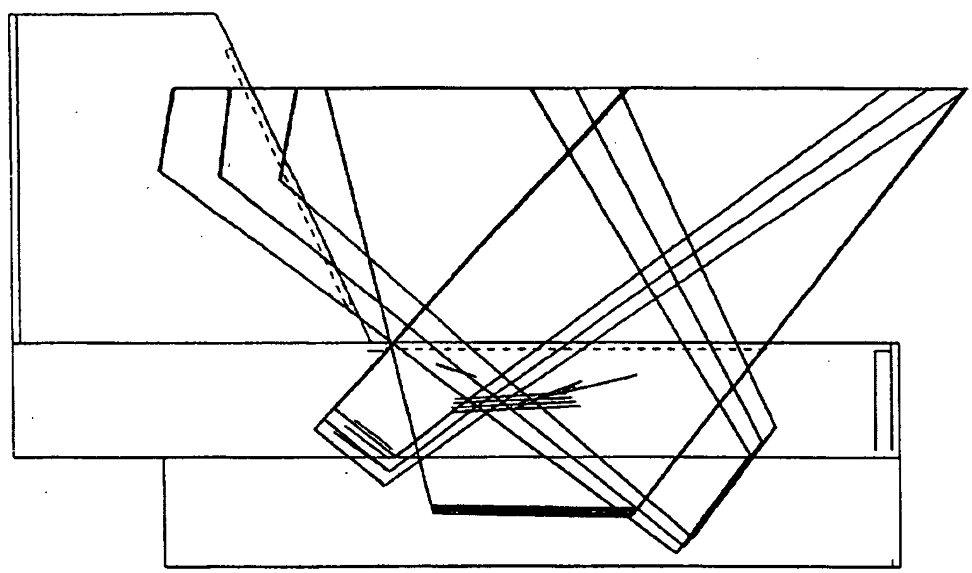

FIG. 5Q5

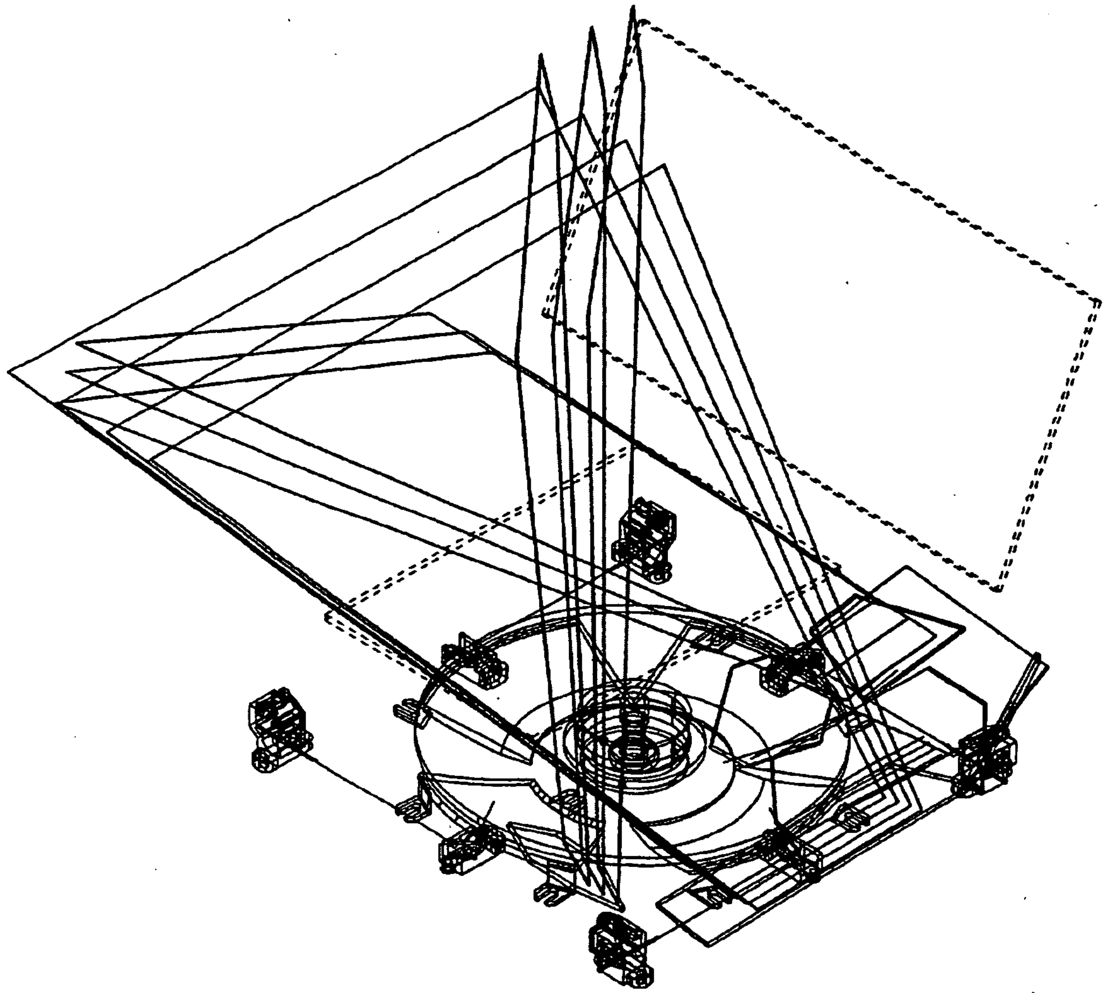

FIG. 5R1

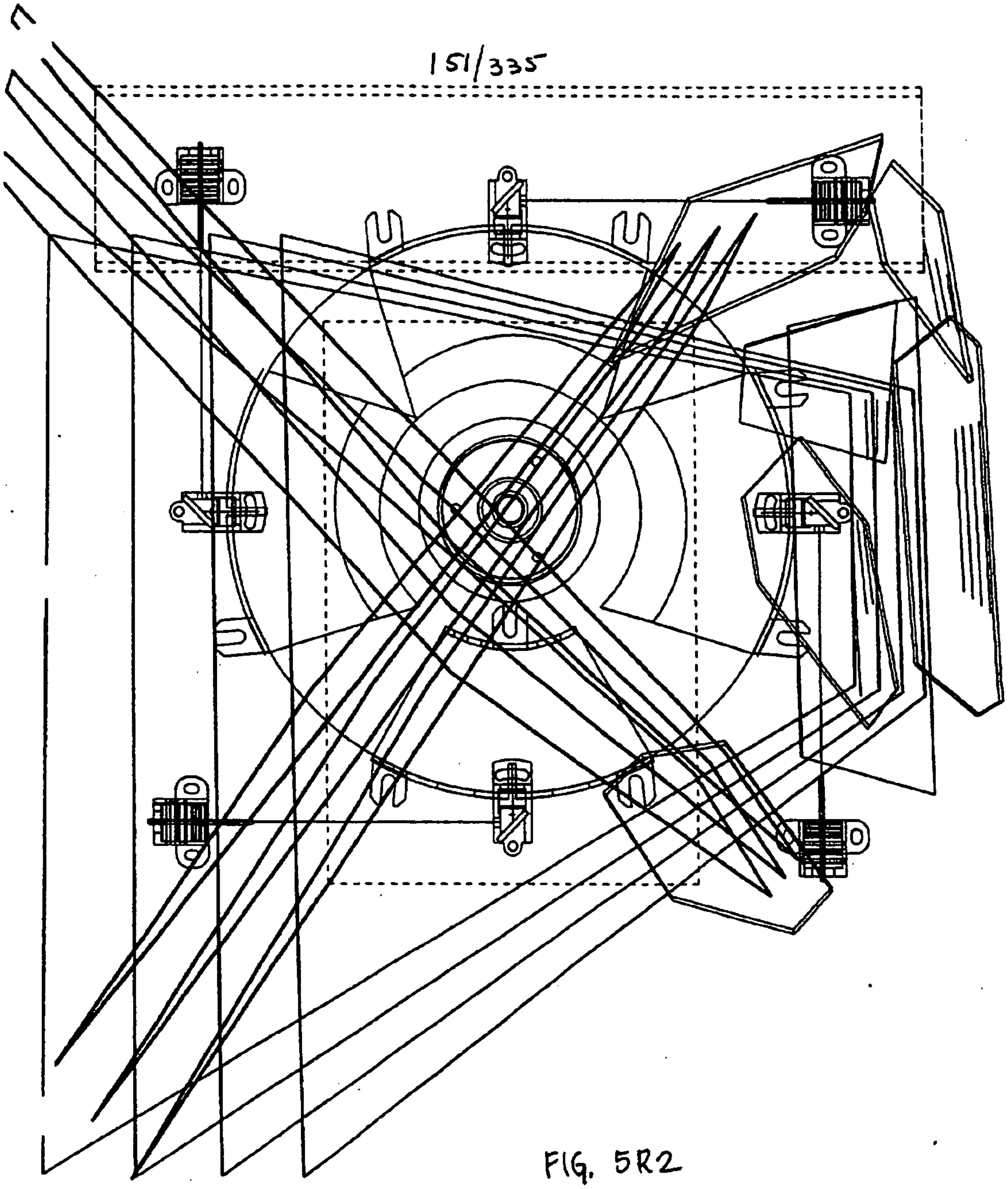

FIG. 5R2

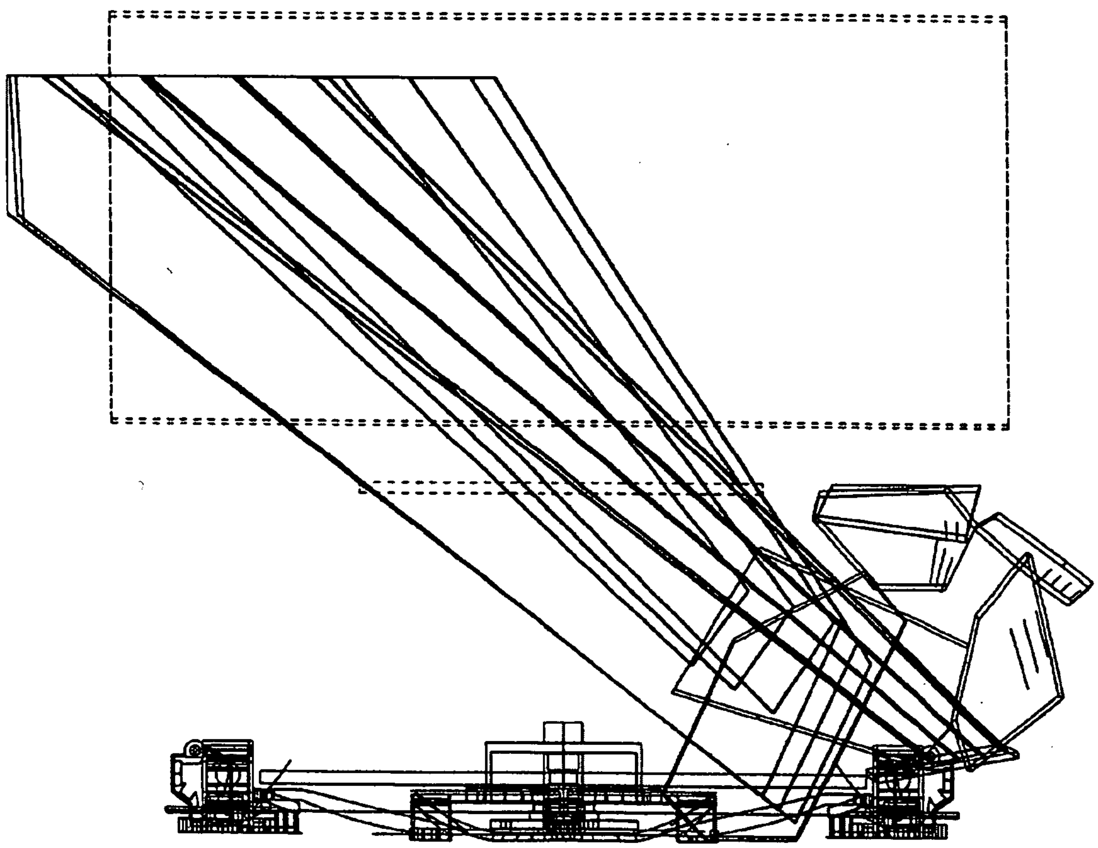

FIG. 5R3

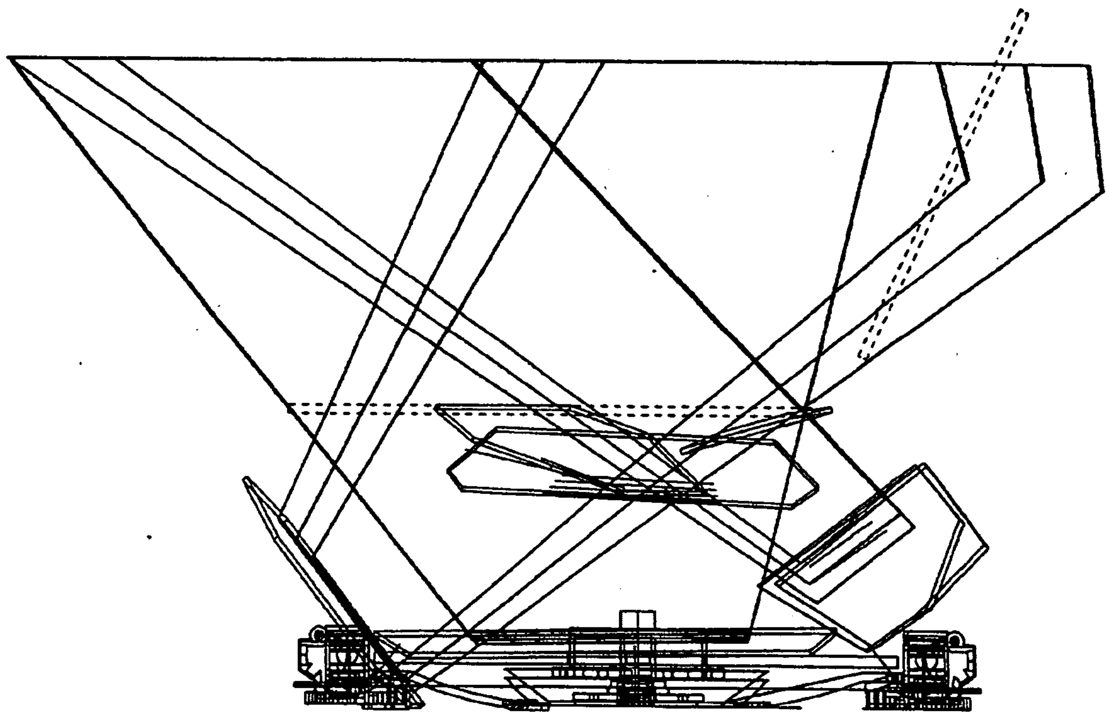

FIG. 5R4

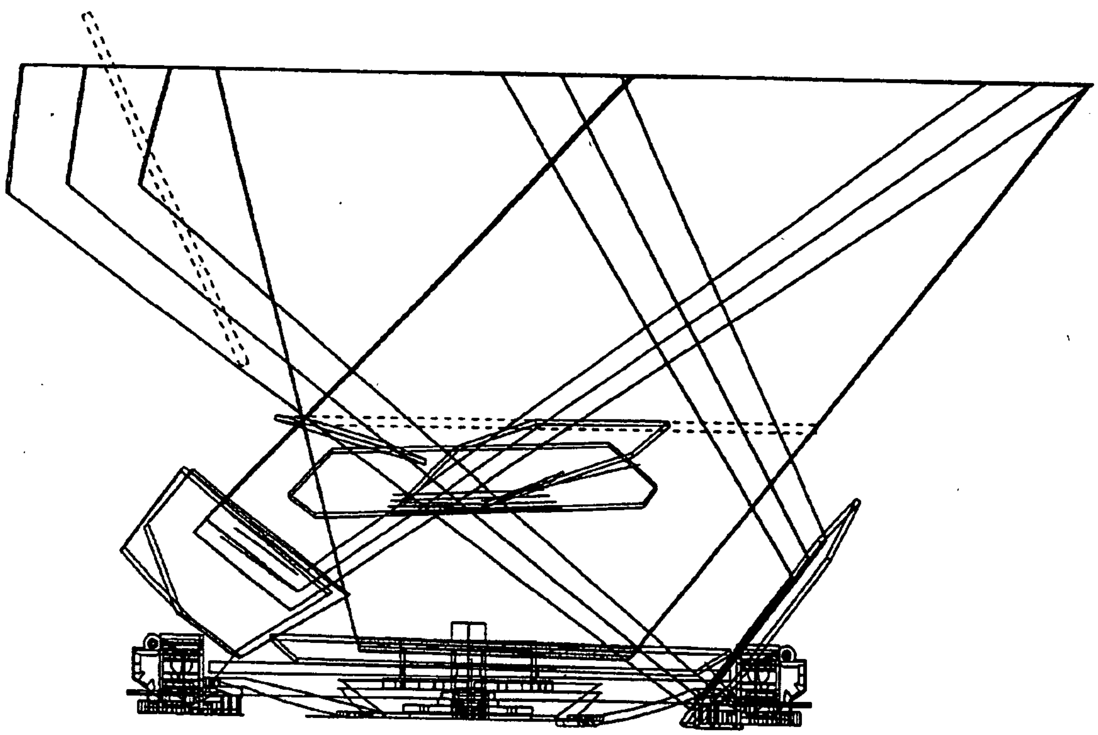

FIG. 5R5

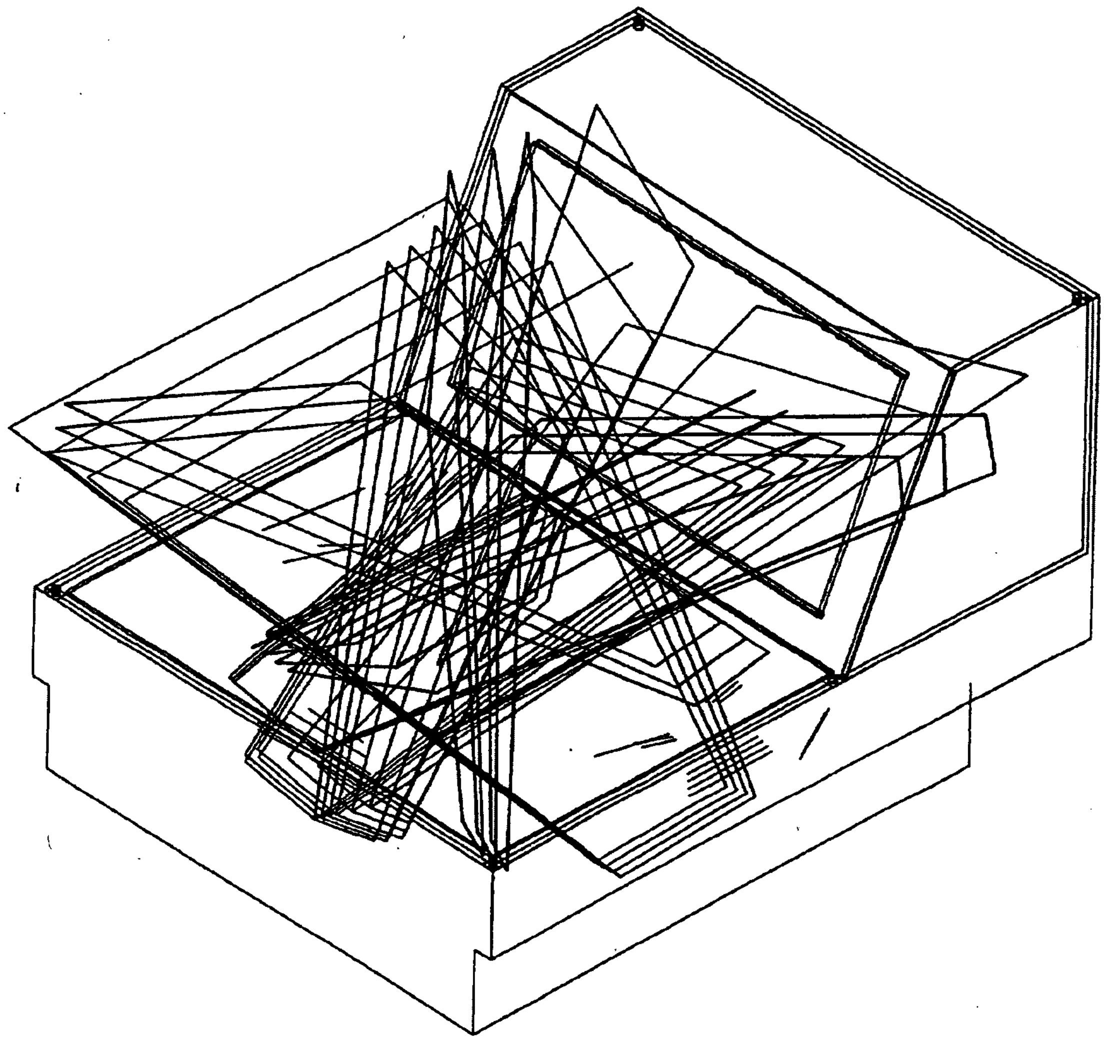

FIG. 581

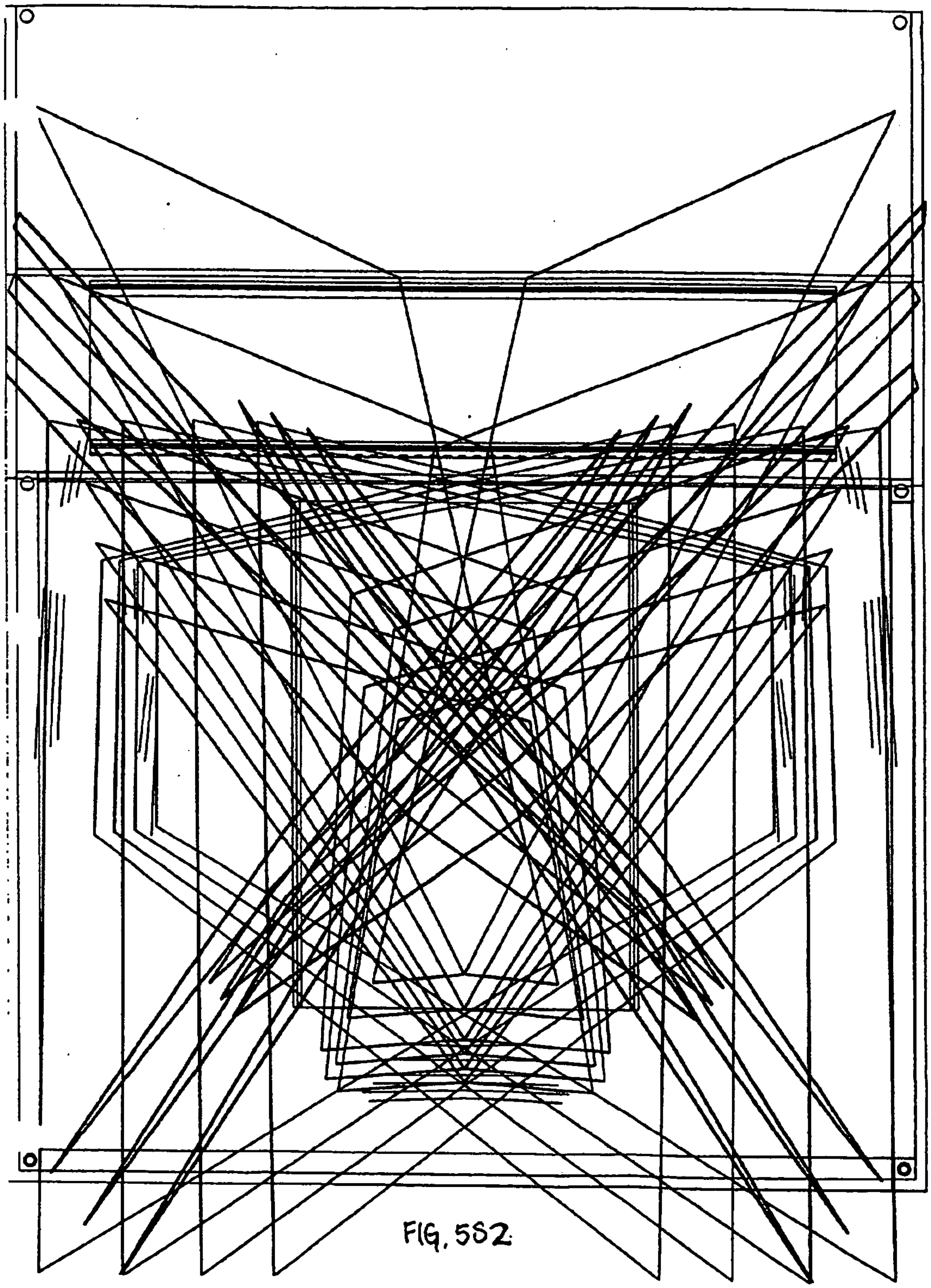

FIG. 552

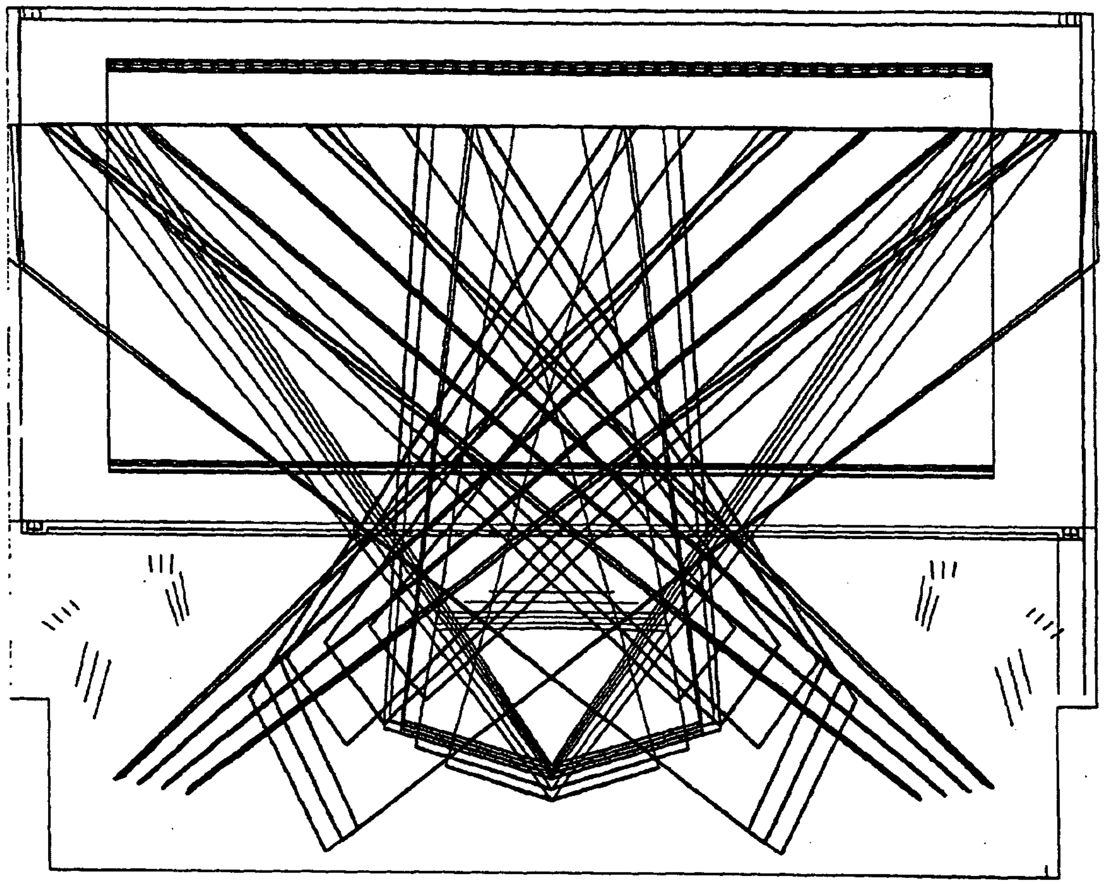

FIG. 553

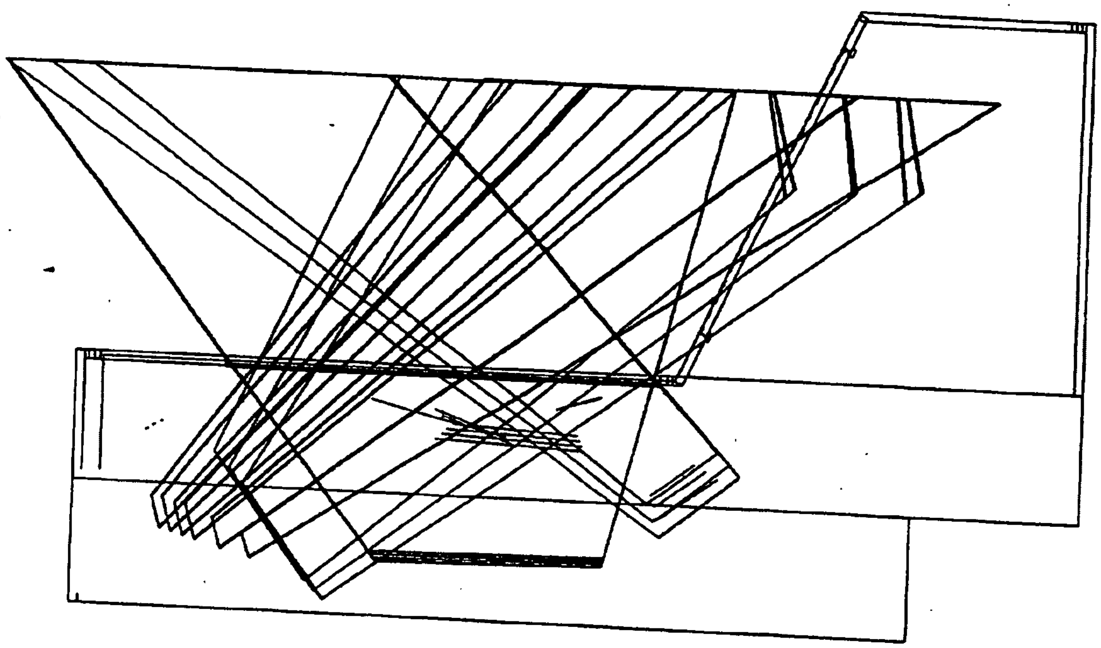

FIG. 584

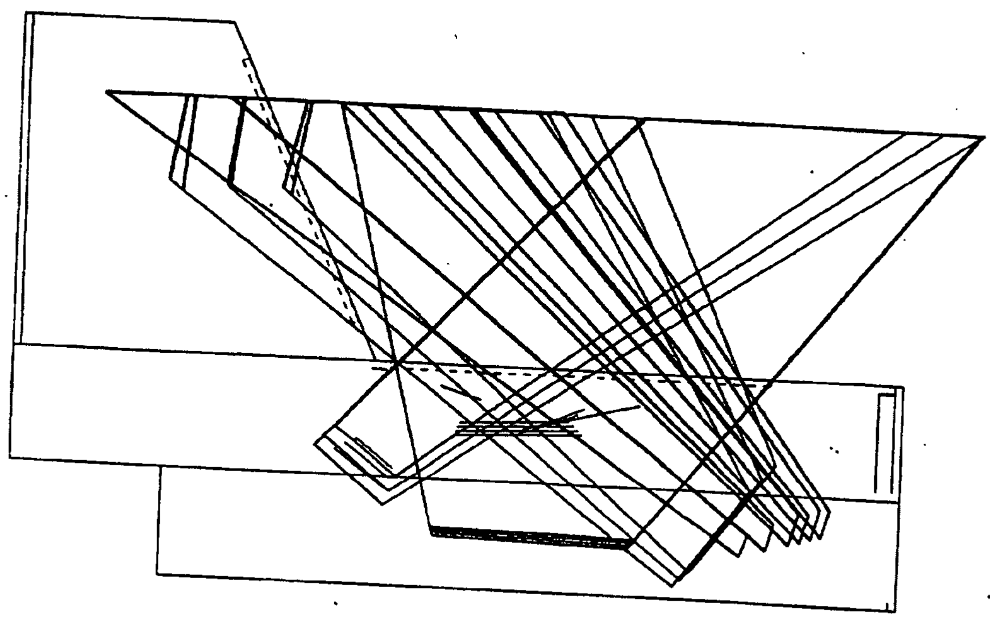

FIG. 555

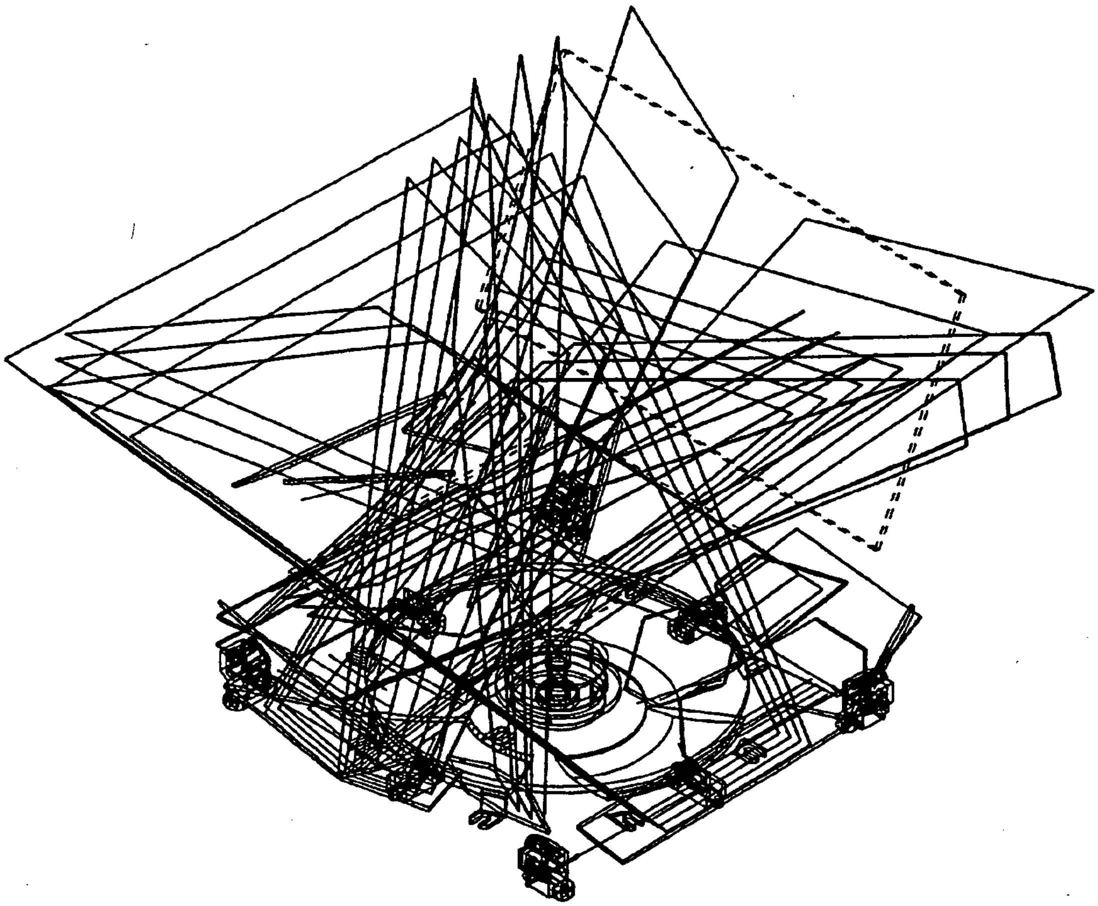

FIG. 5T1

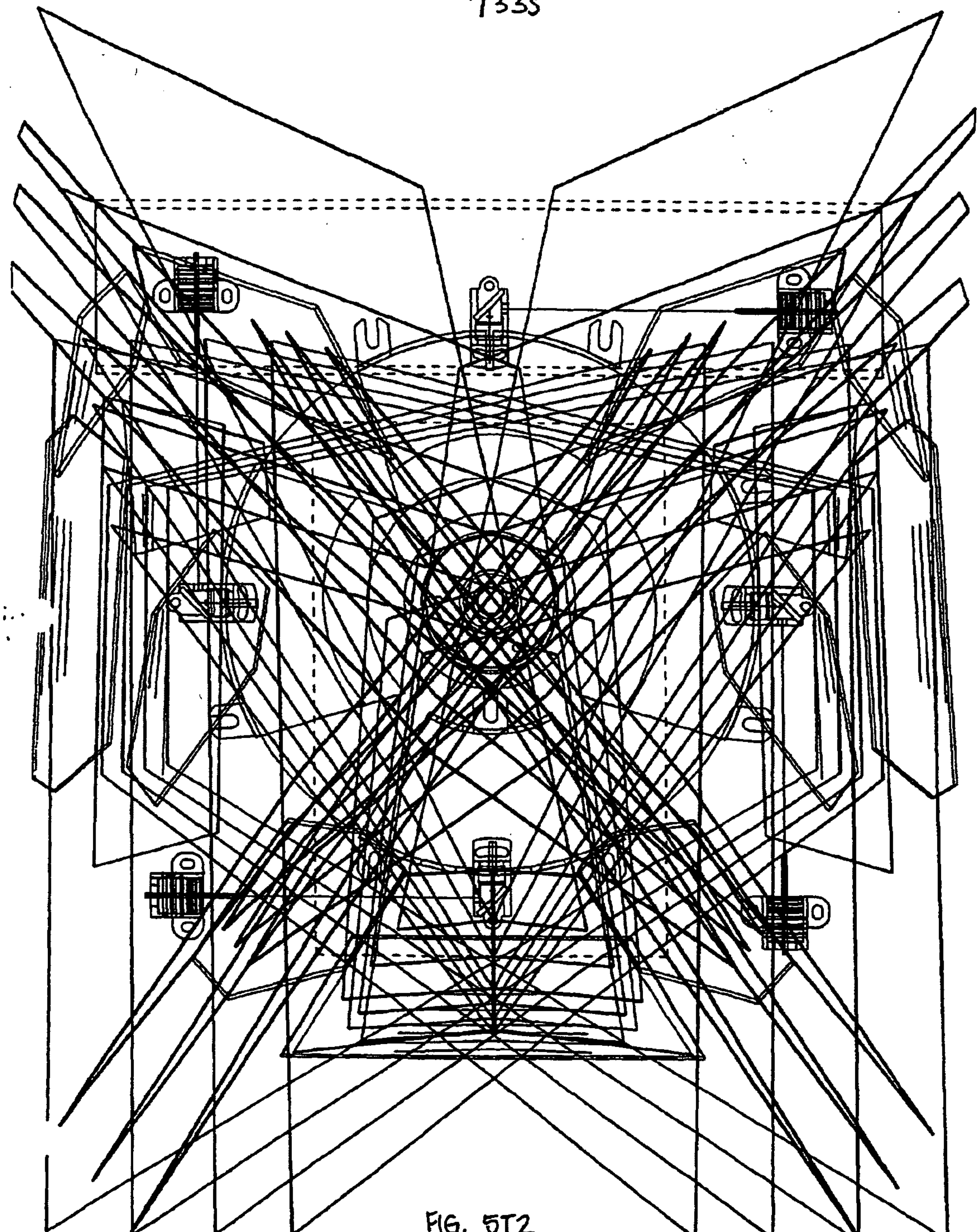

FIG. 5T2

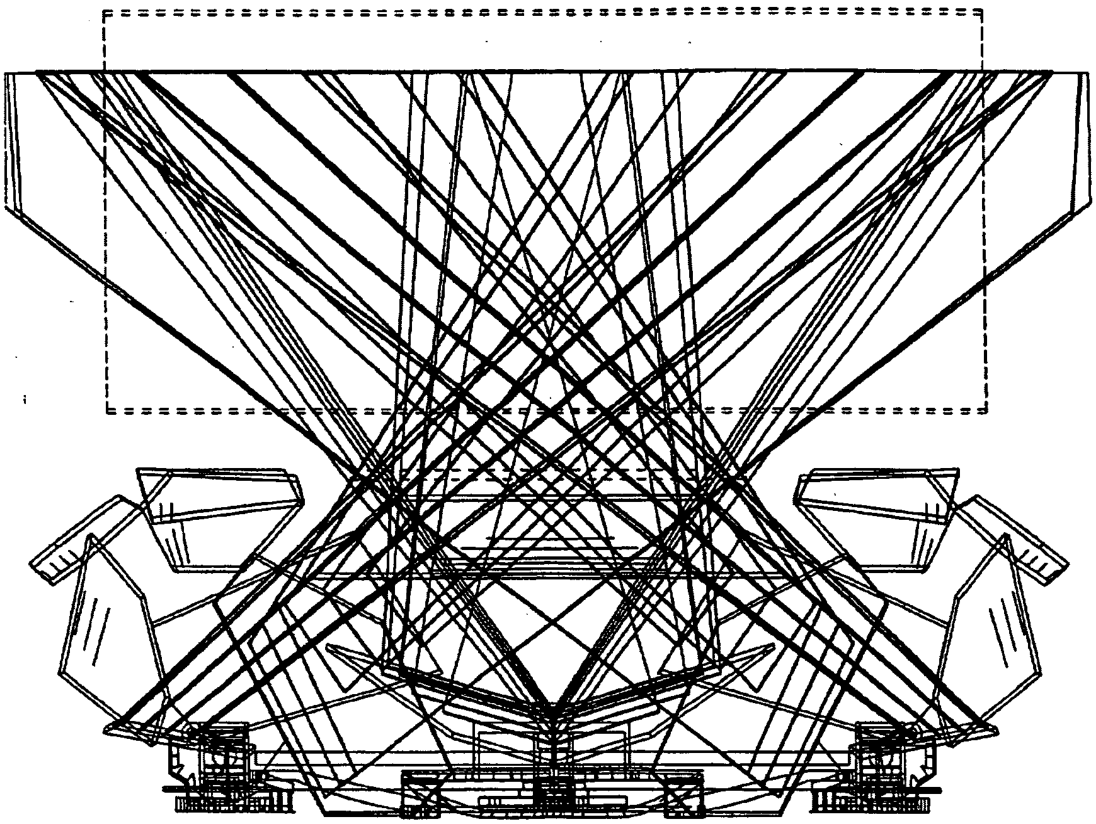

FIG. 5T3

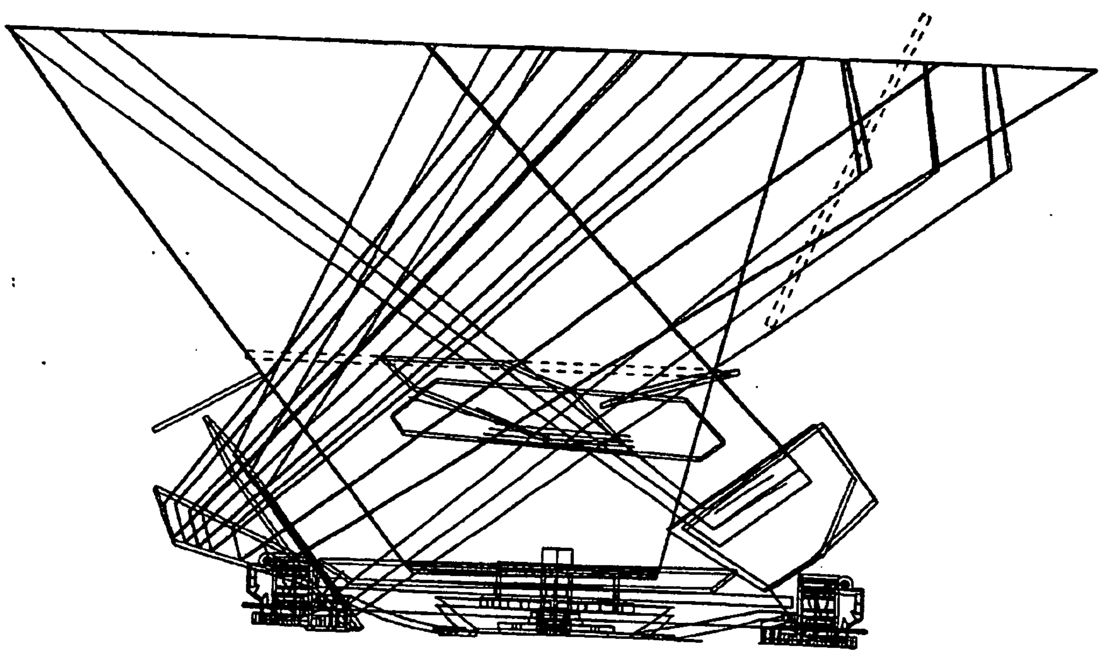

FIG. 5T4

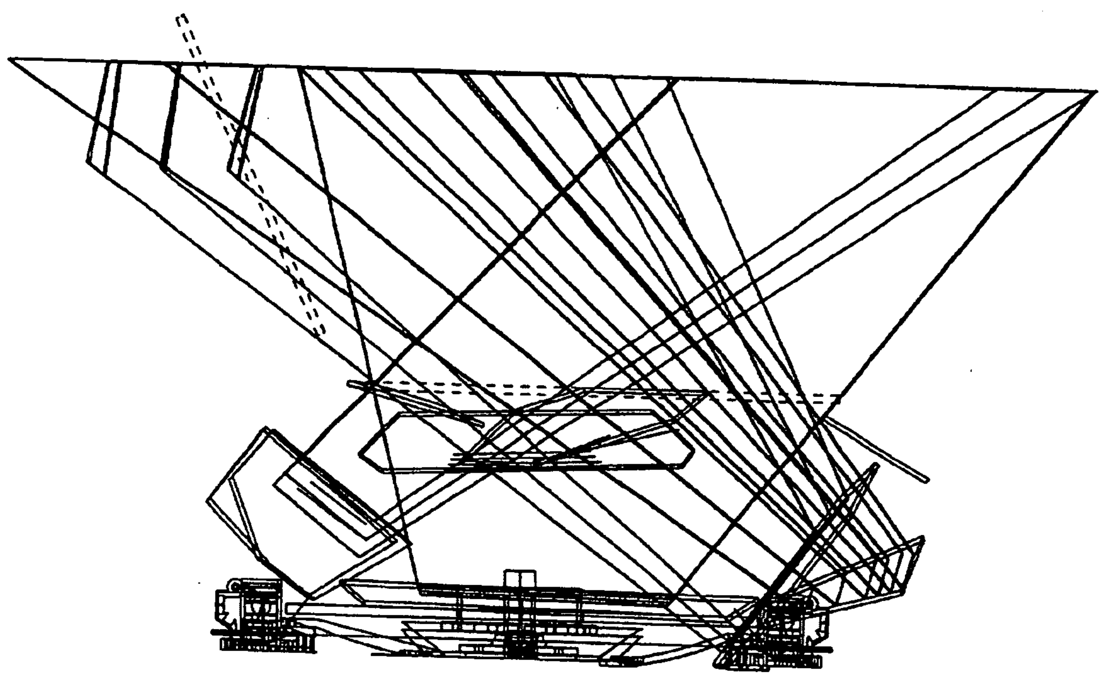

FIG. 5T5

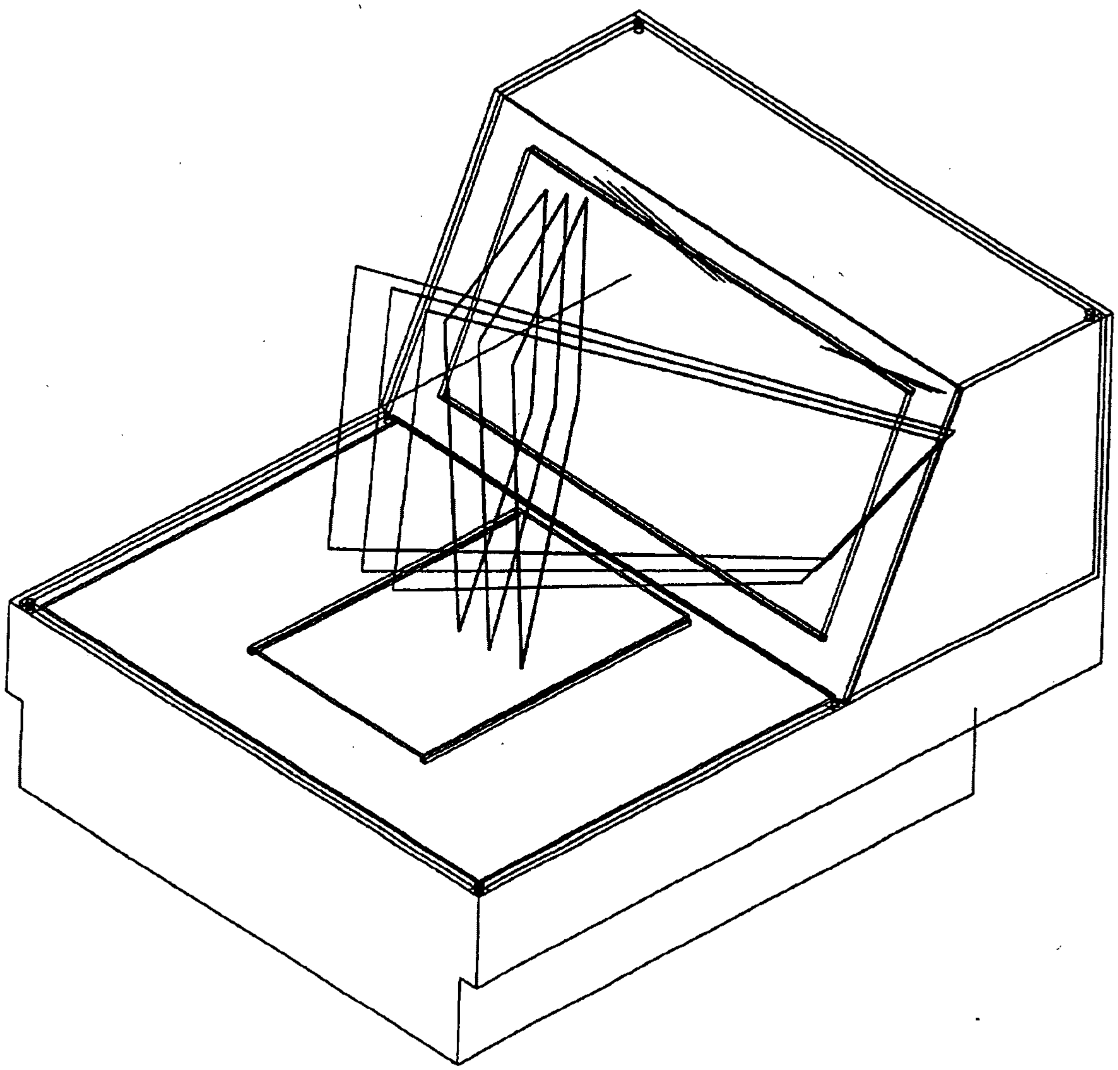

FIG. 5U1

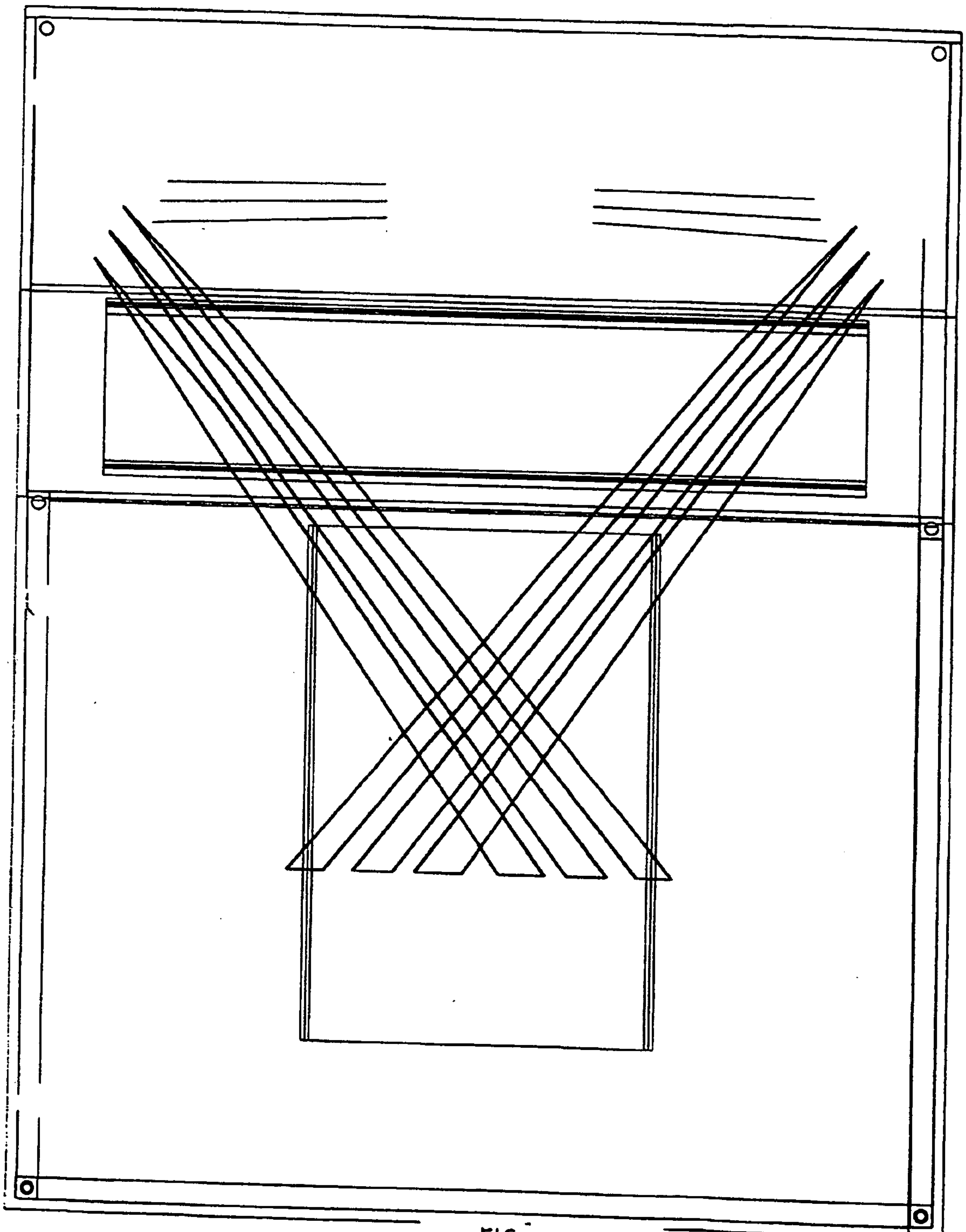

FIG. 5U2

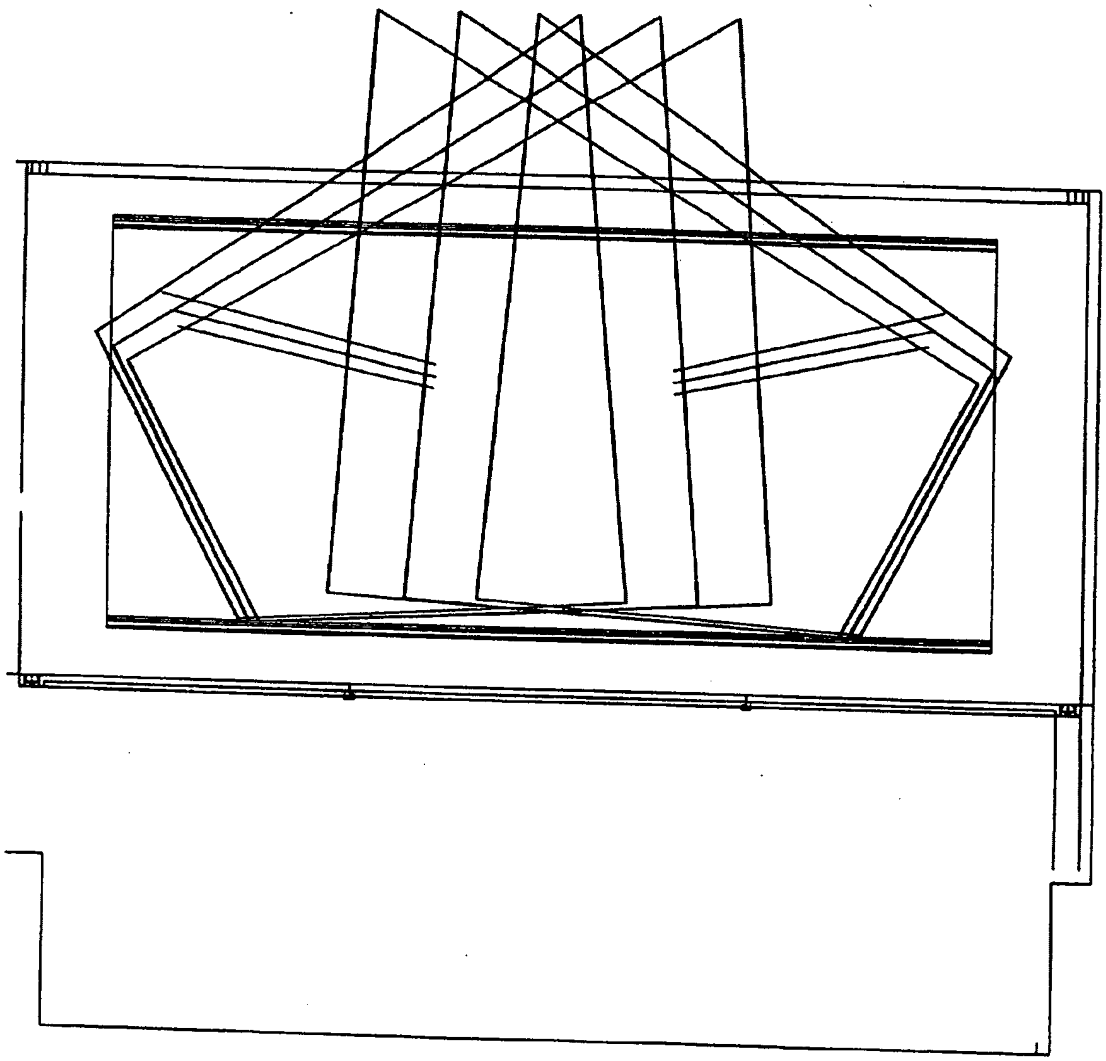

FIG. 5U3

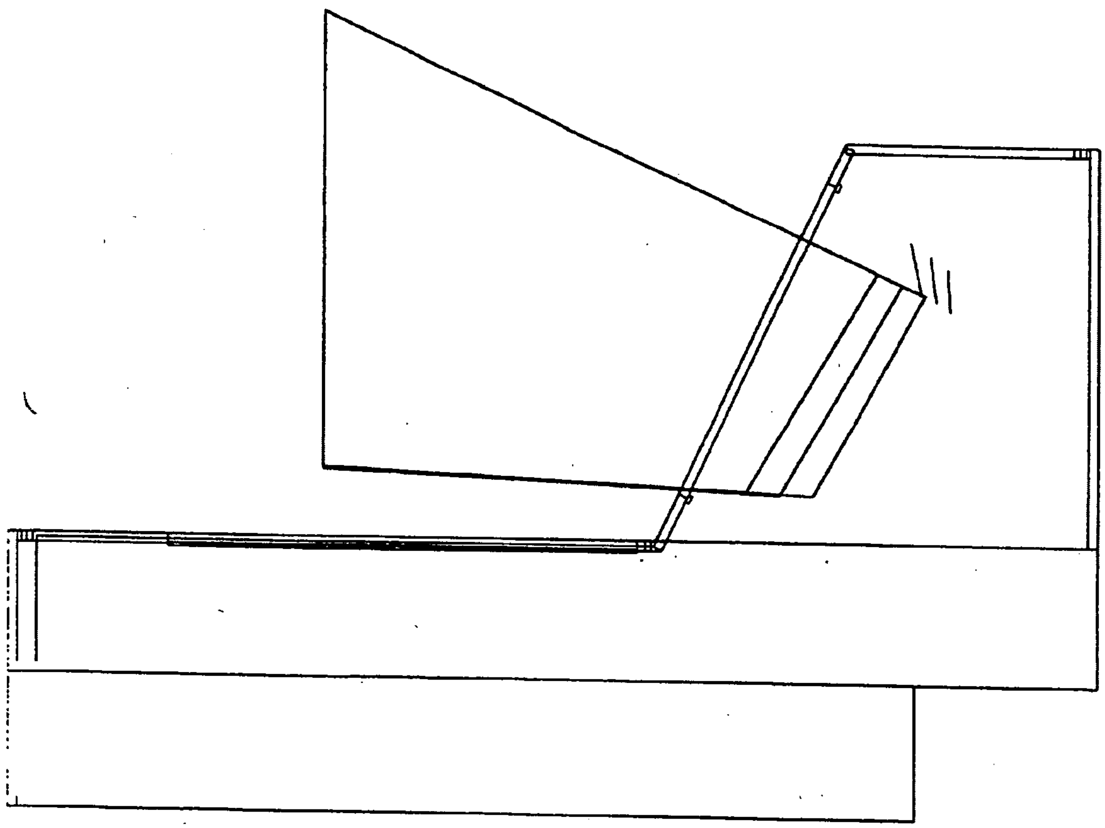

FIG. 504

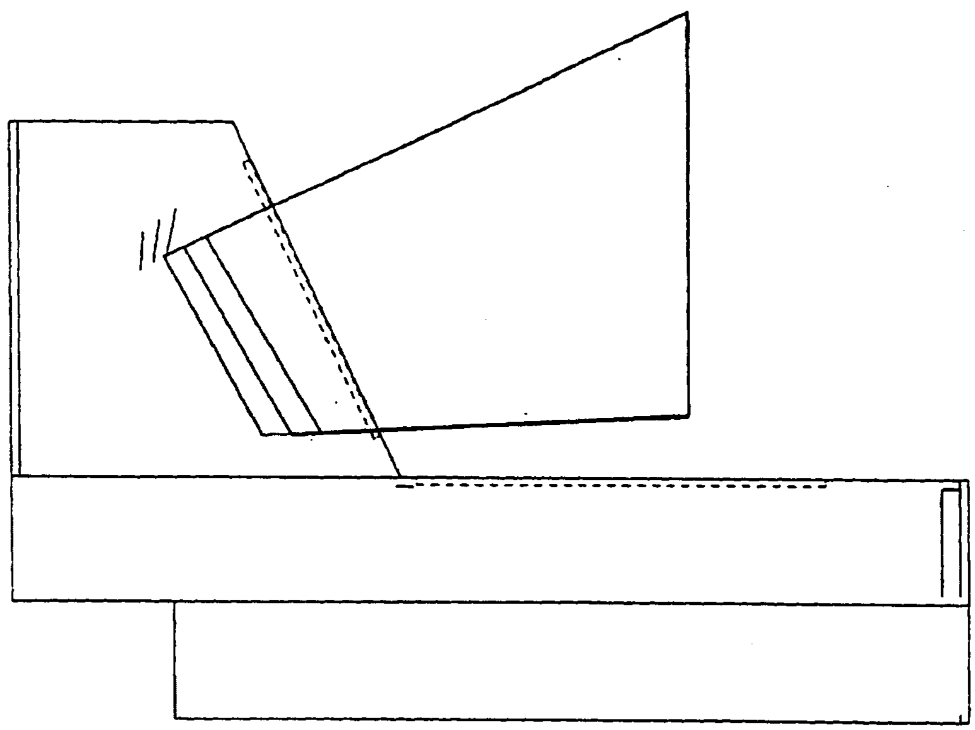

FIG. 5U5

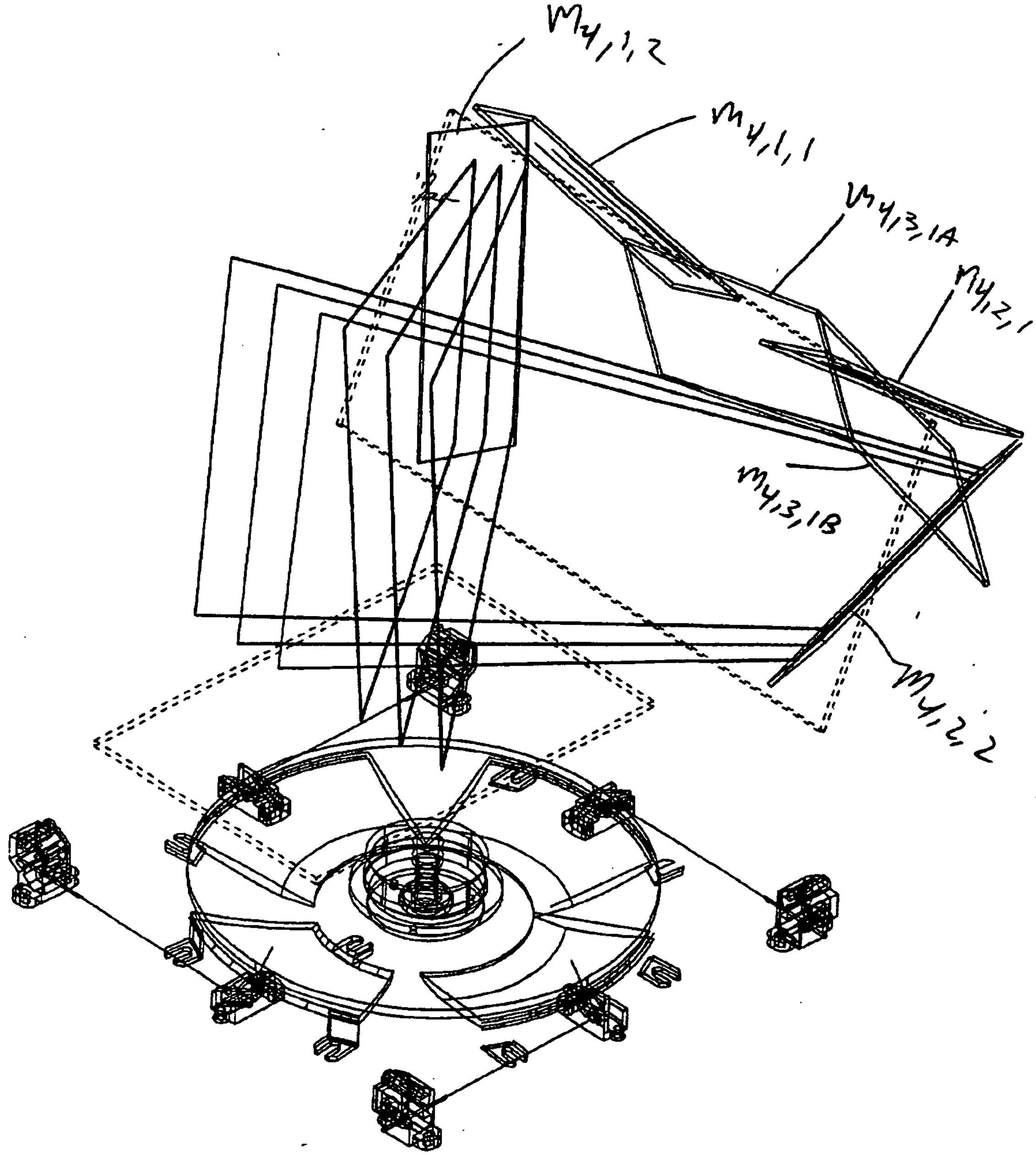

FIG. 5V1

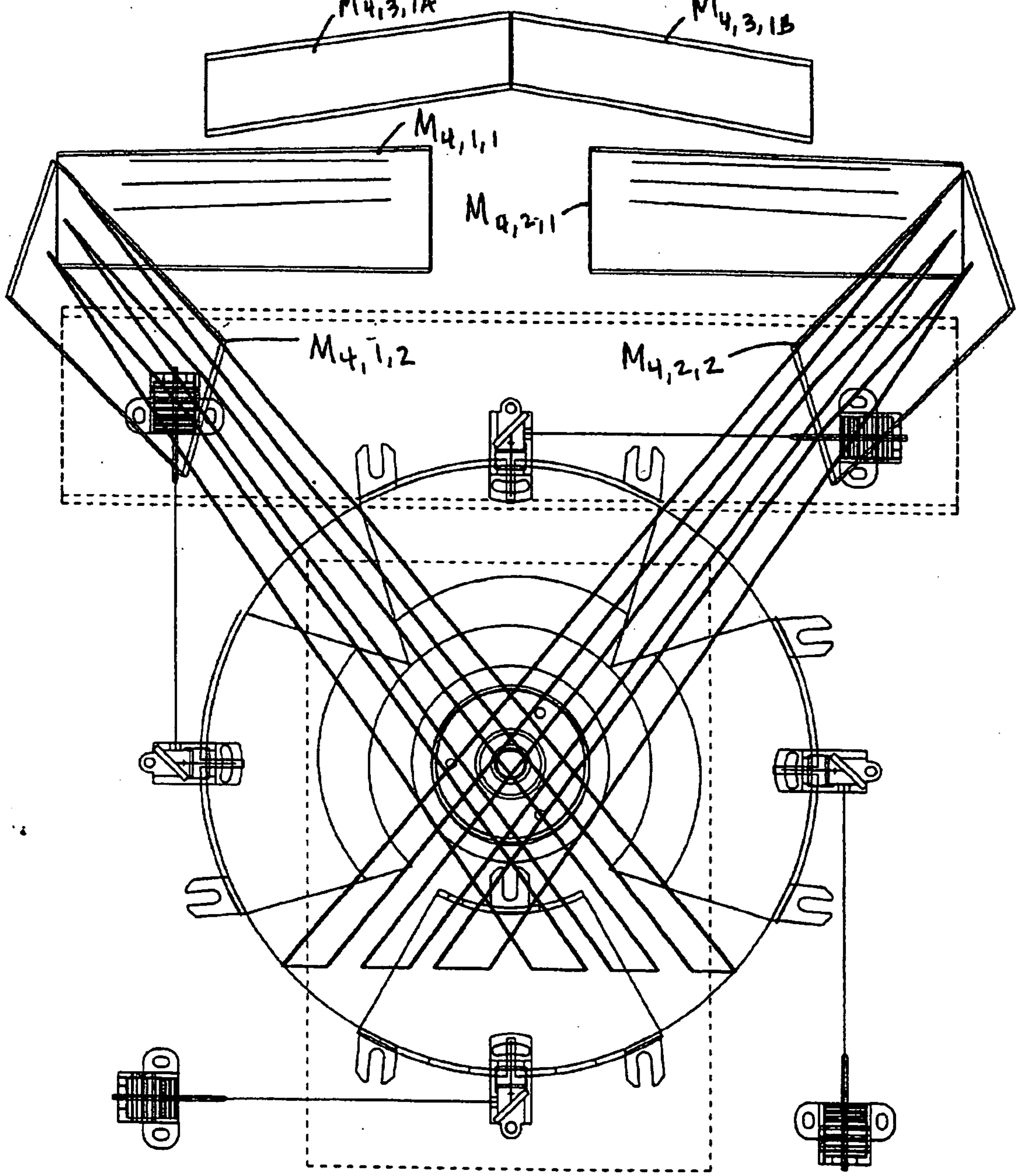

FIG. 5V2

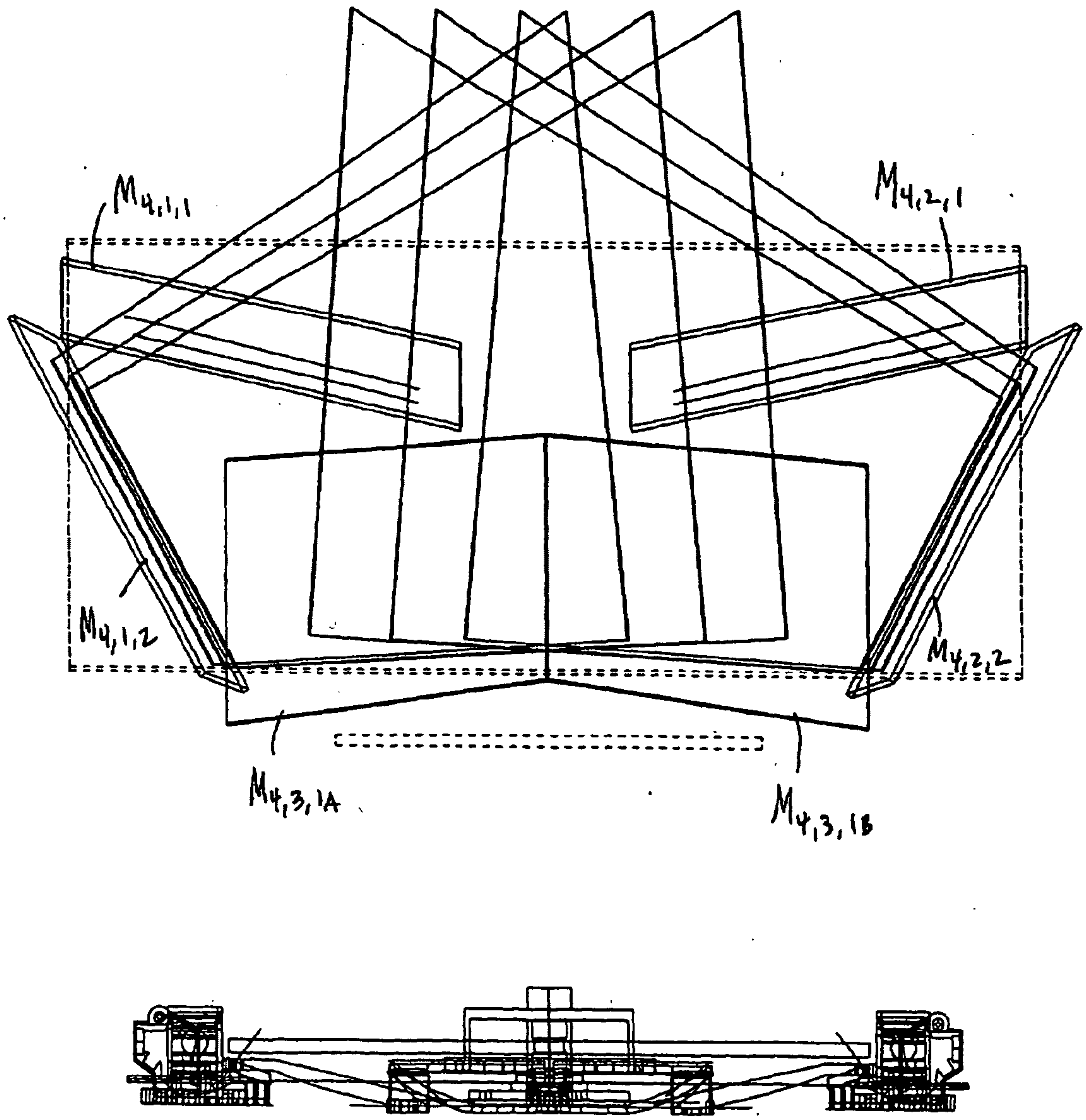

FIG. 5V3

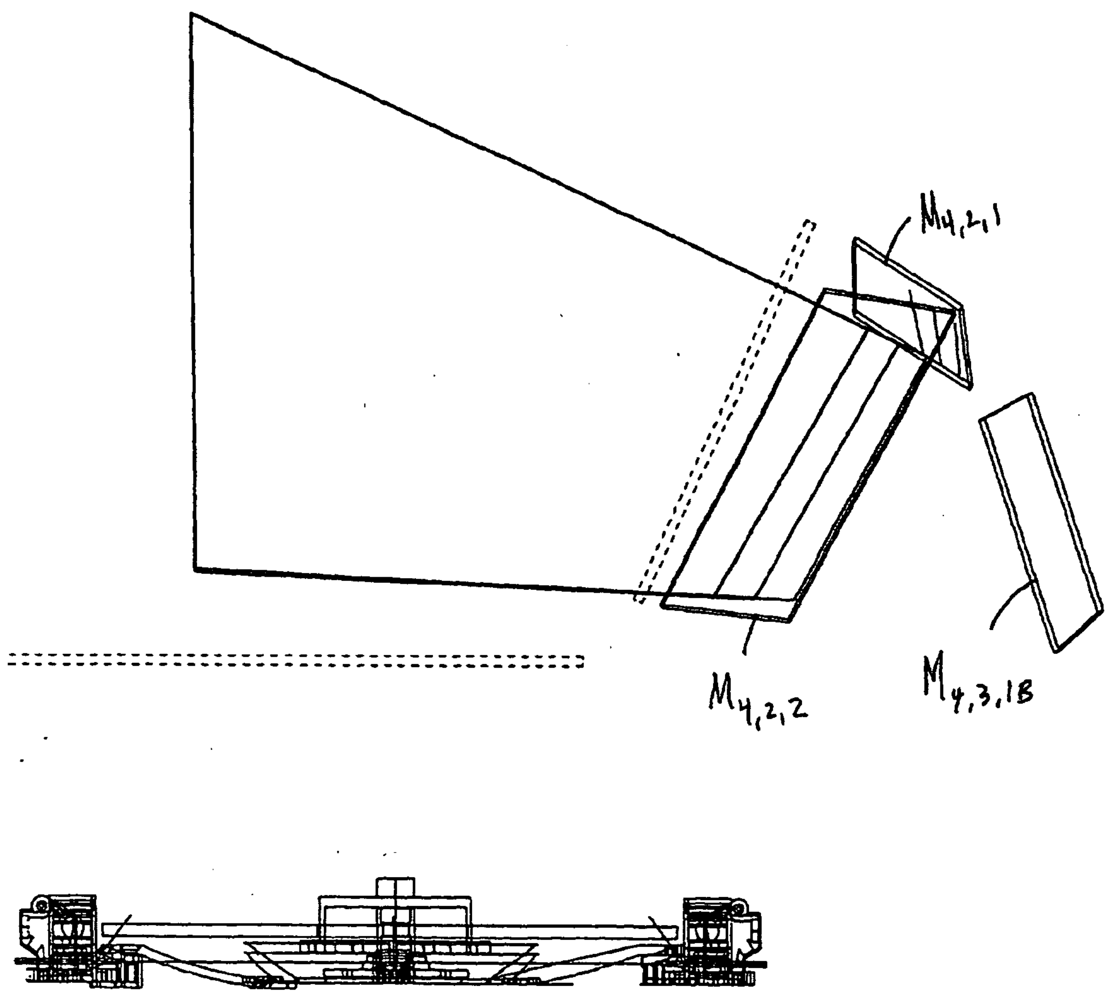

FIG. 5Y4

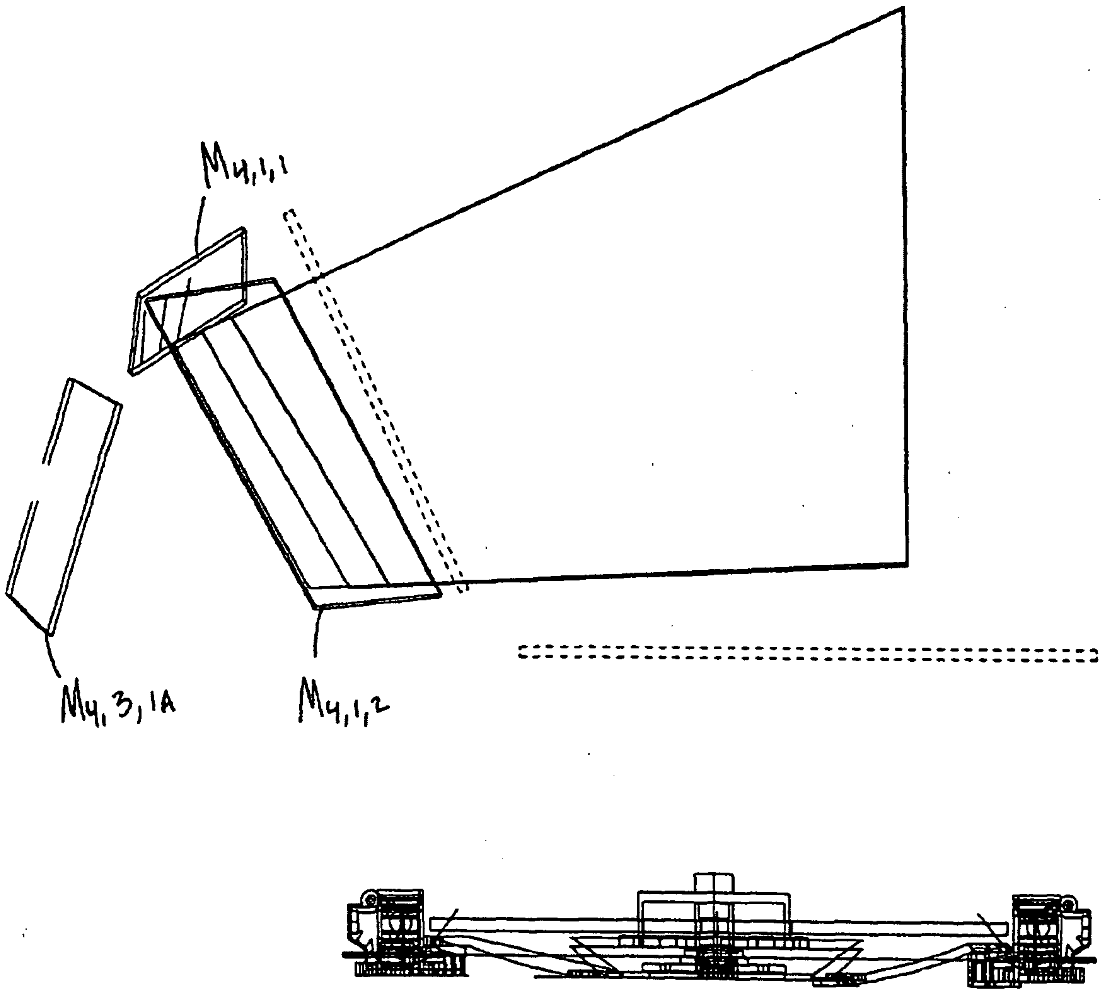

FIG. 5V5

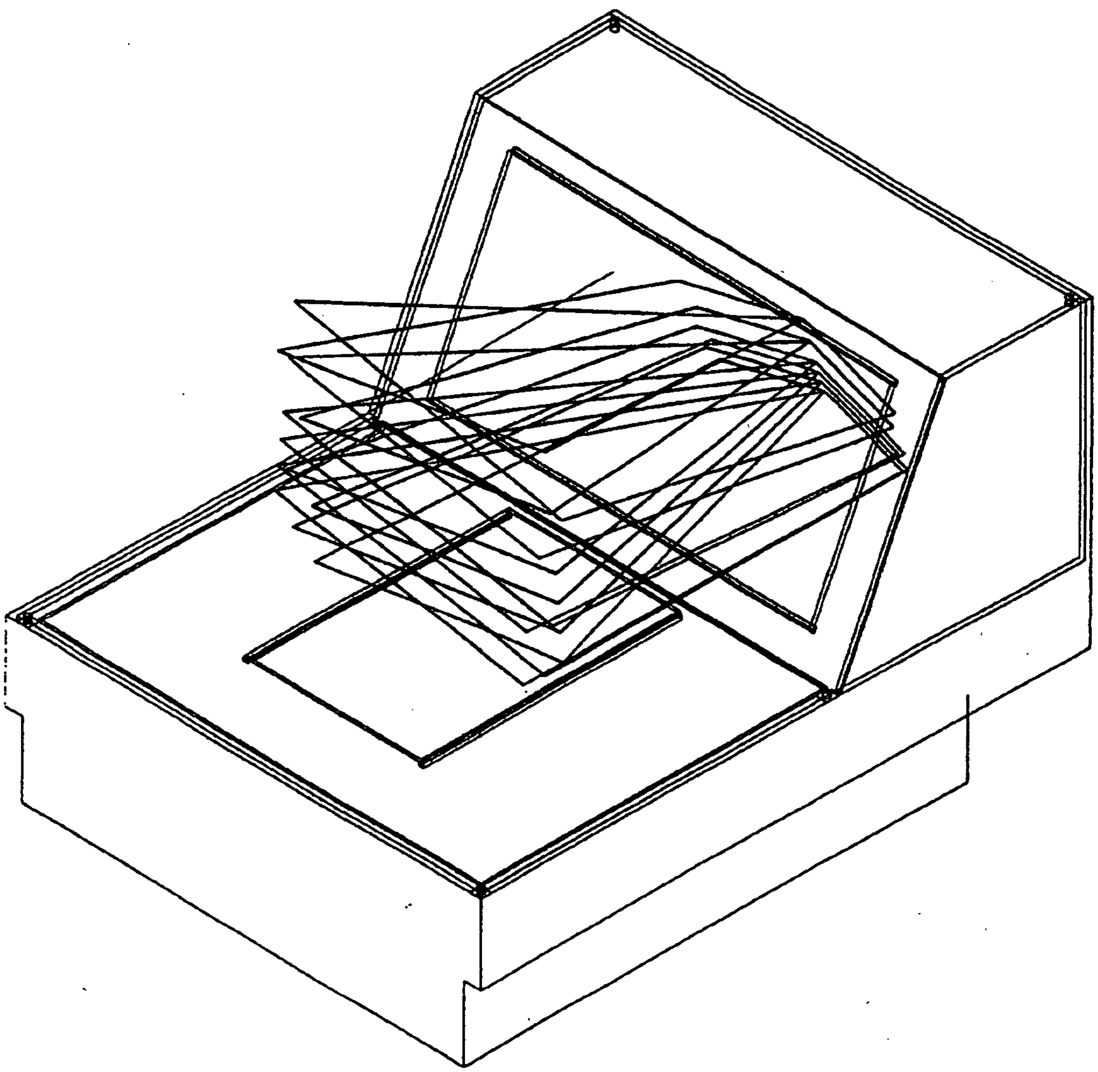

FIG. 5W1

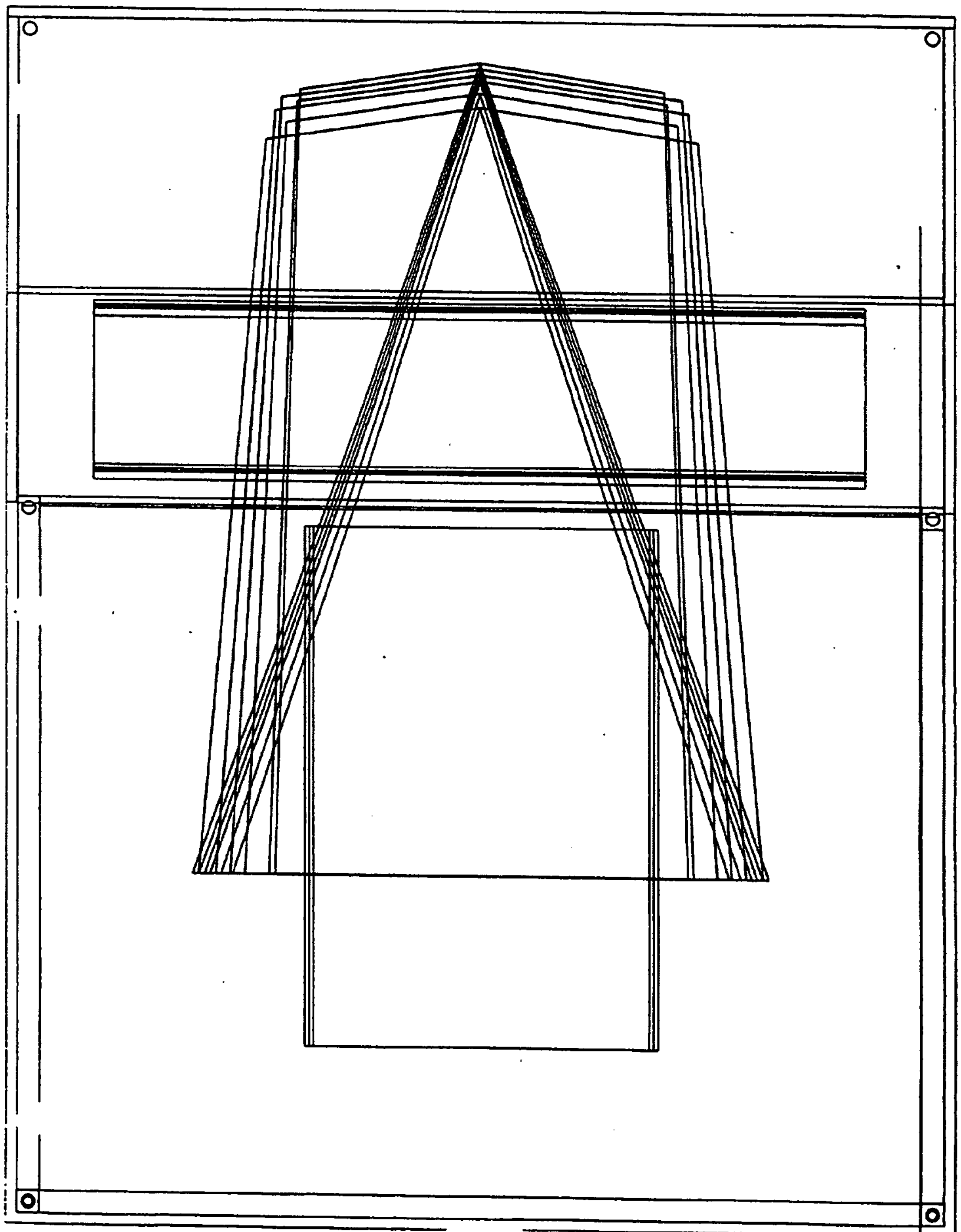

FIG. 5N2

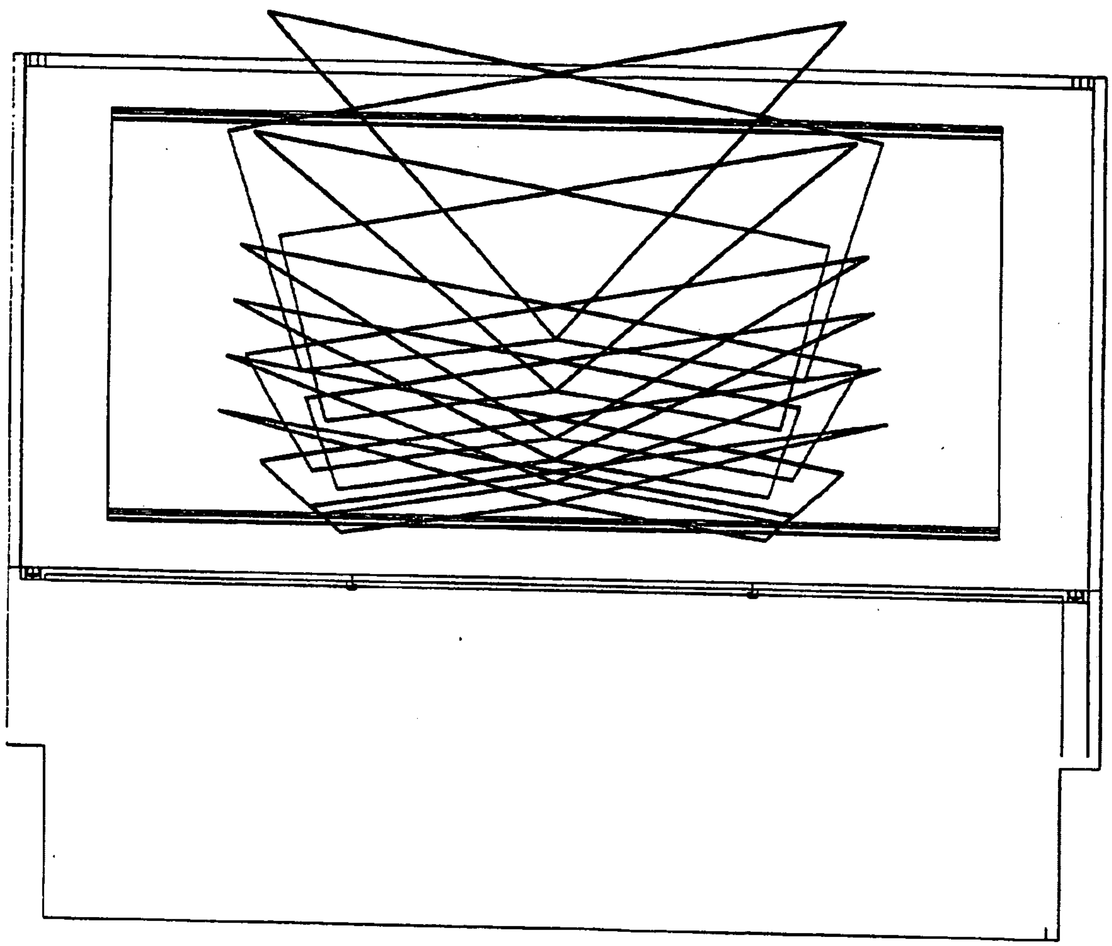

FIG. 5N3

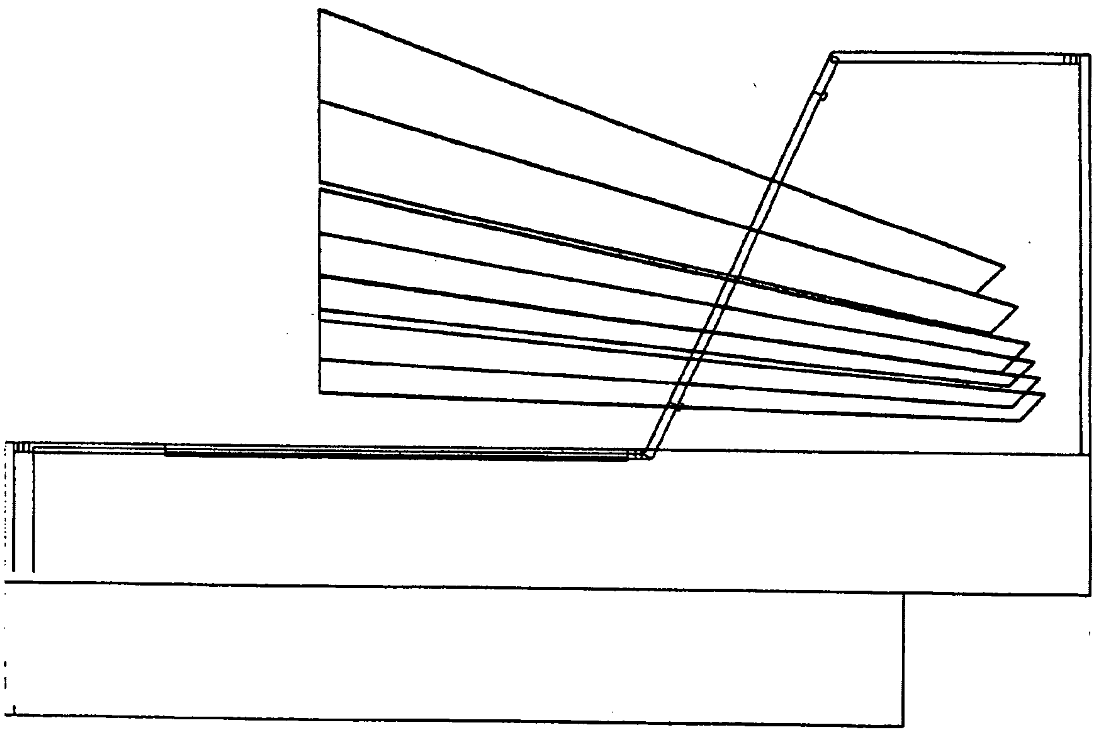

FIG. 5W4

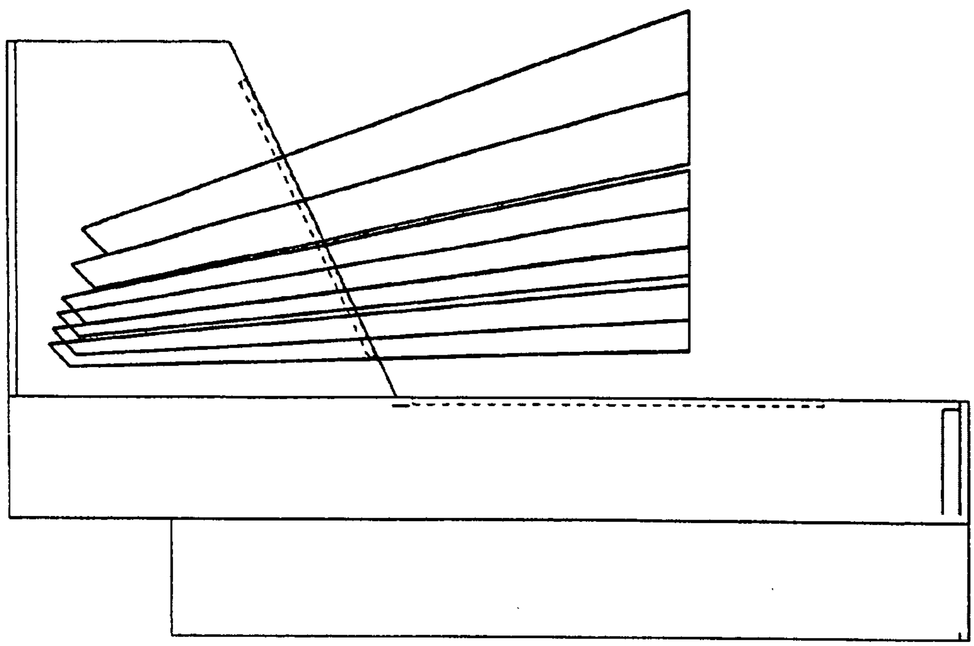

FIG. 5N5

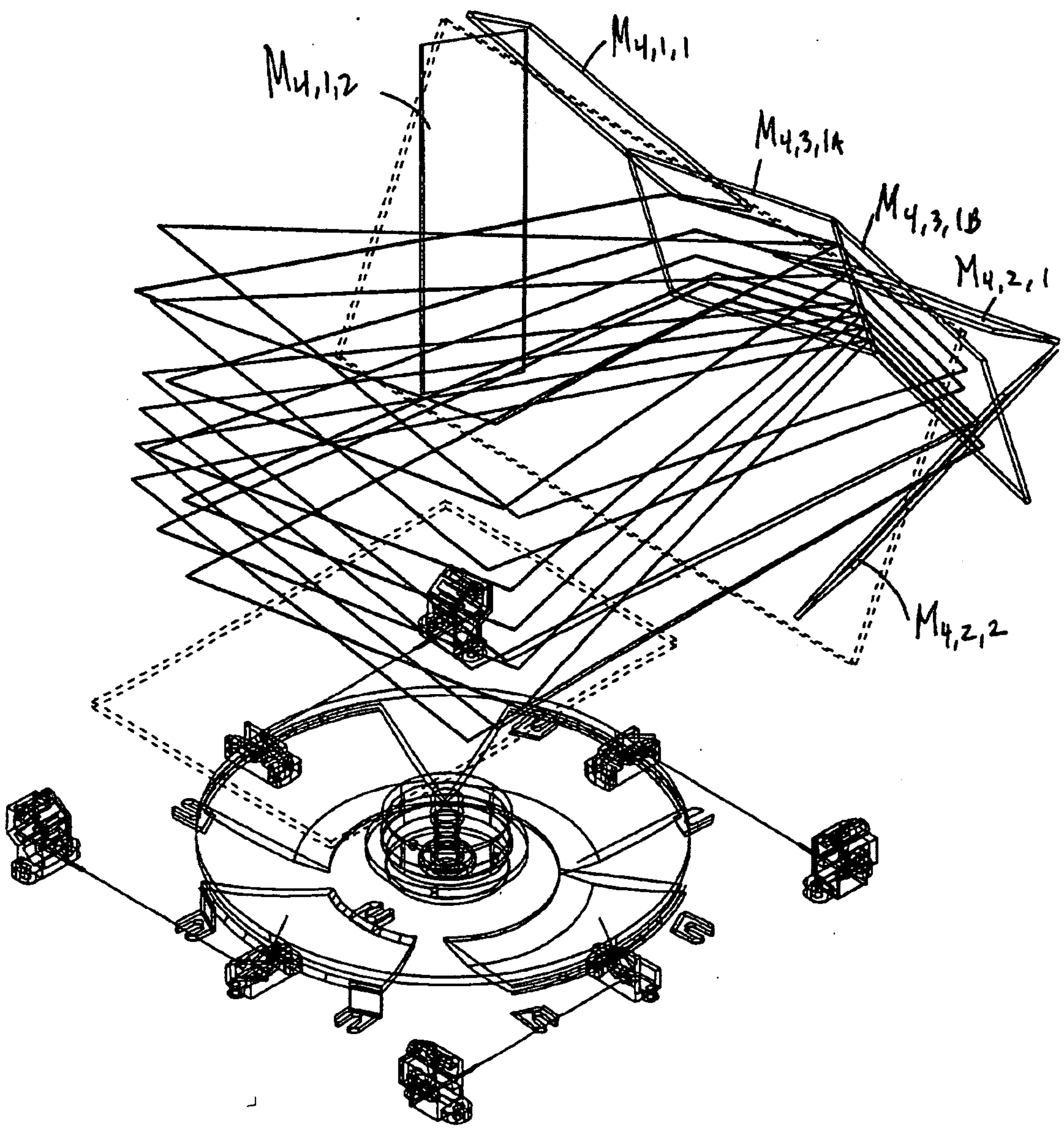

FIG. 5X1

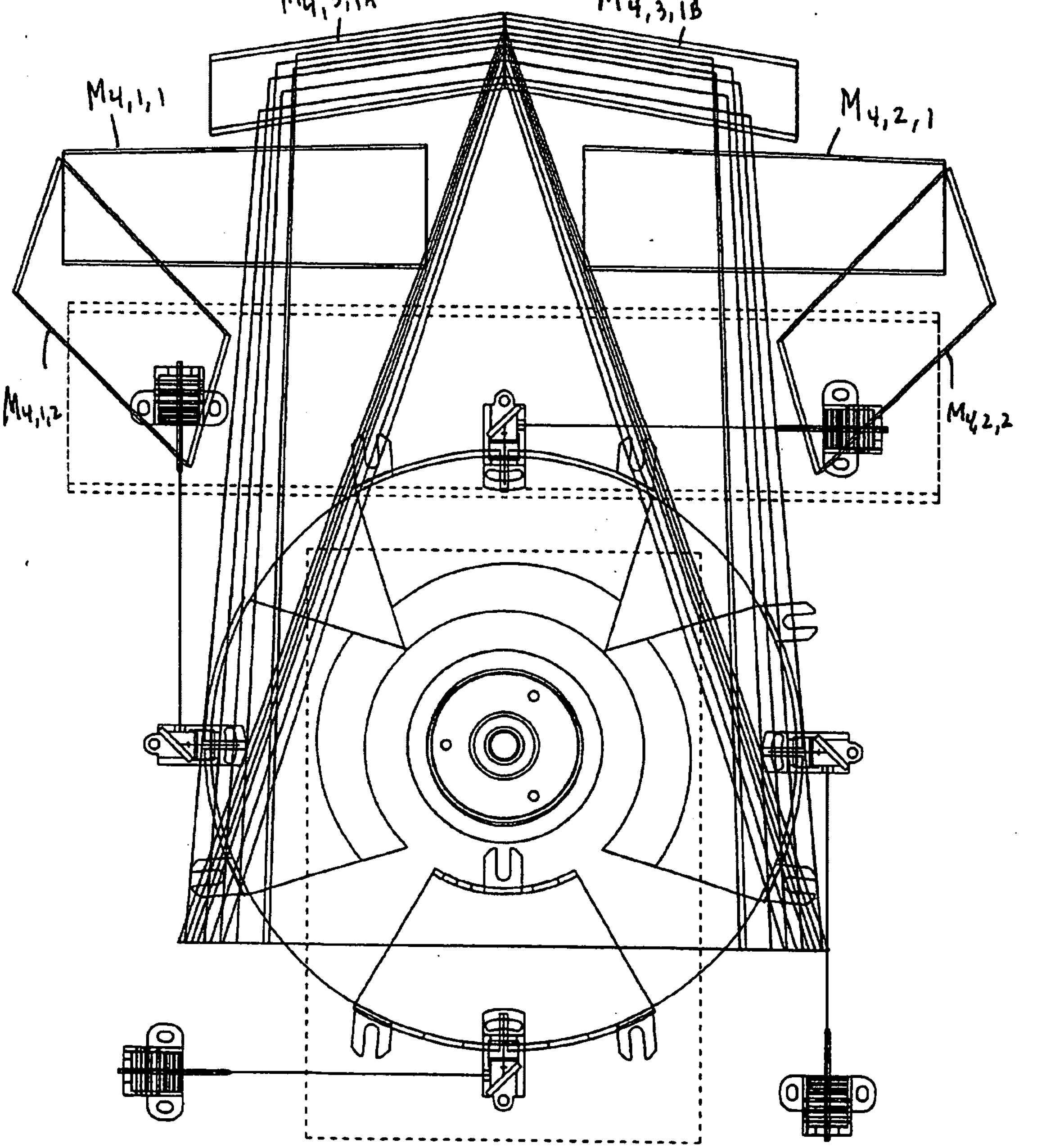

FIG. 5X2

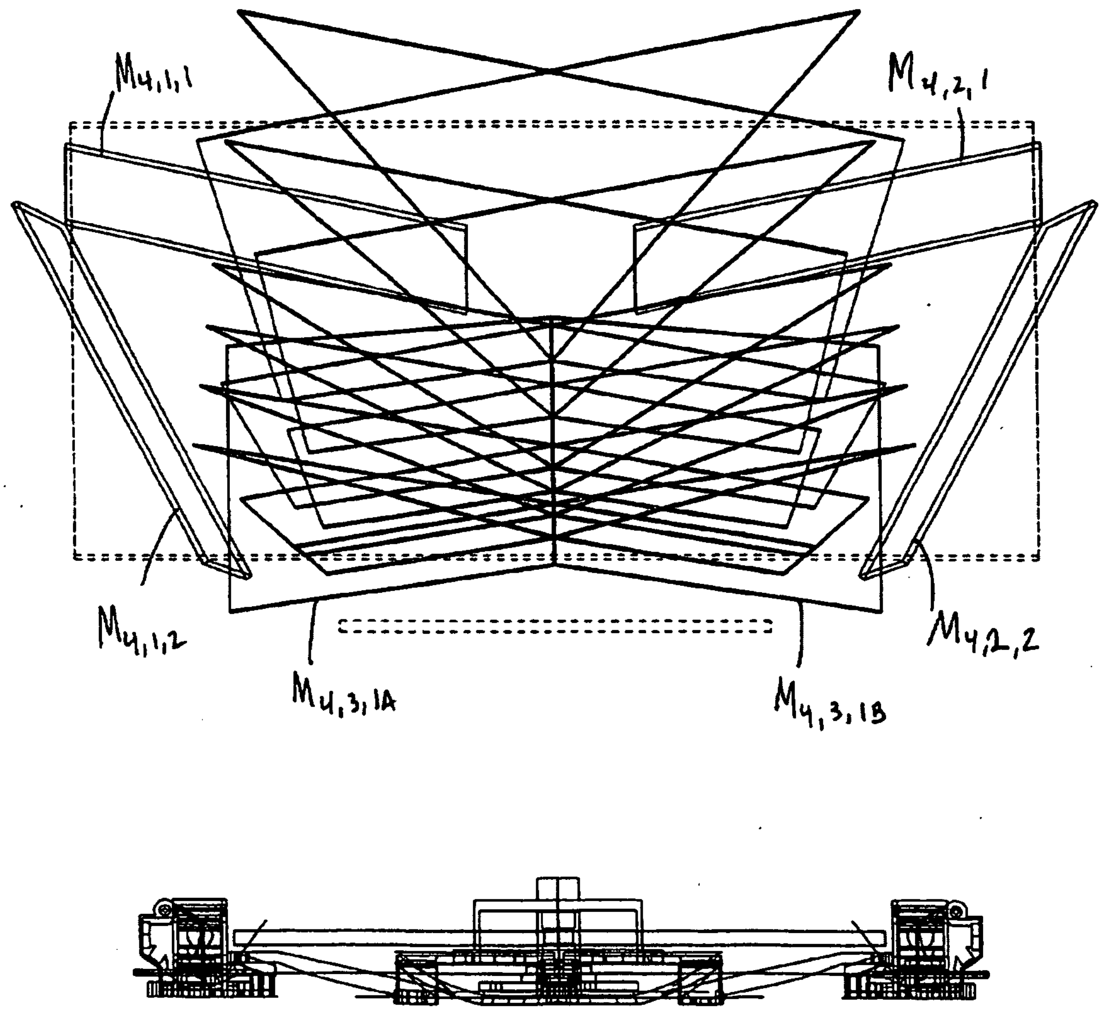

FIG. 5X3

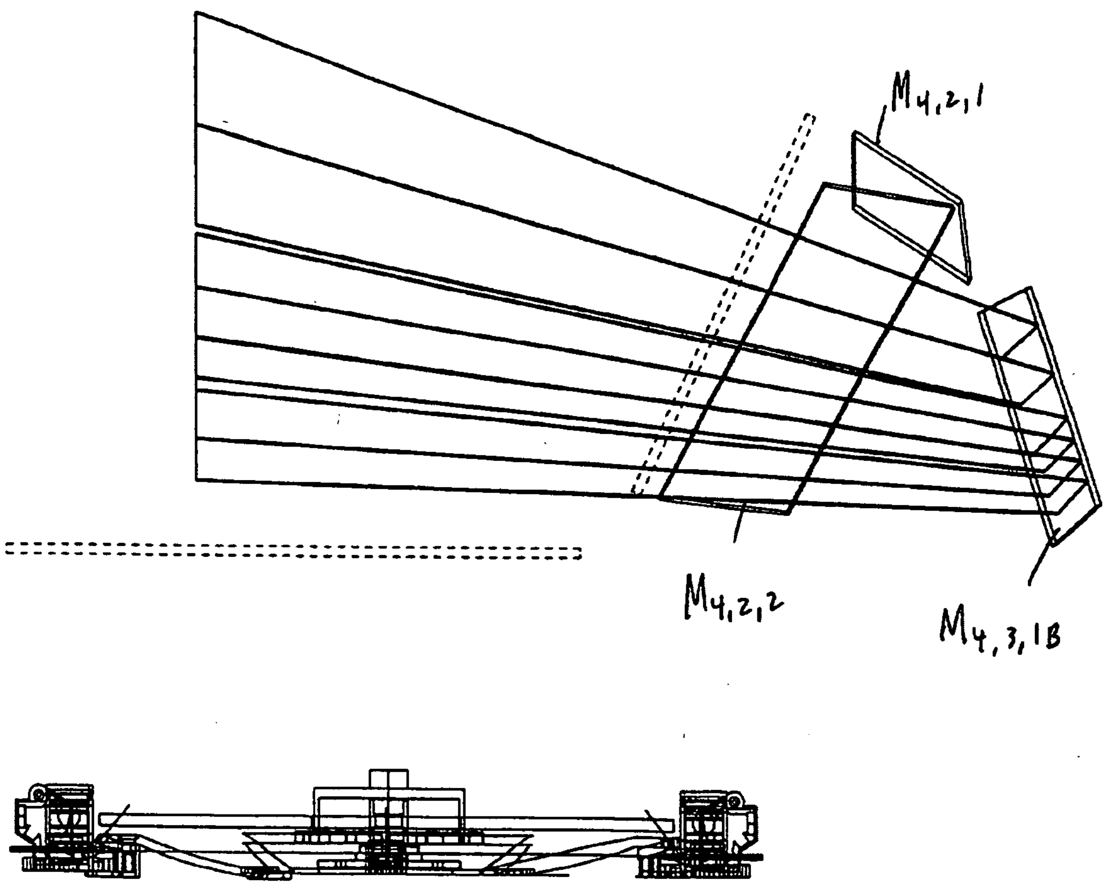

FIG. 5X4

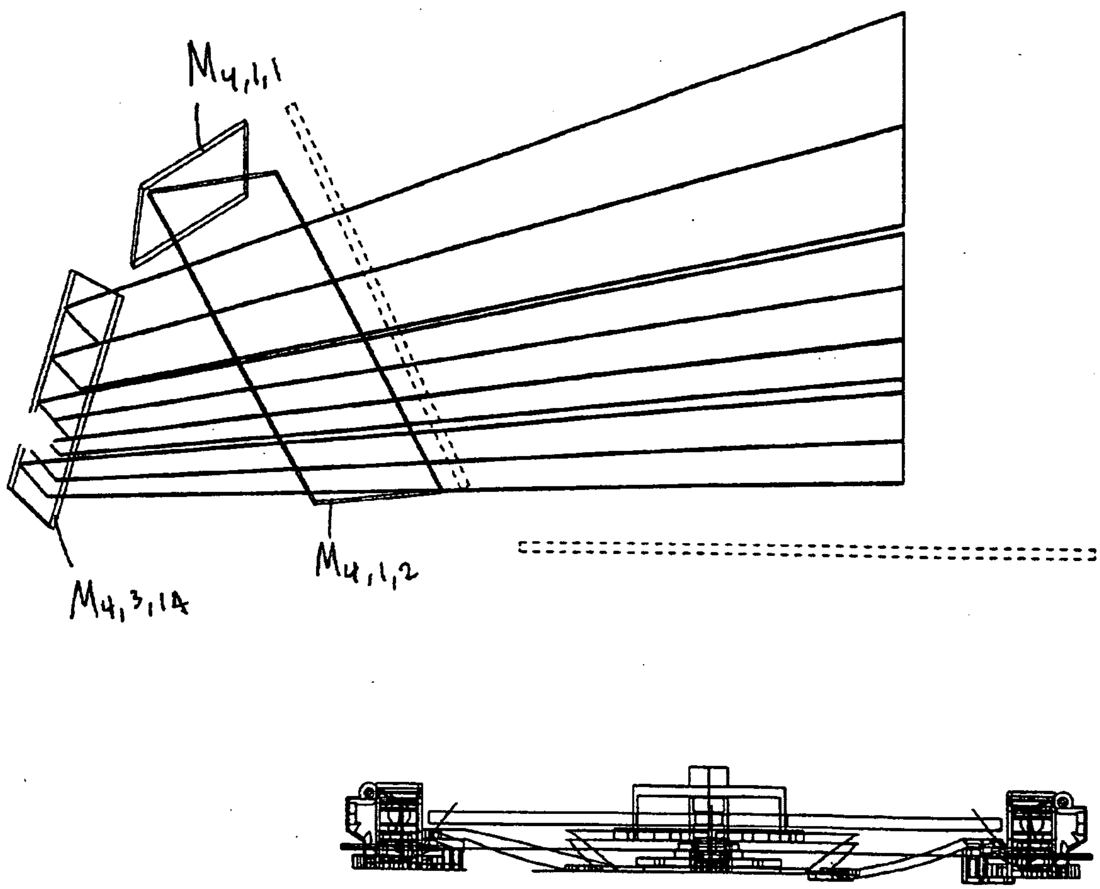

FIG. 5X5

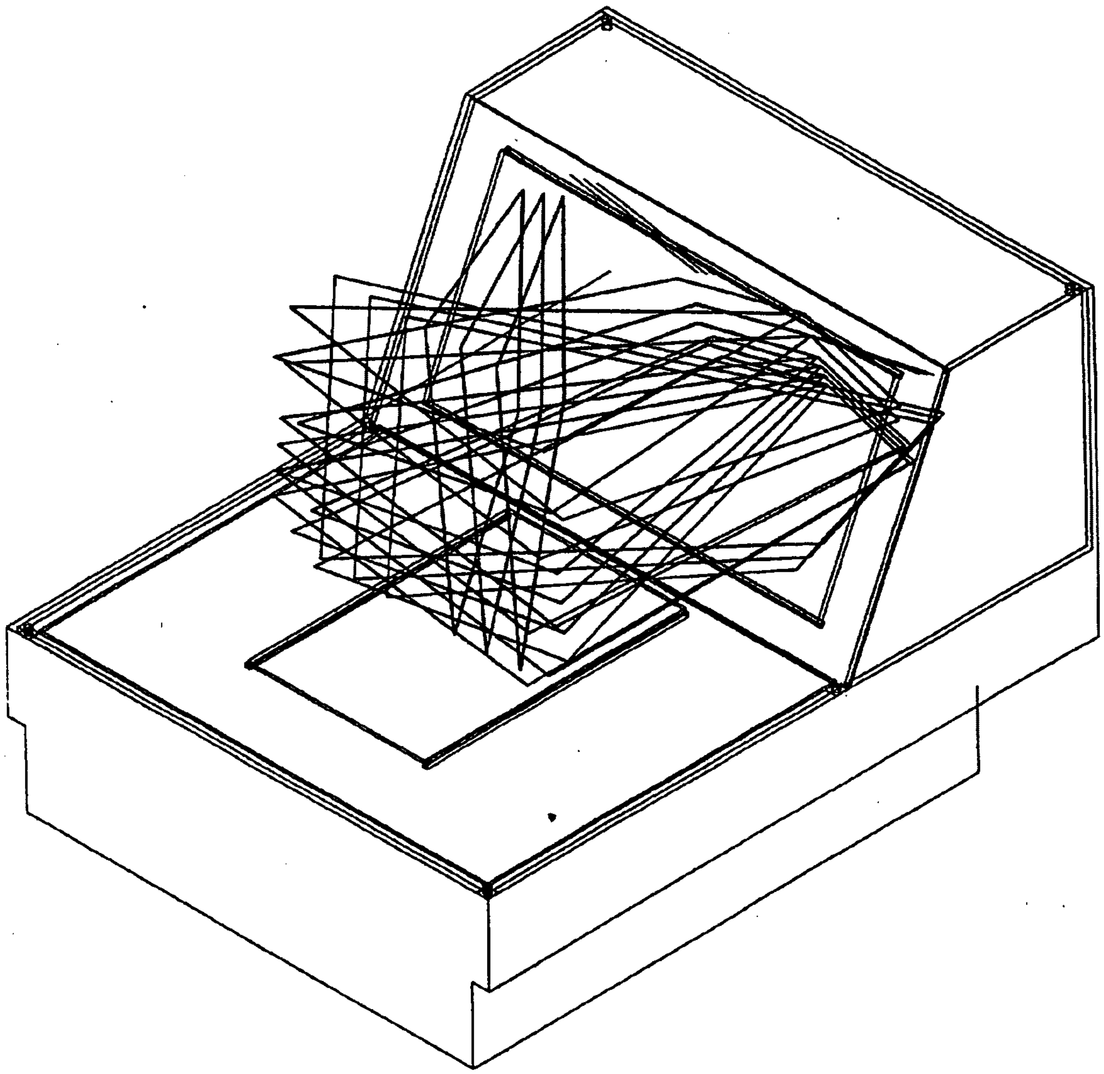

FIG. 5Y1

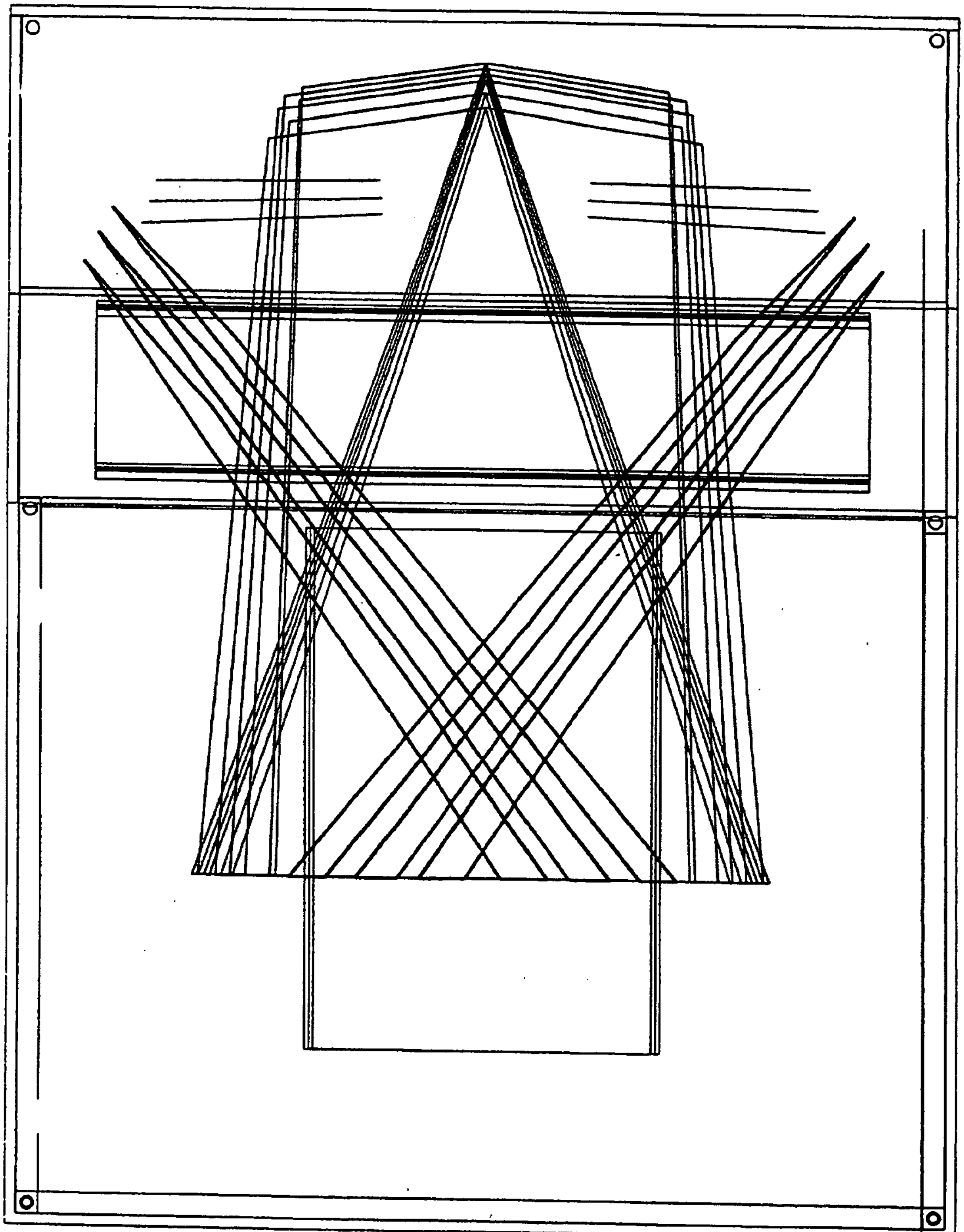

FIG. 5Y2

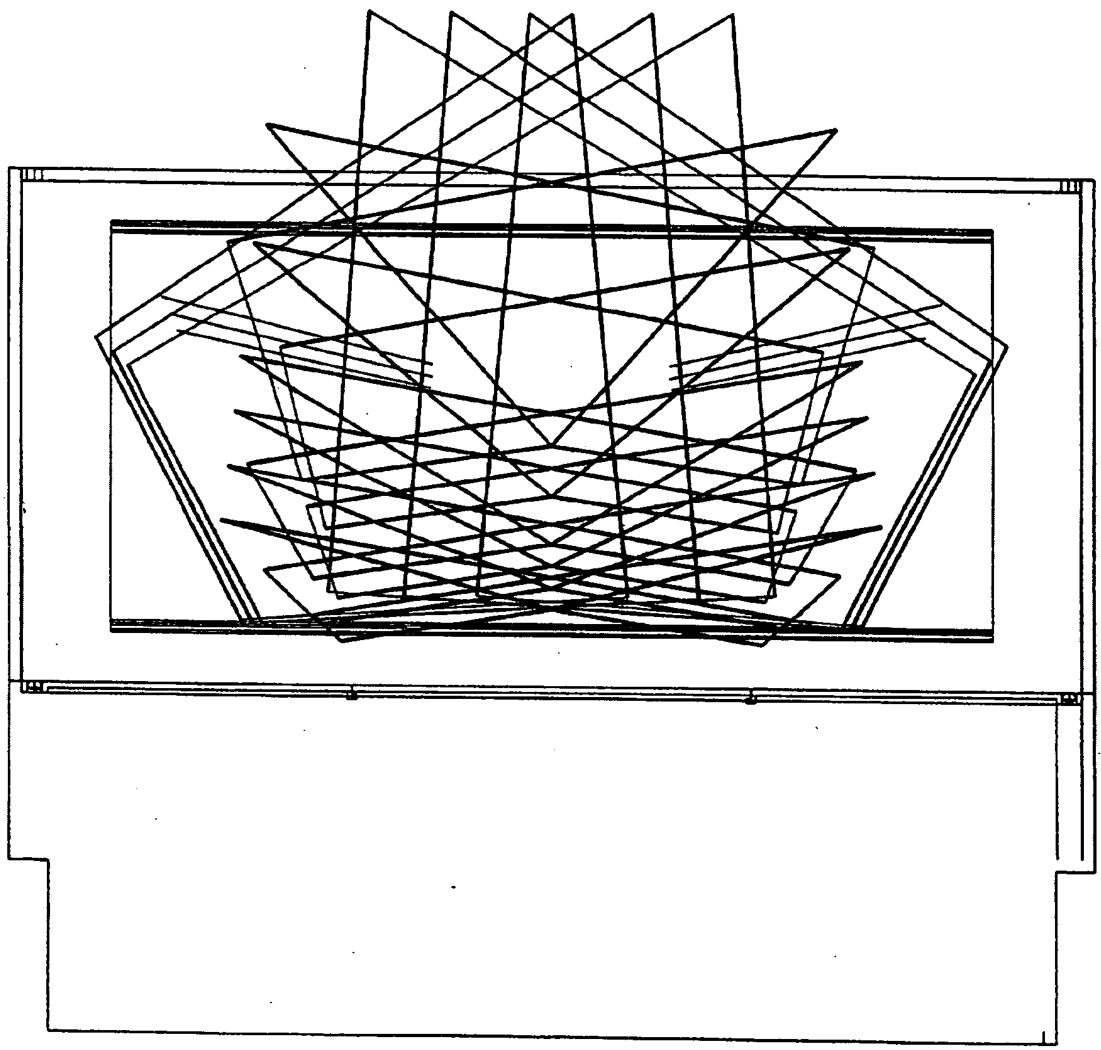

FIG. 5Y3

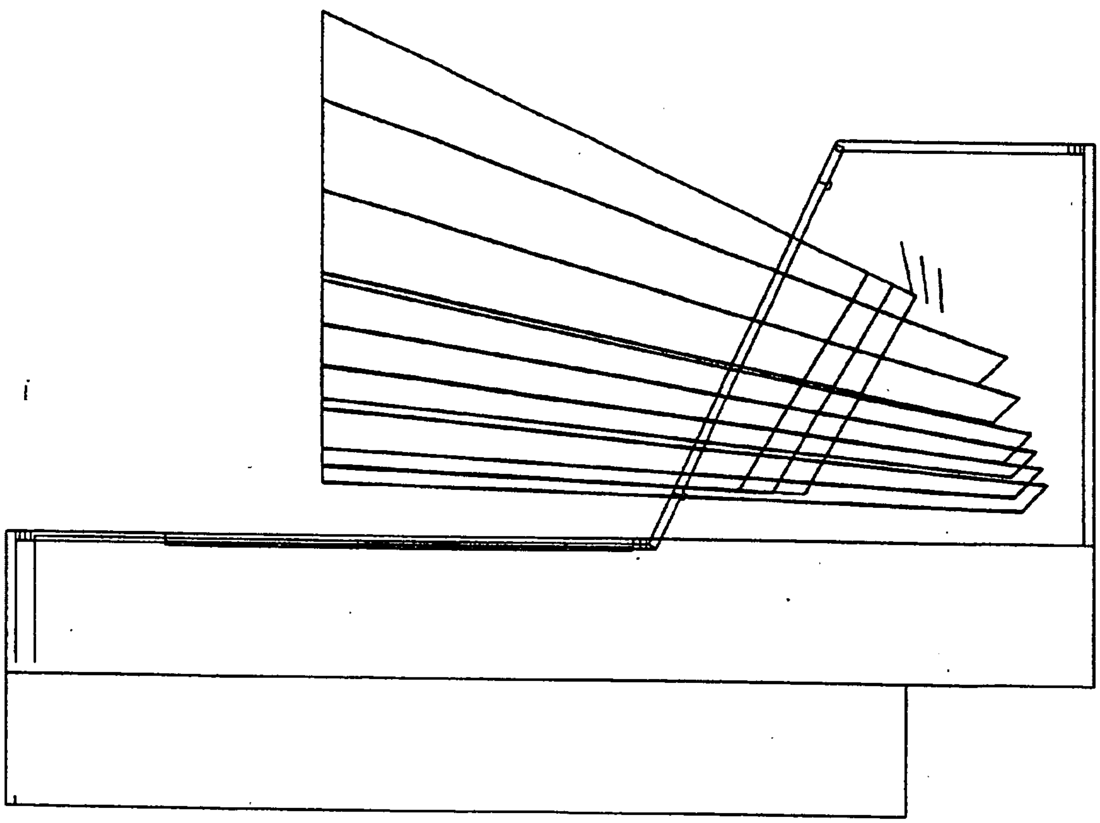

FIG. 5Y4

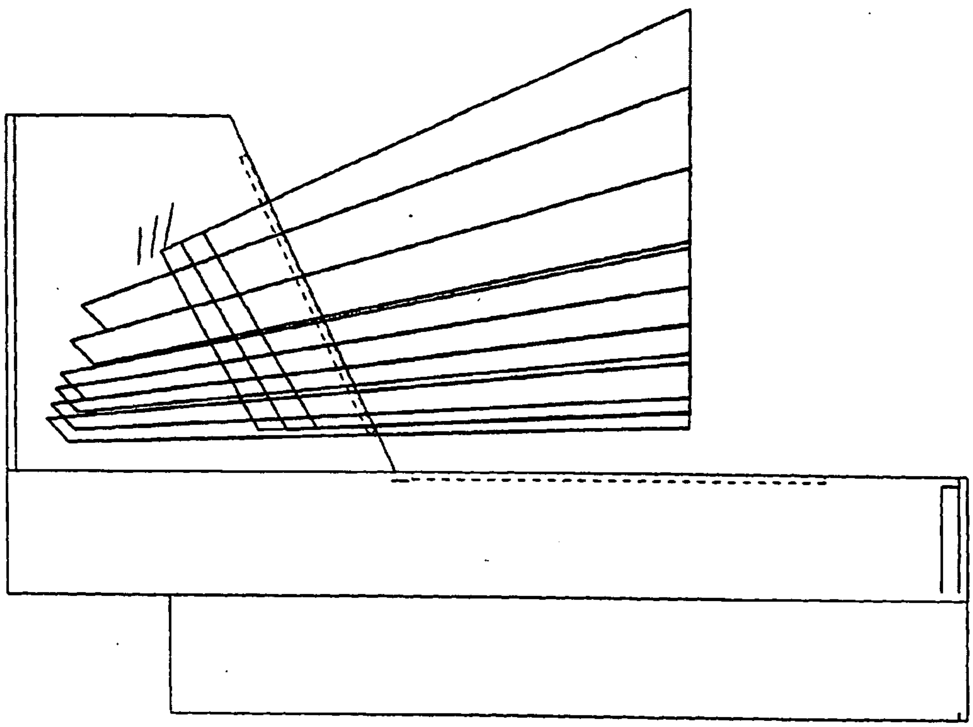

FIG. 5Y5

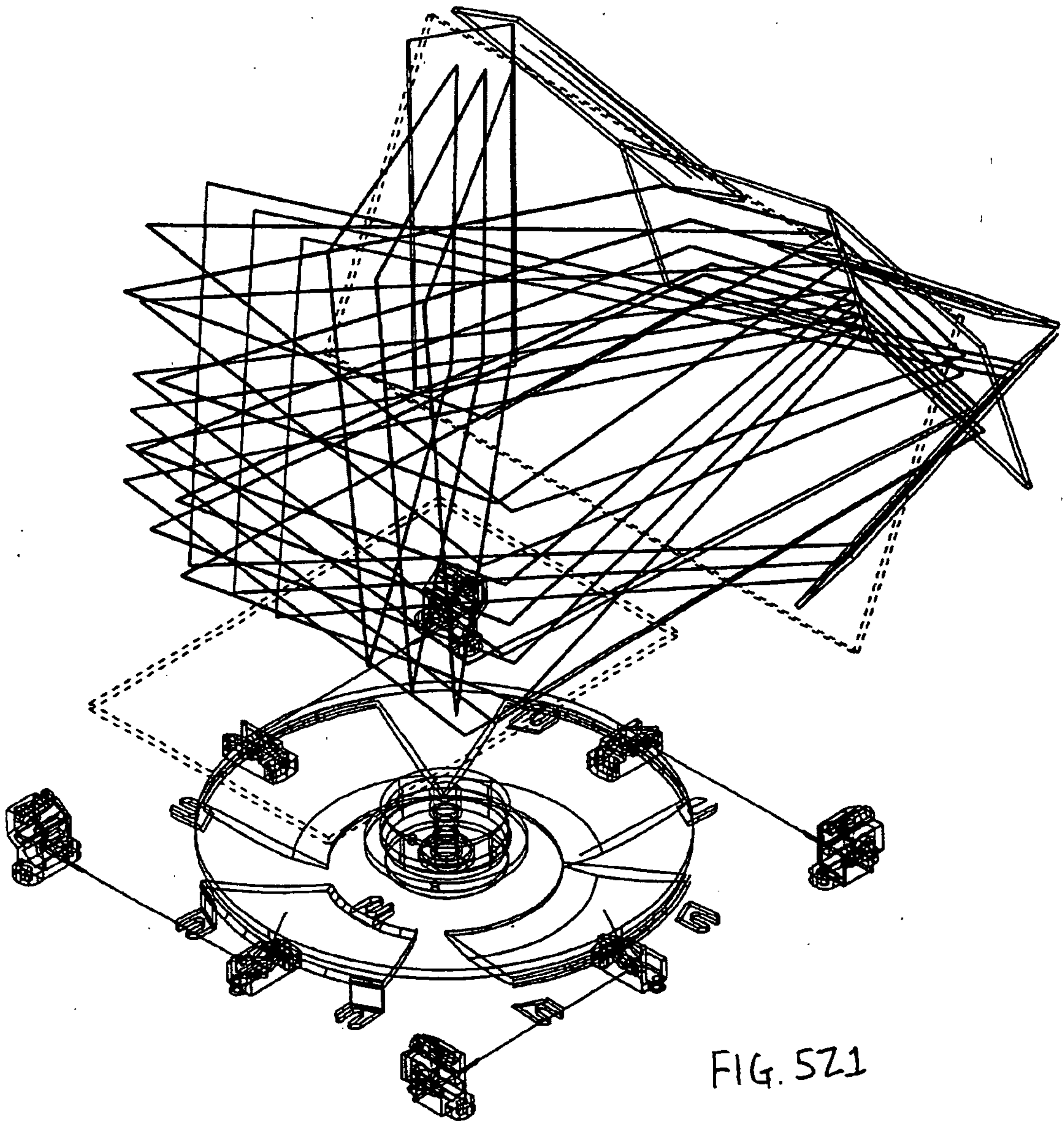

FIG. 521

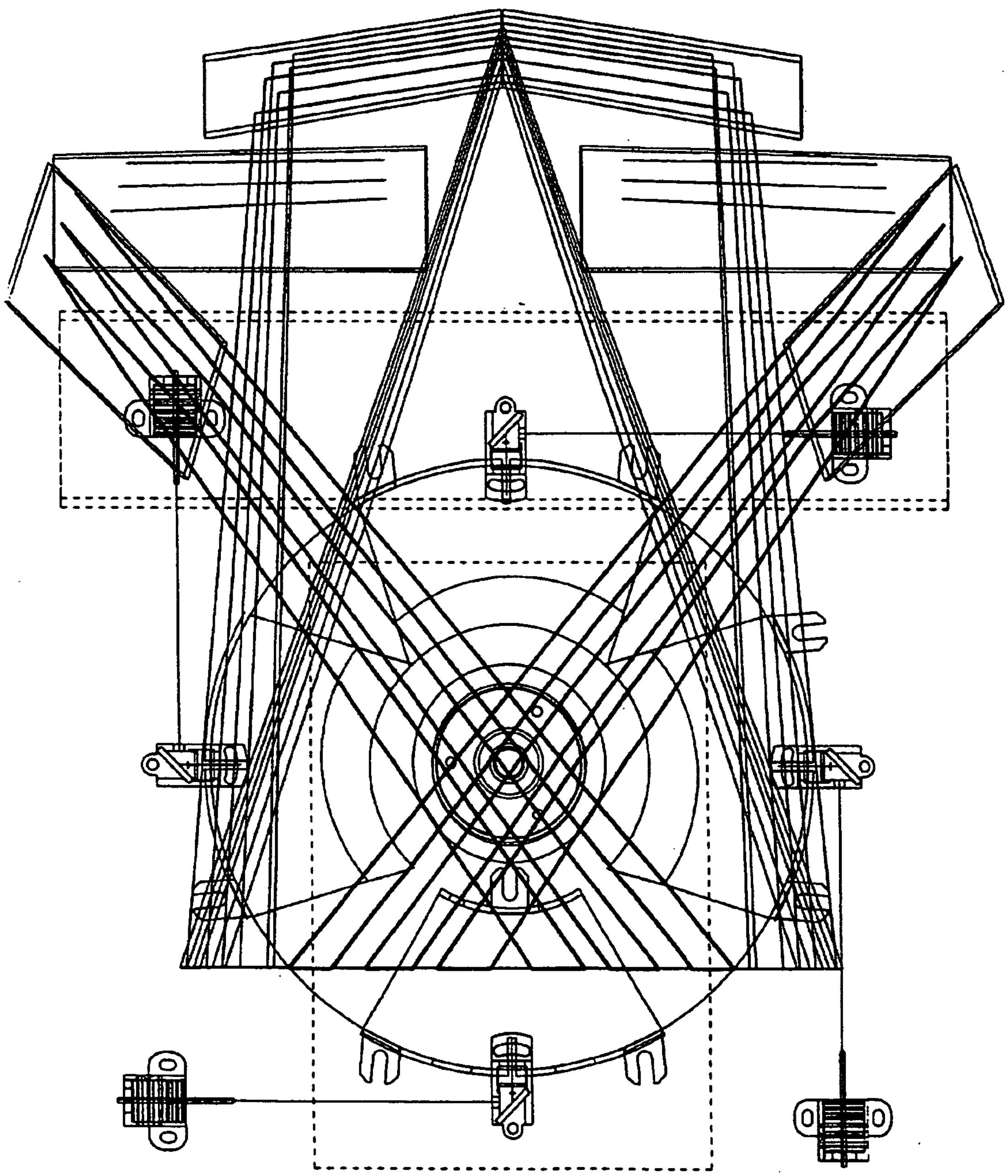

FIG. 522

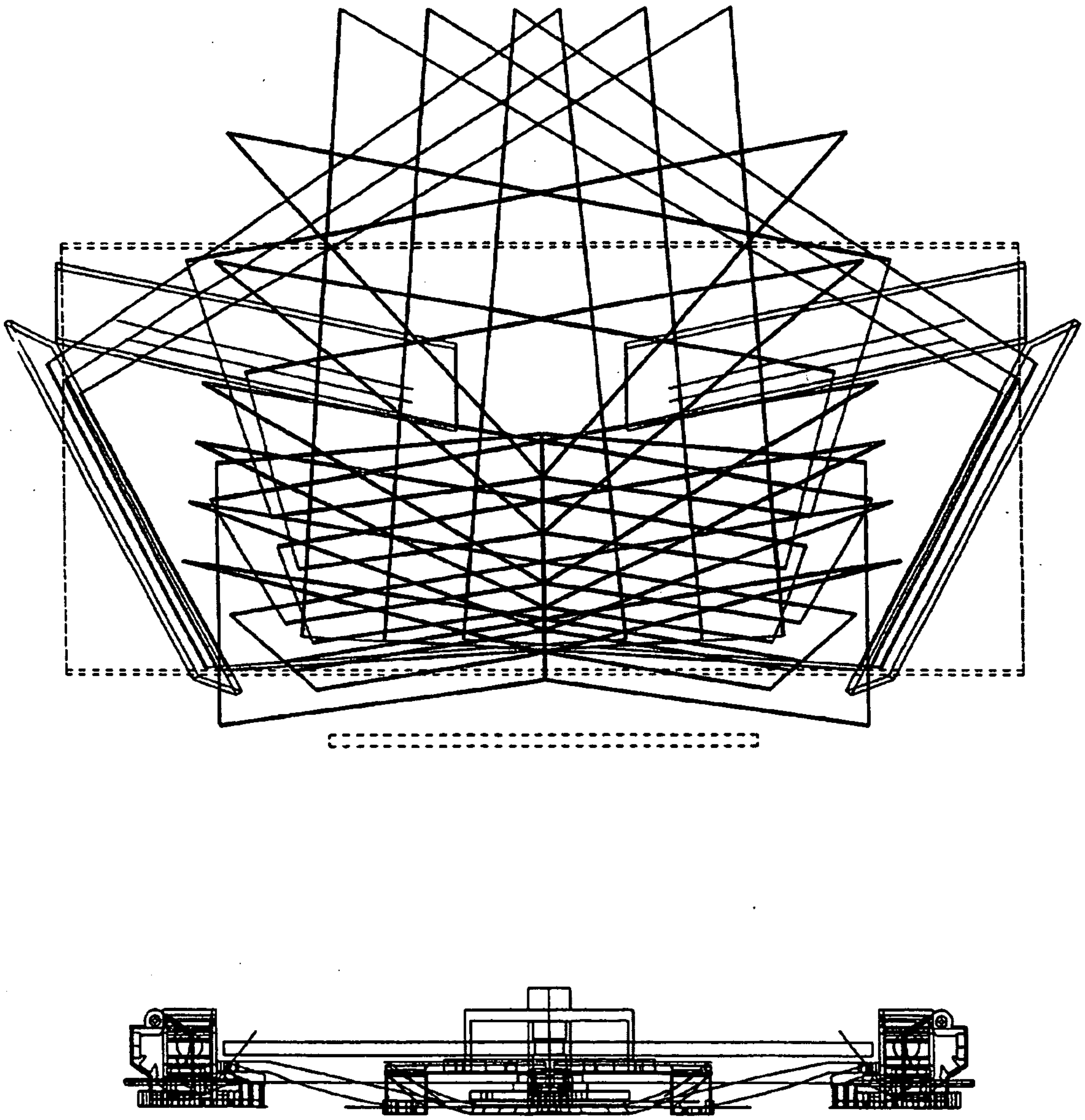

FIG. 523

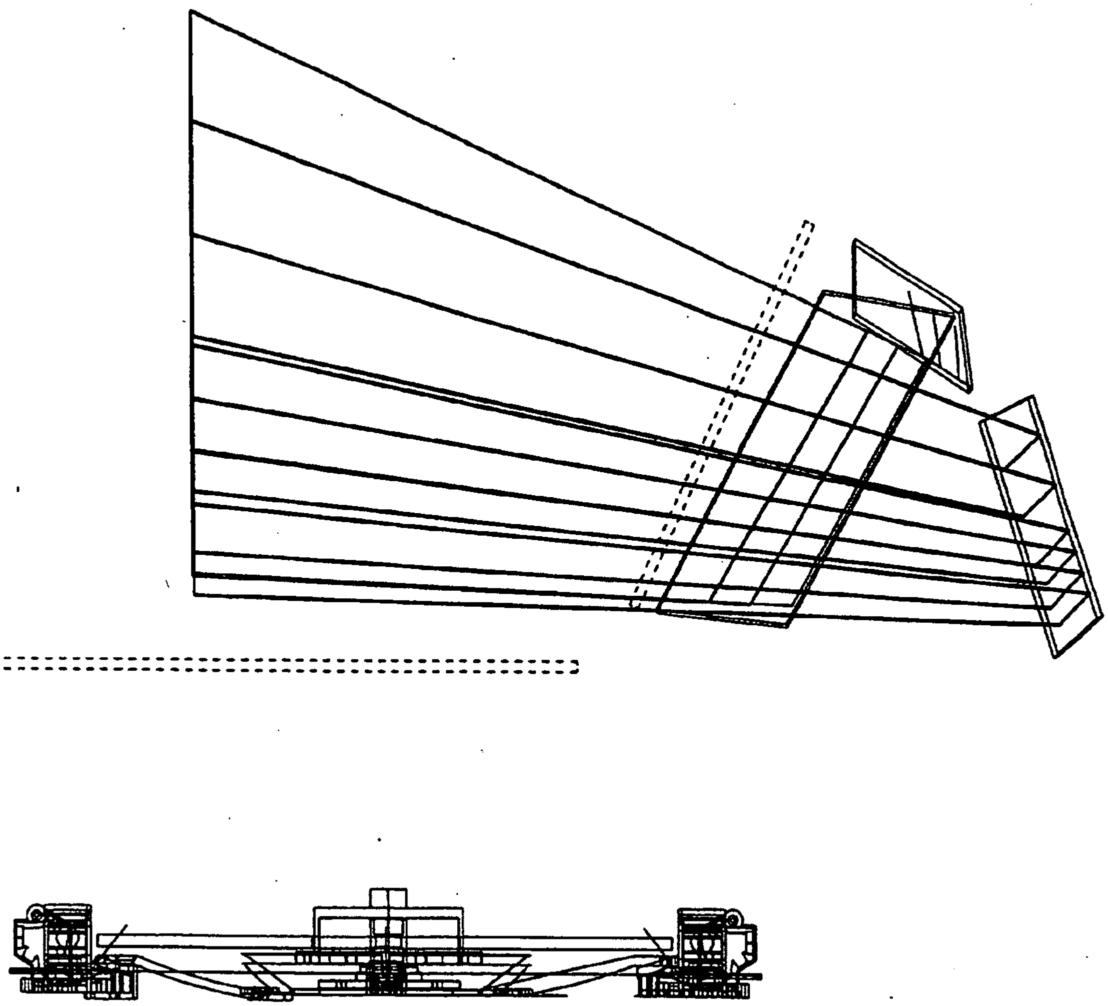

FIG. 524

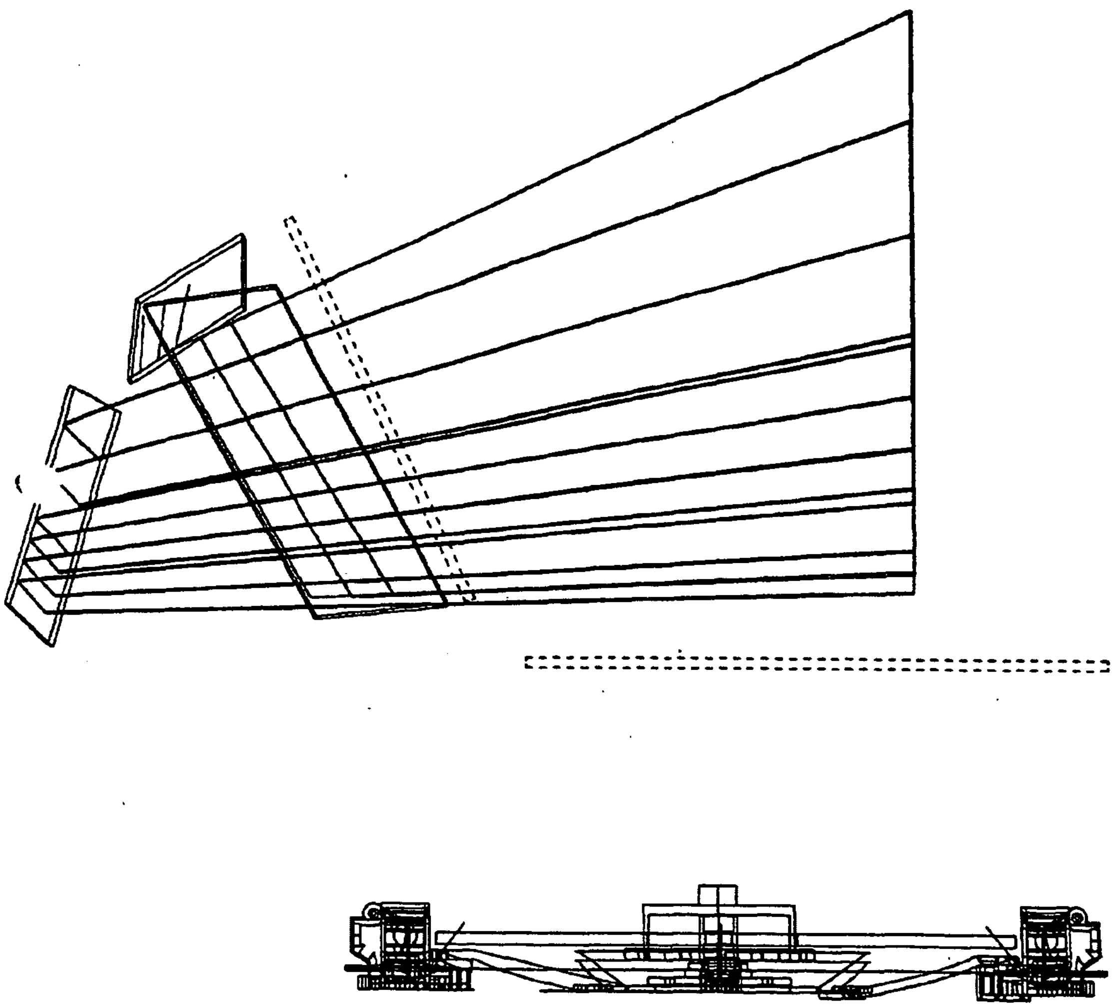

FIG.525

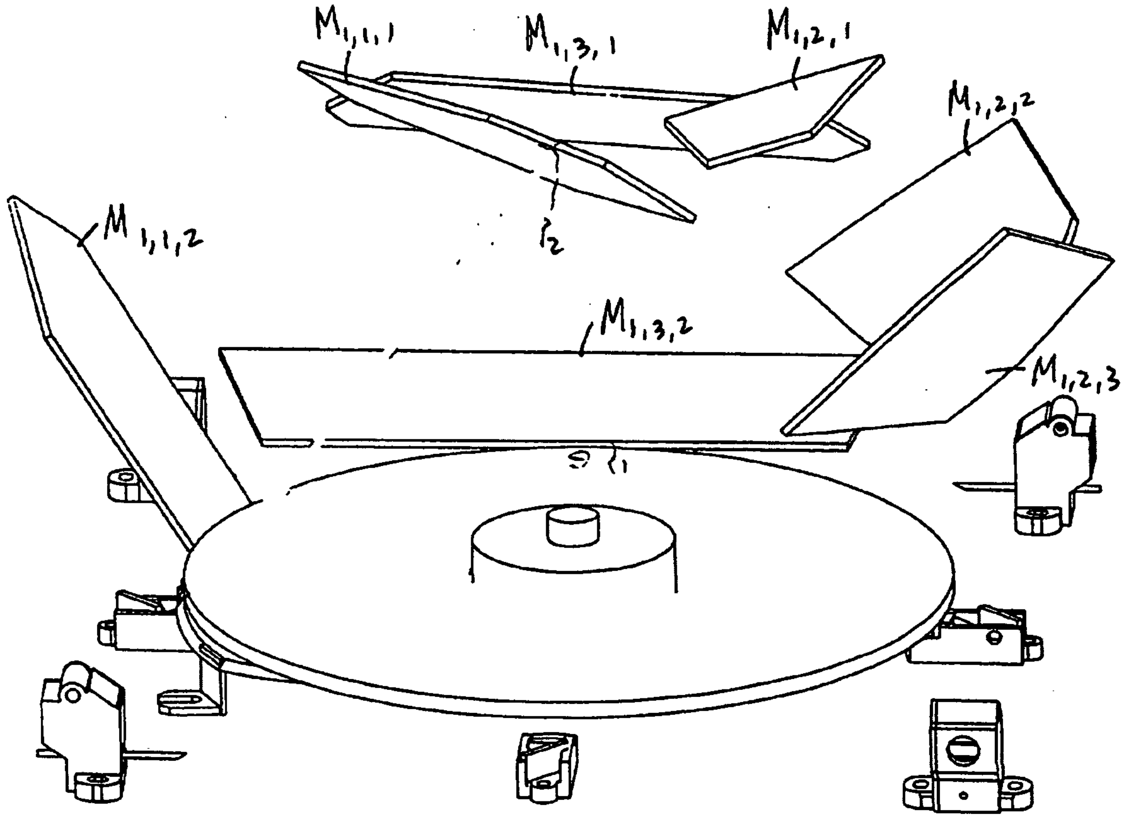

FIG. 6A1

	N	O	P	Q	R	S	T	U	V	W	X
1											
2											
3											
4	Facet	7									
5	x	y	z								
6	-0.616	0.000	0.788								
7	End				Middle				End		
8	x	y	z		x	y	z		x	y	z
9	0.419	0.416	0.807		0.468	0.249	0.848		0.494	0.048	0.868
10	-0.253	0.917	-0.310		-0.316	0.832	-0.455		-0.387	0.704	-0.596
11	-0.469	-0.414	0.781		-0.537	-0.527	0.659		-0.603	-0.626	0.494
12											
13											
14	Mirror 1 Corners				Mirror 2 Corners				Mirror 3 Corners		
15	x	y	z		x	y	z		x	y	z
16	3.900	2.436	2.770		1.700	4.102	1.300				
17	4.100	1.879	2.400		3.300	4.400	1.980				
18	3.800	0.137	1.800		3.400	3.990	1.500				
19	3.150	-0.737	1.800		2.300	2.427	-0.625				
20	2.500	-0.159	2.450		1.700	2.524	-0.625				
21	2.650	0.757	2.770		1.050	3.101	-0.050				
22											
23											
24											

FIG. 6A2

Station 1

	A	B	C	D	E	F	G	H	I	J	K	L
1	Station 1											
2												
3												
4	High Elevation Left Skew	Facet	9									
5	(G2)	x	y	z								
6	Vector from Module	-0.616	0.000	0.788								
7			End				Middle				End	
8		x	y	z		x	y	z		x	y	z
9	Output Vectors From Disk	0.378	0.445	0.812		0.441	0.235	0.866		0.464	0.068	0.883
10	First Mirror Reflected Directions	-0.269	0.927	-0.263		-0.349	0.823	-0.448		-0.408	0.717	-0.565
11	Second Mirror Reflected Directions	-0.479	-0.367	0.797		-0.566	-0.512	0.647		-0.621	-0.595	0.510
12	Third Mirror Reflected Directions											
13												
14			Mirror 1 Corners				Mirror 2 Corners				Mirror 3 Corners	
15		x	y	z		x	y	z		x	y	z
16	1	3.900	2.436	2.770		1.700	4.102	1.300				
17	2	4.100	1.879	2.400		3.300	4.400	1.980				
18	3	3.800	0.137	1.800		3.400	3.990	1.500				
19	4	3.150	-0.737	1.800		2.300	2.427	-0.625				
20	5	2.500	-0.159	2.450		1.700	2.524	-0.625				
21	6	2.650	0.757	2.770		1.050	3.101	-0.050				
22	7											
23	8											

FIG. 6A3

	Z	AA	AB	AC	AD	AE	AF	AG	AH	AI	AJ
1											
2											
3											
4	Facet	11									
5	x	y	z								
6	-0.616	0.000	0.788								
7		End				Middle				End	
8	x	y	z		x	y	z		x	y	z
9	0.333	0.476	0.814		0.415	0.220	0.883		0.433	0.086	0.897
10	-0.284	0.935	-0.211		-0.382	0.813	-0.440		-0.429	0.728	-0.535
11	-0.487	-0.316	0.814		-0.594	-0.496	0.633		-0.638	-0.564	0.524
12											
13											
14	Mirror 1 Corners				Mirror 2 Corners				Mirror 3 Corners		
15	x	y	z		x	y	z		x	y	z
16	3.900	2.436	2.770		1.700	4.102	1.300				
17	4.100	1.879	2.400		3.300	4.400	1.980				
18	3.800	0.137	1.800		3.400	3.990	1.500				
19	3.150	-0.737	1.800		2.300	2.427	-0.625				
20	2.500	-0.159	2.450		1.700	2.524	-0.625				
21	2.650	0.757	2.770		1.050	3.101	-0.050				
22											
23											
24											

FIG. 6A4

Station 1

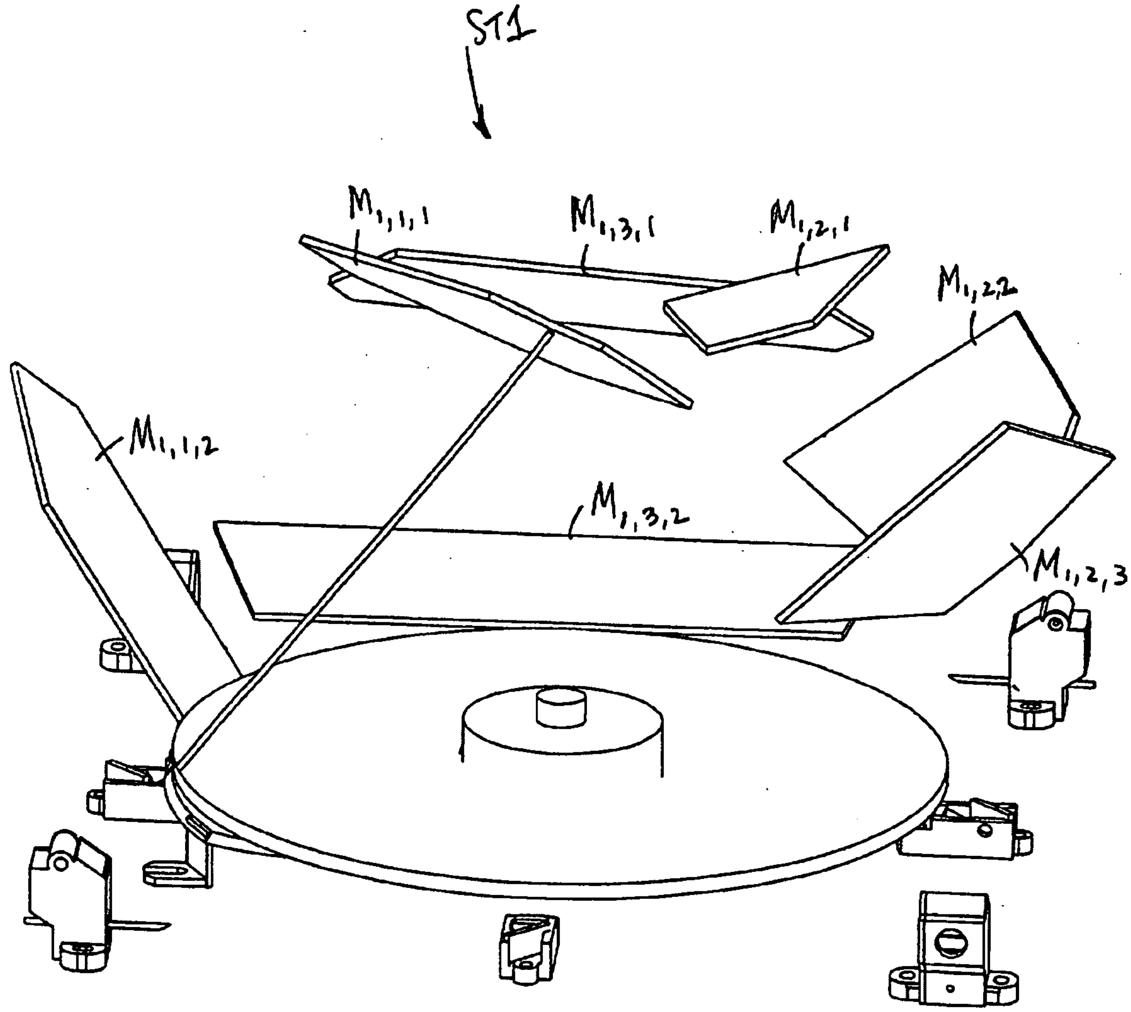

FIG. 6B1

	N	O	P	Q	R	S	T	U	V	W	X
25	Facet	8									
26	x	y	z								
27	-0.616	0.000	0.788								
28		End				Middle				End	
29	x	y	z		x	y	z		x	y	z
30	0.468	-0.249	0.848		0.468	-0.249	0.848		0.430	-0.387	0.816
31	0.408	-0.675	-0.614		0.408	-0.675	-0.614		0.375	-0.774	-0.510
32	-0.999	0.012	-0.034		-0.999	0.012	-0.034		-0.993	-0.106	0.054
33	-0.616	0.531	0.582		-0.616	0.531	0.582		-0.605	0.419	0.677
34											
35											
36											
37											
38											
39											
40											
41											
42											
43											
44											
45											

FIG. 6B2

Station 1

	A	B	C	D	E	F	G	H	I	J	K	L
25	High Elevation Right Skew	Facet	10									
26	(G1)	x	y	z								
27	Vector from Module	-0.616	0.000	0.788								
28			End				Middle				End	
29		x	y	z		x	y	z		x	y	z
30	Output Vectors From Disk	0.441	-0.235	0.866		0.441	-0.235	0.866		0.398	-0.391	0.830
31	First Mirror Reflected Directions	0.380	-0.673	-0.635		0.380	-0.673	-0.635		0.343	-0.784	-0.517
32	Second Mirror Reflected Directions	-0.998	0.000	-0.067		-0.998	0.000	-0.067		-0.991	-0.133	0.033
33	Third Mirror Reflected Directions	-0.589	0.553	0.589		-0.589	0.563	0.589		-0.578	0.426	0.697
34												
35			Mirror 1 Corners				Mirror 2 Corners				Mirror 3 Corners	
36		x	y	z		x	y	z		x	y	z
37	1	2.550	-1.630	2.650		4.000	-2.630	0.049		3.746	-3.750	1.000
38	2	4.150	-2.267	2.770		4.900	-1.400	0.775		1.371	-3.300	2.100
39	3	3.950	0.196	2.060		4.600	-3.150	2.118		1.159	-1.600	0.800
40	4	2.420	-0.309	2.270		3.800	-3.900	1.067		2.824	-2.000	0.100
41	5									3.771	-2.700	0.100
42	6											
43	7											
44	8											
45												

FIG. 6B3

Station 1

	Z	AA	AB	AC	AD	AE	AF	AG	AH	AI	AJ
25	Facet	12									
26	x	y	z								
27	-0.616	0.000	0.788								
28		End				Middle				End	
29	x	y	z		x	y	z		x	y	z
30	0.415	-0.220	0.883		0.415	-0.220	0.883		0.369	-0.387	0.845
31	0.351	-0.669	-0.655		0.351	-0.669	-0.655		0.312	-0.788	-0.530
32	-0.995	-0.012	-0.099		-0.995	-0.012	-0.099		-0.988	-0.153	0.007
33	-0.562	0.574	0.596		-0.562	0.574	0.596		-0.550	0.439	0.710
34											
35		Mirror 1 Corners				Mirror 2 Corners				Mirror 3 Corners	
36	x	y	z		x	y	z		x	y	z
37	2.550	-1.630	2.650		4.000	-2.630	0.049		3.746	-3.750	1.000
38	4.150	-2.267	2.770		4.900	-1.400	0.775		1.371	-3.300	2.100
39	3.950	0.196	2.060		4.600	-3.150	2.118		1.159	-1.600	0.800
40	2.420	-0.309	2.270		3.800	-3.900	1.067		2.824	-2.000	0.100
41									3.771	-2.700	0.100
42											
43											
44											
45											

FIG. 6B4

Station 1

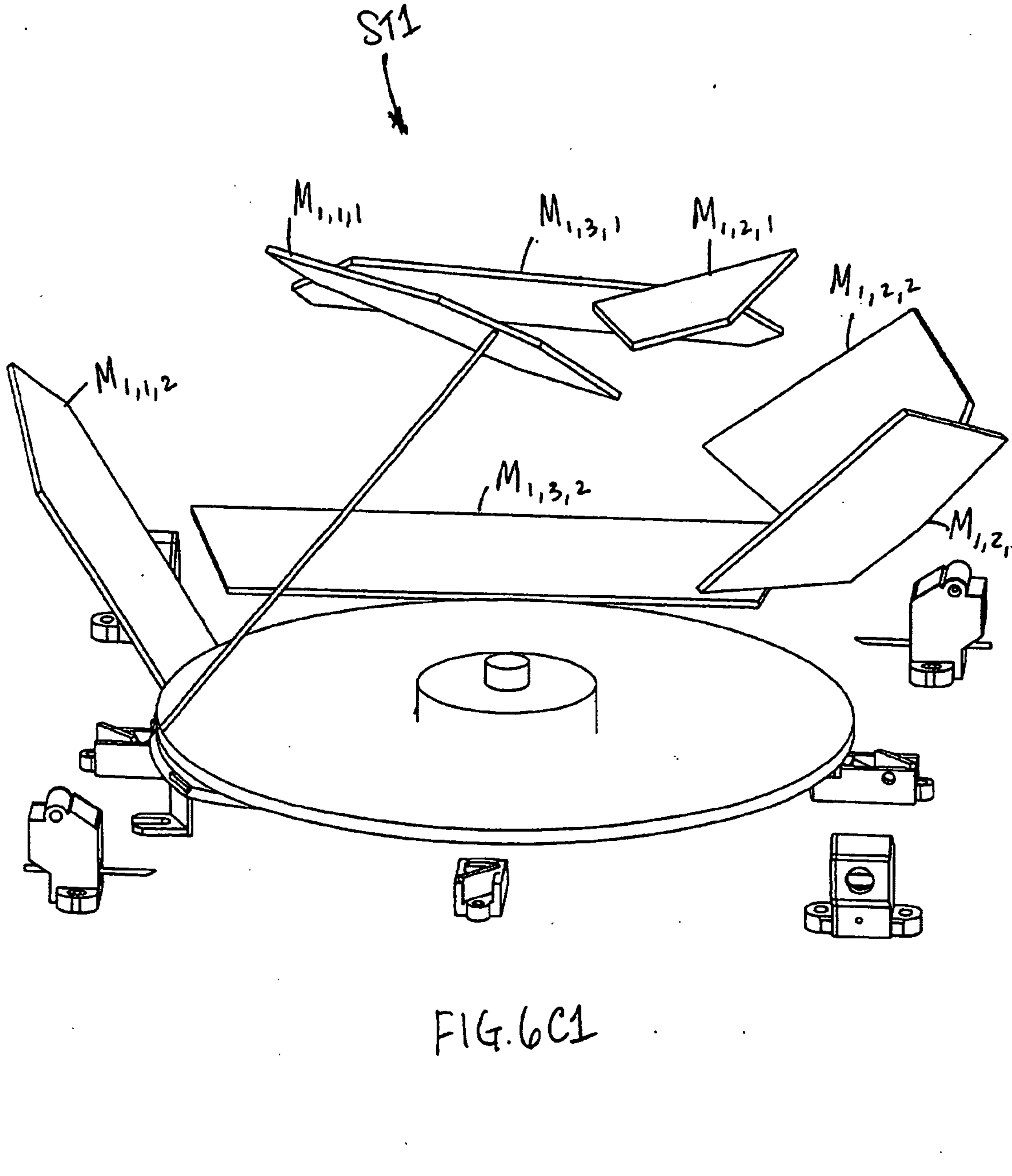

FIG.6C1

	N	O	P	Q	R	S	T	U	V	W	X
46	Facet	1									
47	x	y	z								
48	-0.616	0.000	0.788								
49		End				Middle				End	
50	x	y	z		x	y	z		x	y	z
51	0.753	0.321	0.575		0.788	0.000	0.616		0.753	-0.321	0.575
52	-0.366	0.443	-0.819		-0.425	0.132	-0.896		-0.421	-0.193	-0.887
53	-0.574	0.468	0.672		-0.653	0.160	0.740		-0.648	-0.165	0.743
54											
55											
56		Mirror 1 Corners				Mirror 2 Corners				Mirror 3 Corners	
57	x	y	z		x	y	z		x	y	z
58	4.250	1.500	2.547		3.150	2.450	0.030				
59	4.950	2.000	2.029		4.500	2.800	0.213				
60	5.150	1.800	1.851		4.350	-2.200	0.277				
61	5.000	-1.800	1.656		3.050	-1.850	0.089				
62	4.750	-1.950	1.844								
63	4.100	-1.500	2.405								
64											
65											

FIG. 6C2

Station 1

	A	B	C	D	E	F	G	H	I	J	K	L
46	Low Elevation	Facet	2									
47	(G3)	x	y	z								
48	Vector from Module	-0.616	0.000	0.788								
49			End				Middle				End	
50		x	y	z		x	y	z		x	y	z
51	Output Vectors From Disk	0.734	0.305	0.607		0.766	0.000	0.643		0.731	-0.319	0.604
52	First Mirror Reflected Directions	-0.402	0.429	-0.809		-0.456	0.133	-0.880		-0.453	-0.190	-0.871
53	Second Mirror Reflected Directions	-0.607	0.454	0.653		-0.679	0.161	0.716		-0.675	-0.162	0.719
54	Third Mirror Reflected Directions											
55												
56			Mirror 1 Corners				Mirror 2 Corners				Mirror 3 Corners	
57		x	y	z		x	y	z		x	y	z
58	1	4.250	1.500	2.547		3.150	2.450	0.030				
59	2	4.950	2.000	2.029		4.500	2.800	0.213				
60	3	5.150	1.800	1.851		4.350	-2.200	0.277				
61	4	5.000	-1.800	1.656		3.050	-1.850	0.089				
62	5	4.750	-1.950	1.844								
63	6	4.100	-1.500	2.405								
64	7											
65	8											

FIG. 6C3

Station 1

	Z	AA	AB	AC	AD	AE	AF	AG	AH	AI	AJ
46	Facet	3									
47	x	y	z								
48	-0.616	0.000	0.788								
49		End				Middle				End	
50	x	y	z		x	y	z-		x	y	z
51	0.714	0.290	0.638		0.743	0.000	0.669		0.709	-0.311	0.633
52	-0.438	0.416	-0.797		-0.487	0.134	-0.863		-0.485	-0.181	-0.855
53	-0.638	0.440	0.632		-0.704	0.161	0.692		-0.702	-0.155	0.695
54											
55											
56	Mirror 1 Corners				Mirror 2 Corners				Mirror 3 Corners		
57	x	y	z		x	y	z		x	y	z
58	4.250	1.500	2.547		3.150	2.450	0.030				
59	4.950	2.000	2.029		4.500	2.800	0.213				
60	5.150	1.800	1.851		4.350	-2.200	0.277				
61	5.000	-1.800	1.656		3.050	-1.850	0.089				
62	4.750	-1.950	1.844								
63	4.100	-1.500	2.405								
64											
65											

FIG. 6C4

Station 1

	AL	AM	AN	AO	AP	AQ	AR	AS	AT	AU	AV
46	Facet	4									
47	x	y	z								
48	-0.616	0.000	0.788								
49		End				Middle				End	
50	x	y	z		x	y	z		x	y	z
51	0.692	0.275	0.667		0.719	0.000	0.695		0.686	-0.307	0.660
52	-0.472	0.402	-0.784		-0.517	0.135	-0.846		-0.516	-0.176	-0.838
53	-0.667	0.426	0.611		-0.728	0.161	0.666		-0.727	-0.151	0.670
54											
55											
56		Mirror 1 Corners				Mirror 2 Corners				Mirror 3 Corners	
57	x	y	z		x	y	z		x	y	z
58	4.250	1.500	2.547		3.150	2.450	0.030				
59	4.950	2.000	2.029		4.500	2.800	0.213				
60	5.150	1.800	1.851		4.350	-2.200	0.277				
61	5.000	-1.800	1.656		3.050	-1.850	0.089				
62	4.750	-1.950	1.844								
63	4.100	-1.500	2.405								
64											
65											

FIG. 6C5

Station 1

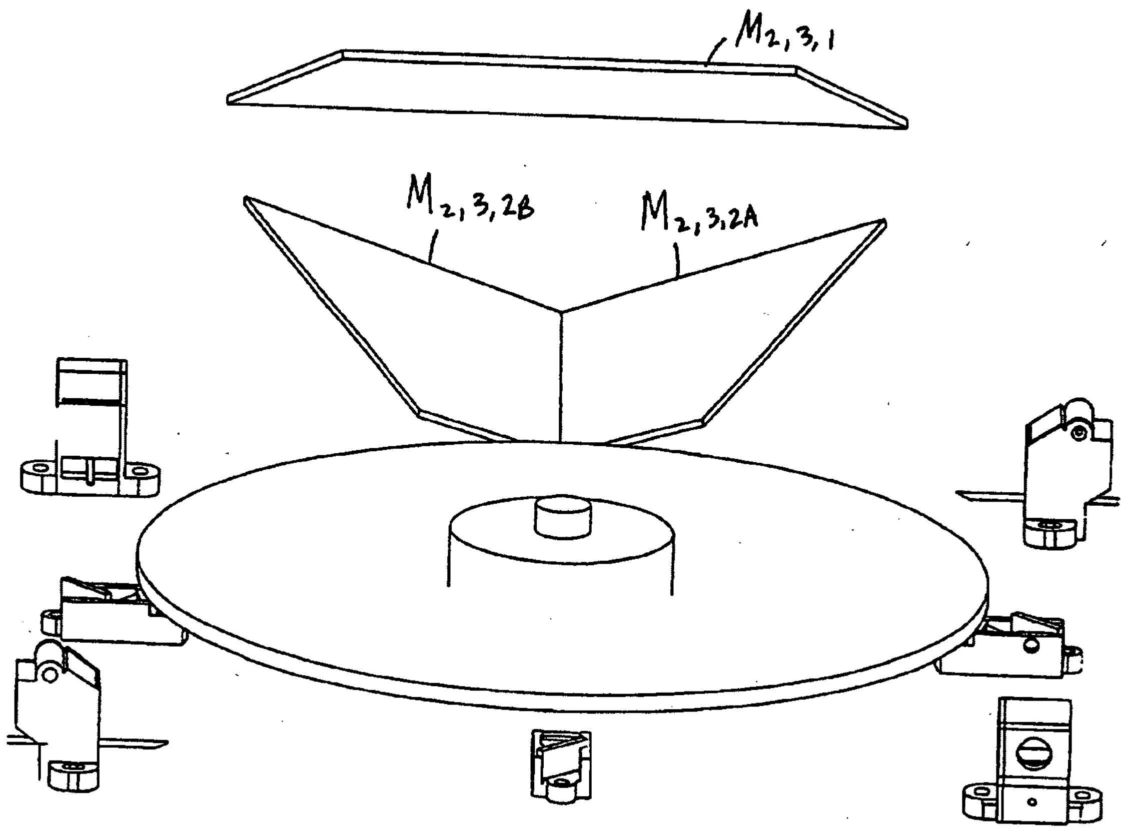

FIG. 6D1

	N	O	P	Q	R	S	T	U	V	W	X
46	Facet	1									
47	x	y	z								
48	-0.616	0.000	0.788								
49		End				Middle				End	
50	x	y	z		x	y	z		x	y	z
51	0.788	0.000	0.616		0.788	0.000	0.616		0.741	-0.367	0.562
52	-0.140	0.000	-0.990		-0.140	0.000	-0.990		-0.117	-0.367	-0.923
53	-0.595	0.448	0.667		-0.595	0.448	0.667		-0.590	0.098	0.801
54											
55											
56		Mirror 1 Corners				Mirror 2 Corners				Mirror 3 Corners	
57	x	y	z		x	y	z		x	y	z
58	3.750	-1.600	2.509		3.000	0.000	-0.112				
59	5.100	-2.400	1.728		4.800	0.000	0.382				
60	5.100	2.400	1.728		5.071	-2.256	1.066				
61	3.750	1.600	2.509		5.071	-2.256	1.066				
62					3.060	-1.000	0.175				
63											
64											
65											
66											
67											
68											
69	This station uses a split mirror for mirror #2. The second part of mirror 2 is the abo										
70											
71					3.000	0.000	-0.112				
72					4.800	0.000	0.382				
73					5.071	2.256	1.066				
74					5.071	2.256	1.066				
75					3.060	1.000	0.175				
76											

FIG. 6D2

Station 2

	Z	AA	AB	AC	AD	AE	AF	AG	AH	AI	AJ
46	Facet	2									
47	x	y	z								
48	-0.616	0.000	0.788								
49		End				Middle				End	
50	x	y	z		x	y	z		x	y	z
51	0.766	0.000	0.643		0.766	0.000	0.643		0.711	-0.395	0.581
52	-0.175	0.000	-0.985		-0.175	0.000	-0.985		-0.149	-0.395	-0.907
53	-0.623	0.440	0.647		-0.623	0.440	0.647		-0.614	0.062	0.787
54											
55											
56	Mirror 1 Corners				Mirror 2 Corners				Mirror 3 Corners		
57	x	y	z		x	y	z		x	y	z
58	3.750	-1.600	2.509		3.000	0.000	-0.112				
59	5.100	-2.400	1.728		4.800	0.000	0.382				
60	5.100	2.400	1.728		5.071	-2.256	1.066				
61	3.750	1.600	2.509		5.071	-2.256	1.066				
62					3.060	-1.000	0.175				
63											
64											
65											
66											
67											
68											
69	This station uses a split mirror for mirror #2. The second part of mirror 2 is the abo										
70											
71					3.000	0.000	-0.112				
72					4.800	0.000	0.382				
73					5.071	2.256	1.066				
74					5.071	2.256	1.066				
75					3.060	1.000	0.175				
76											

FIG. 6D3

Station 2

	A	B	C	D	E	F	G	H	I	J	K	L
46	Low Elevation	Facet	3									
47		x	y	z								
48	Vector from Module	-0.616	0.000	0.788								
49			End				Middle				End	
50		x	y	z		x	y	z		x	y	z
51	Output Vectors From Disk	0.743	0.000	0.669		0.743	0.000	0.669		0.697	-0.362	0.619
52	First Mirror Reflected Directions	-0.209	0.000	-0.978		-0.209	0.000	-0.978		-0.189	-0.362	-0.913
53	Second Mirror Reflected Directions	-0.649	0.433	0.625		-0.649	0.433	0.625		-0.648	0.089	0.757
54	Third Mirror Reflected Directions											
55												
56			Mirror 1 Corners				Mirror 2 Corners				Mirror 3 Corners	
57		x	y	z		x	y	z		x	y	z
58	1	3.750	-1.600	2.509		3.000	0.000	-0.112				
59	2	5.100	-2.400	1.728		4.800	0.000	0.382				
60	3	5.100	2.400	1.728		5.071	-2.256	1.066				
61	4	3.750	1.600	2.509		5.071	-2.256	1.066				
62	5					3.060	-1.000	0.175				
63	6											
64	7											
65	8											
66												
67												
68												
69	**Note: Special Case!**	This station uses a split mirror for mirror #2. The second part of mirror 2 is the abo										
70												
71	**Second Part of Mirror 2**					3.000	0.000	-0.112				
72						4.800	0.000	0.382				
73						5.071	2.256	1.066				
74						5.071	2.256	1.066				
75						3.060	1.000	0.175				
76												
77												

FIG. 6D4

Station 2

	AL	AM	AN	AO	AP	AQ	AR	AS	AT	AU	AV
46	Facet	4									
47	x	y	z								
48	-0.616	0.000	0.788								
49	End				Middle				End		
50	x	y	z		x	y	z		x	y	z
51	0.719	0.000	0.695		0.719	0.000	0.695		0.664	-0.395	0.635
52	-0.243	0.000	-0.970		-0.243	0.000	-0.970		-0.220	-0.395	-0.892
53	-0.675	0.425	0.603		-0.675	0.425	0.603		-0.668	0.046	0.742
54											
55											
56	Mirror 1 Corners				Mirror 2 Corners				Mirror 3 Corners		
57	x	y	z		x	y	z		x	y	z
58	3.750	-1.600	2.509		3.000	0.000	-0.112				
59	5.100	-2.400	1.728		4.800	0.000	0.382				
60	5.100	2.400	1.728		5.071	-2.256	1.066				
61	3.750	1.600	2.509		5.071	-2.256	1.066				
62					3.060	-1.000	0.175				
63											
64											
65											
66											
67											
68											
69	This station uses a split mirror for mirror #2. The second part of mirror 2 is the abo										
70											
71					3.000	0.000	-0.112				
72					4.800	0.000	0.382				
73					5.071	2.256	1.066				
74					5.071	2.256	1.066				
75					3.060	1.000	0.175				
76											

FIG. 605

Station 2

	AX	AY	AZ	BA	BB	BC	BD	BE	BF	BG	BH
46	Facet	5									
47	x	y	z								
48	-0.616	0.000	0.788								
49		End				Middle				End	
50	x	y	z		x	y	z		x	y	z
51	0.669	0.000	0.743		0.669	0.000	0.743		0.634	-0.311	0.708
52	-0.310	0.000	-0.951		-0.310	0.000	-0.951		-0.298	-0.311	-0.903
53	-0.724	0.407	0.557		-0.724	0.407	0.557		-0.730	0.114	0.673
54											
55											
56	Mirror 1 Corners				Mirror 2 Corners				Mirror 3 Corners		
57	x	y	z		x	y	z		x	y	z
58	3.750	-1.600	2.509		3.000	0.000	-0.112				
59	5.100	-2.400	1.728		4.800	0.000	0.382				
60	5.100	2.400	1.728		5.071	-2.256	1.066				
61	3.750	1.600	2.509		5.071	-2.256	1.066				
62					3.060	-1.000	0.175				
63											
64											
65											
66											
67											
68											
69	This station uses a split mirror for mirror #2. The second part of mirror 2 is the abo										
70											
71					3.000	0.000	-0.112				
72					4.800	0.000	0.382				
73					5.071	2.256	1.066				
74					5.071	2.256	1.066				
75					3.060	1.000	0.175				
76											

FIG. 6D6

Station 2

	BJ	BK	BL	BM	BN	BO	BP	BQ	BR	BS	BT	BU	BV	BW	BX
46	Facet	6													
47	x	y	z												
48	-0.616	0.000	0.788												
49		End				Middle				End					
50	x	y	z		x	y	z		x	y	z				
51	0.616	0.000	0.788		0.616	0.000	0.788		0.596	-0.232	0.769				
52	-0.376	0.000	-0.927		-0.376	0.000	-0.927		-0.369	-0.232	-0.900				
53	-0.770	0.387	0.508		-0.770	0.387	0.508		-0.781	0.173	0.600				
54															
55															
56		Mirror 1 Corners				Mirror 2 Corners				Mirror 3 Corners					
57	x	y	z		x	y	z		x	y	z				
58	3.750	-1.600	2.509		3.000	0.000	-0.112								
59	5.100	-2.400	1.728		4.800	0.000	0.382								
60	5.100	2.400	1.728		5.071	-2.256	1.066								
61	3.750	1.600	2.509		5.071	-2.256	1.066								
62					3.060	-1.000	0.175								
63															
64															
65															
66															
67															
68															
69	This station uses a split mirror for mirror #2. The second part of mirror 2 is the above mirrored about the y axis. I.e.:														
70															
71					3.000	0.000	-0.112								
72					4.800	0.000	0.382								
73					5.071	2.256	1.066								
74					5.071	2.256	1.066								
75					3.060	1.000	0.175								
76															

FIG. 6D7

Station 2

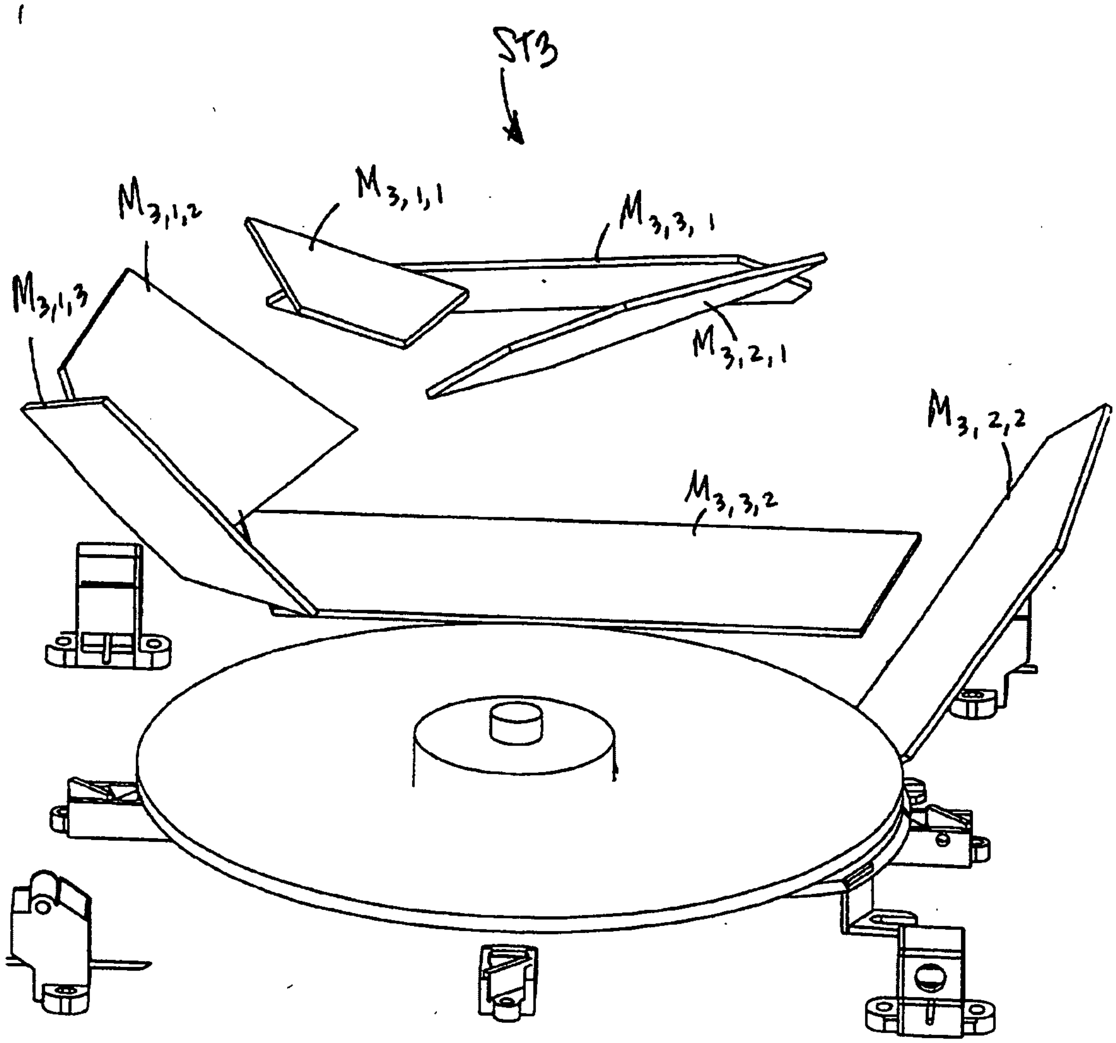

FIG. 6E1

	N	O	P	Q	R	S	T	U	V	W	X
1											
2											
3											
4	Facet	7									
5	x	y	z								
6	-0.616	0.000	0.788								
7		End				Middle				End	
8	x	y	z		x	y	z		x	y	z
9	0.468	0.249	0.848		0.468	0.249	0.848		0.430	0.387	0.816
10	0.408	0.675	-0.614		0.408	0.675	-0.614		0.375	0.774	-0.510
11	-0.999	-0.012	-0.034		-0.999	-0.012	-0.034		-0.993	0.106	0.054
12	-0.616	-0.531	0.582		-0.616	-0.531	0.582		-0.605	-0.419	0.677
13											
14		Mirror 1 Corners				Mirror 2 Corners				Mirror 3 Corners	
15	x	y	z		x	y	z		x	y	z
16	2.550	1.630	2.650		4.000	2.630	0.049		3.746	3.750	1.000
17	4.150	2.267	2.770		4.900	1.400	0.775		1.371	3.300	2.100
18	3.950	-0.196	2.060		4.600	3.150	2.118		1.159	1.600	0.800
19	2.420	0.309	2.270		3.800	3.900	1.067		2.824	2.000	0.100
20									3.771	2.700	0.100
21											
22											
23											
24											

FIG. 6E2

Station 3

	A	B	C	D	E	F	G	H	I	J	K	L
1	Station 3											
2												
3												
4	High Elevation Left Skew	Facet	9									
5	(G2)	x	y	z								
6	Vector from Module	-0.616	0.000	0.788								
7			End				Middle				End	
8		x	y	z		x	y	z		x	y	z
9	Output Vectors From Disk	0.441	0.235	0.866		0.441	0.235	0.866		0.398	0.391	0.830
10	First Mirror Reflected Directions	0.380	0.673	-0.635		0.380	0.673	-0.635		0.343	0.784	-0.517
11	Second Mirror Reflected Directions	-0.998	0.000	-0.067		-0.998	0.000	-0.067		-0.991	0.133	0.033
12	Third Mirror Reflected Directions	-0.589	-0.553	0.589		-0.589	-0.553	0.589		-0.578	-0.426	0.697
13												
14			Mirror 1 Corners				Mirror 2 Corners				Mirror 3 Corners	
15		x	y	z		x	y	z		x	y	z
16	1	2.550	1.630	2.650		4.000	2.630	0.049		3.746	3.750	1.000
17	2	4.150	2.267	2.770		4.900	1.400	0.775		1.371	3.300	2.100
18	3	3.950	-0.196	2.060		4.600	3.150	2.118		1.159	1.600	0.800
19	4	2.420	0.309	2.270		3.800	3.900	1.067		2.824	2.000	0.100
20	5									3.771	2.700	0.100
21	6											
22	7											
23	8											

FIG. 6E3

	Z	AA	AB	AC	AD	AE	AF	AG	AH	AI	AJ
1											
2											
3											
4	Facet	11									
5	x	y	z								
6	-0.616	0.000	0.788								
7		End				Middle				End	
8	x	y	z		x	y	z		x	y	z
9	0.415	0.220	0.883		0.415	0.220	0.883		0.369	0.387	0.845
10	0.351	0.669	-0.655		0.351	0.669	-0.655		0.312	0.788	-0.530
11	-0.995	0.012	-0.099		-0.995	0.012	-0.099		-0.988	0.153	0.007
12	-0.562	-0.574	0.596		-0.562	-0.574	0.596		-0.550	-0.439	0.710
13											
14	Mirror 1 Corners				Mirror 2 Corners				Mirror 3 Corners		
15	x	y	z		x	y	z		x	y	z
16	2.550	1.630	2.650		4.000	2.630	0.049		3.746	3.750	1.000
17	4.150	2.267	2.770		4.900	1.400	0.775		1.371	3.300	2.100
18	3.950	-0.196	2.060		4.600	3.150	2.118		1.159	1.600	0.800
19	2.420	0.309	2.270		3.800	3.900	1.067		2.824	2.000	0.100
20									3.771	2.700	0.100
21											
22											
23											
24											

FIG. 6E4

Station 3

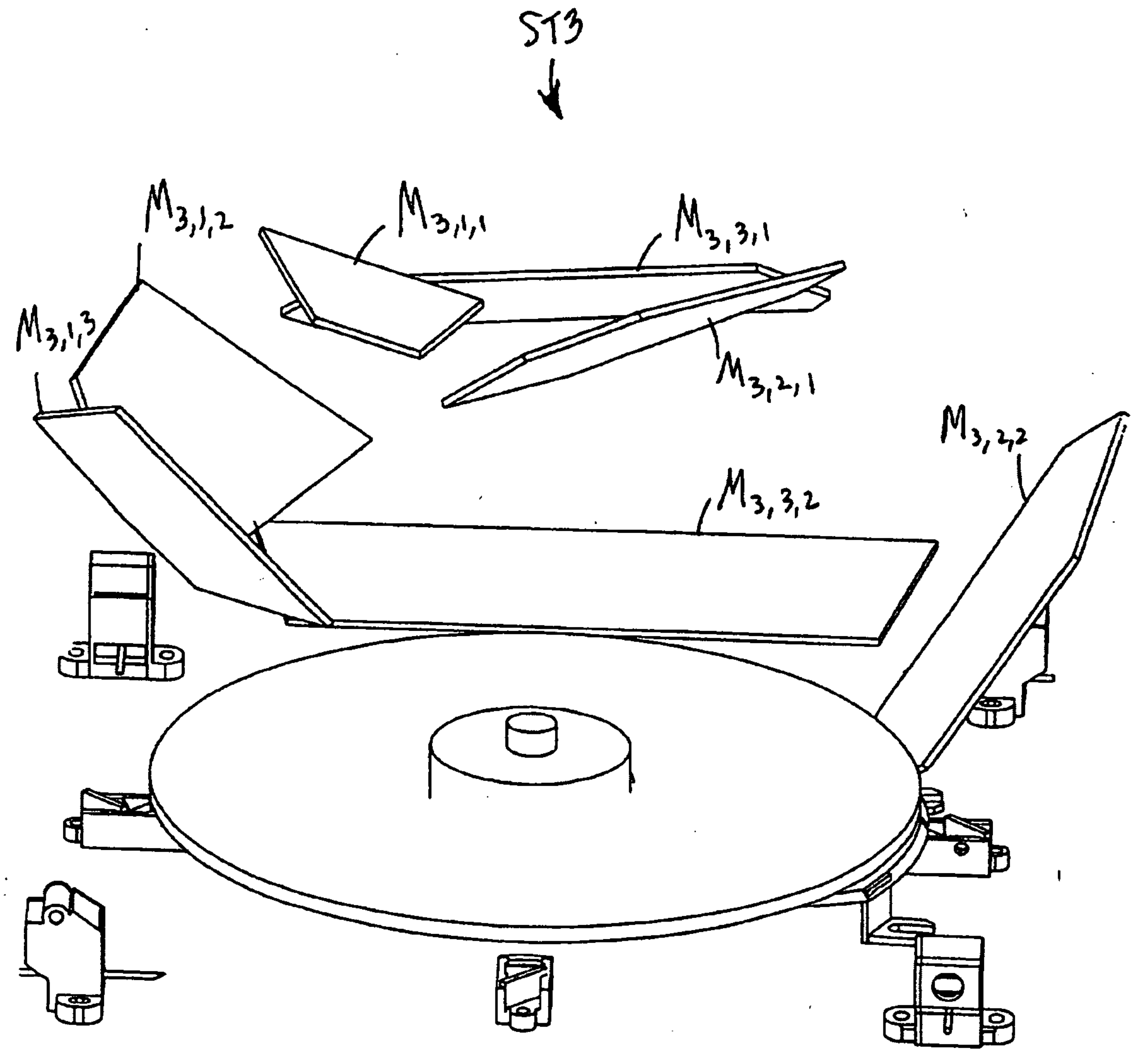

FIG. 6F1

	N	O	P	Q	R	S	T	U	V	W	X
25	Facet	8									
26	x	y	z								
27	-0.616	0.000	0.788								
28		End				Middle				End	
29	x	y	z		x	y	z		x	y	z
30	0.419	-0.416	0.807		0.468	-0.249	0.848		0.494	-0.048	0.868
31	-0.253	-0.917	-0.310		-0.316	-0.832	-0.455		-0.387	-0.704	-0.596
32	-0.469	0.414	0.781		-0.537	0.527	0.659		-0.603	0.626	0.494
33											
34											
35	Mirror 1 Corners				Mirror 2 Corners				Mirror 3 Corners		
36	x	y	z		x	y	z		x	y	z
37	3.900	-2.436	2.770		1.700	-4.102	1.300				
38	4.100	-1.879	2.400		3.300	-4.400	1.980				
39	3.800	-0.137	1.800		3.400	-3.990	1.500				
40	3.150	0.737	1.800		2.300	-2.427	-0.625				
41	2.500	0.159	2.450		1.700	-2.524	-0.625				
42	2.650	-0.757	2.770		1.050	-3.101	-0.050				
43											
44											

FIG. 6F2

Station 3

	A	B	C	D	E	F	G	H	I	J	K	L
25	High Elevation Right Skew	Facet	10									
26	(G1)	x	y	z								
27	Vector from Module	-0.616	0.000	0.788								
28			End				Middle				End	
29		x	y	z		x	y	z		x	y	z
30	Output Vectors From Disk	0.378	-0.445	0.812		0.441	-0.235	0.866		0.464	-0.068	0.883
31	First Mirror Reflected Directions	-0.269	-0.927	-0.263		-0.349	-0.823	-0.448		-0.408	-0.717	-0.565
32	Second Mirror Reflected Directions	-0.479	0.367	0.797		-0.566	0.512	0.647		-0.621	0.595	0.510
33	Third Mirror Reflected Directions											
34												
35			Mirror 1 Corners				Mirror 2 Corners				Mirror 3 Corners	
36		x	y	z		x	y	z		x	y	z
37	1	3.900	-2.436	2.770		1.700	-4.102	1.300				
38	2	4.100	-1.879	2.400		3.300	-4.400	1.980				
39	3	3.800	-0.137	1.800		3.400	-3.990	1.500				
40	4	3.150	0.737	1.800		2.300	-2.427	-0.625				
41	5	2.500	0.159	2.450		1.700	-2.524	-0.625				
42	6	2.650	-0.757	2.770		1.050	-3.101	-0.050				
43	7											
44	8											

FIG. 6F3

Station 3

	Z	AA	AB	AC	AD	AE	AF	AG	AH	AI	AJ
25	Facet	12									
26	x	y	z								
27	-0.616	0.000	0.788								
28		End				Middle				End	
29	x	y	z		x	y	z		x	y	z
30	0.333	-0.476	0.814		0.415	-0.220	0.883		0.433	-0.086	0.897
31	-0.284	-0.935	-0.211		-0.382	-0.813	-0.440		-0.429	-0.728	-0.535
32	-0.487	0.316	0.814		-0.594	0.496	0.633		-0.638	0.564	0.524
33											
34											
35		Mirror 1 Corners				Mirror 2 Corners				Mirror 3 Corners	
36	x	y	z		x	y	z		x	y	z
37	3.900	-2.436	2.770		1.700	-4.102	1.300				
38	4.100	-1.879	2.400		3.300	-4.400	1.980				
39	3.800	-0.137	1.800		3.400	-3.990	1.500				
40	3.150	0.737	1.800		2.300	-2.427	-0.625				
41	2.500	0.159	2.450		1.700	-2.524	-0.625				
42	2.650	-0.757	2.770		1.050	-3.101	-0.050				
43											
44											
45											

FIG. 6F4

Station 3

223/335

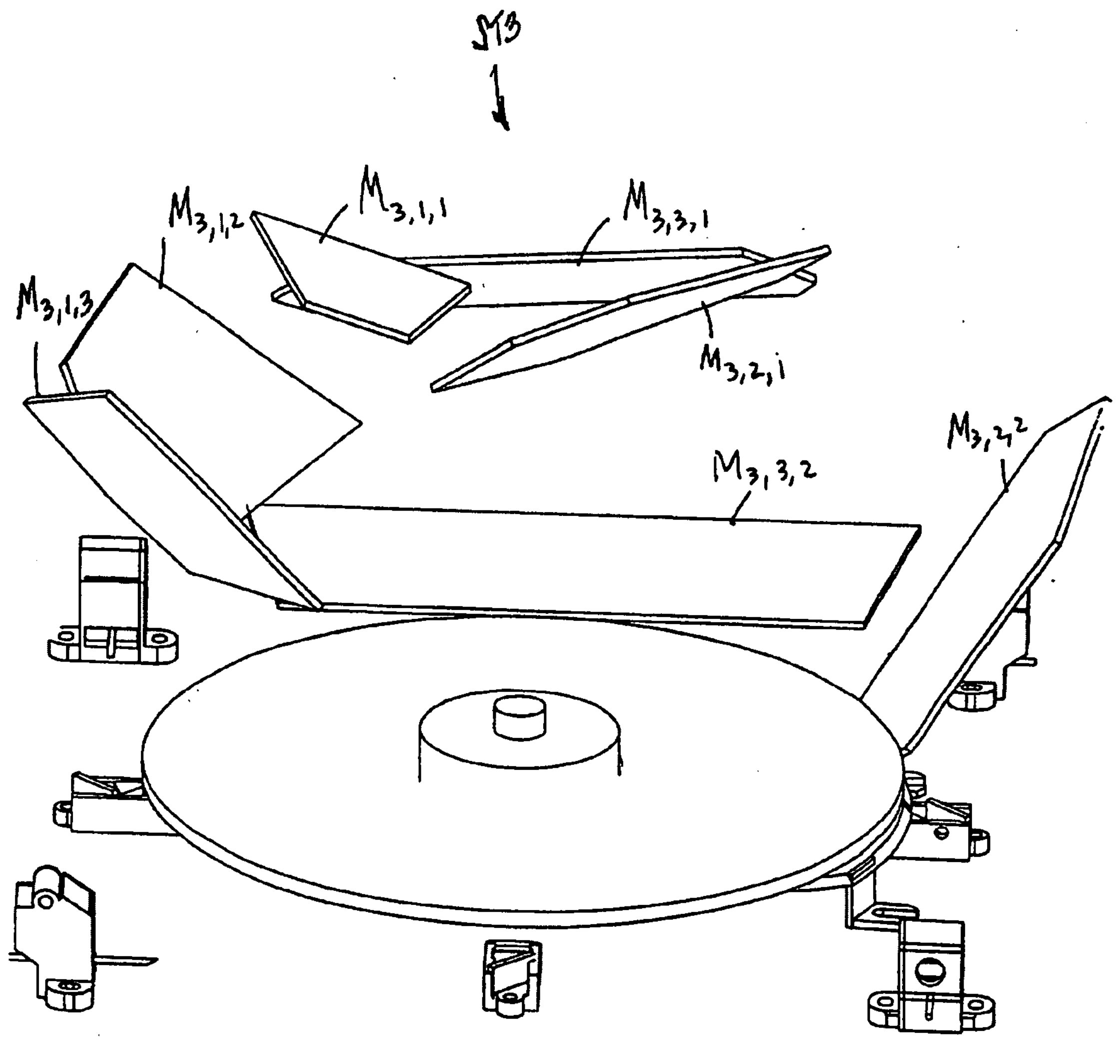

FIG.6G1

	N	O	P	Q	R	S	T	U	V	W	X
46	Facet	1									
47	x	y	z								
48	-0.616	0.000	0.788								
49		End				Middle				End	
50	x	y	z		x	y	z		x	y	z
51	0.753	-0.321	0.575		0.788	0.000	0.616		0.753	0.321	0.575
52	-0.366	-0.443	-0.819		-0.425	-0.132	-0.896		-0.421	0.193	-0.887
53	-0.574	-0.468	0.672		-0.653	-0.160	0.740		-0.648	0.165	0.743
54											
55											
56	Mirror 1 Corners				Mirror 2 Corners				Mirror 3 Corners		
57	x	y	z		x	y	z		x	y	z
58	4.250	-1.500	2.547		3.150	-2.450	0.030				
59	4.950	-2.000	2.029		4.500	-2.800	0.213				
60	5.150	-1.800	1.851		4.350	2.200	0.277				
61	5.000	1.800	1.656		3.050	1.850	0.089				
62	4.750	1.950	1.844								
63	4.100	1.500	2.405								
64											
65											

FIG. 6G2

Station 3

	A	B	C	D	E	F	G	H	I	J	K	L
46	Low Elevation	Facet	2									
47	(G3)	x	y	z								
48	Vector from Module	-0.616	0.000	0.788								
49			End				Middle				End	
50		x	y	z		x	y	z		x	y	z
51	Output Vectors From Disk	0.734	-0.305	0.607		0.766	0.000	0.643		0.731	0.319	0.604
52	First Mirror Reflected Directions	-0.402	-0.429	-0.809		-0.456	-0.133	-0.880		-0.453	0.190	-0.871
53	Second Mirror Reflected Directions	-0.607	-0.454	0.653		-0.679	-0.161	0.716		-0.675	0.162	0.719
54	Third Mirror Reflected Directions											
55												
56			Mirror 1 Corners				Mirror 2 Corners				Mirror 3 Corners	
57		x	y	z		x	y	z		x	y	z
58	1	4.250	-1.500	2.547		3.150	-2.450	0.030				
59	2	4.950	-2.000	2.029		4.500	-2.800	0.213				
60	3	5.150	-1.800	1.851		4.350	2.200	0.277				
61	4	5.000	1.800	1.656		3.050	1.850	0.089				
62	5	4.750	1.950	1.844								
63	6	4.100	1.500	2.405								
64	7											
65	8											
66												

FIG. 6G3

Station 3

	Z	AA	AB	AC	AD	AE	AF	AG	AH	AI	AJ
46	Facet	3									
47	x	y	z								
48	-0.616	0.000	0.788								
49		End				Middle				End	
50	x	y	z		x	y	z		x	y	z
51	0.714	-0.290	0.638		0.743	0.000	0.669		0.709	0.311	0.633
52	-0.438	-0.416	-0.797		-0.487	-0.134	-0.863		-0.485	0.181	-0.855
53	-0.638	-0.440	0.632		-0.704	-0.161	0.692		-0.702	0.155	0.695
54											
55											
56	Mirror 1 Comers				Mirror 2 Comers				Mirror 3 Comers		
57	x	y	z		x	y	z		x	y	z
58	4.250	-1.500	2.547		3.150	-2.450	0.030				
59	4.950	-2.000	2.029		4.500	-2.800	0.213				
60	5.150	-1.800	1.851		4.350	2.200	0.277				
61	5.000	1.800	1.656		3.050	1.850	0.089				
62	4.750	1.950	1.844								
63	4.100	1.500	2.405								
64											
65											

FIG. 6G4

Station 3

	AL	AM	AN	AO	AP	AQ	AR	AS	AT	AU	AV
46	Facet	4									
47	x	y	z								
48	-0.616	0.000	0.788								
49	End				Middle				End		
50	x	y	z		x	y	z		x	y	z
51	0.692	-0.275	0.667		0.719	0.000	0.695		0.686	0.307	0.660
52	-0.472	-0.402	-0.784		-0.517	-0.135	-0.846		-0.516	0.176	-0.838
53	-0.667	-0.426	0.611		-0.728	-0.161	0.666		-0.727	0.151	0.670
54											
55											
56	Mirror 1 Corners				Mirror 2 Corners				Mirror 3 Corners		
57	x	y	z		x	y	z		x	y	z
58	4.250	-1.500	2.547		3.150	-2.450	0.030				
59	4.950	-2.000	2.029		4.500	-2.800	0.213				
60	5.150	-1.800	1.851		4.350	2.200	0.277				
61	5.000	1.800	1.656		3.050	1.850	0.089				
62	4.750	1.950	1.844								
63	4.100	1.500	2.405								
64											
65											

FIG. 6G5

Station 3

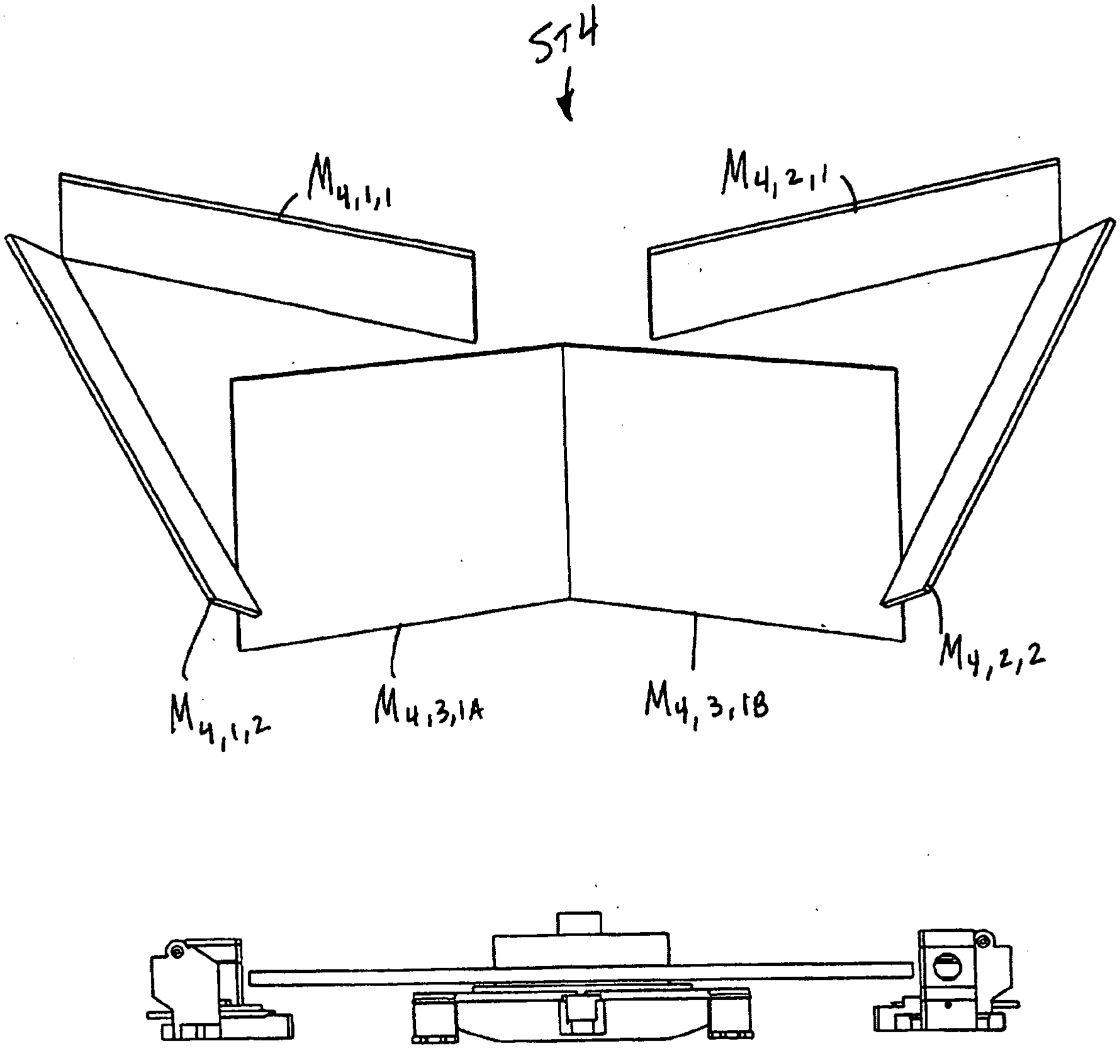

FIG.6H1

	N	O	P	Q	R	S	T	U	V	W	X
1											
2											
3											
4	Facet	7									
5	x	y	z								
6	-0.616	0.000	0.788								
7		End				Middle				End	
8	x	y	z		x	y	z		x	y	z
9	0.399	0.468	0.789		0.468	0.249	0.848		0.481	0.180	0.858
10	-0.433	0.736	-0.519		-0.495	0.559	-0.665		-0.511	0.500	-0.700
11	-0.737	-0.585	0.339		-0.768	-0.631	0.108		-0.771	-0.636	0.038
12											
13											
14		Mirror 1 Corners				Mirror 2 Corners				Mirror 3 Corners	
15	x	y	z		x	y	z		x	y	z
16	4.900	0.800	6.409		2.850	3.200	3.370				
17	6.100	0.800	5.645		4.200	2.800	3.231				
18	6.000	4.500	6.468		5.950	4.500	6.464				
19	4.900	4.500	7.168		4.600	4.950	6.680				
20											
21											
22											
23											

FIG. 6H2

	A	B	C	D	E	F	G	H	I	J	K	L
1	Station 4											
2												
3												
4	High Elevation Left Skew	Facet	9									
5		x	y	z								
6	Vector from Module	-0.616	0.000	0.788								
7			End				Middle				End	
8		x	y	z		x	y	z		x	y	z
9	Output Vectors From Disk	0.366	0.474	0.801		0.441	0.235	0.866		0.452	0.177	0.874
10	First Mirror Reflected Directions	-0.458	0.739	-0.494		-0.525	0.546	-0.653		-0.538	0.496	-0.681
11	Second Mirror Reflected Directions	-0.755	-0.556	0.348		-0.789	-0.606	0.096		-0.792	-0.610	0.037
12	Third Mirror Reflected Directions											
13												
14			Mirror 1 Corners				Mirror 2 Corners				Mirror 3 Corners	
15		x	y	z		x	y	z		x	y	z
16	1	4.900	0.800	6.409		2.850	3.200	3.370				
17	2	6.100	0.800	5.645		4.200	2.800	3.231				
18	3	6.000	4.500	6.468		5.950	4.500	6.464				
19	4	4.900	4.500	7.168		4.600	4.950	6.680				
20	5											
21	6											
22	7											

FIG. 6H3

	Z	AA	AB	AC	AD	AE	AF	AG	AH	AI	AJ
1											
2											
3											
4	Facet	11									
5	x	y	z								
6	-0.616	0.000	0.788								
7		End				Middle				End	
8	x	y	z		x	y	z		x	y	z
9	0.332	0.478	0.813		0.415	0.220	0.883		0.422	0.176	0.889
10	-0.482	0.741	-0.467		-0.554	0.533	-0.640		-0.564	0.494	-0.661
11	-0.773	-0.526	0.356		-0.810	-0.581	0.084		-0.811	-0.583	0.039
12											
13											
14	Mirror 1 Corners				Mirror 2 Corners				Mirror 3 Corners		
15	x	y	z		x	y	z		x	y	z
16	4.900	0.800	6.409		2.850	3.200	3.370				
17	6.100	0.800	5.645		4.200	2.800	3.231				
18	6.000	4.500	6.468		5.950	4.500	6.464				
19	4.900	4.500	7.168		4.600	4.950	6.680				
20											
21											
22											
23											
24											

FIG. 6H4

Station 4

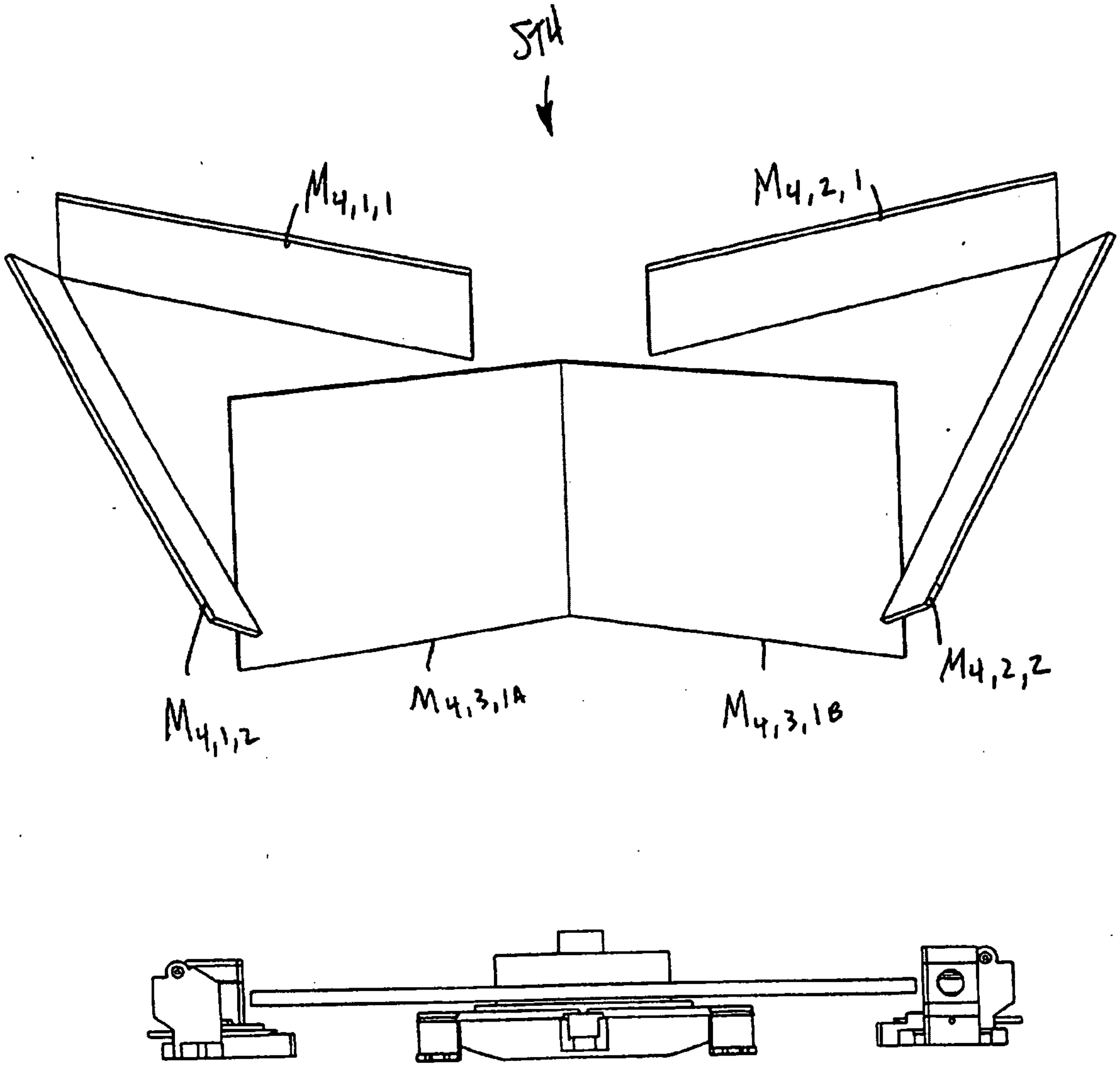

FIG. 6I1

	N	O	P	Q	R	S	T	U	V	W	X
25	Facet	8									
26	x	y	z								
27	-0.616	0.000	0.788								
28		End				Middle				End	
29	x	y	z		x	y	z		x	y	z
30	0.481	-0.180	0.858		0.468	-0.249	0.848		0.399	-0.468	0.789
31	-0.511	-0.500	-0.700		-0.495	-0.559	-0.665		-0.433	-0.736	-0.519
32	-0.771	0.636	0.038		-0.768	0.631	0.108		-0.737	0.585	0.339
33											
34											
35		Mirror 1 Corners				Mirror 2 Corners				Mirror 3 Corners	
36	x	y	z		x	y	z		x	y	z
37	4.900	-0.800	6.409		2.850	-3.200	3.370				
38	6.100	-0.800	5.645		4.200	-2.800	3.231				
39	6.000	-4.500	6.468		5.950	-4.500	6.464				
40	4.900	-4.500	7.168		4.600	-4.950	6.680				
41											
42											
43											
44											

FIG. 6I2

Station 4

	A	B	C	D	E	F	G	H	I	J	K	L
25	High Elevation Right Skew	Facet	10									
26		x	y	z								
27	Vector from Module	-0.616	0.000	0.788								
28			End				Middle				End	
29		x	y	z		x	y	z		x	y	z
30	Output Vectors From Disk	0.452	-0.177	0.874		0.441	-0.235	0.866		0.366	-0.474	0.801
31	First Mirror Reflected Directions	-0.538	-0.496	-0.681		-0.525	-0.546	-0.653		-0.458	-0.739	-0.494
32	Second Mirror Reflected Directions	-0.792	0.610	0.037		-0.789	0.606	0.096		-0.755	0.556	0.348
33	Third Mirror Reflected Directions											
34			Mirror 1 Corners				Mirror 2 Corners				Mirror 3 Corners	
35		x	y	z		x	y	z		x	y	z
36	1	4.900	-0.800	6.409		2.850	-3.200	3.370				
37	2	6.100	-0.800	5.645		4.200	-2.800	3.231				
38	3	6.000	-4.500	6.468		5.950	-4.500	6.464				
39	4	4.900	-4.500	7.168		4.600	-4.950	6.680				
40	5											
41	6											
42	7											
43	8											
44												

FIG. 6I3

	Z	AA	AB	AC	AD	AE	AF	AG	AH	AI	AJ
25	Facet	12									
26	x	y	z								
27	-0.616	0.000	0.788								
28		End				Middle				End	
29	x	y	z		x	y	z		x	y	z
30	0.422	-0.176	0.889		0.415	-0.220	0.883		0.332	-0.478	0.813
31	-0.564	-0.494	-0.661		-0.554	-0.533	-0.640		-0.482	-0.741	-0.467
32	-0.811	0.583	0.039		-0.810	0.581	0.084		-0.773	0.526	0.356
33											
34											
35	Mirror 1 Corners				Mirror 2 Corners				Mirror 3 Corners		
36	x	y	z		x	y	z		x	y	z
37	4.900	-0.800	6.409		2.850	-3.200	3.370				
38	6.100	-0.800	5.645		4.200	-2.800	3.231				
39	6.000	-4.500	6.468		5.950	-4.500	6.464				
40	4.900	-4.500	7.168		4.600	-4.950	6.680				
41											
42											
43											
44											

FIG. 6I4

Station 4

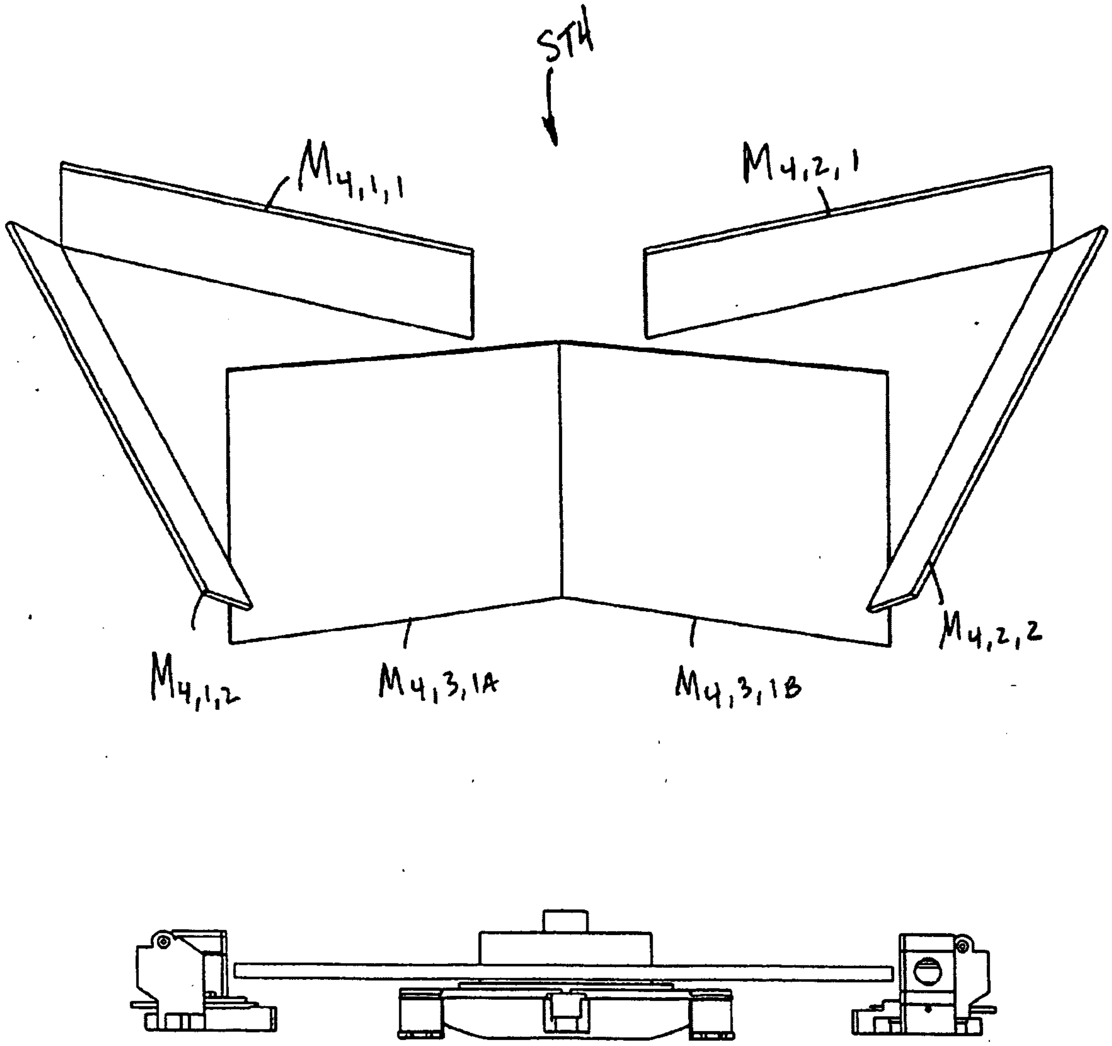

FIG. 6J1

	N	O	P	Q	R	S	T	U	V	W	X
46	Facet	1									
47	x	y	z								
48	-0.616	0.000	0.788								
49		End				Middle				End	
50	x	y	z		x	y	z		x	y	z
51	0.788	0.001	0.616		0.788	0.000	0.616		0.741	-0.367	0.562
52	-0.938	0.335	0.087		-0.939	0.334	0.087		-0.999	-0.031	0.029
53											
54											
55											
56	Mirror 1 Corners				Mirror 2 Corners				Mirror 3 Corners		
57	x	y	z		x	y	z		x	y	z
58	6.700	0.000	5.608								
59	7.400	0.000	3.322								
60	6.950	-3.000	2.897								
61	6.200	-3.000	5.345								
62											
63											
64											
65											
66											

FIG. 6J2

Station 4

	Z	AA	AB	AC	AD	AE	AF	AG	AH	AI	AJ
46	Facet	2									
47	x	y	z								
48	-0.616	0.000	0.788								
49		End				Middle				End	
50	x	y	z		x	y	z		x	y	z
51	0.766	0.000	0.643		0.766	0.000	0.643		0.711	-0.395	0.581
52	-0.936	0.329	0.121		-0.936	0.329	0.121		-0.996	-0.065	0.058
53											
54											
55											
56		Mirror 1 Corners				Mirror 2 Corners				Mirror 3 Corners	
57	x	y	z		x	y	z		x	y	z
58	6.700	0.000	5.608								
59	7.400	0.000	3.322								
60	6.950	-3.000	2.897								
61	6.200	-3.000	5.345								
62											
63											
64											
65											
66											

FIG. 6J3

	A	B	C	D	E	F	G	H	I	J	K	L
46	Low Elevation	Facet	3									
47		x	y	z								
48	Vector from Module	-0.616	0.000	0.788								
49			End				Middle				End	
50		x	y	z		x	y	z		x	y	z
51	Output Vectors From Disk	0.743	0.000	0.669		0.743	0.000	0.669		0.697	-0.362	0.619
52	First Mirror Reflected Directions	-0.933	0.324	0.156		-0.933	0.324	0.156		-0.994	-0.035	0.101
53	Second Mirror Reflected Directions											
54	Third Mirror Reflected Directions											
55			Mirror 1 Corners				Mirror 2 Corners				Mirror 3 Corners	
56		x	y	z		x	y	z		x	y	z
57	1	6.700	0.000	5.608								
58	2	7.400	0.000	3.322								
59	3	6.950	-3.000	2.897								
60	4	6.200	-3.000	5.345								
61	5											
62	6											
63	7											
64	8											
65												
66												

FIG. 6J4

Station 4

	AL	AM	AN	AO	AP	AQ	AR	AS	AT	AU	AV
46	Facet	4									
47	x	y	z								
48	-0.616	0.000	0.788								
49		End				Middle				End	
50	x	y	z		x	y	z		x	y	z
51	0.719	0.000	0.695		0.719	0.000	0.695		0.664	-0.395	0.635
52	-0.929	0.319	0.190		-0.929	0.319	0.190		-0.989	-0.075	0.129
53											
54											
55											
56	Mirror 1 Corners				Mirror 2 Corners				Mirror 3 Corners		
57	x	y	z		x	y	z		x	y	z
58	6.700	0.000	5.608								
59	7.400	0.000	3.322								
60	6.950	-3.000	2.897								
61	6.200	-3.000	5.345								
62											
63											
64											
65											
66											

FIG. 6J5

Station 4

	AX	AY	AZ	BA	BB	BC	BD	BE	BF	BG	BH
46	Facet	5									
47	x	y	z								
48	-0.616	0.000	0.788								
49		End				Middle				End	
50	x	y	z		x	y	z		x	y	z
51	0.669	0.000	0.743		0.669	0.000	0.743		0.621	-0.362	0.695
52	-0.916	0.307	0.257		-0.916	0.307	0.257		-0.977	-0.052	0.206
53											
54											
55											
56	Mirror 1 Corners				Mirror 2 Corners				Mirror 3 Corners		
57	x	y	z		x	y	z		x	y	z
58	6.700	0.000	5.608								
59	7.400	0.000	3.322								
60	6.950	-3.000	2.897								
61	6.200	-3.000	5.345								
62											
63											
64											
65											

FIG. 6J6

Station 4

	BJ	BK	BL	BM	BN	BO	BP	BQ	BR	BS	BT	BU
46	Facet	6										
47	x	y	z									
48	-0.616	0.000	0.788									
49		End				Middle				End		
50	x	y	z		x	y	z		x	y	z	
51	0.616	0.000	0.788		0.616	0.000	0.788		0.561	-0.380	0.735	
52	-0.900	0.293	0.324		-0.900	0.293	0.324		-0.959	-0.086	0.270	
53												
54												
55												
56		Mirror 1 Corners				Mirror 2 Corners				Mirror 3 Corners		
57	x	y	z		x	y	z		x	y	z	
58	6.700	0.000	5.608									
59	7.400	0.000	3.322									
60	6.950	-3.000	2.897									
61	6.200	-3.000	5.345									
62												
63												
64												
65												

FIG. 6J7

Station 4

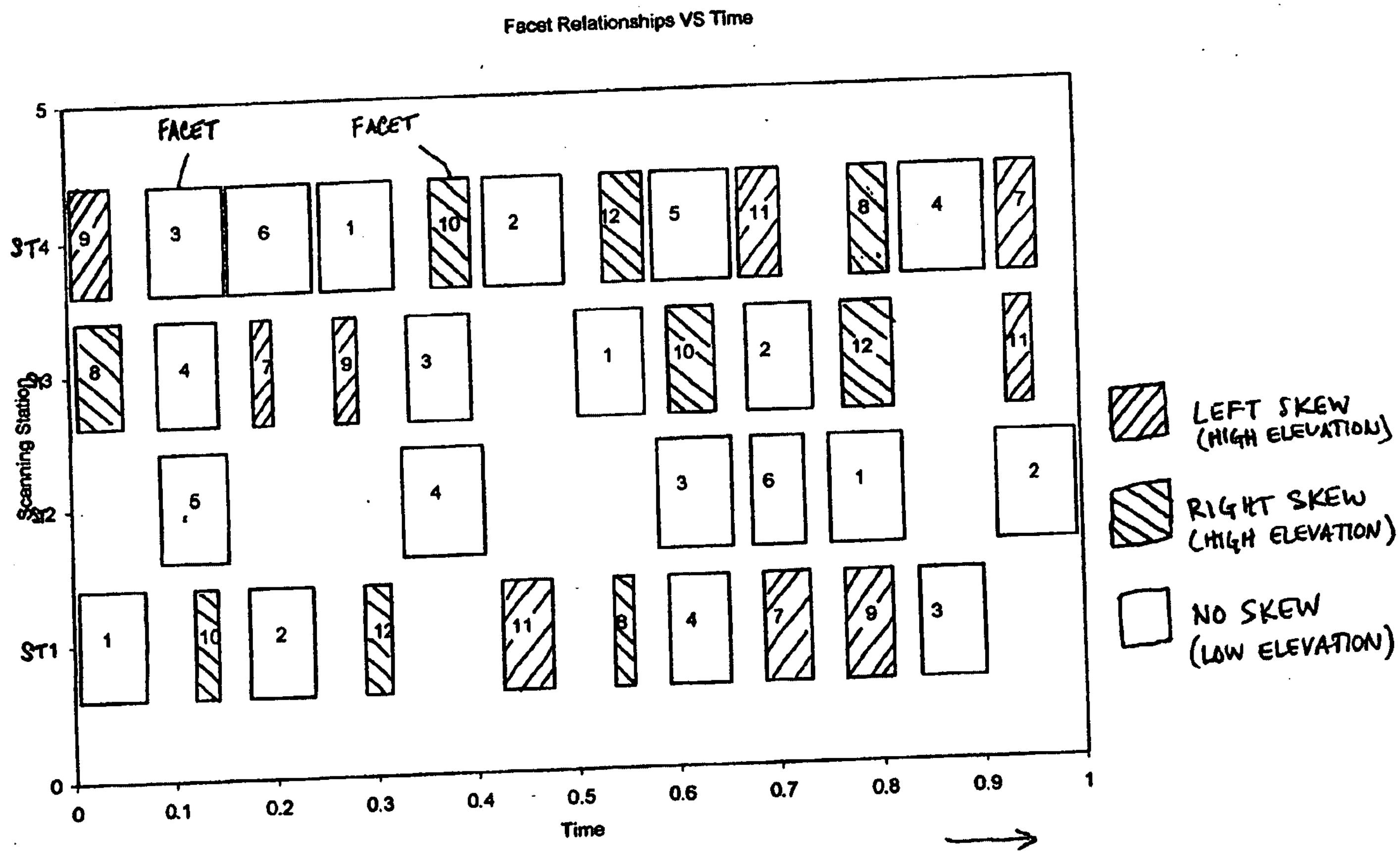
Facet Relationships VS Time
FACET
FACET
Scanning Station
ST4
ST3
ST2
ST1
Time
0
0.1
0.2
0.3
0.4
0.5
0.6
0.7
0.8
0.9
1
5
LEFT SKEW (HIGH ELEVATION)
RIGHT SKEW (HIGH ELEVATION)
NO SKEW (LOW ELEVATION)

FIG. 6K

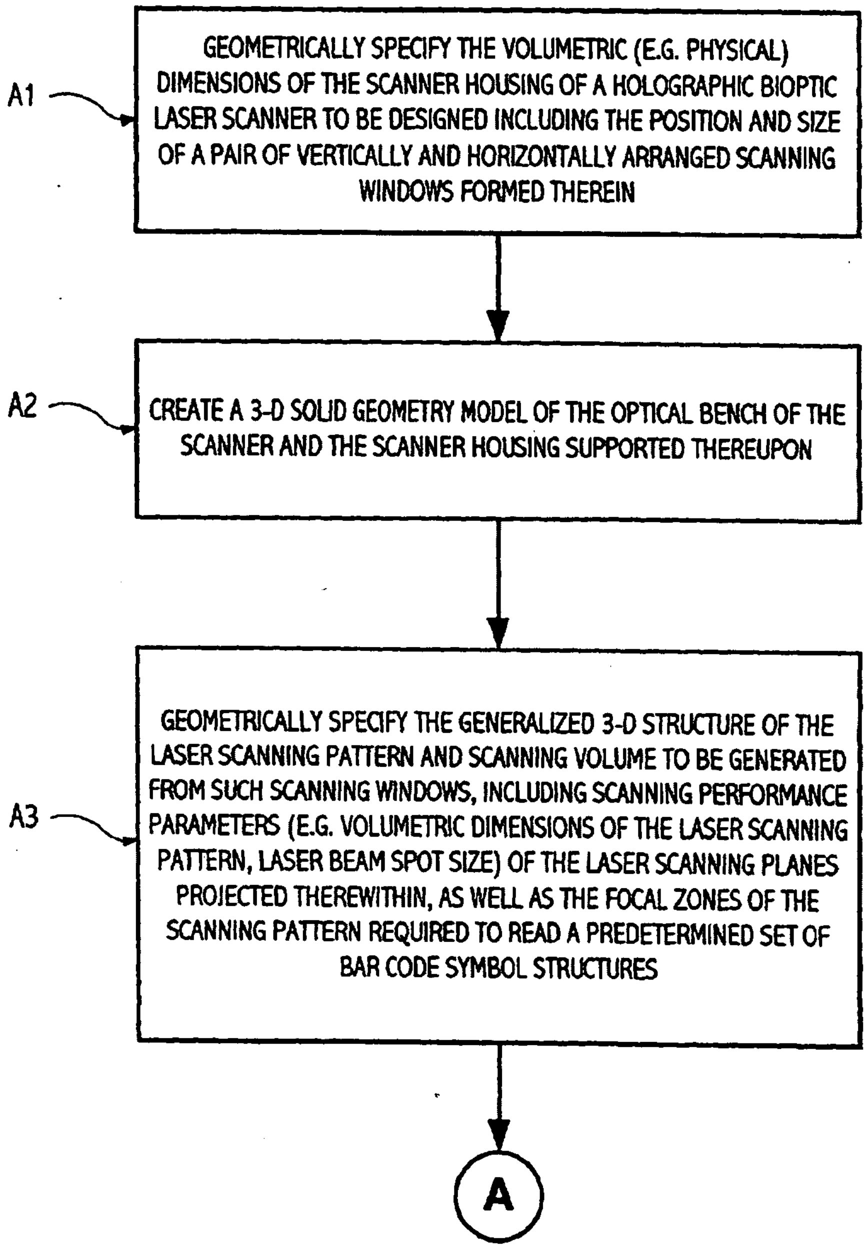
A1
GEOMETRICALLY SPECIFY THE VOLUMETRIC (E.G. PHYSICAL) DIMENSIONS OF THE SCANNER HOUSING OF A HOLOGRAPHIC BIOPTIC LASER SCANNER TO BE DESIGNED INCLUDING THE POSITION AND SIZE OF A PAIR OF VERTICALLY AND HORIZONTALLY ARRANGED SCANNING WINDOWS FORMED THEREIN
A2
CREATE A 3-D SOLID GEOMETRY MODEL OF THE OPTICAL BENCH OF THE SCANNER AND THE SCANNER HOUSING SUPPORTED THEREUPON
A3
GEOMETRICALLY SPECIFY THE GENERALIZED 3-D STRUCTURE OF THE LASER SCANNING PATTERN AND SCANNING VOLUME TO BE GENERATED FROM SUCH SCANNING WINDOWS, INCLUDING SCANNING PERFORMANCE PARAMETERS (E.G. VOLUMETRIC DIMENSIONS OF THE LASER SCANNING PATTERN, LASER BEAM SPOT SIZE) OF THE LASER SCANNING PLANES PROJECTED THEREWITHIN, AS WELL AS THE FOCAL ZONES OF THE SCANNING PATTERN REQUIRED TO READ A PREDETERMINED SET OF BAR CODE SYMBOL STRUCTURES
A

FIG. 7A

A

B1 SELECT AN ARCHITECTURE FOR A HOLOGRAPHIC LASER SCANNING PLATFORM TO BE DESIGNED AND REALIZED UPON THE OPTICAL BENCH WITHIN THE SPECIFIED SCANNER HOUSING

B2 CREATE A 3-D SOLID GEOMETRY MODEL FOR THE HOLOGRAPHIC SCANNING DISC AND EACH LASER SCANNING STATION IN THE HOLOGRAPHIC SCANNING SYSTEM

B3 INTEGRATE THE 3-D SOLID GEOMETRY MODELS OF THE SCANNER HOUSING, OPTICAL BENCH, HOLOGRAPHIC SCANNING DISC, AND LASER SCANNING STATIONS TO FORM A 3-D HOLOGRAPHIC LASER SCANNING SYSTEM

B4 SYMBOLICALLY EMBED A FIRST LOCALLY-DEFINED HYBRID CARTESIAN/POLAR COORDINATE SYSTEM WITHIN THE 3-D SOLID GEOMETRY MODEL OF THE HOLOGRAPHIC LASER SCANNING SYSTEM, IN ORDER TO SPECIFY THE PROPAGATION OF LASER BEAMS GENERATED FROM THE LASER BEAM PRODUCTION MODULE OF LASER SCANNING STATION NO. 1 THROUGH THE FACETS ON THE HOLOGRAPHIC SCANNING DISC, AND OFF THE BEAM FOLDING MIRRORS ASSOCIATED WITH THE LASER SCANNING STATION, THROUGH THE BOTTOM SCANNING WINDOW FORMED IN THE SCANNER HOUSING. WHOSE COORDINATE REFERENCE SYSTEM IS INDICATED BY R_{LOCAL1}

B

FIG. 7B

B

B5 SYMBOLICALLY EMBED A SECOND LOCALLY-DEFINED HYBRID CARTESIAN/POLAR COORDINATE SYSTEM WITHIN THE 3-D SOLID GEOMETRY MODEL OF THE HOLOGRAPHIC LASER SCANNING SYSTEM, IN ORDER TO SPECIFY THE PROPAGATION OF LASER BEAMS GENERATED FROM THE LASER BEAM PRODUCTION MODULE OF LASER SCANNING STATION NO. 2 THROUGH THE FACETS ON THE HOLOGRAPHIC SCANNING DISC, AND OFF THE BEAM FOLDING MIRRORS ASSOCIATED WITH THE LASER SCANNING STATION, THROUGH THE BOTTOM SCANNING WINDOW FORMED IN THE SCANNER HOUSING. WHOSE COORDINATE REFERENCE SYSTEM IS INDICATED BY R_{LOCAL2}

B6 SYMBOLICALLY EMBED A THIRD LOCALLY-DEFINED HYBRID CARTESIAN/POLAR COORDINATE SYSTEM WITHIN THE 3-D SOLID GEOMETRY MODEL OF THE HOLOGRAPHIC LASER SCANNING SYSTEM, IN ORDER TO SPECIFY THE PROPAGATION OF LASER BEAMS GENERATED FROM THE LASER BEAM PRODUCTION MODULE OF LASER SCANNING STATION NO. 3 THROUGH THE FACETS ON THE HOLOGRAPHIC SCANNING DISC, AND OFF THE BEAM FOLDING MIRRORS ASSOCIATED WITH THE LASER SCANNING STATION, THROUGH THE SIDE SCANNING WINDOW FORMED IN THE SCANNER HOUSING. WHOSE COORDINATE REFERENCE SYSTEM IS INDICATED BY R_{LOCAL3}

B7 SYMBOLICALLY EMBED A FOURTH LOCALLY-DEFINED HYBRID CARTESIAN/POLAR COORDINATE SYSTEM WITHIN THE 3-D SOLID GEOMETRY MODEL OF THE HOLOGRAPHIC LASER SCANNING SYSTEM, IN ORDER TO SPECIFY THE PROPAGATION OF LASER BEAMS GENERATED FROM THE LASER BEAM PRODUCTION MODULE OF LASER SCANNING STATION NO. 4 THROUGH THE FACETS ON THE HOLOGRAPHIC SCANNING DISC, AND OFF THE BEAM FOLDING MIRRORS ASSOCIATED WITH THE LASER SCANNING STATION, THROUGH THE SIDE SCANNING WINDOW FORMED IN THE SCANNER HOUSING. WHOSE COORDINATE REFERENCE SYSTEM IS INDICATED BY R_{LOCAL4}

C

FIG. 7C

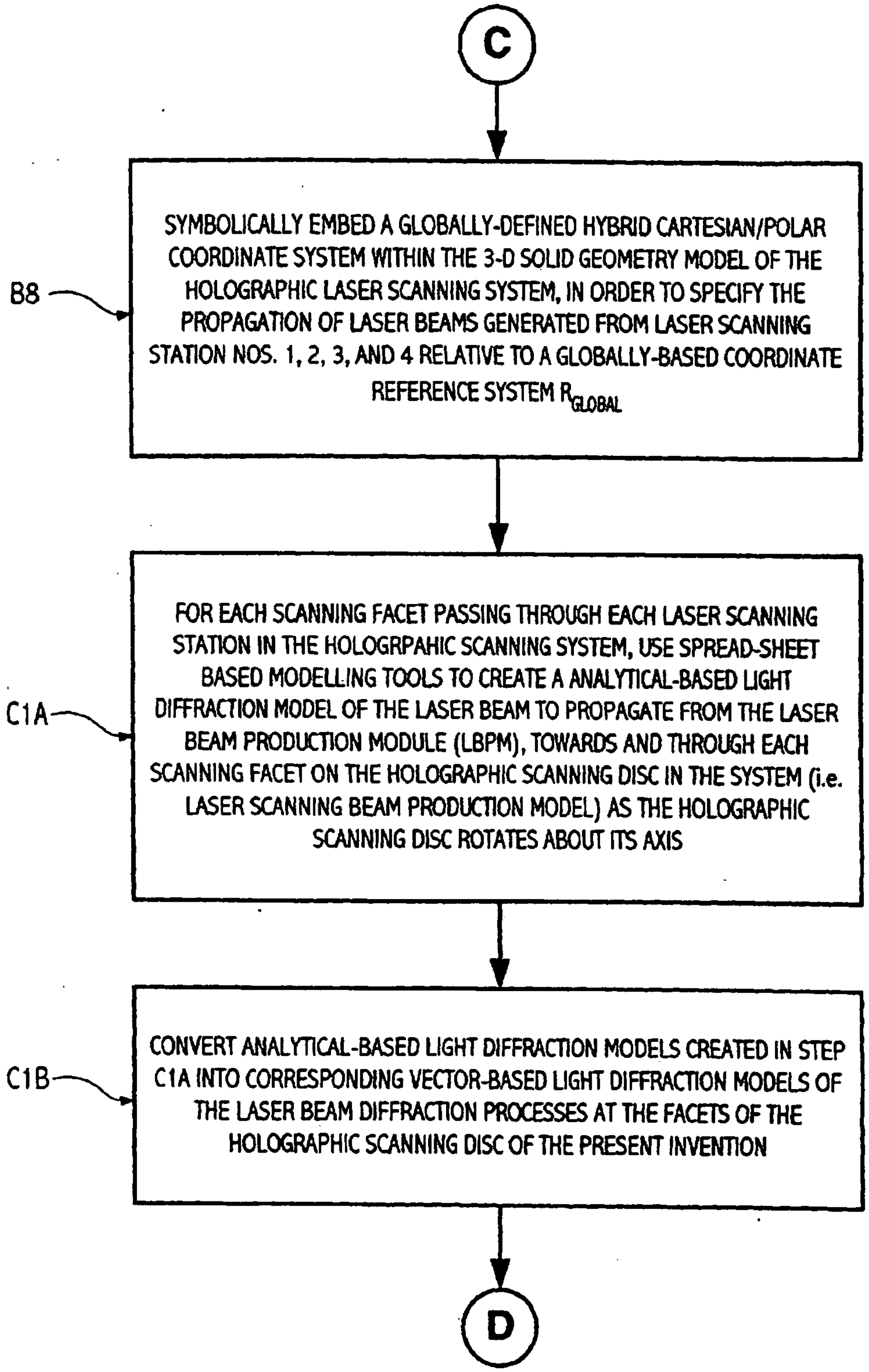
C
B8
SYMBOLICALLY EMBED A GLOBALLY-DEFINED HYBRID CARTESIAN/POLAR COORDINATE SYSTEM WITHIN THE 3-D SOLID GEOMETRY MODEL OF THE HOLOGRAPHIC LASER SCANNING SYSTEM, IN ORDER TO SPECIFY THE PROPAGATION OF LASER BEAMS GENERATED FROM LASER SCANNING STATION NOS. 1, 2, 3, AND 4 RELATIVE TO A GLOBALLY-BASED COORDINATE REFERENCE SYSTEM R_{GLOBAL}
C1A
FOR EACH SCANNING FACET PASSING THROUGH EACH LASER SCANNING STATION IN THE HOLOGRPAHIC SCANNING SYSTEM, USE SPREAD-SHEET BASED MODELLING TOOLS TO CREATE A ANALYTICAL-BASED LIGHT DIFFRACTION MODEL OF THE LASER BEAM TO PROPAGATE FROM THE LASER BEAM PRODUCTION MODULE (LBPM), TOWARDS AND THROUGH EACH SCANNING FACET ON THE HOLOGRAPHIC SCANNING DISC IN THE SYSTEM (i.e. LASER SCANNING BEAM PRODUCTION MODEL) AS THE HOLOGRAPHIC SCANNING DISC ROTATES ABOUT ITS AXIS
C1B
CONVERT ANALYTICAL-BASED LIGHT DIFFRACTION MODELS CREATED IN STEP C1A INTO CORRESPONDING VECTOR-BASED LIGHT DIFFRACTION MODELS OF THE LASER BEAM DIFFRACTION PROCESSES AT THE FACETS OF THE HOLOGRAPHIC SCANNING DISC OF THE PRESENT INVENTION
D

FIG. 7D

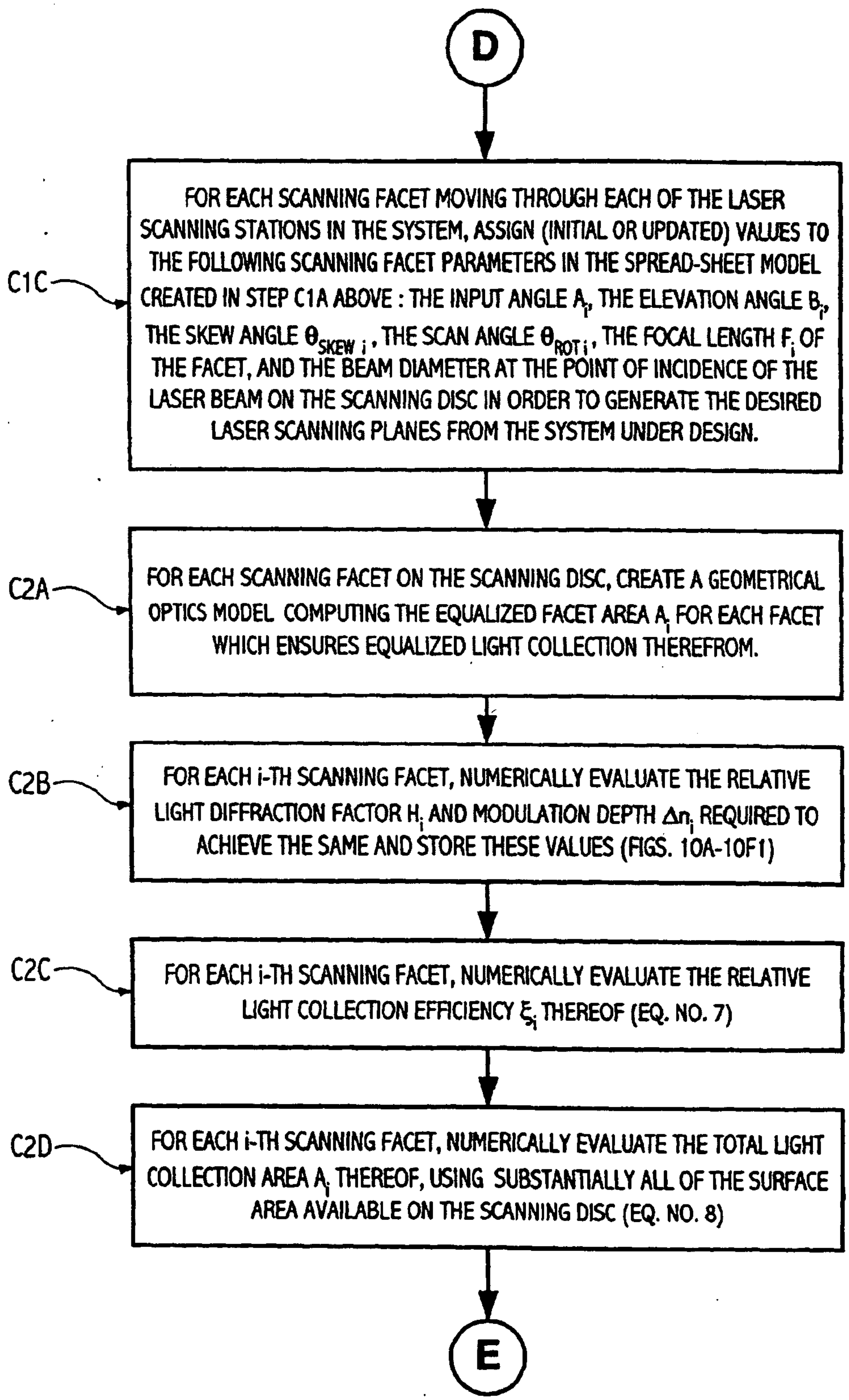
D
C1C
FOR EACH SCANNING FACET MOVING THROUGH EACH OF THE LASER SCANNING STATIONS IN THE SYSTEM, ASSIGN (INITIAL OR UPDATED) VALUES TO THE FOLLOWING SCANNING FACET PARAMETERS IN THE SPREAD-SHEET MODEL CREATED IN STEP C1A ABOVE : THE INPUT ANGLE A_i, THE ELEVATION ANGLE B_i, THE SKEW ANGLE $\theta_{SKEW\ i}$, THE SCAN ANGLE $\theta_{ROT\ i}$, THE FOCAL LENGTH F_i OF THE FACET, AND THE BEAM DIAMETER AT THE POINT OF INCIDENCE OF THE LASER BEAM ON THE SCANNING DISC IN ORDER TO GENERATE THE DESIRED LASER SCANNING PLANES FROM THE SYSTEM UNDER DESIGN.
C2A
FOR EACH SCANNING FACET ON THE SCANNING DISC, CREATE A GEOMETRICAL OPTICS MODEL COMPUTING THE EQUALIZED FACET AREA A_i FOR EACH FACET WHICH ENSURES EQUALIZED LIGHT COLLECTION THEREFROM.
C2B
FOR EACH i-TH SCANNING FACET, NUMERICALLY EVALUATE THE RELATIVE LIGHT DIFFRACTION FACTOR H_i AND MODULATION DEPTH Δn_i REQUIRED TO ACHIEVE THE SAME AND STORE THESE VALUES (FIGS. 10A-10F1)
C2C
FOR EACH i-TH SCANNING FACET, NUMERICALLY EVALUATE THE RELATIVE LIGHT COLLECTION EFFICIENCY ξ_i THEREOF (EQ. NO. 7)
C2D
FOR EACH i-TH SCANNING FACET, NUMERICALLY EVALUATE THE TOTAL LIGHT COLLECTION AREA A_i THEREOF, USING SUBSTANTIALLY ALL OF THE SURFACE AREA AVAILABLE ON THE SCANNING DISC (EQ. NO. 8)
E

FIG. 7E

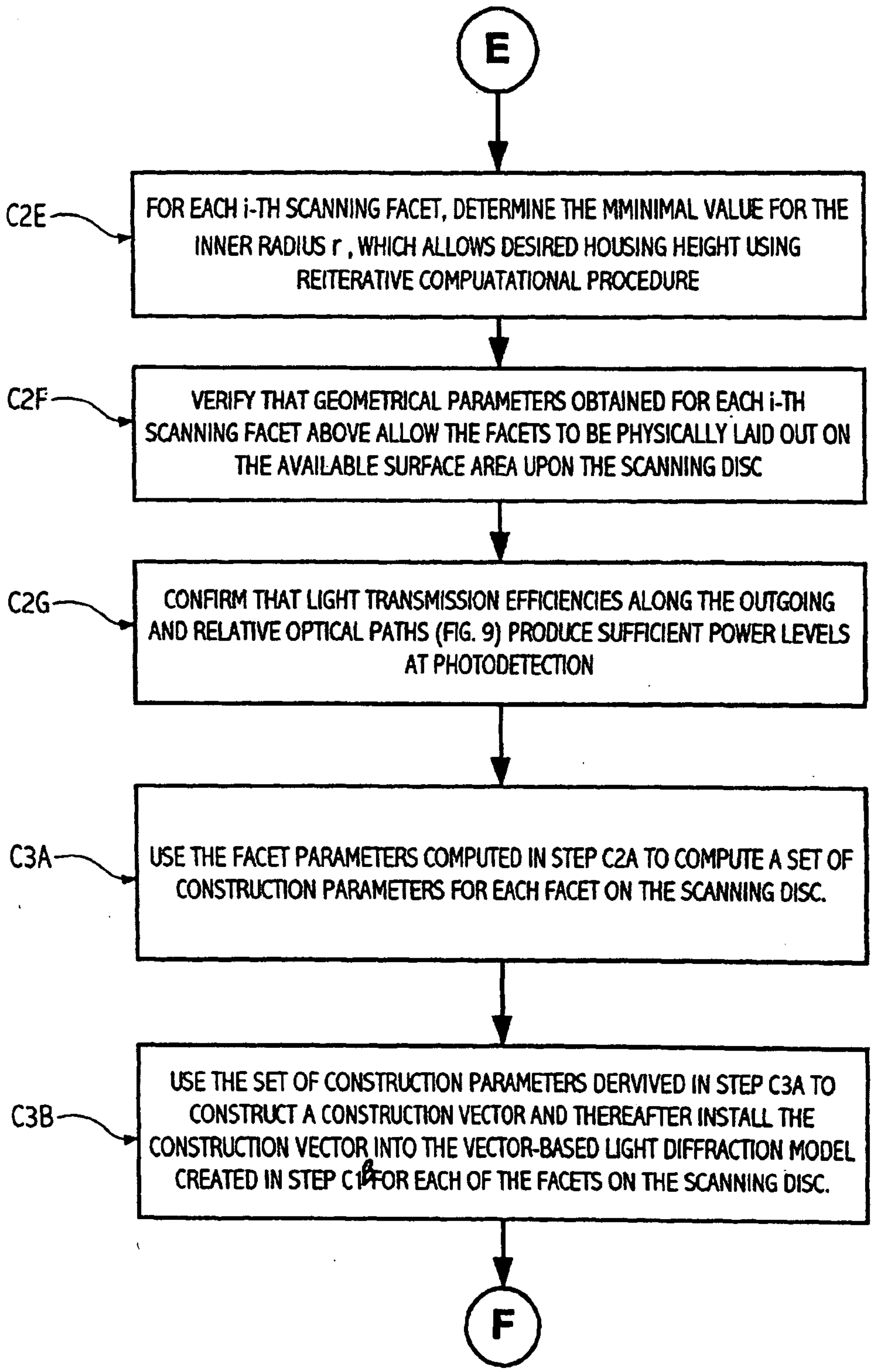
E
C2E
FOR EACH i-TH SCANNING FACET, DETERMINE THE MMINIMAL VALUE FOR THE INNER RADIUS r, WHICH ALLOWS DESIRED HOUSING HEIGHT USING REITERATIVE COMPUATATIONAL PROCEDURE
C2F
VERIFY THAT GEOMETRICAL PARAMETERS OBTAINED FOR EACH i-TH SCANNING FACET ABOVE ALLOW THE FACETS TO BE PHYSICALLY LAID OUT ON THE AVAILABLE SURFACE AREA UPON THE SCANNING DISC
C2G
CONFIRM THAT LIGHT TRANSMISSION EFFICIENCIES ALONG THE OUTGOING AND RELATIVE OPTICAL PATHS (FIG. 9) PRODUCE SUFFICIENT POWER LEVELS AT PHOTODETECTION
C3A
USE THE FACET PARAMETERS COMPUTED IN STEP C2A TO COMPUTE A SET OF CONSTRUCTION PARAMETERS FOR EACH FACET ON THE SCANNING DISC.
C3B
USE THE SET OF CONSTRUCTION PARAMETERS DERVIVED IN STEP C3A TO CONSTRUCT A CONSTRUCTION VECTOR AND THEREAFTER INSTALL THE CONSTRUCTION VECTOR INTO THE VECTOR-BASED LIGHT DIFFRACTION MODEL CREATED IN STEP C1 FOR EACH OF THE FACETS ON THE SCANNING DISC.
F

FIG. 7F

F

C4A

SPECIFY THE DEPTH OF FOCUS (DOF) AND THE MINIMUM BEAM SPOT SIZE (I.E. CROSS-SECTIONAL DIAMETER) OF THE LASER SCANNING PLANES TO BE GENERATED FROM EACH FACET ON THE SCANNING DISC AT EACH OF THE LASER SCANNING STATIONS.

C4B

USING THE RESULTS FROM STEP C4A ABOVE AND INITIAL FACET PARAMETERS, SPECIFY THE FOCAL LENGTH AND NUMERICAL APERTURE OF THE VLD LENS IN THE REFRACTION-BASED MODEL OF THE LASER BEAM PRODUCTION MODULES USED IN THE HOLOGRAPHIC SCANNING SYSTEM SO AS TO PRODUCE LASER SCANNING PLANES HAVING THE DOF AND MINIMUM BEAM SPOT SIZE CHARACTERISTICS SPECIFIED IN STEP C4A.

G

FIG. 7G

251/335

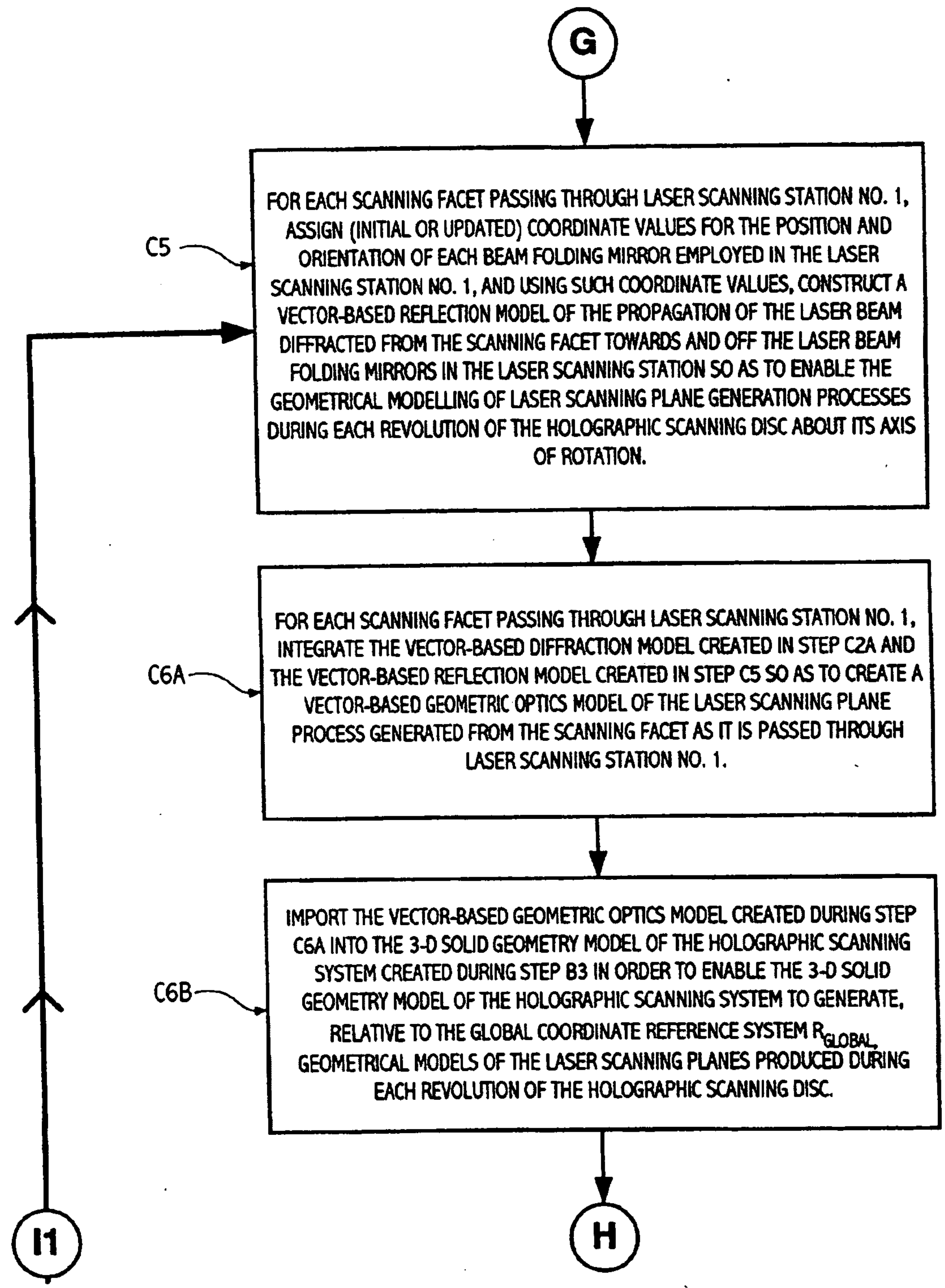

FIG. 7H

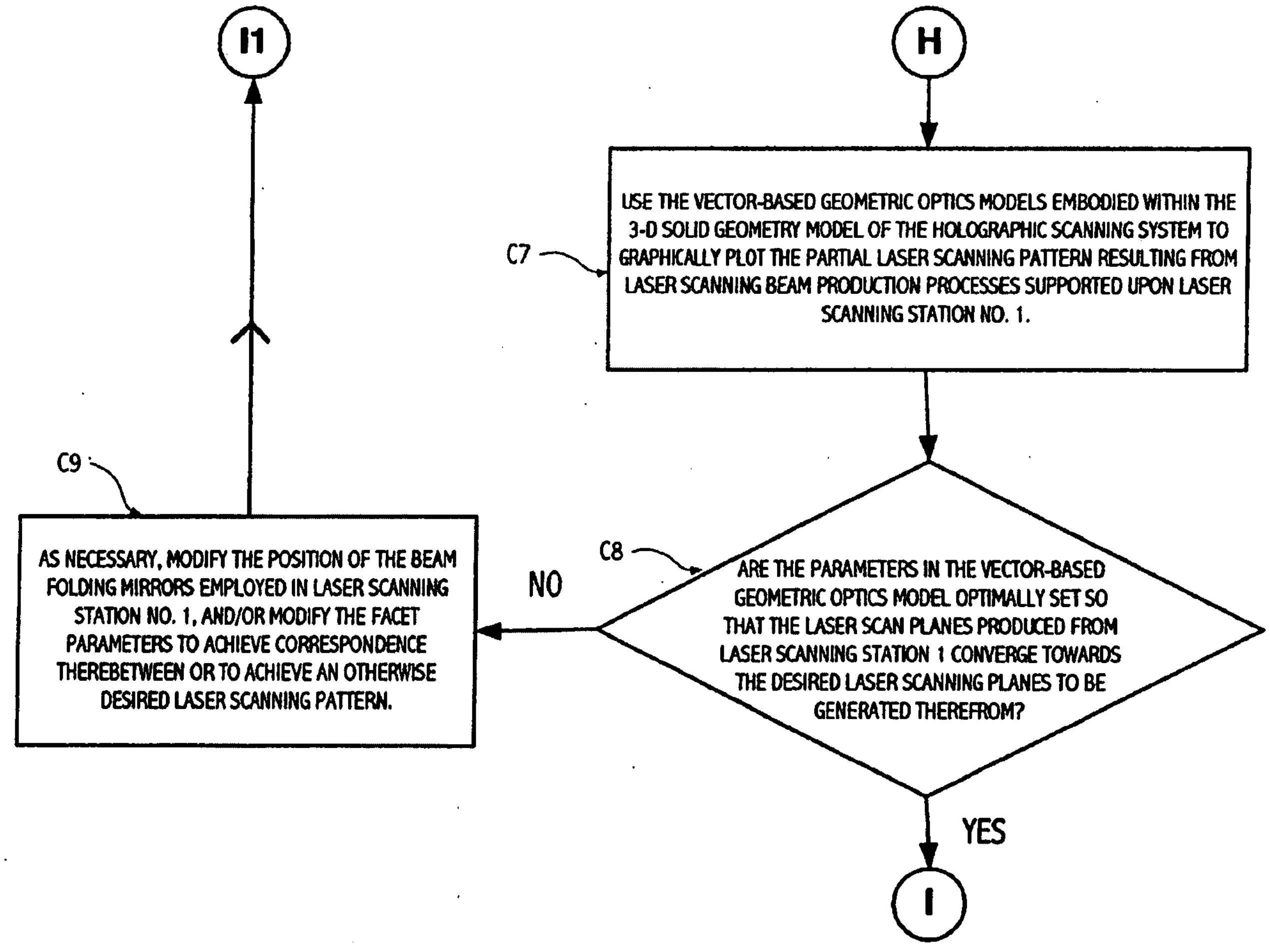
H
USE THE VECTOR-BASED GEOMETRIC OPTICS MODELS EMBODIED WITHIN THE 3-D SOLID GEOMETRY MODEL OF THE HOLOGRAPHIC SCANNING SYSTEM TO GRAPHICALLY PLOT THE PARTIAL LASER SCANNING PATTERN RESULTING FROM LASER SCANNING BEAM PRODUCTION PROCESSES SUPPORTED UPON LASER SCANNING STATION NO. 1.
C7
ARE THE PARAMETERS IN THE VECTOR-BASED GEOMETRIC OPTICS MODEL OPTIMALLY SET SO THAT THE LASER SCAN PLANES PRODUCED FROM LASER SCANNING STATION 1 CONVERGE TOWARDS THE DESIRED LASER SCANNING PLANES TO BE GENERATED THEREFROM?
C8
YES
I
NO
AS NECESSARY, MODIFY THE POSITION OF THE BEAM FOLDING MIRRORS EMPLOYED IN LASER SCANNING STATION NO. 1, AND/OR MODIFY THE FACET PARAMETERS TO ACHIEVE CORRESPONDENCE THEREBETWEEN OR TO ACHIEVE AN OTHERWISE DESIRED LASER SCANNING PATTERN.
C9
I1

FIG. 7I

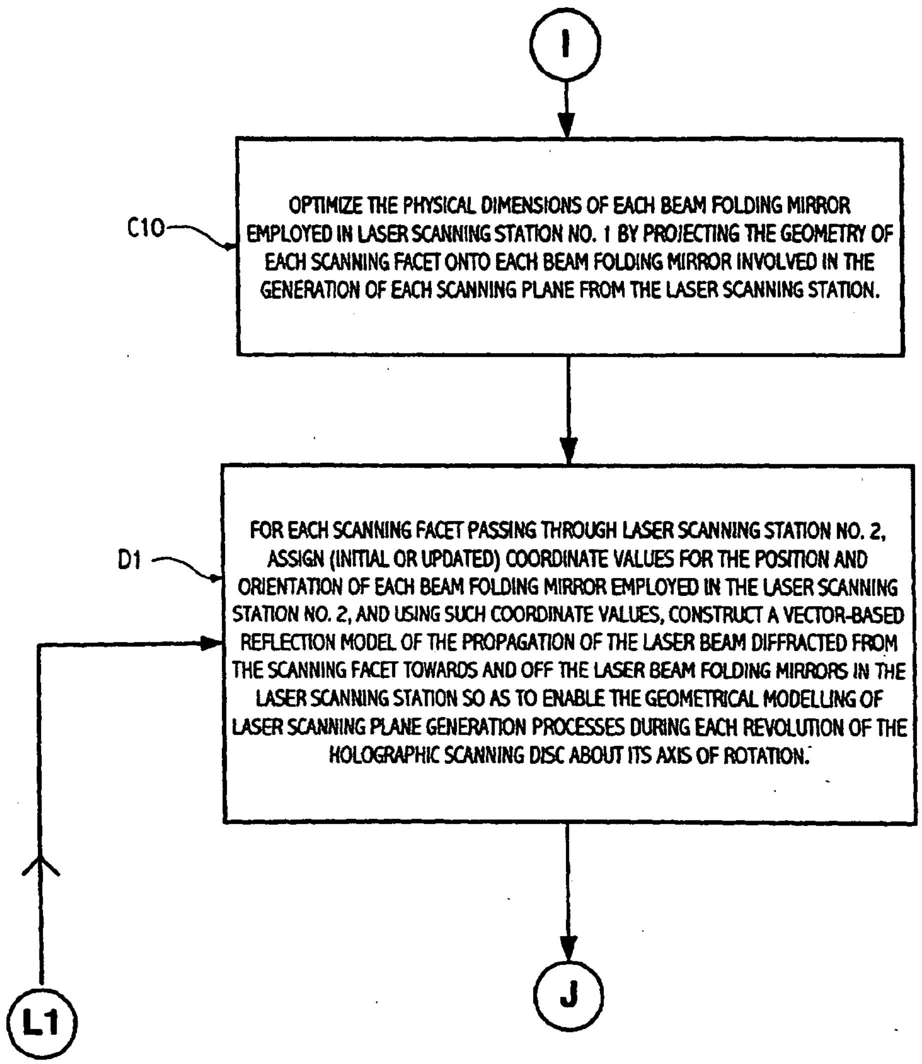
I
C10
OPTIMIZE THE PHYSICAL DIMENSIONS OF EACH BEAM FOLDING MIRROR EMPLOYED IN LASER SCANNING STATION NO. 1 BY PROJECTING THE GEOMETRY OF EACH SCANNING FACET ONTO EACH BEAM FOLDING MIRROR INVOLVED IN THE GENERATION OF EACH SCANNING PLANE FROM THE LASER SCANNING STATION.
D1
FOR EACH SCANNING FACET PASSING THROUGH LASER SCANNING STATION NO. 2, ASSIGN (INITIAL OR UPDATED) COORDINATE VALUES FOR THE POSITION AND ORIENTATION OF EACH BEAM FOLDING MIRROR EMPLOYED IN THE LASER SCANNING STATION NO. 2, AND USING SUCH COORDINATE VALUES, CONSTRUCT A VECTOR-BASED REFLECTION MODEL OF THE PROPAGATION OF THE LASER BEAM DIFFRACTED FROM THE SCANNING FACET TOWARDS AND OFF THE LASER BEAM FOLDING MIRRORS IN THE LASER SCANNING STATION SO AS TO ENABLE THE GEOMETRICAL MODELLING OF LASER SCANNING PLANE GENERATION PROCESSES DURING EACH REVOLUTION OF THE HOLOGRAPHIC SCANNING DISC ABOUT ITS AXIS OF ROTATION.
L1
J

FIG. 7J

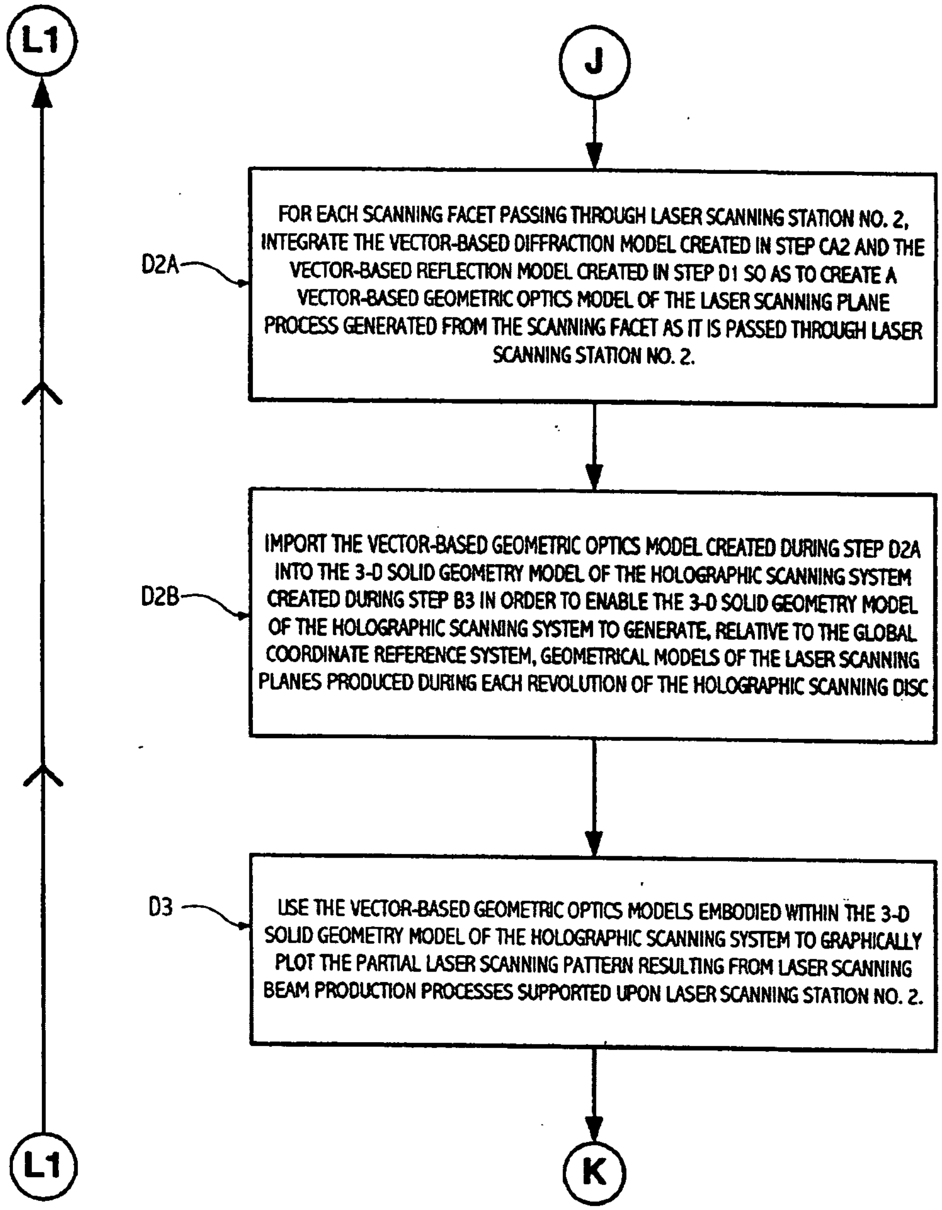
L1
J
FOR EACH SCANNING FACET PASSING THROUGH LASER SCANNING STATION NO. 2, INTEGRATE THE VECTOR-BASED DIFFRACTION MODEL CREATED IN STEP CA2 AND THE VECTOR-BASED REFLECTION MODEL CREATED IN STEP D1 SO AS TO CREATE A VECTOR-BASED GEOMETRIC OPTICS MODEL OF THE LASER SCANNING PLANE PROCESS GENERATED FROM THE SCANNING FACET AS IT IS PASSED THROUGH LASER SCANNING STATION NO. 2.
D2A
IMPORT THE VECTOR-BASED GEOMETRIC OPTICS MODEL CREATED DURING STEP D2A INTO THE 3-D SOLID GEOMETRY MODEL OF THE HOLOGRAPHIC SCANNING SYSTEM CREATED DURING STEP B3 IN ORDER TO ENABLE THE 3-D SOLID GEOMETRY MODEL OF THE HOLOGRAPHIC SCANNING SYSTEM TO GENERATE, RELATIVE TO THE GLOBAL COORDINATE REFERENCE SYSTEM, GEOMETRICAL MODELS OF THE LASER SCANNING PLANES PRODUCED DURING EACH REVOLUTION OF THE HOLOGRAPHIC SCANNING DISC
D2B
USE THE VECTOR-BASED GEOMETRIC OPTICS MODELS EMBODIED WITHIN THE 3-D SOLID GEOMETRY MODEL OF THE HOLOGRAPHIC SCANNING SYSTEM TO GRAPHICALLY PLOT THE PARTIAL LASER SCANNING PATTERN RESULTING FROM LASER SCANNING BEAM PRODUCTION PROCESSES SUPPORTED UPON LASER SCANNING STATION NO. 2.
D3
L1
K

FIG. 7K

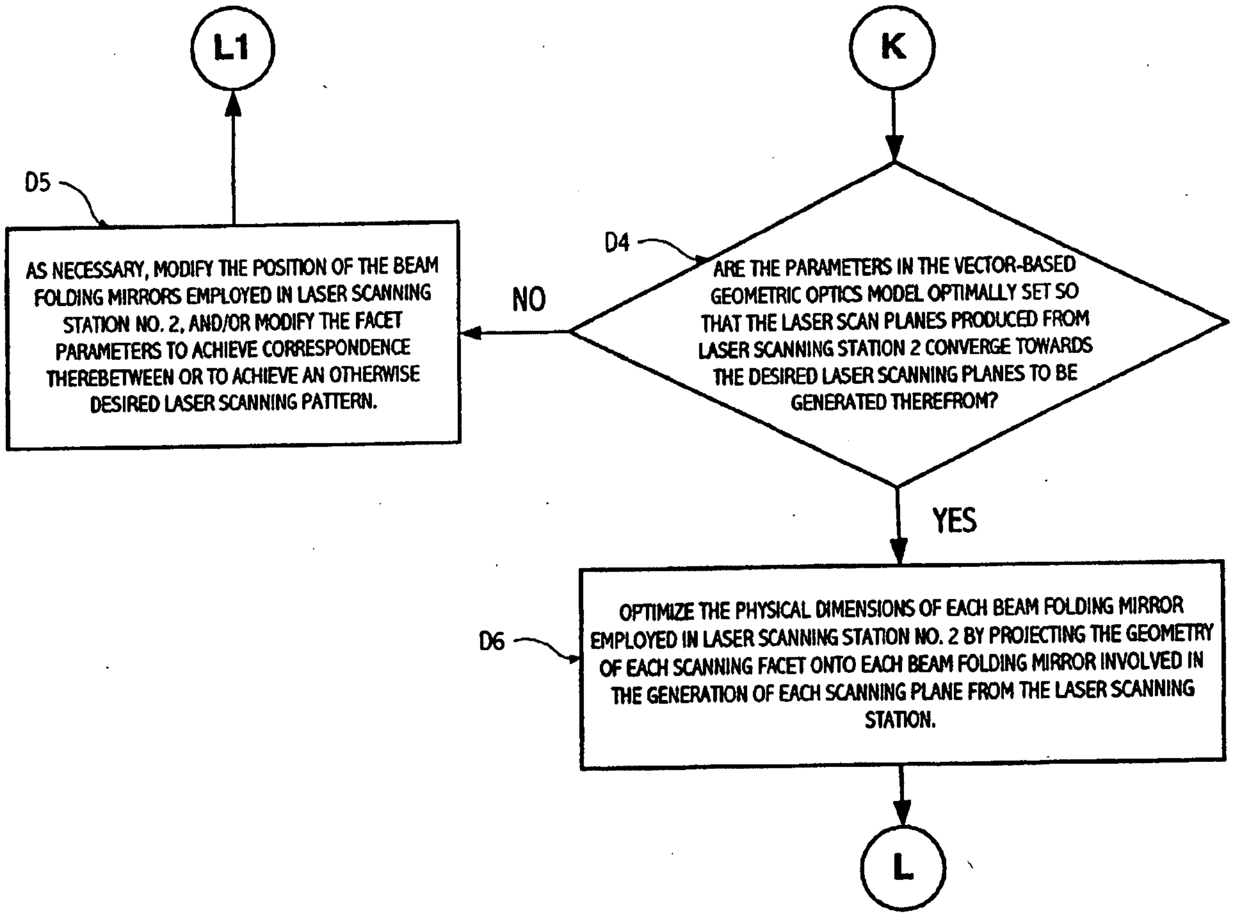
K
D4
ARE THE PARAMETERS IN THE VECTOR-BASED GEOMETRIC OPTICS MODEL OPTIMALLY SET SO THAT THE LASER SCAN PLANES PRODUCED FROM LASER SCANNING STATION 2 CONVERGE TOWARDS THE DESIRED LASER SCANNING PLANES TO BE GENERATED THEREFROM?
NO
D5
AS NECESSARY, MODIFY THE POSITION OF THE BEAM FOLDING MIRRORS EMPLOYED IN LASER SCANNING STATION NO. 2, AND/OR MODIFY THE FACET PARAMETERS TO ACHIEVE CORRESPONDENCE THEREBETWEEN OR TO ACHIEVE AN OTHERWISE DESIRED LASER SCANNING PATTERN.
L1
YES
D6
OPTIMIZE THE PHYSICAL DIMENSIONS OF EACH BEAM FOLDING MIRROR EMPLOYED IN LASER SCANNING STATION NO. 2 BY PROJECTING THE GEOMETRY OF EACH SCANNING FACET ONTO EACH BEAM FOLDING MIRROR INVOLVED IN THE GENERATION OF EACH SCANNING PLANE FROM THE LASER SCANNING STATION.
L

FIG. 7L

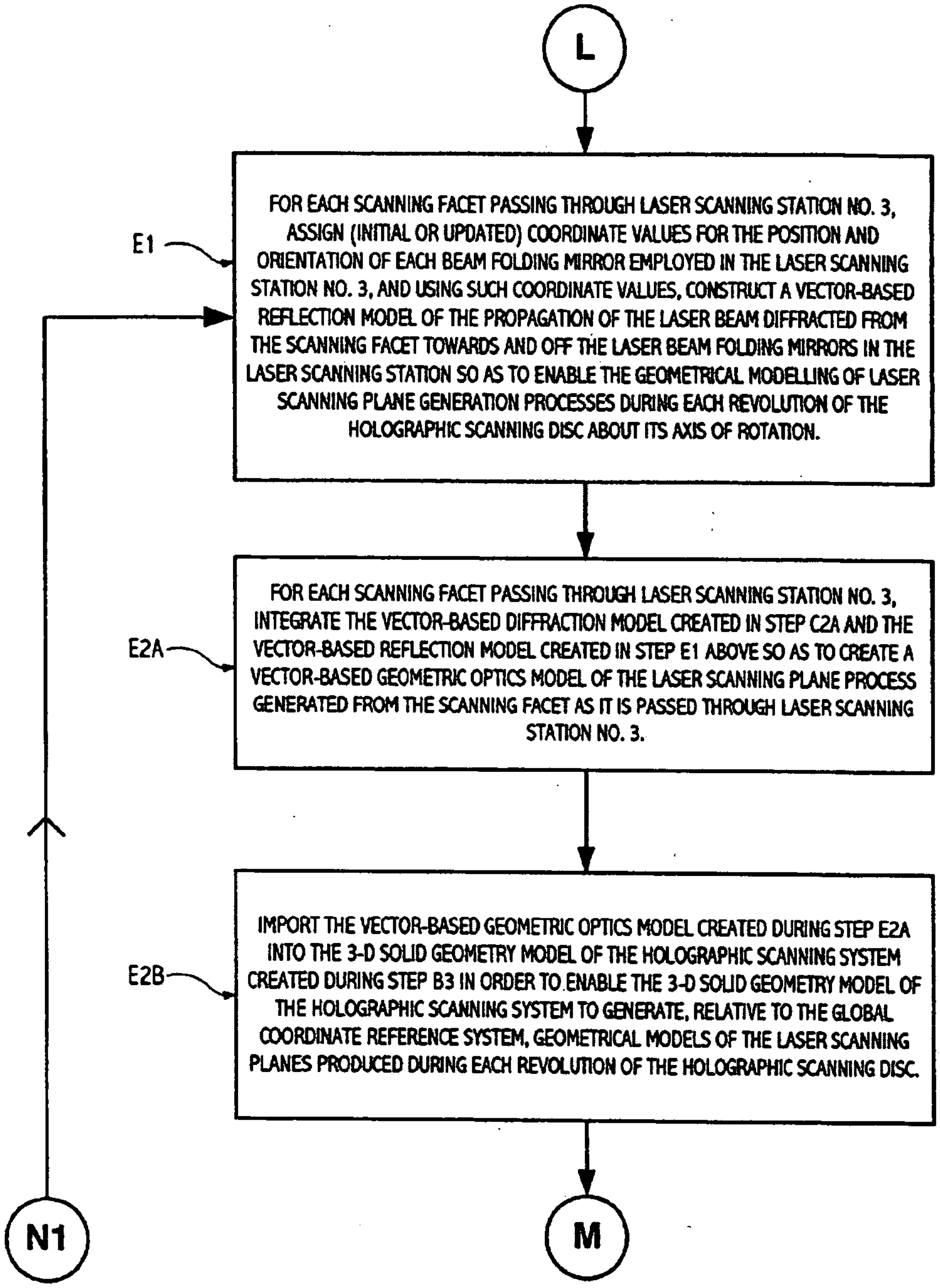
L
E1
FOR EACH SCANNING FACET PASSING THROUGH LASER SCANNING STATION NO. 3, ASSIGN (INITIAL OR UPDATED) COORDINATE VALUES FOR THE POSITION AND ORIENTATION OF EACH BEAM FOLDING MIRROR EMPLOYED IN THE LASER SCANNING STATION NO. 3, AND USING SUCH COORDINATE VALUES, CONSTRUCT A VECTOR-BASED REFLECTION MODEL OF THE PROPAGATION OF THE LASER BEAM DIFFRACTED FROM THE SCANNING FACET TOWARDS AND OFF THE LASER BEAM FOLDING MIRRORS IN THE LASER SCANNING STATION SO AS TO ENABLE THE GEOMETRICAL MODELLING OF LASER SCANNING PLANE GENERATION PROCESSES DURING EACH REVOLUTION OF THE HOLOGRAPHIC SCANNING DISC ABOUT ITS AXIS OF ROTATION.
E2A
FOR EACH SCANNING FACET PASSING THROUGH LASER SCANNING STATION NO. 3, INTEGRATE THE VECTOR-BASED DIFFRACTION MODEL CREATED IN STEP C2A AND THE VECTOR-BASED REFLECTION MODEL CREATED IN STEP E1 ABOVE SO AS TO CREATE A VECTOR-BASED GEOMETRIC OPTICS MODEL OF THE LASER SCANNING PLANE PROCESS GENERATED FROM THE SCANNING FACET AS IT IS PASSED THROUGH LASER SCANNING STATION NO. 3.
E2B
IMPORT THE VECTOR-BASED GEOMETRIC OPTICS MODEL CREATED DURING STEP E2A INTO THE 3-D SOLID GEOMETRY MODEL OF THE HOLOGRAPHIC SCANNING SYSTEM CREATED DURING STEP B3 IN ORDER TO ENABLE THE 3-D SOLID GEOMETRY MODEL OF THE HOLOGRAPHIC SCANNING SYSTEM TO GENERATE, RELATIVE TO THE GLOBAL COORDINATE REFERENCE SYSTEM, GEOMETRICAL MODELS OF THE LASER SCANNING PLANES PRODUCED DURING EACH REVOLUTION OF THE HOLOGRAPHIC SCANNING DISC.
N1
M

FIG. 7M

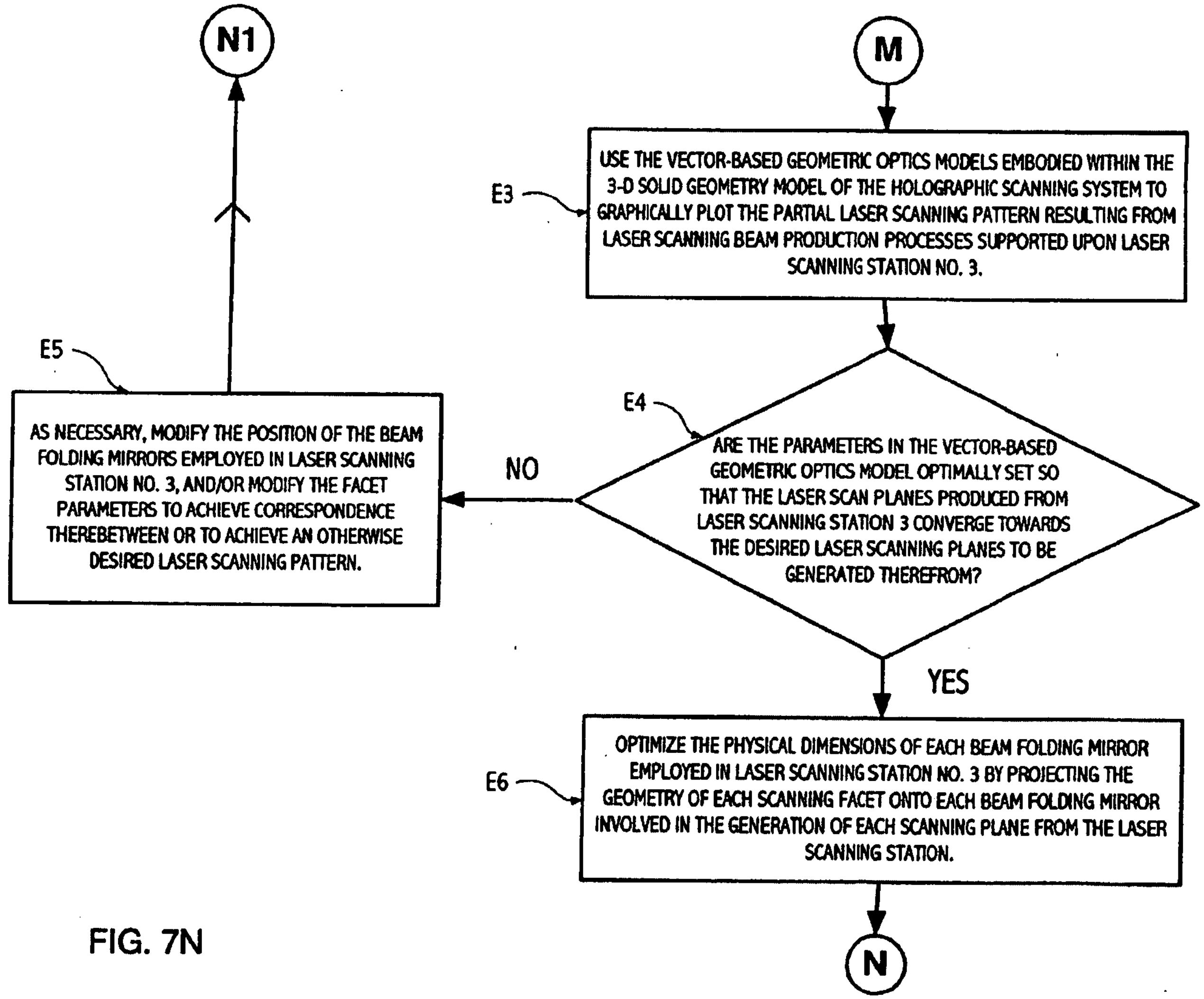
M
E3
USE THE VECTOR-BASED GEOMETRIC OPTICS MODELS EMBODIED WITHIN THE 3-D SOLID GEOMETRY MODEL OF THE HOLOGRAPHIC SCANNING SYSTEM TO GRAPHICALLY PLOT THE PARTIAL LASER SCANNING PATTERN RESULTING FROM LASER SCANNING BEAM PRODUCTION PROCESSES SUPPORTED UPON LASER SCANNING STATION NO. 3.
E4
ARE THE PARAMETERS IN THE VECTOR-BASED GEOMETRIC OPTICS MODEL OPTIMALLY SET SO THAT THE LASER SCAN PLANES PRODUCED FROM LASER SCANNING STATION 3 CONVERGE TOWARDS THE DESIRED LASER SCANNING PLANES TO BE GENERATED THEREFROM?
NO
E5
AS NECESSARY, MODIFY THE POSITION OF THE BEAM FOLDING MIRRORS EMPLOYED IN LASER SCANNING STATION NO. 3, AND/OR MODIFY THE FACET PARAMETERS TO ACHIEVE CORRESPONDENCE THEREBETWEEN OR TO ACHIEVE AN OTHERWISE DESIRED LASER SCANNING PATTERN.
N1
YES
E6
OPTIMIZE THE PHYSICAL DIMENSIONS OF EACH BEAM FOLDING MIRROR EMPLOYED IN LASER SCANNING STATION NO. 3 BY PROJECTING THE GEOMETRY OF EACH SCANNING FACET ONTO EACH BEAM FOLDING MIRROR INVOLVED IN THE GENERATION OF EACH SCANNING PLANE FROM THE LASER SCANNING STATION.
N

FIG. 7N

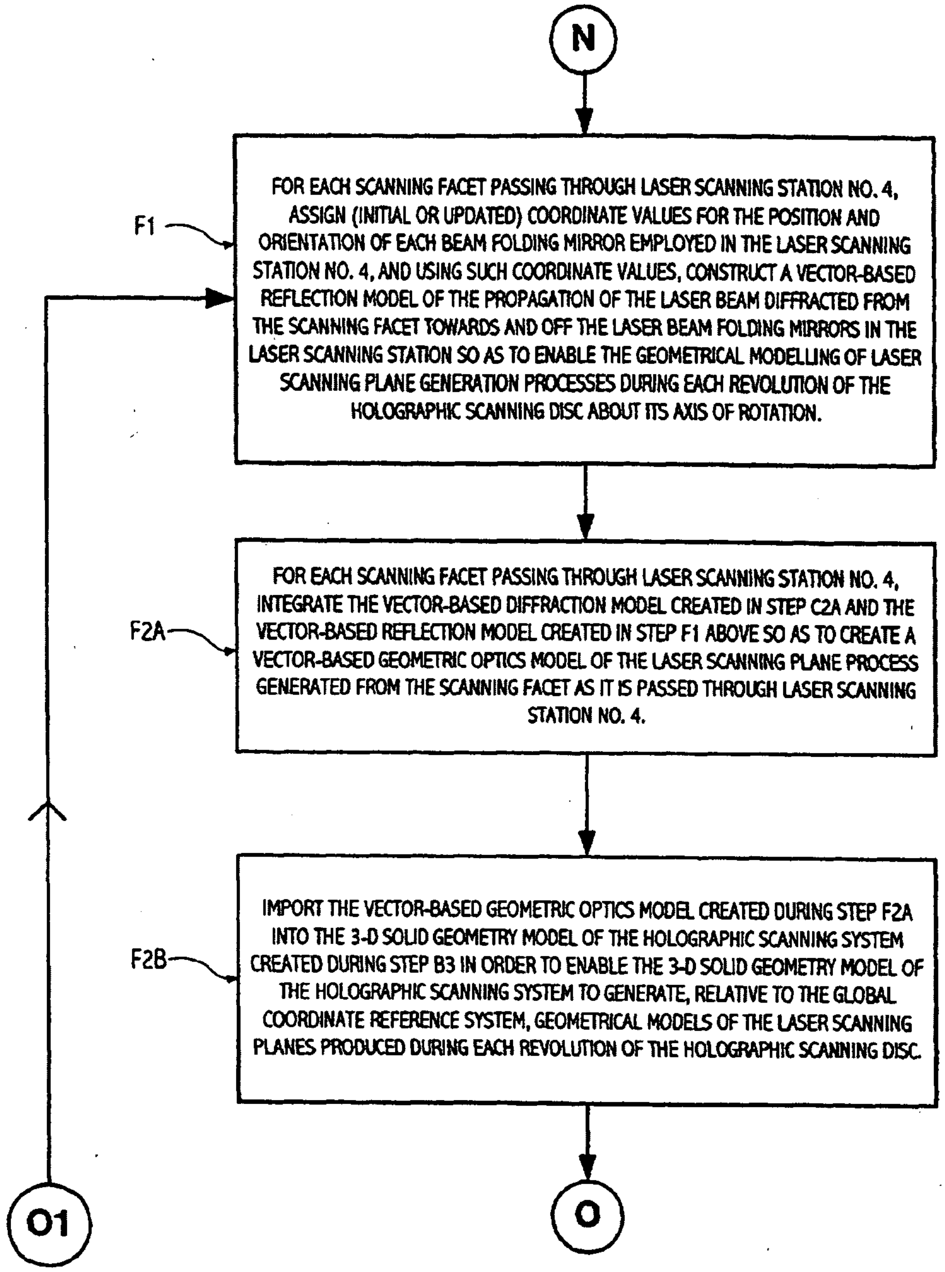
N
F1
FOR EACH SCANNING FACET PASSING THROUGH LASER SCANNING STATION NO. 4, ASSIGN (INITIAL OR UPDATED) COORDINATE VALUES FOR THE POSITION AND ORIENTATION OF EACH BEAM FOLDING MIRROR EMPLOYED IN THE LASER SCANNING STATION NO. 4, AND USING SUCH COORDINATE VALUES, CONSTRUCT A VECTOR-BASED REFLECTION MODEL OF THE PROPAGATION OF THE LASER BEAM DIFFRACTED FROM THE SCANNING FACET TOWARDS AND OFF THE LASER BEAM FOLDING MIRRORS IN THE LASER SCANNING STATION SO AS TO ENABLE THE GEOMETRICAL MODELLING OF LASER SCANNING PLANE GENERATION PROCESSES DURING EACH REVOLUTION OF THE HOLOGRAPHIC SCANNING DISC ABOUT ITS AXIS OF ROTATION.
F2A
FOR EACH SCANNING FACET PASSING THROUGH LASER SCANNING STATION NO. 4, INTEGRATE THE VECTOR-BASED DIFFRACTION MODEL CREATED IN STEP C2A AND THE VECTOR-BASED REFLECTION MODEL CREATED IN STEP F1 ABOVE SO AS TO CREATE A VECTOR-BASED GEOMETRIC OPTICS MODEL OF THE LASER SCANNING PLANE PROCESS GENERATED FROM THE SCANNING FACET AS IT IS PASSED THROUGH LASER SCANNING STATION NO. 4.
F2B
IMPORT THE VECTOR-BASED GEOMETRIC OPTICS MODEL CREATED DURING STEP F2A INTO THE 3-D SOLID GEOMETRY MODEL OF THE HOLOGRAPHIC SCANNING SYSTEM CREATED DURING STEP B3 IN ORDER TO ENABLE THE 3-D SOLID GEOMETRY MODEL OF THE HOLOGRAPHIC SCANNING SYSTEM TO GENERATE, RELATIVE TO THE GLOBAL COORDINATE REFERENCE SYSTEM, GEOMETRICAL MODELS OF THE LASER SCANNING PLANES PRODUCED DURING EACH REVOLUTION OF THE HOLOGRAPHIC SCANNING DISC.
O1
O

FIG. 7O

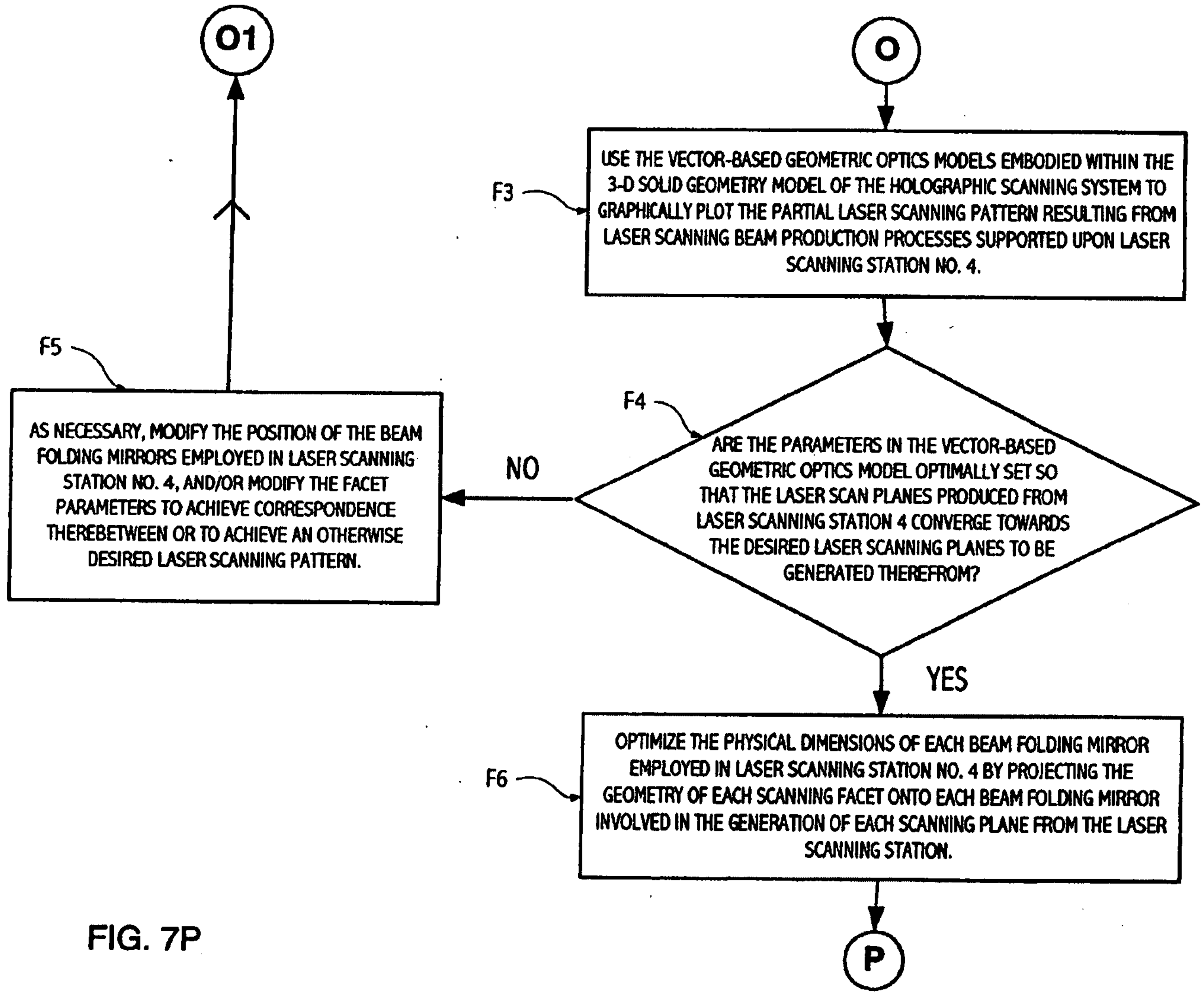
O
USE THE VECTOR-BASED GEOMETRIC OPTICS MODELS EMBODIED WITHIN THE 3-D SOLID GEOMETRY MODEL OF THE HOLOGRAPHIC SCANNING SYSTEM TO GRAPHICALLY PLOT THE PARTIAL LASER SCANNING PATTERN RESULTING FROM LASER SCANNING BEAM PRODUCTION PROCESSES SUPPORTED UPON LASER SCANNING STATION NO. 4.
F3
ARE THE PARAMETERS IN THE VECTOR-BASED GEOMETRIC OPTICS MODEL OPTIMALLY SET SO THAT THE LASER SCAN PLANES PRODUCED FROM LASER SCANNING STATION 4 CONVERGE TOWARDS THE DESIRED LASER SCANNING PLANES TO BE GENERATED THEREFROM?
F4
NO
AS NECESSARY, MODIFY THE POSITION OF THE BEAM FOLDING MIRRORS EMPLOYED IN LASER SCANNING STATION NO. 4, AND/OR MODIFY THE FACET PARAMETERS TO ACHIEVE CORRESPONDENCE THEREBETWEEN OR TO ACHIEVE AN OTHERWISE DESIRED LASER SCANNING PATTERN.
F5
O1
YES
OPTIMIZE THE PHYSICAL DIMENSIONS OF EACH BEAM FOLDING MIRROR EMPLOYED IN LASER SCANNING STATION NO. 4 BY PROJECTING THE GEOMETRY OF EACH SCANNING FACET ONTO EACH BEAM FOLDING MIRROR INVOLVED IN THE GENERATION OF EACH SCANNING PLANE FROM THE LASER SCANNING STATION.
F6
P

FIG. 7P

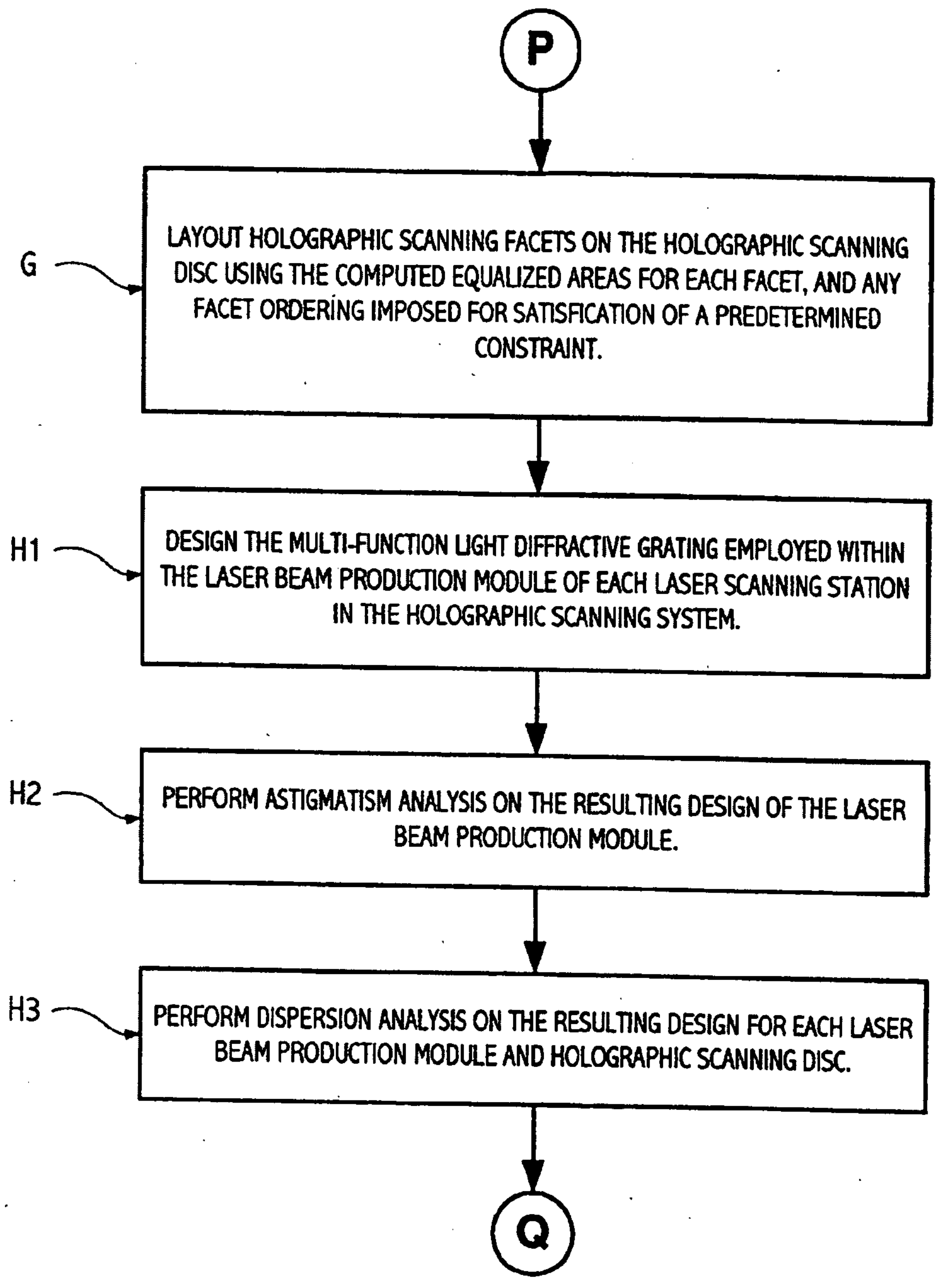
P
G
LAYOUT HOLOGRAPHIC SCANNING FACETS ON THE HOLOGRAPHIC SCANNING DISC USING THE COMPUTED EQUALIZED AREAS FOR EACH FACET, AND ANY FACET ORDERING IMPOSED FOR SATISFICATION OF A PREDETERMINED CONSTRAINT.
H1
DESIGN THE MULTI-FUNCTION LIGHT DIFFRACTIVE GRATING EMPLOYED WITHIN THE LASER BEAM PRODUCTION MODULE OF EACH LASER SCANNING STATION IN THE HOLOGRAPHIC SCANNING SYSTEM.
H2
PERFORM ASTIGMATISM ANALYSIS ON THE RESULTING DESIGN OF THE LASER BEAM PRODUCTION MODULE.
H3
PERFORM DISPERSION ANALYSIS ON THE RESULTING DESIGN FOR EACH LASER BEAM PRODUCTION MODULE AND HOLOGRAPHIC SCANNING DISC.
Q

FIG. 7Q

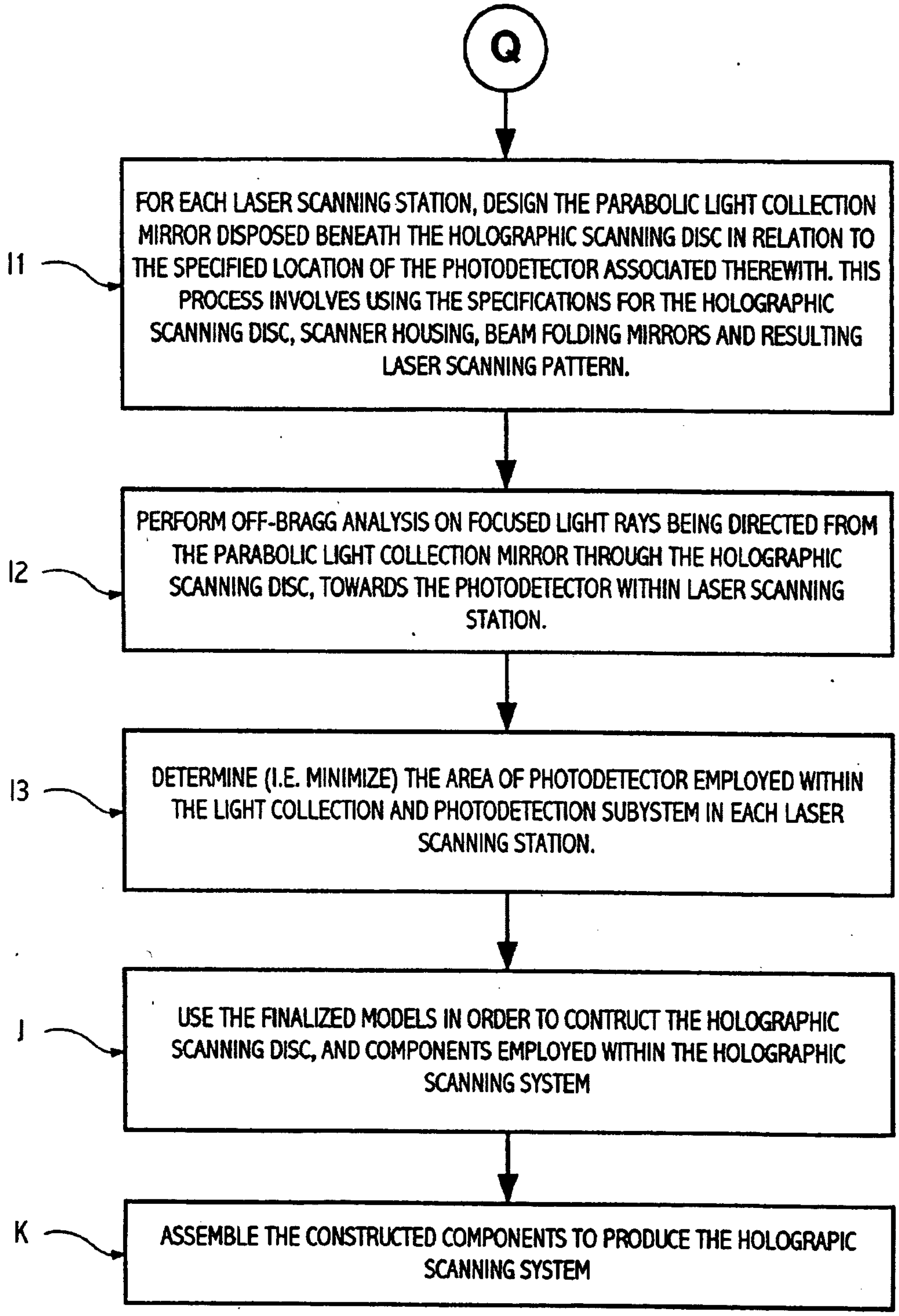
Q
I1
FOR EACH LASER SCANNING STATION, DESIGN THE PARABOLIC LIGHT COLLECTION MIRROR DISPOSED BENEATH THE HOLOGRAPHIC SCANNING DISC IN RELATION TO THE SPECIFIED LOCATION OF THE PHOTODETECTOR ASSOCIATED THEREWITH. THIS PROCESS INVOLVES USING THE SPECIFICATIONS FOR THE HOLOGRAPHIC SCANNING DISC, SCANNER HOUSING, BEAM FOLDING MIRRORS AND RESULTING LASER SCANNING PATTERN.
I2
PERFORM OFF-BRAGG ANALYSIS ON FOCUSED LIGHT RAYS BEING DIRECTED FROM THE PARABOLIC LIGHT COLLECTION MIRROR THROUGH THE HOLOGRAPHIC SCANNING DISC, TOWARDS THE PHOTODETECTOR WITHIN LASER SCANNING STATION.
I3
DETERMINE (I.E. MINIMIZE) THE AREA OF PHOTODETECTOR EMPLOYED WITHIN THE LIGHT COLLECTION AND PHOTODETECTION SUBYSTEM IN EACH LASER SCANNING STATION.
J
USE THE FINALIZED MODELS IN ORDER TO CONTRUCT THE HOLOGRAPHIC SCANNING DISC, AND COMPONENTS EMPLOYED WITHIN THE HOLOGRAPHIC SCANNING SYSTEM
K
ASSEMBLE THE CONSTRUCTED COMPONENTS TO PRODUCE THE HOLOGRAPIC SCANNING SYSTEM

FIG. 7R

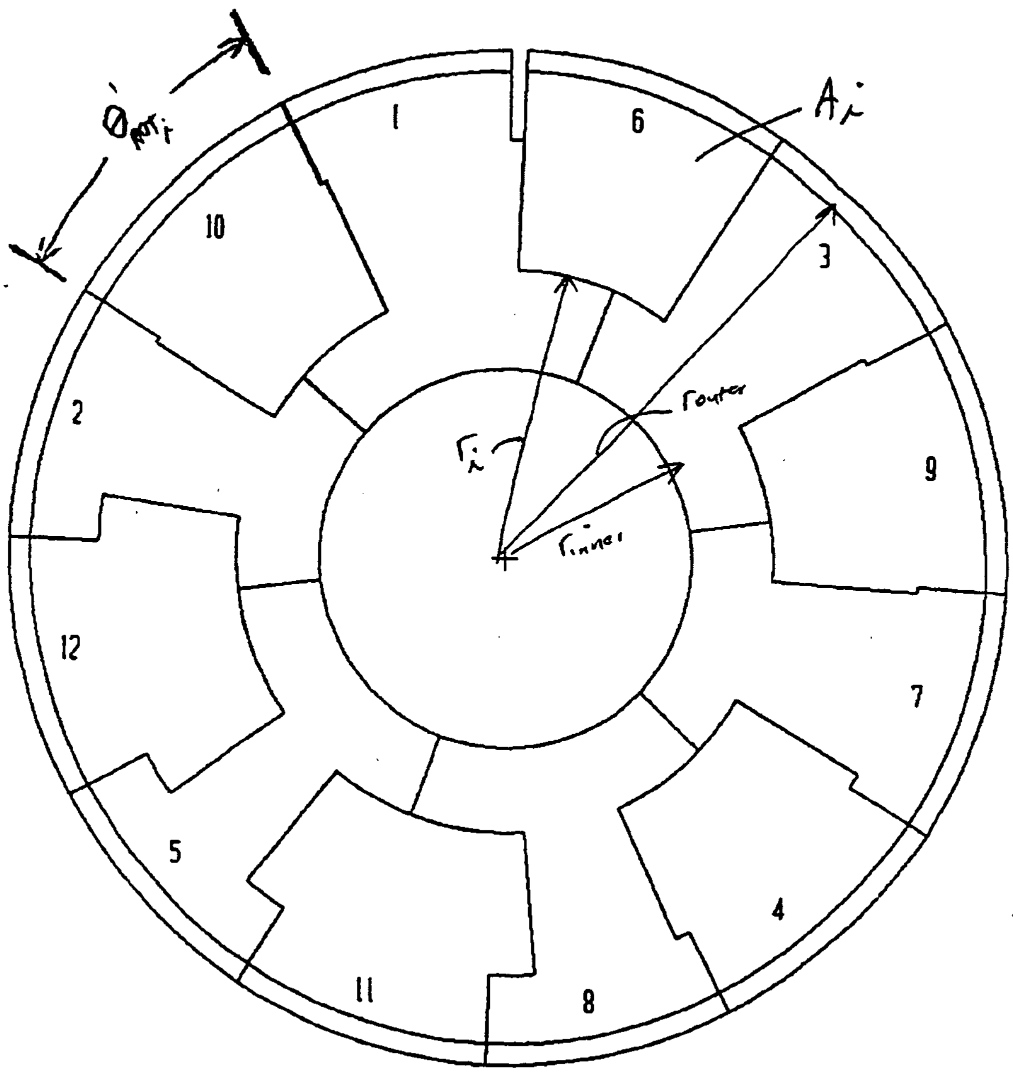

FIG. 8A

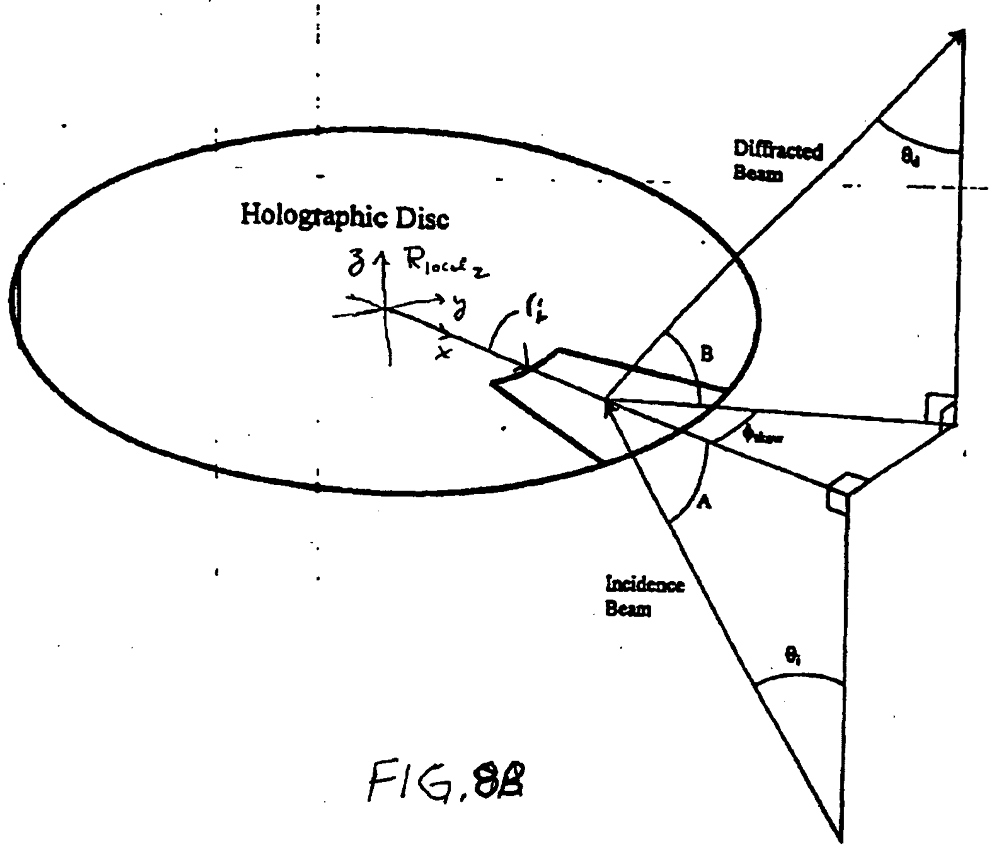
Holographic Disc
z
$R_{local\,z}$
y
x
ϕ_i
Diffracted Beam
θ_d
B
ϕ_{skew}
A
Incidence Beam
θ_i

FIG. 8B

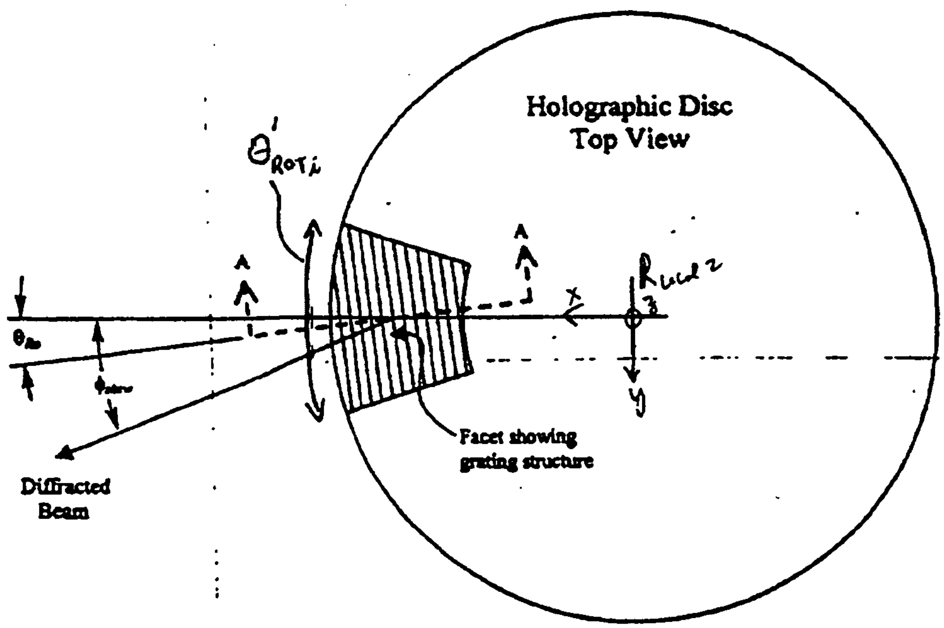
Holographic Disc Top View
θ'_{ROT_i}
A
A
$R_{local\,z}$
x
z
y
θ_{Rot}
ϕ_{skew}
Diffracted Beam
Facet showing grating structure

FIG. 8B

(1) THE RADIUS TO BEAM-INCIDENT-POINT ON THE HOLOGRAPHIC SCANNING DISC, ASSIGNED THE SYMBOLIC NOTATION "r_0"

(2) THE DISTANCE FROM RADIUS TO BEAM-INCIDENT-POINT r_0 TO BEAM FOLDING MIRROR , ASSIGNED THE SYMBOLIC NOTATION "L"

(3) THE FACET NO. ON THE HOLOGRAPHIC SCANNING DISC, ASSIGNED THE SYMBOLIC NOTATION "i"

(4) THE DISTANCE FROM THE BEAM INCIDENT POINT ON THE VIRTUAL SCANNING DISC TO THE FOCAL PLANE WITHIN WHICH THE (i, j)-TH SCANLINE RESIDES, ASSIGNED THE SYMBOLIC NOTATION "f_i"

(5) THE DIAMETER OF THE CROSS-SECTION OF THE LASER BEAM SCANNING STATION, ASSIGNED THE SYMBOLIC NOTATION "d_{BEAM}"

(6) THE ANGULAR GAP BETWEEN ADJACENT HOLOGRAPHIC SCANNING FACETS, ASSIGNED THE SYMBOLIC NOTATION "d_{GAP}"

(7) THE OUTER RADIUS OF THE AVAILABLE LIGHT COLLECTION REGION ON THE HOLOGRAPHIC SCANNING DISC, ASSIGNED THE SYMBOLIC NOTATION "r_{OUTER}"

(8) THE INNER RADIUS OF THE AVAILABLE LIGHT COLLECTION REGION ON THE HOLOGRAPHIC SCANNING FACET, ASSIGNED THE SYMBOLIC NOTATION "r_{INNER}"

(9) THE FOCAL LENGTH OF THE i-TH HOLOGRAPHIC SCANNING FACET FROM THE SCANNING FACET TO THE CORRESPONDING FOCAL PLANE WITHIN THE SCANNING VOLUME, ASSIGNED THE SYMBOLIC NOTATION "f_i"

(10) INCIDENT BEAM ANGLE, ASSIGNED THE SYMBOLIC NOTATION "A_i"

F I G. 8D1

(11) DIFFRACTED BEAM ANGLE, ASSIGNED THE SYMBOLIC NOTATION "B_i"

(12) THE SCAN ANGLE OF THE LASER BEAM , ASSIGNED THE SYMBOLIC NOTATION "θ_{SI}"

(13) THE SCAN MULTIPLICATION FACTOR FOR THE i-TH HOLOGRAPHIC FACET, ASSIGNED THE SYMBOLIC NOTATION "M_i"

(14) THE FACET ROTATION ANGLE FOR THE i-TH HOLOGRAPHIC FACET, ASSIGNED THE SYMBOLIC NOTATION "θ_{ROTI}"

(15) ADJUSTED FACET ROTATION ANGLE ACCOUNTING FOR DEADTIME, ASSIGNED THE SYMBOLIC NOTATION "θ'_{ROTI}"

(16) THE LIGHT COLLECTION EFFICIENCY FACTOR FOR THE i-TH HOLOGRAPHIC FACET, NORMALIZED RELATIVE TO THE 16TH FACET, ASSIGNED THE SYMBOLIC NOTATION "ξ_i"

(17) THE MAXIMUM LIGHT COLLECTION AREA FOR THE i-TH HOLOGRAPHIC FACET, ASSIGNED THE SYMBOLIC NOTATION "$Area_i$"

(18) THE ANGLE OF SKEW OF THE DIFFRACTED LASER BEAM AT THE CENTER OF THE i-TH HOLOGRAPHIC FACET, ASSIGNED THE SYMBOLIC NOTATION "ϕ_{SKEW}"

FIG. 8D2

PARAMETER EQUATION USED IN THE SPREADSHEET DESIGN OF THE SCANNER

(1) f_i Focal Length - $f_{i\text{-th}}$ facet

(2) B_i Elevation Angle; $\theta_{dif}\, i = 90 - B_i$

(3) θ_{Si}

(4) $$M_i \; := \; \frac{r_0}{f_i} \cos(\theta_{skew}) + \cos(\lambda_i) + \cos(B_i)$$

(5) $$\theta_{roti} \; := \; \frac{\theta_{Si}}{M_i}$$

(6) $$\theta'_{roti} \; := \; \theta_{roti} + \underbrace{\frac{d_{beam}}{r_0} + \frac{d_{gap}}{r_0}}_{\Theta_{dead}}$$

(7) $$\xi_i \; := \; \left[\frac{f_i}{f_{20}}\right]^2 \frac{\sin[B_{20}]}{\sin(B_i)} H_i$$

(8) $$\text{Area}_i \; := \; \pi \left[r^2_{outer} + r^2_{inner}\right] \frac{\xi_i}{\sum_{i=1}^{20} [\xi_i]} \qquad i = 1, 2, \ldots 20$$

F I G. 8E

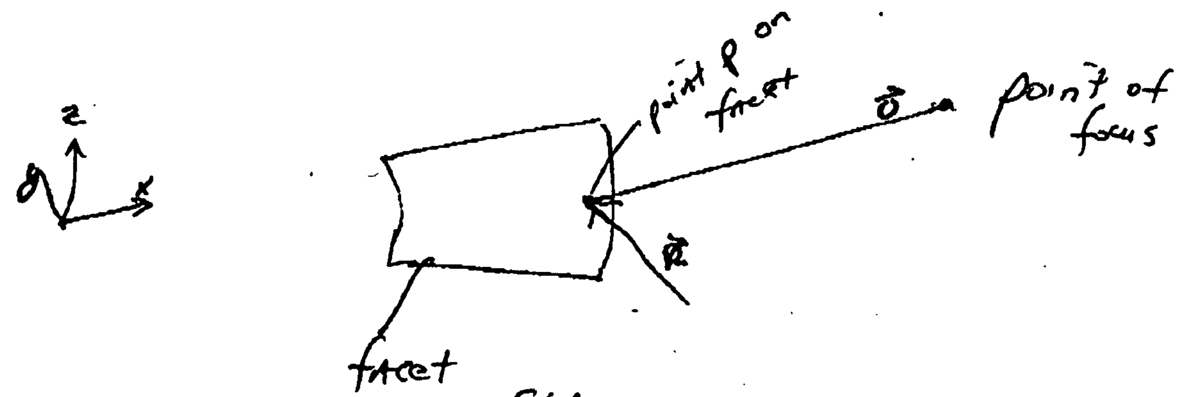

FIG. 8F1

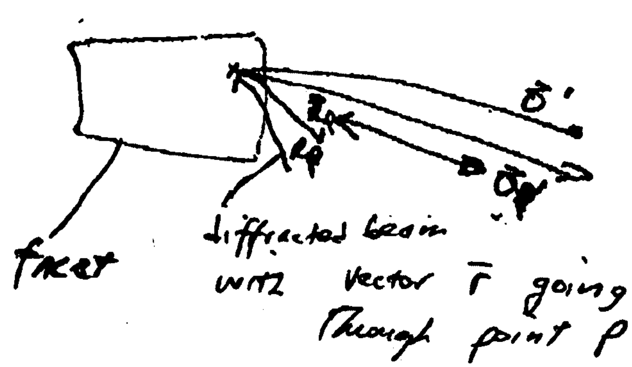

FIG. 8F2

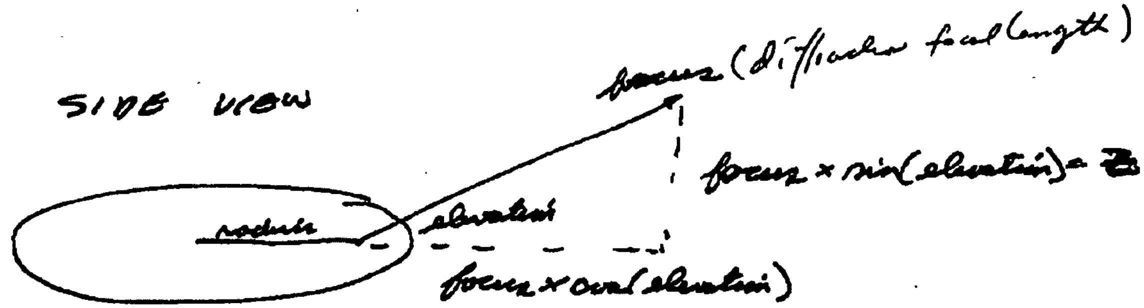

FIG. 8F3

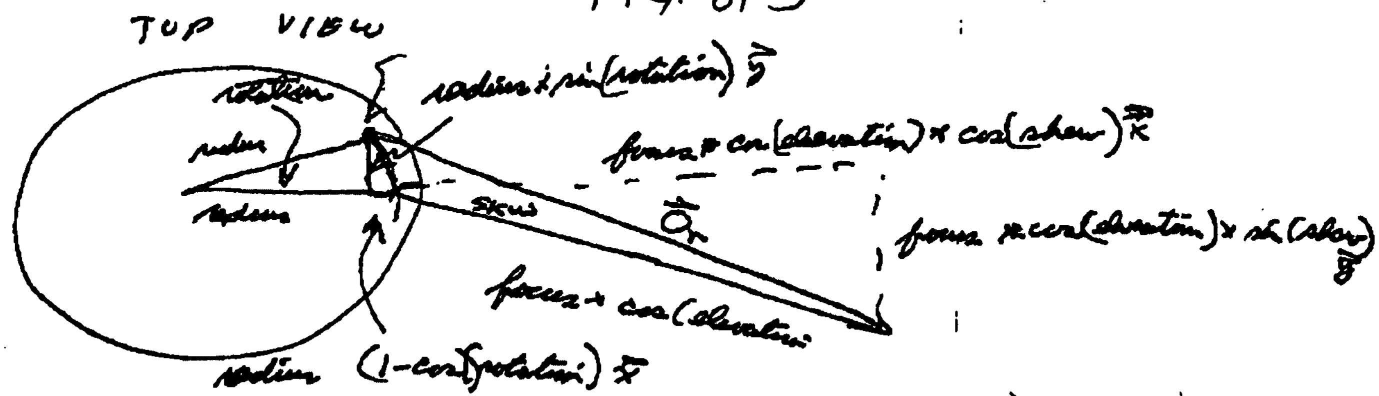

($\vec{O}_r$ is equal to the sum of these components)

FIG. 8F4 8F4

Object ray $\vec{O}_p$ composition:

$$\vec{O}_p = \text{focus} \times \cos(\text{elevation}) \times \cos(\text{skew}) + \text{radius}\,(1 - \cos(\text{rotation}))\ \vec{x}$$
$$+ \text{focus} \times \cos(\text{elevation}) \times \sin(\text{skew}) + \text{radius}\ \cancel{\sin}(\text{rotation})\ \vec{y}$$
$$+ \text{focus} \times \sin(\text{elevation})\ \vec{z}$$

where
- focus = The diffraction
- elevation = elevation angle of face
- skew = Skew angle of face.
- radius = radius to point p
- rotation = START-MIDDLE-END of SCAN RANGES

FIG. 8 F3

*** Optical Power at the Data Detector and Resulting Signal Levels ***

Calculation of the power at the data detector for targets located at the focal planes and targets located at the maximum depth of field limits for each facet.

Assumes average angular offset of: 0.7 degrees

(Offset of outgoing beam from center of facet)

Detector sensitivity (mV/nW): 6.17

Facet	Laser Power (mW)	Transm. of collimating lens	Refl. of first mirror	Diff. Eff. of HF plate	S-diff. eff. of holographic facet	S-refl. of second, third & fourth mirror	Trans. of Window	Lambertian reflectance factor (At focal plane)	Lambertian reflectance factor (At maximum depth of field)	Diffuse Refl. of bar code	Average of P and S-refl. of second, third & fourth mirror	Average of P and S-diff. eff. of holographic facet	Refl. of parabolic mirror	Trans. of hol. based off-Bragg	Trans. of polarizing filter (none used)
	3.30	0.65	0.95	0.86		0.97	0.9			0.9	0.66		0.96	0.93	1
1		(This includes the			0.89			0.0027736	0.0018664			0.66			
2		truncation losses)			0.88			0.0027275	0.0017179			0.70			
3					0.88			0.0026641	0.0017579			0.71			
4					0.90			0.0026434	0.0016637			0.72			
5					0.90			0.0025667	0.0015804			0.75			
6					0.90			0.0024860	0.0016602			0.77			
7					0.90			0.0024122	0.0016459			0.79			
8					0.90			0.0024122	0.0016698			0.79			
9					0.90			0.0023674	0.0015666			0.80			
10					0.90			0.0023674	0.0015666			0.80			
11					0.90			0.0023645	0.0016368			0.81			
12					0.90			0.0023645	0.0016368			0.81			

Facet	Power at window (mW)	Power at detector (nW) (Targets located at the facet focal planes)	Detector signal (Volts) (Targets located at the facet focal planes)	Power at detector (nW) (Targets located at the depth of field limits)	Detector signal (Volts) (Targets located at the depth of field limits)		Facet Collection Area (sq. in.)	Diffraction Angle from Center of Facet (degrees)	Effective Radius of Collection Area (inches)	Light Collection Half-Angle (degrees) (From focal plane)	Light Collection Half-Angle (degrees) (From maximum depth of field)
1	0.86	672	5.47	667	3.96		2.25	52.70	0.85	3.02	2.46
2	0.86	673	5.47	640	3.46		1.79	50.70	0.80	2.90	2.36
3	0.86	674	5.49	572	3.50		2.07	48.70	0.85	2.97	2.40
4	0.86	674	5.49	561	3.46		1.81	46.70	0.80	2.96	2.34
5	0.86	676	5.49	576	3.50		1.77	42.70	0.84	2.90	2.35
6	0.87	677	5.50	582	3.52		1.45	38.70	0.80	2.86	2.29
7	0.87	678	5.51	607	3.80		1.95	32.70	0.72	2.82	2.34
8	0.87	678	5.51	607	3.80		1.95	32.70	0.72	2.82	2.34
9	0.87	680	5.51	606	3.56		1.55	30.70	0.86	2.80	2.29
10	0.87	680	5.51	609	3.59		1.59	30.70	0.86	2.80	2.29
11	0.87	680	5.52	609	3.52		1.86	28.70	0.72	2.79	2.32
12	0.87	680	5.52	609	3.52		1.86	28.70	0.72	2.79	2.32

FIG. 9

GEOMETRICAL OPTICS MODEL FOR HOLOGRAFIC (TOTAL OUT AND BACK) LIGHT DIFFRACTION EFFICIENCY CALCULATIONS

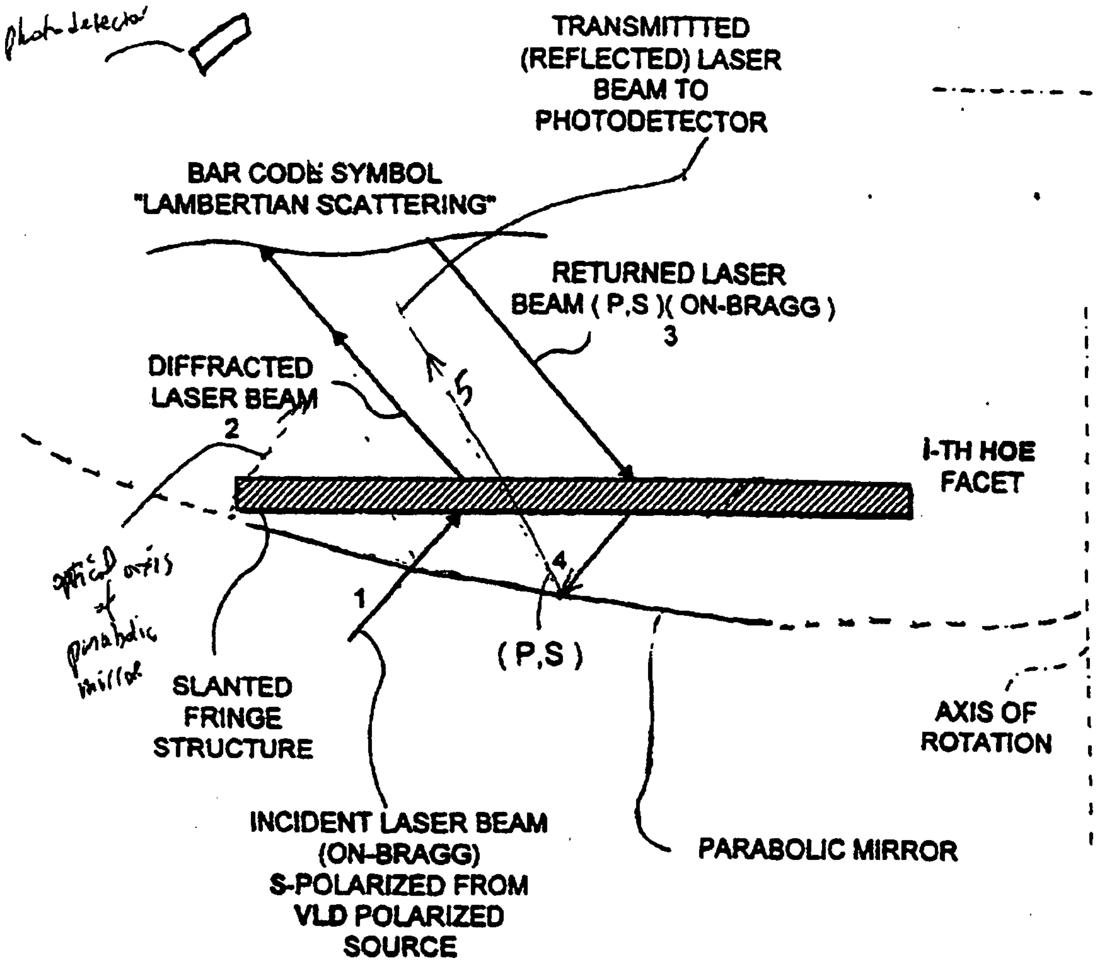

F I G. 10A1

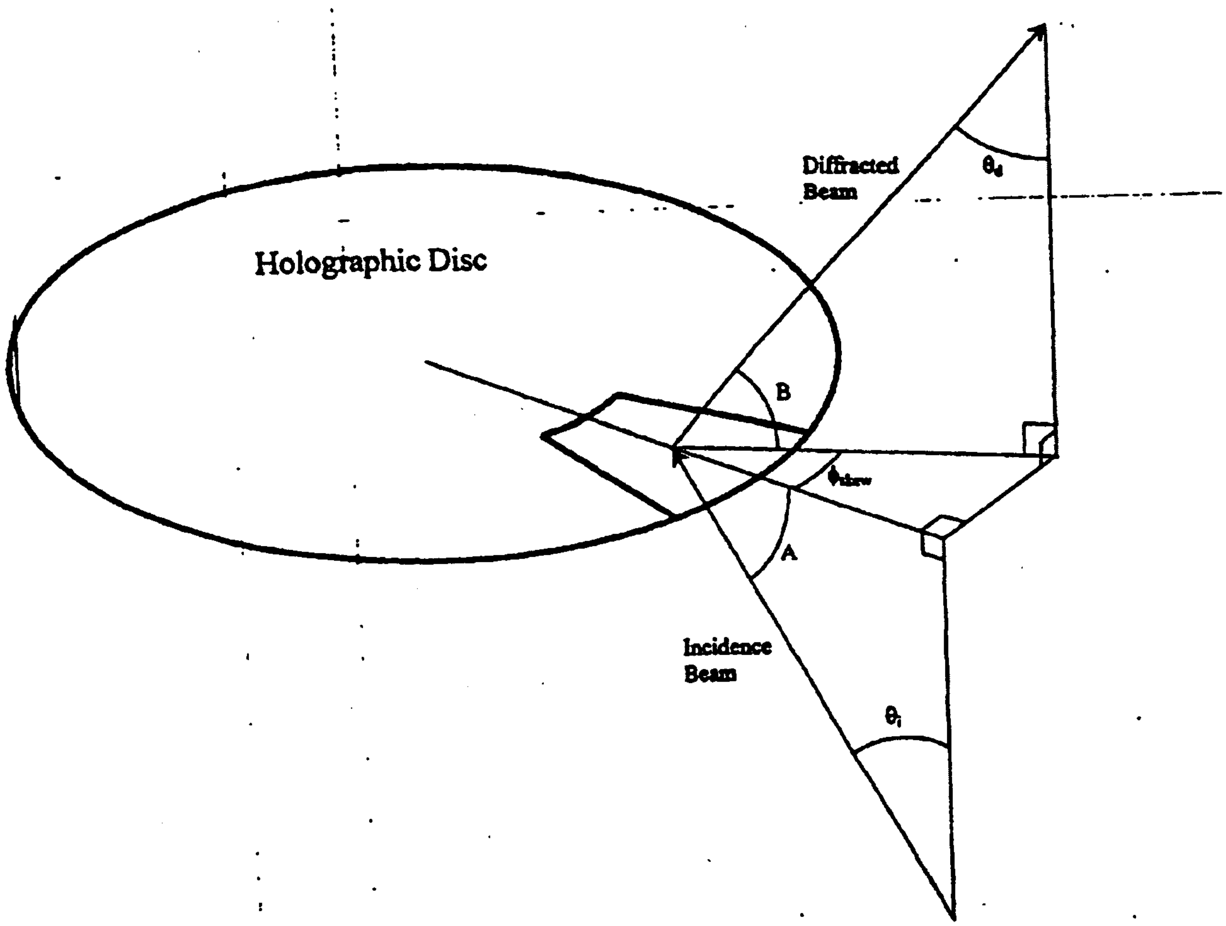
Diffracted Beam
θ_d
Holographic Disc
B
ϕ_{skew}
A
Incidence Beam
θ_i

FIG. 10A2

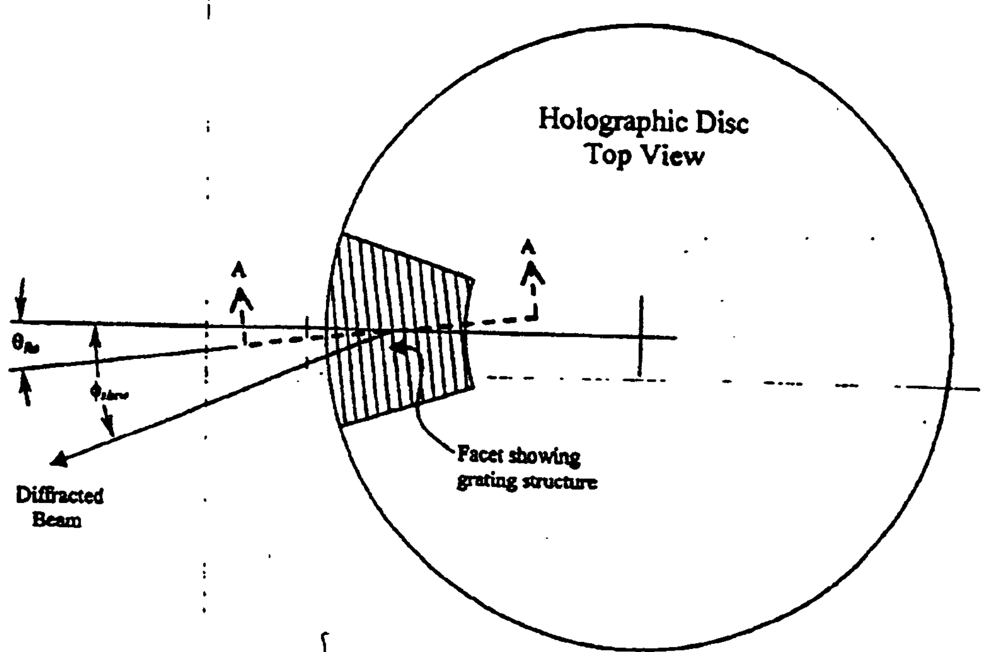

FIG. 10A3

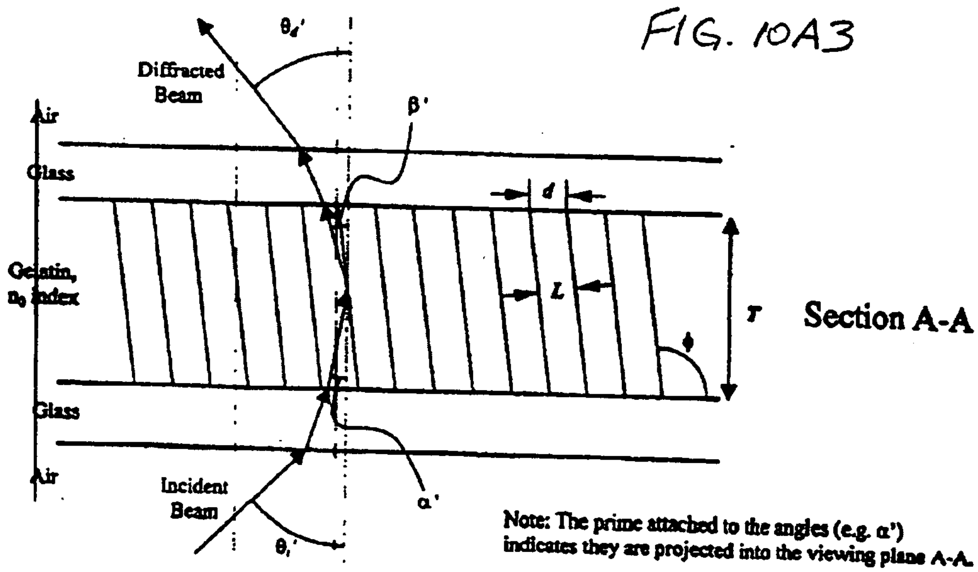

FIG. 10A4

S AND P DIFFRACTION EFFICIENCY ANALYSIS FOR THE MOST GENERAL CASE

The following analysis takes into consideration slanted fringes, skewed design, off-Bragg effects, and disc rotation effects. It is assumed that the wavelength does not deviate from the design, and that all scattering, absorption, and reflection losses are taken into account by the transmission coefficients, t_s and t_p, which are determined by measurement.

Definitions:

θ_i = Angle of incidence outside the HOE ($\theta_i = 90° - A$);

α = Angle of incidence inside the HOE;

θ_d = Angle of diffraction outside the HOE ($\theta_d = 90° - B$);

β = Angle of diffraction inside the HOE;

ϕ_{skew} = Skew angle of the HOE;

ϕ = Tilt of Bragg planes ($\phi = \pi/2$ for no tilt);

θ_R = Rotation angle of HOE grating ($\theta_R = \theta_{Ro}$ when facet is centered);

L = Separation of the Bragg planes;

T = Thickness of the HOE medium;

d = HOE surface fringe spacing;

n_0 = Average refractive index of HOE medium;

n_1 = modulation (i.e. amplitude of periodic variation) of refractive index;

λ_a = Laser wavelength in air;

t_s = Transmission of S-polarization through disc considering losses;

t_p = Transmission of P-polarization through disc considering losses.

FIG. 10B

(1) $\alpha = \arcsin\left(\frac{\sin\theta_i}{n_0}\right)$

(2) $\beta = \arcsin\left(\frac{\sin\theta_d}{n_0}\right)$

(3) $\phi = \arcsin\left(\frac{\cos\beta - \cos\alpha}{\sqrt{2(1 + \sin\alpha\sin\beta\cos\phi_{skew} - \cos\alpha\cos\beta)}}\right) + 90$

(4) $d = \sqrt{\frac{\lambda_a{}^2}{\sin^2\theta_d \sin^2\phi_{skew} + (\sin\theta_i + \sin\theta_d\cos\phi_{skew})^2}}$

(5) $L = d\sin\phi$

(6) $C_R = \cos\alpha$

(7) $C_S = \cos\alpha - \frac{\lambda_a}{n_0 L}\cos\phi$

(8) $N = \pi n_1 \frac{T}{\lambda_a\sqrt{C_R C_S}}$

* (9) $\theta_{Ro} = \arcsin\left(\frac{d}{\lambda_a}\sin\theta_d \sin\phi_{skew}\right)$

(10) $\Gamma = \frac{2\pi(\sin\alpha\sin\phi\cos\theta_{Ro} + \cos\alpha\cos\phi)}{L} - \frac{\pi\lambda_a}{n_0 L^2}$

(11) $S = \Gamma\frac{T}{2C_S}$

Figure 10C1

(12) $\kappa = -\sin\alpha \sin\beta \cos\phi'_{skew} + \cos\alpha \cos\beta$

(13) $E_{par} = \dfrac{\left(\sin\left(\sqrt{N^2 + S^2}\right)\right)^2}{1 + \dfrac{S^2}{N^2}}$

(14) $E_{perp} = \dfrac{\left(\sin\left(\sqrt{(N\kappa)^2 + S^2}\right)\right)^2}{1 + \dfrac{S^2}{(N\kappa)^2}}$

(15) $P_{par} = \dfrac{-\sin\phi \sin\theta_{Ro}}{\sin(\arccos(-\sin\alpha \sin\phi \cos + \cos\alpha \cos\phi))}$

(16) $P_{perp} = 1 - P_{par}$

Diffraction efficiencies E_s and E_p, given losses t_s and t_p which are specific to each polarization and include absorption, scattering, and reflection losses from AR coatings on the outer surfaces of the disc glass.

(17) $E_s = \left(E_{perp}P_{par} + E_{par}P_{perp}\right)t_s$

(18) $E_p = \left(E_{perp}P_{perp} + E_{par}P_{par}\right)t_p$

Total out-and-back efficiency is given by T_s, assuming no polarizer in front of the photodetector

(19) $T_s = E_s \dfrac{E_s + E_p}{2}$

Figure 10C2

(20) $\theta_d\{\theta_R\} = \arcsin\sqrt{\left(\frac{\lambda_a}{d}\right)^2 - 2\frac{\lambda_a}{d}\cos\theta_R \sin\theta_i + \sin^2\theta_i}$

(21) $\phi_{skew}\{\theta_R\} = \arctan\left[\frac{\sin\theta_R}{\cos\theta_R - (d/\lambda_a)\sin\theta_i}\right]$

(22) $T_s\{\theta_{i\max}\}\cos\theta_d\big|_{\theta_R=\theta_{Ro}-\frac{1}{2}\theta_{RON}} = T_s\{\theta_{i\max}\}\cos\theta_d\big|_{\theta_R=\theta_{Ro}+\frac{1}{2}\theta_{RON}}$

The design efficiency of the i[th] facet is given by evaluating T_s at the design incidence angle, θ_i, the design rotation angle, θ_{Ro}, and the index modulation that maximizes the efficiency, $n_{1\max}$, given the true maximum efficiency incidence angle, $\theta_{i\max}$, that results from equation (22). The relative efficiency, H_i, is then given by dividing the total efficiency of the first facet by that of the i[th] facet.

(23) $$H_i = \frac{T_{s1}}{T_{si}\{\theta_i, \theta_{i\max}, \theta_{Ro}, n_{1\max}\}}$$

Figure 10C3

Diffraction Efficiency Variation with Disc Rotation

Facet 1: before optimization

Fixed design parameters:
$\theta_i = 38°$ $\theta_d = 52°$ $\phi_{skew} = 0°$ $\lambda_a = 650$ nm

DCG parameters:
$T = 2.5$ microns $n_0 = 1.40$ $n_1 = 0.121$

Relative signal is equal to $T_s\cos\theta_d$. Note that the relative signal falls off as the rotation angle goes away from zero. This is for a maximum efficiency incidence angle, θ_{imax}, equal to θ_i (38°). This indicates a non-optimum configuration.

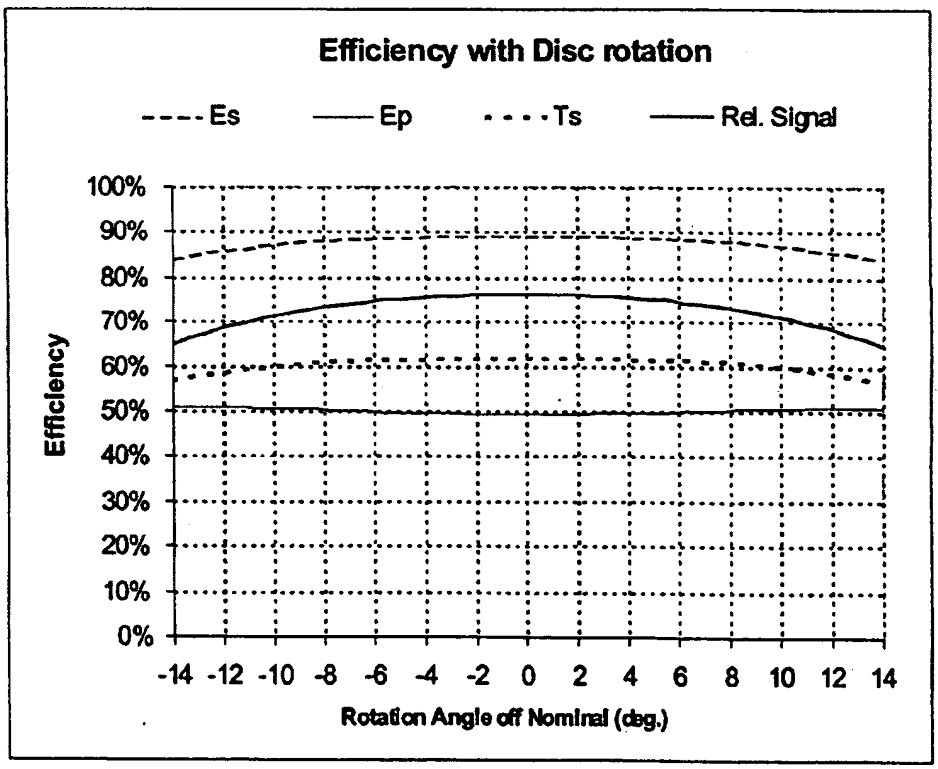

FIG. 10D1

Diffraction Efficiency Variation with Disc Rotation

Facet 1: after optimization

Fixed design parameters:

$\theta_i = 38°$ $\theta_d = 52°$ $\phi_{skew} = 0°$ $\lambda_a = 650$ nm

DCG parameters:

$T = 2.5$ microns $n_0 = 1.40$ $n_1 = 0.121$

Relative signal is equal to $T_s\cos\theta_d$. Note that the relative signal at a rotation angle of +/-13° is equal to the relative signal at 0°. This is achieved when the maximum efficiency incidence angle, θ_{imax}, is 36.3°.

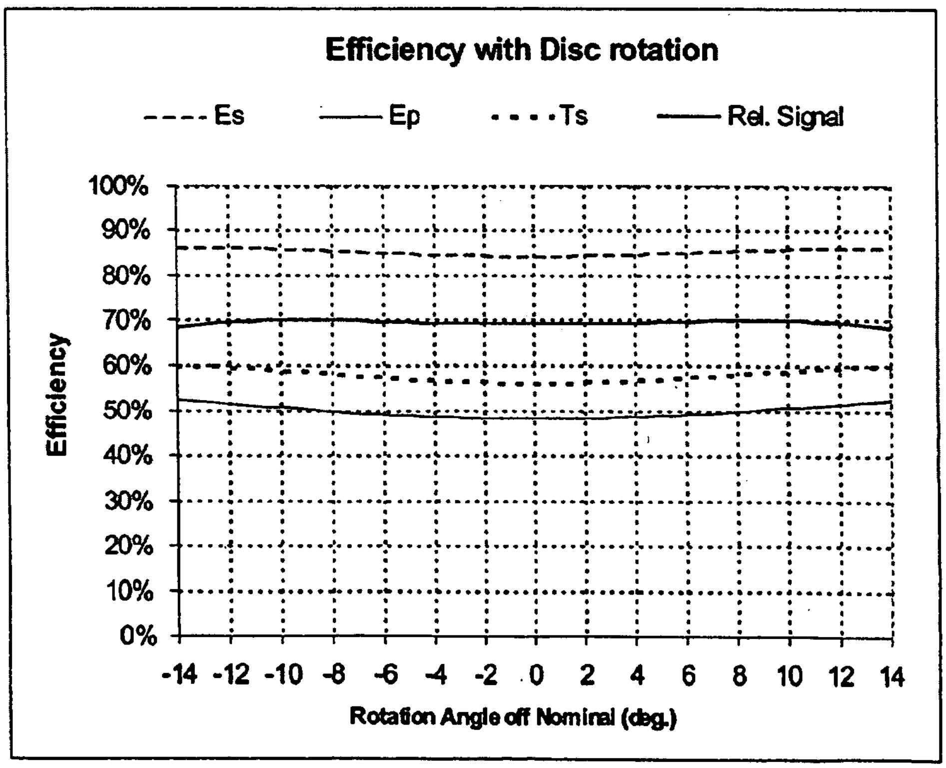

FIG. 10D2

Diffraction Efficiency Variation with Disc Rotation

Facet 7: before optimization

Fixed design parameters:
$\theta_i = 38°$ $\theta_d = 32°$ $\phi_{skew} = 28°$ $\lambda_a = 650$ nm

DCG parameters:
$T = 2.5$ microns $n_0 = 1.40$ $n_1 = 0.121$

Relative signal is equal to $T_s\cos\theta_d$. Note that the relative signal falls off as the rotation angle goes from negative to positive. This is for a maximum efficiency incidence angle, θ_{imax}, equal to θ_i (38°). This indicates a non-optimum configuration.

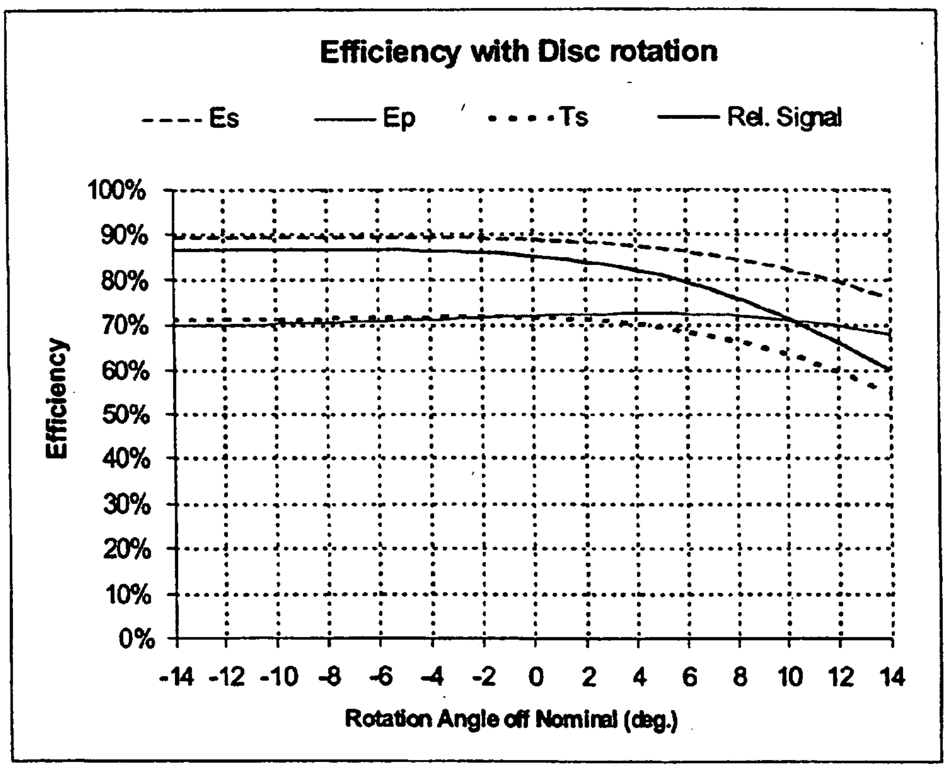

FIG. 10E1

Diffraction Efficiency Variation with Disc Rotation

<u>Facet 7: after optimization</u>

Fixed design parameters:
$\theta_i = 38°$ $\theta_d = 32°$ $\phi_{skew} = 28°$ $\lambda_a = 650$ nm

DCG parameters:
$T = 2.5$ microns $n_0 = 1.40$ $n_1 = 0.121$

Relative signal is equal to $T_s\cos\theta_d$. Note that the relative signal at a rotation angle of -14° is equal to the relative signal at +14°. This is achieved when the maximum efficiency incidence angle, θ_{imax}, is 35.8°.

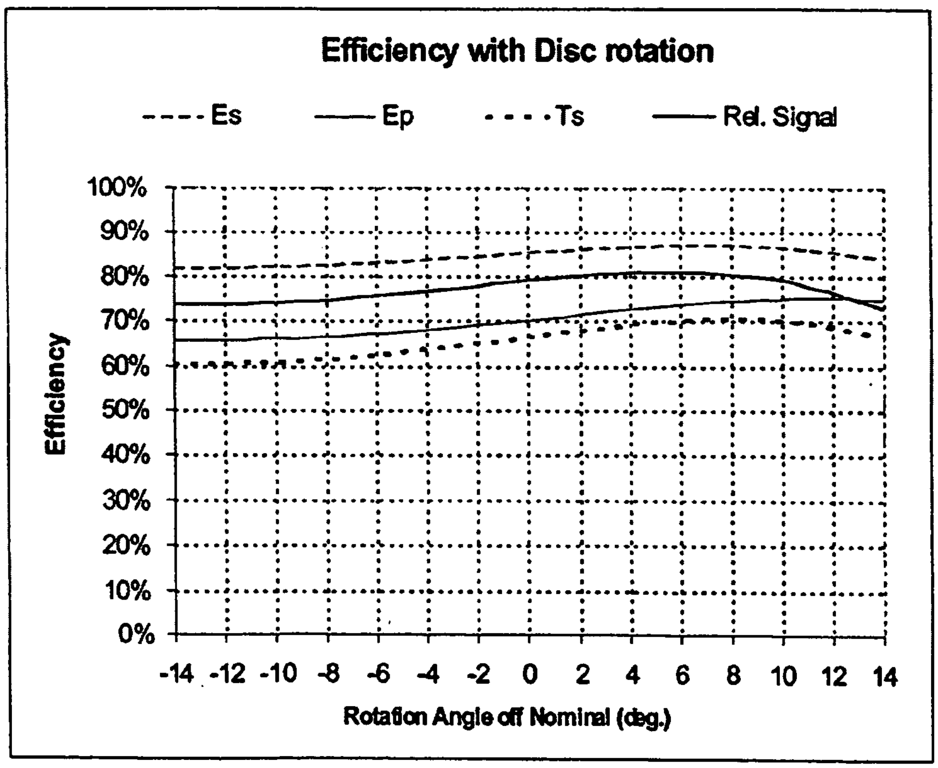

FIG. 10E2

S and P Diffraction Efficiency Calculations

It is assumed that there is no deviation from the nominal wavelength.

Facet-independent design parameters:

Design wavelength:	650 nm
External incidence angle:	38 deg
Internal incidence angle:	26.09 deg
Geletin effective thickness:	2.5 microns
Average bulk refractive index:	1.4
Refractive index modulation:	0.121
S-polarization losses:	10%
P-polarization losses:	10%
degrees to radians conversion:	0.017453

Facet	θ_d (deg.)	β (deg.)	ϕ_{skew} (deg.)	d (nm)	θ_{Ro} (deg.)	$\theta_{i\,max}$ (deg.)	α_{max} (deg.)	β_{max} (deg.)	$\phi_{s\,max}$ (deg.)	ϕ (deg.)	L (nm)	θ_{ROT} (deg.)
1	52.00	34.25	0	463.1	0.00	36.30	25.02	35.43	0.00	84.79	461.2	26.24
2	50.00	33.17	0	470.4	0.00	36.30	25.02	34.34	0.00	85.34	468.9	28.35
3	48.00	32.06	0	478.4	0.00	36.30	25.02	33.21	0.00	85.90	477.1	26.66
4	46.00	30.92	0	486.9	0.00	36.30	25.02	32.05	0.00	86.48	486.0	29.19
5	42.00	28.55	0	505.9	0.00	36.30	25.02	29.66	0.00	87.68	505.5	27.97
6	38.00	26.09	0	527.9	0.00	36.30	25.02	27.17	0.00	88.92	527.8	30.28
7	32.00	22.24	28	584.7	12.93	35.80	24.70	23.45	26.52	90.64	584.6	27.99
8	32.00	22.24	-28	584.7	-12.93	35.80	24.70	23.45	-26.52	90.64	584.6	27.99
9	30.00	20.92	28	600.2	12.52	35.56	24.55	22.26	26.27	91.17	600.1	30.65
10	30.00	20.92	-28	600.2	-12.52	35.56	24.55	22.26	-26.27	91.17	600.1	30.65
11	28.00	19.59	28	617.0	12.08	35.72	24.65	20.83	26.28	91.96	616.6	29.19
12	28.00	19.59	-28	617.0	-12.08	35.72	24.65	20.83	-26.28	91.96	616.6	29.19

FIG. 10F1

C_R:
0.898

C_S	N	θ_d		β		ϕ_{skew}		Γ			S		
		$-½\theta_{ROT}$	$+½\theta_{ROT}$	$-½\theta_{ROT}$	$+½\theta_{ROT}$	$-½\theta_{ROT}$	$+½\theta_{ROT}$	$-½\theta_{ROT}$	θ_{Ro}	$+½\theta_{ROT}$	$-½\theta_{ROT}$	θ_{Ro}	$+½\theta_{ROT}$
0.807	1.718	54.70	54.70	35.66	35.66	-22.98	22.98	0.0634	0.2192	0.0634	0.0982	0.3397	0.0982
0.818	1.706	53.05	53.05	34.81	34.81	-25.05	25.05	0.0380	0.2168	0.0380	0.0581	0.3315	0.0581
0.829	1.695	50.61	50.61	33.51	33.51	-23.91	23.91	0.0586	0.2143	0.0586	0.0885	0.3232	0.0885
0.839	1.684	49.05	49.05	32.65	32.65	-26.45	26.45	0.0285	0.2116	0.0285	0.0424	0.3150	0.0424
0.861	1.663	44.69	44.69	30.16	30.16	-26.20	26.20	0.0438	0.2057	0.0438	0.0636	0.2987	0.0636
0.882	1.643	41.07	41.07	27.99	27.99	-29.30	29.30	0.0176	0.1992	0.0176	0.0250	0.2825	0.0250
0.907	1.620	29.76	38.91	20.76	26.66	-2.39	53.28	0.3498	0.2307	-0.1618	0.4820	0.3180	-0.2230
0.907	1.620	38.91	29.76	26.66	20.76	-53.28	2.39	-0.1618	0.2307	0.3498	-0.2230	0.3180	0.4820
0.914	1.614	27.96	37.62	19.57	25.85	-6.49	55.95	0.3549	0.2510	-0.1726	0.4854	0.3432	-0.2360
0.914	1.814	37.62	27.96	25.85	19.57	-55.95	6.49	-0.1726	0.2510	0.3549	-0.2360	0.3432	0.4854
0.924	1.605	26.06	35.04	18.29	24.21	-6.05	55.44	0.3252	0.2304	-0.1470	0.4400	0.3118	-0.1988
0.924	1.605	35.04	26.06	24.21	18.29	-55.44	6.05	-0.1470	0.2304	0.3252	-0.1988	0.3118	0.4400

FIG. 10F2

κ			E_{par}			E_{perp}			P_{par}			P_{perp}		
$-½\theta_{ROT}$	θ_{Ro}	$+½\theta_{ROT}$	$-½\theta_{ROT}$	θ_{Ro}	$+½\theta_{ROT}$	$-½\theta_{ROT}$	θ_{Ro}	$+½\theta_{ROT}$	$-½\theta_{ROT}$	θ_{Ro}	$+½\theta_{ROT}$	$-½\theta_{ROT}$	θ_{Ro}	$+½\theta_{ROT}$
0.5028	0.4948	0.5028	0.9746	0.9315	0.9746	0.5759	0.5419	0.5759	0.0580	0.0000	0.0580	0.9420	1.0000	0.9420
0.5187	0.5111	0.5187	0.9804	0.9369	0.9804	0.5983	0.5639	0.5983	0.0680	0.0000	0.0680	0.9320	1.0000	0.9320
0.5354	0.5277	0.5354	0.9814	0.9420	0.9814	0.6192	0.5860	0.6192	0.0609	0.0000	0.0609	0.9391	1.0000	0.9391
0.5519	0.5445	0.5519	0.9865	0.9468	0.9865	0.6416	0.6082	0.6416	0.0733	0.0000	0.0733	0.9267	1.0000	0.9267
0.5860	0.5787	0.5860	0.9899	0.9552	0.9899	0.6834	0.6521	0.6834	0.0688	0.0000	0.0688	0.9312	1.0000	0.9312
0.6200	0.6132	0.6200	0.9945	0.9623	0.9945	0.7248	0.6947	0.7248	0.0818	0.0000	0.0818	0.9182	1.0000	0.9182
0.6918	0.6843	0.6906	0.9056	0.9567	0.9773	0.7442	0.7720	0.7946	0.0004	0.0620	0.2446	0.9996	0.9380	0.7554
0.6906	0.6843	0.6918	0.9773	0.9567	0.9056	0.7946	0.7720	0.7442	0.2446	0.0620	0.0004	0.7554	0.9380	0.9996
0.7080	0.7002	0.7068	0.9051	0.9508	0.9755	0.7584	0.7833	0.8093	0.0030	0.0587	0.2614	0.9970	0.9413	0.7386
0.7068	0.7002	0.7080	0.9755	0.9508	0.9051	0.8093	0.7833	0.7584	0.2614	0.0587	0.0030	0.7386	0.9413	0.9970
0.7227	0.7159	0.7221	0.9220	0.9597	0.9828	0.7823	0.8032	0.8276	0.0025	0.0555	0.2452	0.9975	0.9445	0.7548
0.7221	0.7159	0.7227	0.9828	0.9597	0.9220	0.8276	0.8032	0.7823	0.2452	0.0555	0.0025	0.7548	0.9445	0.9975

FIG. 10F3

E_s			E_p			Ts			H_I	Solver
$-½\theta_{ROT}$	θ_{Ro}	$+½\theta_{ROT}$	$-½\theta_{ROT}$	θ_{Ro}	$+½\theta_{ROT}$	$-½\theta_{ROT}$	θ_{Ro}	$+½\theta_{ROT}$		(=0)
85.6%	83.8%	85.6%	53.9%	48.8%	53.9%	59.7%	55.6%	59.7%	1.000	0
85.9%	84.3%	85.9%	56.2%	50.8%	56.2%	61.0%	57.0%	61.0%	0.976	0
86.3%	84.8%	86.3%	57.7%	52.7%	57.7%	62.2%	58.3%	62.2%	0.953	0
86.5%	85.2%	86.5%	60.0%	54.7%	60.0%	63.4%	59.6%	63.4%	0.932	0
87.2%	86.0%	87.2%	63.4%	58.7%	63.4%	65.7%	62.2%	65.7%	0.894	0
87.5%	86.6%	87.5%	67.2%	62.5%	67.2%	67.7%	64.6%	67.7%	0.861	0
81.5%	85.1%	83.9%	67.0%	70.5%	75.5%	60.5%	66.2%	66.9%	0.840	0.020396813
83.9%	85.1%	81.5%	75.5%	70.5%	67.0%	66.9%	66.2%	60.5%	0.840	0.020396813
81.4%	84.7%	83.9%	68.3%	71.4%	76.7%	60.9%	66.1%	67.4%	0.841	0.02187036
83.9%	84.7%	81.4%	76.7%	71.4%	68.3%	67.4%	66.1%	60.9%	0.841	0.02187036
82.9%	85.6%	85.0%	70.4%	73.1%	77.9%	63.6%	67.9%	69.3%	0.819	0.019325482
85.0%	85.6%	82.9%	77.9%	73.1%	70.4%	69.3%	67.9%	63.6%	0.819	0.019325482
										0.255193744

Figure 10F4

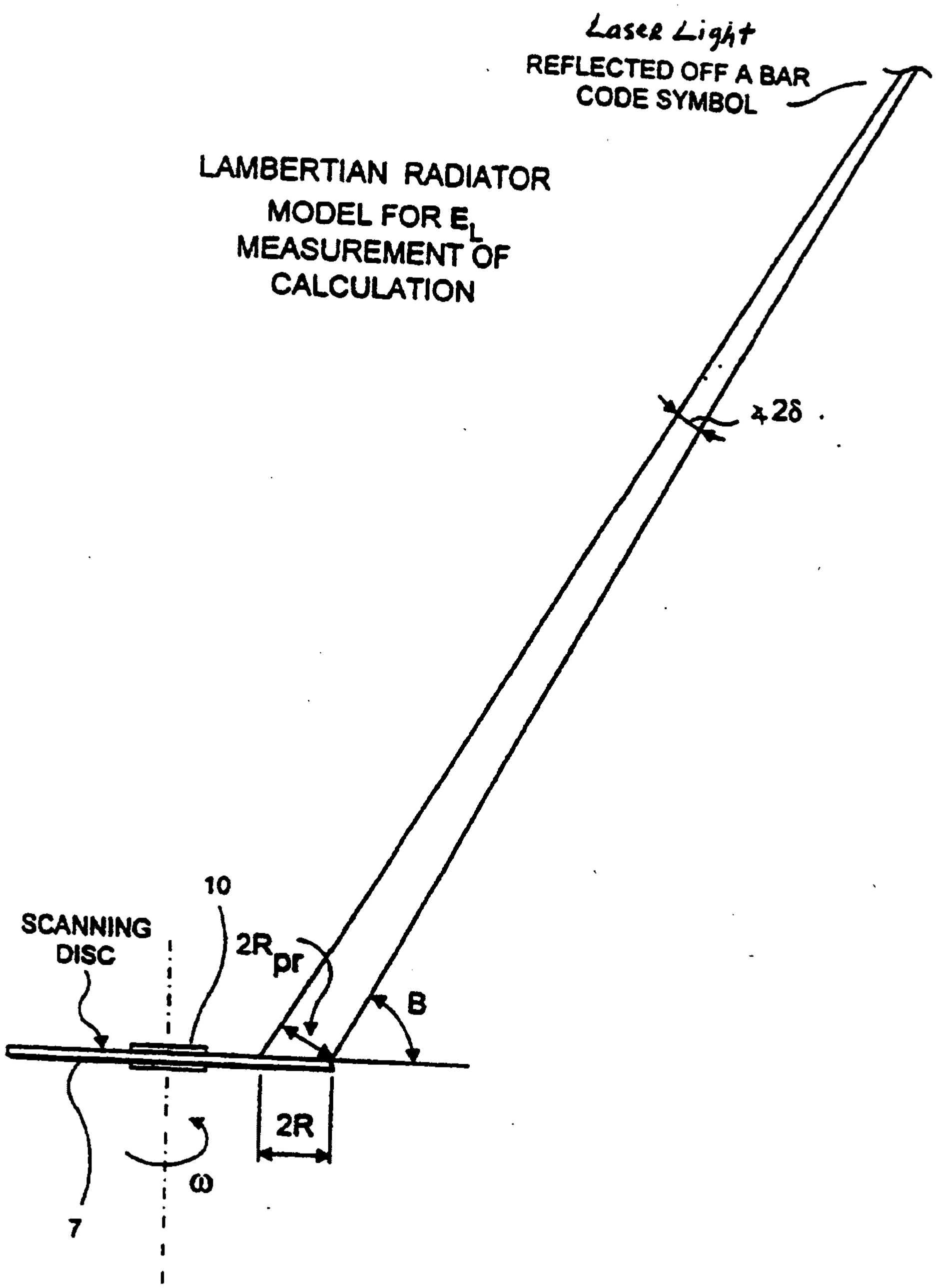
Laser Light
REFLECTED OFF A BAR
CODE SYMBOL
LAMBERTIAN RADIATOR
MODEL FOR E_L
MEASUREMENT OF
CALCULATION
∡2δ
10
SCANNING
DISC
$2R_{pr}$
B
2R
ω
7

FIG. 10G1

FACET LIGHT COLLECTION EFFICIENCY

Z	=	DISTANCE FROM SCAN POINT ON LABEL (MAX = FOCAL) LENGTH PLUS 5 INCHES
Area	=	AREA OF CORRESPONDING FACET
R	=	RADIUS OF EFFECTIVE CIRCULAR APERTURE
R.pr	=	RADIUS OF PROJECTED EFFECTIVE CIRCULAR APERTURE
B	=	ANGLE BETWEEN OUTGOING BEAM AND THE DISC
δ	=	HALF-ANGLE SUBTENDED BY EFFECTIVE PROJECTED CIRCULAR APERTURE
E.L	=	LAMBERTIAN LIGHT COLLECTION EFFICIENCY

FIG. 10G2

$$R_{pr} := \sqrt{\frac{\text{Area } \sin B}{\pi}} \qquad \delta := \operatorname{atan}\left[\frac{R_{pr}}{Z}\right]$$

$$E_L := (\sin(\delta))^2$$

FIG. 10G3

TRNCStratos-6-Pol.xls

Degrees to radians conversion factor: 0.017453293

Truncation analysis. Effect of truncation on the diffraction limited spot size of a Gaussian beam

Given the laser and lens parameters, this spreadsheet will calculate the effect of truncation on the beam
The final result is an "effective diameter." This is an equivalent 1/e-squared diameter that will
produce the same spot size at the focal point as the actual truncated beam. This is also the beam
diameter that will be inserted in the main scanner disk design spreadsheet.
The actual number linked to the main spreadsheet will be a rounded number.
It will usually be rounded up 0.1 to allow for tolerances.

Sony	Wavelength (nm)	650
SLD1137VS	theta-P (degrees)	8
	theta-S (degrees)	30
	Astigmatism (microns)	7

H = Hoya; K = Kodak; P = Philips; G = GelTech
(Alternate choices - from Tom's table)

Lens:		G/350430		K/A397	H/A41	K/77	P/AC062	P/AC325	P/AC320	H/A129	P/777	H/A62	H/AH11	P/AC355	H/A51	H/A123	K/A370	G/350550	G/350430
	focal length (mm)	5		11	10	8.5	9	8	7.5	7	7	6.67	6.25	6.25	6	5.4	4.6	6.1	5
	Numerical Aperture	0.15		0.3	0.33	0.3	0.3	0.3	0.3	0.39	0.3	0.33	0.4	0.35	0.4	0.38	0.3	0.18	0.15
	Clear Aperture (mm)	1.50	lens diam	7.2	8	8.05	6.5	6.5	6.6	6.4	6.3	5.8	6.38	6.5	6.37	5	8.05	2.8	2
	(= 2 x f x NA)		dbeam-eff	4.8	4.7	4.1	3.9	3.5	3.3	3.7	3.1	3.2	3.4	3.1	3.3	2.9	2.1	1.7	1.2
1/e-squared beam diameter at lens (mm)		1.180																	

Aperture factor (m) 1.263 — m = 1 is 1/e-squared truncation; m > 2 is essentially no truncation

1/e-squared beam radius (for normalized aperture) 0.792

Truncation factor. 1.219 — 1/e-squared radius at focal plane is increased by this factor due to truncation.

Z0:	3.078	To determine the effective diameter,
(A(Z0)/A(0))^2 =	0.1353363	vary Z0 until (A(Z0)/A(0))^2 = 0.1353353 or,
Ln((A(Z0)/A(0))^2) =	-2.000000001	equivalently, until Ln((A(Z0)/A(0))^2)=-2
		This can most easily be done by using
		the SOLVER function of Excel Tools:
		Target cell = C31; Value = -2
Effective diameter:	0.97	Change cell = C29
Spreadsheet value:	1.10	This is the effective beam diameter that is linked to the Gaus spreadsheet and the main disk design spreadsheet.

The remaining part of this spreadsheet is simply the numerical integration
of the diffraction equation for A(z) from the Mathcad program.
It includes the evaluation of the functions (A(Z)/A(0))^2 and Ln((A(Z)/A(0))^2).
It also includes a graph of (A(Z)/A(0))^2 vs Z.

			Zn =	0	0.1	0.2	0.3	0.4	0.5	0.6	0.7	0.8	0.9	1	1.1	1.2	1.3	1.4
			delta-Z =	0.1														
delta-r	r	e^-(r/r0)^2		A(Z1)	A(Z2)	A(Z3)	etc.											
0.01	0	1		0	0	0	0	0	0	0	0	0	0	0	0	0	0	0
	0.01	0.9998405		9.99841E-05	1E-04	1E-04	1E-04	1E-04	1E-04	1E-04	1E-04	1E-04	1E-04	1E-04	1E-04	1E-04	1E-04	1E-04
	0.02	0.9993623		0.000199872	0.0002	0.0002	0.0002	0.0002	0.0002	0.0002	0.0002	0.0002	0.0002	0.0002	0.0002	0.0002	0.0002	0.0002
	0.03	0.9985658		0.00029957	0.0003	0.0003	0.0003	0.0003	0.0003	0.0003	0.0003	0.0003	0.0003	0.0003	0.000299	0.000299	0.000299	0.000299
	0.04	0.9974517		0.000399901	0.000399	0.000399	0.000399	0.000399	0.000399	0.000399	0.000399	0.000399	0.000399	0.000399	0.000399	0.000399	0.000399	0.000398
	0.05	0.9960211		0.000498011	0.000498	0.000498	0.000498	0.000498	0.000498	0.000498	0.000498	0.000498	0.000498	0.000498	0.000498	0.000498	0.000497	0.000497
	0.06	0.9942754		0.000596565	0.000597	0.000597	0.000597	0.000596	0.000596	0.000596	0.000596	0.000596	0.000596	0.000596	0.000596	0.000596	0.000596	0.000596
	0.07	0.9922162		0.000694551	0.000695	0.000695	0.000694	0.000694	0.000694	0.000694	0.000694	0.000694	0.000694	0.000694	0.000694	0.000693	0.000693	0.000693
	0.08	0.9898456		0.000791878	0.000792	0.000792	0.000792	0.000792	0.000792	0.000791	0.000791	0.000791	0.000791	0.000791	0.00079	0.00079	0.00079	0.000789
	0.09	0.9871657		0.000888449	0.000888	0.000888	0.000888	0.000888	0.000888	0.000888	0.000888	0.000887	0.000887	0.000887	0.000886	0.000886	0.000885	0.000885
	0.1	0.9841791		0.000984176	0.000984	0.000984	0.000984	0.000984	0.000984	0.000983	0.000983	0.000983	0.000982	0.000982	0.000981	0.000981	0.00098	0.000979
	0.11	0.9808886		0.001078877	0.001079	0.001079	0.001079	0.001078	0.001078	0.001078	0.001077	0.001077	0.001076	0.001076	0.001075	0.001074	0.001073	0.001073
	0.12	0.9772974		0.001172757	0.001173	0.001173	0.001172	0.001172	0.001172	0.001171	0.001171	0.00117	0.001169	0.001169	0.001168	0.001167	0.001166	0.001164
	0.13	0.9734088		0.001265431	0.001265	0.001265	0.001265	0.001265	0.001264	0.001264	0.001263	0.001262	0.001261	0.00126	0.001259	0.001258	0.001256	0.001255
	0.14	0.9692265		0.001358017	0.001357	0.001357	0.001356	0.001356	0.001355	0.001355	0.001354	0.001353	0.001352	0.00135	0.001349	0.001347	0.001346	0.001344

FIG. 11A1

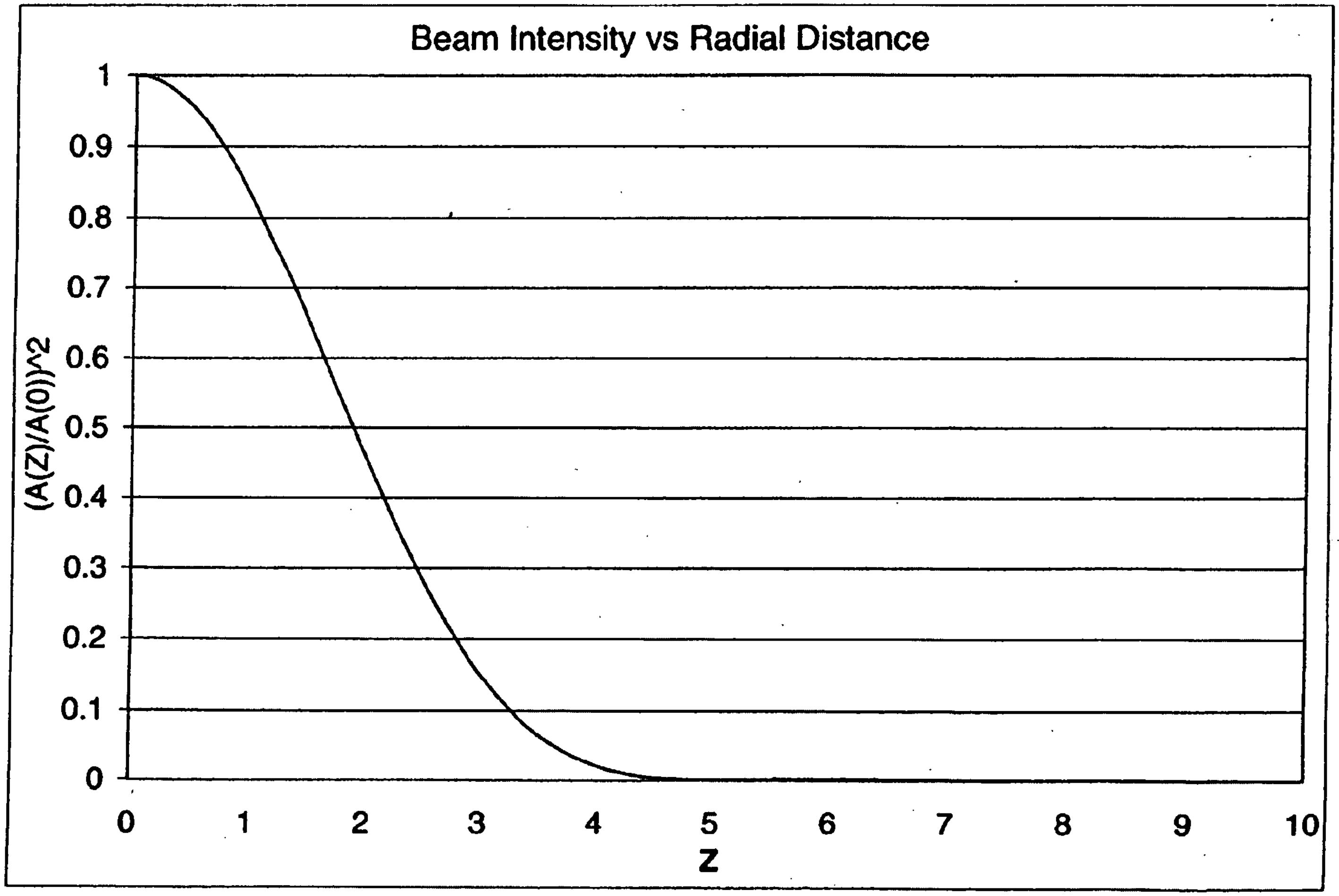
Beam Intensity vs Radial Distance
1
0.9
0.8
0.7
0.6
0.5
0.4
0.3
0.2
0.1
0
(A(Z)/A(0))^2
0
1
2
3
4
5
6
7
8
9
10
Z

FIG. 11A2

FIG 11B1

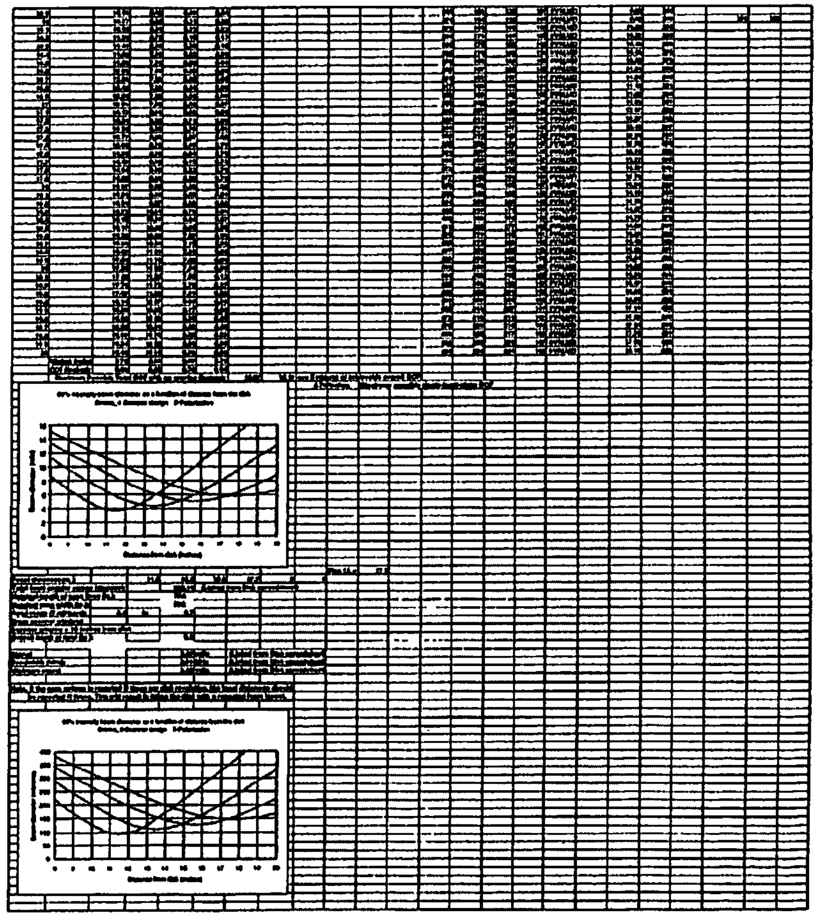

FIG. 11B2

L. 3/23/00

60% intensity beam diameter as a function of distance from the disk
Stratos_4 Scanner design - S-Polarization

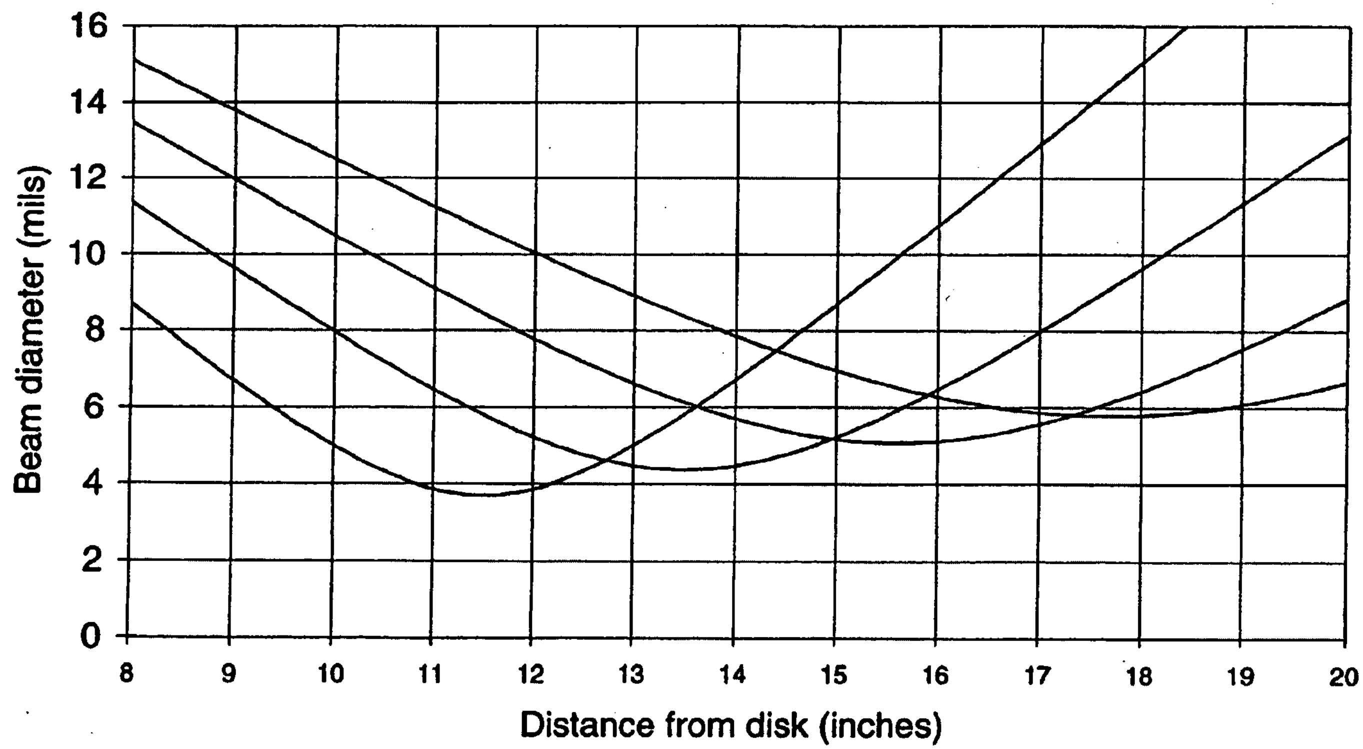

FIG. 11B3

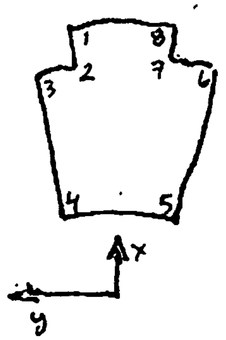

FIG. 12A1

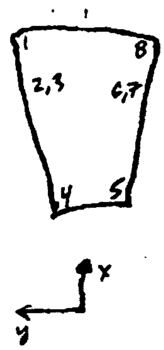

FIG. 12A2

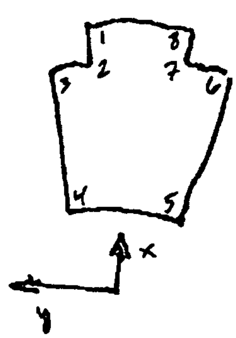

FIG. 12B1

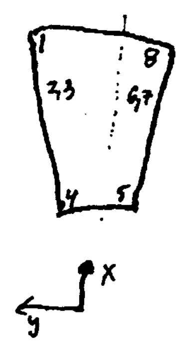

FIG. 12B2

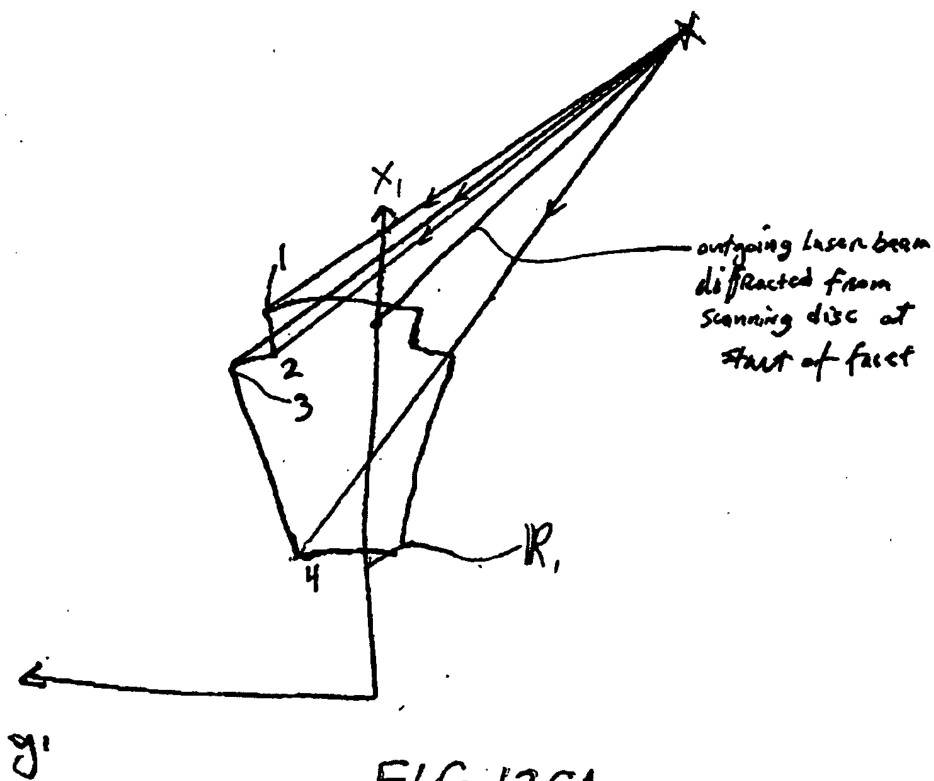

FIG. 12C1

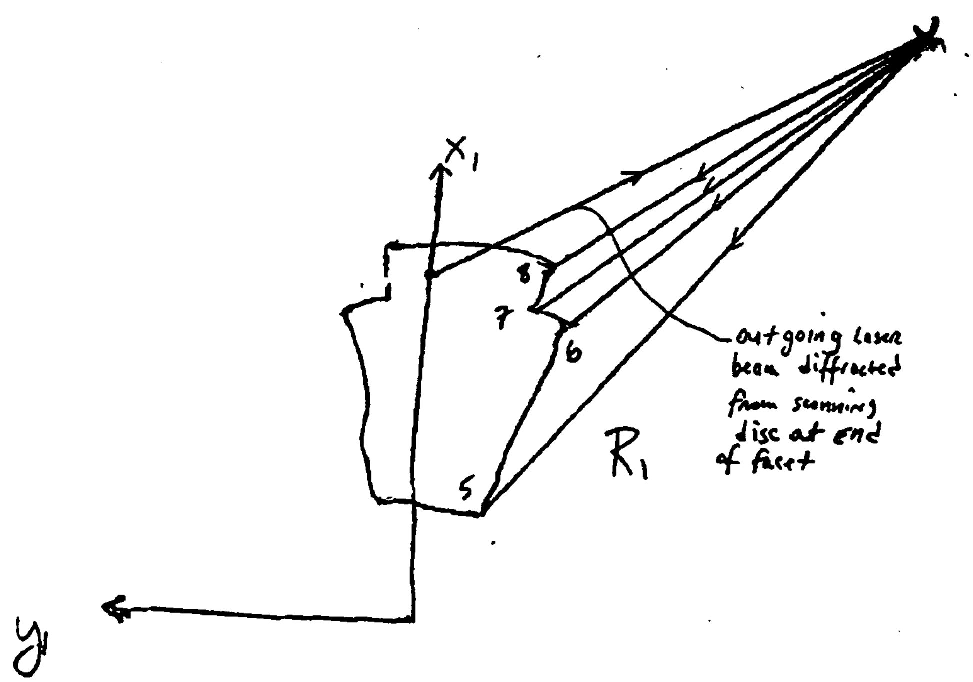

FIG. 12C2

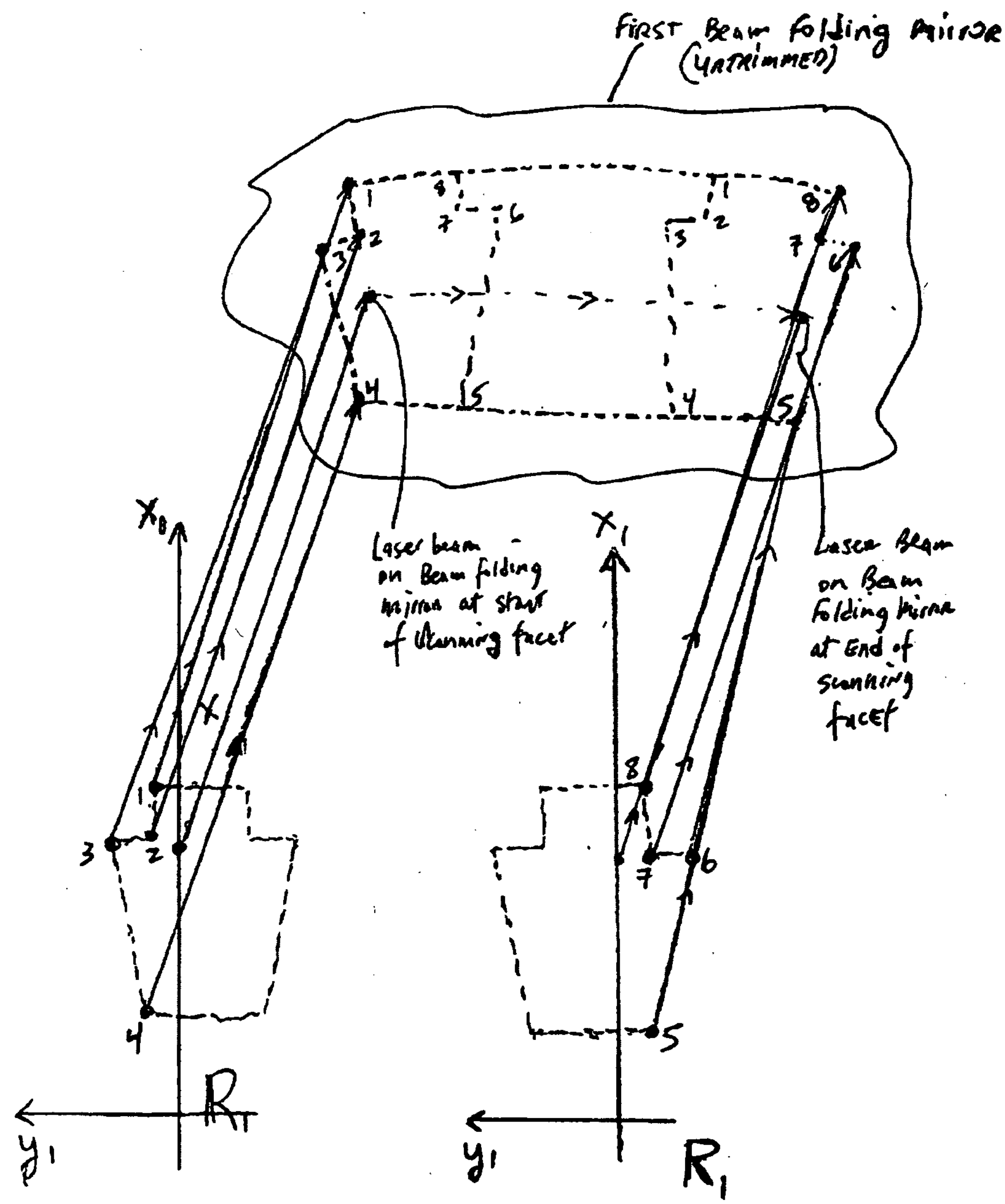
FIRST Beam folding Mirror (UNTRIMMED)
Laser beam on Beam folding mirror at start of scanning facet
Laser Beam on Beam folding mirror at End of scanning facet
X_B
X_1
y_1
y_1
R_T
R_1

FIG 12D

	A	B	C	D	E	F	G	H	I	J
75		1			2			3		
76	[redacted]	Facet			Facet			Facet		
77	G1	8			10			12		
78	Point 1	3.94874	-0.02294	2.12380	3.83250	0.07718	2.09937	3.75358	0.10925	2.09325
79	Point 2	3.65113	-0.12038	2.16443	3.53978	-0.02665	2.14166	3.45010	0.00887	2.13498
80	Point 3	3.61581	-0.03502	2.14098	3.53978	-0.02665	2.14166	3.44555	0.02059	2.13175
81	Point 4	2.64691	-0.40575	2.28887	2.88384	-0.25930	2.23643	2.44051	-0.31915	2.27208
82	Point 5	2.79472	-1.59304	2.62907	3.02644	-1.72489	2.65801	2.54066	-1.56107	2.63017
83	Point 6	3.81419	-2.04371	2.71867	3.69455	-2.02106	2.71697	3.56179	-2.02254	2.72286
84	Point 7	3.82907	-1.96478	2.69504	3.69455	-2.02106	2.71697	3.56439	-2.01174	2.71960
85	Point 8	4.13065	-2.08452	2.71758	3.98553	-2.15005	2.74265	3.86380	-2.14515	2.74622
86	Point 9	3.94874	-0.02294	2.12380	3.83250	0.07718	2.09937	3.75358	0.10925	2.09325
87	Start of scan line	4.02545	-0.67817	2.31174	3.92247	-0.62341	2.30000	3.82454	-0.57134	2.28883
88	Middle of rotation	4.02545	-0.67817	2.31174	3.92247	-0.62341	2.30000	3.82454	-0.57134	2.28883
89	End of scan line	4.04162	-1.16307	2.45250	3.92934	-1.15860	2.45580	3.81937	-1.12321	2.44999
90										

FIG 13.A1

Station 1

MR1

	A	B	C	D	E	F	G	H	I	J
91		Facet			Facet			Facet		
92	G2	7			9			11		
93	Point 1	4.02247	2.19033	2.58609	3.91799	2.45353	2.76685	3.80802	2.74420	2.96322
94	Point 2	3.79236	2.11753	2.69195	3.69690	2.36537	2.86040	3.58337	2.64904	3.05579
95	Point 3	3.78639	2.20453	2.73451	3.69690	2.36537	2.86040	3.58162	2.66095	3.06217
96	Point 4	3.05197	1.92230	3.05003	3.21262	2.17226	3.06533	2.85731	2.34705	3.35743
97	Point 5	2.64347	-0.27369	2.31221	2.81913	-0.34045	2.17660	2.54140	-0.10460	2.44937
98	Point 6	3.25774	-0.84215	1.68794	3.25935	-0.70440	1.74867	3.23044	-0.61969	1.80401
99	Point 7	3.29896	-0.76438	1.69797	3.25935	-0.70440	1.74867	3.23562	-0.60869	1.80582
100	Point 8	3.50262	-0.93172	1.50046	3.46547	-0.87482	1.54830	3.45674	-0.77127	1.59994
101	Point 9	4.02247	2.19033	2.58609	3.91799	2.45353	2.76685	3.80802	2.74420	2.96322
102	Start of scan line	3.88910	1.13139	2.19201	3.81752	1.25640	2.29108	3.73628	1.40993	2.40874
103	Middle of rotation	3.83943	0.57926	1.97459	3.76954	0.54210	2.00000	3.70069	0.50549	2.02503
104	End of scan line	3.77386	0.09914	1.79899	3.72144	0.14315	1.85024	3.66728	0.18290	1.90064
105										

FIG. 13A2

Station 1

MR1

	A	B	C	D	E	F	G	H	I	J	K	L	M
106	[redacted]	Facet			Facet			Facet			Facet		
107	G3	1			2			3			4		
108	Point 1	5.11617	1.95380	1.89155	5.01400	1.88093	1.96716	4.92433	1.81870	2.03365	4.82799	1.75935	2.10576
109	Point 2	4.98460	1.86904	1.98969	4.88136	1.79109	2.06571	4.77964	1.72980	2.14196	4.68407	1.66502	2.21298
110	Point 3	4.94695	2.08109	2.03847	4.88064	1.79549	2.08667	4.76362	1.86942	2.17507	4.68407	1.66502	2.21298
111	Point 4	4.55990	1.69707	2.31542	4.46955	1.51422	2.37191	4.31720	1.51260	2.49402	4.34215	1.44090	2.46771
112	Point 5	4.35785	-1.63559	2.18575	4.29296	-1.52325	2.24765	4.14486	-1.55897	2.36336	4.17995	-1.53887	2.33696
113	Point 6	4.71038	-2.01784	1.86940	4.68022	-1.80322	1.91239	4.54753	-1.91413	2.00915	4.50146	-1.76326	2.05933
114	Point 7	4.77395	-1.80620	1.83693	4.68147	-1.79883	1.91177	4.59009	-1.77513	1.98718	4.50146	-1.76326	2.05933
115	Point 8	4.89971	-1.89063	1.72862	4.80732	-1.88882	1.80291	4.72764	-1.86391	1.86903	4.63750	-1.85821	1.94186
116	Point 9	5.11617	1.95380	1.89155	5.01400	1.88093	1.96715	4.92433	1.81870	2.03365	4.82799	1.75935	2.10576
117	Start of scan line	5.11614	1.00830	1.80678	5.02116	0.94389	1.87935	4.92928	0.88565	1.94798	4.84129	0.83137	2.01383
118	Middle of rotation	5.03523	0.00000	1.78542	4.95474	0.00000	1.85000	4.87537	0.00000	1.91369	4.79689	0.00000	1.97666
119	End of scan line	5.00607	-0.96140	1.72464	4.92129	-0.94701	1.79393	4.83778	-0.91710	1.86356	4.75656	-0.89961	1.93026
120													

FIG. 13A3

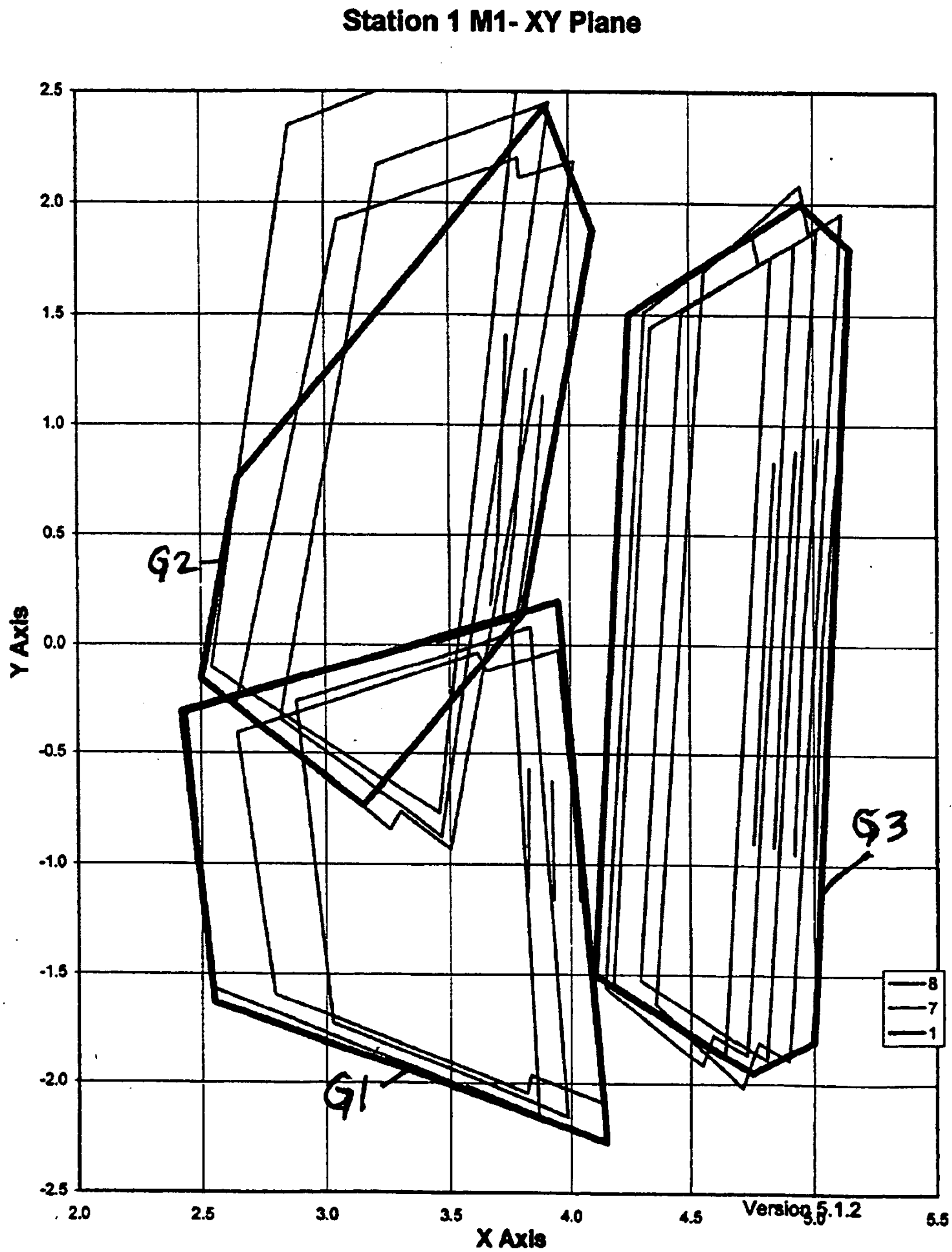

FIG. 13A4

Station 1 MR1.xy

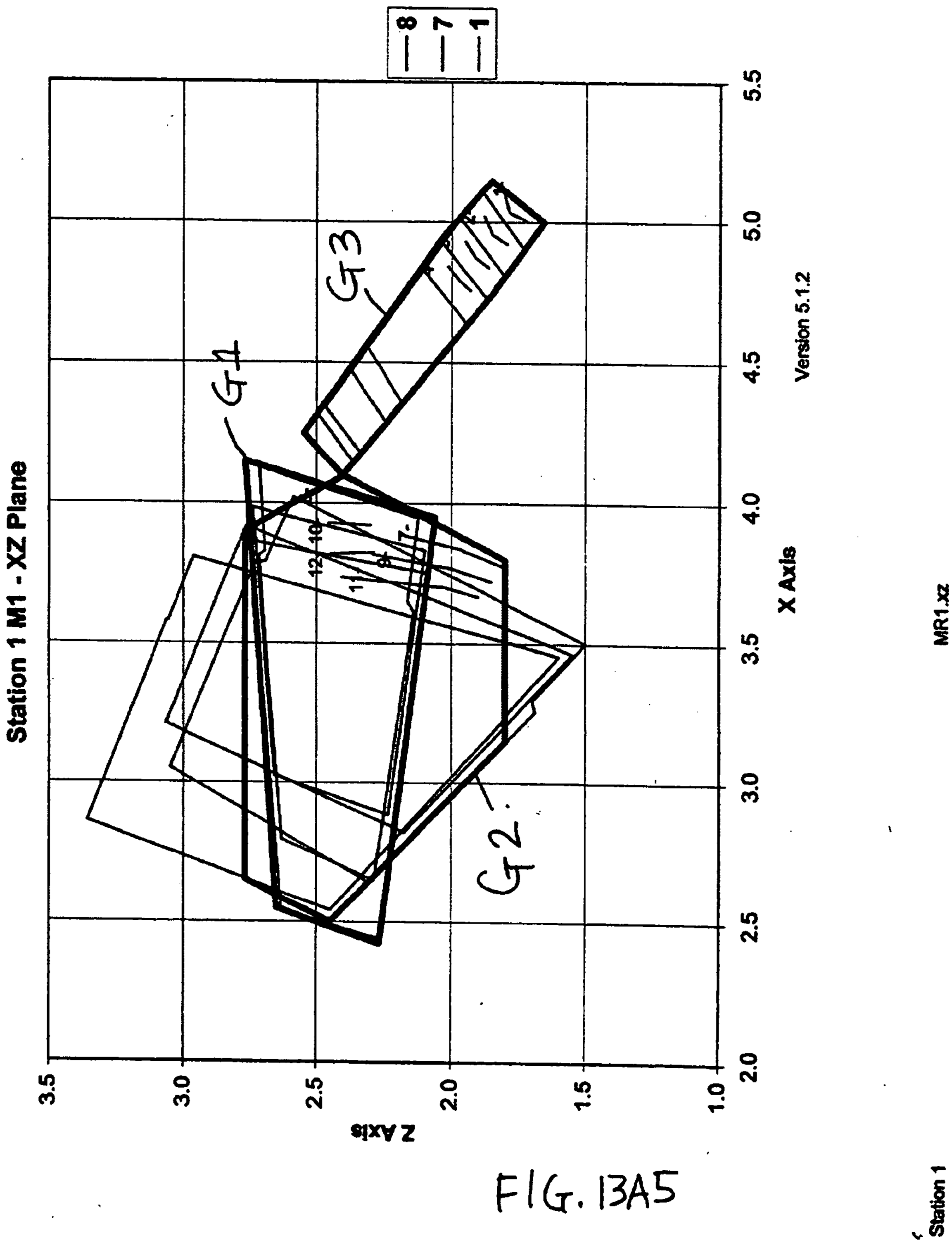
Station 1 M1 - XZ Plane
Z Axis
3.5
3.0
2.5
2.0
1.5
1.0
X Axis
2.0
2.5
3.0
3.5
4.0
4.5
5.0
5.5
8
7
1
G1
G2
G3
Version 5.1.2
MR1.xz
Station 1

FIG. 13A5

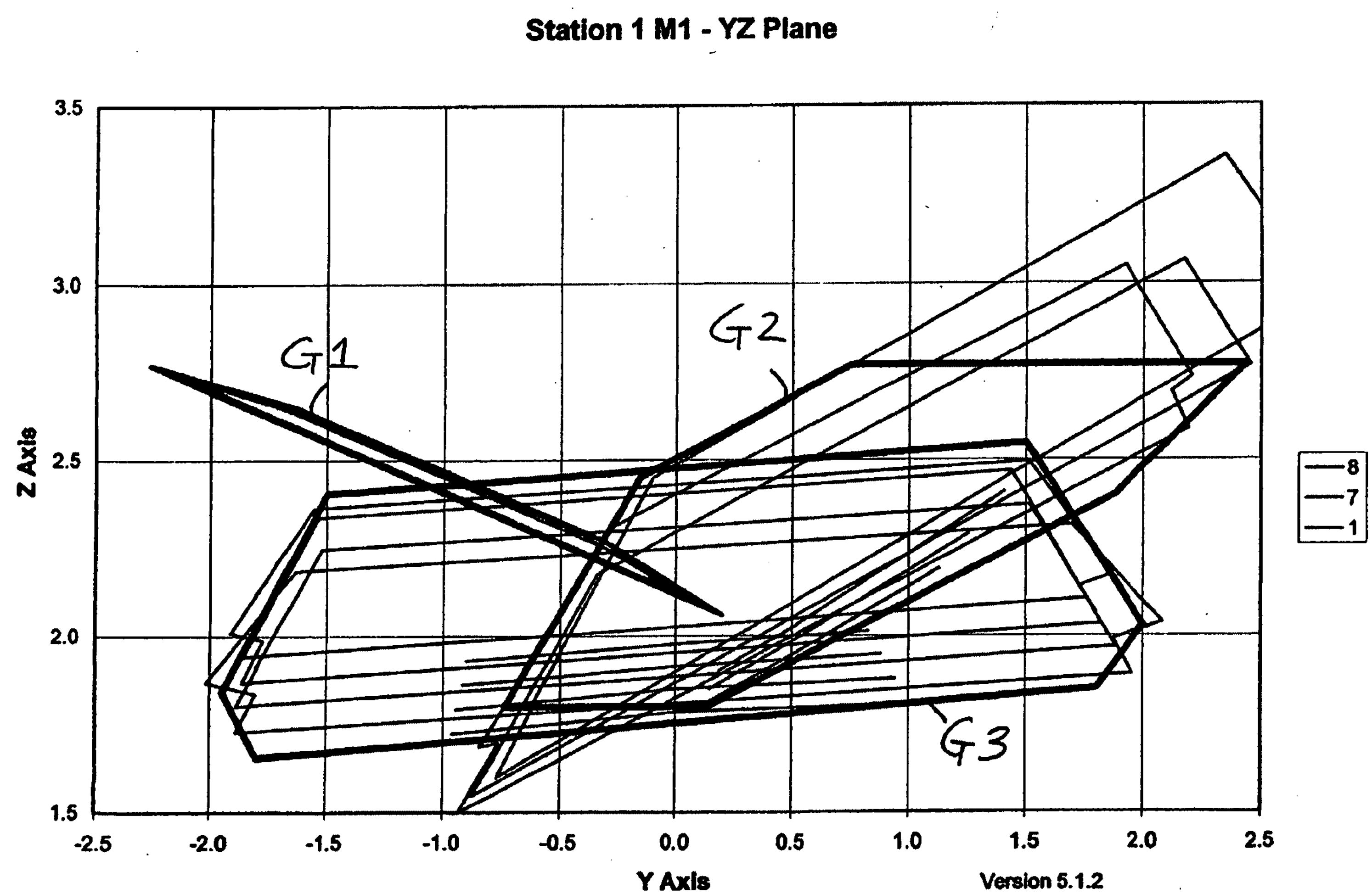

FIG. 13A6

Station 1

MR1.yz4/3/00

	A	B	C	D	E	F	G	H	I	J
75										
76	[redacted]	1			2			3		
77	G1	Facet			Facet			Facet		
78		8			10			12		
79	Point 1	4.83616	-1.58877	0.84115	4.73669	-1.63993	0.66301	4.64314	-1.69543	0.50201
80	Point 2	4.68429	-1.81884	0.74767	4.58926	-1.86587	0.57304	4.48446	-1.93076	0.39587
81	Point 3	4.67878	-1.78796	0.69779	4.58926	-1.86587	0.57304	4.48358	-1.92664	0.38888
82	Point 4	4.22223	-2.50841	0.44377	4.28260	-2.33583	0.38592	4.00469	-2.63997	0.07232
83	Point 5	4.05858	-3.52592	1.25078	4.08790	-3.53306	1.33026	3.80481	-3.82416	0.98868
84	Point 6	4.46417	-3.19384	1.84067	4.36259	-3.30509	1.72614	4.23639	-3.46214	1.60614
85	Point 7	4.48187	-3.13482	1.81374	4.36259	-3.30509	1.72614	4.23895	-3.45403	1.60276
86	Point 8	4.62128	-3.01193	2.00617	4.49650	-3.19395	1.91915	4.38465	-3.33084	1.80981
87	Point 9	4.83616	-1.58677	0.84115	4.73669	-1.63993	0.66301	4.64314	-1.69543	0.50201
88	Start of scan line	4.79136	-1.94631	1.15786	4.70000	-2.00000	1.00000	4.60451	-2.05611	0.83500
89	Middle of rotation	4.79136	-1.94631	1.15786	4.70000	-2.00000	1.00000	4.60451	-2.05611	0.83500
90	End of scan line	4.69056	-2.50111	1.56984	4.58033	-2.64637	1.47458	4.46974	-2.76462	1.34651

FIG. 13B1

Station 1

MR2

	A	B	C	D	E	F	G	H	I	J
91	[redacted]	Facet			Facet			Facet		
92	G2	7			9			11		
93	Point 1	3.38194	4.20092	1.75395	3.24016	4.43917	2.01655	3.11010	4.72655	2.34142
94	Point 2	3.16298	4.26385	1.78738	3.03125	4.49361	2.04162	2.88665	4.78740	2.37142
95	Point 3	3.16739	4.30137	1.83403	3.03125	4.49361	2.04162	2.88663	4.79258	2.37774
96	Point 4	2.50443	4.46930	1.90767	2.59900	4.60627	2.09349	2.21545	4.97231	2.46415
97	Point 5	1.39822	2.79582	-0.35302	1.44696	2.82994	-0.30174	1.08385	3.11226	-0.02918
98	Point 6	1.81707	2.39729	-0.75633	1.73748	2.57459	-0.55577	1.56833	2.71448	-0.41858
99	Point 7	1.85962	2.41646	-0.72451	1.73748	2.57459	-0.55577	1.57414	2.71711	-0.41422
100	Point 8	2.00251	2.29151	-0.84867	1.87437	2.45426	-0.67547	1.73191	2.58895	-0.53935
101	Point 9	3.38194	4.20092	1.75395	3.24016	4.43917	2.01655	3.11010	4.72655	2.34142
102	Start of scan line	3.14045	3.84670	1.27398	3.00728	4.05126	1.49719	2.86346	4.28889	1.75864
103	Middle of rotation	2.81784	3.26851	0.50471	2.60000	3.30000	0.50000	2.37384	3.33269	0.49511
104	End of scan line	2.37758	2.63817	-0.35149	2.22734	2.77029	-0.22004	2.06736	2.89843	-0.09537
105										

FIG. 13B2

	A	B	C	D	E	F	G	H	I	J	K	L	M
106		Facet			Facet			Facet			Facet		
107	G3	1			2			3			4		
108	Point 1	4.36645	2.65376	0.19632	4.13039	2.57939	0.16456	3.89207	2.57127	0.13136	3.63985	2.49916	0.09731
109	Point 2	4.22328	2.62785	0.17673	3.98981	2.54937	0.14541	3.72893	2.54596	0.10897	3.48464	2.46924	0.07610
110	Point 3	4.17479	2.80928	0.16686	3.98888	2.55291	0.14522	3.69351	2.66161	0.10205	3.48464	2.46924	0.07610
111	Point 4	3.78746	2.62732	0.11577	3.58353	2.46410	0.09002	3.24144	2.51989	0.04122	3.13971	2.40274	0.02898
112	Point 5	3.59706	-1.89846	0.16625	3.42901	-1.80124	0.14108	3.10957	-1.84718	0.09718	3.03925	-1.79742	0.08649
113	Point 6	4.00140	-2.16622	0.22737	3.86105	-1.97527	0.20449	3.58373	-2.08109	0.16749	3.40752	-1.93323	0.14032
114	Point 7	4.06710	-1.99138	0.23359	3.86230	-1.97181	0.20460	3.62849	-1.86992	0.17186	3.40752	-1.93323	0.14032
115	Point 8	4.22016	-2.04816	0.25597	4.01328	-2.03180	0.22675	3.80192	-2.02808	0.19711	3.57430	-1.99474	0.16470
116	Point 9	4.36645	2.65376	0.19632	4.13039	2.57939	0.16456	3.89207	2.57127	0.13136	3.63985	2.49916	0.09731
117	Start of scan line	4.40361	1.87032	0.21487	4.17745	1.84317	0.18369	3.94222	1.82246	0.15114	3.70025	1.80404	0.11760
118	Middle of rotation	4.29670	0.23013	0.22786	4.10000	0.25000	0.20000	3.89313	0.27090	0.17070	3.67474	0.29297	0.13978
119	End of scan line	4.30920	-1.28070	0.25535	4.10701	-1.28789	0.22718	3.89234	-1.26997	0.19685	3.66999	-1.27076	0.16575
120													

FIG. 13B3

Station 1

MR2

Station 1 M2- XY Plane

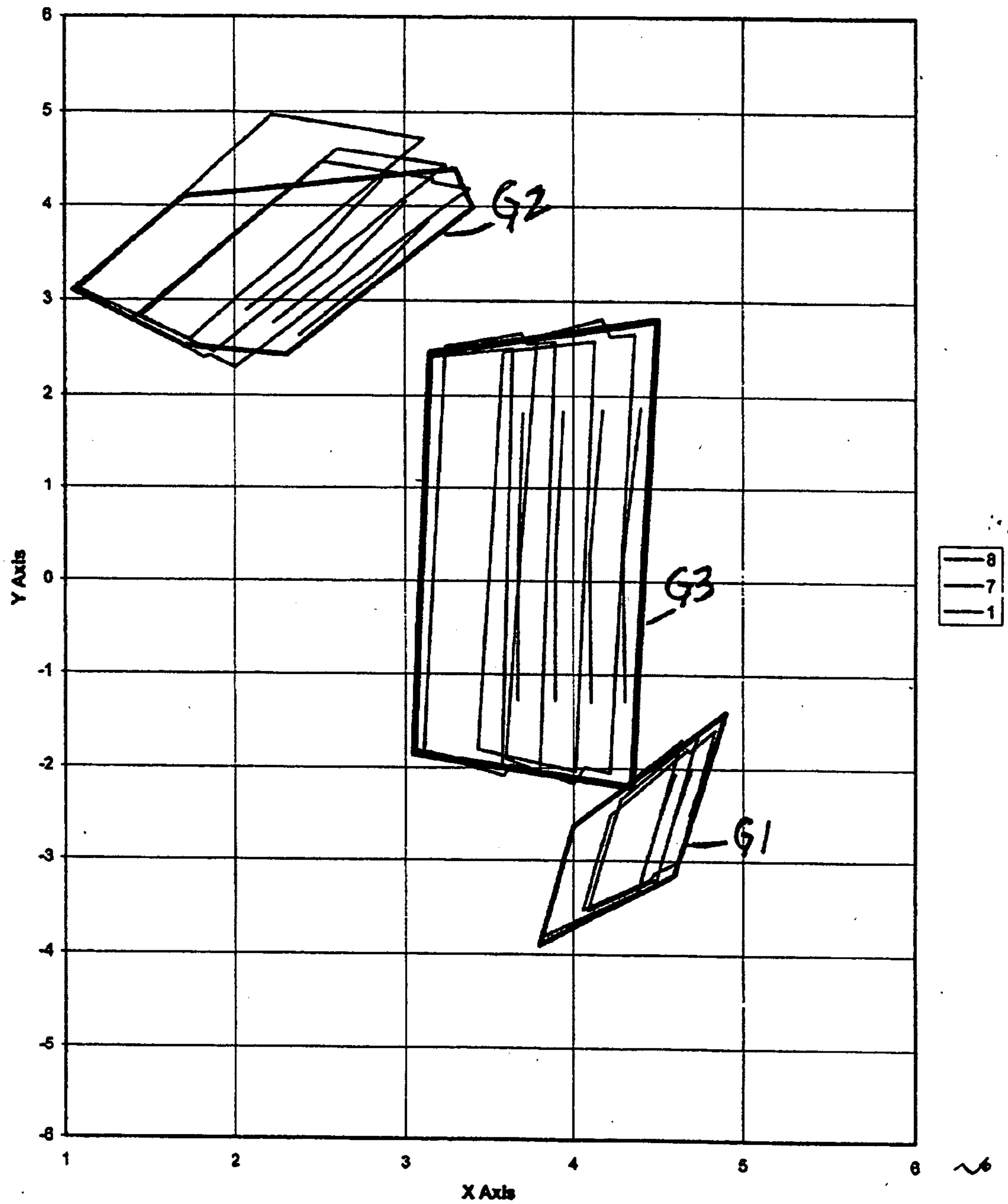

FIG. 13B4

306/335

Station 1 M2 - XZ Plane

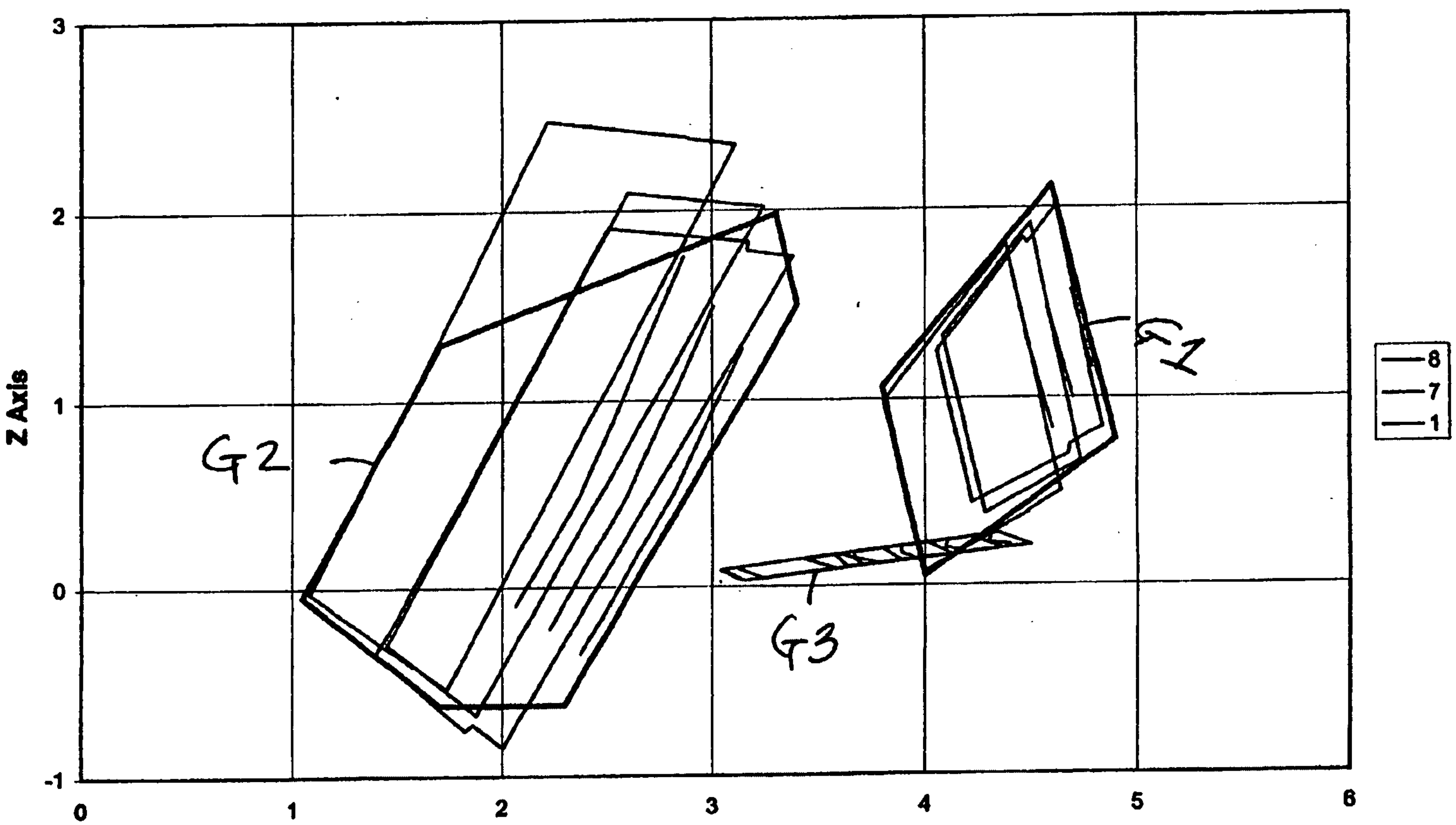

FIG. 13B5

Station 1

MR2.xz

Station 1 M2 - YZ Plane

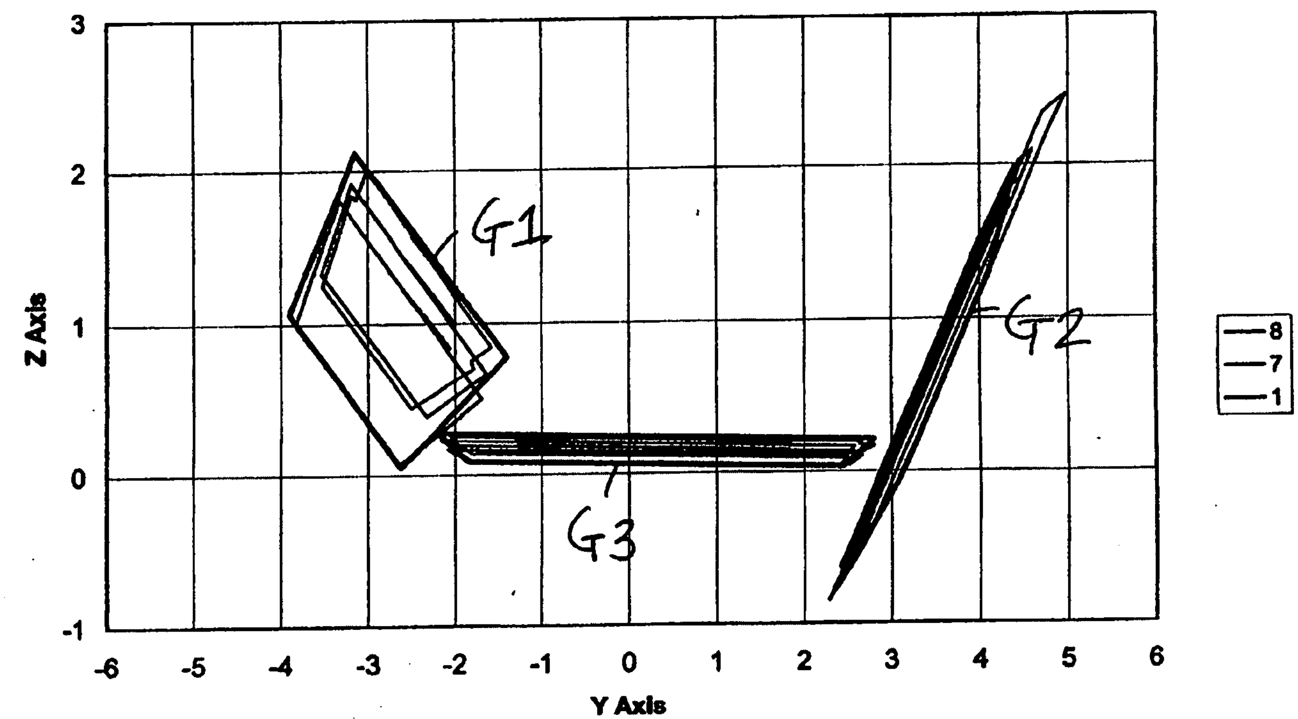

FIG. 13B6

Station 1

MR2.yz

	A	B	C	D	E	F	G	H	I	J
76		Facet			Facet			Facet		
77	G1	8			10			12		
78	Point 1	1.20537	-1.67340	0.83287	1.73454	-1.76256	0.57847	2.18607	-1.81295	0.33975
79	Point 2	1.50717	-1.82194	0.77007	2.01252	-1.90575	0.52600	2.50076	-1.97962	0.28421
80	Point 3	1.53373	-1.80077	0.73570	2.01252	-1.90575	0.52600	2.50470	-1.97622	0.27888
81	Point 4	2.71992	-2.40114	0.50283	2.72609	-2.27331	0.39129	3.72651	-2.62604	0.06549
82	Point 5	2.86809	-3.52973	1.36131	2.87153	-3.57274	1.39541	3.86534	-3.82116	0.98584
83	Point 6	1.66004	-3.29877	1.91900	2.13984	-3.43596	1.73579	2.62296	-3.60007	1.57321
84	Point 7	1.63442	-3.25853	1.90105	2.13984	-3.43596	1.73579	2.61924	-3.59386	1.57029
85	Point 8	1.32257	-3.19447	2.04127	1.85089	-3.38194	1.87021	2.29384	-3.53522	1.72352
86	Point 9	1.20537	-1.67340	0.83287	1.73454	-1.76256	0.57847	2.18607	-1.81295	0.33975
87	Start of scan line	1.19058	-1.90430	1.03659	1.70000	-2.00000	0.80000	2.15170	-2.08486	0.59022
88	Middle of rotation	1.19058	-1.90430	1.03659	1.70000	-2.00000	0.80000	2.15170	-2.08486	0.59022
89	End of scan line	1.33110	-2.85916	1.75349	1.84105	-3.01433	1.56667	2.29073	-3.10310	1.36142
90										

FIG. 13C1

Station 1 M3- XY Plane

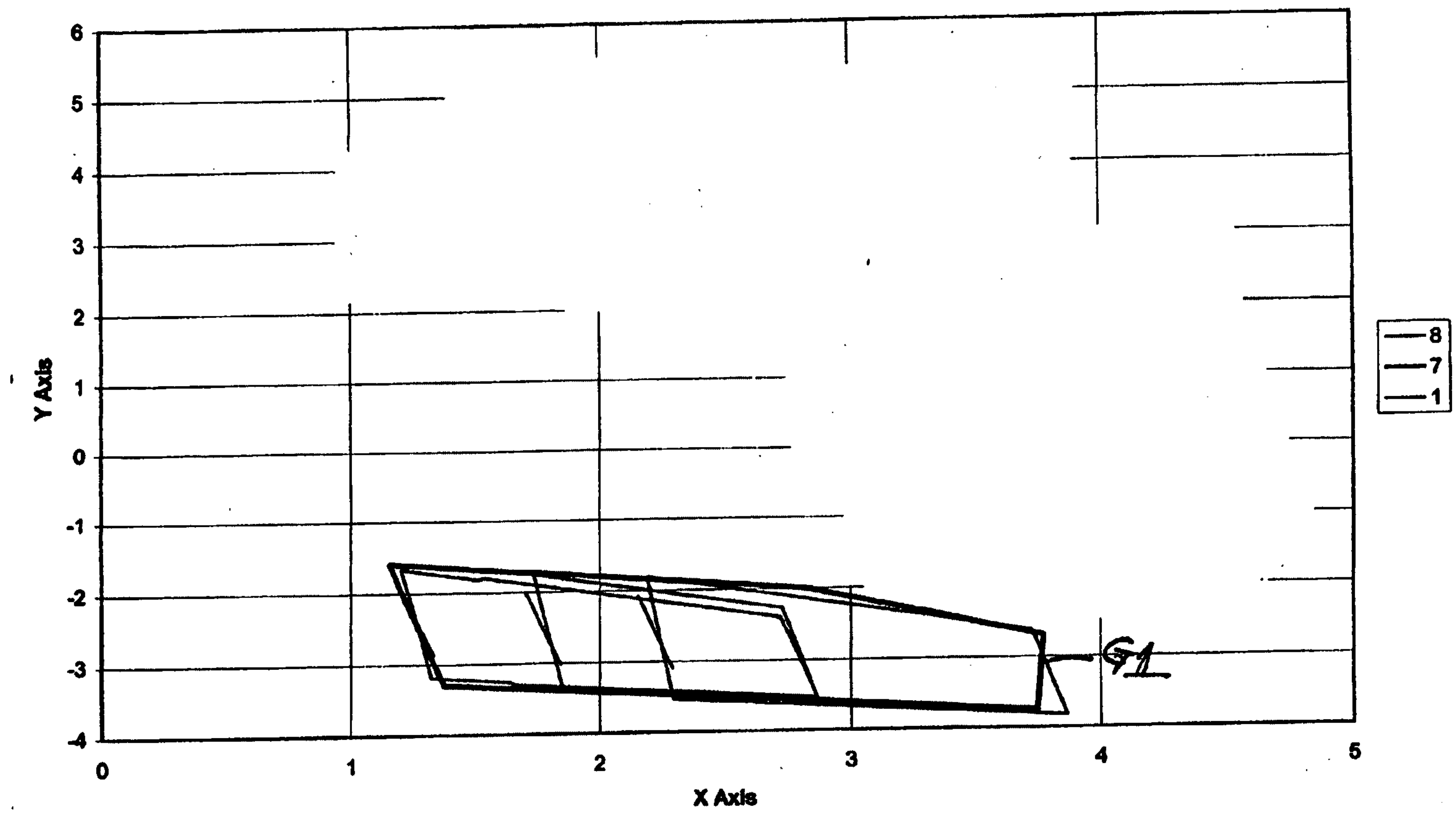

FIG.13C2

MR3.xy

Station 1

Station 1 M3 - XZ Plane

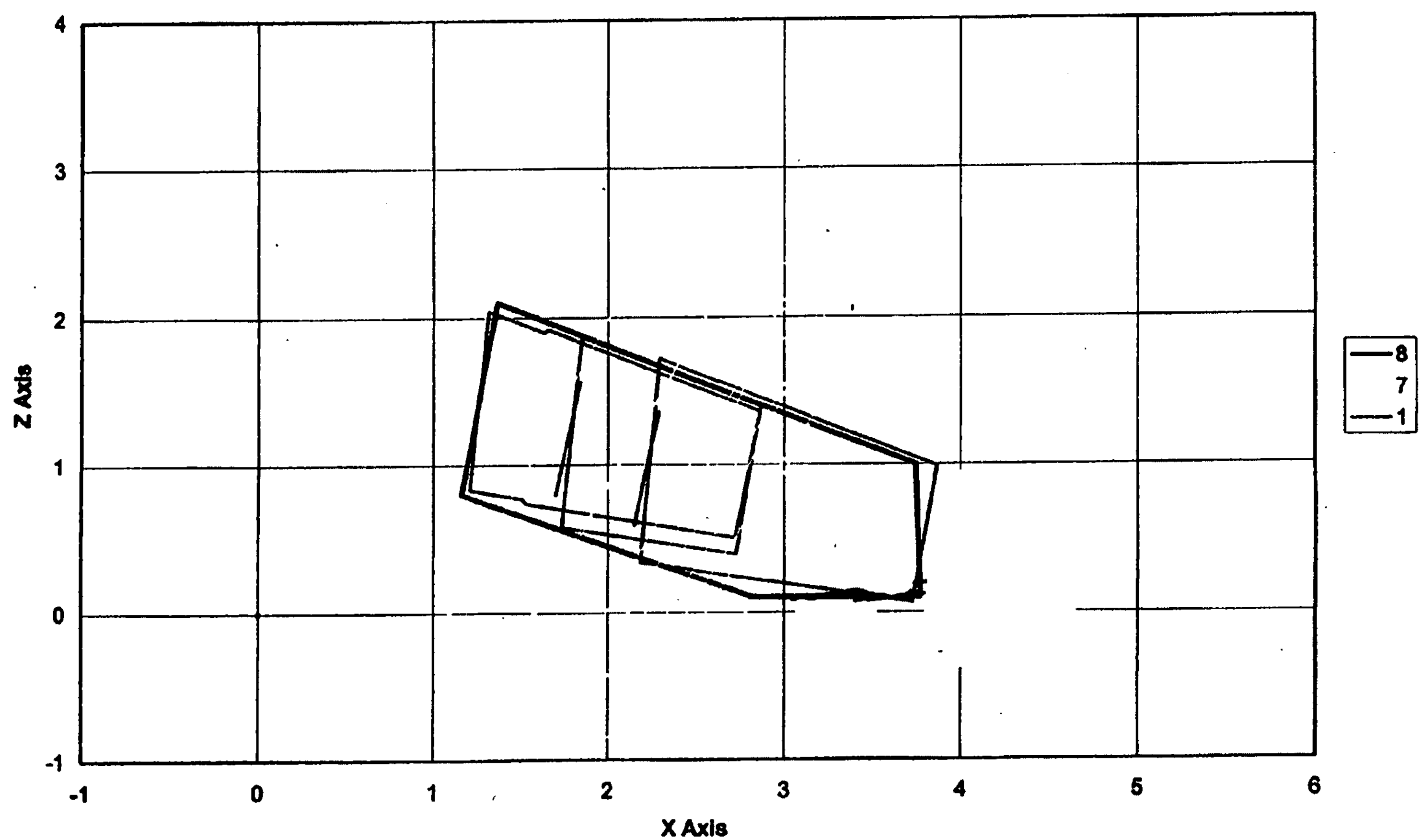

FIG. 13C3

Station 1

MR3.xz

Station 1 M3 - YZ Plane

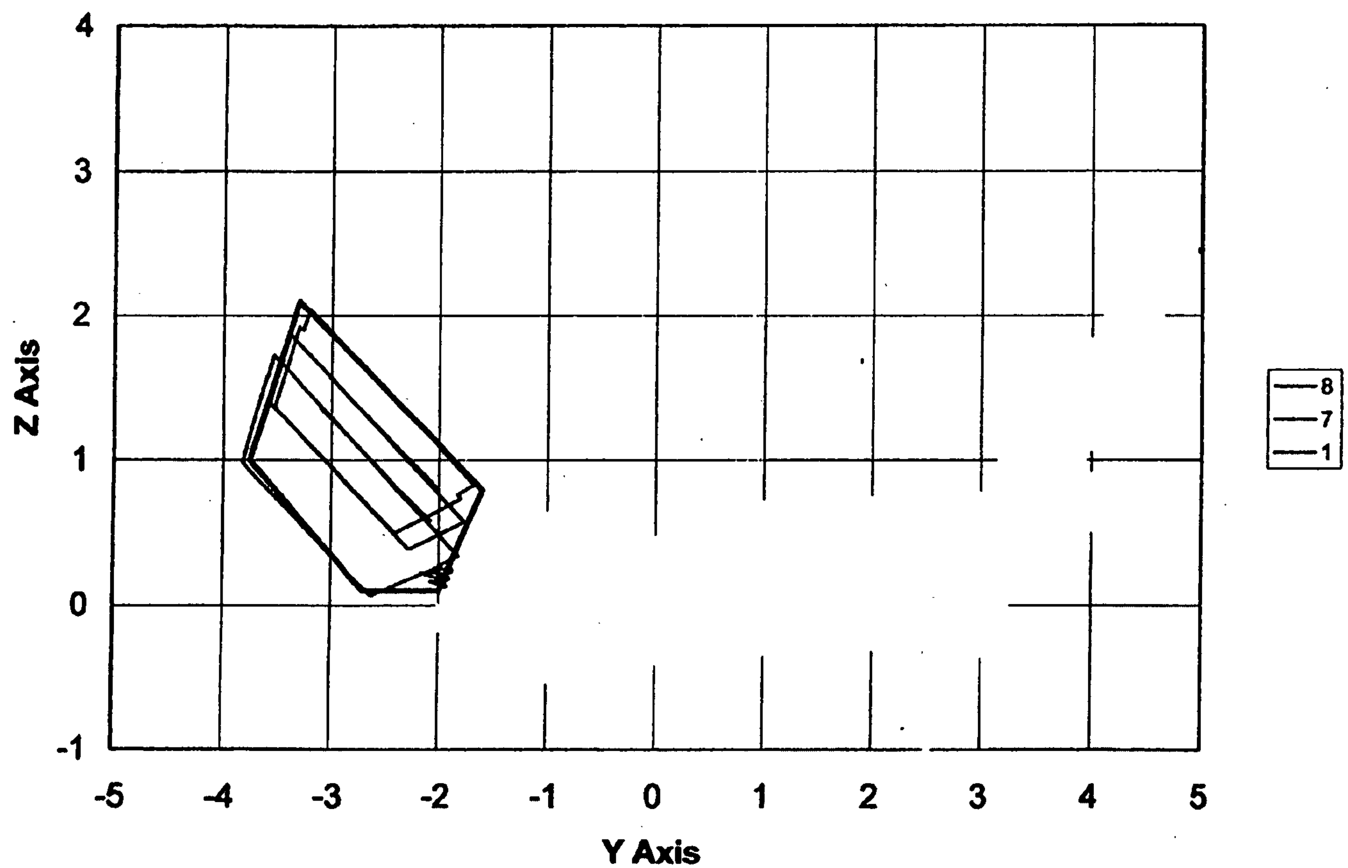

FIG. 13C4

Station 1

MR3.yz

312/335

	A	B	C	D	E	F	G	H	I	J
75		1			2			3		
76	[redacted]	Facet			Facet			Facet		
77	G1	8			10			12		
78	Point 1	1.20537	-1.67340	0.83287	1.73454	-1.76256	0.57847	2.18607	-1.81295	0.33975
79	Point 2	1.50717	-1.82194	0.77007	2.01252	-1.90575	0.52600	2.50076	-1.97962	0.28421
80	Point 3	1.53373	-1.80077	0.73570	2.01252	-1.90575	0.52600	2.50470	-1.97622	0.27888
81	Point 4	2.71992	-2.40114	0.50283	2.72609	-2.27331	0.39129	3.72651	-2.62604	0.06549
82	Point 5	2.86809	-3.52973	1.36131	2.87153	-3.57274	1.39541	3.86534	-3.82116	0.98584
83	Point 6	1.66004	-3.29877	1.91900	2.13984	-3.43596	1.73579	2.62296	-3.60007	1.57321
84	Point 7	1.63442	-3.25853	1.90105	2.13984	-3.43596	1.73579	2.61924	-3.59386	1.57029
85	Point 8	1.32257	-3.19447	2.04127	1.85089	-3.38194	1.87021	2.29384	-3.53522	1.72352
86	Point 9	1.20537	-1.67340	0.83287	1.73454	-1.76256	0.57847	2.18607	-1.81295	0.33975
87	Start of scan line	1.19058	-1.90430	1.03659	1.70000	-2.00000	0.80000	2.15170	-2.08486	0.59022
88	Middle of rotation	1.19058	-1.90430	1.03659	1.70000	-2.00000	0.80000	2.15170	-2.08486	0.59022
89	End of scan line	1.33110	-2.85916	1.75349	1.84105	-3.01433	1.56667	2.29073	-3.10310	1.36142
90										

FIG. 13D1

Station 1

MR4

	A	B	C	D	E	F	G	H	I	J	K	L	M	N	O	P	Q	R	S
105																			
106		Facet			Facet			Facet			Facet			Facet			Facet		
107	G3	1			2			3			4			5			6		
108	Point 1	5.04006	0.62476	1.76314	4.94178	0.55167	1.81997	4.85731	0.53694	1.86881	4.76146	0.57105	1.92423	4.59494	0.56809	2.02061	4.42066	0.60393	2.12116
109	Point 2	4.87042	0.44426	1.86123	4.77196	0.46655	1.91616	4.67548	0.45660	1.97394	4.58109	0.48315	2.02852	4.39766	0.48153	2.13458	4.21828	0.51160	2.23831
110	Point 3	4.83173	0.66283	1.88360	4.77125	0.47110	1.91867	4.65020	0.60068	1.98856	4.58109	0.48315	2.02852	4.39672	0.48704	2.13512	4.21826	0.51160	2.23831
111	Point 4	4.32129	0.26699	2.17673	4.24022	0.20212	2.22561	4.09186	0.25949	2.31139	4.14950	0.27260	2.27807	3.77406	0.21047	2.49515	3.84486	0.34144	2.45421
112	Point 5	4.34770	-1.84845	2.16347	4.26992	-1.86717	2.20644	4.08721	-1.77102	2.31406	4.12497	-1.92124	2.29225	3.74166	-1.46848	2.51366	3.79316	-1.27109	2.48410
113	Point 6	4.77372	-2.25670	1.91714	4.71924	-2.17652	1.94664	4.58410	-2.15769	2.03634	4.49172	-2.17143	2.08019	4.30150	-1.80374	2.19018	4.13935	-1.47056	2.26393
114	Point 7	4.63579	-2.04739	1.88125	4.72049	-2.17219	1.94791	4.80668	-2.01968	2.01372	4.49172	-2.17143	2.08019	4.30312	-1.79644	2.18924	4.13935	-1.47056	2.26393
115	Point 8	4.96278	-2.13965	1.79626	4.86407	-2.27009	1.86490	4.76563	-2.11752	1.92182	4.64469	-2.27678	1.99174	4.48021	-1.90337	2.08665	4.32687	-1.57861	2.17561
116	Point 9	5.04006	0.52476	1.76314	4.94178	0.55167	1.81997	4.85731	0.53694	1.86881	4.76146	0.57105	1.92423	4.59494	0.56809	2.02061	4.42066	0.60393	2.12116
117	Start of scan line	5.02090	0.00000	1.77422	4.92826	0.00000	1.82778	4.83795	0.00000	1.88000	4.74966	0.00000	1.93105	4.57806	0.00000	2.03027	4.41147	0.00000	2.12659
118	Middle of rotation	5.02090	0.00000	1.77422	4.92826	0.00000	1.82778	4.83795	0.00000	1.88000	4.74966	0.00000	1.93105	4.57806	0.00000	2.03027	4.41147	0.00000	2.12659
119	End of scan line	5.06055	-1.14492	1.75129	4.96266	-1.22689	1.80788	4.85432	-1.09333	1.87063	4.76001	-1.19617	1.92507	4.57039	-0.86357	2.03470	4.40142	-0.84218	2.13240
120																			

FIG. 14A1

	A	B	C	D	E	F	G	H	I	J	K	L	M	N	O	P	Q	R	S
105																			
106	[redacted]	Facet			Facet			Facet			Facet			Facet			Facet		
107	G3	1			2			3			4			5			6		
108	Point 1	4.82498	0.44237	0.26978	4.65503	0.44811	0.22157	4.49179	0.44459	0.17770	4.30775	0.44954	0.12583	3.93952	0.44834	0.02505	3.52125	0.44891	-0.08994
109	Point 2	4.66874	0.38963	0.24652	4.50103	0.37345	0.19944	4.31949	0.37132	0.15017	4.14124	0.37427	0.10044	3.74647	0.37385	-0.00784	3.32508	0.37322	-0.12337
110	Point 3	4.62719	0.54811	0.18746	4.50022	0.37701	0.19826	4.28911	0.48536	0.11104	4.14124	0.37427	0.10044	3.74516	0.37803	-0.00933	3.32508	0.37322	-0.12337
111	Point 4	4.18842	-0.22763	0.15299	4.04652	0.15472	0.13371	3.79612	0.20147	0.05234	3.76369	0.20355	0.04286	3.17536	0.15541	-0.10566	2.98199	0.24084	-0.18182
112	Point 5	4.29176	-2.24568	0.84926	4.17480	-2.32513	0.63655	3.90727	-2.24907	0.74455	3.89193	-2.41913	0.78626	3.29187	-2.00085	0.50856	3.10607	-1.64117	0.36043
113	Point 6	4.89167	-2.49257	1.02567	4.58519	-2.46863	0.99272	4.37431	-2.45821	0.92926	4.25097	-2.52865	0.91466	3.86517	-2.15830	0.70794	3.47166	-1.74831	0.48974
114	Point 7	4.74716	-2.30630	0.99034	4.58627	-2.46486	0.99200	4.41150	-2.33743	0.90686	4.25097	-2.52955	0.91466	3.86651	-2.15166	0.70712	3.47166	-1.74631	0.48974
115	Point 8	4.89443	-2.35176	1.04332	4.74099	-2.51341	1.04484	4.57811	-2.36443	0.98529	4.41114	-2.57881	0.97193	4.06339	-2.20429	0.77533	3.68342	-1.81036	0.56463
116	Point 9	4.82498	0.44237	0.26976	4.65503	0.44811	0.22157	4.49179	0.44469	0.17770	4.30775	0.44954	0.12583	3.93952	0.44834	0.02505	3.52125	0.44891	-0.08994
117	Start of scan line	4.82442	0.00000	0.38906	4.66490	0.00000	0.34528	4.50000	-0.00001	0.30000	4.32901	0.00000	0.25305	3.96553	0.00000	0.15325	3.56687	0.00000	0.04380
118	Middle of rotation	4.82442	0.00000	0.38907	4.66490	0.00000	0.34526	4.50000	0.00000	0.30000	4.32901	0.00000	0.25305	3.96553	0.00000	0.15325	3.56687	0.00000	0.04380
119	End of scan line	4.94361	-1.51167	0.82998	4.80210	-1.65515	0.82987	4.62186	-1.53817	0.74880	4.47185	-1.71403	0.75509	4.08637	-1.40033	0.56428	3.67805	-1.09574	0.37020
120																			

FIG. 14B1

	A	B	C	D	E	F	G	H	I	J	K	L	M	N	O	P	Q	R	S
106		Facet			Facet			Facet			Facet			Facet			Facet		
107	G3	1			2			3			4			5			6		
108	Point 1	4.82496	0.44237	0.26978	4.65503	0.44811	0.22157	4.49179	0.44459	0.17770	4.30775	0.44954	0.12583	3.93952	0.44834	0.02505	3.52125	0.44891	-0.06994
109	Point 2	4.66874	0.36963	0.24652	4.50103	0.37345	0.19944	4.31949	0.37132	0.15017	4.14124	0.37427	0.10044	3.74647	0.37386	-0.00784	3.32508	0.37322	-0.12337
110	Point 3	4.62719	0.54811	0.18746	4.50022	0.37701	0.19826	4.28911	0.48536	0.11104	4.14124	0.37427	0.10044	3.74516	0.37602	-0.00833	3.32508	0.37322	-0.12337
111	Point 4	4.16842	0.22763	0.15299	4.04652	0.15472	0.13371	3.79812	0.20147	0.05234	3.76359	0.20355	0.04285	3.17536	0.15541	-0.10566	2.98199	0.24064	-0.16182
112	Point 5	4.29176	-2.24588	0.84926	4.17480	-2.32513	0.83865	3.80727	-2.24907	0.74465	3.89193	-2.41913	0.78626	3.29187	-2.00065	0.50866	3.10607	-1.64117	0.36043
113	Point 6	4.69167	-2.49257	1.02567	4.59519	-2.46863	0.99272	4.37431	-2.45821	0.92926	4.25097	-2.52955	0.91468	3.86517	-2.15630	0.70794	3.47166	-1.74831	0.48974
114	Point 7	4.74716	-2.30530	0.99034	4.59627	-2.48486	0.99200	4.41150	-2.33743	0.90686	4.25097	-2.52955	0.91468	3.86651	-2.15168	0.70712	3.47166	-1.74831	0.48974
115	Point 8	4.89443	-2.35176	1.04332	4.74099	-2.51341	1.04484	4.57811	-2.38443	0.96529	4.41114	-2.67881	0.97193	4.06339	-2.20429	0.77533	3.68342	-1.81036	0.56463
116	Point 9	4.82496	0.44237	0.26978	4.65503	0.44811	0.22157	4.49179	0.44459	0.17770	4.30775	0.44954	0.12583	3.93952	0.44834	0.02505	3.52125	0.44891	-0.06994
117	Start of scan line	4.82442	0.00000	0.38906	4.66490	0.00000	0.34526	4.50000	-0.00001	0.30000	4.32901	0.00000	0.25305	3.96663	0.00000	0.15325	3.56687	0.00000	0.04360
118	Middle of rotation	4.82442	0.00000	0.38907	4.66490	0.00000	0.34526	4.50000	0.00000	0.30000	4.32901	0.00000	0.25305	3.96553	0.00000	0.15325	3.56687	0.00000	0.04360
119	End of scan line	4.94361	-1.51167	0.82996	4.80210	-1.65515	0.82967	4.62168	-1.53817	0.74660	4.47166	-1.71403	0.75509	4.06537	-1.40033	0.56426	3.67805	-1.09574	0.37020
120																			

FIG. 14.C1

315/335

	A	B	C	D	E	F	G	H	I	J	K	L	M	N	O	P	Q	R	S
106		Facet			Facet			Facet			Facet			Facet			Facet		
107	G3	1			2			3			4			5			6		
108	Point 1	4.82498	0.44237	0.26978	4.65503	0.44811	0.22157	4.49179	0.44459	0.17770	4.30775	0.44954	0.12583	3.93952	0.44834	0.02606	3.52125	0.44891	-0.06994
109	Point 2	4.66874	0.36963	0.24652	4.50103	0.37345	0.18944	4.31949	0.37132	0.16017	4.14124	0.37427	0.10044	3.74647	0.37385	-0.00784	3.32508	0.37322	-0.12337
110	Point 3	4.62719	0.54611	0.18746	4.50022	0.37701	0.19826	4.26911	0.48536	0.11104	4.14124	0.37427	0.10044	3.74516	0.37603	-0.00933	3.32506	0.37322	-0.12337
111	Point 4	4.18842	0.22763	0.15299	4.04662	0.15472	0.13371	3.79612	0.20147	0.05234	3.76359	0.20356	0.04286	3.17635	0.15541	-0.10566	2.98199	0.24084	-0.18182
112	Point 5	4.29176	-2.24588	0.84926	4.17480	-2.32513	0.83855	3.90727	-2.24907	0.74466	3.89193	-2.41913	0.78826	3.29187	-2.00065	0.60856	3.10807	-1.64117	0.38043
113	Point 6	4.69167	-2.49257	1.02667	4.59519	-2.46863	0.99272	4.37431	-2.45821	0.92926	4.26097	-2.52966	0.91466	3.86517	-2.15630	0.70794	3.47166	-1.74831	0.46974
114	Point 7	4.74716	-2.30530	0.99034	4.59827	-2.46486	0.99200	4.41150	-2.33743	0.90666	4.26097	-2.52955	0.91486	3.86651	-2.15188	0.70712	3.47166	-1.74631	0.46974
115	Point 8	4.89443	-2.36176	1.04332	4.74099	-2.51341	1.04484	4.67811	-2.38443	0.96529	4.41114	-2.57881	0.97193	4.06339	-2.20429	0.77533	3.68342	-1.81036	0.56463
116	Point 9	4.82498	0.44237	0.26978	4.65503	0.44811	0.22157	4.49179	0.44459	0.17770	4.30776	0.44954	0.12583	3.93952	0.44834	0.02506	3.52125	0.44891	-0.06994
117	Start of scan line	4.82442	0.00000	0.38908	4.66490	0.00000	0.34528	4.60000	-0.00001	0.30000	4.32901	0.00000	0.25306	3.98553	0.00000	0.15325	3.56667	0.00000	0.04380
118	Middle of rotation	4.82442	0.00000	0.38907	4.66490	0.00000	0.34528	4.60000	0.00000	0.30000	4.32901	0.00000	0.25306	3.98553	0.00000	0.15326	3.56687	0.00000	0.04380
119	End of scan line	4.94361	-1.51187	0.82996	4.80210	-1.65516	0.82967	4.62188	-1.53817	0.74880	4.47185	-1.71403	0.76509	4.08537	-1.40033	0.56426	3.67805	-1.09574	0.37020
120																			

FIG. 14D1

	A	B	C	D	E	F	G	H	I	J
75		1			2			3		
76		Facet			Facet			Facet		
77	G1	8			10			12		
78	Point 1	5.95032	-0.72692	5.72516	5.75912	-0.72344	5.84633	5.57831	-0.71341	5.95933
79	Point 2	6.80752	-0.82205	5.83575	5.62511	-0.81564	5.95052	5.42747	-0.80763	6.07464
80	Point 3	5.79099	-0.77284	5.83618	5.62511	-0.81564	5.95052	5.42531	-0.80078	6.07461
81	Point 4	5.35054	-1.10363	6.18430	5.33722	-1.01369	6.17433	4.95130	-1.10154	6.43794
82	Point 5	5.44406	-4.23150	6.76631	6.37166	-4.30055	6.82654	4.94319	-4.40584	7.12079
83	Point 6	5.82668	-4.38204	6.55370	5.60403	-4.39100	6.69722	5.33088	-4.56037	6.90578
84	Point 7	5.83655	-4.33627	6.53803	5.60403	-4.39100	6.69722	5.33250	-4.55423	6.90349
85	Point 8	5.95867	-4.37550	6.46837	5.71110	-4.43267	6.63764	5.45432	-4.60159	6.83568
86	Point 9	5.95032	-0.72592	5.72516	5.75912	-0.72344	5.84633	5.57831	-0.71341	5.95933
87	Start of scan line	5.99623	-1.21758	5.79678	5.80609	-1.19815	5.91380	5.61623	-1.19501	6.03397
88	Middle of rotation	6.00363	-1.72998	5.89717	5.80862	-1.62630	6.00000	5.61481	-1.52325	6.10220
89	End of scan line	5.95828	-3.76722	6.34386	5.72650	-3.84809	6.50794	5.48105	-3.93033	6.68100
90										

FIG. 15A1

	A	B	C	D	E	F	G	H	I	J
91	[redacted]	Facet			Facet			Facet		
92	G2	7			9			11		
93	Point 1	5.95867	4.37550	6.46837	5.71110	4.43267	6.63764	5.45432	4.60159	6.83568
94	Point 2	5.83655	4.33627	6.53803	5.60403	4.39100	6.69722	5.33250	4.55423	6.90349
95	Point 3	5.82668	4.38204	6.55370	5.60403	4.39100	6.69722	5.33088	4.56037	6.90578
96	Point 4	5.44406	4.23150	6.76631	5.37166	4.30055	6.82654	4.94319	4.40584	7.12079
97	Point 5	5.35054	1.10363	6.18430	5.33722	1.01369	6.17433	4.95130	1.10154	6.43794
98	Point 6	5.79099	0.77284	5.83618	5.62511	0.81564	5.95052	5.42531	0.80078	6.07461
99	Point 7	5.80752	0.82205	5.83575	5.62511	0.81564	5.95052	5.42747	0.80763	6.07464
100	Point 8	5.95032	0.72592	5.72516	5.75912	0.72344	5.84633	5.57831	0.71341	5.95933
101	Point 9	5.95867	4.37550	6.46837	5.71110	4.43267	6.63764	5.45432	4.60159	6.83568
102	Start of scan line	5.95828	3.76722	6.34386	5.72650	3.84809	6.50794	5.48105	3.93033	6.68100
103	Middle of rotation	6.00363	1.72998	5.89717	5.80862	1.62630	6.00000	5.61481	1.52325	6.10220
104	End of scan line	5.99623	1.21758	5.79678	5.80609	1.19815	5.91380	5.61623	1.19501	6.03397
105										

FIG. 15A2

	A	B	C	D	E	F	G	H	I	J
106	[redacted]	Facet			Facet			Facet		
107	G3	1			2			3		
108	Point 1	7.36483	0.36621	3.60327	7.31635	0.35437	3.81936	7.25212	0.36293	4.03445
109	Point 2	7.33669	0.30677	3.72290	7.27018	0.28546	3.93269	7.20014	0.30320	4.16642
110	Point 3	7.35066	0.45214	3.76848	7.27046	0.29630	3.93374	7.20660	0.39665	4.19794
111	Point 4	7.19969	0.19069	4.09696	7.13404	0.12287	4.26827	7.04932	0.16475	4.57132
112	Point 5	6.76168	-2.71194	3.69330	6.69269	-2.64072	3.63654	6.61109	-2.72069	4.17939
113	Point 6	6.62336	-2.91744	3.36219	6.76969	-2.95787	3.51164	6.69288	-2.89697	3.80174
114	Point 7	6.86196	-2.76529	3.33225	6.77042	-2.95493	3.51128	6.71618	-2.79611	3.76090
115	Point 8	6.89064	-2.80469	3.21407	6.79682	-2.99436	3.40022	6.75093	-2.83803	3.64675
116	Point 9	7.36483	0.36621	3.60327	7.31636	0.35437	3.81936	7.26212	0.36293	4.03445
117	Start of scan line	7.32361	0.00361	3.57345	7.25690	0.00056	3.78342	7.19246	0.00004	4.00001
118	Middle of rotation	7.32326	0.00000	3.57301	7.25662	0.00000	3.78335	7.19245	0.00000	4.00000
119	End of scan line	7.01771	-2.11473	3.23472	6.92439	-2.31840	3.41071	6.87655	-2.14504	3.66987
120										

	A	K	L	M	N	O	P	Q	R	S
106	[redacted]	Facet			Facet			Facet		
107	G3	4			5			6		
108	Point 1	7.17687	0.35054	4.26573	7.03506	0.35961	4.74102	6.87159	0.34512	5.26544
109	Point 2	7.13030	0.29192	4.38726	6.97694	0.30016	4.86659	6.81701	0.28706	5.40695
110	Point 3	7.13030	0.29192	4.38726	6.97921	0.30354	4.86784	6.81701	0.28706	5.40695
111	Point 4	7.02005	0.15684	4.66313	6.81266	0.12498	5.31804	6.72143	0.18544	5.65479
112	Point 5	6.65131	-2.93734	4.23771	6.36745	-2.80040	4.92441	6.22148	-3.08048	5.23666
113	Point 6	6.61699	-3.02659	3.96692	6.47664	-2.92071	4.49196	6.26421	-3.12902	4.96658
114	Point 7	6.61699	-3.02659	3.96692	6.47758	-2.91719	4.49112	6.26421	-3.12902	4.96656
115	Point 8	6.64613	-3.06818	3.84679	6.51493	-2.95743	4.34377	6.32024	-3.16838	4.84610
116	Point 9	7.17687	0.35054	4.26573	7.03506	0.35961	4.74102	6.87159	0.34512	5.26544
117	Start of scan line	7.12389	-0.00002	4.22361	6.97902	0.00007	4.69680	6.82144	0.00006	5.21121
118	Middle of rotation	7.12389	0.00000	4.22362	6.97901	0.00000	4.69679	6.82143	0.00000	5.21120
119	End of scan line	6.77390	-2.39484	3.85364	6.64346	-2.28763	4.35990	6.44631	-2.50435	4.64743
120										

FIG. 15A3

	A	B	C	D	E	F	G	H	I	J
75		1			2			3		
76	[redacted]	Facet			Facet			Facet		
77	G1	8			10			12		
78	Point 1	4.09124	-2.79379	3.18258	3.69818	-2.92223	3.24153	3.24420	-3.02504	3.23954
79	Point 2	4.01214	-2.84817	3.23834	3.63983	-2.96298	3.28365	3.16721	-3.07489	3.28909
80	Point 3	3.98793	-2.83938	3.21628	3.63983	-2.96298	3.28365	3.16395	-3.07385	3.28633
81	Point 4	3.75453	-3.01427	3.40306	3.51489	-3.05022	3.37382	2.92561	-3.22999	3.44252
82	Point 5	5.22942	-4.63324	6.41511	5.13129	-4.70247	6.48702	4.61719	-4.94977	6.68618
83	Point 6	5.73352	-4.52709	6.42964	5.43660	-4.63666	6.49349	5.13524	-4.83496	6.69231
84	Point 7	5.72839	-4.50585	6.39515	5.43660	-4.63666	6.49349	5.13464	-4.83220	6.68785
85	Point 8	5.89808	-4.46565	6.39317	5.58735	-4.60417	6.49668	5.31142	-4.79243	6.68904
86	Point 9	4.09124	-2.79379	3.18258	3.69818	-2.92223	3.24153	3.24420	-3.02504	3.23954
87	Start of scan line	4.26503	-2.91167	3.42532	3.84166	-3.00957	3.42658	3.41287	-3.12422	3.45169
88	Middle of rotation	4.65630	-3.25182	4.08689	4.20000	-3.30000	4.00000	3.71220	-3.35150	3.90711
89	End of scan line	5.66800	-4.26040	5.99609	5.37598	-4.41413	6.12962	5.05851	-4.57920	6.27163
90										

FIG. 15B1

	A	B	C	D	E	F	G	H	I	J
90										
91	[redacted]	Facet			Facet			Facet		
92	G2	7			9			11		
93	Point 1	5.89808	4.46565	6.39317	5.58735	4.60417	6.49668	5.31142	4.79243	6.68904
94	Point 2	5.72839	4.50585	6.39515	5.43660	4.63666	6.49349	5.13464	4.83220	6.68785
95	Point 3	5.73352	4.52709	6.42964	5.43660	4.63666	6.49349	5.13524	4.83496	6.69231
96	Point 4	5.22942	4.63324	6.41511	5.13129	4.70247	6.48702	4.61719	4.94977	6.68618
97	Point 5	3.75453	3.01427	3.40306	3.51489	3.05022	3.37382	2.92561	3.22999	3.44252
98	Point 6	3.98793	2.83938	3.21628	3.63983	2.96298	3.28365	3.16395	3.07385	3.28633
99	Point 7	4.01214	2.84817	3.23834	3.63983	2.96298	3.28365	3.16721	3.07489	3.28909
100	Point 8	4.09124	2.79379	3.18258	3.69818	2.92223	3.24153	3.24420	3.02504	3.23954
101	Point 9	5.89808	4.46565	6.39317	5.58735	4.60417	6.49668	5.31142	4.79243	6.68904
102	Start of scan line	5.66800	4.26040	5.99609	5.37598	4.41413	6.12962	5.05851	4.57920	6.27163
103	Middle of rotation	4.65630	3.25182	4.08689	4.20000	3.30000	4.00000	3.71220	3.35150	3.90711
104	End of scan line	4.26503	2.91167	3.42532	3.84166	3.00957	3.42658	3.41287	3.12422	3.45169
105										

FIG. 15B2

	A	B	C	D	E	F	G	H	I	J	K	L	M	N	O	P	Q	R	S
106		Facet			Facet			Facet			Facet			Facet			Facet		
107	G3	1			2			3			4			5			6		
108	Point 1	7.38483	0.38621	3.60327	7.31636	0.35437	3.81936	7.25212	0.36293	4.03445	7.17887	0.36064	4.26573	7.03606	0.35681	4.74102	6.87159	0.34512	5.26544
109	Point 2	7.33669	0.30877	3.72290	7.27018	0.29848	3.93269	7.20014	0.30320	4.16642	7.13030	0.29192	4.38726	6.97894	0.30016	4.88659	6.81701	0.28706	5.40695
110	Point 3	7.36086	0.45214	3.76848	7.27046	0.29830	3.93374	7.20880	0.39686	4.19794	7.13030	0.29192	4.38726	6.97921	0.30354	4.88784	6.81701	0.28706	5.40695
111	Point 4	7.19989	0.19089	4.09896	7.13404	0.12287	4.26827	7.04932	0.16475	4.57132	7.02005	0.15884	4.66313	6.61288	0.12498	5.31804	6.72143	0.18544	5.65479
112	Point 5	6.76168	-2.71194	3.69330	6.69289	-2.84072	3.83654	6.61109	-2.72089	4.17939	6.55131	-2.93734	4.23771	6.38745	-2.80040	4.92441	6.22148	-3.06048	5.23686
113	Point 6	6.82335	-2.91744	3.36219	6.76969	-2.95787	3.51184	6.69286	-2.89597	3.60174	6.61699	-3.02659	3.96692	6.47584	-2.92071	4.49196	6.28421	-3.12902	4.96658
114	Point 7	6.86196	-2.76529	3.33226	6.77043	-2.96483	3.51128	6.71818	-2.79611	3.78080	6.61699	-3.02659	3.96692	6.47758	-2.91719	4.49112	6.28421	-3.12902	4.96658
115	Point 8	6.89054	-2.80469	3.21407	6.79682	-2.99436	3.40022	6.75093	-2.63603	3.64876	6.64613	-3.06618	3.84679	6.51493	-2.95743	4.34377	6.32024	-3.16836	4.84610
116	Point 9	7.38483	0.38621	3.60327	7.31636	0.35437	3.81936	7.25212	0.36293	4.03445	7.17887	0.35064	4.26573	7.03606	0.36961	4.74102	6.87159	0.34512	5.26544
117	Start of scan line	7.32381	0.00361	3.67345	7.25890	0.00056	3.78342	7.19246	0.00004	4.00001	7.12369	-0.00002	4.22381	6.97902	0.00007	4.69680	6.82144	0.00006	5.21121
118	Middle of rotation	7.32325	0.00000	3.67301	7.25882	0.00000	3.78335	7.19246	0.00000	4.00000	7.12369	0.00000	4.22382	6.97901	0.00000	4.69679	6.82143	0.00000	5.21120
119	End of scan line	7.01771	-2.11473	3.23472	6.92439	-2.31840	3.41071	6.87855	-2.14504	3.66987	6.77390	-2.39464	3.85364	6.64346	-2.26763	4.35990	6.44631	-2.50436	4.84743
120																			

FIG. 15B3

	A	B	C	D	E	F	G	H	I	J
75		1			2			3		
76		Facet			Facet			Facet		
77	G1	8			10			12		
78	Point 1	4.09124	-2.79379	3.18258	3.69818	-2.92223	3.24153	3.24420	-3.02504	3.23954
79	Point 2	4.01214	-2.84817	3.23834	3.63983	-2.96298	3.28365	3.16721	-3.07489	3.28909
80	Point 3	3.98793	-2.83938	3.21628	3.63983	-2.96298	3.28365	3.16395	-3.07385	3.28633
81	Point 4	3.75453	-3.01427	3.40306	3.51489	-3.05022	3.37382	2.92561	-3.22999	3.44252
82	Point 5	5.22942	-4.63324	6.41511	5.13129	-4.70247	6.48702	4.61719	-4.94977	6.68618
83	Point 6	5.73352	-4.52709	6.42964	5.43660	-4.63666	6.49349	5.13524	-4.83496	6.69231
84	Point 7	5.72839	-4.50585	6.39515	5.43660	-4.63666	6.49349	5.13464	-4.83220	6.68785
85	Point 8	5.89808	-4.46565	6.39317	5.58735	-4.60417	6.49668	5.31142	-4.79243	6.68904
86	Point 9	4.09124	-2.79379	3.18258	3.69818	-2.92223	3.24153	3.24420	-3.02504	3.23954
87	Start of scan line	4.26503	-2.91167	3.42532	3.84166	-3.00957	3.42658	3.41287	-3.12422	3.45169
88	Middle of rotation	4.65630	-3.25182	4.08689	4.20000	-3.30000	4.00000	3.71220	-3.35150	3.90711
89	End of scan line	5.66800	-4.26040	5.99609	5.37598	-4.41413	6.12962	5.05851	-4.57920	6.27163
90										

FIG. 15C1

	A	B	C	D	E	F	G	H	I	J
91		Facet			Facet			Facet		
92	G2	7			9			11		
93	Point 1	5.89808	4.46565	6.39317	5.58735	4.60417	6.49668	5.31142	4.79243	6.68904
94	Point 2	5.72839	4.50585	6.39515	5.43660	4.63666	6.49349	5.13464	4.83220	6.68785
95	Point 3	5.73352	4.52709	6.42964	5.43660	4.63666	6.49349	5.13524	4.83496	6.69231
96	Point 4	5.22942	4.63324	6.41511	5.13129	4.70247	6.48702	4.61719	4.94977	6.68618
97	Point 5	3.75453	3.01427	3.40306	3.51489	3.05022	3.37382	2.92561	3.22999	3.44252
98	Point 6	3.98793	2.83938	3.21628	3.63983	2.96298	3.28365	3.16395	3.07385	3.28633
99	Point 7	4.01214	2.84817	3.23834	3.63983	2.96298	3.28365	3.16721	3.07489	3.28909
100	Point 8	4.09124	2.79379	3.18258	3.69818	2.92223	3.24153	3.24420	3.02504	3.23954
101	Point 9	5.89808	4.46565	6.39317	5.58735	4.60417	6.49668	5.31142	4.79243	6.68904
102	Start of scan line	5.66800	4.26040	5.99609	5.37598	4.41413	6.12962	5.05851	4.57920	6.27163
103	Middle of rotation	4.65630	3.25182	4.08689	4.20000	3.30000	4.00000	3.71220	3.35150	3.90711
104	End of scan line	4.26503	2.91167	3.42532	3.84166	3.00957	3.42658	3.41287	3.12422	3.45169

FIG. 15C2

	A	B	C	D	E	F	G	H	I	J	K	L	M	N	O	P	Q	R	S
106	[redacted]	Facet			Facet			Facet			Facet			Facet			Facet		
107	G3	1			2			3			4			5			6		
108	Point 1	7.38483	0.36821	3.60327	7.31635	0.35437	3.81936	7.25212	0.36293	4.03445	7.17887	0.35054	4.26573	7.03508	0.35961	4.74102	6.87159	0.34512	5.26544
109	Point 2	7.33869	0.30677	3.72290	7.27016	0.29548	3.93289	7.20014	0.30320	4.16642	7.13030	0.29192	4.38726	6.97894	0.30016	4.86659	6.81701	0.28706	5.40686
110	Point 3	7.35086	0.45214	3.76848	7.27046	0.29830	3.93374	7.20860	0.38686	4.19794	7.13030	0.29192	4.38726	6.97921	0.30354	4.88784	6.81701	0.28708	5.40686
111	Point 4	7.19969	0.19069	4.09696	7.13404	0.12287	4.28827	7.04932	0.16475	4.57132	7.02005	0.15884	4.66313	6.81288	0.12498	5.31804	6.72143	0.16644	5.65479
112	Point 5	6.76168	-2.71194	3.69330	6.69289	-2.84072	3.83654	6.61109	-2.72069	4.17839	6.55131	-2.93734	4.23771	6.36746	-2.80040	4.92441	6.22146	-3.06046	5.23666
113	Point 6	6.62336	-2.91744	3.36219	6.76969	-2.95787	3.51164	6.69286	-2.89597	3.80174	6.61698	-3.02659	3.96692	6.47684	-2.92071	4.49196	6.26421	-3.12902	4.96858
114	Point 7	6.66196	-2.76529	3.33225	6.77043	-2.95493	3.51126	6.71618	-2.78811	3.78090	6.61698	-3.02659	3.96692	6.47758	-2.91719	4.49112	6.26421	-3.12902	4.96858
115	Point 8	6.69064	-2.80469	3.21407	6.79682	-2.98436	3.40022	6.75093	-2.83603	3.64676	6.64613	-3.06818	3.84679	6.51493	-2.95743	4.34377	6.32024	-3.16838	4.84610
116	Point 9	7.38483	0.36821	3.60327	7.31635	0.36437	3.81936	7.25212	0.36293	4.03445	7.17887	0.35054	4.26573	7.03508	0.35961	4.74102	6.87159	0.34512	5.26544
117	Start of scan line	7.32361	0.00361	3.57345	7.25690	0.00066	3.78342	7.19248	0.00004	4.00001	7.12369	-0.00002	4.22361	6.97902	0.00007	4.69680	6.82144	0.00006	5.21121
118	Middle of rotation	7.32325	0.00000	3.57301	7.25682	0.00000	3.78336	7.19246	0.00000	4.00000	7.12369	0.00000	4.22362	6.97901	0.00000	4.69679	6.82143	0.00000	5.21120
119	End of scan line	7.01771	-2.11473	3.23472	6.92439	-2.31640	3.41071	6.87856	-2.14504	3.86967	6.77390	-2.39464	3.85384	6.84346	-2.26763	4.35990	6.44631	-2.50436	4.84743
120																			

FIG. 15C3

	A	B	C	D	E	F	G	H	I	J
75		1			2			3		
76		Facet			Facet			Facet		
77	G1	8			10			12		
78	Point 1	4.09124	-2.79379	3.18258	3.69818	-2.92223	3.24153	3.24420	-3.02504	3.23954
79	Point 2	4.01214	-2.84817	3.23834	3.63983	-2.96298	3.28365	3.16721	-3.07489	3.28909
80	Point 3	3.98793	-2.83938	3.21628	3.63983	-2.96298	3.28365	3.16395	-3.07385	3.28633
81	Point 4	3.75453	-3.01427	3.40306	3.51489	-3.05022	3.37382	2.92561	-3.22999	3.44252
82	Point 5	5.22942	-4.63324	6.41511	5.13129	-4.70247	6.48702	4.61719	-4.94977	6.68618
83	Point 6	5.73352	-4.52709	6.42964	5.43660	-4.63666	6.49349	5.13524	-4.83496	6.69231
84	Point 7	5.72839	-4.50585	6.39515	5.43660	-4.63666	6.49349	5.13464	-4.83220	6.68785
85	Point 8	5.89808	-4.46565	6.39317	5.58735	-4.60417	6.49668	5.31142	-4.79243	6.68904
86	Point 9	4.09124	-2.79379	3.18258	3.69818	-2.92223	3.24153	3.24420	-3.02504	3.23954
87	Start of scan line	4.26503	-2.91167	3.42532	3.84166	-3.00957	3.42658	3.41287	-3.12422	3.45169
88	Middle of rotation	4.65630	-3.25182	4.08689	4.20000	-3.30000	4.00000	3.71220	-3.35150	3.90711
89	End of scan line	5.66800	-4.26040	5.99609	5.37598	-4.41413	6.12962	5.05851	-4.57920	6.27163
90										

FIG. 15D1

	A	B	C	D	E	F	G	H	I	J
91	[redacted]	Facet			Facet			Facet		
92	G2	7			9			11		
93	Point 1	5.89808	4.46565	6.39317	5.58735	4.60417	6.49668	5.31142	4.79243	6.68904
94	Point 2	5.72839	4.50585	6.39515	5.43660	4.63666	6.49349	5.13464	4.83220	6.68785
95	Point 3	5.73352	4.52709	6.42964	5.43660	4.63666	6.49349	5.13524	4.83496	6.69231
96	Point 4	5.22942	4.63324	6.41511	5.13129	4.70247	6.48702	4.61719	4.94977	6.68618
97	Point 5	3.75453	3.01427	3.40306	3.51489	3.05022	3.37382	2.92561	3.22999	3.44252
98	Point 6	3.98793	2.83938	3.21628	3.63983	2.96298	3.28365	3.16395	3.07385	3.28633
99	Point 7	4.01214	2.84817	3.23834	3.63983	2.96298	3.28365	3.16721	3.07489	3.28909
100	Point 8	4.09124	2.79379	3.18258	3.69818	2.92223	3.24153	3.24420	3.02504	3.23954
101	Point 9	5.89808	4.46565	6.39317	5.58735	4.60417	6.49668	5.31142	4.79243	6.68904
102	Start of scan line	5.66800	4.26040	5.99609	5.37598	4.41413	6.12962	5.05851	4.57920	6.27163
103	Middle of rotation	4.65630	3.25182	4.08689	4.20000	3.30000	4.00000	3.71220	3.35150	3.90711
104	End of scan line	4.26503	2.91167	3.42532	3.84166	3.00957	3.42658	3.41287	3.12422	3.45169
105										

FIG. 15D2

	A	B	C	D	E	F	G	H	I	J	K	L	M	N	O	P	Q	R	S
106		Facet			Facet			Facet			Facet			Facet			Facet		
107	G3	1			2			3			4			5			6		
108	Point 1	7.38483	0.36621	3.60327	7.31636	0.35437	3.81936	7.25212	0.36293	4.03445	7.17687	0.35054	4.26573	7.03506	0.35961	4.74102	6.67159	0.34512	5.26544
109	Point 2	7.33669	0.30677	3.72290	7.27018	0.29548	3.93269	7.20014	0.30320	4.16642	7.13030	0.29192	4.38726	6.97694	0.30016	4.86669	6.81701	0.28708	5.40695
110	Point 3	7.35065	0.45214	3.76646	7.27046	0.29830	3.93274	7.20660	0.39685	4.19794	7.13030	0.29192	4.38726	6.97921	0.30354	4.86784	6.81701	0.28708	5.40695
111	Point 4	7.19969	0.19069	4.09695	7.13404	0.12267	4.26827	7.04932	0.16476	4.57132	7.02006	0.15684	4.66313	6.81266	0.12496	5.31604	6.72143	0.18544	5.65479
112	Point 5	6.76166	-2.71194	3.69330	6.69289	-2.84072	3.83654	6.61109	-2.72069	4.17939	6.55131	-2.93734	4.23771	6.36745	-2.80040	4.82441	6.22148	-3.06046	5.23666
113	Point 6	6.82336	-2.91744	3.36219	6.76969	-2.95787	3.51184	6.69266	-2.89697	3.80174	6.61699	-3.02659	3.96692	6.47664	-2.92071	4.49196	6.26421	-3.12802	4.98656
114	Point 7	6.86196	-2.76529	3.33226	6.77043	-2.95493	3.51126	6.71818	-2.79611	3.76090	6.61629	-3.02659	3.96692	6.47756	-2.91719	4.49112	6.26421	-3.12802	4.98656
115	Point 8	6.89054	-2.80469	3.21407	6.79662	-2.89436	3.40022	6.75093	-2.83603	3.84875	6.64613	-3.06618	3.84679	6.51493	-2.95743	4.34377	6.32024	-3.16838	4.84610
116	Point 9	7.38483	0.36621	3.60327	7.31635	0.35437	3.81936	7.25212	0.36293	4.03445	7.17687	0.35054	4.26573	7.03506	0.35961	4.74102	6.67159	0.34512	5.26544
117	Start of scan line	7.32361	0.00361	3.67346	7.25690	0.00056	3.78342	7.19246	0.00004	4.00001	7.12369	-0.00002	4.22361	6.97902	0.00007	4.69680	6.82144	0.00006	5.21121
118	Middle of rotation	7.32325	0.00000	3.67301	7.25662	0.00000	3.78336	7.19245	0.00000	4.00000	7.12369	0.00000	4.22362	6.97901	0.00000	4.69679	6.82143	0.00000	5.21120
119	End of scan line	7.01771	-2.11473	3.23472	6.82439	-2.31840	3.41071	6.87655	-2.14504	3.66987	6.77390	-2.39464	3.85364	6.64346	-2.26763	4.35990	6.44831	-2.50435	4.64743

FIG. 15D3

A — CREATE 3-D GEOMETRICAL MODEL OF HOLOGRAPHIC LASER SCANNER BASED ON PARAMETERS OBTAINED FROM PRIOR STAGES OF SCANNER DESIGN METHOD, EXCLUDING PARABOLIC LIGHT COLLECTION MIRRORS AND PHOTODETECTORS

B — PERFORM BRAGG SENSITIVITY ANALYSIS ON EACH HOLOGRAPHIC FACET USING THE HSD WORKSTATION TO DETERMINE THE RANGE OF INCIDENCE ANGLES OFF BRAGG, AT WHICH LIGHT RAYS REFLECTED OFF THE PARABOLIC MIRROR WILL BE TRANSMITTED THROUGH THE FACETS WITH MINIMUM DIFFRACTION (I.E. MAXIMUM TRANSMISSION) TOWARDS THE PHOTODETECTOR DURING LIGHT COLLECTION OPERATIONS

C — USE THE HSD WORKSTATION TO TRACE ALL INCOMING LIGHT RAYS REFLECTED OFF A BAR CODE SYMBOL ANYWHERE IN THE SPECIFIED SCANNING VOLUME ONTO THE FACETS OF THE PREDESIGNED SCANNING DISC, AND BASED ON THIS ANALYSIS, IDENTIFY A POINT(S) ABOVE THE SCANNING DISC AND BELOW TOP EDGE OF ASSOCIATED BEAM FOLDING MIRROR, WHICH IS FREE OF INCOMING LIGHT RAYS

D — LOCATE THE POSITION (I.E. CENTER AND OPTICAL AXIS ORIENTATION) OF THE PHOTODETECTORS USING THE "RAY FREE POINT" INFORMATION ACQUIRED DURING BLOCK C ABOVE

FIG. 16A

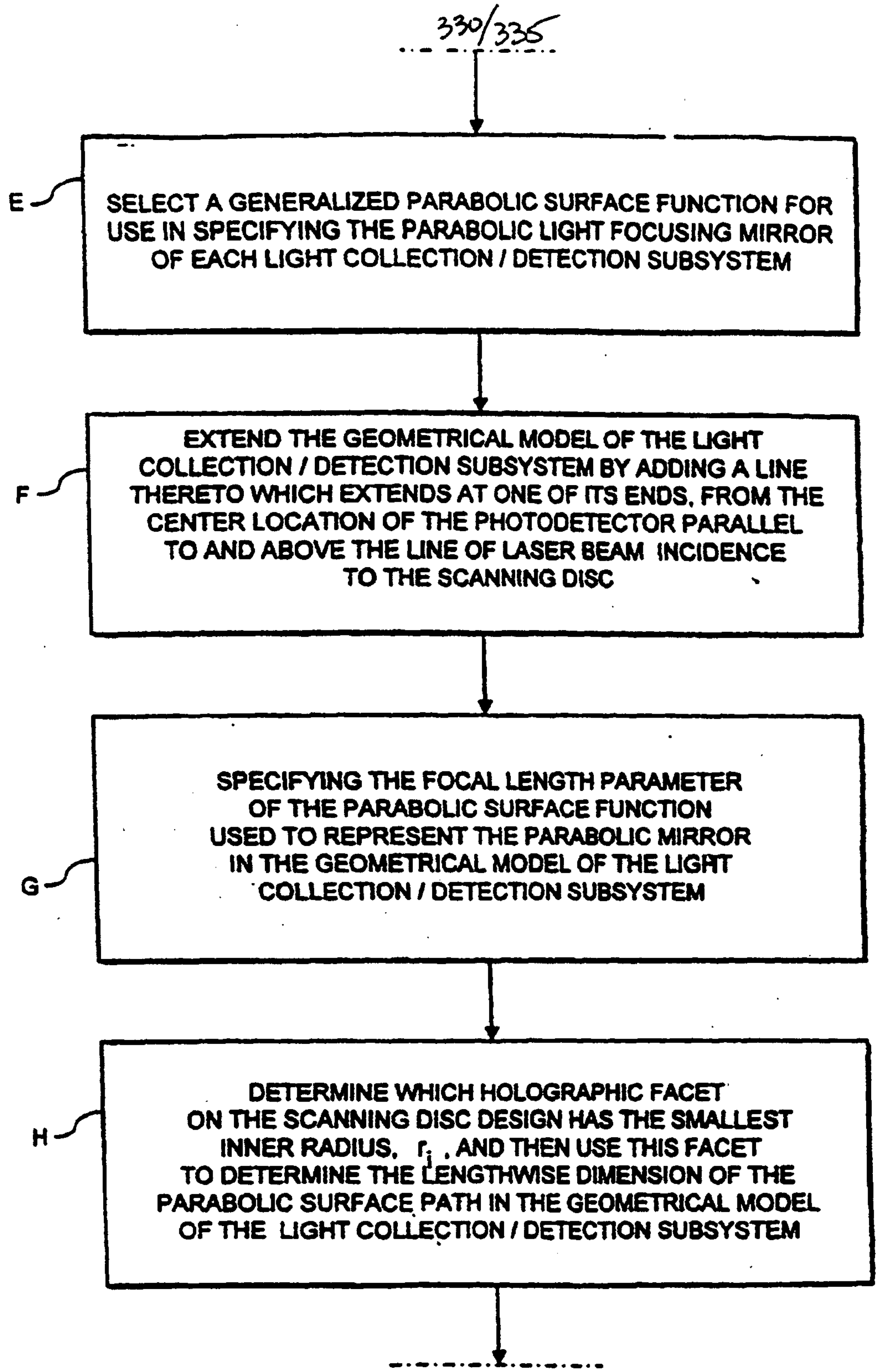
330/335
E
SELECT A GENERALIZED PARABOLIC SURFACE FUNCTION FOR USE IN SPECIFYING THE PARABOLIC LIGHT FOCUSING MIRROR OF EACH LIGHT COLLECTION / DETECTION SUBSYSTEM
F
EXTEND THE GEOMETRICAL MODEL OF THE LIGHT COLLECTION / DETECTION SUBSYSTEM BY ADDING A LINE THERETO WHICH EXTENDS AT ONE OF ITS ENDS, FROM THE CENTER LOCATION OF THE PHOTODETECTOR PARALLEL TO AND ABOVE THE LINE OF LASER BEAM INCIDENCE TO THE SCANNING DISC
G
SPECIFYING THE FOCAL LENGTH PARAMETER OF THE PARABOLIC SURFACE FUNCTION USED TO REPRESENT THE PARABOLIC MIRROR IN THE GEOMETRICAL MODEL OF THE LIGHT COLLECTION / DETECTION SUBSYSTEM
H
DETERMINE WHICH HOLOGRAPHIC FACET ON THE SCANNING DISC DESIGN HAS THE SMALLEST INNER RADIUS, r_i, AND THEN USE THIS FACET TO DETERMINE THE LENGTHWISE DIMENSION OF THE PARABOLIC SURFACE PATH IN THE GEOMETRICAL MODEL OF THE LIGHT COLLECTION / DETECTION SUBSYSTEM

FIG. 16B

I — DETERMINE THE HOLOGRAPHIC FACET HAVING THE GREATEST ANGULAR SWEEP Θ_{SWEEP} ON THE SCANNING DISC

J — USE THE GEOMETRICAL MODEL OF THE SUBSYSTEM AND THE FACET HAVING THE GREATEST ANGULAR SWEEP TO DETERMINE THE LEFT AND RIGHT SURFACE BOUNDARIES TO BE IMPOSED ON THE WIDTHWISE DIMENSIONS OF THE PARABOLIC SURFACE PATCH

K — REVISE GEOMETRICAL MODEL OF LIGHT COLLECTION / DETECTION SUBSYSTEM USING THE COMPLETE SPECIFICATION OF THE PARABOLIC SURFACE PATCH FOR THE PARABOLIC LIGHT FOCUSING MIRROR

L — ANALYZE THE REVISED GEOMETRICAL MODEL ON THE HSD WORKSTATION TO CONFIRM THAT ALL LIGHT RAYS REFLECTED OFF THE PARABOLIC FOCUSING MIRROR ARE TRANSMITTED THROUGH THE RESPECTIVE HOLOGRAPHIC FACETS OFF BRAGG, TO ENSURE THAT MAXIMUM OPTICAL POWER IS TRANSMITTED TO THE PHOTODETECTOR (AT THE FOCAL POINT OF THE MIRROR) FOR DETECTION

FIG. 16C

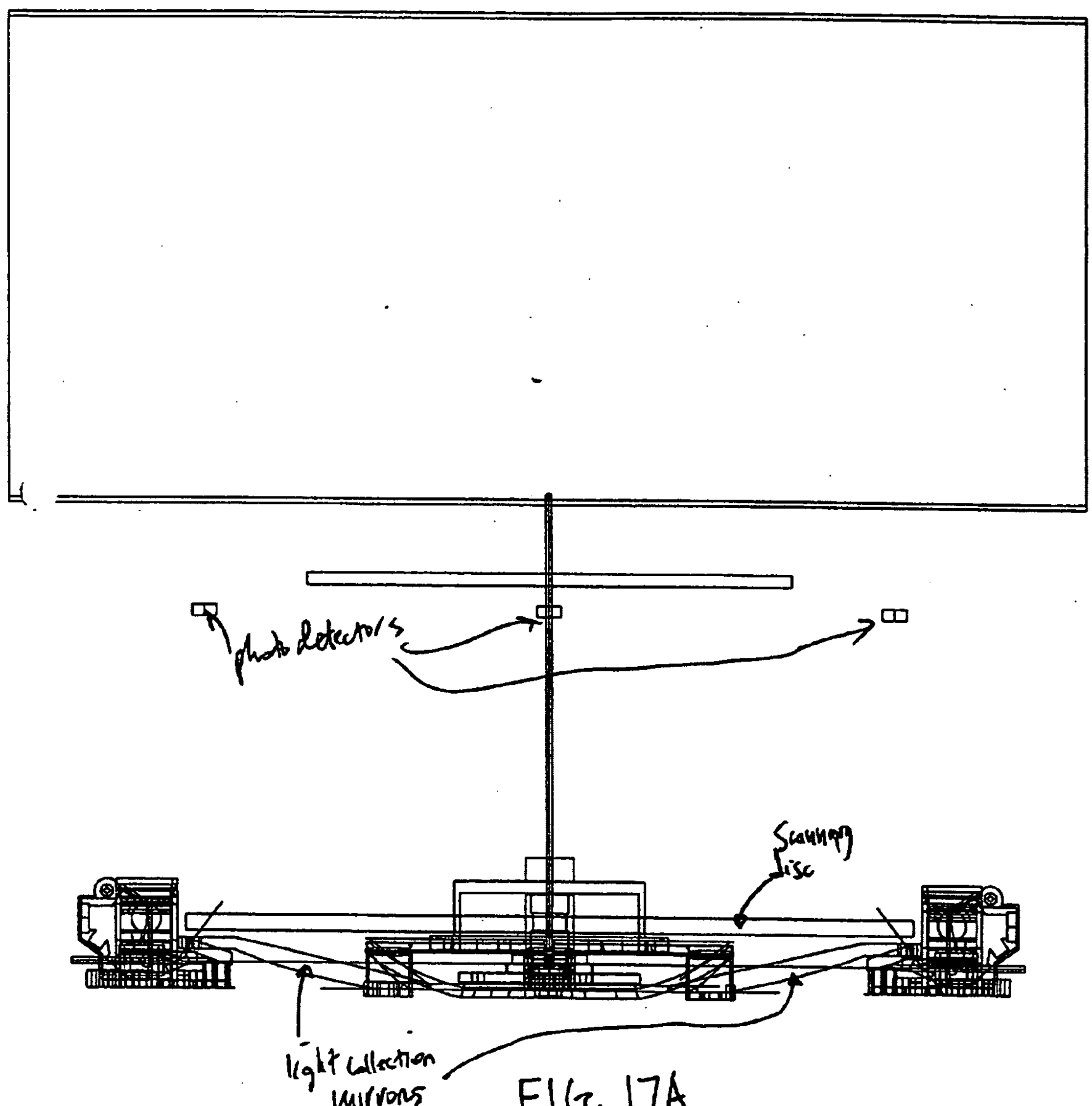

FIG. 17A

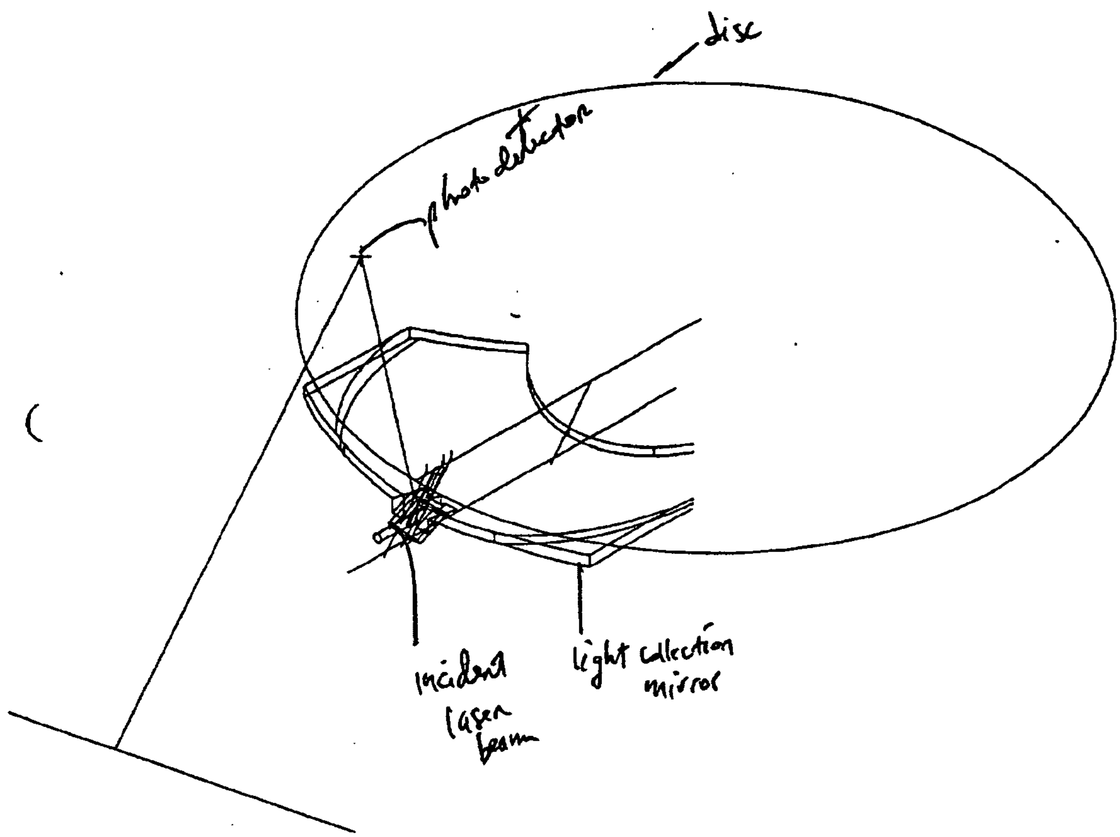
disc
photodetector
incident laser beam
light collection mirror

FIG. 17B

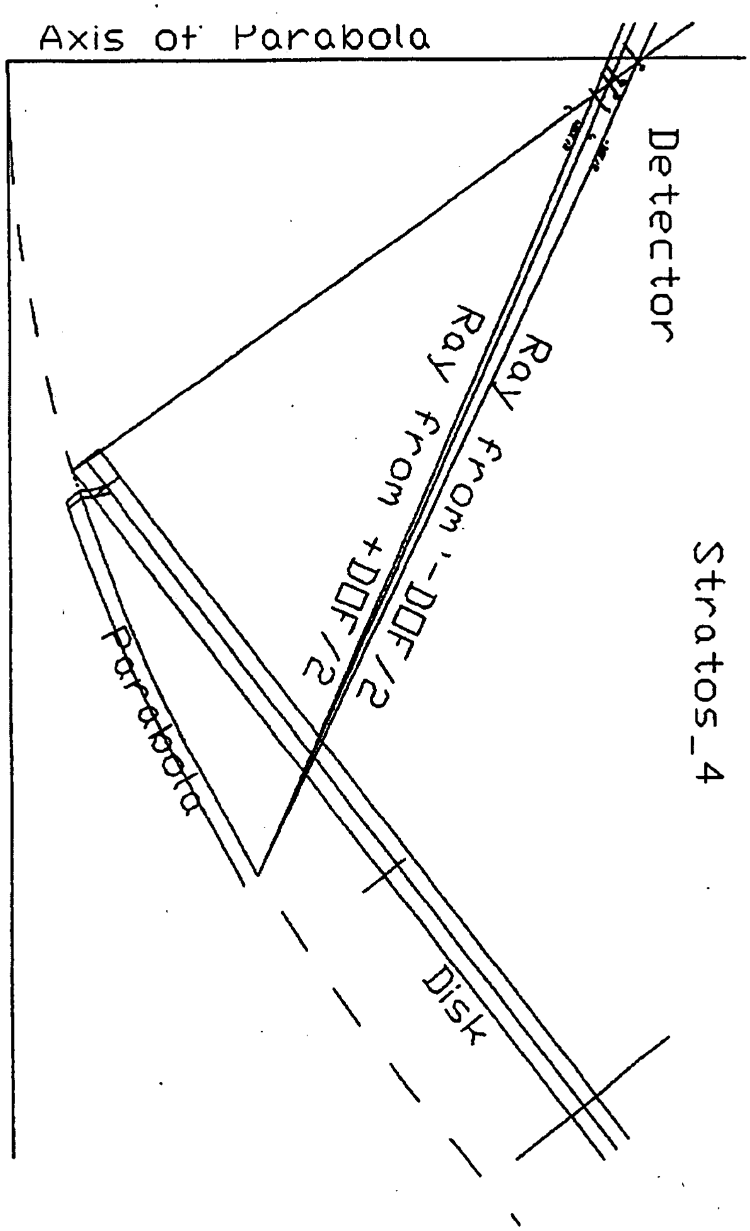
Axis of Parabola
Detector
Ray from -DOF/2
Ray from +DOF/2
Stratos_4
Parabola
Disk

FIG. 17C

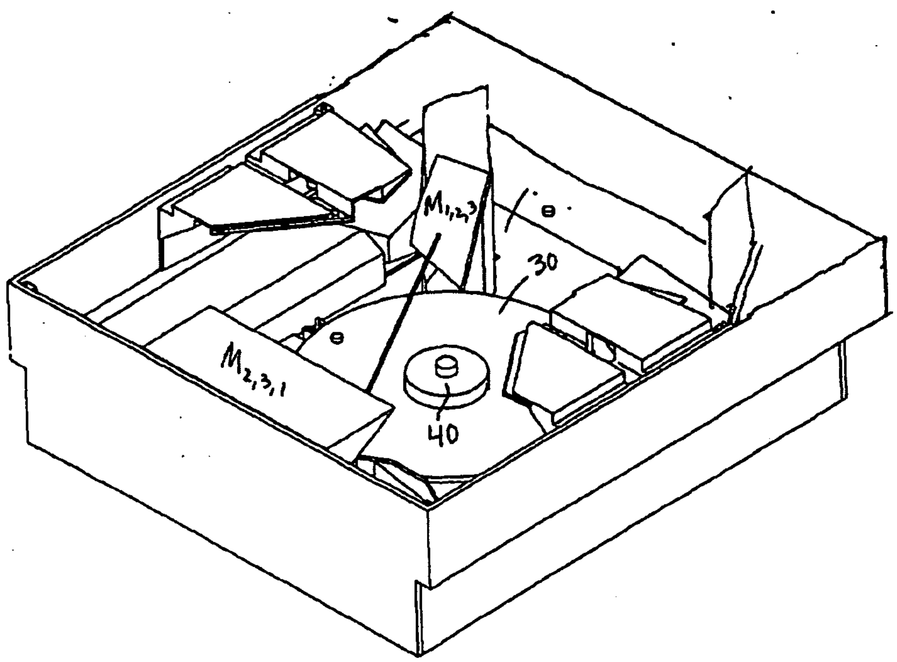

FIG. 18